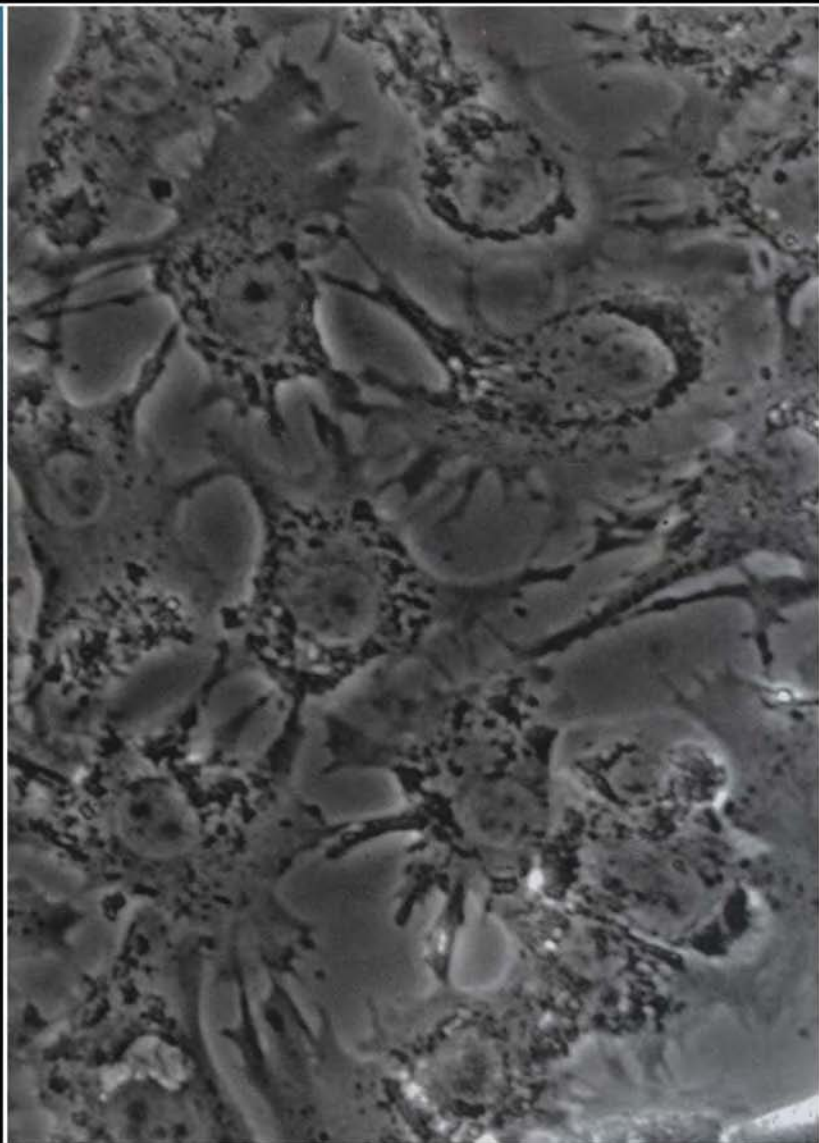


ENDOCRINE METHODS



Edited by John A. Thomas



**ENDOCRINE
METHODS**

This Page Intentionally Left Blank

ENDOCRINE METHODS


EDITED BY **JOHN A. THOMAS**

UNIVERSITY OF TEXAS HEALTH SCIENCE CENTER
SAN ANTONIO, TEXAS



Academic Press

San Diego *New York* *Boston* *London* *Sydney* *Tokyo* *Toronto*

This book is printed on acid-free paper. 

Copyright © 1996 by ACADEMIC PRESS, INC.

All Rights Reserved.

No part of this publication may be reproduced or transmitted in any form or by any means, electronic or mechanical, including photocopy, recording, or any information storage and retrieval system, without permission in writing from the publisher.

Academic Press, Inc.

A Division of Harcourt Brace & Company
525 B Street, Suite 1900, San Diego, California 92101-4495

United Kingdom Edition published by
Academic Press Limited
24-28 Oval Road, London NW1 7DX

Library of Congress Cataloging-in-Publication Data

Thomas, J. A. (John A.), date.

Endocrine methods / by John A. Thomas.

p. cm.

Includes index.

ISBN 0-12-688460-9 (alk. apper)

1. Endocrinology--Methodology. 2. Endocrine toxicology--Methodology. 3. Hormones--Analysis. I. Title.

QP187.T46 1996

612.4'0028--dc20

95-30012
CIP

PRINTED IN THE UNITED STATES OF AMERICA

96 97 98 99 00 01 BB 9 8 7 6 5 4 3 2 1

CONTENTS

Contributors	xvii
Preface	xxi

I Assay Techniques Available for the Toxicologist

Barry D. Albertson, J. Robert Swanson

Introduction	1
Colorimetric Assays	3
Bioassays	3
Radioreceptor Assays	6
Radioimmunoassay	9
Antibodies	13
Radiolabels	18
Separation of the Bound-from-Free Fractions	21
Data Display and Antibody/Receptor Binding Characteristics	26
Assay Quality Control and Validation	28
Nonradiometric Assays	32
Basic ELISA Formats	35
The Heterogenous Assays	37
Homogeneous Enzyme Assays	40
Fluorescence Assays	44
Chemiluminescent Assays	51
Other Assay Techniques	55
Appendix 1: Selected Hormone Marker Assays	
Useful to the Toxicologist	60
Lipid-Soluble Hormones (Steroids/ Vitamin D/Thyroid Hormones)	60
Water-Soluble Hormones	64
Conclusion/Addendum	68
References	69

2 Longitudinal Bone Growth: Experimental Methods

Jeffrey Baron

Principles of Longitudinal Bone Growth 81

Measurement of Longitudinal Bone
Growth 82

Growth Plate Infusion 85

References 87

3 Measurement of Steroid Receptor Binding to DNA

Franklin G. Berger, Gordon Watson

Introduction 89

Mobility Shift Analysis 90

Materials 91

Procedures 91

Comments 92

DNase I Footprinting 94

Materials 95

Procedures 95

Comments 96

Methylation Interference 97

Materials 98

Procedures 98

Comments 99

References 99

4 Hypophysical Grafts beneath the Renal Capsule: A Model to Study Endocrine Control Systems

Gary T. Campbell, Martha A. Steele, Charles A. Blake

History and Utility of Pituitary Grafts 101

Comparison of the Pituitary Allograft Model
with Studies Using Pituitary Tissue *in Situ* or
in Vitro 104

Techniques and Considerations for Grafting

Pituitary Tissue beneath the Renal Capsule 105

Methodology 105

Selection of Hosts 108

Selection of Donor Tissue 110

Allografts of Control Tissue	112
Removal of Allograft Tissue	112
Summary of the Status of the Host and the Allograft Tissue	113
Status of Host	113
Status of Allograft	113
References	113

5 Prolactin Secretion from Single Cells: Analysis by Reverse Hemolytic Plaque Assays

Fredric R. Boockfor

Introduction 115

Establishment of a Prolactin Plaque
Assay 117

Procedures 117

 Reagents, Materials, and Equipment 117

 Preparation for Assay 118

 Assay Performance 121

Advantages of Using RHPA Analysis 125

Application of Plaque Assays to Assess Toxic
Influence 126

References 128

6 Application of Fluorescence Techniques to Bone Biology

Akimitsu Miyauchi, Akira Fujimori, Roberto Civitelli

Introduction 131

Cell Cultures 132

 Osteoblastic Cells 132

 Osteoclastic Cells 134

Analyses in Cell Populations 135

 Applicative Considerations 135

 Sample Preparation 136

 Cytosolic Calcium 137

 Intracellular pH 138

 Membrane Potential 139

 Cell-Cell Communication 141

Analyses in Single Cells 142

 Applicative Considerations 142

 Sample Preparation 144

Cytosolic Calcium	144
Intracellular pH	146
Intracellular Cyclic AMP	147
Cell Coupling	149
References	150

7 Measurement of Thyroid Hormone and Related Molecules

Edward J. Diamond

Introduction	157
Laboratory Measurements to Assess Thyroid Function	158
Total Thyroxine (T4) and Triiodothyronine (T3)	158
Free Thyroid Hormone Measurements	159
Thyroid-Stimulating Hormone (Thyrotropin)	169
Autoimmune Processes That Influence Thyroid Gland Function and Hormone Measurements:	
Serum Thyroid Autoantibodies	173
Autoantibodies to Thyroid Peroxidase and Thyroglobulin	173
Antibodies to the TSH Receptor	175
Measurement of Serum Thyroglobulin	176
Conclusions	177
References	178

8 Uptake Measurements of Thyroid Hormones and Amino Acids in Cultured Cells

Vadivel Ganapathy, Puttur D. Prasad, Frederick H. Leibach

Introduction	187
Amino Acid Transport Systems	188
Substrate Specificity and Driving Forces	188
Interaction between Thyroid Hormones and Amino Acids during Transport	189
Strategies to Establish the Identity of the Transport System for Any Particular Amino Acid	190
Uptake Measurements in Cultured Cells	191
Cell Culture	191
Uptake Measurement	192

Determination of Incorporation of Amino Acids into Cellular Proteins during Uptake	194
Differentiation between Transmembrane Transport and Cell-Surface Binding	194
Differentiation between Passive and Active Transport	195
Determination of Cell Number and Protein Content	195
Plasma Membrane Vesicles Derived from Cultured Cells for Uptake Measurements	196
Advantages of the Use of Membrane Vesicles	196
Isolation of Plasma Membrane Vesicles from Cultured Cells	196
Uptake Measurement in Plasma Membrane Vesicles	197
Differentiation between Passive Transport and Active Transport	199
Conclusion	199
References	200

9 Two-Dimensional Gel Electrophoresis of Proteins

Chung Lee, Yi Qian, Julia A. Sensibar, Harold H. Harrison	
Introduction	203
Sample Preparation	204
Solubilizing Agents	204
Preparation of Solid Tissues for 2D	204
Preparation of Cells for 2D	205
Preparation of Fluid Specimens for 2D	205
The First Dimension: The ISO System	205
Alternate First Dimension: The IPG System	207
The Second Dimension: The DALT System	207
Detection of Protein Spots in 2D Gels	209
Coomassie Blue Dye Staining	209
Silver Staining	209
Fluorography	212
Protein Blotting	212

Support Membranes and Transfer Buffer	213
Electroblotting	213
Staining for Total Proteins on Membranes	213
Detection of Specific Proteins by Western Blotting	214
Detection of Glycoconjugates and Glycoproteins Using Digoxigenin-Labeled Lectins	216
Analysis of 2D Protein Profiles by Computer- Based Image Analysis Systems	217
Summary	218
References	219

10 Effects of *in Vivo* Exposure to Glucocorticoids on Pituitary, Serum, and Messenger Ribonucleic Acid Levels of the Gonadotropin Hormones FSH and LH in Male and Female Rats

Joanne M. McAndrews, Sonia J. Ringstrom

Introduction	221
Methodologies	223
Hormone Pellet Construction	223
Surgeries	224
Subcutaneous Injections	225
Tissue Dissection and Serum Collection	225
Pituitary Hormone Content Extraction	225
Radioimmunoassays	226
Pituitary Total RNA Extraction	227
Northern Blot Analysis	227
Experimental Protocols	228
Experiment 1	228
Experiment 2	228
Experiment 3	229
Results	229
Serum Levels of Cortisol (F) and Corticosterone (B)	229
Gonadotropin Hormone Subunit Messenger RNA Levels	232
Summary	235
References	238

11 Glutamate Receptor Autoradiography and *in Situ* Hybridization

Rick Meeker

Introduction	239
Glutamate Receptors and CNS Pathology	239
Glutamate Receptor Neurotoxins	240
Neuroendocrine Effects of Excitotoxins	242
Receptor Plasticity	243
Methods for Studying Glutamate Receptor	
Expression	244
Dealing with Multiple Receptor Subtypes	244
The Glutamate Receptor Binding Assay	249
General Considerations	249
Materials	250
Glutamate Receptor Autoradiography	251
Nonspecific Binding	252
Indirect Glutamate Receptor Subtype Analysis	252
Direct Glutamate Receptor Subtype Analysis	254
Saturation Binding	255
The Glutamate Transporter and	
Nonspecific Binding	256
Standards	257
Automated Densitometry and Grain Counting	259
Identification of Glutamate Receptor Subtypes	
by <i>In Situ</i> Hybridization Analysis	260
The Basic <i>in Situ</i> Hybridization Protocol for	
Glutamate Receptors	260
Maximizing the <i>in Situ</i> Hybridization	
Reactions	266
Autoradiography and Analysis	267
Troubleshooting and Elimination of Nonspecific	
Hybridization	268
Stock Solutions for <i>in Situ</i> Hybridization	270
References	271

12 Chromatographic Methods for Analyzing β -Endorphin and Related Peptides

William R. Millington, Amy B. Manning

Introduction	281
Procedures	285

Tissue Extraction Procedures	285
Procedures for Separating β -Endorphin from β -Lipotropin and POMC	289
Analysis of Individual β -Endorphin Peptides	291
Analysis of β -Endorphin Peptides in the Human Pituitary	294
Conclusions	295
References	296

13 Detection of Autoantibodies to the Thyrotropin Receptor

John S. Dallas, Bellur S. Prabhakar

The Thyrotropin Receptor and Normal Thyroid Function	299
The Structure of the Thyrotropin Receptor	299
The Function of the Thyrotropin Receptor	300
The Thyrotropin Receptor and Autoimmune Thyroid Diseases	301
Thyrotropin Receptor Antibody-Mediated Thyroid Diseases	301
Clinical Usefulness of Thyrotropin Receptor Antibody Assays	302
Methods to Detect Autoantibodies to the Thyrotropin Receptor	303
Radioreceptor Assays	303
Bioassay Methods	306
Correlations between Radioreceptor and Bioassay Methods	310
Future Directions for Detection of Thyrotropin Receptor Antibodies	311
References	315

14 Measurement of Intracellular Glucocorticoid and Mineralocorticoid Receptors

Andrew S. Meyer, Thomas J. Schmidt

Introduction	319
Overall Goal	319
Physiological Effects of Adrenal Corticosteroids	320

Intracellular Mode of Action of Adrenal Corticosteroids	323
Autoregulation of Corticosteroid Receptors	326
Measurement of Intracellular GR and MR	327
Quantitation of GR and MR Binding Levels	327
Quantitation of GR and MR Protein Levels	331
Quantitation of GR and MR mRNA Levels	335
Autoregulation of Rat Colonic GR and MR	340
Introduction	340
Effects of Adrenalectomy of GR and MR Ligand Binding Levels	341
Effects of Adrenalectomy on GR and MR Protein Levels	342
Effects of Adrenalectomy and Exogenous Ligands on GR and MR mRNA Levels	345
Conclusions	348
References	350

15 Use of Transfection Techniques for Studying the Function of the D₂ Dopamine Receptors

Susan E. Senogles, Michael W. Quasney

Introduction	355
Importance of Dopamine in Regulating Prolactin Secretion from the Pituitary	355
Dopamine Receptor Signaling	356
Dopamine Receptor Expression	356
Why Use Transfection Techniques	357
Transfection of Clonal Pituitary Cell Lines	357
Choice of Parent Cell Line	357
Stable Transfection in GH4C1 with Constitutive Expression	358
Inducible Expression of D ₂ Dopamine Receptors in AtT20 Cells	364
Transient Expression in HEK 293 Cells	365
Conclusions	366
The Potential of Using Transfection for Study of Structure–Function Relationships of Receptors	366
The Potential for the Study of Cellular Processes by Individual Receptor Subtypes	367
References	368

16 Quantitation of Metallothionein

Michael P. Waalkes

- The Physiology and Toxicology of Metallothionein 371
 - Structure and Biological Characteristics 372
 - Possible Functions 374
 - Toxicity 377
- Quantitation of Metallothionein 377
 - General Comments 377
 - Metal Saturation Assays 378
 - Immunological Assays 380
- Analysis of Metallothionein mRNA 381
- Use of Metallothionein Analysis in Endocrine Toxicology 382
- Summary and Conclusions 383
- References 385

17 Primary Culture of Bovine and Human Adult Adrenocortical Cells

Matthias M. Weber, Patrick Michl

- Introduction 393
- Materials and Reagents 394
 - Equipment and Supplies 394
 - Reagents and Solutions 394
- Cell Culture of Bovine Adrenocortical Cells 396
 - Source of Bovine Adrenal Glands 396
 - Dissection of Bovine Adrenocortical Tissue 396
 - Preparation of Bovine Fasciculata Cell Suspensions 397
 - Purification of Bovine Fasciculata Cells by Percoll Centrifugation 399
 - Monolayer Cell Culture of Bovine Adrenocortical Cells 400
- Cell Culture of Human Adrenocortical Cells 401
 - Source of Human Adrenal Glands 403
 - Dissection of Human Adrenocortical Tissue 403
 - Isolation and Purification of Human Fasciculata Cells 404

Monolayer Cell Culture of Human Adrenocortical Cells	404
Diagnostic Evaluation of Adrenocortical Cell Cultures	405
Proliferation Studies	405
Steroidogenic Response	409
Conclusions	414
References	415

18 Assays for Vasopressin

Arnold M. Moses, Carol Jones	
Background	417
Methodology	420
Handling Specimens	421
Extraction Procedures	422
Radioimmunoassay	423
Techniques of Determining Amount of Unknown AVP Following Gamma-Counter Counting	428
Normal Values in Humans	428
Currently Utilized Methods in Authors' Laboratory	429
Application of RIA for Vasopressin	433
Normal Regulation of Arginine Vasopressin Secretion	434
Metabolism of AVP	435
Role of AVP in Disease States	436
<i>In Vitro</i> Studies	439
References	440

Index	447
--------------	-----

This Page Intentionally Left Blank

CONTRIBUTORS

Numbers in parentheses indicate the pages on which the authors' contributions begin.

- Barry D. Albertson** (1), Department of Medicine, Division of Endocrinology, Diabetes, and Clinical Nutrition and Department of Pathology, Oregon Health Sciences University, Portland, Oregon 97201
- Jeffrey Baron** (81), Developmental Endocrinology Branch, National Institute of Child Health and Human Development, National Institutes of Health, Bethesda, Maryland 20892-1862
- Franklin G. Berger** (89), Department of Biological Sciences, University of South Carolina, Columbia, South Carolina 29208
- Charles A. Blake** (101), Department of Cell Biology and Neuroscience, University of South Carolina School of Medicine, Columbia, South Carolina 29208
- Fredric R. Boockfor** (115), Department of Cell Biology and Neuroscience, University of South Carolina School of Medicine, Columbia, South Carolina 29208
- Gary T. Campbell** (101), Department of Cell Biology and Neuroscience, University of South Carolina School of Medicine, Columbia, South Carolina 29208
- Roberto Civitelli** (131), Division of Bone and Mineral Diseases, Washington University School of Medicine, St. Louis, Missouri 63110
- John S. Dallas** (299), Department of Pediatrics, The University of Texas Medical Branch, Galveston, Texas 77555
- Edward J. Diamond** (157), Department of Medicine, Division of Endocrinology, Mt. Sinai School of Medicine, New York, New York 10029
- Akira Fujimori** (131), Department of Artificial Kidney, Konan Hospital, Kobe, Japan
- Vadivel Ganapathy** (187), Department of Biochemistry and Molecular Biology, Medical College of Georgia, Augusta, Georgia 30912-2100
- Harold H. Harrison** (203), Genetrix, Inc. and Southwest Biomedical Research Institute, Scottsdale, Arizona 85251

- Carol Jones** (417), Department of Medicine, State University of New York, Syracuse, New York 13210
- Chung Lee** (203), Department of Urology, Northwestern University Medical School, Chicago, Illinois 60611
- Frederick H. Leibach** (187), Department of Biochemistry and Molecular Biology, Medical College of Georgia, Augusta, Georgia 30912-2100
- Amy B. Manning** (281), Division of Molecular Biology and Biochemistry, University of Missouri-Kansas City, Kansas City, Missouri 64018
- Joanne M. McAndrews** (221), Department of Neurobiology and Physiology, Northwestern University, Evanston, Illinois 60208
- Rick Meeker** (239), Department of Neurology, University of North Carolina, Chapel Hill, North Carolina 27599
- Andrew S. Meyer** (319), Department of Physiology and Biophysics, College of Medicine, The University of Iowa, Iowa City, Iowa 52242
- Patrick Michl** (393), Medical Department II, Laboratory of Endocrine Research, Klinikum Großhadern University of Munich, 81377 Munich, Germany
- William R. Millington** (281), Division of Molecular Biology and Biochemistry, University of Missouri-Kansas City, Kansas City, Missouri 64018
- Akimitsu Miyauchi** (131), National Sanatorium, Hyogo Chuo Hospital, Sanda, Hyogo, Japan
- Arnold M. Moses** (417), Department of Medicine, State University of New York, Syracuse, New York 13210
- Bellur S. Prabhakar** (299), Department of Microbiology and Immunology, The University of Texas Medical Branch, Galveston, Texas 77555
- Puttur D. Prasad** (187), Department of Biochemistry and Molecular Biology, Medical College of Georgia, Augusta, Georgia 30912-2100
- Yi Qian** (203), Department of Urology, Northwestern University Medical School, Chicago, Illinois 60611
- Michael W. Quasney** (355), Department of Pediatrics, Division of Critical Care, LeBonheur Children's Medical Center, University of Tennessee, Memphis, Tennessee 38103
- Sonia J. Ringstrom** (221), Department of Neurobiology and Physiology, Northwestern University, Evanston, Illinois 60611
- Thomas J. Schmidt** (319), Department of Physiology and Biophysics, College of Medicine, The University of Iowa, Iowa City, Iowa 52242
- Susan E. Senogles** (355), Department of Biochemistry, University of Tennessee, Memphis, Tennessee 38163
- Julia A. Sensibar** (203), Department of Urology, Northwestern University Medical School, Chicago, Illinois 60611
- Martha A. Steele** (101), Department of Cell Biology and Neuroscience, University of South Carolina School of Medicine, Columbia, South Carolina 29208

J. Robert Swanson (1), Department of Pathology, Division of Clinical Pathology, Oregon Health Sciences University, Portland, Oregon 97201

Michael P. Waalkes (371), Inorganic Carcinogenesis Section, Laboratory of Comparative Carcinogenesis, Division of Basic Sciences, National Cancer Institute, Frederick Cancer Research and Development Center, Frederick, Maryland 21702-1201

Gordon Watson (89), Children's Hospital, Oakland Research Institute, Oakland, California 94609

Matthias M. Weber (393), Medical Department II, Laboratory of Endocrine Research, Klinikum Großhadern, University of Munich, 81377 Munich, Germany

This Page Intentionally Left Blank

PREFACE

Endocrine Methods is a continuing and important contribution to the toxicology field. The contributors represent leading authorities in their respective fields of endocrinology. The use of advanced methodological assays has further extended scientific knowledge surrounding important endocrine events. Such selected methods or assays are not only valuable in understanding physiological processes, but also for enhancing the knowledge of how cellular perturbations caused by toxic agents lead to endocrine disruptions. Advances in molecular endocrinology are inseparable with state-of-the-art technology and sophisticated biochemical methods.

Endocrine Methods offers a wide spectrum of assays important to several areas of hormone research. Methodologies involve organs such as the thyroid, the adrenal, and the pituitary glands. Several techniques for studying receptors (e.g., steroids, thyrothropin, dopamine, etc.) and for examining osteoblast activity and the measurement of parathyroid hormone are described. Methods for examining and analyzing specific proteins and peptides related to the endocrine system are likewise important topics that may be useful to the toxicologist seeking to better understand chemical-/drug-induced changes in the hormonal environment. A number of approaches, some involving *in vitro* assays, cell culture techniques, and *in situ* methods can be utilized to study aspects of the endocrine system. *Endocrine Methods* encompasses a host of important research tools that can be exploited by the toxicologist and other biomedical scientists.

John A. Thomas

This Page Intentionally Left Blank

1

Assay Techniques Available for the Toxicologist

Barry D. Albertson

Department of Medicine

*Division of Endocrinology, Diabetes, and
Clinical Nutrition and*

Department of Pathology

Oregon Health Sciences University

Portland, Oregon 97201

J. Robert Swanson

Department of Pathology

Division of Clinical Pathology

Oregon Health Sciences University

Portland, Oregon 97201

INTRODUCTION

Over the past 50 years toxicology has evolved to become a very precise discipline. And as in other changing research areas, the ability to measure useful and important toxicological end points has taken on a greater significance. Endocrine toxicology encompasses the study of drugs and chemicals that can disquiet the delicate balance of hormones and metabolic processes, causing serious perturbations in the function of many endocrine organs. To study and evaluate the many toxicological forces on endocrine and nonendocrine systems, one must be aware of the tools and reagents available to accurately and precisely monitor toxicological effects.

Prior to 1960 it was relatively uncommon for the concentrations of hormones in biological fluids to be measured. A few steroids could be reckoned with reasonable accuracy, but large volumes of plasma or urine were required and researchers (including toxicologists) were obliged to withstand exacting procedures and invest large amounts of time to get results. Measuring the water-soluble or other lipid-soluble hormones were at best a nightmare and at worst a pipe dream (1). It was in 1959 and 1960

that scientists at two well-known research centers, one at the Veterans Administration Hospital in the Bronx, New York, and the other at the Middlesex Hospital Medical School in London, broke through the barriers and published what are now considered “the” classic papers describing the radioimmunoassay (2,3). For several years Drs. Rosalyn Yalow and Solomon Berson had been investigating the immunological characteristics and metabolism of insulin in both diabetic and nondiabetic patients. In this effort they characterized a specific insulin antibody and used it as a key reagent in their insulin assay. Oddly enough, the initial attempt to publish their results was met with rejection at the hands of *The Journal of Clinical Investigation* (4). Roger Ekins, on the other hand, pursued more general microanalytical techniques that were amenable to a wide group of biological compounds, and in this endeavor relied on a naturally occurring protein, thyroxine binding globulin, as the specific reagent in his thyroid hormone assay. Interestingly, both of these investigative efforts were hampered by the lack of appropriate radioactive markers possessing adequate specific activity. So it is no surprise that the birthplace of these immunoassays was at “specialized radioisotope centers” (5).

The radioimmunoassay, or RIA, and other, newer assay methodologies have added new weapons to the arsenal of endocrine toxicologists and have given the practitioners of toxicology tools with which to monitor the endocrine effects of toxic agents. But for this single technology to capture the attention of scientists worldwide, other events had to fall into place. One of these was the development of a novel protein radioiodination technique, using the oxidant chloramine T and relatively small amounts of ^{131}I . This one refinement by Greenwood *et al.* in 1963 (6) enabled virtually any reputable laboratory to radiolabel polypeptide hormones with high specific activity. ^{14}C -radiolabeling of steroids came earlier, twenty years or so, but readily available ^3H - and ^{14}C -labeled steroid hormones possessing high specific activities for RIA use were developed coincidentally with that of the peptide hormones (7).

Fractions of cell membranes (8) and cell receptors (9,10) were also employed as “reagents” in these new assays with the hope of imparting a greater degree of specificity. Instead of these, however, it was unique antibody production that played a second crucial role in the development of RIAs. Reagent-class antibodies opened the door to the generation of assays for a vast number of peptide, polypeptide, and glycoprotein hormones. Nonprotein hormones (and a few other compounds or haptens) fell short in terms of their “intrinsic antigenicity,” for example, the steroids, thyroid hormones, cyclic nucleotides, and prostaglandins (5). Antibodies for these delinquent hormones soon were available owing to some sophisticated

chemical manipulations that disguised these hormones so that highly specific and sensitive antibodies could be obtained.

Finally, but certainly not the least important, was the isolation and purification of protein, peptide, steroid, and other hormones and factors from tissues and blood so that radioligands, antibodies, and assay standards could be generated. The women and men who gave hour upon hour of laboratory tedium for this end have never been given adequate credit.

Thus, with all the pieces available to put the puzzle together, curiosity and necessity stoked the fire that led to what today is a triumph of scientific ingenuity. Thousands of endocrine and nonendocrine toxicologists use the techniques and reagents described in the following, this enterprise being fueled by a billion dollar endocrine diagnostic, research, and development industry that produces state-of-the-art reagents, and newer and better assays and assay reagents. The overview presented here is a compilation of the published work and words of many pioneering investigators in hormone assay technology.

COLORIMETRIC ASSAYS

During the years that sophisticated bio- and radioimmunoassays were being developed, clinical chemists and biochemists, using advances in chemical manipulation, provided the expertise and technology to measure a wide variety of compounds in blood and biological fluid that were important to both clinicians and researchers. An excellent review of many of these assays was published by Gold in 1975 (11).

Though these assays began as laborious manual methods, they have remained in the armamentaria of hospital laboratories, evolving to what are now automated (autoanalyzer) analysis systems. These tests measure the molecules that hormones affect, like glucose, urea nitrogen, uric acid, calcium, phosphorous, and many others. Two representative colorimetric assays that are frequently used quantitate serum cholesterol and triglycerides. The principles of these assays, as with all colorimetric assays, are based on the chemical structure and metabolism of the molecules in question and on the addition of specific reagents, including enzymes, to generate quantitative color changes (usually measured spectrophotometrically) that are specific for that particular compound (Figure 1).

BIOASSAYS

Bioassays represent some of the earliest assays available to toxicologists. They usually involved the injection of specific agents into live animals and

4 Chapter 1 Assay Techniques Available for the Toxicologist

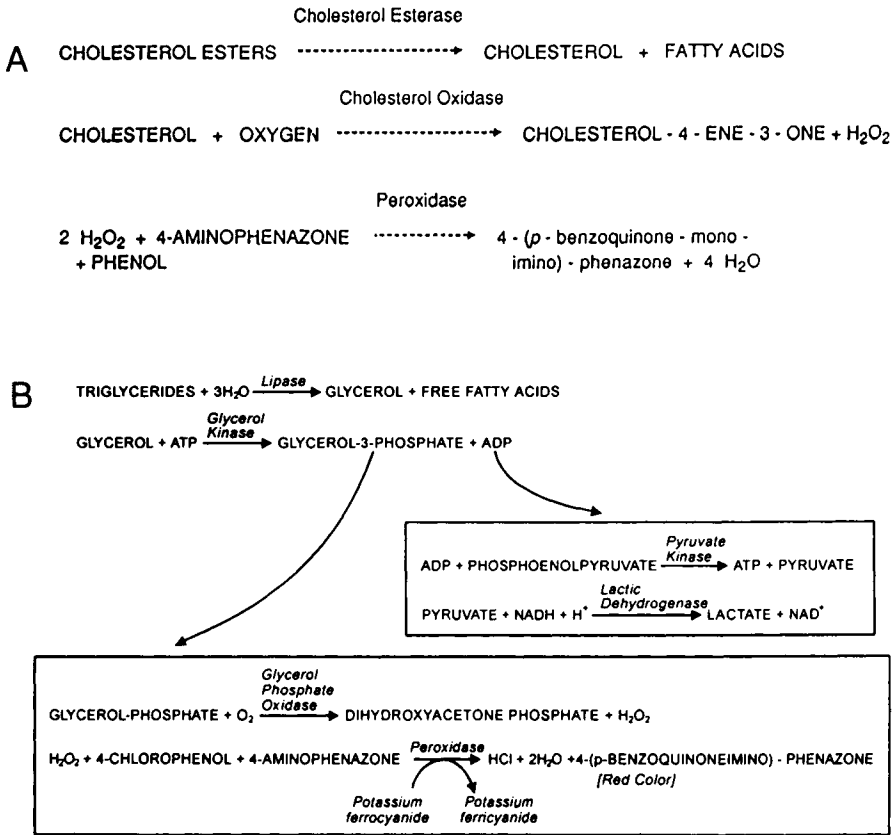


FIGURE 1. Colorimetric assay methodology for measuring serum cholesterol and triglycerides. (A) Cholesterol is produced enzymatically by the use of cholesterol esterase, which effectively hydrolyzes cholesterol esters. Then, in the presence of oxygen, free cholesterol is oxidized by cholesterol oxidase to cholest-4-ene-3-one and stoichiometric amounts of hydrogen peroxide (H₂O₂). The H₂O₂ subsequently reacts with phenol and 4-aminophenazone in the presence of peroxidase to form 4-(p-benzoquinone-monoimino)-phenazone, which is pink in color. The intensity of the color formed is proportional to the cholesterol concentration of the original sample and is measured photometrically at 500–600 nM. (Used with permission, Boehringer-Mannheim Diagnostics, Division of Boehringer-Mannheim Corporation, Indianapolis, IN, 1988.) (B) Similarly, serum triglycerides can be completely hydrolyzed to free glycerol and free fatty acids using microbial lipase. The stoichiometrically formed glycerol is subjected to glycerol kinase in the presence of ATP, forming glycerol-3-phosphate and ADP. This generated ADP plus phosphoenol pyruvate in the presence of pyruvate kinase produces ATP and pyruvate, which in the presence of NADH, H⁺, and LDH produces lactate and NAD⁺. The disappearance of NADH in this final reaction, monitored at between 340–380 nM, is a stoichiometric measure of the glycerol formed from the original triglyceride in the sample. (Abbott Laboratories, Diagnostic Division, Abbott Park, Chicago, IL, 1984.)

ultimately measured specific end organ responses. Both *in vivo* and *in vitro* bioassays have been developed over the years, often involving complex biological phenomena such as enzyme activities, gene products, growth factor production, synthesis of complex macromolecules, and the production or inhibition of hormones. For example, bioassays for growth hormone have been based on body weight changes, the incorporation of amino acids into proteins, or the addition of smaller chemical groups to larger macromolecules (12). On the other hand, bioassays for luteinizing hormone (LH) and/or follicle-stimulating hormone (FSH) usually require the production of only a single hormone from a tissue or isolated cell population (13).

In vitro bioassays have been classified as either proximal or distal (14) depending on whether the response is an intermediary one, like the stimulation of cAMP, adenylate cyclase, or other second messenger, or an end response, such as the product of a steroid or protein hormone via trophic stimulation (Figure 2) (15). Both proximal and distal type bioassays provide

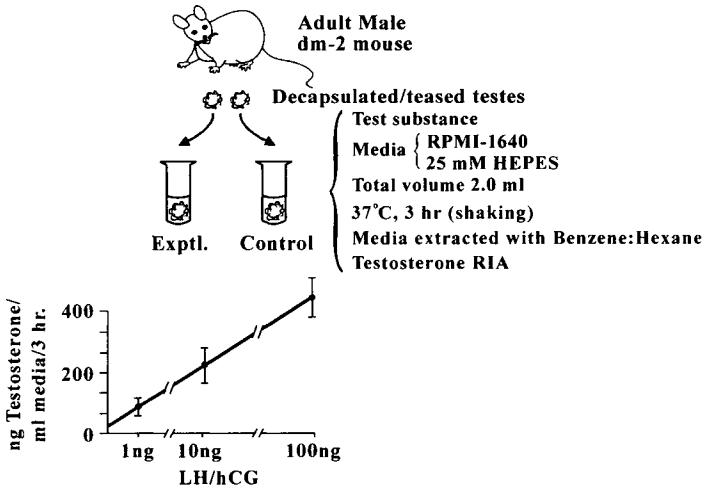


FIGURE 2. *In vitro* gonadotropin bioassay. The whole-mouse testis bioassay for gonadotropin activity was developed by Chubb and colleagues (15). The dm-2 strain of mouse is used. Adult males are castrated, and the testes are decapsulated, teased apart, and placed into assay tubes. The two testes from a single animal act as the experimental and control for a particular test agent (because of the potentially large intra-animal variability). Culture media (RPMI-1640 plus 25 mM HEPES) are added followed by the drug, hormone, or test substance. The testes are incubated for 180 minutes at 37°C, and the media are removed, extracted with benzene:hexane, and measured for testosterone by RIA. The depicted standard curve plots the dose of luteinizing hormone (LH) or human chorionic gonadotropin (hCG) tested versus testosterone produced by the testes into the media.

investigators with applications that can offer a wide variety of endocrine tissues to choose from. Other classifications include bioassays that elicit mitogenic or cytochemical responses. These encompass some of the most sensitive bioassays currently available and often require that investigators have access to permanent endocrine responsive cell lines.

In vivo bioassays were used initially for the quantitative standardization of many hormones (14). These include the murine hypoglycemia test for insulin, the rat tibial growth response for growth hormone, the pigeon crop-sac assay for prolactin, the rat ovarian weight response for gonadotropins, rat uterine weight response for estrogens, release of labeled thyroid iodide for thyroid-stimulating hormone (TSH), and the adrenal depletion of ascorbic acid for adrenocorticotrophic hormone (ACTH) (16), to mention a few. Unfortunately, *in vivo* assays may be fraught with insensitivity, nonspecificity, and values with broad confidence limits. But in spite of these flaws, *in vivo* bioassays are indispensable for the detection of hormones, drugs, or toxic chemical factors unseen by other bio- or immunoassays. Testimony to this fact has been the description of a novel, blood-borne, testis-stimulating factor by Manasco *et al.* (17) from boys with gonadotropin-independent precocious puberty, that is, familial male precocious puberty (FMPP), using a live intact male monkey bioassay (Figure 3).

The major complication of the bioassay is validation. For example, most tissues and cells respond to stimulating and inhibitory substances, both of which may be contaminants of the compounds or agents to be tested. Moreover, assay requirements can be quite stringent, requiring enzyme inhibitors, antioxidants, rigorous buffering, and consistency in cell types, tissues, or animal strains. But, despite these drawbacks, bioassays furnish a unique form of compound assessment and quantification and provide information not available from other assays (12).

RADIORECEPTOR ASSAYS

Radioreceptor assays are the first cousin of the RIA, measuring the interaction of a ligand hormone, not with the use of an antibody, but with specific receptor sites for that hormone on cells or cell membrane preparations that manifest the action of the hormone (Figure 4) (18). Thus, the radioreceptor assay shares a kindred with the bioassay, that is, both are functional hormone assays. The first radioreceptor assays were developed for ACTH by the Dr. Ira Pastan research group (19,20). The new technology rapidly spread to a variety of hormone and nonhormone molecules (18,21–23). The circumstances under which radioreceptor assays distinguish themselves have been described by Gordon and Weintraub (14): (1) as a supplement

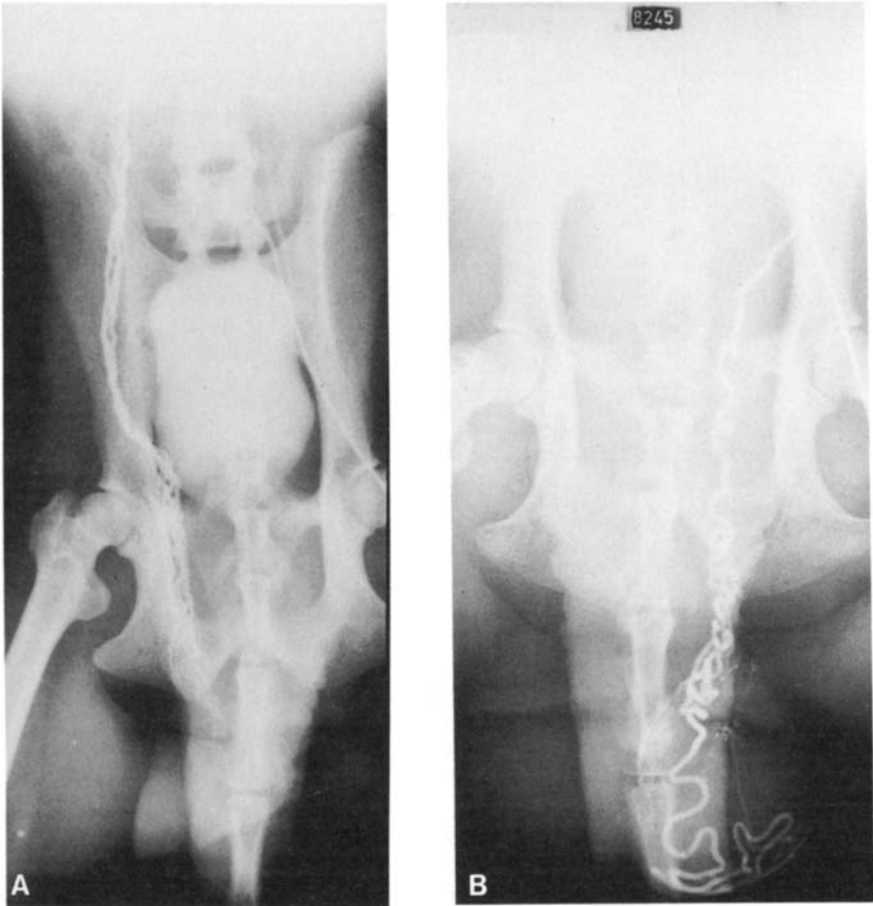


FIGURE 3. Bioassay of testis-stimulating activity. A unique *in vivo* bioassay using live intact male cynomolgus monkeys to detect gonadotropinlike testis-stimulating activity in the blood of boys with familial male precocious puberty (FMPP). Anesthetized monkeys are catheterized via jugular vein to access the spermatic vein (A, note venous plexus) and via femoral artery to access the spermatic artery (B). Plasma from FMPP boys that have no bioactivity in classic gonadotropin bioassays (rat leydig cell, etc.) stimulates monkey testis testosterone production after acute injection into the spermatic artery. Vessels are shown by prior injection of radio-paque contrast dye.

to RIA data providing (with bioassays) additional indices of biological activity, for example, in determining steroid hormone analog potency for the glucocorticoid receptor; (2) in measuring hormonally active substances for which other assays have not yet been established; and (3) in providing

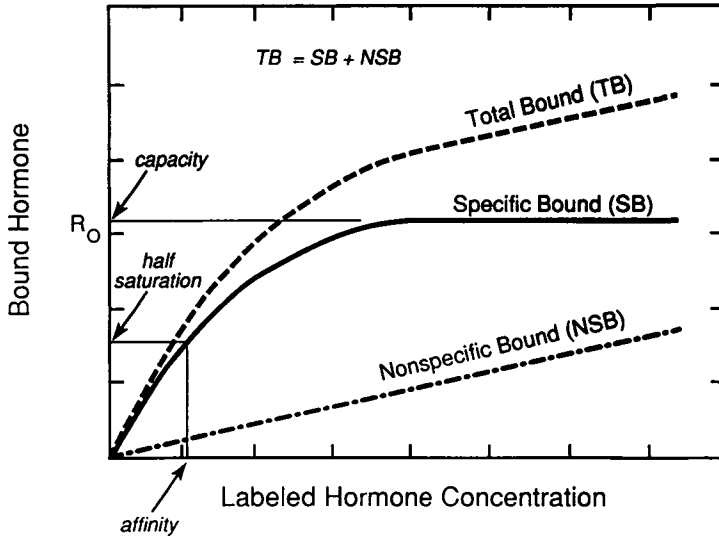


FIGURE 4. Saturation curve of a typical radioreceptor assay showing total binding (TB) and nonspecific binding (NSB) at different concentrations of labeled hormone [$TB - NSB =$ specific binding (SB)]. Extrapolation of the asymptotic saturation line to the Y axis indicates the total number of receptor sites (R_0) per cell or milligram of receptor protein. The concentration of hormone at half-saturation of receptor sites gives a measure of affinity. (From G. P. Chrousos, Radioreceptor assay of steroids and assay of receptors. In "15th Training Course: Syllabus. Hormonal Assay Techniques." The Endocrine Society, Bethesda, Maryland, 1989.)

insight into endocrine disorders that involve hormone receptor abnormalities or autoantibodies to hormone receptors.

Hormone target tissues are usually chosen as the source of the receptor preparation, with enzyme-dispersed cells or cell membrane preparations often being employed. ^3H and ^{14}C have been frequently used as radiolabels, however, the higher specific activity of ^{125}I makes this the isotope of choice for labeling both steroid and polypeptide hormones. Like bioassays, specific conditions must be met when using radioreceptor assays. For example, enzyme inhibitors like aprotinin (Kallikrein/Trasylol) may be needed for biological samples to inhibit intrinsic protease activities, however, these preparations can actually damage peptide hormone tracers, inhibit binding of the tracer to the receptor, or potentially invalidate the assay in unknown or nonspecific ways. Low incubation temperatures have been used in some receptor assays to minimize assay component degradation, and special buffering systems are often required since radioreceptor reactions are often pH and ionic strength dependent. Radioreceptor assays can be very precise,

accurate, and quite specific, but, like all other assays, must be rigorously validated before the data are accepted as sound.

Taken together, bioassays and radioreceptor assays provide information to the investigator that other assays do not, that is, an approximation of the true biologic or toxic activity of the agent in question. Moreover, bioassays along with radioreceptor assays measure not only the first step in the biologic cascade, but intermediate and final steps, giving an excellent representation of the full effect of these molecules, from receptor binding or receptor inhibition to cell response. Because no other assays have this power, bioassays and radioreceptor assays will continue to be used as essential tools in the toxicologist's arsenal. However, they come at a high cost in terms of time, money, and assay complexity (12).

RADIOIMMUNOASSAY

The principles of radioimmunoassays and techniques involved in their development have not changed for twenty-five years. Detailed treatises of all aspects of the RIA can be found in a variety of publications, textbooks, and assay manuals (11,20,24–33). Because of their specificity, sensitivity, and ease of performance, RIAs have been the benchmark of most, if not all, hormone assays, and continue to be the gold standard of hormone measurement for endocrine and nonendocrine toxicologic diagnosis and research. However, if carried out in a casual or cavalier manner, results from the RIA can not only be inaccurate, but misleading. Oddly enough, the basic tenets of RIAs have not changed from their inception, evidenced by the fact that many renowned research laboratories continue to use the RIA techniques they established and validated twenty or more years ago. What has changed is the production of better reagents, that is, antibodies with greater specificity (both polyclonal and monoclonal), tracers with higher specific activities giving greater precision and sensitivity (e.g., multi-labeled ^3H and ^{125}I isotopic incorporation into steroids as well as proteins), and the availability of RIA kits, produced by both large and small manufacturers, that include virtually everything an investigator needs to “get results.”

The basic principle of the RIA is the competitive inhibition of the binding of a labeled hormone to a “specific” antibody by the same unlabeled hormone that is contained in prepared standards or unknown samples (Figures 5A and 5B) (12). A typical radioimmunoassay is performed by the addition of standards or unknown samples into assay tubes. To these tubes, a fixed amount of radiolabeled antigen is added, and then antibody. After an appropriate reaction or incubation time, antibody bound and

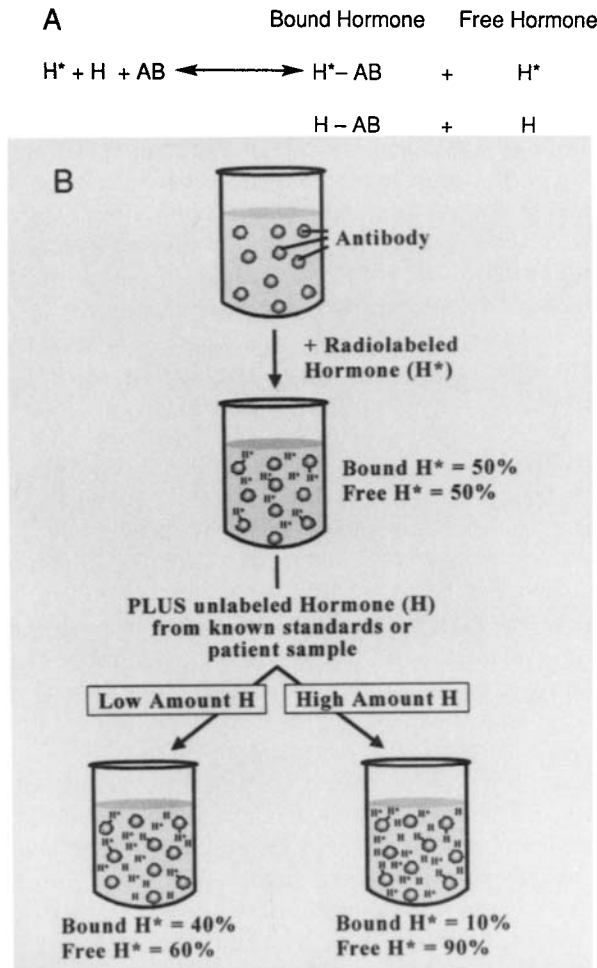


FIGURE 5. Generalized scheme of a RIA. (A) Radiolabeled hormone (H^*) and antibody (AB) are combined such that the percent binding is between 30 and 50%, usually established during assay setup experiments. The addition of unlabeled hormone in the form of standards or in an unknown sample perturbs (decreases) the $H^* - AB$ binding equilibrium dynamics depending on the unlabeled hormone concentration (B). As more standard hormone or hormone in the sample is added, the final amounts (after a period of incubation for equilibrium to be established) or percent of bound radiolabeled hormone to free labeled hormone changes. The final step, separation of bound hormone from free hormone, gives ultimate hormone quantitation (measured as radioactivity, H^*) in bound (pellet) or free fraction (supernate) after centrifugation or another physical separation procedure. In practice, all the components (H , H^* , and AB) are added together until equilibrium is established. However, the late addition of tracer (H^*) can improve assay sensitivity. [Modified from B. D. Albertson, Hormone assay methodology: Present and future prospects. In "Clinical Obstetrics and Gynecology," Vol. 33, No. 3, "Reproductive Endocrinology Update" (E. Y. Adashi, ed.). Lippincott Co., Philadelphia, Pennsylvania, 1990.]

unbound labeled antigen are separated by a variety of physical or chemical techniques, a final step that can well determine the ultimate success or failure of the assay (33).

RIAs have been modified by the incorporation of solid-phase-linked reagents and novel radiolabeling procedures that have improved the stability and ease of performing these assays. For example, immunoradiometric assays, or IRMAs, have become proverbial. These differ from classic RIAs in that the antibody, usually an IgG or monoclonal antibody, is labeled instead of the hormone. Moreover, the IRMA classically uses a "sandwich" format (Figure 6). When a primary antibody (often linked to some solid-phase matrix like polystyrene) that can recognize a unique binding site or epitope of a large polypeptide molecule (like ACTH) and a second labeled (often ^{125}I) antibody that is specific to another epitope of the molecule are used, the resulting noncompetitive assay delivers increased specificity and sensitivity over standard RIAs. The advantage of this perturbation is that iodinated secondary immunoglobulins or monoclonal antibodies can be more stable than iodinated hormones. But IRMA assays have some drawbacks. For example, they can produce standard curves that have an upper level "hook effect" (24), that is, when high concentrations of the hormone are present in the reaction mixture, a hook in the standard curve and in the unknown samples reverses the slope of the response curve caused by a decrease in bound counts with labeled antibody at the higher hormone concentrations. Thus, biologic samples suspected of being elevated should be measured at more than one dilution to be certain that the hormone concentrations are within the linear portion of the standard dose-response range of the assay (24,32). These assays also have the distinction of being too specific, that is, being able to detect only a single biologic form of a protein. This has become evident in the lack of measurable levels of ACTH and hGH produced by ectopic tumors.

Other drawbacks of these immunoassay technologies are linked to (1) limitations of the radioactive tracer component, including short and fragile reagent life; (2) the cost of equipment for measuring gamma or beta particles; (3) radiation exposure to users; (4) radioisotope licensing; and (5) a serious long-range, environmental problem, namely, isotope disposal. On the other hand, assays incorporating radioactive tracers have provided researchers and clinicians with the tools to measure a host of hormones to concentrations of picograms or even femtograms per milliliter of plasma, serum, or culture media. Thus, it is no surprise that these assays are some of the most popular and enjoy widespread use.

Sensitive RIAs have been successfully developed and commercialized for the accurate measuring of low circulating levels of hormones, requiring relatively small volumes of biologic fluids. These assays incorporate:

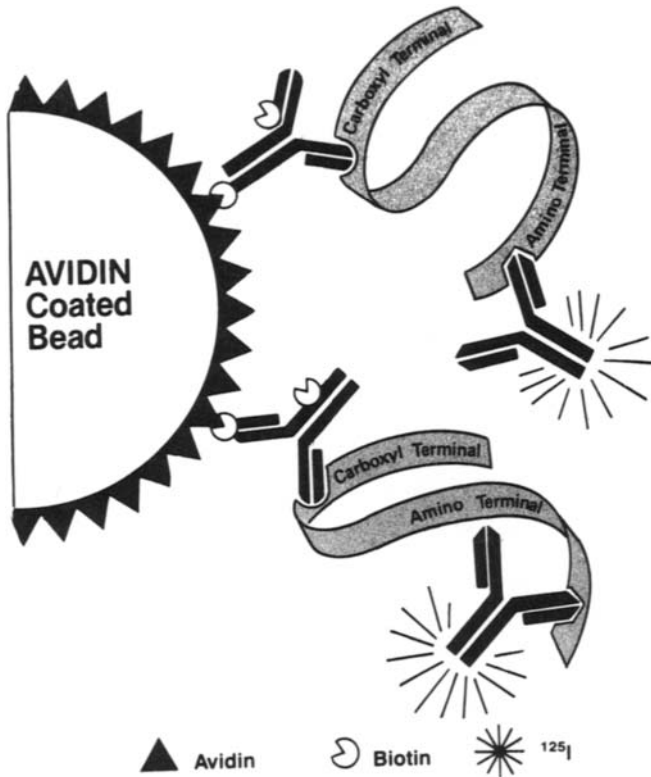


FIGURE 6. Schematic depiction of a typical IRMA. An avidin-coated polystyrene bead is combined with standards (pure ACTH) or patient sample ACTH and a biotin-conjugated primary or first antibody (here generated against the carboxyl terminus of the ACTH molecule). A second antibody (with a ^{125}I label attached) generated against the amino terminus of the ACTH molecule is added to this system, creating an antibody-hormone-antibody "sandwich" (called the two-site sandwich method). Separation of the bound and free fractions is made easy because of the use of the solid-phase bead and the high-affinity interaction between biotin and avidin. (Courtesy of Nichols-Corning Diagnostics, San Juan Capistrano, CA.)

(1) purified radiolabeled hormones with high specific activities so that only trace amounts of hormone need be added; (2) labeled hormones or antibodies that do not affect the specificity or immunoreactivity of the reagents; (3) antibodies (polyclonal and monoclonal) with high affinities and specificities to measure low levels of the desired hormone; and (4) appropriate reference preparations against which the concentration of unknown sample

may be dose-interpolated. Features of the key components of RIAs are elaborated in the following sections.

Antibodies

The power of the RIA (or other immunoassays) is married to the quality and specificity of the antibodies employed. The more specific the antibody, the better one is able to accurately measure the hormone of interest. Antibodies most commonly used for RIAs have been selected from the immunoglobulin class called gammaglobulin or IgG (Figure 7) (34). IgGs are made up of two heavy polypeptide (approximately 450–700 amino acids) and

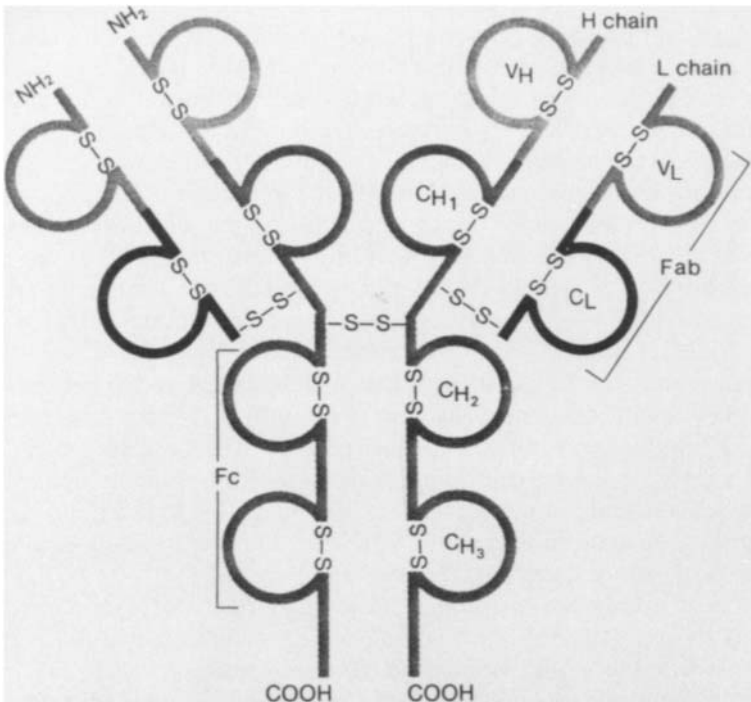


FIGURE 7. Immunoglobulin model. Immunoglobulin molecules (IgG) are composed of two heavy (H) and two light (L) chain polypeptides. Each IgG has two antigen-binding sites (Fab) and a complement fixing site (Fc). Variable regions of the heavy and light chain are shown by solid and gray loops. Folded loops of the protein chains and the chains themselves are joined by disulfide bonds (S-S). [From R. D. Guttman (ed.) "Immunology: A Scope Publication" The Upjohn Company, Kalamazoo, MI, 1981.]

two light polypeptide (approximately 214 amino acids) chains symmetrically arranged and covalently linked to each other by disulfide bridges. Because these IgGs possess antibody reaction sites along with antigen determination sites, the IgGs themselves serve as antigens when injected into an animal of another species, an important characteristic used in the production of second antibodies for RIAs.

Although the concentration or titer of a desired antibody is important, the principal determinants of a great antibody are its affinity and specificity for the desired hormone. The antibody–antigen interaction is derived by the combination of events involved in the intricate “locking” of the antigen in a complementary way to the combining site of the antibody through electrostatic, hydrogen-bonding, and van der Waals interactions (24,32,35,36).

The synthesis of specific antihormone IgGs is accomplished by injecting highly purified hormone preparations into laboratory animals. Protein or polypeptide immunogens are usually injected into guinea pigs, rabbits, sheep, goats, chickens, or other animals that will recognize the immunogens as “foreign” molecules. If the hormone immunogen has a molecular weight of less than 1000, it must be linked or chemically conjugated to a carrier molecule to establish immunogenicity in the animal of choice. A number of carrier molecules, usually ones with intrinsic immunogenicity, have been successfully used for this task, including bovine serum albumin, thyroglobulin, and hemocyanin. Steroids, thyroid hormones, and vitamin D and its precursors must be conjugated to immunogenic carrier molecules for adequate antibody production. For example, steroids differ from each other by small changes in their structure, usually in hydroxyl and/or ketone radicals. An intimate understanding of the chemistry of these reactive sites enabled coupling reactions to be devised (37). The best known are the mixed-anhydride and the carbodiimide reaction. And, as mentioned earlier, the choice of the exact molecular site of conjugation is essential, that is, through that reactive moiety of the molecule that is least likely to alter its characteristic stereospecificity (Figure 8) (24,32).

The most widely used method of inducing antibody formation has been to inject the antigen or antigen–conjugate in Freund’s adjuvant (32,38,39), a mixture of mineral oil (included to delay resorption), waxes, and killed bacilli (to sensitize the animal). The technique involves injecting the merangue-like adjuvant–hormone emulsion intradermally or subcutaneously on the back along the para-aortic lymphatic chain (Figure 9). Initially large amounts of antigen were thought to be essential for good antibody production, but the studies of Vaitukaitis *et al.* (40) demonstrated that very small doses of antigens can be used. Moreover, low doses of immunogen often produce antibodies with the highest affinity; conversely, higher dose

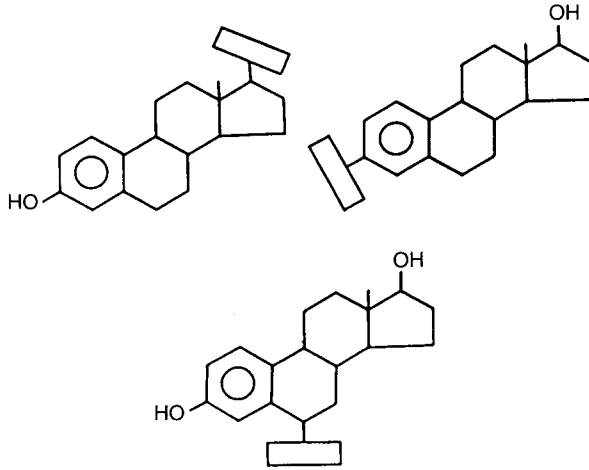


FIGURE 8. Molecular site of conjugation on estradiol. Conjugation on carbon 17 (top, left), carbon 3 (top, right), and carbon 6 (lower) to retain immunogenicity of estradiol for the generation of a specific antibody.

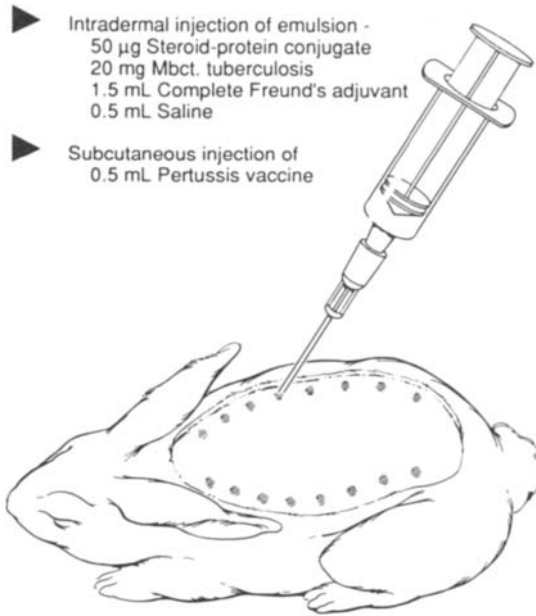


FIGURE 9. Immunization of a rabbit for production of steroid antibodies for RIA.

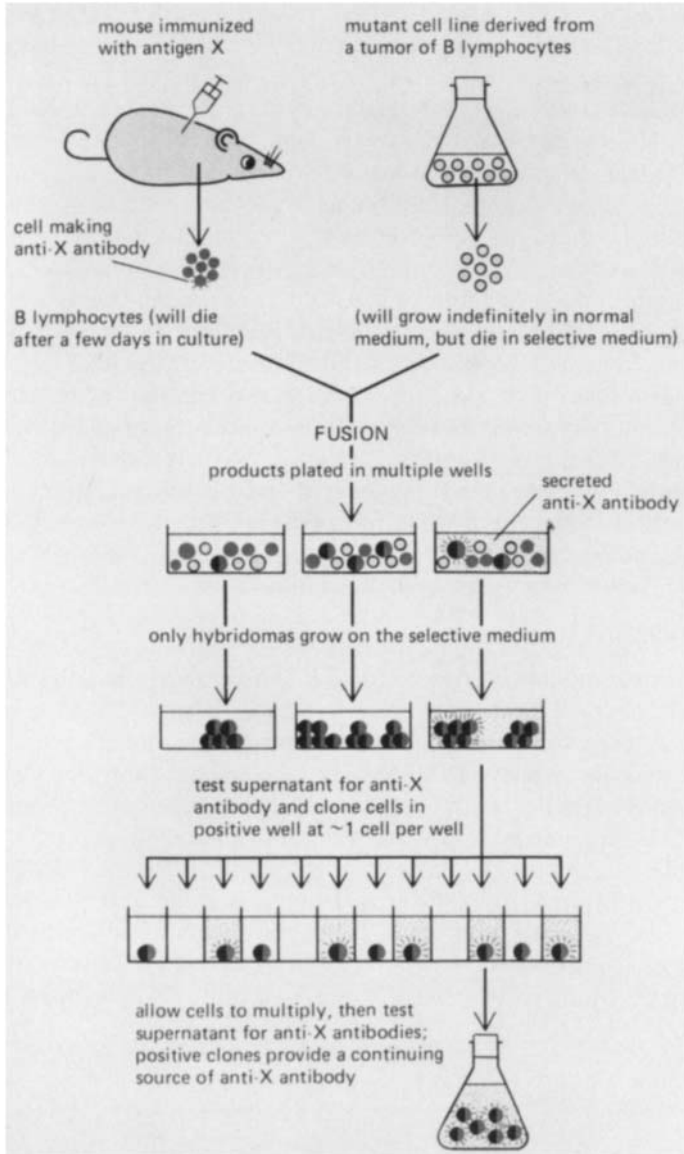
immunogens produce antibodies with lower affinities. High-dose immunization can also induce “tolerance” in the immunized animal, resulting in very low or no measurable antibody titer (24,27,32).

Primary immunizations are usually begun with complete Freund’s (with mycobacteria added) or similar adjuvant and usually takes about 8 weeks for significant levels of antibodies to be detected. Titers and affinities usually peak within 3 to 4 months (32,41). Blood samples from the animals are obtained by cardiac puncture, by retro-orbital sinus puncture, or by “nicking” tail veins or the marginal veins of rabbits with a sterile scalpel blade. The serum is screened for antibody titer, specificity, and affinity using an appropriate radiolabeled ligand.

Several alternative “non-Freund’s” adjuvants have been used recently and are selected based on the type of cellular response desired. These include alum compounds (especially aluminum hydroxide, Alhydrogel), water-in-oil emulsions employing micro-particulate stabilized emulsions containing nontoxic, metabolizable oils like squalene (Hunter’s TiterMax, Cytrx Corp., Norcross, GA), oil-in-water-based adjuvants (RIBI Adjuvant System, Immunochem Research, Inc., Hamilton MN), Bentonite, trehalose-dimycolate, vinyl acetate copolymers, muramyl dipeptide, liposomes, and pristane (2,6,10,11-tetramethylpentadecane).

The antisera produced in animals is actually a heterogeneous population of immunoglobulins with different affinities and specificities. Thus, each individual animal that is immunized with antigen may produce totally different antibody populations with different titers, affinities, and specificities. This often means that a single rabbit, for example, may be the sole source of

FIGURE 10. Production of monoclonal antibodies. Animals (usually rats or mice) are injected with an antigen or antigen–conjugate. Once serum levels of “polyclonal antibodies” are detected, that animal’s spleen is removed surgically and the spleen cells are fused with a nonimmunoglobulin-secreting mouse myeloma cell line. Clones are selected from the hybridoma on the basis of antigen specificity and affinity and can be grown ad infinitum for assay application. Although monoclonal antibodies have been widely used and applied to polypeptide and protein hormone assays, their unique specificity can make them problematical for the measurement of altered forms of circulating hormones. Preparation of hybrid cells or hybridomas is carried out, which secrete homogeneous monoclonal antibodies against a particular hormone or antigen (X). Selective growth medium contains an inhibitor (aminopterin) that blocks the normal biosynthetic pathways by which nucleotides are made. The cells must therefore use a bypass pathway to synthesize their nucleic acids, and this pathway is defective in the mutant cell line to which the normal B lymphocytes are fused. Because neither cell type used for the initial fusion can grow on its own, only the cell hybrids survive. [From Alberts, Bray, Lewis, Raff, Roberts, and Watson (eds.), “The Molecular Biology of the Cell” 2nd Ed. Garland Publishing, Inc., New York and London, 1989.]



a “great antibody” and could elevate that particular animal to an invaluable status. The loss of such an animal could be devastating. This fact, among other particulars, has led to the replacement of polyclonal antibodies with monoclonal antibodies that represent a single immunoglobulin with a unique affinity and specificity for a single antigenic site of a hormone or other hapten (Figure 10) (42,43).

In general, monoclonal antibodies have improved RIAs and IRMAs because (1) they can be produced in large quantity with high titers; (2) they are consistently similar or identical over long time periods of hybridoma clone production; and (3) they are (or can be) quite specific for the hormone of interest, and (as already mentioned) almost to a fault. For example, in the development of a specific antibody for ACTH, monoclonal antibodies have been produced that are so specific for native pituitary ACTH that they sometimes do not cross-react with other bioactive ACTH molecules, like fragments of ACTH or “big” ACTH found in ectopic ACTH syndromes (44). Several companies are currently producing and distributing antibodies in either kit or bulk form that provide the user with the ability to pick and choose the best antibody for their particular application (12).

Radiolabels

The most commonly used isotopes in RIAs are shown in Table I with some of their physical characteristics. Of these, ^3H and ^{125}I have been most routinely used (45). Historically, tritium has been the “tracer” of choice for steroid and vitamin D RIAs since the specific activities available are reasonably high, the labeling procedures are carried out by reputable commercial companies that provided assurance of activity and purity, and the costs are sufficiently low to keep budgets intact. ^{14}C -labeled steroids have been used in RIAs, but the long isotope half-life and thus low specific activity of these nuclides made them unsatisfactory in terms of yielding good assay sensitivities. Six- and eight-labeled tritiated steroids are available and greatly improve assay sensitivities, often into the low picogram or high

TABLE I. Isotopes Used in RIAs

Isotope	$T_{1/2}$	Decay particle	Detection efficiency (%)	Specific activity
^{14}C	5568 y	β	80	10–50 mCi/mmol
^3H	12.35 y	β	55	50–200 Ci/mmol
^{75}Se	121 d	$\gamma + x$	90	100–300 Ci/mmol
^{125}I	60 d	$\gamma + x$	90	2000 Ci/mmol
^{131}I	8 d	γ	45	2000 Ci/mmol

femtogram range. Recently, steroids have been introduced into the market that are iodinated, providing even higher specific activities and greater sensitivities for assay applications.

The most commonly used tracers for polypeptide and thyroid hormones have been isotopes of iodine, beginning with the use of ^{131}I . However, this tracer's 8-day half-life and rather low specific activity quickly led to its substitution with ^{125}I , which has a 60-day half-life (45–48). As with tritium, iodination of protein and thyroid hormones is carried out commercially by several reputable companies that ship reagents to laboratories on a frequent basis. However, some investigators continue to iodinate their own hormone preparations in an effort to minimize tracer costs or when only precious amounts of a highly purified hormone are available. Dedicated iodination areas (usually modified chemical fume hoods) are required for these preparations, along with gamma particle monitoring devices and labeled antigen purification systems, including powdered cellulose absorbent, gel filtration, dialysis, ion-exchange chromatography, cross-linked dextrans (sephadexes), or anion-exchange resins. Purification of the newly labeled hormones by chromatographic methods may be required to reduce "nonspecific" assay binding. Prewashing sephadex columns with albumin has been used to help saturate absorption sites, and the addition of 2-mercaptoethanol has been used to stabilize a variety of labeled protein hormones during purification and storage (49,50). In cases where the original antigenic preparation is not pure or when significant antigenic degradation occurs during radiolabeling, additional purification (like starch gel and polyacrylamide gel electrophoresis, or high-performance liquid chromatography may be necessary (49–56).

Routinely used iodination procedures include: (1) use of the potent oxidizing agent chloramine T (originally marketed as a disinfectant) by Greenwood *et al.* (6), which converts $\text{Na } ^{125}\text{I}$ to free iodine (a simple mixing of the peptide, sodium iodide, and chloramine T is required, with the reaction being terminated by the addition of the reducing agent, frequently sodium metabisulfite); (2) the lactoperoxidase method of Marchalonis (57), in which this enzyme in the presence of a trace of H_2O_2 transfers ^{125}I -labeled NaI to free iodine with selective incorporation into tyrosyl or histidyl residues [the addition of glucose oxidase to this cocktail, which generates H_2O_2 from glucose *in situ*, minimizes the potential for protein or peptide damage; a reducing agent is not required to stop the reaction since sample dilution is sufficient (58)]; (3) the Bolton Hunter or conjugation labeling technique (Figure 11) (59), where an intermediate derivative, 3-(*p*-hydroxyphenyl)propionic acid *N*-hydroxysuccinimide ester, is iodinated by the chloramine T reaction and then subsequently condensed with amino groups on the polypeptide hormone; (4) the iodogen method of Fraker and Speck (60), in which a relatively insoluble soluble oxidizing agent

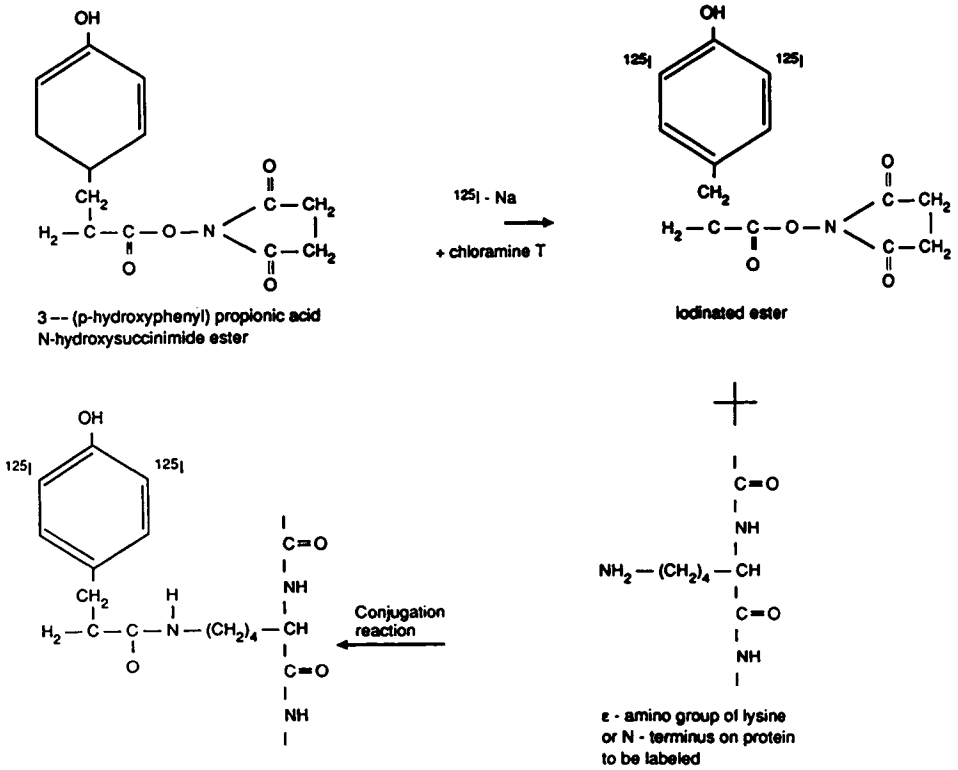


FIGURE 11. Bolton Hunter iodination scheme. Schematic representation of the iodination scheme of Bolton and Hunter using chloramine T. (From T. Chard, "An Introduction to Radioimmunoassay and Related Techniques," p. 56. Elsevier Biomedical Press, Amsterdam, 1982.)

(1,3,4,6-tetrachloro-3 α ,6 α -diphenyl glycouril) is evaporated onto the walls of a reaction vessel from a solution in chloroform or methylene chloride [the polypeptide and ^{125}I are added, and the reaction is terminated when the mixture is removed from the vessel without requiring addition of a reducing agent (27)]; (5) chlorine/sodium hypochlorite oxidation (61); (6) iodine monochloride (60); (7) iodine vaporization (60); and (8) electrolysis (62,63). Each of these techniques has the potential of chemically damaging the hormone to be iodinated if vigorous reaction conditions are used. Thus, gentle iodination procedures have been adopted, for example, hormone damage can be minimized when labeling with the lactoperoxidase method if the H_2O_2 is added in two or three small aliquots since this is such a harsh oxidizing reagent.

Small polypeptide molecules that do not contain histidyl or tyrosyl residues may be modified by substituting a tyrosyl group within the polypeptide or at the nonfunctional end of the molecule. Similar approaches have been employed with steroids, but in this case iodination is located at a site distant from the active hydroxyl or ketone groups. This position must be carefully chosen so as not to affect the molecule's native conformation. These new tyrosyl analogs can be iodinated by several of the techniques described in the foregoing.

The final specific activity of the newly labeled antigen can be estimated by determining the disintegrations per minute of radioactivity found in the molecules at various stages during radiolabeling. By comparing the dpm of the isotopes before labeling with the total dpm of the various labeled fractions (e.g., labeled antigen and free isotope), one can determine the percent recovery. Knowing this recovery, and the amount of antigen and label initially present, one can estimate the specific activity of the newly formed tracer (50). One may also wish to check for immunoreactive changes of the labeled antigen using a quick RIA screen by assaying the radiolabeled antigen alone and then diluted with unlabeled antigen. A decrease in the immunoreactivity of the tagged hormone would indicate that the molecule had suffered some insult during the labeling procedure (50).

It must be mentioned that specific precautions must be met if attempting to perform peptide or polypeptide radio-iodinations in the laboratory. Gamma monitoring must be carried out continuously when preparing for and carrying out in-lab iodinations. Approved, well-ventilated fume hoods should be used for all iodinations. Charcoal traps should be used where indicated (e.g., for venting the radioactive iodine vials, etc.). Investigators should protect themselves with the appropriate shielding (lead or other high Z material), eye and face protection, lab coat, disposable gloves (double gloving is recommended and gloves should be changed frequently or whenever possible contamination occurs), and a working knowledge of the isotope they are using. The practice of drinking a solution of saturated potassium iodide to block the thyroid gland has been abandoned by most radiation safety committees.

Separation of the Bound-from-Free Fractions

Once the primary hormone-antibody reaction reaches equilibrium, it is necessary to determine the distribution of the hormone between the free and bound forms. This usually requires that the bound fraction be physically separated from the free fraction so that the radioactivity of either the bound or free phase can be accurately measured (64). Essential in this is the premise that the separation techniques used do not disturb the initial equi-

librium attained between hormone and antibody (or receptor). All the techniques devised to perform this final all-important step of the RIA exploited physical-chemical differences between the hormone in its free and bound forms. A perfect separation system would completely divide the two components of the assay. In practice, this is never achieved because (1) the free hormone almost always can behave like it is bound, that is, constituting what is commonly referred to as “nonspecific binding,” and (2) there is invariably incomplete separation of the bound-hormone complex (27). Classic immunological methods for separation of bound from free hormone fractions have been based on spontaneous precipitation of antigen–antibody complexes since molar concentrations of these complexes permitted simplistic approaches (33). RIAs, because of their much lower assay sensitivities, utilize very low molar concentrations of reagents and thus demand specific assay steps that will effect the separation of antibody-bound and free antigens (65). In considering the best approach to the separation of bound from free, several factors should be weighed: the speed of the procedure, simplicity, applicability, effectiveness, and cost.

The earliest methods used for separation of bound and free fractions in RIAs were electrophoretic, including paper chromatoelectrophoresis, starch gel, cellulose acetate, and polyacrylamide gel electrophoresis. The extremely cumbersome nature of these approaches led to techniques that involved nonspecific fractional precipitation of the hormone–antibody complex itself using salts or organic solvents. Reagents used included ethanol, acetone, dioxane, sodium sulfite, ammonium sulfate (Figure 12) (27), trichloroacetic acid (TCA), and polyethylene glycol (PEG) (50). Although these procedures were immediate and needed no second “incubation step,”

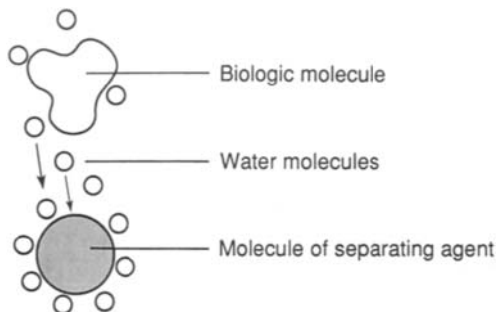


FIGURE 12. Fractional precipitation of bound and free with ammonium sulfate. The ammonium sulfate molecule takes up water molecules, depriving the protein of its protective hydration shell. (From T. Chard, “An Introduction to Radioimmunoassay and Related Techniques,” p. 125. Elsevier Biomedical Press, Amsterdam, 1982.)

fractional precipitation techniques may have a tendency to “bring down” other proteins or assay components, causing an incomplete separation of the two fractions.

Solid-phase bonding of either the hormone or antibody components of the RIA was attempted in the mid-1970s. The solid-phase antibody technique made use of antibodies covalently bonded or fixed to insoluble polymers covalently cross-linked to one another or physically adsorbed to plastic. These immunosorbents included bentonite particles (66), bromoacetyl cellulose (66), sephadex (67), sepharose (68), enzacrlyl AA (68), and polyacrylamide gels. Although this approach has the advantage that all the components of the assay (antibody, hormone-tracer, and the means of separating bound from free simply by decanting or low-speed centrifugation) are within one unit, it necessitated the producer of these reagents to have large quantities of antisera available. And even though attaching an antibody to a solid-phase component does not, in itself, require high amounts of antibody especially if the format is competitive, excess antibody is needed in the “sandwich assays” in order that all of the analyte will be bound (particularly if there is a large amount of that analyte in the sample). The use of solid-phase separation techniques like antibody attachment to polystyrene beads (common in IRMA formats) or capture in a mesh of polyacrylamide gel has provided the simplest and most user foolproof approaches to separation of bound and free. But these concoctions are wasteful of antibody and very difficult to produce, especially in relation to batch to batch consistency. If unlimited amounts of antibody are available, these approaches can offer true simplicity of this final assay step to the point of being almost instantaneous and automatic.

Physical adsorption of antibodies to polypropylene or polystyrene discs, plastic tubes, or small beads has been developed particularly for protein hormones and has yielded reproducible and highly sensitive RIA and IRMA assays in which the adsorbed antibodies have a very long shelf life. Separation by solid-phase antigen precipitation has also been successful, being simple, economical, quick, and reproducible.

Adsorption of free antigens has been and probably remains the gold standard for steroid and steroid metabolite RIAs. Free hormone is bound to specific adsorbents that are then precipitated by centrifugation. Powdered talc and florasil (magnesium silicates), kaolin, Fuller’s earth, Lloyd’s reagent (aluminum silicates), and cellulose were some of the earliest of these adsorbents, many of which were originally employed by chemists as decolorizing agents. But one, dextran-coated charcoal, has remained one of the most used for RIAs (Figure 13) (27). Used primarily in steroid, vitamin D, and small peptide RIAs, this adsorbent combines all the best features of the earlier methods, but more importantly has endured the test of time in

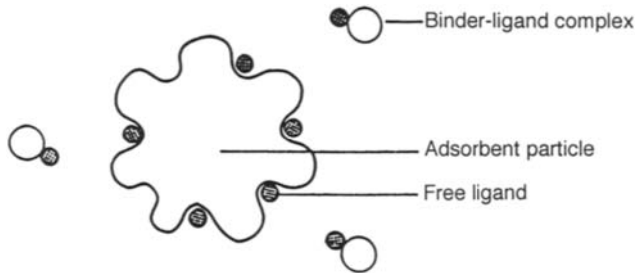


FIGURE 13. Adsorption separation using powdered charcoal. Free hormone enters “crevices” on the charcoal particle and is firmly adsorbed. Antibody-bound hormone cannot enter the crevices and thus remains in the liquid phase. (From T. Chard, “An Introduction to Radioimmunoassay and Related Techniques,” p. 121. Elsevier Biomedical Press, Amsterdam, 1982.)

its use by many established research and clinical laboratories. There are, however, some requirements for charcoal separation steps to perform well: (1) the preparation of the charcoal (usually Norit A, Norit SG, or G-60) must be rigorous, with multiple washings in distilled water or assay buffer to segregate the “fine” particles from the usable heavier granules, [dextran (T-70 or T-80) is often used to produce dextran-coated charcoal, although the need for dextran has been found to be optional for good charcoal separation]; (2) the determination of the conditions (e.g., incubation times and temperature) under which the separation is complete with minimal stripping of the hormone from its antibody. This is true especially when one is processing large batches of assay tubes, where the incubation time for the first tube and the last tube may be significantly different and possibly add some error to the assay results. And (3) establishing optimal centrifugation conditions so that decanting the supernate into counting vials from the assay tubes does not result in contamination with the pelleted charcoal.

Because the initial binding step in polypeptide hormone RIAs produces a soluble hormone–antibody complex, simple centrifugation may not be adequate for separating bound from free fractions. The second antibody, generated against the IgG of the animal species in which the first antibody was generated, is added after equilibrium has been reached in the first antibody–hormone reaction. This second antibody–primary antibody–hormone complex is an insoluble species and the bound hormone can be separated by centrifugation. For protein or polypeptide hormones, the use of double antibodies (i.e., a primary antibody generated against the hormone to be measured and a secondary antibody generated against the primary antibody) is usually the method of choice. Generally, polypeptide hormone assays use radiolabeled (or nonradiometric tracer labeled) second

antibodies (monoclonal antibodies) in a sandwich IRMA format, which, coupled with solid-phase chemistry, simplifies the separation of bound from free fractions (Figure 14) (27). Secondary antibodies are routinely harvested in large domestic animals like sheep or goats since relatively large amounts of antibody (i.e., blood plasma or serum) are often required, especially when hundreds or thousands of samples are to be analyzed. Goat or sheep anti-rabbit or anti-rat IgGs are the most common type of second antibody used (although IgA and IgM fractions have found application) and give excellent separation of the original rabbit, rat, or other IgG species of primary antisera–antigen complex from free hormone.

The ability to generate large amounts of monoclonal antibodies has further enhanced and simplified the bound from free separation step. These uniform populations of antibodies can be bound to the walls of plastic assay tubes or microtiter plates, making a simple decanting step the method of separating bound from free in some IRMA systems.

Magnetic field separation of bound hormones has also been developed. In this application, ferric oxide is conjugated to the first or primary antibody and a magnetic field, usually in the form of a strong permanent magnet imbedded in the base or sides (and near the bottom) of an assay tube rack or holder. After the initial incubation of reagents of the RIA is completed and the reactants have reached equilibrium, the assay tubes are placed into the magnetic tray and allowed to stand for several minutes. The assay tubes can be singly or simultaneously decanted, blotted, and then counted, thus effectively separating the free from bound fraction in mass. Both steroid and polypeptide hormones can be assayed using magnetic separation tech-

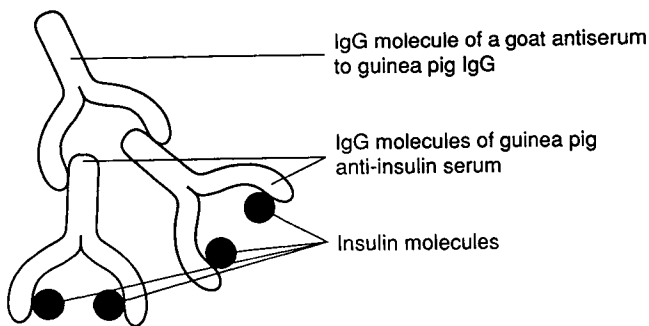


FIGURE 14. Second antibody separation of bound and free in an insulin RIA. Primary IgG antibodies are raised in guinea pigs against human insulin. Each primary antibody binds two insulin molecules. A secondary antibody produced in a goat is an anti-guinea pig IgG, and binds two primary antibodies. (From T. Chard, "An Introduction to Radioimmunoassay and Related Techniques," p. 128. Elsevier Biomedical Press, Amsterdam, 1982.)

niques, providing simplicity and quick turn-around time for laboratories performing large numbers of assays (12).

Data Display and Antibody/Receptor Binding Characteristics

There are a variety of methods for handling the data derived from RIAs (24,32,69–78). Standard curves are routinely generated and can be displayed graphically as either hyperbolic functions or straight lines depending on the mathematical manipulation of the data. The simplest of these are depicted in Figure 15 (24,27).

The basic dose–response or standard curve is constructed by placing the bound over free activity (B/F) or any other partition index between bound and free on the ordinate and the unlabeled antigen or ligand concentration on the abscissa. A log scale of the abscissa yields a sigmoid curve. One of the most used curve-fitting response variables is the logit transformation:

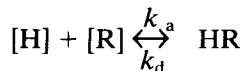
$$\text{Logit } B/B_0 = \text{Log } e \ B/B_0 / 1 - B/B_0$$

where

$$\begin{aligned} B &= \text{antibody-bound radioactivity of each sample} \\ B_0 &= \text{antibody-bound radioactivity at the zero dose.} \end{aligned}$$

On the abscissa is plotted the log scale of the unlabeled hormone and on the ordinate the logit (log base e) of B/B_0 (24).

Hormone receptor or antibody binding interactions have also been mathematically analyzed by a variety of approaches. In general, when hormone $[H]$ interacts with a specific receptor or antibody $[R]$, a reversible reaction at equilibrium can be defined as



where HR is the hormone–antibody (receptor) complex.

The affinity of the hormone for its antibody or receptor can also be expressed using a rearrangement:

$$K_a = k_a/k_d = [\text{HR}]/[H] [R] = 1/K_d$$

where

$$\begin{aligned} K_a &= \text{the equilibrium constant in liters per mole} \\ k_a &= \text{the association constant rate} \\ k_d &= \text{the dissociation rate} \\ K_d &= \text{the equilibrium dissociation constant in} \\ &\quad \text{liters per mole.} \end{aligned}$$

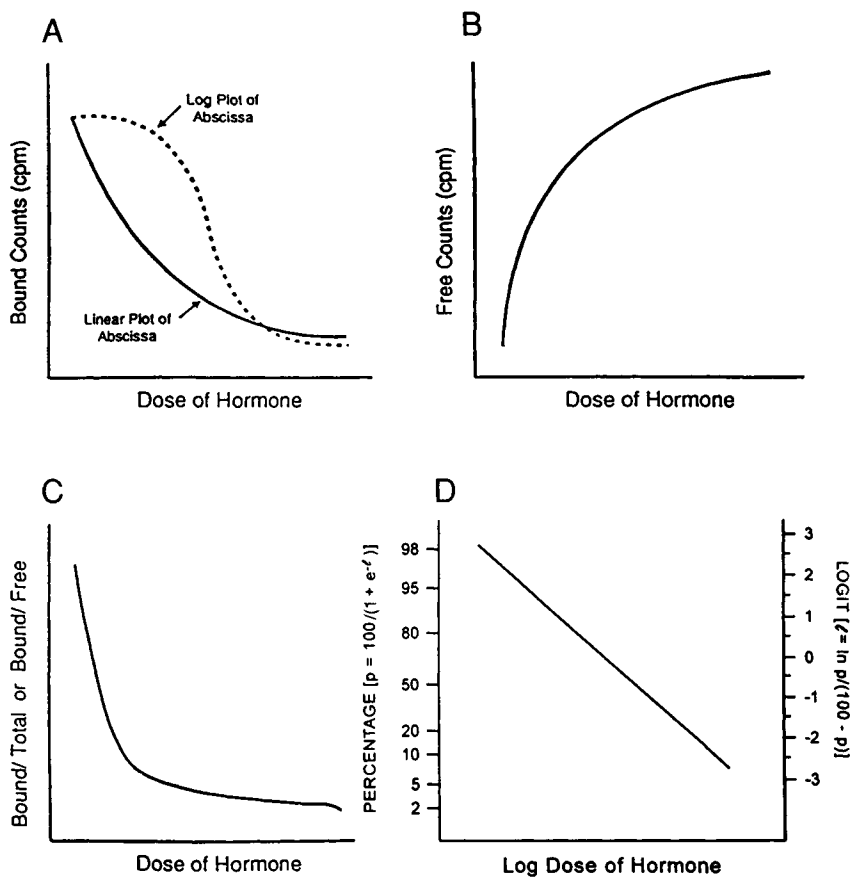


FIGURE 15. RIA standard curve presentations. A variety of techniques have been used to graph data for RIAs. The simplest of these is shown in panels A and B, where either bound or free counts per minute (cpm) or radioactive disintegrations per minute (dpm) are plotted against the dose of nonlabeled hormone (standard curve). Panel C shows nonlabeled hormone plotted against either the bound over free hormone calculated or the bound over total hormone calculation. All of these plots enable the investigator to determine unknown sample concentrations based on the standard curve generated, but all of these generate curvilinear plots making actual hormone levels difficult to estimate, especially when the slope of the plot is flat. Several approaches have been used to linearize these plots, making the determination of unknown samples at the extremes of the standard curve more valid. The most popular of these is the log-percentage or log-logit plot (D). This plot employs the number of counts bound to antibody normalized to the maximum number of bound counts, B_0 , when only antibody and labeled hormone (i.e., no unlabeled hormone) are incubated together. Nonspecific counts, which reflect physically trapping hormone in the assay tube, are subtracted from both total and bound counts. The resulting log-logit plot is usually a straight line and simplifies visual dose interpolation of unknown samples. [From J. L. Vaitukaitis, *Hormone assays*. In "Endocrinology and Metabolism" (P. Felig, J. D. Baxter, A. E. Broadus, and L. A. Frohman, eds.), p. 164. McGraw-Hill, New York, 1987; and T. Chard, "An Introduction to Radioimmunoassay and Related Techniques," p. 20. Elsevier Biomedical Press, Amsterdam, 1987.]

When the number of occupied receptors or antibody sites is related to the total number of antibodies or receptors, the relationship is

$$[R_0] = [HR] + [R]$$

or

$$[R] = [R_0] - [HR]$$

where

R_0 = the total number of antibodies/receptors
 HR = the bound receptors or antibodies
 R = the free receptors or antibodies.

By rearranging these equations, one can generate a final equation that when plotted results in a straight-line relationship of the hormone bound to its receptor or antibody, that is,

$$HR/H = -1/K_d [HR] + [R_0]/[K_d]$$

or

$$HR/H = -K_a [HR] = [K_a] [R_0].$$

This represents the Scatchard plot, regarded as the most frequently used transformation of receptor or antibody hormone binding data (Figure 16) (32,79,80).

From hormone receptor or antibody binding data, one can generate several important binding parameters, including: R_0 or the total binding sites per cell or protein prep, that is, the binding capacity, found from the lines intercept of the abscissa or x axis; the K_a or equilibrium association constant for the hormone and its receptor or antibody obtained from the lines intercept of the ordinant or y axis and from the slope of the generated line; and the K_d or equilibrium dissociation constant also obtained from the slope of the line.

Scatchard plots are theoretically linear, but when actual binding data are graphed, many are not (Figure 17) (27,28). Nonlinearity can be the result of allosterism between the receptor after initial hormone binding (positive cooperativity) or the converse (negative cooperativity), multiple binding sites per cell or antibody moiety, artifacts of nonequilibrium conditions, inaccurate estimates of assay measurements (e.g., nonspecific binding), and bound and free measurements and different affinities of labeled and nonlabeled hormone or other molecules (28,69,81–83).

Assay Quality Control and Validation

Optimal utilization and interpretation of radioimmunoassay data require knowledge of the precision and reproducibility of the methodology. Early

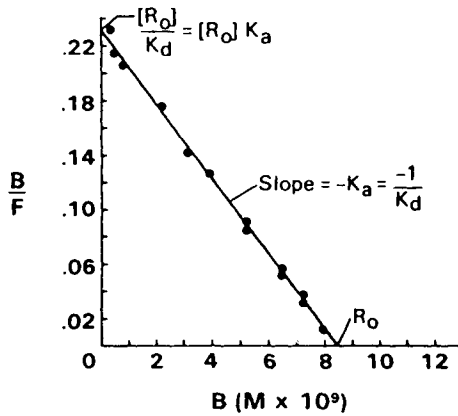


FIGURE 16. Scatchard analysis of hormone binding data. Bound counts divided by free counts are plotted against the dose of the bound counts. The X intercept of the line drawn through the data points indicates the total binding capacity of cells or membrane protein receptors (R_0). The Y intercept of the plot indicates the binding equilibrium association constant $[R_0]K_a$. The slope of the line gives the binding affinity ($-K_a$). [From J. L. Vaitukaitis, *Hormone assays. In "Endocrinology and Metabolism"* (P. Felig, J. D. Baxter, A. E. Broadus, and L. A. Frohman, eds.), p. 164. McGraw-Hill, New York, 1987.]

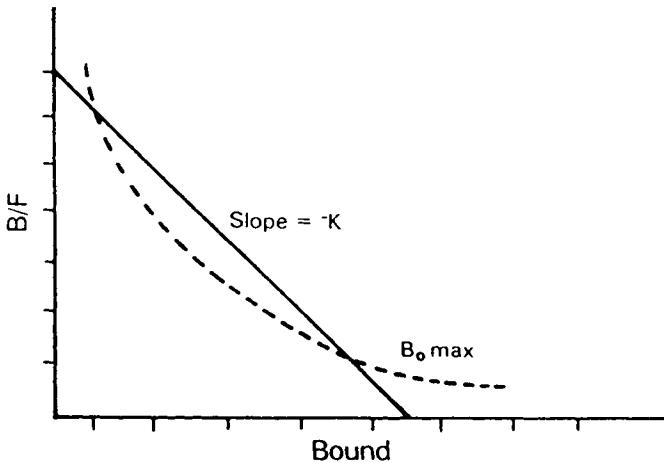


FIGURE 17. Theoretical and actual Scatchard analysis of data. The straight line shows the theoretical straight-line relationship; the dashed line indicates the often observed actual Scatchard data. (From F. S. Ashkar, "Radiobioassays," Vol. 1. CRC Press, Boca Raton, Florida, 1983.)

radioimmunoassay data often measured and quantitated very large changes in hormone levels in response to various stimuli, and assay validation and quality control were often ignored. It was no surprise that some laboratories produced results from a single blood sample that showed a 10-fold difference from each other (84). Thus, the incorporation of proper and adequate quality control became habitual. Several quality control techniques can be used, involving parameters derived from assay results, pool sample results, standard curve results, and commercially supplied “plasma or serum” standards. The most commonly utilized quality control parameters for radioimmunoassays (and that can be applied to all assays) are: (1) specific activity of the tracer (hormone or antibody); (2) amount of tracer; (3) total counts per minute; (4) nonspecific background counts; (5) slope of the standard curve; (6) intercept of the standard curve; (7) the percentage of bound counts in the absence of unlabeled hormone, that is, bound over total counts (B/T_0); (8) within-assay variance; and (9) between-assay variance (85). The first three parameters relate to the labeling procedure and to the amount of tracer present, both of which are known to influence assay sensitivity. B/T_0 is affected by the binding capacity or titer of the antibody, the binding affinity of the antisera, the immunoreactivity of the tracer (an index of “damage”), and the assay incubation conditions (84). The slope of the standard curve line can be calculated by linear regression analysis or determined graphically. Intercept gives a measure of assay sensitivity. Confidence limits for potency estimates of unknowns are derived from within-assay variance calculations. These parameters and the mathematics involved in determining them are discussed in detail elsewhere (69–72,84).

Because RIAs are dependent on the precise interaction of chemicals in accordance with the laws of mass action, the principles of RIA appear quite simple. But a host of nonspecific factors and cross-reacting molecules constantly threaten to interfere with these reactions, jeopardizing the validity of the results (64). This necessitates the user to validate each assay. Several criteria must be met to assume assay validity:

1. The assay should be specific, that is, measure only the hormone of interest. Assay specificity can be defined as the degree of freedom from interfering substances. Specificity of the antibody for the antigen is influenced by heterogeneity or the absence of purely specific antibodies, cross-reaction with other antigens or metabolic fragments that retain immunoreactive sites, and possible influences of the antigen–antibody reaction owing to the presence of low-molecular-weight substances that may alter the environment of the reaction (5). Cross-reactivity measurements are an index of assay specificity, that is, evaluation of the uniqueness of the antibody for a specific antigen. Antibody cross-reactivity can occur between antigenic

determinants on similar hormones or between multiple hormones, their precursors, fragments, or metabolites, and between different types of steroid molecules. Cross-reactivity may also exist to varying degrees between the same hormones in two different animal species. Cross-reactivity problems with antibodies are minimized by using chromatographic separation procedures to “purify” the sample containing the antigen or hormone.

2. The assay should be sensitive enough to measure levels of a hormone under conditions when concentrations are known to be low, but meaningful. Sensitivity can be defined as the smallest amount of unlabeled antigen that can be distinguished from “no” antigen. This also can be defined by the slope of the dose–response curve with the formula

$$S = \frac{B/F}{1.1} \times \text{slope } B/F$$

or sensitivity (S) equals the mean difference between duplicate estimates (B/F) divided by 1.1 times the slope of the dose–response curve at B/F .

3. The assay should be accurate. Accuracy is the ability of an assay to measure exactly in a quantitative way the amount of hormone in a biologic fluid or tissue, when that amount is known. However, until the precise chemical structure and properties of the antigen are known, one can only approximate this “true” value by evaluating a “relative” accuracy. Accuracy is routinely determined by the ability of the assay to correctly measure the amount of hormone “spiked” into a blank sample.

4. The assay must be precise. Precision is defined as the ability to have an assay perform consistently in reference to hormone antibody binding characteristics, separation of bound from free fractions, and so on, over long periods of time, assay after assay. As stated by Midgley *et al.* (81), “Assay precision is the extent to which a given set of measurements of the same sample agrees with the mean of that set, i.e., the amount of variation in the estimation of unlabeled antigen.”

5. Reproducibility. The main factor influencing reproducibility, that is, the duplication of the values within or between assays, is the difference in individual techniques in carrying out the same operation.

Proper validation of the assay also requires that the apparent hormone content of an unknown sample be independent of the dilution at which it is assayed, establishing in a sense that all the components of the assay are performing optimally and as expected. Simply stated, the concentration of the unknown must decrease linearly with dilution, or alternatively a dilution curve of the unknown is superimposable on a dilution curve of the standard over a wide (100-fold or more) concentration range. Lack of exact superimposability can be due to experimental errors. Superimposability does not

prove immunochemical identity of the unknown and standards, but represents a large nail in the coffin. A lack of superimposability can be caused by a variety of specific and nonspecific factors, and implies that the assay lacks quantitative validity, although it still may be useful clinically (33).

The actual performance of the RIAs or IRMAs and the nuances of each step, from preparing assay reagents to data reduction, are too numerous to elucidate in a single volume. In fact, the subtle distinctions of immunoassay procedures are usually omitted in written texts and syllabuses. True understanding and expertise come from months or years of training and frequently only in discussions with those who helped father and establish each essential step. These must be mastered if the user expects valid quantitation of extremely small amounts of hormones, regardless of whether assays are set up from scratch in the laboratory or generated from a commercially prepared kit (86).

NONRADIOMETRIC ASSAYS

Many informative books and journal review articles on nonradiometric assays have been published over the course of the last decade, covering a wide range of methodologies for enzyme immunoassays, electrochemical sensors, bioluminescence assays, fluoroimmunoassays, and chemiluminescent assays (12,30,87–128). Of these assays, the enzyme immunoassay (EIA) or enzyme-linked immunosorbent assay (ELISA) best typifies the evolution of endocrine assays from radiometric to nonradiometric approaches.

Several factors led to the change from isotopic to nonisotopic assay methodologies in routine work: (1) the critical separation of bound from free step in RIAs was an obstacle to RIA automation; (2) the cost of reagents, including radioisotopes and equipment; and (3) the fact that RIAs require radioactive tracers. Researchers and clinical chemists realized the need to protect lab personnel and come to grips with the problems of generating large volumes of radioactive waste. The result has been a search for alternative approaches to hormone assay technology.

The principle of the enzyme immunoassay depends on the ability to assay the concentration of a hormone or other analyte by measuring the activity of an associated “enzyme” that is conjugated to either a primary or secondary antibody (25). The detection systems required for EIAs range from visual to photometric, quantifying colored, fluorescence, or luminescent products. Reviews of these assays have been published by Voller *et al.* (114) and Albertson and Hazeltine (26), and others (90,116,117,125–127).

The ELISA, first described by Engvall and Perlman in 1971 (128), has been subject to many modifications and refinements. In the ELISA, the

basic tenets of immunoassays are conserved, those being the interaction between an antibody and a corresponding antigen. The novelty is that an enzyme that can be easily quantitated acts as the tracer. This enzyme is covalently linked to either the hormone or one of the antibodies in the reaction. After an appropriate incubation period with either standard hormone or sample and a step separating the bound from free fraction (which under certain circumstances may not be necessary), the enzyme activity is measured through the addition of a specific enzyme substrate or chromogen that turns color in the presence of the enzyme in a dose-responsive relationship, that is, the more enzyme, the darker the color. Assay quantitation can often be made with the naked eye, however, spectrophotometric analysis provides more precise readings and significantly quickens result turn-around time. There are several obvious advantages in the use of enzyme labels. Particular enzymes can be purchased with no licensing regulations, are available in very pure form, are quite inexpensive, and have long shelf lives. A variety of enzymes can be used to provide sensitive assays owing to the amplification effect of these enzymes. Some EIAs have been automated. And, enzymes (as well as the chromogens used) are nontoxic and safe, posing no disposal problems.

Because the antibody moiety carries the “label” in the EIA, polypeptide or proteins were the first hormones routinely measured by these techniques. This was based on the fact that sandwich or double antibody assays could be developed that utilized antibodies directed toward different antigenic epitopes of the hormone (like IRMA formats). New assays based on different antigenic sites of subunits of a hormone have also exploited EIA technology. For example, Schwall and colleagues have devised an EIA scheme that detects two related gonadal peptides, inhibin and activin (Fig. 18) (129).

The basic EIA or ELISA procedure entails sandwiching the hormone between two specific and different antibodies: the primary or capture antibody is usually linked to a solid-phase matrix, sometimes a polystyrene tube, microfilm plate well, or sphere; and a separate secondary antibody is conjugated to the enzyme tracer. This approach is most frequently applied to molecules that have an appropriate topographical distribution of antigenic determinants and are large enough to bind to two different antibodies without affecting either the binding reaction or affinity. By using microtiter plate and plate reader (or ELISA reader), one can get results from 96 individual assays in about 70 seconds (even shorter for the newer “state-of-the-art” ELISA plate readers).

The ultimate challenge for EIAs was to be able to measure a variety of polypeptide and steroid hormones and other molecules and achieve the same or better assay sensitivity, specificity, accuracy, and precision as that

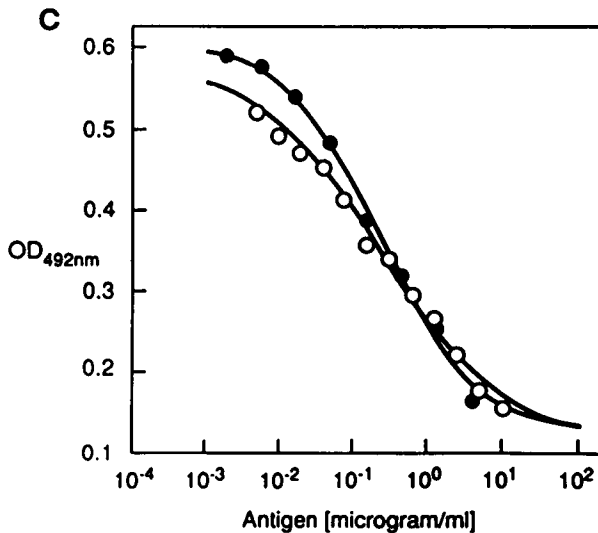
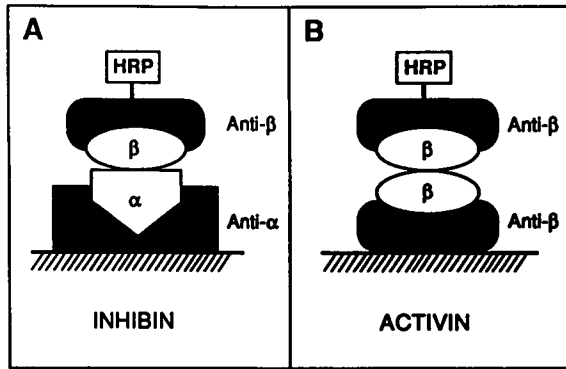


FIGURE 18. Application of ELISA technology for the measurement of inhibin and activin. For this and other EIAs, 96-well or ELISA plates are frequently used with one of the two antibodies used being coated to the wells. Because inhibin is a heterodimer, a second antibody, generated against a separate unique binding site, can be conjugated to an enzyme (in this case, horseradish peroxidase, HRP) and added as a unique reagent. The amount of enzyme/second antibody bound in this system is directly proportional to the amount of hormone in the sample. After the ELISA plate is washed, the enzyme activity is quantitated with the addition of *o*-phenylenediamine, the reaction is stopped with sulfuric acid, and the absorbance is measured at 492 nm in an ELISA plate reader. (A, B) Orientation of the assay and its components to measure inhibin or activin by changing the solid-phase-linked anti-alpha (anti- α) or antibody against the beta chain (anti- β). (C) Competition ELISA of porcine follicular inhibin (solid circles) or pure porcine inhibin (1–30) (open circles) when a multiwell ELISA plate was coated with pure porcine inhibin (1–30). [From R. Schwall, L. N. Bald, E. Szonyi, A. S. Mason, and K. Nikolics, Approaches to non-radiometric assays for inhibin and activin. *In* “Non-radiometric Assays: Technology and Application in Polypeptide and Steroid Hormone Detection” (B. D. Albertson and F. Haseltine, eds.), pp. 205–220. John Wiley & Sons, New York, 1988.]

achieved by RIAs and IRMAs. This was not an insurmountable task, and has been achieved in many circumstances.

If the particular protein hormone exists as a monomer and if highly purified preparations of the protein are available, a competitive-type EIA or ELISA can be used. For example, purified antigen is coated to the ELISA plate wells in an overnight incubation step. Limiting amounts of the specific hormone antibody and either pure hormone standards or sample are added. Nonspecific binding can be minimized with the addition of blocking agents like phosphate-buffered saline-Tween. After an overnight incubation the plate is washed and the antibody-antigen mixture is added to antigen-coated 96-well plates and incubated for 1 hr. During this final incubation, any antibody that did not bind to the hormone is washed from the wells and the bound component of the assay is quantitated. One drawback of microtiter plates is the limited surface area available through which to bind hydrophobic compounds. To solve this limitation a variety of "macro" beads have been used, including latex or polystyrene, polycarbonate, polyacrylamide, and copolymer beads (124). The beads can be linked to antibodies, then incubated with the hormone, with excess reagent removed by washing.

The preparation of enzyme protein conjugates is critical. The functional residues and stabilities of both the enzyme used and the molecule to be coupled will determine the precise chemical cross-linking approach used. Because enzymes themselves are proteins, conjugation methods are as likely to produce enzyme to enzyme complexes or protein to protein complexes as the desired enzyme to protein conjugate. Several approaches have been described by O'Sullivan *et al.* (87) and include the one-step glutaraldehyde method, 2-step glutaraldehyde method, periodate method, and the use of *N,N'*-*o*-phenylenedimaleimide or *m*-maleimidobenzoyl-*N*-hydroxy succinimide (MBS) (Figure 19) (87). Hapten-enzyme conjugate coupling reactions are often similar to those used for protein-enzyme cross-linking. Experts recommend the avoidance of linking enzyme molecules to hapten (e.g., steroid) antigenic sites and to use a different site and cross-linking method when preparing the enzyme label from that used to prepare the immunogen. Common methods employed are the mixed anhydride method, carbodiimide, and bifunctional imidates like MBS (Figure 20) (87).

Basic ELISA Formats

Enzyme or other nonradiometric assays can be subdivided into two groups:

1. heterogeneous—in which assay formats require a bound from free separation step and where the enzyme activity is not influenced by the hormone-antibody reaction; and

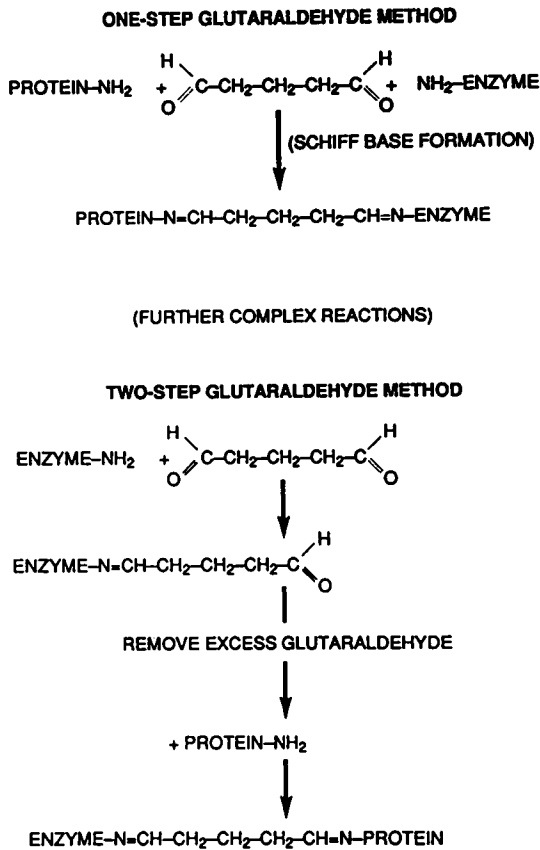


FIGURE 19. Enzyme-protein hormone conjugations. In the one-step glutaraldehyde method, the dialdehyde, glutaraldehyde, links through the protein amino residues to form a Schiff's base. In the one-step method this is followed by further reactions, the details of which are described elsewhere (90). Alkaline phosphatase and horseradish peroxidase are common enzymes used here. In the two-step method, horseradish peroxidase is the best enzyme candidate, because of its relative unreactivity toward glutaraldehyde (probably a result of alkyl isocyanate found in horseradish, which blocks the majority of its amino groups). This horseradish peroxidase is "activated" by glutaraldehyde and not self-polymerized. After removing excess glutaraldehyde, the active enzyme is further reacted with antigens or antibodies containing amino residues. [From M. J. O'Sullivan, J. W. Bridges, and V. Marks, *Enzyme immunoassay: A review. Anal. Clin. Biochem.* **16**, 223 (1979).]

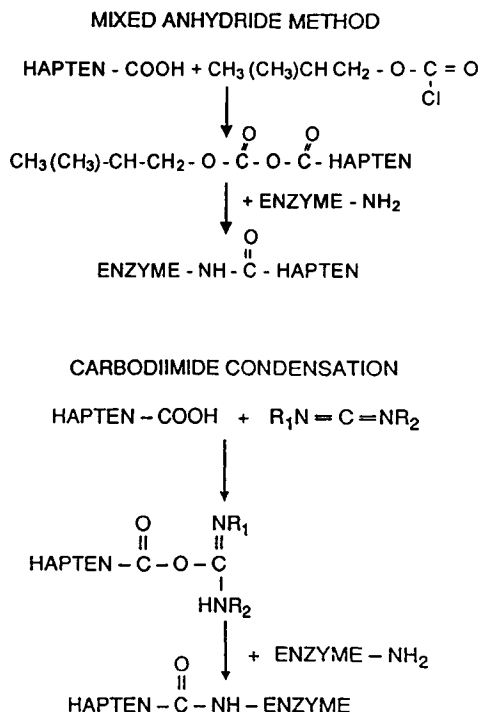


FIGURE 20. Enzyme-steroid conjugation methods. These reactions have been successfully used for steroids, for example, estradiol using the mixed anhydride, and testosterone and cortisol with carbodiimide. [From M. J. O'Sullivan, J. W. Bridges, and V. Marks, *Enzyme immunoassay: A review. Anal. Clin. Biochem.* **16**, 226 (1979).]

2. homogeneous—where the enzyme activity of the conjugate is influenced by the hormone-antibody, and in which a distinct step for separation of bound from free is not required.

The Heterogeneous Assays

The basic design of several simple heterogeneous enzyme assays is shown in Figure 21 (106). The competitive enzyme assay (Fig. 21A) is analogous to classic radioimmunoassays. Enzyme-labeled hormone and unlabeled (sample) hormones (H) compete for the binding sites of a limited number of solid-phase bound antigen-specific antibodies (AB). Antibody saturation occurs simultaneously providing all reactants are incubated together (106).

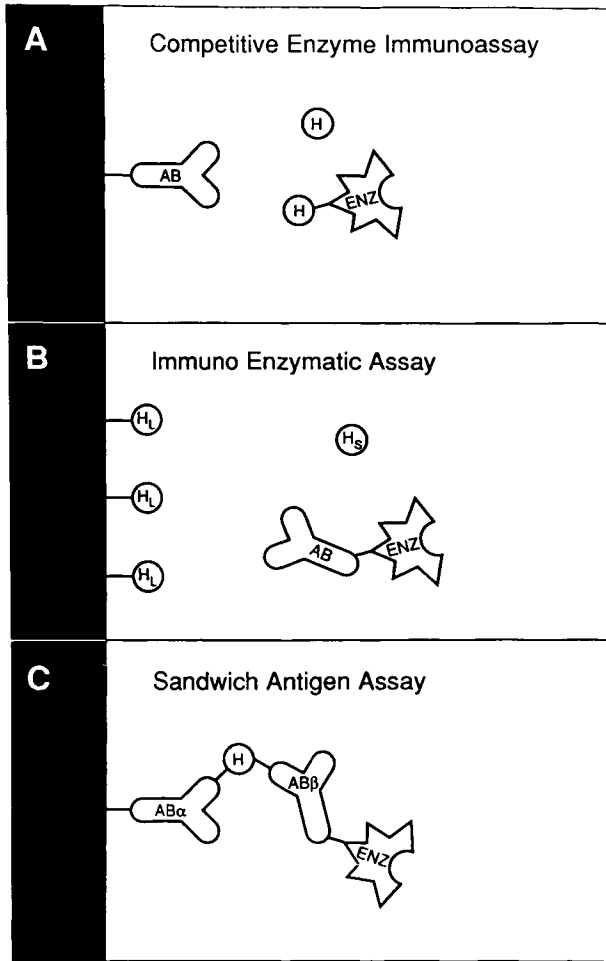


FIGURE 21. Typical heterogeneous enzyme immunoassay formats. (A) Competitive enzyme immunoassay; (B) immunoenzymatic assay; (C) the sandwich antigen assay format. Hormone moiety (H) and enzyme (ENZ) can be coupled to the hormone or antibody (AB). The left side of each panel represents a solid-phase support material. [From M. Oellerich, Enzyme immunoassay: A review. *J. Clin. Chem. Clin. Biochem.* **22**, 895–904 (1984).]

Sequential saturation may be preferred if the hormone to be measured is in very low concentrations in the fluid to be tested (130), however, this often reduces the specificity of the assay (131). The amount of enzyme-labeled antigen bound by the antibody is inversely proportional to the concentration of unlabeled antigen present in the sample (90).

The reverse of the competitive enzyme immunoassay is the inhibition enzyme immunoassay in which the antigen-antibody interaction between a solid-phase linked hormone (H_1) is inhibited by free sample hormone (H_s). This modification is called the immunoenzymatic assay (Figure 21B). Here, enzyme-labeled antibody is reacted with antigen, and excess solid-phase antigen is then added. Sample hormone (H_s) is added and binds to the enzyme-antibody complex. The remaining free enzyme-labeled antibody is subsequently separated by binding to a solid-phase coupled antigen also added in excess. The enzyme activity detected on the solid-phase matrix after separation of bound and free is inversely proportional to the amount of antigen in the sample.

Sandwich assays have also been developed (Figure 21C). Large protein or polypeptide hormones with several dissimilar epitopes or antibody binding sites are particularly suitable for this sandwich antigen assay. Obviously, for this approach, the two assay antibodies should not react with each other, only their unique epitopes on the hormone (H). In addition to these are several modifications, that is, assay designs that employ multiple ligand hormones and antibodies that ultimately give either a direct or indirect measure of the particular hormone in question (128,130,131).

The overall quality of the ELISA or EIA depends on the specific characteristics of the enzyme label chosen. For example, in heterogeneous assays, the enzyme activity is usually measured on the washed bound phase. Therefore, interfering serum or plasma sample factors are usually removed by the washing procedure, making the pretreatment of samples unnecessary. In general, highly purified enzyme preparations produce the most sensitive assays. The most commonly used enzymes meeting this criteria are alkaline phosphatase, horseradish peroxidase, β -D-galactosidase, glucose oxidase, carbonic anhydrase, acetylcholinesterase, catalase, and glucoamylase (87,128). Although the actual detection of this assay end point, that is, measuring enzyme activity, is usually performed by photometry, chemical luminescence- and fluorogenic-producing substrates have also been used (see later sections).

Enzymes are coupled to the assay antibodies or antigens by a variety of chemical techniques, including carbodiimide and mixed-anhydride formation, glutaraldehyde, periodate, or N,N' -*o*-phenylene dimaleimide. The goal is to incorporate as much enzyme as possible onto the hormone or antibody without compromising its activity or the properties of the coupled complex. The acid test of this step comes in generating a standard curve after the enzyme conjugation is completed (87).

Systems used in heterogeneous assays to separate bound from free assay fractions usually incorporate a solid-phase matrix, like polystyrene beads (bound to one of the antibodies), cellulose, and magnetic polyacrylamide

agarose particles (106,128). Precipitation can also be used, for example, with second antibodies or polyethylene glycol.

Homogeneous Enzyme Assays

The principal design of the simplest homogeneous enzyme assays have been described by Oellerich and others (106,128). Because homogeneous assays do not require a separation step, they are more susceptible to plasma or serum interferences, making the selection of enzyme labels critical. The rule is to choose one that is absent from and unaffected by such biological sample factors. Those routinely used are lysozyme, malate dehydrogenase, glucose-6-phosphate dehydrogenase, and β -D galactosidase. The most common homogeneous assay format is the enzyme multiplied immunoassay technique, abbreviated as EMIT (Figure 22) (106). Two very basic approaches can be used, in which the activity of the enzyme label is enhanced by antigen in the sample (Fig. 22A) or inhibited (Figure 22B) as the single hormone (H) increases if the conjugate is bound to the antibody (131,132). In EMIT assays, an enzyme-labeled antigen is required and the ability of the enzyme to catalyze a substrate (S) to a product (P), which is the final factor to be quantitated, is compromised by the hormone–enzyme conjugation binding to an antibody. Configuration of the enzyme to the hormone does not destroy the enzymatic activity; however, binding of the hormone-specific antibody to the enzyme inhibits the enzyme activity. Free hormone in the sample relieves this inhibition by competing for antibody. Therefore, in the presence of antibody, enzyme activity is proportional to the concentration of free hormone (87). The reverse of this mechanism is found in an EMIT for thyroxine that uses thyroxine–malate dehydrogenase. Here the thyroxine–malate dehydrogenase conjugate is enzymatically inactive basally, but is activated when bound by thyroxine antibodies (87,133). There are many variations of these basic principles, eloquently described by Oellerich (106).

A variety of enzyme labels have been used in homogeneous enzyme immunoassays. EMIT assays invariably use an NAD-dependent glucose-6-phosphate dehydrogenase or other dehydrogenases. They are available in very pure form, are inexpensive, and have activities that can be easily quantitated photometrically. Reviews of EMIT assays have been published by O'Sullivan (87), Scharpe *et al.* (89), and others (128,133,134).

The final reagent in the EIA or ELISA format is the chromogen, that is, the enzyme substrate or substrate-associated molecule that actually effects the color change. In an assay where β -amylase might be used as the enzyme, starch could be the final indicator, producing a clear end product from a dark black/violet starting point. Other more classic chromogens

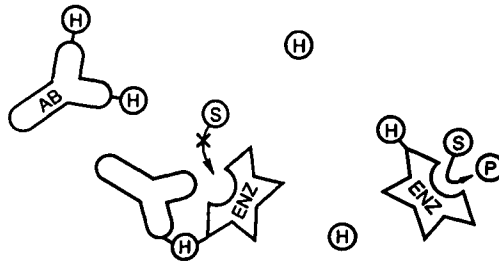
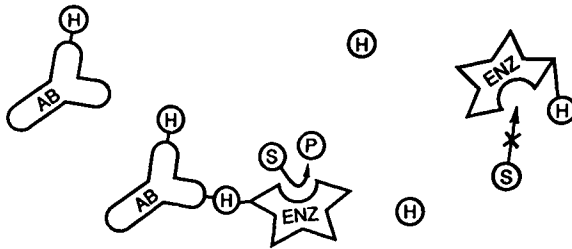
A Enhanced Enzyme Multiplied Immunoassay (EMIT)**B** Inhibited Multiplied Immunoassay (EMIT)*

FIGURE 22. Typical homogeneous enzyme immunoassay formats (EMITs). (A) Enhanced enzyme multiplied immunoassay; (B) inhibited multiplied immunoassay. All the reactants are present in a single reaction medium. Hormone (H) and enzyme (ENZ) can be linked to a hormone or an antibody (AB). Substrate (S) of the enzyme can be converted to product (P) if the enzyme is available for this conversion step. $S \rightarrow P$ indicates the completion of the conversion by the enzyme, and $S - x \rightarrow P$ indicates the inability of the enzyme to catalyze the conversion. [From M. Oellerich, Enzyme immunoassay: A review. *J. Clin. Chem. Clin. Biochem.* **22**, 895-904 (1984).]

commonly used are 2-nitrophenol (with β -D-galactosidase), 4-nitrophenol phosphate (with alkaline phosphatase), and *o*-phenylene-diamine (with peroxidase).

Enzyme immunoassays have been used in virtually all previous RIA and IRMA applications. Assays for the detection of plasma and serum proteins, tumor antigens, drugs, hormones and other haptens, antigens, and antibodies have been developed (87,106,126,128). Likewise, EIA accuracy is affected by the same factors that influence RIAs, plus potentially others. When directly comparing enzyme immunoassays with RIAs, one finds that they are comparable in terms of both assay accuracy and precision. Coefficients of variation for inter- and intraassay variability are between 2 and 10% when midstandard curve range values are evaluated (125,128).

Assay performance, however, can be perturbed owing to inherent interference of the enzyme or immunological reactions in these assay formats. Endogenous enzymes in biological fluids to be tested may interfere with “assay reagent” enzyme activities and other plasma or serum factors (e.g., proteins), probably far more in these settings than with RIAs. Thus, pretreatment of some serum or plasma samples may be necessary to avoid problematic assay interferences.

EIA and ELISA assay cross-reactivity (as with the RIA) is primarily dependent on the specificity of the antibodies used and, as in all assays, must be rigorously validated. The sensitivity of enzyme immunoassays has also been shown to rival classic RIAs (125,128,135). For endocrine assays, EIA and ELISA hormone values ranging from 0.2 to 50 fmol/tube are not uncommon. Some heterogeneous enzyme immunoassays can detect analytes in the amol/tube (10^{-18} mol) range, for example, ornithine- δ -aminotransferase or mouse myeloma IgG (136–138).

In general, to increase the sensitivity of an assay further, the number of substrate conversions per unit time must be increased by introducing a suitable multiplier in the assay “sandwich” structure (124). Streptavidin (and the homologous protein avidin) is remarkable for its ability to bind up to four molecules of biotin with exceptionally high binding affinity. By incorporating a biotin label on a second antibody, it is theoretically possible to increase the number of labels per sandwich by a factor of three. Further manipulation using more monoclonal antibodies can increase this to four (Figure 23) (124,139). One other approach to improve assay sensitivity is through substrate amplification by enzymatic cycling. For example, by replacing the alkaline phosphatase substrate *p*-nitrophenyl phosphate with NADP and adding an enzyme cycling system, a significant increase in signal intensity can be obtained (Figure 24) (124). Even better sensitivities have been reported when fluorescent substrates are used to detect end points of enzyme activity (139). It appears, however, that the sensitivity of heterogeneous EIAs for hormones is linked to the procedures used to separate bound from free fractions. Solid-phase systems using sepharose-coupled antisera often lack good sensitivities. Although microcrystalline cellulose-coupled antibodies combined with second antibody separation steps have sensitivities similar to or better than those of RIAs, generally EIA sensitivities for protein hormones are better than analogous RIA sensitivities. Steroid EIAs possess sensitivities and reproducibilities related to the steroid conjugates used and antisera employed. Combinations in which the same steroid derivative is used for the preparation of immunogen as label (homologous systems) are more specific, but often less sensitive. But comparable specificities, sensitivities, and reproducibilities to RIAs are obtainable with EIAs when the optimal combination of antisera, conjugates, and enzyme

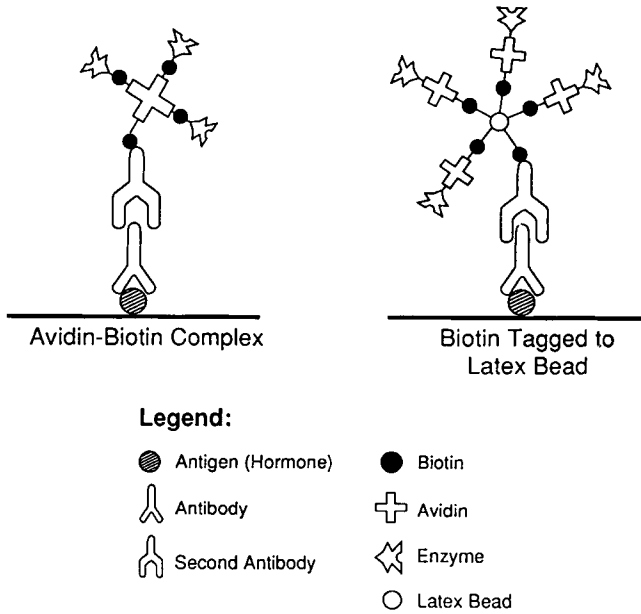


FIGURE 23. Avidin–biotin enhancement. With the incorporation of avidin and biotin as reagent multipliers, signals can be increased by three- or fourfold, depending on the specific application. [From B. Nilsson, *Curr. Opin. Immunol.* 2, 898–904 (1990).] Copyright Current Biology Ltd., ISSN 0952-7915.)

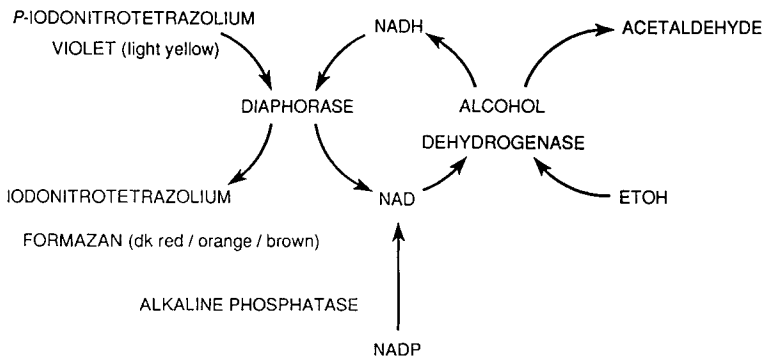


FIGURE 24. Substrate amplification by enzyme cycling. By substituting NADP as a substrate for alkaline phosphatase in place of *p*-nitrophenyl phosphate, and incorporating an enzymatic regenerating system, the color end point of the EIA can be magnified with the production of increased iodonitrotetrazolium formazan by cycling reduced nicotinamide adenine dinucleotide (NADH/NAD). [From B. Nilsson, *Curr. Opin. Immunol.* 2, 898–904 (1990).] Copyright Current Biology Ltd., ISSN 0952-7915.)

labels is chosen (87). Homogeneous assays can perform even better under optimal circumstances. Wide detection limits using EMIT assays for thyroxine and a number of drugs have been reported to be between 0.1 and 10,000 pmol/ml.

The real advantage of the enzyme-linked substrate immunoassay is the elimination of the issues of using radioactivity, including costs (in both direct and disposal costs), contamination concerns in the lab, and lab personnel exposures. With state-of-the-art automation procedures, turn-around time for large-scale enzyme assays will improve dramatically, enabling 400–500 patient samples to be assayed daily for any particular hormone (antigen/ligand/hapten). References to a thousand samples a day (e.g., antibody detection for *Trichinella spiralis*) have been made in the literature (140).

The future of EIAs and ELISAs is dependent on improvement of critical areas of the assay: Production of better enzyme labels, employment of better cross-linking chemistry, developing a better understanding of interfering substances in biological samples, implementing monoclonal antibodies in the assay formats, and developing more automated detection systems.

FLUORESCENCE ASSAYS

Concurrent with the development of EIAs and ELISAs was the emergence of a variety of other nonradiometric assays applicable to the toxicologist. Fluorometric methods and fluorescent probes have gained increasing interest and use over the past several years since they too can be incorporated into rapid and sensitive assays that offer inexpensive, stable, and safe reagents. Their attractiveness is associated with the fact that, like EIAs, a single label can produce many detectable “events” per label molecule depending on turnover (for enzymes), or in the case of fluorescence, one molecule can cycle many times through the excited and ground state during a short measurement period (141,142).

Fluoroimmunoassays (FIA) and immunofluorometric assays (IFMA) are based on labeling of the immunoreactants with fluorescent probes. The techniques of labeling proteins or antibodies with fluorescent probes are certainly not new. As early as 1941, Coons *et al.* (143) were describing the immunological properties of antibodies containing fluorescent groups. The high sensitivity of the fluorescence measurement, combined with the ability of the fluorescent probes to change depending on its environment, offered the possibility for developing heterogeneous assays in which the concentration of an analyte or hormone could be monitored directly in the reaction mixture (144), not to mention homogeneous assay formats where the concentration of an analyte can be measured directly in the reaction mixture.

The problems with fluorescence immunoassay methods historically centered around their inferior assay sensitivities, usually a result of high background in the fluorometric measurement. The recent development of solid-phase separation systems, new fluorescent probes, and automated instrumentation has improved the sensitivities of these assays, making them equal or better than that found in RIAs or EIAs.

The basic principle of fluorescence is shown by the simplified Jablonski diagram in Figure 25 (144). Luminescent molecules capable of absorbing

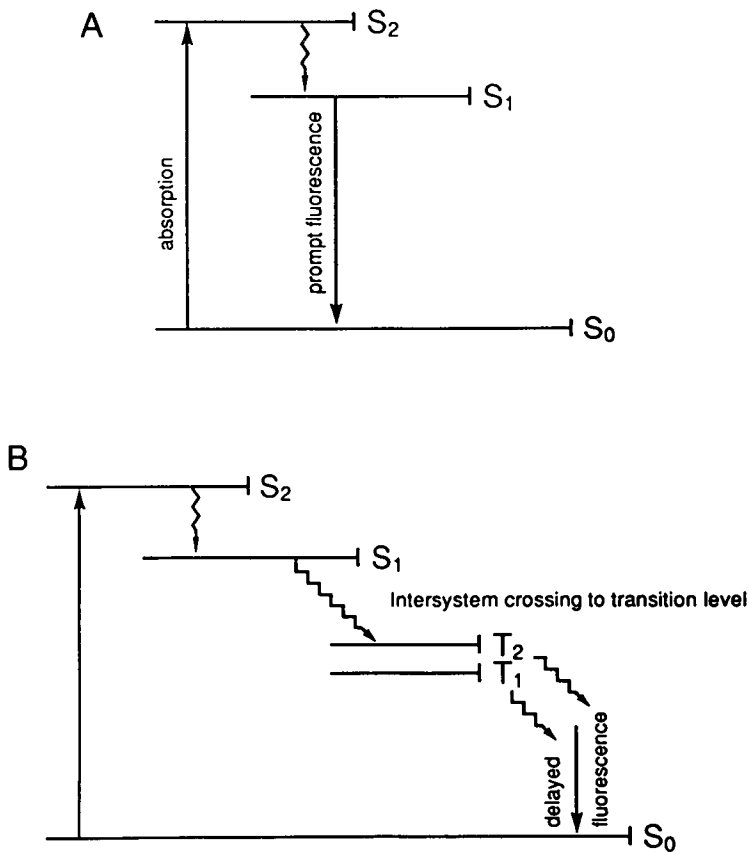


FIGURE 25. Energy levels and transitions in a typical fluorescent organic molecule (A) and in a fluorescent rare earth chelate (B). S_0 = ground state, S_1 , S_2 = excited singlets, T_1 , T_2 = triplets. Straight arrows indicate radiative energy transfer, and wavy arrows are nonradiative energy transfer. [From I. Hammila, *Fluoroimmunoassays and immunofluorometric assays. Clin. Chem.* **312**, 359–370 (1985).]

energy can transfer that energy within its molecular structure, releasing it as a photon. The absorbed energy excites the electronic field of the molecule from its ground-state singlet (S_0) to a higher electronic state (S_1 , S_2 , S_3 , etc.). The excited state then releases or unloads this energy in various forms, and often as fluorescence. After energy unloading the molecule returns directly back to the ground state (S_0) (Figure 25A). The small loss of energy in luminescence, that is, the difference between excitation and emission energies, or wavelengths, is determined as the Stokes shift. This shift is about 30–50 nm for fluorescent organic molecules, but longer for other fluorescent molecules like the lanthanide chelates (Figure 25B). The ratio between absorbed energy and emitted energy is called the quantum yield. This parameter, along with others like the fluorescence molecules' absorption spectra, emission spectra, and fluorescence lifetime (i.e., the decay rate of the excited state), is quite variable, dependent on a host of physical and chemical factors (e.g., temperature, polarity, pH, quenching, and so forth), and is key in the selection of an appropriate fluorescent marker (144).

However, as in all assay formats, fluorescence analysis is not without unique problems. When organic fluorescent probes with narrow Stokes shifts are used, very high background fluorescence can be observed because of light scattering of the excitation beam, for both soluble molecules (Rayleigh and Raman scattering) and insoluble material (Tyndall scattering). The very nature of biological fluids having high concentrations of protein makes them difficult candidates for use in fluorimetric assays. These interfering fluorescence wavelength emissions are usually between 320 and 350 nm and can be as high as 430–470 nm. Thus, the specific emission of usable fluorescent probes should be greater than 500 nm. Pretreatment of plasma and serum samples with proteolytic enzymes and oxidizing or denaturing agents can help eliminate this background contamination. Solid-phase support structures like microbeads with intrinsically low fluorescence backgrounds can also eliminate nonspecific serum background (144).

Biological fluids also contain a host of factors that can quench the fluorescence yields. pH, polarity of the probes, and the oxidation state of nearby molecules or heavy ions can also alter fluorescence yields. Some molecules carrying the fluorescence probes can even be self-quenching.

In spite of these potential problems, a variety of fluorescent probes have proved satisfactory. These probes have a high fluorescence intensity, that is, their fluorescence signal is easily distinguished from background, and their unique chemical characteristics enable them to be bound to antigens (hormones) or antibodies without adversely affecting their properties.

Fluorescence intensity depends on both the absorption of excitation and the quantum yield. The molar absorptivity of the probe must be high

(greater than 10,000), with as high a quantum yield as possible. Moreover, the emission energy of the probe must be easily and clearly distinguished from background. Thus, probes with emissions of greater than 500 nm and large Stokes shifts (greater than 50 nm) are essential.

Coupling of fluorescence probes to other molecules is not unlike other coupling requirements. Immunoreactants must have available functional groups like carboxylic acid, aromatic, hydroxyl, sulfonic acid, or aliphatic amine groups. Reactive intermediates like esters, isocyanates, acid anhydrides, isothiocyanates, or *N*-hydroxyl succinimides have been successfully used (144). Fluorescein or rhodamine derivative probes (having very high fluorescence intensities) are widely used, with isothiocyanate fluorescein derivatives being most popular (145,146). Umbelliferone, a 7-hydroxycoumarin compound, has also been applied to fluorescence assays. Though its fluorescence intensity is not as good as that of fluorescein, it has a larger Stokes shift, enabling it to be used to label polymers like polylysine to increase the yield of steroid tracers (147,148). These and other fluorescent labels that have endocrine applications are shown in Figure 26. Each of these compounds has its own strong and weak points in specific applications; some have excellent quantum yields, high Stokes shifts, and

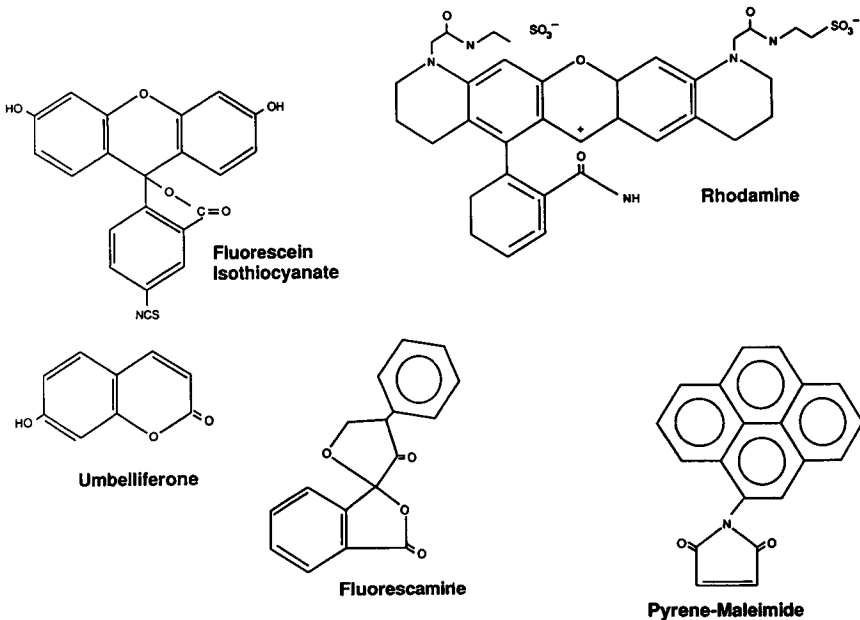


FIGURE 26. Typical fluorescent compounds used in fluorescence immunoassays.

good photostabilities, but some can also be sensitive to scattering of light, sensitive to background interferences, and self-quenching. Fluorescamine and *N*-pyrene-maleimide have been used in fluorescence assays because of their excellent fluorescence enhancement and long fluorescence lifetimes (hundreds of nanoseconds) (145,148,149). Naturally occurring fluorescent phyco-biliproteins from algae, along with porphyrins and chlorophylls, have unique fluorescent properties that make them excellent candidates for fluorescent assay applications (144,148,150–158).

Unfortunately, fluorescein- and rhodamine-labeled tracers are applicable for assaying analytes and hormones that are found in nanomolar ranges, that is, because of the intrinsic detection limitations, picomolar ranges are not accessible. Recently, metal chelates, in particular the fluorescent rare earth ions, have been exploited for application in fluorescence assays because of their excellent fluorescent properties and high detection sensitivity (10^{-13} to 10^{-14} mol/liter). Most notable of these are the lanthanides, europium (Eu-III) and terbium (Tb-III). When these lanthanides are chelated with organic ligands like 4,7-bis(chlorosulfo-phenyl)-1,10-phenanthroline-2,9-dicarboxylic acid (BCPDA), the resulting compound fluorescence is often characterized by broad excitation in the absorption region of the ligand (250 to 360 nm), reduced fluorescence quenching, decreased serum autofluorescence, large Stokes shifts (greater than 250 nm; fluorescein is about 30 nm), and long fluorescence lifetimes (100 to 1000 μ sec) (141,144,159).

Application with this chelating compound has been made in the Cyberfluor System (Cyberfluor Inc., Toronto), can be labeled to streptavidin without loss of biological activity, and can be carried out in microtiter plate wells with final fluorescence measuring on a solid phase using specially designed equipment (160–163). By delaying the measurement of fluorescence after a flash excitation of the sample, background short-lived fluorescence due to serum, solvents, cuvettes, and reagents is essentially eliminated.

However, these lanthanides do not form particularly stable (i.e., chemically inert) chelates, especially in aqueous biological fluids, and they also have a tendency to dissociate and be quenched by water (144). These flaws or shortcomings have been partially corrected by the development of aqueous stabilized chelate systems by polymerization of the chelate to latex particles that are covalently bound to antibodies or antigens (144). Polyamino-polycarboxylate chelates of lanthanides have been used more than any other type of complex in producing usable fluorescent assays. Terbium and europium chelated to IgGs using diazophenyl EDTA, to thyroxine using ethylenediaminetetraacetic acid and sulfosalicylic acid, or to specific antibodies using EDTA and β -diketones have been the first steps in producing usable and efficient fluorescent labels for routine laboratory use (144,164).

The use of separate steps for lanthanide dissociation and simultaneous development after the specific immunoreaction has been perfected by LKB-Wallac (Turku, Finland) in their Delfia time-resolved system (Dissociation Enhanced Lanthanide Fluorescence Immunoassay), making it possible to use nonfluorescence bifunctional complexes such as the derivatives of aminophenyl-EDTA or aminobenzyl-diethylenetriamine tetraacetate for europium labeling (144,165–175).

The Arcus time-resolved fluorometer (LKB-Wallac) is essentially identical to other conventional instruments, except that it has added a system for time-gated measurements of only a portion of the total fluorescence emission cycle. During a critical portion of the emission cycle the photomultiplier is inactive, thus unwanted events are undetected. An example of the sequence might be: excitation light flash (1 μ sec), time delay during which short-lived or unwanted fluorescence is decayed (400 μ sec), actual measuring time with active photomultiplier (400 μ sec), and recovery time before the next cycle (200 μ sec). This makes about 1000 flashes (or a 1-msec full cycle) for the 1-sec well measuring time (141). Newer gated fluorometers use lasers (often nitrogen lasers) as the excitation source, enabling these instruments to measure fluorescence from a solid-phase matrix rather than limited to measurements from solutions.

Fluorescence assay principles are identical to those of the radioimmunoassay and enzyme-linked assays with respect to reaction conditions, separation of bound from free fractions, assay validation, and so on. Fluorescence assays are also similarly classified like RIAs and EIAs, that is, those with labeled antigen versus labeled antibodies, those featuring competition between antigens (tracer and free) for a limited amount of antibody versus noncompetitive or excess reagent assays, or as heterogeneous (requiring a separation of bound from free fraction) or homogeneous (not requiring a separation step) assays (144). Competitive assays using limited amounts of antibodies are similar to most standard RIAs.

Solid-phase-based sandwich assays using labeled antibodies are most common and are called immunofluorometric assays and are analogous to IRMAs. These provide the user with simple procedures and low background fluorescence. Polyacrylamide beads, polysaccharide microbeads, and magnetized cellulose particle compounds have seen application in these assay formats (144,176–178). Like the IRMA, immunofluorometric assays use fluorescent probe-labeled antibodies in excess (i.e., an excess reagent assay). In these assays the fluorescent signal is directly proportional to the analyte or hormone concentration. The use of excess reagents can shorten the incubation time, provide greater sensitivity, and widen the measurement range of the assay (144,179).

As in EIAs, fluorescence assays can be used to measure protein of

polypeptide hormones having two or more distinct epitopic antibody binding sites, like TSH of hCG (180–184). The primary or capture antibody is immobilized on a solid matrix, like polyacrylamide beads or cellulose nitrate or acetate discs. This can then, in turn, be quantitated by a second antibody. Common separation techniques used in RIAs (double antibody, PEG, ammonium sulfate precipitation, etc.) are rarely used in heterogeneous fluorescence assays because of their intrinsic background fluorescence properties. Thus, solid-phase separations are most often used. Obviously all the solid-phase materials employed in the separation step of these formats must provide ease of handling (i.e., easily washed) throughout the assay procedure, as well as intrinsic low fluorescence, scatter, and quench properties (144). Microbeads composed of polysaccharides (176), polyacrylamides (185–187), or magnetizable cellulose particles (178,187) have received the widest application. The use of polyacrylamide and polystyrene beads and magnetizable particles can eliminate the centrifugation steps during washing sequences, and polyacrylamide and polystyrene beads can be applied to homogeneous assay formats because of their low fluorescence and scattering properties. Dipstick or surface technology can be applied to fluorescence assays by employing cellulose acetate-nitrate substrate or polymethylmethacrylate. Obviously special fluorometers are needed to measure the fluorescence from these solid-state applications (144).

Homogeneous fluorescence assay formats do not require a “bound from free” separation step to enable final fluorescent measurement, owing to the reaction mixtures direct effect on the fluorescence properties of the labeled antibody or antigen. These assays are simple and rapid, like their RIA and EIA counterparts, but fall short in terms of assay sensitivities seen using heterogeneous assays because of interference from serum samples and by the chemical nature of the actual assay immunoreaction. Thus, homogeneous fluorescence assays are usually found in applications where analytes or hormones are known to be in relatively large concentrations, for example, drugs and hormones like cortisol and estradiol. Most of these homogeneous fluorescence assays are of the competitive type in which antibody binding induces some change in the labeled antigen fluorescence properties, usually in fluorescence wavelength. Detailed descriptions and useful modifications of both homogeneous and heterogeneous fluorescence assays are provided by numerous investigators (141,144,148,155,182).

Currently, fluorescent assays with sensitivities equal to or greater than RIAs or EIAs have been developed. This has been fueled by the development of better reagents (antibodies, fluorescent probes, cleaner separation techniques, etc.) and more sophisticated and automated instrumentation. The use of poly-fluorescein, rhodamine, and chelated rare earth lanthanides used in time-resolved measurement fluorometers has enabled fluorescent assays to achieve sensitivities similar to or better than those of the best

RIAs and EIAs Background fluorescence, always a potential problem in fluorescence assays, can be decreased with acidic or enzymatic pretreatment of the biological sample. Instrumentation has also improved dramatically over the past several years, which has increased the signal-to-noise ratios using improved fluorescence optics, better fluorescence detectors and signal-processing hardware, and special fluorescence filters. The formats of these systems range from carrying out assays in flow cells (188,189), disposable cuvettes (190), microtiter plates, or microtiter strips or plastic strip surfaces (e.g., dipstick formats) (144). The replacement of continuous light with pulsed excitation and lasers greatly improves the versatility and sensitivity of these assays. Time-resolved fluorescence assays have also been established using terbium (Tb^{3+}) and samarium (Sm^{3+}), as well as europium (Eu^{3+}) (190–192). For conventional fluorescence immunoassays, assay sensitivity is not limited by instrumentation, but by the signal-to-noise ratio of the sample. Appropriate filtering must be used to decrease background fluorescence in addition to implementing unique measuring systems, depending on the fluorescence assay system supplier. It becomes as no surprise that virtually each supplier has its own unique measurement system using polarization, surface, kinetic, and time-resolved measurements (144,159–163,167,169,174–181,193).

CHEMILUMINESCENT ASSAYS

Another more recent modification of the original immunoassay scheme employs the utilization of chemiluminescent end points as opposed to colorimetric and fluorometric end point determinations. Research using chemiluminescent molecules as immunoassay reagents has been ongoing for over a decade, but the implementation of these assay techniques in routine endocrine measurements is relatively new (194–203).

Chemiluminescence differs from fluorescence in that it involves excited state formation as the product of an exoergic chemical reaction (194). The excited state product molecule relaxes to a ground state and in so doing emits photons. Chemiluminescence incorporates a population of excited states of specific molecules as a consequence of the thermodynamics of the oxidative chemical reaction involved. The photoefficiency of this reaction or the number of photons emitted per molecule of reactant is called the chemiluminescence quantum yield (195). The kinetics of these reactions can be varied by modifying the chemical reactions involved so the photon emission can occur immediately (within one or two seconds) or be slightly delayed (within several seconds to minutes). The actual kinetics of the reactions varies according to the concentration of initiating reagents, but usually is characterized by a very rapid rise in emission intensity (measured

in fractions of a second) followed by a gradual decay (measured over a few seconds) as the excited states become depolarized.

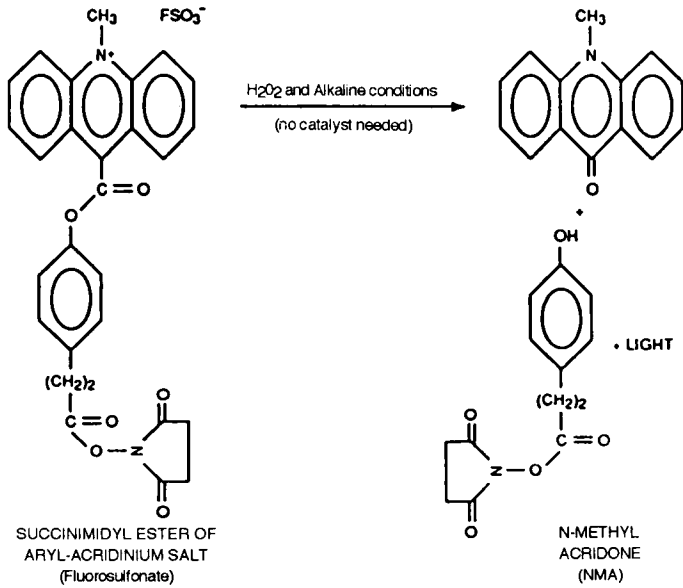
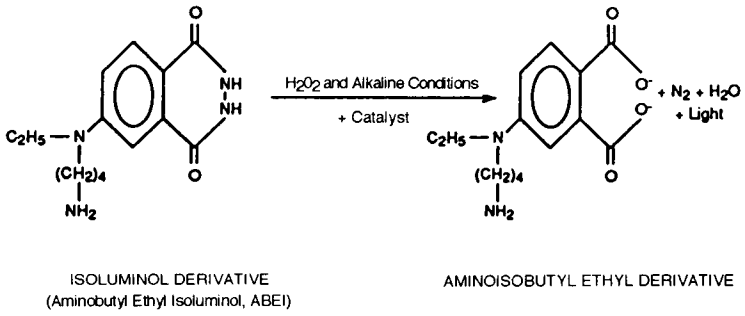
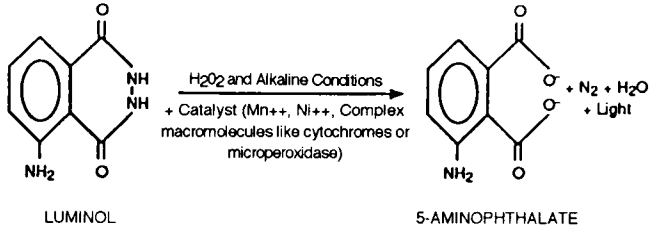
Good chemiluminescence quantitative techniques have only recently become a reality. The search for efficient luminometry has centered around improving nonspecific luminescence and interferences from the assay system itself. Light detection is achieved using high-efficiency photomultiplier tubes, but still remains in the 20–30% efficiency range. Events are treated in either digital or analog manner, depending on the type of instrument being used. Digital systems operate on a “one photon–one event–one pulse” basis, with the number of pulses per time being a function of light intensity. Analog systems involve treating the photomultiplier output as a photocurrent, the magnitude of which is proportional to light emission intensity (195). New automated luminometric systems must incorporate a sample transportation system, an elevator mechanism that translocates each sample to a light-free chamber near the photomultiplier tube, and an automatic injection system to dispense initiating reagents, all integrated with software programs for operation and data reduction.

Though instrumentation and electronic signal interpretation are important, the success of chemiluminometric assays depends on the ability to produce stable conjugates between the antigen, antibody, and the label. The first assay prototypes employing chemiluminescent probes encountered assay interferences from a variety of factors that influenced assay catalytic reagent requirements and microenvironmental quenching.

Most of the early published work on chemiluminometric assays has been on small molecules, usually steroids. This is due to the well-established procedures for producing externally labeled steroid molecules. The conjugation chemistries (succinate or glucuronide bridging) have also been developed. The derivatives of luminol (e.g., isoluminol) (Figure 27) (195) make conjugation with minimal loss of quantum yield a reality (196).

Chemiluminescent molecules are covalently linked to either the assay antigen (hormone) or antibody, and as in other assays these reagents can

FIGURE 27. Chemiluminescent molecules (luminol, isoluminol, and an acridinium derivative) and their reactions to produce light. Simplified chemical reactions of common “labels” in chemiluminescence assays. Luminol and isoluminol require catalysts like Mn^{2+} or Ni^{2+} , or complex macromolecules like cytochromes, horseradish peroxidase, or microperoxidase. Acridinium derivatives offer certain advantages since the reaction does not require catalysts, making the reaction less susceptible to background and interference effects, and the NMA produced in this reaction has a higher chemiluminescence quantum yield because the yield is independent of the chemical modifications required to conjugate the acridinium salt to assay components. [From I. Weeks and J. Woodhead, Chemiluminescence immunoassay. *J. Clin. Immunol.* **7**, 82–89 (1984).]



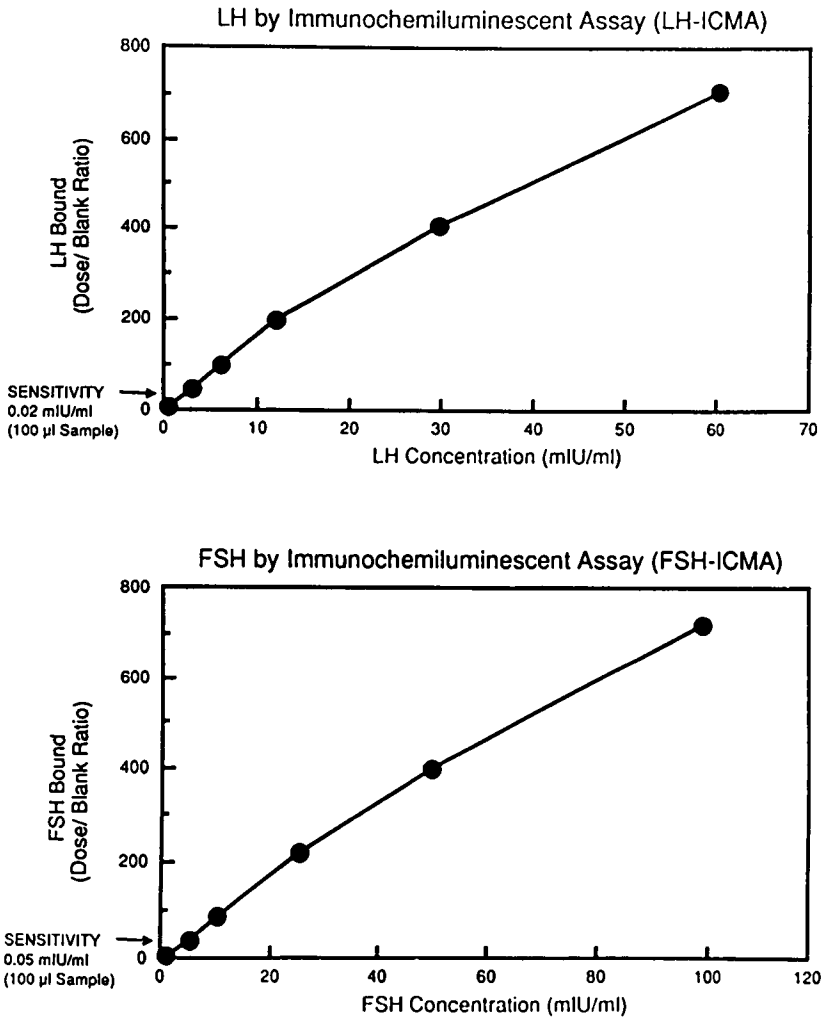


FIGURE 28. Typical standard curves of chemiluminescence assay of LH and FSH. Sensitivities for comparable radioimmunoassays are: LH, 4.0 mIU/ml using 100- μ l sample; FSH, 0.5 mIU/ml using 100- μ l sample. (From Dr. Darrel Mayes, Endocrine Sciences, Calabassas Hills, CA, 1992.)

be adapted to either a homogeneous system or heterogeneous format. Although the homogeneous assays provide simplicity, heterogeneous formats provide higher assay sensitivity.

Endocrine assays have been developed by Kohen and her colleagues for several steroid hormones and their urinary metabolites, including pro-

gesterone (204–206), estradiol (207), estrone-glucuronide (208) estriol glucuronide (209), and pregnanediol glucuronide (210), reaching and/or surpassing assay performance and sensitivities of the best EIA and RIAs (211). These assays have adapted solid-phase methodologies, making the removal of interfering serum factors or other quenchers a part of the assay dynamics. Conjugation of aminobutylethylisoluminol (ABEI) to antibodies posed some significant problems in terms of quenching and loss of quantum yield. Most investigators have overcome this by adding a dissociation step just prior to luminometry. This usually involves high temperatures and the addition (incubation) of strong alkali. The use of acridium esters may eliminate this quench, and thus the extra assay step.

Polypeptide assays can be flawed (as stated earlier) when labels are linked to these proteins, thus producing greatly reduced quantum yields. Other isoluminol derivatives (e.g., aminohexylethylisoluminol, AHEI) have partially overcome this obstacle (195,197). The incorporation of acridinium derivative labels has been attempted with encouraging results (212). Examples of this are gonadotropin assays (Figure 28) that incorporate paired monoclonal antibodies linked to an acridinium ester, providing highly sensitive and specific procedures when directly compared to analogous IRMA formats. Similarly, assays for TSH, thyroxine (T_4), and free T_4 have been developed, also employing monoclonal antibodies and an acridinium chemiluminescence label (Figure 29) (194,195,213,214).

Photons or light intensity can be accurately and precisely measured using commercially available luminometers. The earliest models were crude in design, in essence being small shoe-box-sized darkrooms requiring the manual dispensing of catalysts and other luminescent reagents by the operator, and measuring only one assay sample at a time. Current state-of-the-art luminometers can automatically dispense reagents and measure light intensity at a variety of postreaction time intervals, integrate this intensity, and report results through computerized data-processing systems.

OTHER ASSAY TECHNIQUES

There are several other assay approaches available to the toxicologist for the measurement of important molecules. Fluorescence polarization immunoassays have been developed into homogeneous assay format systems that currently are among the most common clinical methods for measuring therapeutic drug concentrations in serum (215,216). These are competitive immunoassays in which drug and drug labeled with a fluoroprobe compete for binding with a specific antibody.

The mechanism of this technique is quite straightforward. If a stationary fluoroprobe absorbs plane polarized light, the resulting fluorescense will

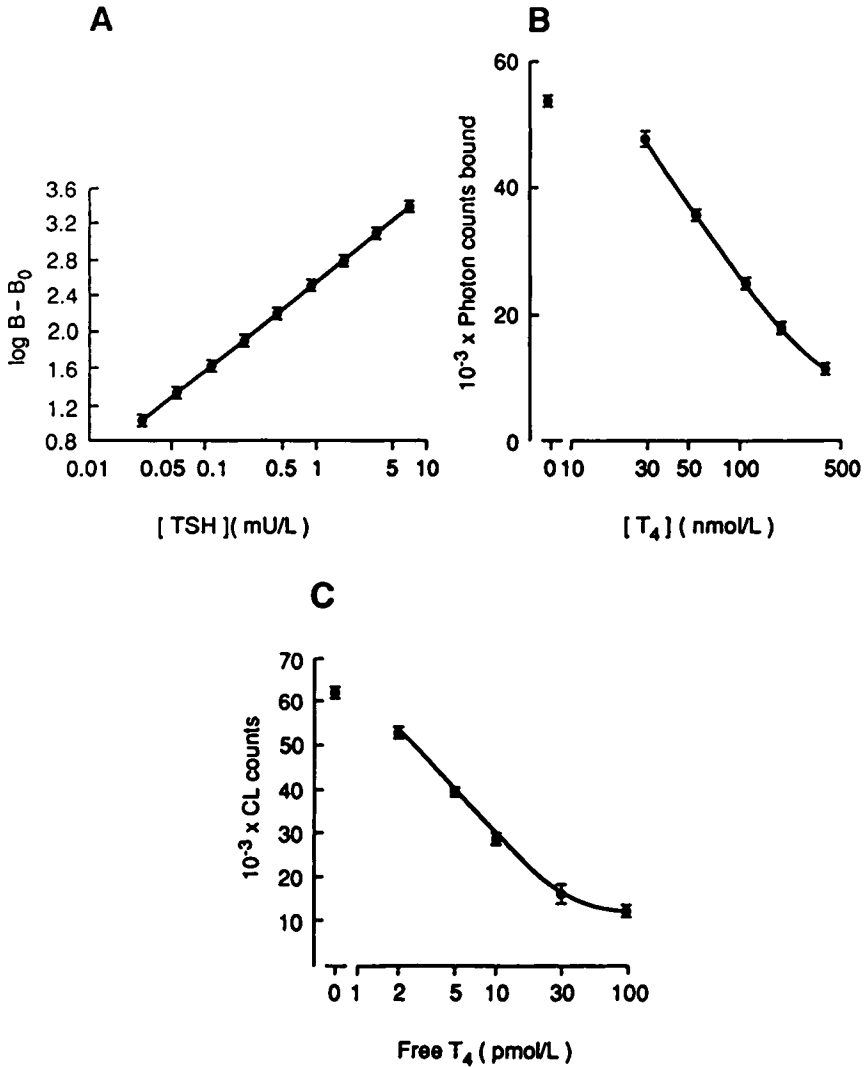


FIGURE 29. Chemiluminescent assay standard curve for the measurement of thyroid-stimulating hormone (TSH), thyroxine (T₄), and free (T₄). (A) Dose-response curve of a two-site immunochemoluminometric assay for human TSH using a high-affinity monoclonal antibody labeled with 3 moles of acridinium ester per mole of antibody. The assay format comprises: (1) mixing sample with labeled antibody (2 hr), (2) solid-phase polyclonal antibody added (1 hr), and (3) a final wash step with mild detergent to help reduce nonspecific binding (background) to less than 0.1% of added activity. Luminescence of the acridinium component is evaluated with the addition of alkaline hydrogen peroxide. Light intensity is quantitated over a 1- to 2-sec period, being directly proportional to the sample's

also be plane polarized. A molecule that rotates between the time of the absorption and emission events will not maintain plane polarization of the emitted light. Thus, the assay system takes advantage of the fact that large fluorescent molecules, such as the fluorophore–drug bound to an antibody, rotate slowly in solution and that when irradiated with plane polarized light will emit light that is still polarized. Small molecules such as the drug–fluoroprobe rotate much more rapidly and their emitted fluorescence will be considerably depolarized relative to the larger molecules. The fluorescence polarization instrument measures the polarization of the fluorescence, which is related to the ratio of free to bound fluorophore. A dose–response curve is constructed that relates standard drug concentration to the fluorescence polarization signal. Several advantages to these assay systems are that the reagents are stable for long periods of time and assay calibrations are typically good for several weeks. In addition, these are homogeneous assays, so no separation of bound and free forms is required. Serum can usually be assayed directly without any pretreatment of sample and a batch of assays can be performed with relatively little technologist time required.

Electrochemical immunoassays combine the sensitivity of bioselective electrode detection with the specificity of the antigen–antibody interaction. Electrochemical methods are not plagued by problems of sample turbidity, quenching, or interferences from the many absorbing or fluorescing compounds found in biological samples that interfere with other spectroscopic techniques. Both potentiometric, that is, assays based on charge separation across the sample electrode surface, with a slow recovery and response time, and amperometric, that is, assays based on redox reactions at the electrode surface, resulting in fast response times, assay approaches can be used to monitor immunoassays to provide both rapid and specific analyte analysis (217). Although these methods adapt to flow-through procedures, sensor fouling remains a common problem and represents a serious limita-

TSH concentration. The ordinate is expressed as the log of specific antibody-bound light emission. (B, C) Similar assays for total thyroxine and serum-free thyroxine using an acridinium-labeled thyroxine antibody incubated with a solid-phase-conjugated thyroxine moiety, and the unknown sample or standard. After centrifugation to separate the solid-phase immune complexes, chemiluminescence is measured with the concentration of thyroxine in the sample or standard being inversely proportional to the emission of light intensity (195). Free T₄ assays are technically difficult, but can be simplified, as in this case, by the introduction of labeled hormone analogs that bind to the antibody but not to serum proteins. [From I. Weeks, M. L. Sturgess, and J. S. Woodhead, Chemiluminescence immunoassay: An overview. *Clin. Sci.* **70**, 403–408 (1986).]

tion to these techniques. Potentiometric immunoassays (PIAs) have proven themselves over the years, but amperometric devices appear to be more promising. Amperometric electrodes have a better long-term stability, show little if any interference, and can produce linear responses in an analyte's physiologic range. For example, electrochemical detection can be linked to an enzyme label, that is, an enzyme that is available in very pure form and is inexpensive. The product of the enzyme reaction should be nontoxic and easily detected at low levels (218). One example is alkaline phosphatase, used to catalyze the conversion of an electroinactive substance (phenylphosphate) to phenol (Figure 30). Phenol is separated by chromatography (usually HPLC) and is detected by oxidation in a thin-layer electrochemical cell with a carbon paste working electrode (218). This gives an extremely sensitive method of quantitating alkaline phosphatase activity, and thus an application for EIA or ELISA techniques using this or other enzymes. These assays can be formatted as either competitive or sandwich types, and can attain sensitivities using amperometric detections equal to those of other immunoassay techniques (e.g., low pg/ml range on a 20- μ l sample volume). Automation of these approaches is currently under investigation.

Other biosensors based on optical (light scattering) or piezoelectric or mass to frequency transducers (mechanical vibrations translated to electrical signals) have been recently developed (12,219,220). Capacitative affinity sensors can measure changes in dielectric properties in response to the presence of a particular analyte encompassed on a silicon chip (12). Pocket-sized blood glucose biosensors utilize a ferrocene-mediated response to glucose oxidase. Field effect transistors have been produced that work by loading or unloading charges to an insulating gate in the transistor. This change in charge alters the net current of the transistor and can ultimately reflect the level of an analyte or chemical in solution. Light-addressable potentiometric sensors (12,220) use an alternating photocurrent through an electrolyte-insulator semiconductor interface to provide a means of measuring small potential changes. A closed circuit is made with a variable

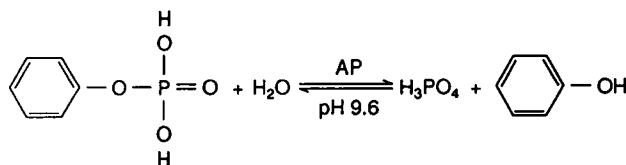


FIGURE 30. Conversion of phenylphosphate (electroinactive) to phenol (electroactive) for immunoassays with electrochemical detection. [From W. R. Heineman, H. B. Halsall, K. R. Wehmeyer, M. J. Doyle, and D. S. Wright, Immunoassay with electrical detection. *In* "Methods of Biochemical Detection" (D. Glick, ed.), Vol. 32, p. 349. John Wiley & Sons, New York, 1987.]

voltage source, an electrode, an ammeter, and a biosensor consisting of a silicon wafer covered with an insulating layer that is stable in the presence of biological solutions. Specific enzymes on the biosensor's surface can produce detectable shifts in the surface potential in the presence of specific molecules of interest (12). Solid-state or dipstick assays are also currently being designed and improved, as shown by the semiquantitative colorimetric products currently available for monitoring urinary LH and hCG (12,220,221).

Nephelometry, or the measurement of scattered light, provides a convenient means of quantifying immunoprecipitation reactions. Light scattering occurs as a result of elastic collisions of particles of all sizes with light quanta. The amount and nature of the scatter depend on the size and shape of the particles, the wavelength of light, and the refractive index of the medium (222). The time course of the nephelometry signal is depicted in Figure 31. Reaction conditions can be selected to cause a maximum of the steepest portion of the curve, that is, the rate curve, to occur within seconds of the injection of the triggering reagent. The use of the rate of change of light scattering is called "rate nephelometry" (223). Rate nephelometry has proven itself to be precise and accurate, measuring proteins such as immunoglobulin, complements C3 and C4, and prealbumin, albumin, and microalbumin (223). Nephelometric measurements of small nonantigenic hormones (or haptens) requires a variant approach called nephelometric inhibition (223,224). Though drugs are the most commonly measured hap-

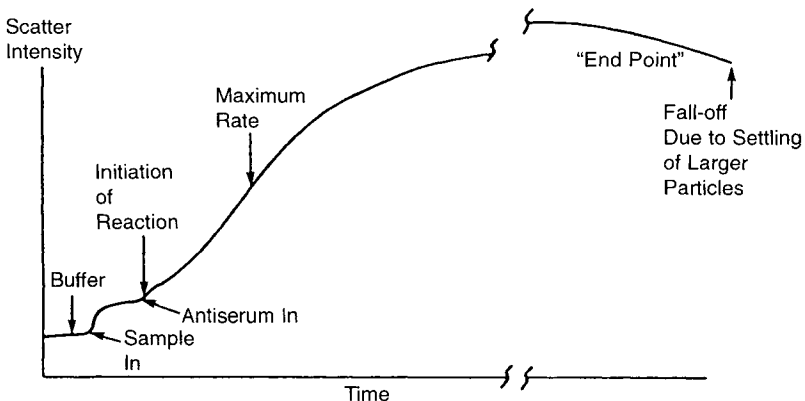


FIGURE 31. Time course of an immunoprecipitation reaction showing variation of intensity of scattered light versus time. [From J. C. Sternberg, Rate nephelometry. In "Manual of Clinical Laboratory Immunology" (N. R. Rose, H. Freidman, and J. L. Fahey, eds.), 3rd Ed., p. 34. American Society of Microbiology, Washington, D.C., 1986.]

tens using nephelometric inhibition, investigators are pursuing the measurement of hormones by this technique (223).

Particle-enhanced immunoassays, employing erythrocytes, clay, or polymer latex as an inert solid support reagent to increase sensitivities, are based on the measurement of the agglutination of an antigen and its corresponding antibody as a function of the concentration of one of these components (225). As the immune complex of the antigens and antibodies grows in size, its light-scattering properties change. This change is monitored by visual, spectrophotometric, or nephelometric approaches. Singer and Plotz (226) were the first to describe this approach in detail, in following rheumatoid factor in patients. Currently, commercially available kits and automated instrumentation systems are available, but are usually only qualitative or semiquantitative, for example, the β -hCG assay.

Analogous to these are the particle-counting immunoassays (227,228) that have been used to measure pregnancy-specific β_1 -glycoprotein, thyroid-stimulating hormone, thyroglobulin, thyroid-binding globulin, placental lactogen, somatotropin, thyroxine, tri-iodothyronine, and others (227–229). Briefly, antigens are quantitated by mixing a biological sample with antibody-coated latex particles (0.8 μm diameter) suspended in a suitable buffer. Antigen in the sample agglutinates some of the latex particles, so that the number of remaining, dispersed particles decreases. Sample antigen concentration is thus inversely proportional to the unagglutinated particle content (Figure 32) (227).

APPENDIX 1: SELECTED HORMONE MARKER ASSAYS USEFUL TO THE TOXICOLOGIST

Lipid-Soluble Hormones (Steroids/Vitamin D/ Thyroid Hormones)

Most steroid hormones and the steroid pro-hormones are measured using radioimmunoassay techniques. However, fluorescent and chemiluminescent assays have been developed for specific steroids and are currently being introduced into the market. The most frequently measured steroid hormones and their assay approaches are discussed in the following.

Cortisol

Classic RIA procedures are routinely used, incorporating an initial sample heat-methanol thermodestruction step to eliminate transcortin interference. ^{125}I -labeled cortisol and polypropylene-immobilized antibody simplify the separation of bound from free, versus the classic dextran-coated char-

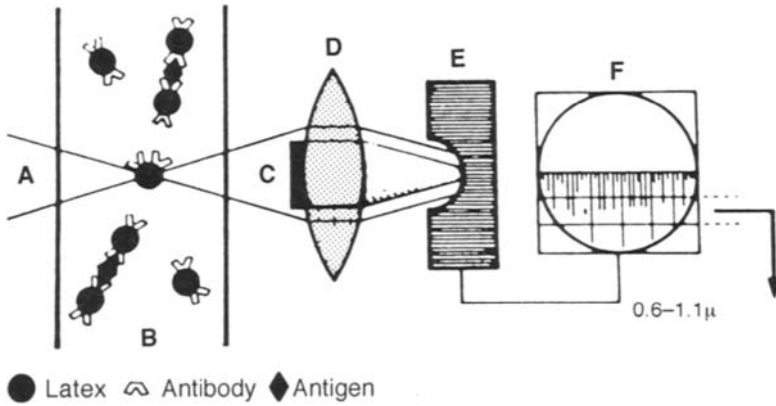


FIGURE 32. Quantitation of antigens using particle counting. A collimated beam of white light focused to a diameter of $7.5 \mu\text{m}$ passes through a flow cell (B) and impinges on a black spot (C). When a particle passes through this beam, light is diffracted past the black spot, collected by the lens (D), and focused onto the photomultiplier (E). The impulse from E, shown on the oscilloscope (F), is proportional to the size of the particle. Only agglutinated particles are electronically counted, thus separating bound from free. No physical separation is necessary, making this particular format a homogeneous assay system. (From P. L. Masson and H. W. Holy, *Immunoassay by particle counting*. In "Manual of Clinical Laboratory Technology" (N. R. Rose, H. Freidman, and J. L. Fahey, eds.), 3rd Ed., p. 44. American Society of Microbiology, Washington, D.C., 1986.]

coal approach. The best RIAs incorporate extraction and chromatographic steps, but the latter have often been eliminated owing to the availability of high-quality specific antisera. Cortisol can also be measured using a fluorometric enzyme immunoassay format based on competitive immunoassay methodology. Alkaline phosphate-conjugated cortisol is mixed with sample and ANS on a fiber glass filter. Anti-cortisol antibodies are immobilized in the filter. Filter washing removes unbound cortisol. Alkaline phosphate substrate is subsequently added during the wash steps and surface fluorescence is measured from the ensuing reaction with ANS. Cortisol assay sensitivities range from 0.2 to $1.0 \mu\text{g/dl}$; fluorescence assays can be as low as $0.1 \mu\text{g/dl}$. Cortisol methodology has recently been included in the chemiluminescent assay class. These provide excellent specificity, sensitivity (on the order of 1.0 – $1.5 \mu\text{g/dl}$), and accuracy, with less than 1 day turn-around times.

Dehydroepiandrosterone (DHA) and Dehydroepiandrosterone Sulfate (DHAS)

The best assays are RIAs, employing extraction and chromatography. Assay sensitivity is 5 – 20 ng/dl for DHA and 2 – $5 \mu\text{g/dl}$ for DHAS. New reagents

employing chemiluminescent immunoassay technology are available from Diagnostic Products Corporation.

Dihydrotestosterone (DHT)

Extraction and chromatography are used in the best RIAs since most antisera do not distinguish DHT from testosterone. Sensitivity is 2–4 ng/dl.

Estradiol

Standard RIA techniques and antibody-coated tube RIA procedures are available. Magnetic solid-phase RIAs employing magnetic particle second antibodies are also used with good results. Estradiol assay limitations are usually related to assay sensitivities since estradiol circulates and is biologically active in very low serum concentrations. Thus multiple ^3H - or ^{125}I -labeled tracers are employed. Recrystallization of estradiol standards is also encouraged, with the use of very specific estradiol antisera. Extraction and chromatography steps help provide the best results. The best assay sensitivities using “routine” procedures are between 5–20 pg/ml. However, ultrasensitive assays can achieve sensitivities in the fg/ml range. Estradiol radioreceptor assay kits are available (Diagnostic Systems Laboratories, Inc. Webster, TX) that can discriminate estrogen receptor capacity between 3 and 1000 fmol/mg protein. Several companies (Nichols and Diagnostic Products Corporation) have estradiol assays available on random access chemiluminescent immunoassay systems, with assay sensitivities in the 10–15 pg/ml range.

Progesterone

Standard ^3H - and ^{125}I -labeled progesterone RIAs using extraction and chromatography are the most common assay formats being used, although most kit formatted assays are direct measurement assays. Antibodies used have been linked to the walls of polypropylene assay tubes, simplifying the separation of bound from free fraction. Magnetic polymer particles have also been used with antibodies, again to simplify the bound from free separation step. The urinary metabolite pregnanediol-3-glucuronide (PDG) can be directly assayed by RIA and ELISAs. Several ELISA formats have been modified to a semiquantitative “matrix pad” assembly so that the best can be run in a “nonlaboratory” environment. Progesterone is also available on random access chemiluminescent immunoassay systems. Good assays report sensitivities in the 0.1–0.5 ng/ml range.

Testosterone

New ^{125}I -labeled testosterone RIAs are now available, along with multilabeled ^3H assays, combined with antibodies coated to the walls of assay tubes. Serum-free testosterone assays incorporate unique tracer molecules (testosterone analogs) that are designed not to bind to steroid hormone transport proteins, and antisera with affinities slightly less than that of SHBG. Good assay sensitivities are in the 3–10 ng/dl range.

Vitamin D, its derivatives and metabolites, and the substituted tyrosine or adenosine molecules (thyroxine, tri-iodothyronine, reverse T_3 , and the cyclic nucleotides) are included in the lipid-soluble category. Like the steroids, these hormones are also principally measured by RIAs, and are elucidated in the following.

25-Hydroxy Vitamin D

^3H -labeled vitamin D RIAs using charcoal separation of bound from free are most common, usually including a sample extraction step. Sensitivity is 5 ng/ml.

1,25-Dihydroxy Vitamin D

Sample extraction as, with 25-OH vitamin D, is common and can include acetonitrile with an 18-OH column chromatography step. RIAs and radioreceptor assays are available. Sensitivities should approach 10 pg/ml.

Triiodothyronine (T_3) and Thyroxine (T_4)

Standard T_3 and T_4 RIAs are common, some incorporating magnetic particles bound to antibodies, others with antibodies bound to plastic assay tubes or beads. T_3 and T_4 linked magnetic particle/ T_3 or T_4 monoclonal acridinium ester antibody assays are also available for chemiluminescent end point assays (Diagnostic Products Corporation). Pretreatment of samples often includes 8-anilino-naphthalenesulfonic acid and NaOH to release T_3/T_4 from serum protein binders. Fluorometric enzyme immunoassays have been developed using sequential saturation methods, that is, alkaline phosphate-labeled T_3 or T_4 is added to reaction discs after the sample. The disc contains incorporated specific T_3/T_4 antibodies. Unbound T_3/T_4 is washed free. Enzyme and substrate, 4-methyl umbelliferyl phosphate, generate surface fluorescence. Sensitivities of the best assays are 10–15 ng/dl for T_3 and 0.5–1.0 $\mu\text{g}/\text{dl}$ for T_4 .

Free T₄

Direct equilibrium dialysis methods (followed by a sensitive T₄ RIA) provide the most accurate estimates of free T₄. There are ⁵⁷Co-labeled T₄-derivative IRMA assays designed so that these unique labels do not disrupt and preexisting equilibrium between serum bound and free T₄. Direct competitive assays are also available that utilize very high specific activity ¹²⁵I-T₄ tracers combined with monoclonal T₄ antibodies bound to magnetizable particles for simple bound-from-free separation. Fluorometric enzyme immunoassays and chemiluminescent assays are also available. Sensitivities in the 0.05–0.2 ng/dl range are not uncommon.

T₄ and T₃ Resin Uptake

T₃ antisera-coated plastic tubes and spheres can be incubated with ¹²³I-T₃ and finally competed with thyroid binding globulin (TBG) in patient's samples, giving a simple one-step immunoassay of T₃ uptake. Similar approaches use the partition of ¹²⁵I-T₃ between TBG and a suspension of macroaggregated albumin. The ¹²³I-T₃ absorbed macroaggregated albumin relationship can be shifted by serum proteins like TBG. T₄-conjugated solid-phase magnetic particles and acridinium ester-labeled monoclonal antibodies generated against TBG have been combined in chemiluminescent and magnetic-chemiluminescent assay formats. Fluorometric enzyme immunoassays are also available in which a fixed amount of T₄ is added to the sample to be tested. After incubation the serum protein unbound T₄ fraction is captured on glass filter discs containing immobilized T₄ antibodies. An alkaline phosphate-labeled T₄ conjugate is added to the disc and binds to any unoccupied T₄ antibodies. Unbound T₄ is washed away. Surface fluorescence is measured by alkaline phosphatase action on 4-methyl-umbelliferyl phosphate in the wash solution.

Water-Soluble Hormones

The research and application of nonradiometric endocrine assays have concentrated on the protein and polypeptide hormones. Although most protein hormones have and are currently measured by standard RIA and IRMA techniques, ELISA, fluorometric, and chemiluminescent assay formats have been developed for many of these hormones and are discussed in the following sections.

ACTH

Double antibody ¹²⁵I RIAs and IRMAs are currently the most popular. Specific monoclonal antibodies for ACTH 1-39 give sensitivities in the range of 1.0 pg/ml.

Calcitonin

Calcitonin is routinely measured by RIA with ^{125}I tracer and the double antibody approach. Separation of bound and free fractions can be accomplished with a polyethylene glycol-assisted second antibody step. Assay sensitivities should be in the 2–10 pg/ml range. Calcitonin assays are notorious for producing nonlinear results, thus it is advised that patient or research samples be assayed “neat” and diluted to ensure parallelism.

Follicle-Stimulating Hormone

FSH is measured by a wide spectrum of assay approaches. Classic double antibody, ^{125}I -labeled RIA formats are common. Modifications employing monoclonal and polyclonal antibodies are in use. IRMAs are also available in which ^{125}I -labeled primary antibody is used in concert with an immobilized second (often monoclonal) anti-FSH antibody. The second antibody can be solid-phase-linked to polystyrene beads or tubes. Magnetic separation assays are available in which the magnetic particles are bound to the second antibody. Fluorometric enzyme immunoassays are available using a two-site sandwich immunoassay format. Chemiluminometric assays are also being introduced into the market, having a succinimide derivative of acridinium conjugated to anti-beta human subunit second antibody. Good assay sensitivities are between 0.1 and 0.8 mIU/ml. Fluorescence and chemiluminometric assays can provide sensitivities in the 0.01–0.05 mIU/ml range.

Growth Hormone (Somatotropin)

Routine double antibody, ^{125}I RIAs are most common. IRMA approaches are available using ^{125}I -labeled primary antibodies. Specific second antibodies (usually monoclonal) are then added, sometimes on covalently linked polystyrene beads or on the surface of polystyrene assay tubes. Sensitivities can approach the 0.05–0.2 ng/ml range.

Human Chorionic Gonadotropin(hCG, and Subunits)

hCG was originally measured by standard double antibody, ^{125}I -labeled hormone RIAs. Currently, this approach has been modified to an IRMA format with polyclonal first antibody labeled with ^{125}I and a solid-phase capture second antibody (monoclonal). These offer ease of performance, greater sensitivity, and convenience in terms of separation of bound from free fractions. Another modification of this basic theme is the use of three monoclonal antibodies, each specific for a different epitope on the hCG molecule. One is ^{125}I -labeled for detection, the others are biotinylated and

serve as capture antibodies. One is beta subunit specific, whereas the other is specific for intact hCG. Avidin-coated beads are subsequently added to this reaction mixture to provide ease of separation of bound from free in segregating the hCG sandwich complex. Similar IRMA formats are available that do not include avidin–biotin complexing. Two-site chemiluminometric (sandwich) magnetic immunoassays are also available. Monoclonal antibodies specific for the beta chain are labeled with acridinium ester. A second polyclonal antibody directed against the beta chain is coupled to magnetic particles for ease of bound from free separation. Specific alpha and beta subunit assays are double antibody, ^{125}I -labeled RIAs, and can be classic RIA formats or IRMAs. All of these assays are very specific, with assay sensitivities ranging from 0.5 to 2.0 mIU/ml. hCG can be measured semiquantitatively by ELISAs, the reagents incorporated into dipstick formats for “at home” pregnancy determination.

Insulin

Double antibody, ^{125}I -labeled insulin RIAs are most commonly used. Procedures can be simplified by conjugating specific insulin antibodies to polystyrene beads or tubes. Assay sensitivities are between 0.5 and 5 $\mu\text{IU/ml}$. Precautions pertaining to cross-reactivity of insulin in proinsulin RIAs should be taken. C-peptide assays are usually double antibody RIAs using ^{125}I -labeled C-peptide. PEG is often added in the separation of bound from free. Sensitivities are in the 0.05–0.1 ng/ml range.

Luteinizing Hormone

Assay formats for LH are essentially identical to those for FSH. Several companies have produced very good RIAs and IRMAs. ELISAs have been developed providing semiquantitative LH estimation for the prediction of ovulation. These assays range in complexity from the user having several steps to perform to a simple urine dipstick requiring one reagent addition step. Good LH assays can detect between 0.1 and 2.0 mIU/ml. As with the best FSH assays, (fluorescence and chemiluminometric), 0.01–0.02 mIU/ml levels are obtained.

Osteocalcin (Bone γ -Glutamic Acid Protein)

Classic double antibody, ^{125}I -labeled osteocalcin RIAs are most common. Sensitivities of 0.2–0.5 ng/ml are reported.

Prolactin

^{125}I -labeled prolactin RIAs are available that use standard double antibody approaches. Solid-phase IRMA assays are also available that employ polystyrene bead or tube-linked second antibodies, providing a noncentrifugational step for separating bound from free. Avidin–biotin enhancement is often used in these IRMA approaches. Chemiluminescence assays are also being offered by the better laboratories. RIA and IRMA assay sensitivities should be in the 0.5–2.0 ng/ml range. More sensitive assay techniques are reporting 0.1–0.2 ng/ml.

Parathyroid Hormone (N-terminal, Measuring Intact and N-terminal Fragments; C-terminal or Midmolecule Specific, Measuring Midregion Fragments and C-terminal Fragments; and Intact Assays, Measuring Only the Intact Molecule)

Standard double antibody RIAs and IRMAs using ^{125}I tracers are available. Some employ avidin–biotin enhancement (e.g., avidin-coated polystyrene beads). Protease inhibitors are often required for initial sample treatment in these assays. Sensitivities are: N terminus 5.0 pg/ml; midmolecule or C terminus, 40 pg/ml; and intact, 2–3 pg/ml.

Sex Hormone Binding Globulin (SHBG, Testosterone/Estradiol Binding Globulin)

Double antibody ^{125}I -labeled SHBG RIAs and enhanced or amplified IRMAs using ^{125}I -labeled antibodies are available with sensitivities in the 0.05–1.0 nmol/liter range. Competitive binding assays give sensitivities of around 100 $\mu\text{g}/\text{dl}$.

IgF-1 (Somatomedin C)

Standard double antibody ^{125}I -labeled IgF-1 RIAs are the most common. Somatomedin C binding proteins can interfere with these assays, resulting in cumbersome separation steps, including acid-ethanol extraction, acid-gel chromatography, or octodeca-salicylic acid (Sep-Pak) columns. Sensitivities can reach 0.05–1.0 ng/ml in extracted/chromatographed samples.

Thyroglobulin

Assay sensitivities of 1.0–2.0 ng/ml are achieved with standard ^{125}I -labeled thyroglobulin double antibody RIAs. These assays use sheep or goat anti-rabbit second antibodies for separation of bound from free.

Thyroid-Stimulating Hormone

Probably one of the first and most used endocrine tests, TSH assays cover the continuum from isotopic to nonisotopic. Standard double antibody ^{125}I -labeled TSH assays were common some years ago and are available today. Currently, IRMA procedures are more widespread, some using three monoclonal TSH antibodies each with specificity for different epitopic sites on the TSH molecule. One is ^{125}I -labeled, and the others are coupled to biotin-avidin-coated plastic beads allowing specific and quantitative binding and simplicity in the separation of bound from free fractions. Partition fluorometric dissociation-enhanced lanthanide fluoroimmunoassays incorporating europium labels and solid-phase separation of bound from free on microtiter plates are also available. Another assay is the two-site immunoluminescence for TSH that employs acridinium esters as the chemiluminescence label, two mouse monoclonal TSH antibodies, and a final magnetic separation of bound from free step. A chemiluminometric assay designed for pediatric samples is also available. First- and second-generation assay sensitivities were in the 1.0 mIU/ml range, however, sensitivities around 0.01 mIU/ml are now possible with the third-generation chemiluminescence system.

CONCLUSION/ADDENDUM

Assays available to the toxicologist or endocrine toxicologist provide state-of-the-art schemes for the measurement of hormones and endocrine-related molecules for research and clinical uses. They have evolved from very simple bench manipulations to assays encompassing complex and sophisticated automated technology. Many important endocrine tests describing sophisticated end points have not been described here. These include the evaluation of gamete structure and function (in particular that of spermatogenesis), biological assays of sperm function (swim-up, hamster oocyte penetration, and others), and gross, histological, and cytological changes in tissues and cells. Assays that evaluate the end points of stress (in its many forms) can use the hormones of the hypothalamic-pituitary-adrenal axis and other molecules like cytokines (especially IL-1 and IL-6), and tests to evaluate carbohydrate metabolism using blood glucose levels or insulin and/or glucagon assays. Frequent improvements in these assays have stimulated and propagated newer and even more elegant improvements, usually related to the speed of analysis, precision, and sensitivity of the assay. The result of this effort sometimes appears to be the commercial production of newer kits and/or “perfect” instrumentation systems that are fast, precise,

inexpensive, fully automated, versatile, and foolproof (230). Simplification and miniaturization of these assays will be a great advantage to some of these efforts, along with user-safe and sink-disposable reagents. The linchpin for success of every assay is inherent in its validation, which is perhaps the essential part of any new immunoassay's development. Greatly improved sensitivities, possibly exceeding clinical or research need, will be obtained, but hopefully not at the cost of diminishing assay specificities. Many more advances in the assays will appear by the turn of the century. Only time will tell whether the new methodologies will encompass true improvements over current schemes. As long as the founding principles of immuno- or other assays remain central components of the formula, endocrine investigations and discoveries can only advance.

ACKNOWLEDGMENTS

The authors would like to acknowledge the skillful talent of Ms. Kathryn Derrickson for her preparation of several of the illustrations and figures used in this manuscript.

REFERENCES

1. J. D. N. Nabarro, Radioimmunoassay and saturation analysis. *Br. Med. Bull.* **30**, 1-2 (1974).
2. R. P. Ekins, The estimation of thyroxine in human plasma by an electrophoretic technique. *Clin. Chim. Acta* **5**, 453-459 (1960).
3. R. S. Yalow and S. A. Berson, Assay of plasma insulin in human subjects by immunological methods. *Nature (London)* **184**, 1648-1649 (1959).
4. R. S. Yalow, Remembrance project: Origins of RIA. *Endocrinology (Baltimore)* **129**, 1694-1695 (1991).
5. R. P. Ekins, Basic principles and theory. Radioimmunoassay and saturation analysis. *Br. Med Bull* **30**, 3-11 (1974).
6. F. C. Greenwood, W. M. Hunter, and J. S. Glover, The preparation of ¹³¹I-labelled human growth hormone of high specific radioactivity. *Biochem. J.* **89**, 114-123 (1963).
7. B. E. P. Murphy, Some studies of the protein-binding of steroids and their applications to routine micro and ultramicro measurement of various steroids in body fluids by competitive-protein binding. *J. Clin. Endocrinol. Metab.* **27**, 973-990 (1967).
8. R. J. Lefkowitz, J. Roth, and I. Pastan, Radioreceptor assay of adrenocorticotrophic hormone: New approaches to assay of polypeptide hormones in plasma. *Science* **170**, 633-635 (1970).
9. S. G. Korenman, Radio-ligand binding assay of specific estrogens using a soluble uterine macromolecule. *J. Clin. Endocrinol. Metab.* **28**, 127-130 (1968).
10. B. L. Brown, R. P. Ekins, and W. Tampion, The assay of adenosine 3'-5'-cyclic monophosphate by saturation analysis. *Biochem. J.* **120**, 8 (1970).
11. J. J. Gold, Endocrine laboratory procedures and available tests. In "Gynecologic Endocrinology" (J. J. Gold, ed.), 2nd Ed., pp. 647-667. Harper & Row, Hagerstown, Maryland, 1975.

12. B. D. Albertson, Hormone assay methodology: Present and future prospects. *In* "Clinical Obstetrics and Gynecology, Reproductive Endocrinology Update" (E. Y. Adashi, ed.), Vol. 33, No., 3, pp. 591–610. 1990.
13. M. L. Dufau, C. R. Mendelson, and K. J. Catt, A highly sensitive *in vitro* bioassay for LH and CGs: Testosterone production by dispersed Leydig cells. *J. Clin. Endocrinol. Metab.* **39**, 610–616 (1974).
14. P. Gordon and B. D. Weintraub, Radioreceptor and other functional hormone assays. *In* "William's Textbook of Endocrinology" (J. D. Wilson and D. W. Foster, eds.), 7th Ed., pp. 133–146. Saunders, Philadelphia, Pennsylvania, 1985.
15. C. Chubb, personal communication (1993).
16. M. A. Sayers, G. Sayers, and L. A. Woodbury, The assay of adrenocorticotrophic hormone by the adrenal ascorbic acid-depletion method. *Endocrinology (Baltimore)* **42**, 379–393 (1948).
17. P. Manasco, M. E. Girton, R. L. Diggs, J. L. Doppman, P. P. Feuillan, G. B. Cutler, Jr., D. L. Loriaux, and B. D. Albertson, A novel testis-stimulating factor in familial male precocious puberty. *N. Engl. J. Med.* **324**, 227–231 (1991).
18. G. P. Chrousos, Radioreceptor assay of steroids and assay of receptors. *In* "Hormonal Assay Techniques," 15th Training Course Syllabus p. 214. The Endocrine Society, Bethesda, Maryland 1989.
19. R. J. Lefkowitz, J. Roth, and I. Pastan, Radioreceptor assay of ACTH: A new approach to assay polypeptide hormones in plasma. *Science* **170**, 633–635 (1970).
20. R. J. Lefkowitz, J. Roth, and I. Pastan, Effects of Ca^{++} on ACTH stimulation of the adrenals: Separation of hormone binding from adenyl cyclase activation. *Nature (London)* **228**, 864–866 (1970).
21. S. I. Taylor, Principles of radioimmunoassay. *In* "Hormone Assay Techniques," 15th Training Course Syllabus, pp. 31–49. The Endocrine Society, Baltimore, Maryland, 1989.
22. M. L. Dufau, Radioassays and bioassays of gonadotropins. *In* "Hormone Assay Techniques," 15th Training Course Syllabus, pp. 130–146. The Endocrine Society, Baltimore, Maryland, 1989.
23. K. J. Catt, Radioassays of angiotensins I and II. *In* "Hormone Assay Techniques," 15th Training Course Syllabus, pp. 146–169. The Endocrine Society, Baltimore, Maryland, 1989.
24. J. L. Vaitukaitis, Hormone assays. *In* "Endocrinology and Metabolism" (P. Felig, J. D. Baxter, A. E. Braodus, and L. A. Frohman, eds.), p. 164. McGraw-Hill, New York, 1987.
25. H. R. Behrman, A History of hormone assays. *In* "Nonradiometric Assays: Technology and Application in Polypeptide and Steroid Hormone Detection" (B. D. Albertson and F. P. Haseltine, eds.), pp. 1–14. Wiley, New York, 1988.
26. B. D. Albertson and F. P. Haseltine, "Non-radiometric Assays: Technology and Application in Polypeptide and Steroid Hormone Detection." Wiley, New York, 1988.
27. T. Chard, An introduction to radioimmunoassay and related techniques. *In* "Laboratory Techniques in Biochemistry and Molecular Biology" (T. S. Work and E. Work, eds.). Elsevier, Amsterdam, New York, and Oxford, 1982.
28. F. S. Ashkar, "Radiobioassays," Vol. 1. CRC Press, Boca Raton, Florida, 1985.
29. W. T. Newton and R. M. Donati, "Radioassay in Clinical Medicine." Thomas, Springfield, Illinois, 1974.
30. Radioimmunoassay and related procedures in medicine—1977. Proceedings of a Symposium (Berlin, 1977). Volume 1, International Atomic Energy Agency, Vienna, 1978.
31. B. M. Jaffe and H. R. Behrman, "Methods of Hormone Radioimmunoassay," 2nd Ed., Academic Press, New York, 1979.

32. B. D. Weintraub (director), "Hormone Assay Techniques," 15th Training Course Syllabus. The Endocrine Society, Bethesda, Maryland, 1989.
33. R. S. Yalow, Radioimmunoassay of hormones. In "Textbook of Endocrinology" (J. D. Wilson and D. W. Foster, eds.), 7th Ed., pp. 123–132. Saunders, Philadelphia, Pennsylvania 1985.
34. R. D. Guttman (ed.), "Immunology : A Scope Publication," p. 9. Upjohn, Kalamazoo, Michigan, 1981.
35. D. R. Davies, E. A. Padlan, and D. M. Segal, Three dimensional structure of immunoglobulins. *Annu. Rev. Biochem.* **44**, 639–667 (1975).
36. R. J. Poljak, L. M. Amzel, B. L. Chen, Y. Y. Chiu, P. P. Phizackerly, F. Saul, and X. Yserm, Three dimensional structure and diversity of immunoglobulins. *Cold Spring Harbor Symp. Quant. Biol.* **41** (Part 2), 639–645 (1977).
37. D. L. Loriaux, Steroid radioimmunoassay. In "Hormone Assay Techniques." 15th Training Course Syllabus, pp. 237–240. The Endocrine Society, Baltimore, Maryland, 1989.
38. J. Freund, Some aspects of active immunization. *Annu. Rev. Microbiol.* **1**, 291–308 (1947).
39. J. Freund, The effect of paraffin oil and mycobacteria on antibody formation and sensitization. *Am. J. Clin. Pathol.* **21**, 645–656 (1951).
40. J. L. Vaitukaitis, J. B. Robbins, E. Nieschlag, and G. T. Ross, A method for producing specific antisera with small doses of immunogen. *J. Clin. Endocrinol. Metab.* **33**, 988–991 (1971).
41. H. N. Eisen and G. W. Siskind, Variation in affinities of antibodies during the immune response. *Biochemistry* **3**, 996–1008 (1964).
42. B. Alberts, D. Bray, J. Lewis, M. Raff, K. Roberts, and J. D. Watson (eds.), "The Molecular Biology of the Cell," 2nd Ed. Garland, New York and London, 1989.
43. S. I. Taylor, Monoclonal antibodies. In "Hormone Assay Techniques," 15th Training Course Syllabus, pp. 165–170. The Endocrine Society, Baltimore, Maryland, 1989.
44. H. Raff and J. W. Findling, A new immunoradiometric assay for corticotropin evaluated in normal subjects and patients with Cushing's syndrome. *Clin. Chem.* **35**, 596–600 (1989).
45. S. W. Rosen, Iodination and other labelling techniques. In "Hormone Assay Techniques," 15th Training Course Syllabus, pp. 84–107. The Endocrine Society, Baltimore, Maryland, 1989.
46. J. J. Thorell and B. G. Johansson, Enzymatic iodination of polypeptides with ¹²⁵I to high specific activity. *Biochim. Biophys. Acta* **251**, 363–369 (1971).
47. A. S. McFarlane, Efficient trace labelling of proteins with iodine. *Nature (London)* **182**, 53 (1958).
48. W. R. Butt, The iodination of follicle stimulating and other hormones for radioimmunoassay. *J. Endocrinol.* **55**, 453–454 (1972).
49. T. Shjian and H. Arman, Jr., Immunoassay of thyrocalcitonin. I. The method and its serological specificity. *Endocrinology (Baltimore)* **84**, 140–141 (1969).
50. D. S. Skelly, L. P. Brown, and P. K. Besch, Radioimmunoassay. *Clin. Chem.* **19**, 146–186 (1973).
51. P. Franchimont, Dosage radio-immunologique des hormones luteinisantes chorionique et hypophysaire. *Ann Endocrinol.* **27**, 273–280 (1966).
52. A. R. Midgley, Jr., G. D. Niswender, V. L. Gay, and L. E. Reichart, Jr., Use of antibodies for characterization of gonadotropins and steroids. *Recent Prog. Horm. Res.* **27**, 235–302 (1971).
53. S. A. Berson, R. S. Yalow, A. Bauman, M. A. Rothschild, and K. Newerly, Insulin ¹³¹I metabolism in human subjects: Demonstration of insulin binding globulin in the circulation of insulin treated subjects. *J. Clin. Invest.* **35**, 170–190 (1956).

54. A. R. Midgley, Jr., Radioimmunoassay for human follicle stimulating hormone. *J. Clin. Endocrinol. Metab.* **27**, 295–299 (1967).
55. W. D. Odell, A. C. Charters, W. D. Davidson, and J. C. Thompson, Radioimmunoassay for human gastrin as an antigen. *J. Clin. Endocrinol. Metab.* **78**, 1840–1842 (1968).
56. S. M. Glick and A. Kagan, Combined immunoassay of insulin and human growth hormone. *J. Clin. Endocrinol. Metab.* **27**, 133–136 (1967).
57. J. J. Marchalonis, An enzymatic method for the trace iodination of immunoglobulins and other proteins. *Biochem. J.* **113**, 299–305 (1969).
58. Y. Miyachi, J. L. Vaitukaitis, E. Nieschlag, and M. B. Lipsett, Enzymatic iodination of gonadotropins. *J. Clin. Endocrinol. Metab.* **34**, 23–28 (1972).
59. A. E. Bolton and W. M. Hunter, The labelling of protein to high specific activity radioactivity by conjugation to a ¹²⁵I-containing acylating agent. *Biochem. J.* **133**, 529–539 (1973).
60. P. J. Fraker and J. C. Speck, Jr., Protein and cell membrane iodination with a sparingly soluble chloroamide 1,3,4,6-tetrachloro-3 α ,6 α -diphenylglycoluril. *Biochem. Biophys. Res. Commun.* **80**, 849–857 (1978).
61. M. R. Redshaw and S. S. Lynch, An improved method for the preparation of iodinated antigens for radioimmunoassay. *J. Endocrinol.* **60**, 527–528 (1974).
62. U. Rosa, G. A. Scassellati, F. Pennisi, N. Riccioni, P. Gianoni, and R. Giordani, Labelling of human fibroinogen with ¹³¹I by electrolytic iodination. *Biochim. Biophys. Acta* **86**, 519–526 (1964).
63. S. T. Nielsen, P. Q. Barrett, M. W. Neuman, and W. F. Neuman, The electrolytic preparation of bioactive radioiodinated parathyroid hormone of high specific activity. *Anal. Biochem.* **92**, 67–73 (1979).
64. B. D. Weintraub, Separation techniques and validation of radioimmunoassay. In “Hormone Assay Techniques,” 15th Training Course Syllabus, pp. 25–30. The Endocrine Society, Bethesda, Maryland, 1989.
65. R. S. Yalow, Radioimmunoassay methodology: Applications to problems of heterogeneity of peptide hormones. *Pharmacol. Rev.* **25**, 161–178 (1973).
66. W. R. Butt and S. S. Lynch, Some observations on the radioimmunoassay of follicle stimulating hormone. In Proceedings of the International Peptide Symposium on Protein and Polypeptide Hormones” (M. Margoules, ed.), p. 134. Ed Excerpta Medica, Amsterdam, 1969.
67. L. Wide and J. Porath, Radioimmunoassay of proteins with the use of Sephadex-coupled antibodies. *Biochim. Biophys. Acta* **130**, 257–260 (1966).
68. P. H. Moore, Jr., and L. R. Axelrod, A solid phase radioimmunoassay for estrogen by estradiol-17 β antibody covalently bound to a water insoluble synthetic polymer (Enzacrilyl AA). *Steroids* **20**, 199–212 (1972).
69. D. Rodbard, Mathematics of hormone receptor interaction. I. Basic principles. *Adv. Exp. Med. Biol.* **36**, 289–326 (1973).
70. D. Rodbard, Theory of hormone receptor interaction. 3. The endocrine target cell as a quantal response unit: A general control mechanism. *Adv. Exp. Med. Biol.* **36**, 342–364 (1973).
71. D. Rodbard and R. E. Bertino, Theory of radioimmunoassays and hormone receptor interactions. II. Simulation of antibody divalency, cooperativity, and allosteric effects. *Adv. Exp. Med. Biol.* **36**, 327–341 (1973).
72. D. Rodbard, G. H. Weiss, and L. E. M. Miles, Theory of immunoradiometric (labelled antibody) assays. *Fed. Proc.* **31**, A807 (1972).
73. D. Rodbard, H. J. Ruder, J. Vaitukaitis, and H. S. Jacobs, Mathematical analysis of radioligand assays: Improved sensitivities obtained by delayed addition of labelled ligand. *J. Clin. Endocrinol.* **33**, 343–359 (1971).

74. D. Rodbard and K. J. Catt, Mathematical theory of radioligand assays: Kinetics of separation of bound from free. *J. Steroid Biochem.* **3**, 255–273 (1972).
75. D. Rodbard and J. E. Lewald, Computer analysis of radioligand assay and RIA data. *Acta Endocrinol. (Copenhagen)* **64**(Suppl. 147), 79–103 (1970).
76. D. Rodbard and G. H. Weiss, Mathematical theory of immunoradiometric (labelled antibody) assays. *Anal. Biochem.* **52**, 10–44 (1973).
77. H. Feldman, D. Rodbard, and D. Levine, Mathematical theory of crossreactive radioimmunoassay and ligand binding systems at equilibrium. *Anal. Biochem.* **45**, 530–556 (1972).
78. D. Rodbard, H. Feldman, and D. Levine, Statistical quality control and routine processing for RIAs and IRMAs. *Clin. Chem.* **20**, 1255–1270 (1974).
79. G. Scatchard, The attraction of proteins for small molecules and ions. *Ann. N.Y. Acad. Sci.* **51**, 660–672 (1949).
80. G. Scatchard, J. S. Coleman, and A. L. Shen, Physical chemistry of protein solutions. VII. The binding of some small anions to serum albumin. *J. Am. Chem. Soc.* **79**, 12–20 (1957).
81. A. R. Midgley, Jr., G. D. Niswender, and R. W. Rebar, Principles for the assessment of the reliability of radioimmunoassay methods (precision, accuracy, sensitivity, specificity). *Acta Endocrinol. (Copenhagen)* **63**(Suppl. 142), 163–184 (1969).
82. G. B. Cutler, Jr., General features of steroid receptor assays. In “Hormone Assay Techniques,” 15th Training Course Syllabus, pp. 277–293. The Endocrine Society, Baltimore, Maryland, 1989.
83. G. P. Chrousos, Radioreceptor assay of steroids and assay of receptors. In “Hormone Assay Techniques,” 15th Training Course Syllabus, pp. 241–276. The Endocrine Society, Baltimore, Maryland, 1989.
84. G. S. Challand and T. Chard, Quality control in a radioimmunoassay: Observations on the operation of a semi-automated assay for human placental lactogen. *Clin. Chim. Acta* **46**, 133–138 (1973).
85. D. Rodbard, P. L. Rayford, J. A. Cooper, and G. T. Ross, Statistical quality control of radioimmunoassays. *J. Clin. Endocrinol.* **28**, 1412–1418 (1968).
86. R. M. Dauphinais, Solving and preventing problems in ligand assays. In “Manual of Clinical Laboratory Techniques” (N. R. Rose, H. Freidman, and J. P. Fahey, eds.), 3rd Ed., pp. 88–98. American Society of Microbiology, Washington, D.C., 1986.
87. M. J. O’Sullivan, J. W. Bridges, and V. Marks, Enzyme immunoassay: A review. *Ann. Clin. Biochem.* **16**, 221–240 (1979).
88. A. Voller and B. Bidwell, Enzyme linked immunosorbent assays. In “Manual of Clinical Laboratory Immunology” (N. R. Rose, H. Friedman, and J. L. Fahey, eds.), 3rd Ed., American Society of Microbiology, Washington, D.C., 1986.
89. S. L. Scharpe, W. M. Cooreman, W. J. Blomme, and G. M. Laekeman, Quantitative enzyme immunoassay. *Clin. Chem.* **22**, 733–738 (1976).
90. A. Voller, A. Bartlett, and D. Bidwell, (eds.), “Immunoassays for the 80s.” MTP Press, Lancaster, U.K., 1981.
91. W. R. Butt (ed.), “Practical Immunoassay. The State of the Art.” Decker, New York, 1984.
92. S. B. Pak (ed.), “Immunoassay Technique,” Vol. 2., de Gruyter, Berlin, 1986.
93. D. W. Chan and M. T. Perlstein (eds.), “Immunoassay: A Practical Guide.” Academic Press, New York, 1987.
94. R. Malvanop (ed.), “Immunoenzymatic Assay Techniques.” Martinus Nijhoff, The Hague, 1980.
95. E. T. Maggio, (ed.), “Enzyme-Immunoassay.” CRC Press, Boca Raton, Florida, 1980.
96. E. Ishikawa, T. Kawai, and K. Miyai (eds.), “Enzyme Immunoassay.” Igaku-Shoin, Tokyo, 1981.

97. S. P. Avrameas, P. Dueut, R. Masseyeff, and G. Feldman, "Immunoenzymatic Techniques." Elsevier, Amsterdam, 1983.
98. T. T. Ngo and H. M. Lenhoff (eds.), "Enzyme-Mediated Immunoassay." Plenum, New York, 1985.
99. D. M. Kemeny and S. J. Chalmers (eds.), "ELISA and Other Solid Phase Immunoassays." Wiley, Chichester, U.K., 1988.
100. T. T. Ngo (ed.), "Electrochemical Sensors in Immunological Analysis." Plenum, New York, 1987.
101. W. P. Collins (ed.), "Alternative Immunoassays." Wiley, Chichester, U.K., 1985.
102. W. P. Collins (ed.), "complementary Immunoassays." Wiley, Chichester, U.K. 1988.
103. J. J. Langone and H. Van Vunakis (eds.), "Methods in Enzymology, Immunochemical Techniques. Part E. Monoclonal Antibodies and General Immunoassay Methods," Vol. 92. Academic Press, New York, 1983.
104. P. Tijssen, "Practice and Theory of Enzyme Immunoassays." Elsevier, Amsterdam, 1985.
105. G. B. Wisdom, Recent progress in the development of enzyme immunoassays (Review). *Ligand Rev.* **3**, 44–49 (1981).
106. M. Oellerich, Enzyme-immunoassay; A review. *J. Clin. Chem. Clin. Biochem.* **22**, 895–904 (1984).
107. D. S. Smith, M. H. H. Al-Hakim, and J. Landon, A review of fluoroimmunoassay and immunofluorometric assay. *Ann. Clin. Biochem.* **18**, 253–274 (1981).
108. I. Hammila, Fluoroimmunoassays and immunofluorometric assays (Review). *Clin. Chem.* **31**, 359–370 (1985).
109. E. P. Diamandis, Immunoassays with time resolved fluorescence spectroscopy: Principles and applications (Review). *Clin. Biochem.* **21**, 139–150 (1988).
110. L. J. Kricka and G. H. G. Thorpe, Luminescent immunoassays (Review). *Ligand Rev.* **3**, 17–24 (1981).
111. W. R. Seitz, Immunoassay labels based on chemoluminescence and bioluminescence (Review). *Clin. Biochem.* **17**, 120–125 (1984).
112. I. Weeks and J. S. Woodhead, Chemiluminescence immunoassay (Review). *J. Clin. Immunoassay.* **7**, 82–89 (1984).
113. A. H. W. M. Schuurs and B. K. VanWeemen, Enzyme immunoassay. *Clin. Chem. Acta* **81**, 1–40 (1977).
114. A. Voller, A. Bartlett, and D. E. Bidwell, Enzyme immunoassays with special reference to ELISA techniques. *J. Clin. Pathol.* **31**, 507–520 (1978).
115. M. Oellerich, Enzyme immunoassay in clinical chemistry: Present status and trends. *J. Clin. Chem. Clin. Biochem.* **18**, 197–220 (1980).
116. D. Monroe, Enzyme immunoassay. *Anal. Chem.* **56**, 920A–931A (1984).
117. C. Blake and B. J. Gould, Use of enzymes in immunoassay techniques: A review. *Analyst* **109**, 533–547 (1984).
118. C. P. Price, K. Spencer, and J. Whicher, Light scattering immunoassay of specific hormones: A review. *Ann. Clin. Biochem.* **20**, 1–14 (1983).
119. J. F. Place, R. M. Sutherland, and C. Dahne, Opto-electronic immunosensors: A review of optical immunoassay at continuous surfaces (Review). *Biosensors* **1**, 321–353 (1985).
120. M. J. Green, Electrochemical immunoassays (Review). *Philos. Trans. R. Soc. London Ser. B* **B316**, 135–142 (1987).
121. R. F. Schwall, Jr., and H. J. Tenoso, Alternatives to radioimmunoassay: Labels and methods (Review). *Clin. Chem.* **27**, 1157–1164 (1981).
122. I. Weeks, M. L. Sturgess, and J. S. Woodhead, Chemiluminescence immunoassay: An overview. *Clin. Sci.* **70**, 403–408 (1986).

123. J. P. Gosling, A decade of development in immunoassay methodology. *Clin. Chem.* **36**(8), 1408–1427 (1990).
124. B. Nilsson, Enzyme linked immunosorbent assays. *Curr. Opin. Immunol.* **2**, 898–904 (1990).
125. M. Oellerich, Enzyme immunoassays in clinical chemistry. Present status and trends. *J. Clin. Chem. Clin. Biochem.* **18**, 197–208 (1980).
126. A. H. W. N. Schuurs and B. K. Van Weemen, Enzyme immunoassay. *Clin. Chim. Acta* **81**, 1–40 (1977).
127. O. B. Wisdom, Enzyme immunoassay. *Clin. Chem.* **22**, 1243–1255 (1976).
128. E. Engvall and P. Perlman, Enzyme-linked immunosorbent assay (ELISA) of immunoglobulin G. *Immunochemistry* **8**, 871–874 (1971).
129. R. Schwall, L. N. Bald, E. Szonyi, A. J. Mason, and K. Nikolics, Approaches to non-radiometric assays for inhibin and activin. In “Non-radiometric Assays: Technology and Application in Polypeptide and Steroid Hormone Detection” (B. D. Albertson and F. P. Haseltine, eds.), pp. 205–220. Wiley, New York, 1988.
130. A. Zettner and P. E. Duly, Principles of competitive binding assays (saturation analyses). II. Sequential saturation. *Clin. Chem.* **20**, 5–14 (1974).
131. T. T. Ngo and H. M. Lenhoff, New approach to heterogeneous enzyme immunoassay using tagged enzyme-ligand conjugates. *Biochem. Biophys. Res. Commun.* **99**, 496–503 (1981).
132. K. E. Rubenstein, R. S. Schneider, and E. F. Ullman, “Homogeneous” enzyme immunoassay. A new immunochemical technique. *Biochem. Biophys. Res. Commun.* **47**, 846–851 (1972).
133. J. F. Burd, R. C. Wong, J. E. Feeney, R. J. Carrico, and R. C. Boguslaski, Homogeneous reactant-labelled fluorescent immunoassay for therapeutic drugs exemplified by gentamicin determination in human serum. *Clin. Chem.* **23**, 1402–1408 (1977).
134. T. T. Ngo, R. J. Carrico, R. C. Boguslaski, and J. F. Burd, Homogeneous substrate-labelled fluorescent immunoassay for IgG in human serum. *J. Immunol. Methods* **42**, 93–103 (1981).
135. M. Oellerich, A. Haindl, and R. Haeckel, Evaluation of enzyme immunoassays (EMIT and ENZYMN) for detection of thyroxine and of thyroid binding index. *J. Clin. Chem. Clin. Biochem.* **17**, 483–488. (1979).
136. E. Ishikawa, Enzyme immunoassay. *Nippon Rinsho* (Suppl.), 2202–2203 (1978).
137. E. Ishikawa, Y. Yamada, Y. Hamaguchi, S. Yoshitake, K. Shiomi, T. Ota, Y. Yanamoto, and K. Tanaka, Enzyme labelling with maleimides and its application to the immunoassay of peptide hormones. In “Enzyme Labeled Immunoassay of Hormones and Drugs” (S. B. Pal, ed.). de Gruyter, Berlin, 1978.
138. A. Shalev, A. H. Greenberg, and P. J. McAlpine, Detection of attograms of antigen by a high-sensitivity enzyme-linked immunosorbent assay (HS-ELISA) using a fluorogenic substrate. *J. Immunol. Methods* **38**, 125–139 (1980).
139. W. F. Cassano, Murine monoclonal anti-avidin antibodies enhance the sensitivity of avidin-biotin immunoassays and immunohistologic staining. *J. Immunol. Methods* **117**, 169–174 (1989).
140. E. J. Ruitenberg, P. A. Steerenberg, B. J. M. Brosi, and J. Buys, Sero-diagnosis of *Trichinella spiralis* infections in pigs by enzyme-labelled immunosorbent assays. *Bull W. H. O.* **51**, 108–109 (1974).
141. E. P. Diamandis, Immunoassays with time-resolved fluorescence spectroscopy: Principles and applications. *Clin. Biochem.* **21**, 139–150 (1988).
142. A. R. Neurath and F. Strick, Enzyme linked fluorescence immunoassays using β -galactosidase and antibodies covalently bound to polystyrene plates. *J. Virol. Methods* **3**, 155–165 (1981).

143. A. H. Coons, H. J. Creech, and R. N. Jones, Immunological properties of an antibody containing a fluorescent group. *Proc. Soc. Exp. Biol. Med.* **47**, 200–202 (1941).
144. I. Hemmila, Fluoroimmunoassays and immunofluorometric assays. *Clin. Chem.* **31**, 359–370 (1985).
145. G. Handley, J. N. Miller, and J. W. Bridges, Development of fluorescence immunoassay methods of drug analysis. *Proc. Anal. Div. Chem. Soc.* **16**, 26–29 (1979).
146. T. H. The and T. R. Feltkamp, Conjugation of fluorescein isothiocyanate to antibodies. *Immunology* **18**, 865–873 (1970).
147. G. J. Steinbach and H. Mayersbach, Characterization of fluorescein isothiocyanate. II. Absorption and fluorescence after conjugation to human- and rabbit-gamma globulins and bovine albumin. *Acta Histochem.* **55**, 110–123 (1976).
148. P. Brandtzarg, Conjugates of immunoglobulin G with different fluorochromes: I and II. *Scand. J. Immunol.* **2**, 273–290 and 333–348 (1973).
149. R. P. Liburdy, Antibody induced fluorescence enhancement of an *N*-(3-pyrene) maleimide conjugate of rabbit antihuman immunoglobulin G. *J. Immunol. Methods* **28**, 233–242 (1979).
150. D. Blakeslee and M. Baines, Immunofluorescence using dichlorotriazinyl-amino fluorescein (DTAF): Preparation and fractionation of labelled IgG. *J. Immunol. Methods* **13**, 305–320 (1976).
151. M. Hassan, J. Landon, and D. S. Smith, Multifluorescein-substituted polymers as potential labels in fluoroimmunoassays. *FEBS Lett.* **103**, 339–341 (1979).
152. P. Brandtzarg, Rhodamine conjugates: Specific and nonspecific binding properties in immunochemistry. *Ann. N.Y. Acad. Sci.* **254**, 35–54 (1975).
153. R. M. McKinney and J. T. Spellane, An approach to quantitation in rhodamine isothiocyanate labelling. *Ann. N.Y. Acad. Sci.* **254**, 55–64 (1975).
154. C. S. Chadwick, M. G. McEntegard, and R. C. Mairin, A trial of new fluorochromes and the development of an alternative to fluorescein. *Immunology* **1**, 315–326 (1958).
155. G. I. Ekeke and D. Exley, The assay of steroids by fluoroimmunoassay. In “Enzyme Labelled Immunoassay of Hormones and Drugs” (S. B. Pal, ed.), pp. 195–205. de Gruyer, Berlin, 1978.
156. D. Exley and G. I. Ekeke, Fluoroimmunoassay of 5 α -dihydrotestosterone. *J. Steroid Biochem.* **14**, 1297–1302 (1981).
157. M. N. Kronick and P. D. Grossman, Immunoassay techniques with fluorescent phycobili-protein conjugates. *Clin. Chem.* **29**, 1582–1586 (1983).
158. J. L. Hendrix, Porphyrins and chlorophylls as probes for fluoroimmunoassay. *Clin. Chem.* **29**, 103 (1983) (Letter).
159. R. A. Evangelista, A. Pollak, B. Allore, E. M. Templeton, R. C. Morton, and E. P. Diamandis, A new europium chelate for protein labelling and time-resolved fluorometric applications. *Clin. Biochem.* **21**, 173–178 (1988).
160. M. A. Chan, A. C. Bellem, and E. P. Diamandis, Time resolved immunofluorometric assay of alpha-fetoprotein in serum and amniotic fluid with a novel detection system. *Clin. Chem.* **33**, 2000–2003 (1988).
161. M. J. Khosravi and E. P. Diamandis, Immunofluorometry of hCG by time-resolved fluorescence spectroscopy with a new europium chelate as label. *Clin. Chem.* **33**, 1994–1999 (1988).
162. E. P. Diamandis, V. Bhayana, K. Conway, E. Reichstein, and A. Papanastasiou-Diamandis, Time resolved fluoroimmunoassay of cortisol in serum with a europium chelate as label. *Clin. Biochem.* **21**, 291–296 (1988).
163. E. Reichstein, R. C. Morton, and E. P. Diamandis, Sensitive time-resolved immunofluorometric assay of thyrotropin in serum. *Clin. Biochem.* **22**, 23–29 (1989).

164. K. H. Milby and R. N. Zare, Antibodies, lasers, and chromatography. *Int. Clin. Products Rev.* **3**, 10–18 (1984).
165. I. Hemmila, S. Dakubu, V.-M. Mukkala, H. Siitari, and T. Lövgren, Europium as a label in time resolved immuno-fluorometric assay. *Anal. Biochem.* **137**, 335–342 (1984).
166. M. W. Sundberg, C. F. Mears, D. A. Goodwin, and C. I. Diamanti, Selective binding of metal ions to macromolecules using bifunctional analogs of EDTA. *J. Med. Chem.* **17**, 1304–1307 (1974).
167. O. H. Meurman, I. A. Hemmila, T. N. E. Lovgren, and P. E. Halonen, Time resolved fluoroimmunoassay: A new test for Rubella antibodies. *J. Clin. Immunol.* **15**, 920–925 (1982).
168. H. Siitari, I. A. Hemmila, E. Soini, and T. N. E. Lovgren, Detection of hepatitis B surface antigens using time resolved fluoroimmunoassay. *Nature (London)* **301**, 258–260 (1983).
169. K. Pettersson, H. Siitari, I. A. Hemmila, E. Soini, T. Lovgren, V. Hanninen, P. Tanner, and V.-H. Stenman, Time resolved fluoroimmunoassay of hCG. *Clin. Chem.* **29**, 60–64 (1983).
170. M. T. Karp, A. I. Suominen, I. A. Hemmila, and P. I. Mantsala, Time resolved europium fluorescence in enzyme activity measurements. A sensitive protease assay. *J. Appl. Biochem.* **5**, 399–403 (1983).
171. J. U. Eskola, T. J. Nevalainen, and N. C. Lovgren, Time resolved fluoroimmunoassay of human pancreatic phospholipase A₂. *Clin. Chem.* **29**, 1777–1780 (1983).
172. J. A. Vilpo, S. Rasi, E. Suvanto, and L. M. Vilpo, Time resolved fluoroimmunoassay of 5-methyl-2'-deoxycytidine. *Anal. Biochem.* **154**, 436–440 (1986).
173. T. Lovgren, I. A. Hemmila, K. Pettersson, J. V. Eskola, and E. Bertoft, Determination of hormones by time-resolved fluoroimmunoassay. *Talanta* **31**, 909–916 (1984).
174. T. Lovgren, I. A. Hemmila, K. Pettersson, and P. Halonen, Time-resolved fluorimetry in immunoassay. In "Alternative Immunoassays" (W. P. Collins, ed.), pp. 203–217. Wiley, New York, 1985.
175. E. Toivonen, I. A. Hemmila, J. Marnieme, P. N. Jorgensen, J. Zeuthen, and T. Lovgren, Two-site time-resolved immunofluorometric assay of human insulin. *Clin. Chem.* **32**, 637–640 (1986).
176. G. I. Ekeke, D. Exley, and R. Abuknesha, Immunofluorometric assay of oestradiol-17 β . *J. Steroid Biochem.* **11**, 1597–1600 (1979).
177. Y. Kobayashi, M. Yamata, I. Watanabe, and K. Miyai, A solid phase fluoroimmunoassay of serum cortisol. *J. Steroid Biochem.* **16**, 521–524 (1982).
178. M. Pourfarzaneh and R. D. Nargessi, Composite polyacrolein-coated cellulose magnetizable particles: An "autoreactive" magnetizable solid phase with superior buoyancy properties. *Clin. Chim. Acta* **111**, 61–63 (1981).
179. E. F. Ullman, Recent advances in fluorescence immunoassay techniques. In "Ligand Assay" (J. Langan and J. J. Clapp, eds.), pp. 113–136. Masson, New York, 1981.
180. N. Lawson, N. M. R. Wilson, and H. Pandov, Assessment of a time-resolved fluoroimmunoassay for thyrotropin in routine clinical practice. *Clin. Chem.* **32**, 684–686 (1986).
181. N. Paterson, E. M. Biggart, R. S. Chapman, and G. H. Beastall, Evaluation of a time-resolved immunofluorometric assay for serum TSH. *Ann. Clin. Biochem.* **22**, 606–611 (1983).
182. J. Arends and B. Norgaard-Pedersen, Immunofluorometry of thyrotropin, for whole-blood spots on filter paper to screen for congenital hypothyroidism. *Clin. Chem.* **32**, 1854–1856 (1986).
183. R. John and J. S. Woodhead, An automated immunoradiometric assay of TSH in dried blood filter paper spots. *Clin. Chim. Acta* **125**, 329–340 (1982).

184. H. Alfthan, Comparison of immunoradiometric and immunofluorometric assay for serum hCG. *J. Immunol. Methods* **88**, 239–244 (1986).
185. Y. Kobayashi, M. Yamata, I. Watanabe, and K. Miyai, A solid phase fluoroimmunoassay of serum cortisol. *J. Steroid Biochem.* **16**, 521–524 (1982).
186. L. A. Kaplan, I. W. Chen, N. Gau, J. Fearn, H. Maxon, C. Volle, and E. A. Stein, Evaluation and comparison of fluorescence and enzyme-linked immunoassays with radioimmunoassay for serum thyroxine. *Clin. Biochem. Anal.* **14**, 182–186 (1981).
187. R. E. Curry, H. Heitzman, D. H. Riege, R. V. Sweet, and M. G. Simonsen, A systems approach to fluorescence immunoassay, general principles and representative applications. *Clin. Chem.* **25**, 1591–1595 (1979).
188. P. J. Lisi, C. W. Huang, R. A. Hoffman, and J. A. Tempel, A fluorescence immunoassay for soluble antigens employing flow cytometric determinations. *Clin. Chim. Acta* **120**, 171–179 (1982).
189. M. G. Simonsen and R. L. Curre, A fluorescent immunoassay system: The automated instrumentation. *Clin. Chem.* **25**, 1116 (Abstract 269) (1979).
190. J. E. Kuo, K. H. Milby, W. D. Hindsberg III, P. R. Poole, V. L. McGuffin, and R. N. Zare, Direct measurement of antigens in serum by time-resolved fluoroimmunoassay. *Clin. Chem.* **30**, 50–53 (1985).
191. H. Dechaud, R. Bador, F. Claustrat, and C. Desuzinges, Laser excited immunofluorometric assay of prolactin, with the use of antibodies coupled to lanthanide-labelled diethylenetriaminepenta acetic acid. *Clin. Chem.* **32**, 1323–1327 (1986).
192. R. Bador, H. Dechard, F. Claustrat, and C. Desuzinges, Europium and samarium as labels in time-resolved immunofluorometric assay of follitropin. *Clin. Chem.* **33**, 48–51 (1987).
193. S. R. Popelka, D. M. Miller, J. T. Holen, and D. M. Kelso, Fluorescence polarization immunoassay. II. Analyzer for rapid precise measurement of fluorescence polarization with the use of disposable cuvettes. *Clin. Chem.* **27**, 1198–1201 (1981).
194. J. Weeks, M. L. Sturgess, and J. S. Woodhead, Chemiluminescence immunoassays: An overview. *Clin. Sci.* **70**, 403–408 (1986).
195. I. Weeks and J. S. Woodhead, Chemiluminescence immunoassay. *J. Clin. Immunoassay* **7**, 82–89 (1984).
196. H. R. Schroeder, R. C. Boguslaski, R. J. Carrico, and R. T. Buckler, Monitoring specific protein-binding reactions with chemiluminescence. In “Methods in Enzymology” (M. A. DeLuca and W. D. McElroy, eds.), Vol. 57, pp. 424–444. Academic Press, New York, 1978.
197. L. J. Krika, P. E. Stanley, G. H. G. Thorpe, and T. P. Whitehead (eds.), “Analytical Applications of Bioluminescence and Chemiluminescence.” Academic Press, London, 1984.
198. F. Kohen, M. Pazzagli, M. Serio, J. DeBoever, and D. Vanderkerckhove, Chemiluminescence and bioluminescence immunoassays. In “Alternative Immunoassays” (W. P. Collins, ed.), pp. 103–122. Wiley, New York, 1985.
199. G. J. R. Barnard, J. B. Kim, and J. L. Williams, Chemiluminescence immunoassays and immunochemiluminometric assays. In “Alternative Immunoassays” (W. P. Collins, ed.), pp. 123–152. Wiley, New York, 1985.
200. A. K. Campbell, A. Roberts, and A. Patel, Chemiluminescence energy transfer: A technique for homogeneous immunoassay. In Alternative Immunoassays. (W. P. Collins, ed.), pp. 153–184. Wiley, New York, 1985.
201. W. R. Seitz, Immunoassay labels based on chemiluminescence and bioluminescence. *Clin. Biochem.* **17**, 120–125 (1984).
202. I. Weeks, M. L. Sturgess, and J. S. Woodhead, Chemiluminescence immunoassays: An overview. *Clin. Sci.* **70**, 403–408 (1986).

203. W. G. Wood, Luminescence immunoassays: Problems and possibilities. *J. Clin. Chem. Clin. Biochem.* **22**, 905–918 (1984).
204. F. Kohen, M. Pazzagli, J. B. Kim, and H. R. Lindner, An assay procedure for plasma progesterone based on antibody enhanced chemiluminescence. *FEBS Lett.* **104**, 201–205 (1979).
205. M. Pazzagli, J. B. Kim, G. Nessler, G. Martinazza, F. Kohen, F. Franceschetti, A. Tommasi, R. Salerno, and M. Serio, Luminescent assay (LIA) for progesterone in a heterologous system. *Clin. Chim. Acta* **115**, 287–296 (1981).
206. F. Kohen, J. B. Kim, H. R. Lindner, and W. P. Collins, Development of a solid phase chemiluminescence immunoassay for plasma progesterone. *Steroids* **38**, 73–88 (1981).
207. J. B. Kim, G. J. Barnard, W. P. Collins, F. Kohen, H. R. Lindner, and Z. Eshhar, The measurement of plasma estradiol-17 beta by a solid phase chemiluminescence immunoassay. *Clin. Chem.* **28**, 1120–1124 (1982).
208. D. A. Weerasekera, J. B. Kim, G. J. Barnard, W. P. Collins, F. Kohen, and H. R. Lindner, Monitoring ovarian function by a solid phase chemiluminescence immunoassay. *Acta Endocrinol.* **101**, 254–263 (1982).
209. G. J. Barnard, W. P. Collins, F. Kohen, and H. R. Lindner, The measurement of urinary estriol-16 alpha-glucuronide by a solid phase chemiluminescence immunoassay. *J. Steroid Biochem.* **14**, 941–948 (1981).
210. Z. Eshhar, J. B. Kim, G. Barnard, W. P. Collins, S. Olad, H. R. Lindner, and F. Kohen, Use of monoclonal antibodies to pregnanediol-3 α -glucuronide to the development of a solid phase chemiluminescence immunoassay. *Steroids* **38**, 89–109 (1981).
211. W. P. Collins, G. J. Barnard, J. B. Kim, and F. Kohen, Chemiluminescence immunoassays for plasma steroids and urinary steroid metabolites. In “Immunoassays for Clinical Chemistry” (W. M. Hunter and J. E. T. Corrie, eds.), 2nd Ed., pp. 373–397. Churchill Livingstone, London, 1983.
212. I. Weeks, I. Beheshti, F. McCapra, A. K. Campbell, and J. S. Woodhead, Acridinium esters as high specific activity labels in immunoassays. *Clin. Chem.* **29**, 1474–1479 (1983).
213. I. Weeks, M. L. Sturgess, K. Siddle, M. K. Jones, and J. S. Woodhead, High sensitivity immunochemiluminometric assay for thyrophenin. *Clin. Endocrinol.* **20**, 489–495 (1984).
214. I. Weeks, I. Beheshti, F. McCapra, A. K. Campbell, and J. S. Woodhead, Acridinium esters as high specific activity labels in immunoassays. *Clin. Chem.* **29**, 1474–1479 (1983).
215. M. E. Jolley, S. D. Stroupe, K. S. Schwenzer, *et al.* Fluorescence polarization immunoassay. III. An automated system for therapeutic drug determination. *Clin. Chem.* **27**, 1575–1579 (1981).
216. M. E. Jolley, S. D. Stroupe, C. J. Wang, *et al.* Fluorescence polarization immunoassay. I. Monitoring aminoglycoside antibiotics in serum and plasma. *Clin. Chem.* **27**, 1190–1197 (1981).
217. D. Monroe, Amperometric immunoassay. *Crit. Rev. Clin. Lab. Sci.* **28**, 1–18 (1990).
218. W. R. Heineman, H. B. Halsall, K. R. Wehmeyer, M. J. Doyle, and D. S. Wright, Immunoassay with electrochemical detection. *Methods Biochem. Anal.* **32**, 345–393 (1990).
219. J. E. Place, R. M. Sutherland, and C. Dahne, Opto-electronic immunosensors: A review of optical immunoassays at continuous surfaces. *Biosensor* **1**, 321–353 (1985).
220. D. G. Hafeman, J. W. Parce, and H. M. McConnell, Light addressable potentiometric sensor for biochemical systems. *Science* **240**, 1182–1184, (1985).
221. B. D. Albertson and M. J. Zinaman, Review article: The prediction of ovulation and monitoring of the fertile period. *Adv. Contracept.* **3**, 263–290 (1987).
222. K. L. Campbell, Solid state assays: Reagents and film technology for dip-stick assays. In “Non-radiometric Assays: Technology and Application in Polypeptide and Steroid

- Hormone Detection” (B. D. Albertson and F. P. Haseltine, eds.), pp. 237–287. Wiley, New York, 1988.
223. J. C. Sternberg, Rate nephelometry. *In* “Manual of Clinical Laboratory Immunology” (N. R. Rose, H. Freidman, and J. L. Fahey, eds.), 3rd Ed., pp. 33–37. American Society of Microbiology, Washington, D.C., 1986.
 224. H. Riccomi, P. L. Masson, J. P. Vaerman, and J. F. Heremans, An automated nephelometric inhibition immunoassay (NINIA) for haptens. *In* “Automated Immunoprecipitin Reactions” (J. D. Hamm, ed.), pp. 9–11. Technicon Instruments Corporation, Tarrytown, 1972.
 225. J. P. Galvin, Particle enhanced immunoassay. *In* “Manual of Clinical Laboratory Immunology” (N. R. Rose, H. Freidman, and J. L. Fahey, eds.), 3rd Ed., pp. 38–42. American Society of Microbiology, Washington, D.C., 1986.
 226. J. M. Singer and R. M. Plotz, The latex fixation test—Application to rheumatoid arthritis. *Am. J. Med.* **21**, 888–892 (1956).
 227. P. I. Masson and H. W. Holy, Immunoassay by particle counting. *In* “Manual of Clinical Laboratory Technology” (N. R. Rose, H. Freidman, and J. L. Fahey, eds.), 3rd Ed., pp. 43–48. Society of Microbiology, Washington, D.C., 1986.
 228. P. L. Masson, C. L. Cambiaso, D. Collet-Cassart, C. G. M. Magnusson, C. B. Richards, and J. C. M. Sindic, Particle-counting immunoassay (PACIA). *In* “Methods in Enzymology” (J. J. Langone and H. V. Vanakis, eds.), Vol. 74, pp. 106–139. Academic Press, New York, 1981.
 229. O. C. Fagnart, J. C. Mareschal, C. L. Cambiaso, and P. L. Masson, Particle counting immunoassay (PACIA) of pregnancy specific β_1 glycoprotein. A possible marker of various malignancies and Crohn’s ileitis. *Clin. Chem.* **31**, 397–401 (1985).
 230. R. F. Ritchei, Introduction to general methodology. *In* “Manual of Clinical Laboratory Immunology” (N. R. Rose, H. Freidman, and J. L. Fahey, eds.), 3rd Ed., pp. 1–3. Society of Microbiology, Washington, D.C., 1986.

2

Longitudinal Bone Growth: Experimental Methods

Jeffrey Baron

*Developmental Endocrinology Branch
National Institute of Child Health and
Human Development
National Institutes of Health
Bethesda, Maryland 20892-1862*

PRINCIPLES OF LONGITUDINAL BONE GROWTH

The mammalian embryonic skeleton is composed initially of cartilage. Ossification begins near the midshaft of long bones, and secondary centers of ossification develop near the ends of the bone. Continued enlargement of these ossification centers replaces most of the cartilage with bone. However, the primary and secondary ossification centers remain separated by a thin layer of cartilage, the growth plate, which persists into early postnatal life (1).

The growth plate is responsible for longitudinal bone growth. New bone is formed at the growth plate by endochondral ossification, which involves cartilage formation (chondrogenesis) followed by conversion of the new cartilage into bone (ossification). The chondrogenesis is a result of growth plate chondrocyte proliferation, hypertrophy, and extracellular matrix secretion. In isolation, these processes would lead to progressive widening of the growth plate. However, simultaneously, the metaphyseal border of the growth plate is invaded by blood vessels and bone cell precursors, which remodel the cartilage into bone (2). The two processes, chondrogenesis and ossification, are tightly coupled so that the width of the growth plate

remains relatively constant and new bone is formed at the junction of the growth plate and the metaphyseal bone.

The growth rate at the growth plate depends on the rate at which new proliferative chondrocytes are produced and the length that each of these new cells eventually contributes after it undergoes hypertrophy. Thus, growth rate = $P * H$, where the growth rate is the change in bone length per unit time at a particular growth plate, P is the number of new cells produced per chondrocyte column per unit time, and H is the maximum height of the hypertrophic chondrocyte. This mathematical relationship has been experimentally tested and is at least a reasonable approximation (3).

Early in life, rapid chondrocyte proliferation leads to rapid longitudinal bone growth. With increasing age, chondrocyte proliferation and thus growth rate fall dramatically (4). In the human, the maximal overall linear growth rate, achieved prenatally, is close to 100 cm/yr. By birth, the growth rate has dropped to approximately 50 cm/yr, and by late childhood to 5 cm/yr. In the human, there follows a brief growth acceleration after which the growth decreases gradually to zero (5). This pubertal growth spurt is not seen in nonprimate laboratory animals. In some mammals, including the human and rabbit, the senescent growth plate is replaced by bone. In rodents, the senescent growth plate, although producing essentially no growth, persists.

Growth rate is tightly regulated by endocrine signals. Growth hormone and its principal mediator, insulinlike growth factor 1, positively regulate growth rate as do thyroid hormone and androgen. Estrogen in low dose positively regulates linear growth, at least in the human, whereas high-dose estrogen can negatively regulate growth rate. Excess glucocorticoid is a potent inhibitor of linear growth. Growth rate is also strongly influenced by nutrition. Even modest decreases in nutritional intake can suppress linear growth.

MEASUREMENT OF LONGITUDINAL BONE GROWTH

There are several indirect measures of longitudinal bone growth. In some studies, weight gain is measured, probably because it can be measured easily and with great accuracy. Under many circumstances, increase in length and increase in weight correlate well. However, in other circumstances, such as glucocorticoid excess, these two measures may diverge. Unfortunately, it is difficult to know *a priori* whether gain in weight will accurately reflect gain in length.

Other studies of bone growth employ measurements of growth plate thickness (6). Again, in some circumstances, such as growth hormone defi-

ciency, the width of the growth plate and the rate of bone growth both decrease. However, growth plate width does not depend only on growth velocity. Rather it reflects the lag between chondrogenesis and ossification. Thus, although width may correlate with growth rate in some circumstances, a correlation in any given experimental setting cannot be taken for granted.

In contrast, growth in whole-body length provides a good indirect measure of longitudinal bone growth since it primarily reflects growth of the bones in the lower extremities and vertebral column. Various devices exist or can be constructed for whole-body length measurement in humans (5) or laboratory animals (7,8).

Longitudinal bone growth can also be measured directly by transient administration of a substance that becomes incorporated into newly formed bone (9). When such a substance is administered, it deposits in the area of rapid ossification in the metaphysis adjacent to the growth plate. With time, the growth plate grows away from this band of labeled bone. The animal is killed after some time, t , has elapsed, typically 1 day to 2 weeks. The bones are examined to determine the distance, d , between the growth plate and the band of labeled bone. The growth rate is equal to d/t . Alternatively, two doses of a labeling substance can be administered separated by time Δt . If the distance between the bands is Δd , then the growth rate is equal to $\Delta d/\Delta t$.

Various substances may be used to label newly formed bone, including tetracycline (9), oxytetracycline (9–11), and calcein (12). These substances can be visualized by fluorescence microscopy. Because they incorporate into the bone mineral, the tissue cannot be decalcified and thus tissue sections must be obtained with equipment designed for calcified tissue.

Alternatively, the rate of longitudinal bone growth can be assessed by radiologic methods. These methods have two important advantages. First, if X-ray equipment is available, they are simple to perform. Second, they do not require killing the animal and thus allow serial measurements. The simplest radiologic method is based on whole-bone length measurements (13). The animal is sedated and positioned on a horizontal cassette containing X-ray film. An X-ray point source is placed above the animal, the X-ray exposure is made, and the film is developed. The length, l , of one or more bone images is then measured on the film. The radiographic measurement is repeated after a time interval, t . The growth rate is equal to the change in bone length divided by the time interval, $\Delta l/t$.

To obtain accurate radiologic measurements, the geometric relationships between the animal, the film, and the point source should be optimized. The positioning of the animal on the film cassette should be reproduced precisely during all measurements. The bone or bones of interest should be laid flat along the surface, using tape if necessary. Any tilt will result in

an image shorter than the actual bone. Another possible source of error, parallax, arises because the X rays are not parallel but instead diverge from a point source. Parallax can be minimized by keeping the bone of interest immediately adjacent to the cassette and placing the X-ray source as far from the cassette as possible. We have found ~1 m to be adequate. Similar problems arise if the bone of interest is not placed at the center of the X-ray field. When practical considerations prevent optimization of any geometric parameter, growth rate can still be measured precisely if the nonoptimal condition can be carefully reproduced at each time point. High-resolution film should be used. Finally, replicate radiographs add accuracy. We have found duplicates to be adequate for most purposes. To avoid bias, the labels on the films can be masked so that the observer is blinded as to the identity of the animal and the date of the measurement.

Several methods are suitable to quantitate the length of the bone image. The simplest method is to use an accurate steel ruler alone. Greater precision can be obtained with vernier calipers. Perhaps the greatest precision can be obtained with a steel ruler and a dissecting microscope equipped with an eyepiece micrometer. The microscope is used to verify alignment of a calibration mark on the ruler with one end of the bone. The position of the other end of the bone can be precisely identified using the micrometer to interpolate between marks on the ruler.

Whole-bone length can be measured from the end of one epiphysis to the end of the other. Alternatively, other landmarks, such as the edge of a growth plate, can be selected for measurements. The choice of landmarks will depend on the species and the bone selected.

In the 5-week-old rabbit, tibial growth rate can be measured reliably with an interval of 1 week using a vernier caliper (13). In this model, the mean tibial growth rate was ~5 mm/week and the measurement error for individual animals was approximately 0.2 mm. In the rat, leg length and arm length have been measured radiographically (7).

Greater precision can be obtained by inserting radiopaque markers into the bone of interest. This method provides distinct landmarks with which to make measurements and allows measurement across shorter distances. It also allows the growth rate at a single growth plate to be measured. Various markers have been used, including wires and metal implants (14). The guidelines described here for optimizing accuracy in whole-bone measurements also apply to these methods.

A single marker can be placed in the metaphysis or diaphysis (15). The distance between this marker and a naturally occurring landmark in the bony epiphysis is measured on the radiographs as described earlier. The change in this distance divided by the time interval will reflect growth rate at that growth plate.

We have found that the greatest accuracy can be achieved by inserting markers on both sides of a growth plate (16). To measure growth rate in the 5-week-old rabbit, we surgically implanted three metal pins into the proximal tibia. The pins were prepared by breaking 30-gauge hypodermic needles (Becton Dickinson, Rutherford, NJ) 5 mm from the tip, followed by steam sterilization. Under general anesthesia, the proximal tibia was exposed surgically. The pins were inserted parallel to the growth plate, directed posteriorly. One pin was placed in the bony epiphysis, 2–3 mm proximal to the growth plate. A second pin was placed in the metaphysis, 2–3 mm distal to the growth plate. The third pin was placed in the metaphysis, 5 mm distal to the second pin. To prevent infection, surgery was performed under sterile conditions, and the animals received a single prophylactic intramuscular dose of penicillin G (44,000 IU/kg) immediately prior to surgery.

Serial radiographs were obtained on the day of surgery and on subsequent days. For the radiograph, the animal was sedated and placed in the lateral position on an X-ray cassette. The hindleg of interest was placed closer to the cassette and anterior to the contralateral limb. The extremities were fixed to the cassette with tape. The X-ray source was placed precisely over the proximal tibia of interest at a distance of 91 cm. In different experiments, the time interval between radiographs varied from 1 day (17) to 1 week (18). For the daily measurements, quadruplicate radiographs were obtained at each time point. For less frequent measurements, duplicates were obtained. Each radiograph was examined under a dissecting microscope, and the distance between pins was measured using an eyepiece micrometer. This distance was measured parallel to the long axis of the tibia between the blunt ends of the pins. The distance between the first two pins was used to calculate growth rate. The distance between the second and third pins was expected to remain constant with time and thus served as a control. Even for the daily measurements the error of measurement was small, 0.02 mm, compared to the mean daily growth rate, 0.29 mm/day (17).

GROWTH PLATE INFUSION

The effect of systemic treatments on longitudinal bone growth can be assessed using the technology described in the foregoing (13). However, some substances cannot be administered systemically because of cost, systemic toxicity, or short half-life (19). In these situations, local administration of the substance into the growth plate may provide a practical alternative. For other substances, comparing the effects of local and systemic adminis-

tration can help distinguish direct, local effects on the growth plate from indirect effects (16).

Several methods have been developed to administer substances more directly to the growth plate. In the rat, growth hormone stimulates local bone growth when injected into the proximal tibial growth plate, the articular space of the knee, the proximal tibial bony epiphysis, or the common iliac artery (6,10,20).

We developed a method to infuse substances directly into the rabbit proximal tibial growth plate (16,18,19). Under general anesthesia, an incision was made to expose the proximal anteromedial tibia. Sterile infusion sets, which consisted of a 27-gauge stainless-steel needle attached to a flexible plastic catheter (Baxter Healthcare, Hookset, NH), had been prepared beforehand for implantation. The needle had been bent to place a right angle 2.5 mm from the sharp tip. This tip was then inserted into the proximal tibial growth plate near the junction with the bony epiphysis. The shaft of the needle was bent into a "U" shape, the distal portion of which was sutured to the periosteum of the tibia. The plastic catheter was then tunneled subcutaneously to a second incision over the lower abdomen. The free end of the catheter was attached to an osmotic pump (Alza Corp., Palo Alto, CA). For experiments lasting longer than 1 week, the needle was inserted through the bony epiphysis 1–2 mm above the growth plate, angled such that the tip was within the cartilaginous growth plate (18). The purpose of this modification was to anchor the infusion apparatus in epiphyseal bone. Otherwise, with time the needle would have become situated in metaphyseal bone as a result of growth. To prevent infection, surgery was performed under sterile conditions, and the animals received a single prophylactic intramuscular dose of penicillin G (44,000 IU/kg) immediately prior to surgery.

The effect of a local infusion on growth rate can be determined by combining the methods described here for infusion and growth rate measurement. Alternatively, the effect of the infusion on growth plate histology can be assessed by preparing the proximal tibia for histologic examination at the end of the infusion (19). Serial sections can be cut perpendicular to the path of the needle to search for an affected area near the needle tip. Whether the end point is histology or growth rate, the contralateral proximal tibial growth plate can receive an infusion of vehicle and thus can serve as a control.

The growth plate is a remnant of embryonic cartilage that persists into postnatal life. Within the growth plate, longitudinal bone growth is driven by cellular processes typical of embryonic life: rapid cell proliferation, terminal differentiation, vascular invasion, and cell migration. Thus the growth plate may serve as a model system to explore fundamental develop-

mental processes. Study of this structure has been hampered in the past by methodologic difficulties. It is hoped that the methods described in this chapter, combined with other evolving physiologic, cellular, and molecular approaches, will contribute to this effort.

REFERENCES

1. J. P. Iannotti, Growth plate physiology and pathology. *Orthop. Clin. North Am.* **21**, 1–17 (1990).
2. C. T. Brighton, The growth plate. *Orthop. Clin. North Am.* **15**, 571–595 (1984).
3. H. A. Sissons, Experimental study on the effect of local irradiation on bone growth. In “Progress in Radiobiology” (J. S. Putnam, ed.), p. 436. Oliver & Boyd, Edinburgh, 1955.
4. N. F. Kember and K. V. R. Walker, Control of bone growth in rats. *Nature (London)* **229**, 428–429 (1971).
5. J. M. Tanner and P. S. W. Davies, Clinical longitudinal standards for height and weight velocity for North American children. *J. Pediatr.* **107**, 317–329 (1985).
6. N. L. Schlechter, S. M. Russell, S. Greenberg, E. M. Spencer, C. S. Nicoll, A direct growth effect of growth hormone in rat hindlimb shown by arterial infusion. *Am. J. Physiol.* **250**, E231–E235 (1986).
7. P. C. R. Hughes and J. M. Tanner, *J. Anat.* **106**, 349–370 (1970).
8. I. M. Masoud, A. C. Moses, and F. D. Shapiro, Skeletal growth in the normal rabbit: A longitudinal study of serum somatomedin-C and skeletal development. *Prog. Clin. Biol. Res.* **187**, 233–243 (1985).
9. L. I. Hansson, K. Menander-Sellman, A. Stenström, and K. G. Thorngren, Rate of normal longitudinal bone growth in the rat. *Calcif. Tissue Res.* **10**, 238–251 (1972).
10. J. Isgaard, A. Nilsson, A. Lindahl, J. O. Jansson, and O. G. P. Isaksson, Effects of local administration of GH and IGF-1 on longitudinal bone growth in rats. *Am. J. Physiol.* **250**, E367–E372 (1986).
11. G. J. Breur, B. A. VanEnkevort, C. E. Farnum, and N. J. Wilsman, Linear relationship between the volume of hypertrophic chondrocytes and the rate of longitudinal bone growth in growth plates. *J. Orthop. Res.* **9**, 348–359 (1991).
12. S. Stevenson, E. B. Hunziker, and W. Herrman, Is longitudinal bone growth influenced by diurnal variation in the mitotic activity of chondrocytes of the growth plate? *J. Orthop. Res.* **8**, 132 (1990).
13. C. Heinrichs, J. A. Yanovski, A. H. Roth, Y. M. Yu, H. M. Domene, K. Yano, G. B. Cutler, Jr., and J. Baron, Dexamethasone increases growth hormone receptor messenger ribonucleic acid levels in liver and growth plate. *Endocrinology (Baltimore)* **135**, 1113–1118 (1994).
14. B. G. Sarnat, Growth of bones as revealed by implant markers in animals. *Am. J. Phys. Anthropol.* **29**, 255–286 (1968).
15. H. A. Sissons, Experimental determination of longitudinal bone growth. *J. Anat.* **87**, 228–236 (1953).
16. J. Baron, Z. Huang, K. E. Oerter, J. D. Bacher, and G. B. Cutler, Jr., Dexamethasone acts locally to inhibit longitudinal bone growth in rabbits. *Am. J. Physiol.* **263**, E489–E492 (1992).
17. K. E. Oerter, P. J. Munson, J. D. Bacher, G. B. Cutler, Jr., and J. Baron, Linear growth in the rabbit is continuous, not saltatory. *Endocrinology (Baltimore)* **134**, 1317–1320 (1994).

88 Chapter 2 Longitudinal Bone Growth: Experimental Methods

18. J. Baron, K. O. Klein, M. J. Colli, J. A. Yanovski, J. A. Novosad, J. D. Bacher, and G. B. Cutler, Jr., Catch-up growth after glucocorticoid excess: A mechanism intrinsic to the growth plate. *Endocrinology (Baltimore)* **135**, 1367–1371 (1994).
19. J. Baron, K. O. Klein, J. A. Yanovski, J. A. Novosad, J. D. Bacher, M. E. Bolander, and G. B. Cutler, Jr., Induction of growth plate cartilage ossification by basic fibroblast growth factor. *Endocrinology (Baltimore)* **135**, 2790–2793 (1994).
20. O. G. P. Isaksson, J. O. Jansson, and I. A. M. Gause, Growth hormone stimulates longitudinal bone growth directly. *Science* **216**, 1237–1238 (1982).

3

Measurement of Steroid Receptor Binding to DNA

Franklin G. Berger

*Department of Biological Sciences
University of South Carolina
Columbia, South Carolina 29208*

Gordon Watson

*Children's Hospital
Oakland Research Institute
Oakland, California 94609*

INTRODUCTION

Steroid receptors form a large superfamily of ligand-dependent DNA binding proteins that function in the modulation of gene transcription (for reviews, see Refs. 1–4). Such control of gene expression appears to be the primary mechanism by which steroid receptors play a role in cell growth, development, and differentiation in eukaryotic organisms. Receptor modulation of transcription occurs through binding to specific DNA elements, called steroid response elements; such binding leads to either the activation or repression of RNA synthesis at nearby transcriptional start-sites. Over the last decade, there has been a virtual explosion of information on the structure/function relationships for a variety of steroid receptors, and we now have a fairly detailed picture of the complex mechanism by which receptors enter the nucleus, bind to steroid response elements, and modulate the transcription process (1–4).

Three classes of steroid receptors are currently recognized, and are distinguished on the basis of the DNA sequences of their corresponding response elements, along with the amino acid sequences of domains within them that bind these elements (1,3,4). The first class includes the receptors for glucocorticoids, mineralocorticoids, progesterone, and androgens. The receptors for these hormones bind response elements having consensus

sequence AGAACA NNN TGTTCT, consisting of imperfect inverted repeats separated by three base-pair gaps. The second class comprises the receptors for thyroid hormone, retinoids, and vitamin D, as well as others. This class recognizes a response element containing inverted, everted, or direct repeats having consensus sequence TGACCT and separated by 0–8 nucleotides. Finally, estrogen receptors, which can be considered a subgroup of the second class, bind a response element that is an inverted repeat separated by a three-nucleotide gap; its consensus sequence is GGTCANNN TGACC (1–4).

Critical to the action of steroid receptors is their ability to recognize and bind their cognate response elements. This property is conferred by the DNA binding domain of the protein, which is one of six domains comprising all receptors. The DNA binding domain is approximately 70 amino acids in length, is highly conserved, and folds into two zinc-finger motifs (1–4). Interestingly, three amino acids located at the base of the first finger mediate the receptors' ability to distinguish among various steroid response elements (5).

In this review, we summarize three commonly used methods (mobility shift analysis, DNase I footprinting, and methylation interference) to experimentally measure the binding of steroid receptors to DNA. These methods, which are broadly utilized for analysis of DNA/protein interactions in general, are amenable to use with crude extracts of cell nuclei, as well as with purified preparations of receptors. We refer the reader to Sambrook *et al.* (6) and Ausubel *et al.* (7) for additional details on the protocols described herein.

MOBILITY SHIFT ANALYSIS

DNA fragments bound to receptor protein migrate through an electrophoretic gel more slowly than unbound fragments. This so-called mobility shift provides a basis for identifying complexes between DNA and proteins, and has been very useful in studies of steroid receptor binding to DNA (8–10). Mobility shift assays are relatively simple, rapid, and sensitive, provided that a few precautions are taken to control for nonspecific binding. However, the assay does have limitations. For assays with crude nuclear extracts, the receptor/DNA complex must be at high enough concentrations to be detectable. This is not always the case for steroid receptors. In addition, the complex must be able to survive conditions for gel electrophoresis. Finally, the procedure measures simple complex formation without providing information on the specific region of DNA bound or the actual points of contact between the receptor and the DNA. The accurate identification of the

nucleotides involved in receptor recognition and binding requires other protocols.

Materials

- DNA fragment containing putative binding site
- DNA labeling system, for example, [γ - ^{32}P]ATP and T4 polynucleotide kinase or an [α - ^{32}P]dNTP and the Klenow fragment of DNA polymerase
- Nondenaturing, low-ionic-strength polyacrylamide gel, for example, 4–6% polyacrylamide gel in Tris-acetate or Tris-borate
- Nonspecific DNA, for example, poly (dI-dC)
- Steroid receptor protein, for example, crude nuclear extract or partially purified receptor
- 5 \times HEPES binding buffer (50 mM HEPES-KOH, pH 7.9, 10 mM MgCl_2 , 50% glycerol, 250 mM KCl, 5 mM DTT, 0.5% Triton X-100).

Procedures

Binding Reaction

A variety of reaction mixtures are compatible with DNA/receptor binding. Individual components of the reaction mix must usually be optimized. The HEPES buffer listed here is a reasonable start. Glycerol and Triton X-100 are necessary for loading the sample on the gel; however, the Triton X-100 can be eliminated if it interferes with complex formation. A typical binding reaction contains 5000–20,000 cpm of DNA probe (25–500 pg of DNA, depending on the specific activity), buffer mixture, 0.1–2.0 μg of nonspecific DNA, 1 ng purified receptor, or 20 μg crude extract protein. For the nonspecific DNA, synthetic poly (dI-dC) or poly (dA-dT) is preferred depending on whether the DNA binding site is AT- or GC-rich, respectively. Total DNA (eg., *E. coli* or salmon sperm) can also be used, but it may compete somewhat with specific binding to the probe. It is important that the labeled DNA and the receptor protein not be mixed before the nonspecific DNA is added. If nonspecific binding seems to be a problem, the receptor protein preparation can be incubated with the nonspecific DNA for 15 min before adding the specific, labeled DNA. The final reaction volume is 10–15 μl and incubation is generally 15–30 min at a temperature anywhere from 0° to 30°C. Lower temperatures can retard dissociation of receptor/DNA complexes, but may also stabilize nonspecific binding.

Electrophoresis

After incubating the binding reaction mixture, samples should be loaded on the prerun gel. Bromophenol blue tracking dye can be loaded in a separate lane. Labeled DNA size markers in the outside lanes are also useful. Samples can be run into the gel at higher voltage (e.g., 250 V) for 3–5 min and then allowed to separate at lower voltage (e.g., 150 V) for 1.5–4 hr. The voltage depends on the temperature of the gel, which in turn depends on the current and the dissipation of the heat generated. If the gel is cooled during the run, a higher voltage can be used. The gel should not be allowed to heat up to the point that it feels warm, since this may increase the rate of receptor/DNA complex dissociation. The amount of time will depend on the voltage, the running buffer, and the size of the DNA fragment. If the DNA probe is less than 70 base pairs (bp), electrophoresis should be stopped well before the bromophenol blue reaches the bottom of the gel.

Detection of Bands

After electrophoresis, the gel is transferred to filter paper and dried under vacuum. Positions of labeled DNA bands can be monitored by autoradiography or phosphorimaging.

Comments

Mobility shift assays require labeled DNA fragments of high purity and relatively small size. In general, the shift in mobility is more dramatic as the size of the fragment containing the binding site decreases. The migration of a large DNA fragment may be shifted only imperceptibly by the binding of receptor at a single site. In addition, larger fragments are bigger targets for nonspecific binding. Thus, the practical limits for DNA size are between about 20 and 300 bp.

The source of a DNA fragment containing a putative binding site can be cloned DNA, polymerase chain reaction (PCR)-amplified DNA, or annealed synthetic oligonucleotides. In any case, it is necessary that the DNA fragment be labeled (usually by end-labeling) and purified by gel electrophoresis (6,7). It is important that the labeled DNA be homogeneous and migrate as a single, discrete band.

Theoretically, any cell that responds to a given steroid hormone should be a source of receptor for that hormone. In reality, steroid receptor proteins are often present at too low a concentration to make crude cellular or nuclear extracts effective in binding studies. Thus, partial purification and/

or enrichment of the receptor may be required. Since some receptors are rather unstable under purification conditions, this also can be a problem. However, many steroid receptors cDNAs have been cloned and can be expressed at elevated levels in transfected cells (either bacterial or eukaryotic).

It is not always necessary or even desirable to use a complete receptor in binding studies. A wide variety of truncated, mutated, and chimeric receptors have been used effectively in mobility shift assays (11). It is necessary, however, that the DNA binding domain of the protein be intact. The hormone binding domain is not essential for receptor binding to its response element; however, in the presence of this domain, the addition of steroid hormone can have a marked effect on complex formation (12,13).

The polyacrylamide gel provides for the quick and efficient separation of bound from free DNA in an electrophoretic field. Conditions that destabilize specific binding, such as high ionic strength or denaturants, must be avoided. The ideal conditions, which must be determined empirically, should maximize separation, discourage nonspecific binding, and minimize dissociation of specific receptor/DNA complexes. Typically, a 4% acrylamide gel is used, although 6% gels are preferred when the DNA probe is very small (i.e., near 20 bp). Commonly used ratios of acrylamide : bisacrylamide vary from 30:1 to 80:1. Buffer concentrations range from 10 to 90 mM Tris-acetate or Tris-borate (at pH 8) and contain 1–2 mM EDTA. Gels often contain 2.5% glycerol and sometimes 0.1% Triton X-100. The running buffer for electrophoresis should be the same ionic strength as the gel, and gels should be prerun (90 min at 100 V for a 16-cm gel) before loading samples. It is necessary to recirculate the buffer for the lower-ionic-strength gels.

Once satisfactory conditions for the mobility shift have been established for a given DNA probe and receptor preparation, a competition experiment should be performed to confirm that a shifted band is due to specific binding. First, it is important that the DNA probe be in molar excess over the receptor protein. To determine this, a set of samples having identical amounts of DNA probe and a wide range of receptor protein concentrations are run. Typically, little or no band shift will be observed at the lowest receptor concentration, and virtually complete shift will occur when the receptor is in excess. (Excess protein, particularly if the receptor is not purified, will usually result in a diffuse band of large, nonspecific complexes. These migrate more slowly than either free DNA or specific complexes.) The amount of label in the receptor/DNA band should increase with increasing receptor concentration, plateau as the receptor molar concentration approaches the DNA molar concentration, and then decrease again as the protein concentration becomes excessive, and large nonspecific com-

plexes form. The amount of receptor that provides one-half the maximal signal in the specific, receptor/DNA band is a good working concentration.

For competition experiments, cold DNA identical to the labeled DNA should be added to the binding reaction at a concentration that is 3–250 times the amount of labeled DNA. Receptor should not be added until the competitor and labeled DNA have been preincubated. Increasing amounts of competitor will diminish the signal for specific binding. Any band(s) whose intensity is not affected by cold competitor represent a nonspecific complex.

The relative binding affinities of two different DNAs can be assessed by comparing their abilities to act as competitors. Thus, if it takes five times more of one cold competitor DNA to effectively compete with the labeled DNA, then its relative binding affinity is considered to be 20% less.

The presence of steroid receptor in a shifted complex can be verified with antibody against the receptor. The mobility shift assay is run with and without the addition of the antibody to the binding reaction. If the antibody interferes with the binding of receptor to its DNA site, the band for the complex should disappear. If the antibody does not interfere with DNA binding, a “supershift” will appear, corresponding to a complex with lower mobility as a consequence of the added mass of the antibody.

Another variation of the mobility shift assay is to label the receptor protein rather than the DNA. Usually this is technically more difficult and requires purified receptor. The advantage is an increase in assay sensitivity (14).

DNASE I FOOTPRINTING

As mentioned earlier, one drawback of mobility shift analysis is that it does not provide information on the specific regions or sequences within a DNA molecule that are bound by a protein ligand. Such information is, of course, important in the functional analysis of DNA binding proteins. DNase I footprinting, or protection mapping, is a relatively convenient method for defining the specific sequences involved in protein binding (7,15). The technique is based on the observation that bound proteins protect the phosphodiester backbone of DNA against cleavage by the endonuclease DNase I. This protection can be readily observed by gel electrophoresis of DNA fragments generated by partial DNase I digestion of protein/DNA complexes. Generally, the DNA is end-labelled with ^{32}P at one end, so that the sizes of the resulting fragments represent the distance between the labeled-end and DNase I cleavage sites. Thus, the exact locale of protected regions that result from bound protein(s) can be ascertained. Such protected

regions define the specific binding sites for the protein on the DNA. DNase I footprinting has been broadly used to define the specific nucleotide sequences comprising steroid response elements (16–21).

Materials

- 2X binding buffer (20 mM HEPES, pH 7.9, 4% polyvinyl alcohol, 20% glycerol, 0.2 mM Na₂EDTA, and 1 mM DTT)
- Poly (dA-dT) (1 mg/ml in 10 mM Tris-Cl, pH 8.0, containing 1 mM Na₂EDTA)
- Salt solution (10 mM MgCl₂, 5 mM CaCl₂)
- KCl (1.0 M)
- End-labeled DNA, gel purified and containing a single end-label (7)
- DNase I stock (250 μg/ml in 50 mM TRIS-Cl, pH 7.2, 10 mM MgSO₄, 1 mM DTT, 50% glycerol)
- Stop buffer (1% SDS, 200 mM NaCl, 20 mM Na₂EDTA, 40 μg/ml tRNA, pH 8.0)
- 10X TBE buffer (0.9 M Tris borate, pH 8.3, 20 mM Na₂EDTA)
- Electrophoresis loading buffer (9 mM Tris borate, pH 8.3, 0.2 mM Na₂EDTA, 7 M urea, 0.05% xylene cyanol and bromophenol blue)
- Sequencing gel (6% acrylamide, 7 M urea in 90 mM Tris borate, pH 8.3, containing 2 mM Na₂EDTA)

Procedures

Binding Reaction

The reaction mixture contains 25 μl 2X binding buffer, 0.5 μl poly (dA-dT), 2–4 ng end-labeled fragment (approximately 10,000–15,000 cpm), 3 μl KCl, and receptor protein in a total volume of 50 μl. Mixtures are incubated on ice for 20 min. A control containing no receptor is run in parallel.

DNase I Digestion

Following the incubation, 50 μl of the salt solution and 5 μl of appropriate dilutions of DNase I (containing 0.0005–0.1 Kunitz units/ml) are added. Following a 2-min incubation on ice, digestion reactions are terminated by addition of 100 μl stop buffer. Mixtures are extracted once with phenol/chloroform; nucleic acids are precipitated and washed in ethanol, and dissolved in 5 μl electrophoresis loading buffer.

Electrophoresis

A standard 6% sequencing gel (7) in 1X TBE buffer is prerun for 30 min, and samples are loaded following denaturation of the DNA fragments for 2–5 min at 90°C. Electrophoresis is run under standard conditions of sequencing gels (7).

Detection of Footprint

Following the electrophoresis, the gels are dried and autoradiographed. Footprints are recognized as regions where band intensities are significantly reduced in receptor-containing samples relative to control samples containing no protein.

Comments

The location of the footprint on the DNA template, that is, the exact nucleotides protected from DNase I cleavage by the receptor protein, can be defined by the use of a “G+A ladder.” This involves chemical cleavage of the template at guanine and adenine residues, and running the resulting fragments on the sequencing gels in parallel with the DNase I-treated samples (15). Approximately 200,000 cpm of the end-labeled template are diluted into 30 μ l water, and 2 μ l of 1 M pyridine formate, pH 2.0, are added. After incubation at 37°C for 10–20 min, 150 μ l of 1 M piperidine are added, and the sample is further incubated at 90°C for 30 min. DNA fragments are precipitated twice with ethanol, dissolved in water, lyophilized, and resuspended in 5 μ l electrophoresis loading buffer. The location of footprinted regions is compared to the G+A ladder on the same gel; based on the known sequence of the template DNA, nucleotides that are included in the protected region can be defined.

A significant amount of experimentation is usually required to tailor conditions to the particular DNA and receptor protein utilized. Thus, parameters such as DNase I concentration, time of digestion, receptor concentration, and so on must be varied to maximize conditions for observation of footprint patterns. In addition, other nonspecific competitors, such as poly (dI-dC), calf thymus DNA, or bacterial plasmids, should be tried.

When using crude protein preparations, such as nuclear extracts, higher levels of DNase I are generally required compared to when purified proteins are utilized. This is due to inhibition of DNase I in crude protein preparations. Such variation in rates of cleavage can make

comparisons between control and protein-containing samples a bit more problematic. Thus, care should be exercised in defining footprinted regions when using crude protein preparations.

The DNA template for footprint analysis should be of high quality. In particular, it should be free of single-strand nicks that may be mistaken for DNase I cleavage sites. The integrity of the DNA can be readily monitored by running the footprinting procedure without addition of DNase I; all the DNA should remain near the top of the gel, with no evidence of fragmentation. Problems of DNA integrity can, in general, be avoided by using freshly prepared, gel-purified templates.

Specificity of footprints can be assessed by competition experiments, as described for mobility shift assays (see earlier discussion). Preincubation of the labeled DNA with an excess of unlabeled template prior to the addition of receptor will result in competing out, or removal, of specific footprints. In addition, as with mobility shift assays, such competition can be useful in defining relative affinities between receptor and various response elements.

METHYLATION INTERFERENCE

Chemical modification of DNA bases that come in close contact with a bound protein can impact on that protein's affinity for its binding site on the DNA. Thus, for example, the methylation of purine residues by dimethyl sulfate, and the resulting interference with protein binding, provides an opportunity to precisely define guanine and adenine residues that lie at or near the protein's binding site (7,22). In what is called a methylation interference assay, DNA is partially methylated with dimethyl sulfate, mixed with receptor, and separated into bound and free DNA using the mobility shift protocol. Both the bound and free DNAs are recovered, cleaved at methylated guanine residues with piperidine, and fractionated on a sequencing gel. Gaps in the fragmentation patterns with bound DNA as compared to free DNA represent regions where proteins bind, since such regions must remain unmethylated (and therefore resistant to piperidine) for complex formation to occur.

Methylation interference has a principal advantage over DNase I footprinting in allowing identification of specific bases involved in the interaction between a protein and its binding site on DNA. A number of studies have utilized methylation interference to define critical guanine residues within the response elements for steroid receptors (9,12,13,22,23).

Materials

Solutions and materials for mobility shift assay (see earlier)

Dimethyl sulfate (DMS)

DMS reaction buffer (50 mM Na cacodylate, pH 8.0)

1 mM Na₂EDTA,

DMS stop buffer (1.5 M sodium acetate, pH 7.0, 1 M

β -mercaptoethanol

1 M piperidine

10 mg/ml tRNA

Procedures

DNA Probe

The DNA fragment for methylation interference should be gel-purified, intact, and labeled at only one end (7). Labeled DNA (about 1×10^6 cpm in 5–10 μ l buffer) is added to 200 μ l DMS reaction buffer and 1 μ l DMS. Partial methylation occurs during incubation for 5 min at room temperature, after which 40 μ l of DMS stop buffer and 1 μ l tRNA carrier are added. The methylated DNA is precipitated and washed several times in ethanol (7).

Isolation of DNA/Protein Complexes

The mobility shift assay (see earlier) is used to separate protein-bound from free DNA. The assay is scaled up to allow for the recovery of both free and protein-bound DNA from the gel. The positions of bound and unbound DNA are determined by autoradiography, and both DNAs are cut out and electroeluted (6,7). Alternatively, the bands can be electroblotted onto DEAE paper, identified by autoradiography, cut out, and eluted (7). The recovered DNA is extracted with phenol/chloroform, and precipitated with ethanol.

Chemical Cleavage of DNA

Piperidine cleavage of the recovered DNA is accomplished by resuspending the DNA pellet in 100 μ l of 1 M piperidine, and heating at 90°C for 30 min. Similar to DNase I footprinting (see earlier), the resulting fragments are lyophilized, suspended in gel loading buffer, denatured, and fractionated on a sequencing gel.

Detection of Band Patterns

Acrylamide gels are dried and autoradiographed. Strong bands result from cleavage at guanine residues, whereas weak bands represent cleavage at

adenine residues. The latter are sometimes too weak to be useful. The pattern resulting from free DNA should correspond exactly to the expected pattern based on the known sequence of the DNA substrate used in the assay. Gaps in the banding patterns of receptor-bound, as compared to free, DNA indicate guanine or adenine residues where methylation prevents receptor binding. Such gaps therefore represent points of contact or near contact between the receptor and its DNA binding site.

Comments

On average, each DNA molecule should contain a single methyl group. This can be tested by cleaving the DNA with piperidine (see the following), and running the resulting fragments on a sequencing gel. There should be a series of strong bands corresponding to cleavage at methylated guanine residues; weak bands corresponding to cleavage at methylated adenine residues may also be present. An overmethylated probe will show skewing of bands toward the bottom of the gel, with little or no intact probe near the top; a shorter incubation time with DMS should be used. An undermethylated probe remains uncleaved; in such cases, longer methylation times are necessary.

As with DNase I footprinting, use of probes with a single end-label makes determining the exact location of gaps along a DNA strand relatively simple. However, with such probes only one strand of the DNA can be analyzed. It is useful to determine contact points on both DNA strands, which can be done by repeating the experiment with DNA labeled at the opposite end. Though it is possible to perform the experiment with DNA labeled at both ends (13), the resulting band pattern will be more complex since fragments from the two strands will be superimposed.

Like DNase I footprinting, methylation interference has an advantage over mobility shift in that it identifies areas of contact between DNA and receptor protein. Compared to footprinting, methylation interference is more precise in identifying points of contact. It is also forgiving since all the DNA in the shifted band will be bound to receptor. Thus, unlike footprinting, it is not necessary to saturate the DNA with receptor in the binding reaction.

The concentration of DNA binding proteins of interest can be a limiting factor in methylation interference, since more receptor/DNA complex is required than for other procedures. This is because the complexed DNA must be recovered from one gel, processed, and run on a second gel. The use of purified proteins is advisable, where possible.

REFERENCES

1. R. M. Evans, *Science* **240**, 889 (1988).
2. M. Beato, *Cell (Cambridge, Mass.)* **56**, 335 (1989).

3. B. W. O'Malley, *Mol. Endocrinol.* **4**, 364 (1990).
4. B. M. Forman and H. H. Samuels, *Mol. Endocrinol.* **4**, 1293 (1990).
5. S. Mader, V. Kumar, H. de Verneuil, and P. Chambon, *Nature (London)* **338**, 271 (1989).
6. J. Sambrook, E. F. Fritsch, and T. Maniatis, "Molecular Cloning: A Laboratory Manual." Cold Spring Harbor Laboratory, Cold Spring Harbor, New York, 1989.
7. F. M. Ausubel, R. Brent, R. E. Kingston, D. D. Moore, J. G. Seidman, J. A. Smith, and K. Struhl, "Current Protocols in Molecular Biology." Wiley, New York, 1990.
8. D. Metzger, J. H. White, and P. Chambon, *Nature (London)* **334**, 31 (1988).
9. S. Y. Tsai, J. Carlstedt-Duke, N. L. Weigel, K. Dahlman, J.Å. Gustafsson, M.-J. Tsai, and B. W. O'Malley, *Cell (Cambridge, Mass.)* **55**, 361 (1988).
10. J. Tan, K. B. Marschke, K.-C. Ho, S. T. Perry, E. M. Wilson, and F. S. French, *J. Biol. Chem.* **267**, 4456 (1992).
11. M. C. Rhee, D. D. Dimaculangan, and F. G. Berger, *Mol. Endocrinol.* **5**, 564 (1991).
12. V. Kumar and P. Chambon, *Cell (Cambridge, Mass.)* **55**, 145 (1988).
13. M. Schauer, G. Chalepakis, T. Willmann, and M. Beato, *Proc. Natl. Acad. Sci. U.S.A* **86**, 1123 (1989).
14. A. J. Adler, A. Scheller, Y. Hoffman, and D. M. Robins, *Mol. Endocrinol.* **5**, 1587 (1991).
15. B. Leblanc and T. Moss, *Methods Mol. Biol.* **30**, 1 (1994).
16. F. Payvar, D. DeFranco, G. L. Firestone, B. Edgar, O. Wrangé, S. Okret, J.Å. Gustafsson, and K. R. Yamamoto, *Cell (Cambridge, Mass.)* **35**, 381 (1983).
17. U. Danesch, B. Gloss, W. Schmid, G. Schütz, R. Schüle, and R. Renkawitz, *EMBO J.* **6**, 625 (1987).
18. J. Sap, A. Muñoz, J. Schmitt, H. Stunnenberg, and B. Vennström, *Nature (London)* **340**, 242 (1989).
19. J. Drouin, M. A. Trifiro, R. K. Plante, M. Nemer, P. Eriksson, and Ö. Wrangé, *Mol. Cell. Biol.* **9**, 5305 (1989).
20. P. De Vos, F. Classens, J. Winderickx, P. Van Dijck, L. Celis, B. Peeters, W. Rombauts, W. Heyns, and G. Verhoven, *J. Biol. Chem.* **266**, 3439 (1991).
21. E. P. Slater, G. Redeuilh, and M. Beato, *Mol. Endocrinol.* **5**, 386 (1991).
22. L. Klein-Hitpass, S. Y. Tsai, G. L. Greene, J. H. Clark, M.-J. Tsai, and B. W. O'Malley, *Mol. Cell. Biol.* **9**, 43-49 (1989).
23. L.-H. Wang, S. Y. Tsai, R. G. Cook, W. G. Beattie, M.-J. Tsai, and B. W. O'Malley, *Nature (London)* **340**, 163 (1989).

4

Hypophysial Grafts beneath the Renal Capsule: A Model to Study Endocrine Control Systems

Gary T. Campbell

Martha A. Steele

Charles A. Blake

*Department of Cell Biology
and Neuroscience*

University of South Carolina

School of Medicine

Columbia, South Carolina 29208

This chapter provides an overview of the preparation of allografts of pituitary tissue beneath the renal capsule of the Golden Syrian hamster and a synopsis of the utility of the model for studying endocrine control systems. Because the nature of this publication precludes an extensive reference list, we ask for the indulgence of many authors whom we were not able to cite adequately and refer the reader to the review by Adler (1).

HISTORY AND UTILITY OF PITUITARY GRAFTS

Grafting pituitary tissue into ectopic sites in a variety of hosts has been used as a model to study diverse physiological control systems and the

genesis of pathological states for over 50 years. Early use of pituitary grafts aided in the elucidation of the concept of hypothalamic and neurohormonal control of adenohypophysial cell survival and function. One tenet of this concept is that prolactin (PRL) release by the adenohypophysis is inhibited tonically by the central nervous system. Thus, one hallmark of pituitary grafts is that in most circumstances the lactotrophs in the grafts release PRL excessively. This situation provided a unique opportunity for many investigators to study the mechanisms controlling PRL secretion.

The early investigations using pituitary grafts in the rat established that with the exception of the lactotroph, the other pituitary cell types atrophy in the ectopic site and release only minimal amounts of hormone (1). By using allografts of adult adenohypophysial tissue in the hamster, we have shown trophic influences of luteinizing hormone releasing hormone (LHRH) on gonadotrophs, growth hormone releasing hormone (GHRH) on somatotrophs, and corticotrophin releasing hormone (CRH) on corticotrophs (2–4). These findings supplement prior results indicating the cell-specific trophic effects of the hypothalamic neurohormones.

The use of pituitary allografts also has contributed to our understanding of the development of the adenohypophysis. For instance, studies in the hamster indicate that less than 1% of the cells in the adenohypophysis of a hamster on Day 14 of gestation contain immunoreactive luteinizing hormone (LH), whereas, the gland of a 14-day-old hamster contains approximately 24% LH-containing cells. When hypophyses are removed from similar prenatal hamsters and placed beneath the renal capsule of an adult hypophysectomized-orchidectomized hamster for 16 days, approximately 21% of the graft cells contain LH (5). These findings suggest that the future development of “pregonadotrophs” during the first 2 weeks of life in the hamster is seemingly independent of the trophic influence of the hypothalamus. This is not the case for synthesis of the sister gonadotrophin, follicle-stimulating hormone (FSH), in cells containing LH. Our work indicates that stimulation of the gonadotrophs in the graft with LHRH is required for the accumulation of FSH mRNA in the graft and FSH in LH-containing cells (5–7). This graft model is amenable to studying the mechanisms responsible for continued LH synthesis in cells deprived of LHRH, the amplitude and frequency requirements for effective LHRH induction of FSH synthesis, and the possible influence of other neurohormones such as neuro-peptide Y on gonadotroph development.

Other results have contributed to the understanding of the development of other pituitary cell types. Donor hypophyses removed from neonatal hamsters contain abundant somatotrophs but are virtually devoid of lactotrophs. When allografts of such donor tissue are examined after 8 weeks, the allografts contain appreciable numbers of somatotrophs and lactotrophs.

However, the allografts release minimal amounts of growth hormone (GH) and PRL (8). The lack of GH release most likely can be attributed to the absence of stimulation of the grafts by GHRH. However, the lack of PRL release is perplexing. Previously unpublished results show that donor adenohypophysial tissue removed from 15-day-old hamsters (this donor tissue contains the full complement of lactotrophs) and transplanted beneath the right renal capsules of adult hypophysectomized-orchidectomized hamsters for 14 days releases appreciable amounts of PRL (Table I). Allografts of neonatal hypophyses did not elevate serum PRL levels above those in hypophysectomized-orchidectomized hamsters that had undergone sham transplantation (Table I). These results suggest that the capability of lactotrophs to hypersecrete PRL, after removal from proximity to the hypothalamus, is dependent on either the development of the lactotroph in the normal position *in situ* or exposure of the lactotroph to other stimuli existing during early postnatal development in the hamster.

We think this brief synopsis, focusing on the results of our work with pituitary allografts, indicates the utility of this model for studying endocrine control mechanisms governing pituitary cell function and development. We also have pointed out some of the future lines of research that could be done with this model.

It should be understood that pituitary allografts can be used to provide PRL replacement with accompanying minimal amounts of other pituitary hormones in hypophysectomized hosts or to produce hyperprolactinemia

TABLE I. Serum PRL Levels in Hypophysectomized-Orchidectomized Hamsters Bearing Allografts of Pituitary Glands Removed from Donor Hamsters of Different Ages and Sexes^a

Age of donor	Sex of donor	No. of donor glands/host ^b	No. of hosts	Serum PRL (ng PRL/ml serum)
1 day	Male	10	6	3.3 ± 0.6 ^c
1 day	Female	10	6	2.5 ± 0.5
15 days	Male	5	6	11.8 ± 0.6 ^d
15 days	Female	5	6	12.6 ± 0.9 ^d
50 days	Male	1	12	11.9 ± 0.7 ^d
50 days	Female	1	13	12.4 ± 1.1 ^d

^a The donor tissue was hypophyses removed from 1-day-old hamsters or adenohypophyses removed from 15- or 50-day-old hamsters. Allografts were in place for 14 days.

^b The number of donor glands was varied to equalize the amount of graft tissue.

^c Mean ± SE.

^d These values differ significantly ($P < 0.05$) from the values obtained with allografts of hypophyses removed from 1-day-old hamsters. Serum PRL levels in hypophysectomized-orchidectomized hamsters without hypophysial allografts (sham-transplanted) ranged from 1 to 3 ng/ml serum.

in almost any type of host. In fact, in hamsters, circulating PRL levels can be varied quite easily by selecting the type of donor gland and the numbers of donor glands (Tables I–III). The majority of studies using pituitary allografts in any species have utilized this ability to manipulate circulating PRL levels to study the physiological and pathological roles of PRL. The preponderance of studies have dealt with PRL and reproduction. This work has culminated in the acceptance of PRL's role in the maintenance of pregnancy, regulation of the mammary gland, regulation of gonadal receptors for gonadotrophins, and controlling gonadotrophin secretion. Other investigators have used pituitary allografts to uncover possible physiological roles of PRL in immune function, calcium regulation, and cardiovascular and renal function. Additionally, some of the earliest results implicating PRL in the growth of mammary tumors were obtained using pituitary isografts. Thus, the pituitary-grafted animal has proven to be quite valuable in studying the many actions of PRL (see Ref. 1 for review).

COMPARISON OF THE PITUITARY ALLOGRAFT MODEL WITH STUDIES USING PITUITARY TISSUE *IN SITU* OR *IN VITRO*

In the intact animal, it is often impossible to ascertain whether even a locally administered agent influences pituitary activity by acting directly on the gland or via the central nervous system (CNS). Although disruption of the hypothalamic-pituitary unit is an obvious approach to this set of questions, direct and indirect interplay between the two units (CNS and pituitary) is thought necessary to keep the secretory activities of each in a range in which normal physiological control mechanisms can operate. To date, two genres of methods, designed to expose the pituitary gland to diminished hypothalamic influence, have been applied to the study of regulation of pituitary development and function.

The first category is *in vitro* approaches using incubation of pituitary primordia or pituitary tissue fragments or cell culture of dispersed or cloned pituitary cells. All suffer from inadequacies. Problems due to diffusion into and out of tissue fragments may well account, in part, for the discrepancies that exist between the concentrations of hormones effective *in vitro* and those that appear to circulate in the blood. Dispersed-cell culture partially eliminates diffusion problems, but it suffers from needing defined studies to establish the relevance of findings in cells *in vitro* that have undergone some degree of dedifferentiation or transdifferentiation. Cell culture, using "homogeneous" cell types or cloned cells, completely obviates the possible role(s) of cytoarchitectural arrangements between heterogeneous cell types

in regulating secretory activity. Recent studies using mixtures of “homogeneous” pituitary cell types have partially overcome this inadequacy. Studies using cultured pituitary cells generally are limited to short time intervals because of diminished viability of the cells *in vitro*. Because the duration of binding of endogenous humoral stimuli from the CNS or other tissues and any latent effects these materials may have on pituitary cells existing *in vitro* are unknown, total independence of influences by persistent residual endogenous stimuli to the pituitary cells *in vitro* cannot yet be inferred.

The other genre of method to study pituitary tissue isolated from hypothalamic influence is the use of pituitary tissue transplanted into different ectopic sites in suitable hosts. We have used a preparation in which pituitary tissue removed from hamsters of various ages is transplanted beneath the renal capsules of adult hamsters in different endocrine states. We originally favored the idea that, although we could not regulate all the humoral substances reaching the tissue, at least they would gain access to the tissue via the normal conduits. The investigator can control the number of putative agents reaching the tissue by surgically manipulating the host. For instance, in a hypophysectomized host with one or more pituitary target glands also removed, this model consists of malregulated adeno-hypophysial cells because the cells are not exposed to high concentrations of hypothalamic factors, hormones from the adeno-hypophysis *in situ*, and adeno-hypophysial target gland hormones. The investigator can then supply the agent(s) to be tested in various manners. Pituitary allografts in the hamster are particularly suited for chronic studies because the allografts will survive for nearly a year (322 days) (Figure 1). Additionally, the allograft cells (almost exclusively adeno-hypophysial cells) retain the capacity to form cytoarchitectural arrangements between themselves. Although the allograft model may not be well suited for studying the intracellular mechanisms induced by a particular agent, we think it is optimal for investigating the activity of an agent in a near physiological setting. The following section will deal with minimizing the other drawbacks of this model, that is, optimizing the experimental model to fit the needs of the experiment.

TECHNIQUES AND CONSIDERATIONS FOR GRAFTING PITUITARY TISSUE BENEATH THE RENAL CAPSULE

Methodology

Although transplantation of pituitary tissue into an ectopic site in animals the same age as the donors would be an improvement in technique, we generally use adult animals as hosts because of the convenience of the

surgery and neonates as donors because we especially are interested in the development of the adeno-hypophysial cell types. Although we have not attempted it thoroughly, it is our belief that transplanting tissue beneath the renal capsule of a neonatal hamster would not be feasible. Adult Golden Syrian hamsters of the outbred LVG strain are purchased from Charles River Laboratories, Inc. (Wilmington, MA). The animals to be used as hosts can be housed either individually or communally under appropriate conditions before grafting if they have not undergone recent surgery. Hosts that have been hypophysectomized or been subjected to other surgery should be housed individually at least until sutures and wound clips are removed and surgical wounds are totally healed. Charles River Laboratories, Inc. will perform hypophysectomies and other surgical procedures on animals prior to shipping.

On the day of grafting the host hamster is anesthetized with sodium pentobarbital (75 mg/kg of body weight, intraperitoneally). This dose anesthetizes the hamster for approximately 2 hr. The hamster is weighed and marked for identification. Generally, we use the right kidney as the transplantation site. However, for transplantations of multiple glands from adult donors we use both kidneys as transplantation sites. The following procedure is adaptable for both kidneys. The fur over the right flank is shaved with clippers and the skin cleansed with 70% alcohol and betadine. The hamster then is placed on surgical gauze in front of the surgeon in a well-illuminated area.

The surgical instruments needed are the following: coarse scissors for cutting through the skin, fine scissors for cutting through the muscle, coarse forceps for moving fat and lifting out the kidney, and fine forceps for nicking the renal capsule and placing the donor tissue beneath the renal capsule. The individual doing the surgery can elect to use straight or curved fine forceps. Some individuals prefer to file down the sharp tips of the fine forceps. This minimizes puncturing the renal tissue and the resultant bleeding. However, it is important not to bend the tips of the forceps in a manner that will prevent the surgeon from grasping the renal capsule with the fine forceps. We generally use one set of surgical instruments to perform numerous transplantations. The instruments are autoclaved before the transplantation procedure begins and rinsed with 70% alcohol between transplantations. The surgeon wears gloves.

The surgeon picks up the hamster skin with forceps in his or her left hand. A 1-cm incision is made through the skin dorsal to the right kidney in a caudal-rostral direction. The hyperpigmented area on the fur of the hamster's flank can be used as a guide, as this should be in the center of the 1-cm incision. A similar cut then is made in the muscle dorsal to the right kidney. The small amount of bleeding is stopped by applying pressure

with a disposable sterile cotton-tipped applicator. The cotton tip of a disposable sterile cotton-tipped applicator (the cotton tip had been soaked in sterile saline) is inserted beneath the kidney on the ventral aspect and the right kidney is gently propped up. Generally, if the surgeon rests the applicator against the hamster, the dorsal-lateral surface of the right kidney will be exposed through the slit of the muscle.

The hamster is put in a position that enables the surgeon to gently grasp the capsule with one pair of fine forceps. If the surgeon is right-handed, this is best done with the *left* hand. With a pair of fine forceps in both the left and right hands, the surgeon slightly picks up the capsule with the *left* hand. Once the capsule is elevated above the kidney tissue the surgeon pokes a small hole in the tent of capsular tissue with the tip of the forceps in the *right* hand. *It is important for the surgeon not to lose grasp of the capsule with the forceps in the left hand from this time until after insertion of all donor tissue. Repeated attempts to pick up the capsule will cause tearing of the capsule and there will be nothing to hold the donor tissue in place.* (On a practice host, the surgeon should release the capsule and the capsule will fall back over the kidney. A small opening in the capsule can be observed readily under well-illuminated conditions). *This preparation should be kept moist with saline and is ready for insertion of the donor tissue.*

It is important that another person time the removal of the donor tissue so that as soon as possible after removal it can be placed beneath the host's renal capsule. Donor hypophyses are removed by standard techniques. Generally, when we use adult hamsters as donors, we remove the neural and intermediate lobes and transplant adenohypophysial tissue only. This also can be done when pituitary glands removed from hamsters 15 days old or older are used for donor tissue. However, it is virtually impossible to remove the neural and intermediate lobes from pituitary glands removed from prenatal or neonatal hamsters. Thus, we transplant the entire gland from these donors. In some instances we transplant multiple pituitary glands, particularly when we are transplanting glands from young donor hamsters. Generally, these will fit beneath the right kidney capsule. After removal, the donor tissue is placed in a small petri dish containing sterile saline. When all donor glands have been removed, the petri dish is given to the surgeon.

It is important that the surgeon learn to place the pieces of donor tissue beneath the renal capsule in as few attempts as possible (see the foregoing). This is best done by initially judging the mass of tissue that will fit into the nick in the capsule. We find it works best if the surgeon picks up that amount of tissue from the petri dish with forceps in the right hand. Then the individual gently inserts the moist tissue through the opening and beneath the capsule a little distance from the opening in a direction that

appears to be to the sides of the opening. It is best to have all pieces of donor tissue adhere to the kidney itself as this will facilitate the tissue "sticking" and minimize necrosis. The surgeon should release the capsule, which generally falls in a manner such that it covers the donor tissue. At this point, if the surgeon places a small drop of sterile saline on the area of the capsule covering the graft and the graft is securely positioned beneath the capsule, the graft will not move. Figure 2 illustrates the preparation at the time of insertion of the donor tissue.

After all donor tissue has been put in place, the surgeon removes the cotton-tipped applicator prop and the kidney usually falls back into place. The muscle is closed with two or three stitches of sterile 3-0 chromic gut surgical suture. It is important not to stitch through any of the attending fat. The skin is closed with metal wound clips and swabbed with betadine, and the animals are allowed to recuperate from anesthesia without any special postoperative care. After surgery the hosts should be housed individually to prevent cannibalism.

Selection of Hosts

We have used adult hamsters of either sex subjected to various other surgical manipulations as hosts depending on the aim of the experiment. We have used *intact* adult male or female hamsters to study the effects of *hyperprolactinemia* on the hypothalamic-pituitary unit *in situ*, the activities of the gonads, and the response of splenocytes to mitogens. Intact males generally make better hosts because they have less fat attendant to the right kidney, which makes the transplant surgery easier, causes less adherence of the kidney to other internal organs, and facilitates finding and removing the graft at the termination of the experiment. Serum PRL levels can be varied easily in these animals by altering the amount of donor tissue allografted. It should be pointed out that intact male hosts with multiple female (Tables II and III) or male adeno-hypophysial allografts gain significantly less body weight than controls. No special care is needed for the intact hosts.

When we wish to obviate the effects of hormones from the pituitary gland *in situ* on allograft responses to various agents given to the hosts, we use *hypophysectomized* hamsters as hosts. This also allows us to more accurately assess the hormonal output by allograft cells using radioimmunoassay for serum hormones. Hypophysectomized hamsters are remarkably healthy. Some of them can gain weight at a rate comparable to that of intact hamsters (9). The drinking water for hypophysectomized hamsters is supplemented with 5.0% sucrose to stimulate drinking because the animals generally display symptoms of lack of antidiuretic hormone.

TABLE II. Serum PRL and ACTH Levels and Body Weight (BW) Changes in Intact Male Hamsters Bearing Autografts of Muscle Tissue or Allografts of Muscle Tissue or of Adenohypophyses Removed from Adult Male or Female Hamsters

Type of graft ^a	Serum		Changes in BW (g)
	PRL (ng/ml) ^b	ACTH (pg/ml)	
1 male muscle piece Autograft (<i>n</i> = 8)	10.8 ± 1.1 ^c	191 ± 24	34.8 ± 2.8
1 male muscle piece Allograft (<i>n</i> = 8)	12.5 ± 1.0	200 ± 35	32.9 ± 3.3
1 male adenohypophysial Allograft (<i>n</i> = 8)	18.1 ± 1.4	161 ± 10	30.3 ± 2.8
1 female muscle piece Allograft (<i>n</i> = 8)	12.4 ± 1.1	154 ± 08	33.5 ± 4.3
1 female adenohypophysial Allograft (<i>n</i> = 8)	38.5 ± 5.0 ^d	198 ± 25	23.6 ± 2.6
4 female muscle pieces Allograft (<i>n</i> = 8)	9.3 ± 2.0	176 ± 10	30.0 ± 1.9
4 female adenohypophysial Allograft (<i>n</i> = 8)	113.8 ± 6.7 ^d	147 ± 04	15.6 ± 2.9 ^d

^a These grafts were in place for 21 days.

^b Serum PRL levels in intact male hamsters without grafts ranged from 7 to 15 ng/ml serum.

^c Mean ± SE.

^d Differ significantly ($P < 0.05$) from all other groups.

TABLE III. Serum PRL Levels and Body Weight (BW) Changes in Intact Male Hamsters Bearing Allografts of Muscle or Adenohypophyses Removed from Adult Female Hamsters

Type of allograft ^a	Serum PRL (ng/ml)	Changes in BW (g)
1 female muscle piece Allograft (<i>n</i> = 8)	15.5 ± 1.2 ^b	11.4 ± 1.2
4 female muscle pieces Allograft (<i>n</i> = 8)	16.1 ± 1.4	9.5 ± 1.6
1 female adenohypophysial Allograft (<i>n</i> = 8)	37.6 ± 4.2 ^c	4.4 ± 1.6 ^c
2 female adenohypophysial Allograft (<i>n</i> = 8)	64.1 ± 5.6 ^c	1.6 ± 0.8 ^c
4 female adenohypophysial Allograft (<i>n</i> = 8)	111.9 ± 9.2 ^c	2.1 ± 0.6 ^c

^a These allografts were in place for 14 days.

^b Mean ± SE.

^c Differ significantly ($P < 0.05$) from groups with muscle allografts.

If the experimental design requires it, other circulating influences on the allograft can be removed by further surgical manipulation of the host. For instance, in our studies on the effects of LHRH on gonadotrophs in the allografts we wished to remove possible influences of hormones from the pituitary gland *in situ* and of gonadal hormones. Thus, we used *hypophysectomized-gonadectomized* hosts. No problems are associated with the use of orchidectomized hosts. However, the prior ovariectomies, which are done through flank incisions, cause problems during the transplantation procedure because of tissue inflammation caused by the prior ovariectomy.

Selection of Donor Tissue

The one consistent thing about our selection of donor tissue is that we use allografts within the outbred LVG strain of hamsters. One reason for this is that inbred hamsters of the LSH strain are no longer available commercially. If one wished to use homografts, one can obtain breeding stock of the LSH strain from the National Institutes of Health. Fortuitously, the putative diminished immunogenicity of endocrine tissue and the immune system of the LVG hamster allows allografts of hypophysial tissue to be accepted quite well. We have studied several thousand allografts and seldom have observed loss of allografts beneath the renal capsule due to immune rejection. This also is evidenced by the long-term survival of allografts. Even in the few times in the past when we did use homografts in LSH hamsters, we did not find that they were better suited than allografts in LVG hamsters for endocrine studies. Autografts of pituitary tissue simply are not feasible in some studies, particularly when the donor tissue is removed from perinatal hamsters. The use of homografts or autografts of adult pituitary tissue would obviate subtle immune disturbances associated with allografts if one were studying immune phenomena.

The selection of the appropriate amount and type of donor pituitary tissue depends on the aim of the experiment. If the aim is to produce varying degrees of *hyperprolactinemia*, then we suggest one use *adenohypophyses removed from adult female hamsters*. *Adenohypophyses removed from adult donors are cut into at least four pieces before insertion beneath the renal capsule to minimize necrosis*. To illustrate this suggestion we refer the reader to Tables II and III. The data in Table II show that: (a) control allografts of pieces of muscle tissue similar in size to those of pituitary tissue do not elevate circulating PRL levels; (b) an allograft of a single adenohypophysis from a female hamster elevates circulating PRL above those levels produced by an allograft of a single adenohypophysis removed from an adult male hamster; (c) circulating PRL levels can be elevated

even further by allografting multiple adenohypophyses; (d) neither muscle nor adenohypophysial allografts alter circulating ACTH levels; and (e) adenohypophysial allografts can result in diminished weight gain. The data in Table III illustrate that a dose-response relationship between circulating PRL levels and the amount of adult adenohypophysial tissue allografted can be achieved. A similar situation can be achieved in hypophysectomized hosts with or without additional endocrine ablative surgery. One also would want to use allografts of adult adenohypophysial tissue if one wished to study the effects of various agents on reducing hypersecretion by lactotrophs or on the maintenance of structure and function of adenohypophysial cells other than the lactotroph (2-4).

However, if the goal of the experiment is to study the *development of adenohypophysial cells*, then the investigator should use *hypophyses removed from prenatal or neonatal hamsters*. This type of design is a little more difficult to implement because the hypophyses without accompanying tissue of a prenatal hamster cannot be removed until about 14 days of gestation (about 2 days prior to parturition). Additionally, the neural and intermediate lobes are nearly impossible to remove from the adenohypophysis of a prenatal or early neonatal hamster. However, donor tissue from a prenatal hamster must be used if the investigator wants to make certain that the cellular product to be identified by immunohistochemistry or *in situ* hybridization in the grafts is not present in the donor tissue. For instance, we have used donor tissue removed as early as the 13th day of gestation (before LH and FSH cells are identifiable with immunohistochemistry) and found that LH cells, but not FSH cells, were observed in grafts of 2 weeks duration. In this particular situation, we subsequently observed that we could identify the effects of LHRH on allograft gonadotrophs by using donor hypophyses removed from neonatal hamsters (those less than 24 hr after birth).

The number of donor hypophyses that needs to be used depends on the end point of the experiment. If one wishes to identify cellular products by *in situ* hybridization or immunohistochemistry, then generally two to four donor neonatal hypophyses will provide enough surviving allograft tissue to complete the experiment. If one wishes to challenge the allografts with a particular agent (e.g., LHRH) and measure release of an allograft product into the blood by radioimmunoassay (in this case, LH), then one generally needs about eight to twelve donor neonatal hypophyses. It should be pointed out that allografts of hypophyses removed from perinatal hamsters do not release enough PRL to elevate circulating PRL levels above those found in hypophysectomized hamsters. Thus, this donor tissue can be used to study the development of abnormal lactotroph morphology and one particular hypersecreting syndrome of the adenohypophysis.

Generally, we do not attempt to measure the allograft concentration of a cellular product because the allograft comprises varying amounts of what readily appears to be nonadenohypophysial tissue. Most often, what happens when multiple pieces of donor tissue are used (either pieces of adult glands or multiple glands from young donors) is that areas of adenohypophysial tissue are separated from one another by strands of fibrous tissue. Additionally, cysts, which are probably remnants of cells of the intermediate lobe, are observed. Occasionally, some lymphoid tissue is present. Thus, even though allografts can be removed and weighed, the wet weight may not be determinant of the wet weight of adenohypophysial tissue.

Allografts of Control Tissue

If we are beginning a new project, we will include a group of hosts that received allografts of control tissue. We routinely use pieces of flank muscle removed from the donor animals as control tissue for hypophysial donor tissue. We transplant approximately the same amount of muscle tissue as hypophysial tissue. We have yet to observe any effect of transplanted muscle tissue. In experiments similar to prior ones in which we did not observe any effects of control muscle allografts, we often will use sham-transplanted animals as controls. These animals are subjected to all surgical procedures, except for insertion of tissue beneath the renal capsule.

Removal of Allograft Tissue

Generally, our experiments are terminated by decapitation of the host. Allografts can be removed quickly and studied. The skin and muscle are opened and the kidney is visualized. If we wish to study the allograft with histological procedures, we cut around the periphery of the allograft with fine scissors and deep beneath the allograft through kidney tissue. After removal of this piece of tissue, most of the kidney tissue is sliced off with a razor blade and the appropriate tissue put into fixative.

Because hypophysial allografts adhere to the capsule and not to kidney tissue and do not infiltrate kidney parenchyma markedly, the allograft and overlying capsule can be removed. We do this if we want to determine the content of a cellular product in the allograft. The capsular membrane along the periphery of the allograft is cut with a pair of Barraquer-DeWecker or similar scissors. One edge of the capsule is picked up with fine forceps and the capsule and adherent allograft are gently peeled off the renal parenchyma.

SUMMARY OF THE STATUS OF THE HOST AND THE ALLOGRAFT TISSUE

Status of Host

We have noticed only a few particular aspects about the host animals. First, they should be housed individually to keep one animal from gnawing at another animal's wound. Second, intact hosts need no other special requirements. Third, the drinking water of hosts that are hypophysectomized should be supplemented with 5.0% sucrose.

Status of Allograft

It is our opinion that the model of hamster hypophysial tissue allografted beneath the renal capsule of other hamsters is amenable for studying almost any aspect of control of pituitary function. Cellular morphology, synthesis of hormone mRNA and hormone, and release of hormone all can be studied using this model (2–9). Allografts can survive for nearly a year. Thus, it is particularly useful for studying the chronic effects of (a) removal of the pituitary gland from direct influence of the hypothalamus; (b) exposure of malregulated adenohypophysial cells to various agents; and (c) the physiological and pathological effects of PRL.

ACKNOWLEDGMENTS

We thank Janice Burns for her expert assistance. This work was supported by NIH Grant HD 22687.

REFERENCES

1. R. A. Adler, The anterior pituitary-grafted rat: A valid model of chronic hyperprolactinemia. *Endocr Rev.* **7**, 302 (1986).
2. M. J. Horacek, G. T. Campbell, and C. A. Blake, Luteinizing hormone (LH)-releasing hormone: Effects on maintenance of immunoreactive follicle-stimulating hormone and LH in adenohypophysial cells. *Endocrinology (Baltimore)* **126**, 653 (1990).
3. M. J. Horacek, G. T. Campbell, and C. A. Blake, Effects of growth hormone-releasing hormone on somatotrophs in anterior pituitary gland allografts in hypophysectomized, orchidectomized hamsters. *Cell Tissue Res.* **253**, 287 (1988).
4. M. J. Horacek, G. T. Campbell, and C. A. Blake, Effects of corticotrophin-releasing hormone on corticotrophs in anterior pituitary gland allografts in hypophysectomized, orchidectomized hamsters. *Cell Tissue Res.* **258**, 65 (1989).

5. M. J. Horacek, G. T. Campbell, and C. A. Blake, Luteinizing hormone (LH)-releasing hormone: Effects on induction of LH, follicle-stimulating hormone, and prolactin cell differentiation. *Endocrinology (Baltimore)* **124**, 1800 (1989).
6. G. T. Campbell, J. N. Southard, F. Talamantes, and C. A. Blake, Gonadotropin-releasing hormone-induced accumulation of follicle-stimulating hormone β -subunit messenger ribonucleic acid in adeno-hypophysial cells developing in an ectopic position. *Endocrinology (Baltimore)* **130**, 1180 (1992).
7. K. A. Gregerson, and G. T. Campbell, Influences of luteinizing hormone releasing hormone, hypophysectomy and orchidectomy on the differentiation of luteinizing hormone and follicle-stimulating hormone cells in an ectopic pituitary in the hamster. *Biol. Reprod.* **27**, 169 (1982).
8. G. T. Campbell, J. Wagoner, P. Colosi, M. J. Soares, and F. Talamantes, Development and retention of phenotypically specialized cells in pituitary allografts in the hamster (*Mesocricetus auratus*). *Cell Tissue Res.* **251**, 215 (1988).
9. M. L. Wolf, G. T. Campbell, and C. A. Blake, The response of splenic lymphocytes removed from hypophysectomized-orchidectomized hamsters to phytohemagglutinin correlates with somatic growth but not with circulating prolactin levels. *Endocrinology (Baltimore)* **126**, 2046 (1990).

5

Prolactin Secretion from Single Cells: Analysis by Reverse Hemolytic Plaque Assays

Fredric R. Boockfor
*Department of Cell Biology and
Neuroscience
University of South Carolina
School of Medicine
Columbia, South Carolina 29208*

INTRODUCTION

The release of prolactin from the anterior pituitary is under the regulatory control of a number of different factors. Several of these originate in the hypothalamus, travel down the hypothalamo-hypophyseal portal system, and act directly on prolactin cells in the pituitary. Some of the most well-studied of these hypothalamic substances are thyrotropin releasing hormone (TRH), dopamine, γ -amino butyric acid, vasoactive intestinal polypeptide, and serotonin (1,2). Other types of modulators also influence prolactin release. Certain gonadal hormones such as estrogens are potent modulators of prolactin cell development and function (3–5). The levels of these hormones change during reproductive cyclicity and are present in high concentrations during certain reproductive states such as pregnancy. Finally, hormones involved with stress can cause a marked elevation in prolactin release (6). This may include endorphins, catecholamines, or specific substances such as ACTH or corticoids. The influence of such a wide variety of substances not only demonstrates the complexity of the control

of prolactin, but also suggests that a change in one of these systems may be detectable by a change in prolactin release. For this reason, the use of prolactin secretion as an end point for study provides a sensitive and versatile index to evaluate many different types of toxic substances; some that may disrupt one of these systems or others that may modify or mimic one of these regulators of secretion.

The use of *in vitro* preparations of pituitary cells provides an excellent means of assessing pituitary prolactin secretion. Several different techniques such as organ and explant culture have been explored, but the most commonly used approach is the preparation and use of monolayer cell cultures. With this tool, it is possible to investigate chronic and acute influences of a number of different types of modulators of prolactin secretion (7–9). This is accomplished mainly by adding the substance(s) to the cultures, and then collecting the medium after incubation and subjecting it to radio- or enzyme-linked immunoassays for prolactin quantification. The use of such an approach provides an excellent system for study and analysis of a specific agent in question, especially if it has a potent influence on secretion or acts on a large proportion of the prolactin-secreting cell population. However, it is quite possible that secretory changes induced in small proportions of the cells present may remain undetected because prolactin levels in the medium would represent an average of that released by all cells in culture. Moreover, it has become increasingly clear during the last decade that not all prolactin cells function in a similar manner. In fact, findings of differential responsiveness between prolactin cells in a variety of physiological states (10–14) suggest that a method enabling assessment of stimulatory or inhibitory influences on a cell by cell basis may be one of the most effective methods to detect or study substances that alter secretory function.

The reverse hemolytic plaque assay (RHPA) is an immunological tool that enables study of prolactin release from individual cells (11,15,16). The principle of this assay is quite simple and depends on the recognition of antigen release from secreting cells by a hormone-specific antibody. This antibody, when bound to the antigen, will attach to the surface of indicator cells that are nearby. In the presence of complement, these indicator cells will lyse, forming a zone of hemolysis or “plaque” around the secretors. Because each prolactin-secreting cell can be identified microscopically, it is possible to evaluate changes in release that occur even in very small parts of the prolactin cell population. The ability of plaque assays to detect even modest secretory changes, when coupled with the usefulness of prolactin as an end point to identify alterations in several different physiological systems, suggests strongly that RHPAs for prolactin will serve well as a sensitive and versatile approach for the identification and study of a variety of toxic substances.

ESTABLISHMENT OF A PROLACTIN PLAQUE ASSAY

The establishment of a prolactin plaque assay depends mainly on the quality of the antibody and the ability to obtain a viable single-cell population (11,15). The antibody should be of a high titer and specific for prolactin. The use of an antiserum that cross-reacts with other pituitary hormones will compromise the specificity of the assay. The antiserum used must also be able to fix complement in order for the lytic reaction to be initiated. In addition to antibody requirements, the pituitary cells used in the assay must be viable, actively secreting, and responsive to stimulatory and inhibitory influences. The following discussion contains suggestions for attaining these conditions. Most of the work performed in our laboratory has employed cells and reagents for the evaluation of rat prolactin secretion and will serve as the basis for this discussion. Prolactin plaque assays have also been developed for other species and may prove useful in the evaluation of toxic substances (29). These assays follow principles similar to those discussed in the following.

PROCEDURES

Reagents, Materials, and Equipment

Reagents and Media

- Sheep red blood cells in Alsevier's solution (Colorado Serum, Denver, CO) (cells must be no more than 2 weeks old)
- Sodium chloride (Sigma Chemical Co., St Louis, MO)
- Protein-A (Sigma)
- Trypsin, 1 : 250 (Difco, Detroit, MI)
- Guinea pig serum (Gibco, Grand Island, NY)
- Glutaraldehyde (Sigma)
- Poly-*l*-lysine, MW 380,000 (Sigma)
- Chromium chloride (III) hexahydrate (Sigma)
- Dimethyl sulfoxide (DMSO) (Sigma)
- Assay medium (DMEM+): Dulbecco's Modified Eagle's Medium (Gibco), supplemented with:
 - Bovine serum albumin (BSA, 0.1%, Fraction V) (Sigma)
 - Penicillin G (100 U/ml)/streptomycin sulfate (100 mg/ml) (Gibco)
 - Cell acquisition medium (MEM+): Minimum Essential Medium (Gibco), supplemented with BSA and antibiotics as for DMEM

Materials

- Glass microscope slides, precleaned 25 × 75 mm (Clay Adams, Becton Dickinson Labware, Lincoln Park, NJ)

- Glass coverslips, No. 1, 22 mm square (Corning through Baxter Scientific Products, McGaw Park, IL)
- Double-stick tape, 12.7 mm wide (Scotch, St. Paul, MN)
- Pasteur pipets (borosilicate glass) (Baxter Diagnostics, Inc., McGaw Park, IL) (need to be siliconized and flame-polished)
- Kimwipes (Kimberly Clark, Roswell, GA)

Equipment

- Laminar flow hood for sterile tissue acquisition
- Inverted microscope (with 10X, 20X, and 40X objectives)
- Incubator (CO₂-injected, water-jacketed, 37°C)

Preparation for Assay

Blood Cell Conjugation

The attachment of protein-A to the surface of sheep red blood cells is performed as described previously (16). Briefly, sheep red blood cells in Alsevier's solution (6.5 ml) are centrifuged (200g for 10 min), the supernatant is removed, and saline (10 ml of a 0.9% solution) is added. The cells are resuspended and again centrifuged. This saline wash step is repeated twice to remove all traces of the blood cell storage solution. The erythrocytes are then resuspended in 10 ml of conjugation solution consisting of chromium chloride (0.1 mg/ml) and protein-A (0.05 mg/ml) in saline. Chromium chloride is prepared as a double-strength solution (0.2 mg/ml in saline) that is allowed to stabilize for at least 2 weeks prior to use. When needed, this is combined with saline and protein-A (0.5-mg aliquot) that has been freshly prepared or stored frozen. The mixture is allowed to incubate for 1 hr at 30°C with mixing at 15-min intervals. After incubation, the cells are washed twice in fresh saline and once in assay medium (DMEM+). The erythrocytes are then placed into 50 ml of fresh DMEMH+ and passed repeatedly into and out of a Pasteur pipet to break up aggregated cells. This suspension of conjugated sheep red blood cells (2.0% solution) is refrigerated and should be used within 5 days of conjugation.

Antibody Preparation

Polyclonal antibodies obtained commercially or raised by the investigator may be able to be used without modification. However, if problems occur with titer or cell viability, the preparation should be IgG purified or at least removed from other serum components by ammonium sulfate precipitation.

A standard precipitation and desalting procedure can be followed. In addition, it is often necessary to reduce nonspecific antibody attachment to sheep red blood cells by preabsorbing the antibody with fresh (nonconjugated) erythrocytes before performing a plaque assay. This can be accomplished by incubating 1 ml of the undiluted antiserum with an equal volume of packed red blood cells for 1 hr at 4°C. This procedure should reduce the nonspecific lysis of the indicator cells, which would appear as a general thinning of the assay monolayer. The mixture is centrifuged to remove the cells and the supernatant (antibody) is aliquoted and stored at -70°C until needed for plaque assays.

Slide Chamber Preparation

Plaque assays are conducted in an apparatus known as a Cunningham chamber (17) that is constructed using a glass slide, a coverslip, and double-stick tape. One of the most important requirements of a successful plaque assay is to use glass slides that are devoid of dirt, grease, or biological contaminants. To accomplish this, the slides are first soaked in two changes of 95% ethanol each for 15 min, followed by incubation in a solution of dimethylsulfoxide (DMSO) (1:100 in water) for 30 min. The DMSO is removed by four washes in distilled deionized water and the slides are dried in an oven at approximately 75°C. Care should be taken to store the slides in a clean, dust-free environment. This cleaning procedure is necessary for most commercially available slides, even those that are labeled pre-cleaned.

On the day of an assay, the portion of the slide on which the chamber is to be constructed is subjected to a solution of poly-*l*-lysine (0.5 mg/ml) for 20 min. The slides are then soaked in two changes of distilled water for 5 min each and air-dried. Two pieces of double-stick tape are applied to the slide, one above and one below the area treated with poly-*l*-lysine. A coverslip is then suspended over the slide and pressed onto each piece of double-stick tape. This provides a chamber (illustrated in Figure 1) with a volume of about 30 μ l, consisting of a poly-*l*-lysine-treated floor that facilitates cell adherence, two walls composed of double-stick tape, and a glass coverslip that forms a roof. The remaining two sides of the chamber are open to enable infusion and removal of reagents during the assay.

Cell Acquisition

Prolactin-secreting cells to be used in the assay can be obtained from pituitary tissue or from cultures of several continuous cell lines. Because plaque assays enable determination of prolactin release from single cells,

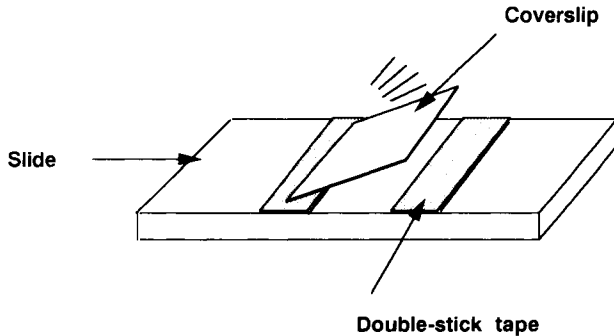


FIGURE 1. Diagram of a plaque assay chamber. A chamber is constructed by placing two strips of double-stick tape on a glass slide about 2 cm apart and then gently pressing a coverslip to the tape. The tape forms the walls, the slide becomes the floor, and the coverslip forms the roof of this structure. Assay components are then passed into and out of the chamber through the sides not bound by tape.

it is very important to use an enzymatic or mechanical procedure that provides a population of single cells rather than aggregates or cell clumps. The procedure used in our laboratory is a trypsin dispersion protocol and is conducted as described by Hymer *et al.* (18) with minor modifications. Rat anterior pituitaries are sliced into 0.5 to 1.0-mm fragments and incubated for 2 hr at 37°C in a trypsin solution (0.1% in MEM+) with constant stirring. Every 30 min during this procedure, the fragments are drawn into and out of a flame-polished Pasteur pipette approximately 20 times. This combination of enzymatic and mechanical disaggregation provides a population of cells that are monodispersed and continue to exhibit a high degree of viability. The cells can be used immediately in plaque assays or placed into culture and used at a later time. In situations in which other dispersion protocols must be used or only aggregates can be obtained, it is possible to place the cells into culture for a period of time during which the aggregates will attach and spread, forming a monolayer. The cells can then be recovered in a monodispersed state by subjecting the cultures to brief treatment with a dilute solution of trypsin (0.025% in MEM+ for 10 min).

Several continuous lines of prolactin-secreting cells are also available for toxicological studies. A few of the most common ones include GH₁, GH₃ (available at ATTC, Rockville, MD), and GH₄C₁ cells. These lines contain cells that not only secrete prolactin, but are also quite sensitive to a number of modulatory agents (19,20). Moreover, they can be fairly easily propagated, providing a continuous and highly accessible source of cells for study. For plaque assays, monodispersed cells from these cultures can

be obtained by gentle trypsin treatment as described earlier for aggregated cells plated prior to recovery (21).

Assay Performance

Formation of Cell Monolayer

On the day of an assay, 6 ml of the 2% protein-A-coated sheep red blood cell solution is centrifuged at 200g for 10 min. The supernatant is removed and the red blood cell pellet resuspended in 1 ml of fresh assay medium. This preparation is combined with an equal volume of pituitary cells (5×10^5 cells/ml), thoroughly mixed, and then infused into plaque assay chambers. Care is taken to fill the chambers evenly, leaving only a small excess of cell solution at the edge. The slides are then placed into a humidified incubator at 37°C in an atmosphere of 5% CO₂: 95% air and allowed to incubate for 45 min. During this period, the blood and pituitary cells settle to the bottom of the chamber and attach owing to the presence of poly-*l*-lysine. Fresh assay medium is then infused by placing a fluid-filled pipet at one opening of the chamber and a folded Kimwipe at the opposite opening. This enables the medium to be drawn through the chamber by capillary action, removing any unattached cells or debris. When completed, this process yields a continuous monolayer of cells attached to the chamber floor that consists of pituitary cells surrounded by indicator erythrocytes.

Assay Reagent Sequence and Incubation Times

A solution that contains a working dilution of prolactin antibody is then infused into the assay chambers. The concentration of this reagent depends on the characteristics of the antiserum employed. In our hands, rabbit anti-rat prolactin antiserum at a concentration of approximately 5 ng/ml of antibody protein is diluted with assay medium in a range of 1:40 to 1:320 before use in the assay (12,21). The most effective concentration will depend on various factors such as pituitary cell source, incubation time, and experimental treatment imposed. Following antibody infusion, the chambers are incubated at 37°C in a humidified atmosphere of 5% CO₂: 95% air for 0–8 hr. The incubation time(s) will be dictated by the design of the experiment and the index used for evaluation. During incubation, the antibody molecules present bind to prolactin that is released from the pituitary cells. These antibody/antigen complexes then attach to the surface of surrounding erythrocytes. In this portion of the assay, various test substances that will stimulate or inhibit hormone release from pituitary cells can be included in the incubation mixture. At the end of this period, guinea pig serum,

which serves as a source of complement, is infused. The concentration of this reagent also varies in different assay systems but is usually diluted with DMEM+ at 1:20 to 1:80. The chambers are incubated for an additional 45–60 min, during which lysis occurs of indicator cells that contain attached antibody/antigen complexes. Finally, the reaction is terminated by infusion of a fixative such as glutaraldehyde (2.0% in saline).

Assessment of Results

The results of a typical plaque assay are presented in Figure 2. As shown, an area of lysed indicator erythrocytes or “plaque” surrounds a prolactin-secreting cell. Cells that do not form plaques can be identified using a background stain. A saturated solution of toluidine blue in saline is infused, allowed to incubate for 15 min, and washed from the chambers. The slides can be immersed in fixative for storage.

Plaque formation is evaluated in one of two ways (Figure 3). First, direct counts are made of plaque-forming and nonplaque-forming cells. This is performed on slides incubated for a period sufficient to induce maximal plaque formation (6–8 hr), providing a determination of the total secreting cells in the population. Direct counts are also used to determine the rate of plaque formation. It is well recognized that a threshold amount of hormone must be released before plaque formation will begin (22). This does not occur with each cell at the same time. Therefore, an evaluation of the percentage of plaque-forming cells identifiable with increasing incubation periods provides an estimate of the rate of hormone release from secreting cells in the population (12). To accomplish this, antibody is added to each of several companion chambers followed by complement development and termination of the reaction at progressive time intervals. The periods that are most effective in assessing changes in the rate of plaque formation are usually within the first hour of incubation. A second index that can be used to evaluate plaque formation is a measurement of plaque size (11). Plaques are circular and quite uniform throughout most of their formation. Microscopic measurement of plaque diameter using an ocular micrometer enables calculation of plaque area. These measurements are believed to closely reflect the amount of prolactin released by the cells (11). The quantification of the percentage of plaque formers or a measurement of plaque size can be evaluated manually with an inverted microscope or can be automated by integrating an image analysis system.

The establishment of a new plaque assay system requires careful attention to control results and possible artifacts. As would be anticipated, the removal of any reagent (antibody, complement, protein-A-conjugated cells, etc.) should result in an abolition of plaque formation. It is also

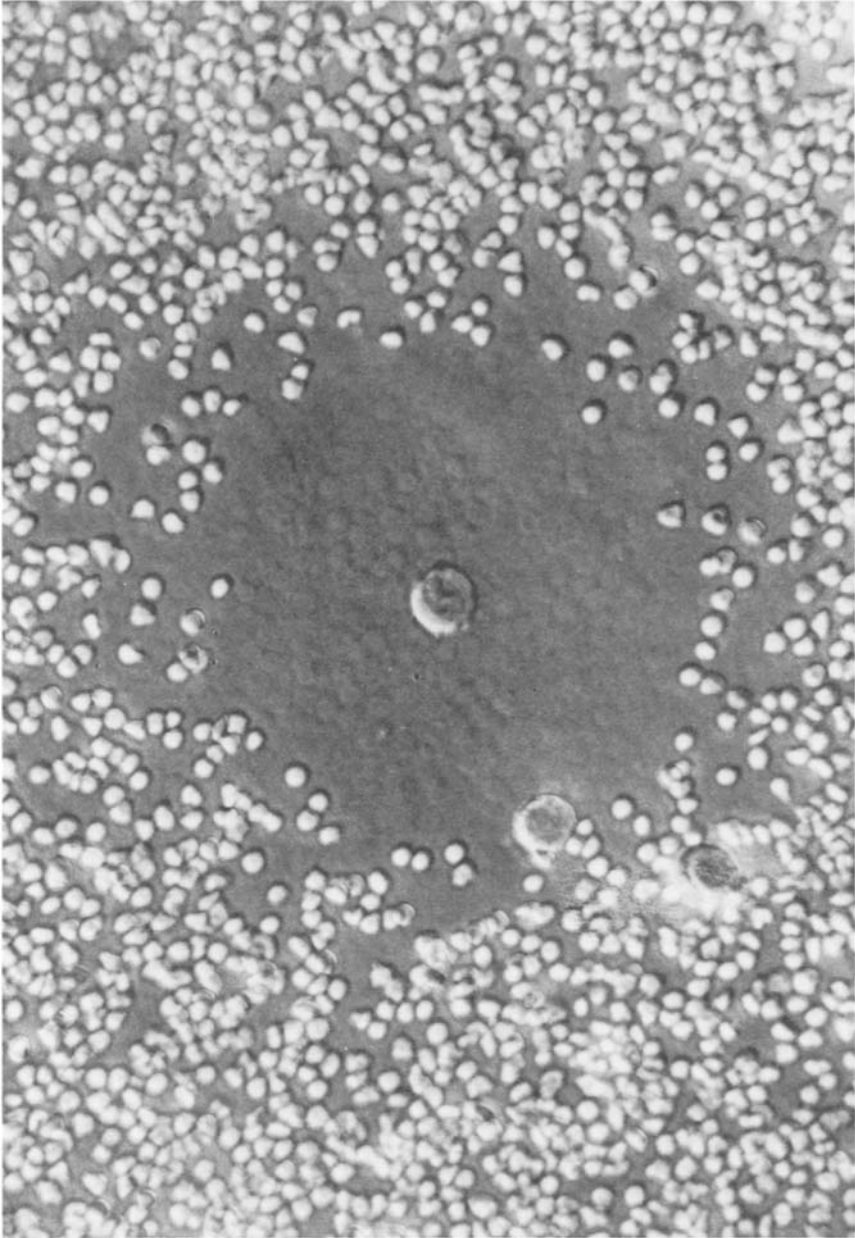


FIGURE 2. Example of a plaque-forming cell. The large cell in the center of the field (pituitary cell) is surrounded by an area devoid of smaller cells (indicator erythrocytes). The presence of this zone of hemolysis or "plaque" identifies this cell as a prolactin secretor. Photomicrograph taken using Nomarski optics; magnification $\times 430$.

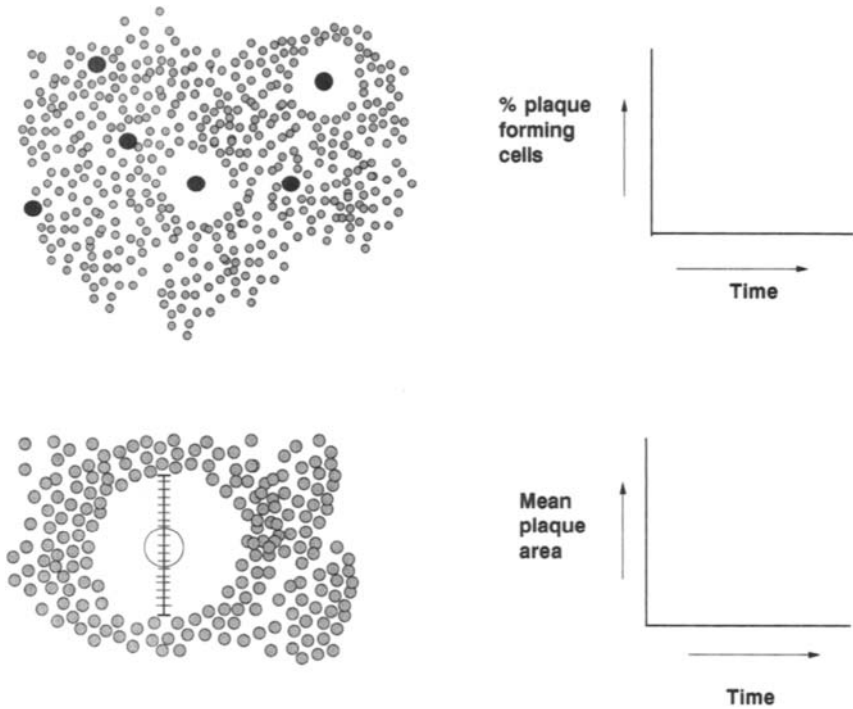


FIGURE 3. Evaluation of plaque assay results. Plaque assays can be quantified using one of two methods. First, the percentage of all cells forming plaques can be determined by microscopic counting procedures (top panel). These counts can be performed after various incubation times or when maximal plaque formation is attained. Second, plaque diameter measurements can be made using an ocular micrometer or equivalent microscopic measuring device and the mean plaque area calculated (bottom panel). This provides a relative index of the amount of prolactin released. See text for further details.

important to determine the specificity of plaque formation by conducting preabsorption controls. The incubation of antibody with purified prolactin before use in an assay should result in a complete absence of plaque formation (11). The continued formation of plaques when any of these conditions are imposed would suggest a reevaluation of the specific reagents employed or a modification of the environment or conditions in which the assay is performed. The assay uses a number of reagents that must be fresh. A lack of attention to this requirement may result in procedural artifacts.

ADVANTAGES OF USING RHPA ANALYSIS

Plaque assays provide one of the only techniques in which individual cell secretion can be studied in a living state. The reagents employed in the assay do not compromise cell viability (11,12). In fact, a modification of the standard plaque assay protocol, called the sequential assay, involves the sequential performance of two plaque assays on the same hormone-secreting cells (23,24). Because the reagents used in either assay do not impair cell function, it is possible to reverse the order of the individual assay components or to perform a complete assay and then return the cells to culture for evaluation at a later time. It must be noted that the indicator blood cells in this type of procedure are not attached with poly-*l*-lysine, allowing their removal and replacement with each assay performed. This type of approach allows the function of individual cells to be monitored repeatedly over long periods.

The sensitivity and rapidity of plaque assays provide additional incentive for their use as a functional assay. It has been estimated in the case of another pituitary hormone, luteinizing hormone, that a small plaque represents as little as 5 pg of hormone released (15). This is far below the sensitivity of most procedures. In addition, plaque assay analysis is quite rapid, producing results within a few hours. This is particularly useful in such instances as the screening of a number of substances for detailed study at a later time.

Plaque assays are quite compatible with several other molecular and cell biological techniques. One of the most common of these is immunocytochemistry. Results obtained using immunocytochemical analysis are virtually identical to those obtained with plaque assays in relation to the identification of a particular cell type (12,23). In fact, immunocytochemical analysis can be performed directly on slides that have been subjected to plaque assays (15). This provides a way to correlate hormone storage and secretion in the same population of cells. Another procedure, *in situ* hybridization, is quite compatible with plaque assays and can be conducted on slides in which plaque assays have been performed (25). From such an approach, it is possible to correlate mRNA and hormone release in specific cells. Finally, as mentioned briefly earlier, a plaque assay modification such as the sequential assay can be utilized to analyze other hormones at the same time as prolactin. The results of such an application may provide insight to not only the direct influence of an agent on prolactin, but also some of the changes that are occurring in the basic function capabilities of the cell in question. For example, a reduction in prolactin cells with a concomitant increase in growth hormone cells (as identified with sequential assays in several different pituitary cell prepara-

tions) suggests that an interconversion of these two cell types may be responsible for changes in secretion (5,21). When taken together, the unique ability to integrate plaque assays with other tools enables several functional parameters to be studied on the same cell. This provides a powerful means to address questions that have previously remained unanswered, but that may be critical in understanding the mode of action of agents that alter secretory function.

APPLICATION OF PLAQUE ASSAYS TO ASSESS TOXIC INFLUENCE

The prolactin plaque assay should provide a valuable approach for assessing the influence of suspected toxins or for further study of established toxic agents. Using this tool, agents can be tested for acute or chronic influences. An acute effect would be evaluated by including the agent in question in the antibody incubation step. The ability to influence prolactin release in this manner is reflected in a change in the rate at which plaque formation occurs. An example of the detection of acute sensitivity to stimulatory input is presented in Figure 4 (26). As shown, the addition of thyrotropin releasing hormone, a known stimulator of prolactin secretion, resulted in

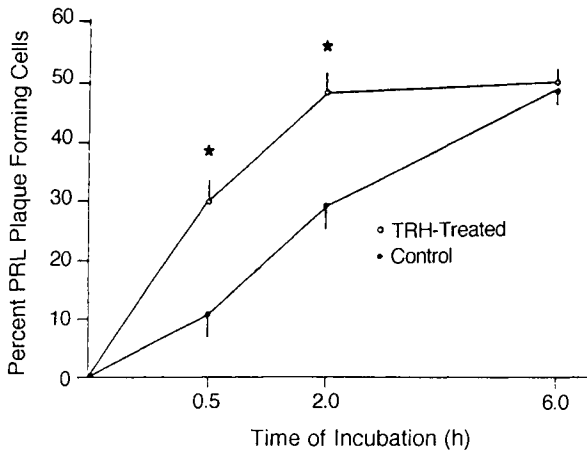


FIGURE 4. Demonstration of the ability to detect acute stimulatory input using the prolactin plaque assay. Cells obtained from portions of Day 10 lactating rat pituitaries were subjected to plaque assays conducted in the presence or absence of TRH ($1 \times 10^{-7}M$) for 0.5, 2, or 6 hr followed by complement incubation for 50 min. Each point reflects the mean \pm SE of four separate experiments from which at least 400 cells were counted. Asterisk indicates $P < 0.05$. As shown, the rate of plaque formation was markedly increased in the presence of TRH. [From Boockfor and Frawley (26) with permission.]

a marked increase in the rate of prolactin plaque formation. This can be detected by at least 30 min of incubation. It is also possible to detect acute inhibitory influences with the prolactin plaque assay. This is illustrated in Figure 5. Our use of the prolactin inhibitor dopamine caused a decrease in the rate at which prolactin plaques formed. These effects could be clearly detected during the first 2 hr of incubation. The identification of chronic influences can also be accomplished with plaque assays but requires a modification in the experimental design. The most effective means to test this type of influence is to culture cells in the presence of the agents in question and then subject the cells to plaque assays to determine whether or not secretion was affected. Figure 6 shows results of experiments in which such a chronic paradigm was used. As shown, both stimulatory and inhibitory influences can be detected. Of particular interest to the study of toxic agents is the effect of estrogen on these cells. Prolactin release is quite sensitive to estrogenic modulation, suggesting that this system would be particularly useful in elucidating the influences of environmental estrogens or other toxins that have a similar mode of action (27,28).

Plaque assay analysis is also applicable to *in vivo* as well as *in vitro* studies. Suspected toxins can be administered by various routes, a single

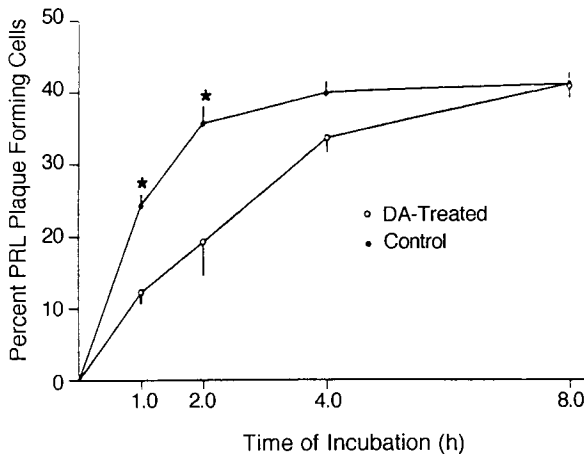


FIGURE 5. Example of the use of plaque assays to detect acute inhibitory input. Pituitary cells from Day 10 lactating rats were first incubated for 2 hr with dopamine ($1 \times 10^{-7} M$). The cells were then subjected to plaque assays with or without the same dopamine concentration for 2, 4, or 8 hr followed by complement incubation for 50 min. Each point reflects the mean \pm SE of four separate experiments in which at least 400 cells were counted. Asterisk indicates $P < 0.05$. In this experiment, dopamine induced a clear decrease in the rate of plaque formation. [From Boockfor and Frawley (26) with permission.]

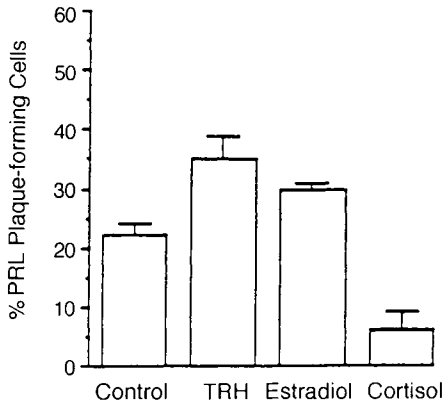


FIGURE 6. Demonstration of the use of plaque assays to detect chronic influences. In these experiments, GH₃ cultures were incubated with TRH (2.5 μ M), 17 β -estradiol (0.1 μ M), or cortisol (5 μ M) for 6 days. The cells were then recovered and subjected to plaque assays. The values represent the mean \pm SE of four separate experiments in which 800 cells were counted for each data point. As shown from these results, chronic influences of either stimulatory (TRH and estradiol) or inhibitory (cortisol) agents can be identified using plaque assay analysis. [From Boockfor *et al.* (21) with permission.]

or multiple times, or in random or carefully regimented patterns. After administration, the pituitary can be recovered and subjected to plaque assays. In this type of study, it would be possible to simulate the type of environmental exposure that is characteristic of the agent under investigation without giving up the versatility and sensitivity provided with plaque assays. It must also be emphasized that the added possibility of establishing plaque assay systems with cells from different species and from normal or tumor tissue provides a number of additional avenues for investigation (29–31). When taken together, it is clear that prolactin plaque assays provide a unique and adaptable tool that should be quite important in the future for the evaluation of an ever-growing list of substances that are known or suspected environmental toxins.

REFERENCES

1. J. D. Neill, In "Frontiers in Neuroendocrinology" (L. Martini and W. F. Ganong, eds.), p. 129. Raven, New York, 1980.
2. L. S. Frawley and J. D. Neill, In "The Anterior Pituitary Gland" (A. S. Bhatnager, ed.), p. 253. Raven, New York, 1983.
3. I. E. Strattman, C. Ezrin, E. A. Sellers, *Cell Tissue Res.* **152**, 229 (1974).

4. M. E. Lieberman, R. A. Maurer, P. Claude, and J. Gorski, *Mol. Cell. Endocrinol.* **25**, 277 (1982).
5. F. R. Boockfor, J. P. Hoeffler, and L. S. Frawley, *Am. J. Physiol.* **250**, E103 (1986).
6. G. L. Noel, H. K. Suh, J. G. Stone, and A. G. Frantz, *J. Clin. Endocrinol. Metab.* **35**, 840 (1972).
7. C. K. Hopkins and M. G. Farquhar, *J. Cell Biol.* **59**, 276 (1973).
8. A. Morin, A. Tixier-Vidal, and D. Gourdj, *Mol. Cell. Endocrinol.* **3**, 351 (1975).
9. C. Denef, L. Swennen, and M. Andries, *Int. Rev. Cytol.* **76**, 225 (1982).
10. A. M. Walker and M. G. Farquhar, *Endocrinology (Baltimore)* **107**, 1095 (1980).
11. J. D. Neill and L. S. Frawley, *Endocrinology (Baltimore)* **112**, 1135 (1983).
12. F. R. Boockfor, J. P. Hoeffler, and L. S. Frawley, *Neuroendocrinology* **42**, 64 (1986).
13. F. R. Boockfor and L. S. Frawley, *Endocrinology (Baltimore)* **120**, 874 (1987).
14. G. M. Nagy, F. R. Boockfor, and L. S. Frawley, *Endocrinology (Baltimore)* **128**, 786 (1991).
15. J. D. Neill, P. F. Smith, E. H. Luque, M. Munoz de Toro, G. Nagy, and J. J. Mulchahey, *Recent Prog. Horm. Res.* **43**, 175 (1987).
16. P. F. Smith, E. H. Luque, and J. D. Neill, In "Methods in Enzymology" (P. M. Conn, ed.), Vol. 124, p. 443. Academic Press, Orlando, Florida, 1986.
17. A. J. Cunningham and A. Szenberg, *Immunology* **14**, 599 (1968).
18. W. C. Hymer, W. H. Evans, J. Kracier, A. Mastro, J. Davis, and E. Griswold, *Endocrinology (Baltimore)* **92**, 275 (1983).
19. A. H. Tashjian, Jr., Y. Yasuma, L. Levine, G. H. Sato, and M. L. Parker, *Endocrinology (Baltimore)* **82**, 342 (1968).
20. D. Gourdj, C. Tougard, and A. Tixier-Vidal, in "Frontiers in Neuroendocrinology" (W. F. Ganong and L. Martini, eds.), p. 317. Raven, New York, 1982.
21. F. R. Boockfor, J. P. Hoeffler, and L. S. Frawley, *Endocrinology (Baltimore)* **117**, 418 (1985).
22. N. K. Jerne, C. Henry, A. A. Nordin, A. M. Koros, and I. Leftkovits, *Transplant. Rev.* **18**, 130 (1974).
23. L. S. Frawley, F. R. Boockfor, and J. P. Hoeffler, *Endocrinology (Baltimore)* **116**, 734 (1985).
24. F. R. Boockfor and L. K. Schwarz, *Endocrinology (Baltimore)* **122**, 762 (1988).
25. K. Scarbrough, N. G. Weiland, G. H. Larson, M. A. Sortino, S. Chiu, A. N. Hirshfield, and P. M. Wise, *Mol. Endocrinol.* **5**, 134 (1991).
26. F. R. Boockfor and L. S. Frawley *Endocrinology (Baltimore)* **120**, 874 (1987).
27. J. R. Levy, K. A. Faber, L. Ayyash, and C. L. Hughes, Jr., *Proc. Soc. Exp. Biol. Med.* **208**, 60 (1993).
28. K. A. Faber and C. L. Hughes, Jr., *Biol. Reprod.* **45**, 649 (1991).
29. R. D. Kineman, W. J. Faught, and L. S. Frawley, *Endocrinology (Baltimore)* **127**, 2229 (1990).
30. R. J. Lloyd, D. Anagnostou, M. Cano, A. L. Barkan, and W. F. Chandler, *J. Clin. Endocrinol. Metab.* **66**, 1103 (1988).
31. R. V. Lloyd, K. Coleman, K. Fields, and V. Nath, *Cancer Res.*, 47 (1987).

This Page Intentionally Left Blank

6

Application of Fluorescence Techniques to Bone Biology

Akimitsu Miyauchi

*National Sanatorium
Hyogo Chuo Hospital
Sanda, Hyogo, Japan*

Akira Fujimori

*Department of Artificial Kidney
Konan Hospital
Kobe, Japan*

Roberto Civitelli

*Division of Bone and Mineral Diseases
Washington University
School of Medicine
St. Louis, Missouri 63110*

INTRODUCTION

We describe methodologies based on the use of fluorescent indicators that have been employed to explore intracellular events in live bone cells. The development of fluorescent probes sensitive to the concentration of ions, and more recently to cAMP, has enabled investigators to study real-time rapid events occurring after hormonal stimulation, or after changes in the extracellular environment. Fluorescence techniques have also been used to analyze the mechanisms of cell–cell communication through gap junctions. Application of these techniques to bone biology has led to fundamental discoveries in several areas, including signal transduction of calcitropic hormones, regulation of intracellular pH homeostasis, cell coupling, and signaling by cell–matrix contact. There are two general experimental approaches to the application of fluorescence technique: one involves the use of bulk cell suspensions, and the other applies light microscopy to adherent

cell layers. In the former instance, the signal reported by the fluorescent probe represents the average of a phenomenon occurring in a large number of cells, whereas in the latter, events can be monitored and recorded in individual cells. The two methods offer features that can be exploited for particular experimental needs. This chapter will review the application of fluorescence techniques to bone biology, with emphasis on the peculiar methodological issues imposed by the biologic characteristic of such specialized cell systems. The investigator that approaches this field for the first time may find the short introductory overview of the currently available models of bone cells useful to devise the most appropriate experimental system. References to pertinent literature are given for those who are interested in more in-depth information about tissue culture of bone cells and for details on specific methodological issues.

CELL CULTURES

Most of the cell models currently available in bone biology can be effectively used for fluorometric studies of live cells. The available technology can provide suitable *in vitro* cultures of osteoblasts, bone marrow stromal cells, and osteoclasts. Osteocytes, which are very abundant in bone, remain very difficult to isolate and study in culture. Transformed osteoblastic cell lines and primary cultures derived from bone explants are commonly used as models of cells of the osteoblastic lineage. Although several methods have been proposed to prepare cultures of normal osteoblastic cells, no one procedure can yield a pure population of well-differentiated osteoblasts. Part of the problem relates to the natural heterogeneity of bone-forming cells, whose phenotypic features change in normal bone as they progress from committed osteoprogenitor of the bone marrow to the terminally differentiated bone lining cells and osteocytes (1,2). Osteoclasts are multinucleated, terminally differentiated cells that do not proliferate. Cell lines with osteoclastic features derived from tumors have been proposed as models of osteoclasts for *in vitro* studies, but not all of these cell lines are able to resorb bone under standard conditions. Because of this limitation, osteoclastic cells freshly isolated from the bone marrow are more commonly used. Marrow-derived osteoclast precursors are also employed, but the functional properties of these preosteoclastic cells do not reflect a fully featured osteoclast.

Osteoblastic Cells

A relatively large number of osteoblastic cell lines are available, and all can be cultured for use with fluorometric techniques. These cell lines express

different degrees of osteoblastic phenotypic features, perhaps representing cells fixed at certain stages of differentiation. Despite their transformed nature and the substantial phenotypic differences among cell lines, osteogenic sarcoma cells have provided the basic tools for the early, breakthrough studies on signal transduction of calciotropic hormones, on intracellular pH homeostasis and membrane potential, and for the analysis of some aspects of direct cell–cell interactions. Even though analysis of rapid intracellular events in these cell lines has undoubtedly led to fundamental discoveries in these areas, caution should be exercised in extrapolating observations obtained in transformed cell lines to a specific osteoblast function. The finely tuned, time-regulated relationship between the proliferative and differentiation phases that characterizes normal osteoblast development is disrupted, and the regulation of osteoblast-specific genes is aberrant in transformed cell lines (3–5). Of more direct relevance to normal physiology are studies that utilize primary cells derived from either rat calvaria or human trabecular bone specimens or bone marrow. However, preparation of primary cell cultures requires specimens of normal bone tissue. Adult human bone specimens may not be easily available to all laboratories and, unfortunately, normal bone cells do not lend themselves to subculturing because their proliferative activity is usually low. More importantly, they tend to lose their phenotypic features after a few replicative cycles. In addition, cell cultures derived from normal bone tissue are inherently heterogeneous, which limits their use to single-cell studies, and carries the obvious interpretative problems related to the use of heterogeneous cell populations. As in many other cell systems, the suitability of any of the available models of osteoblasts depends on the biological question that is being asked. Obviously, knowledge of the limitations of each model is essential for a correct interpretation of the results obtained, a concept that also applies to osteoclastic cell models.

The most widely used *osteogenic sarcoma cells* are the rat UMR 106-01 (6,7) and the ROS 17/2.8 (8,9). They both express several common osteoblastic features, such as alkaline phosphatase and response to PTH, but they differ in some other characteristics. Because they do not produce the bone matrix protein osteocalcin (10), the UMR 106-01 are commonly considered osteoblasts in an early stage of differentiation, compared to the ROS 17/2.8, which may represent a more differentiated phenotype. The mouse MC3T3-E1 cell line has also gained respectable popularity. These are considered osteoblast precursors that under certain conditions can differentiate with time in culture (11,12). As such, they are used as a model of osteoblast differentiation, although it is not certain whether the time-related developmental sequence of events occurring during normal osteoblast maturation is maintained in this cell line. A number of human osteogenic sarcoma cells

exist, and like the rat cell models, they also differ between each other for certain phenotypic features (13,14). A recent comparative characterization of the most commonly used human osteosarcoma cells revealed that the SaOS-2 cells exhibit the most differentiated characteristics, whereas other cell lines, such as the MG-63 or the U2O, express a less mature osteoblastic phenotype (15).

Normal osteoblastic cells can be isolated and cultured from normal bone of animals and humans. Rat calvaria cells are isolated from periosteum-free frontal bones of 1- to 2-day-old rats, or from fetuses of 16-18 days of gestational age, using sequential collagenase digestion methods (5,16). This procedure results in cultures highly enriched in osteoblasts, as demonstrated by intense alkaline phosphatase staining and cAMP production stimulated by parathyroid hormone (PTH) (5,16). This system has been used to characterize the sequential progression of the osteoblast maturation process (5). A similar, although not identical system has been proposed for human osteoblast, utilizing bone marrow stromal cells of adult donors as providers of osteoprogenitor cells. These cells can be induced to differentiate into more mature osteoblasts by treatment with steroids, and represent an *in vitro* model of human osteoblast differentiation (17,18). More differentiated cells, perhaps representing bone lining cells or even osteocytes, can be cultured from collagenase-digested fragments of human trabecular bone (19–22). These cells represent a reliable and relatively homogeneous osteoblastic model, and can be cultured for a long time until calcification of the bone matrix ensues. All of these cell models have been used in fluorescence microscopy studies. Other approaches have been taken to produce human osteoblasts, including immortalization of trabecular bone cells by transfection with the SV-40 large T antigen gene (23–25). See also Ref. 26 for a recent review on models of osteoblasts.

Osteoclastic Cells

Osteoclasts are characteristically large, multinucleated cells normally found on a resorption lacuna. A mature osteoclast expresses tartrate-resistant acid phosphatase, harbors calcitonin receptors or binding sites, the vitronectin receptor, and, above all, should be able to resorb bone [see Refs. 27 and 28 for review]. Osteoclasts of different species may express a different repertoire of these characteristics, perhaps reflecting species differences in the mechanisms of recruitment, differentiation, and regulation of bone-resorbing cells. These differences should be borne in mind when extrapolating to human physiology.

Chicken osteoclastlike cells can be isolated from femurs and tibias of calcium-deficient laying hens (29,30). Large, multinucleated cells are sepa-

rated on a Ficoll-Hypaque density gradient and directly cultured for analysis. This methods may yield very homogeneous populations of multinucleated osteoclastlike cells. The major limitation of avian osteoclasts is the lack of calcitonin receptors, which is instead an invariable feature of mammal bone-resorbing cells. Using similar methods, osteoclasts are also obtained from *rabbit* and *rat* long bones (31–33). Because these techniques are essentially based on the purification of existing multinucleated, differentiated cells, the yield is usually low. Osteoclasts can also be generated from mononucleated precursors of the bone marrow. A very popular mouse model is based on the induction of differentiation *in vitro*, using co-cultures of nonadherent bone marrow cells with stromal cells (34). Although the cultures are obviously heterogeneous, the large, multinucleated osteoclastic cells can be easily distinguished from the much smaller stromal cells, thus making this system suitable for single-cell recordings, as we have demonstrated (35). A marrow culture system has also been developed to identify the committed mononuclear precursors of osteoclasts. In the presence of certain growth factors and culture conditions, these precursors can differentiate into mature bone-resorbing cells, thus representing human osteoclasts (36,37).

ANALYSES IN CELL POPULATIONS

Applicative Considerations

Fluorometric techniques were first developed and applied for bulk cell preparations, usually kept in suspension in media or buffers. The relatively simple hardware and the powerful potentials of these techniques allowed a rapid diffusion to many fields of cell biology. Virtually any type of cell that can be grown in culture and released in a homogeneous suspension is suitable for dye loading and fluorescence analysis. Osteoblastic cell lines have been widely employed by several investigators in a variety of experimental endeavors, including monitoring of $[Ca^{2+}]_i$ as signal transduction pathways of calciotropic hormones, studies of intracellular pH homeostasis and membrane potential, and cell–cell communication. Because of the limited number of osteoclasts that can be generated using the available isolation procedures and the heterogeneity of these cultures, cell population-based studies are not suitable for osteoclasts.

Fluorometry of cell populations is a very useful tool that can be used when the effect of a stimulator, or a changing environmental condition, is to be studied in a certain cell type. For example, averaging the effect of a hormone on a large number of cells can overcome the problem of heteroge-

neity of receptor expression or signal-transducing elements, which may arise either from nonhomogenous primary cell preparations or from selection of more proliferative subclones in cell lines after prolonged subculturing. Although the analysis of hormonal responses in individual cells may provide additional important information on the biologic characteristics of the cell type examined, assessment of responses in a large number of cells of the same type may provide an indication of the physiologic relevance of the phenomenon observed. On the other hand, the large number of cells required for the preparation of cell suspension imposes some limits to the applicability of these techniques. Cell types that are difficult to culture, or are available in limited numbers, such as primary cultures of osteoblasts or osteoclasts, are not suited for these experiments. The other major limitation is constituted by the manipulations required for the preparation of the sample, which necessarily alter the cytoskeletal structure of the cells and remove the cell-to-cell and cell-to-matrix contacts that are formed in tissue cultures. This issue is becoming increasingly important, since the integrity of the cytoskeleton and the maintenance of attachment structures are believed to be important for certain biologic phenomena, including cell signaling. As we shall see, fluorometric techniques have been applied to the study of cell-to-cell communication using cell suspensions, providing an additional tool for investigation in this area.

The detection system for fluorescence measurements in cell suspensions is relatively simple and consists in a spectrofluorometer that can deliver the appropriate monochromatic excitation light. Emission is recorded by photomultipliers, after filtering through suitable interference filters. The ideal system should have user-selectable excitation and emission monochromators and dual excitation or emission capability, in order to take full advantage of the spectral properties of each dye. Because of the growing popularity of single-cell methodologies (discussed later), fluorometric systems dedicated to cell population studies have not evolved as rapidly as fluorescence microscopy and video imaging systems. Nonetheless, this relatively simple technique still provides useful tools for rapid screening of large numbers of cells.

Sample Preparation

Osteoblastic cells can be grown in monolayer to confluence on plastic flasks using standard tissue culture medium, usually supplemented with fetal bovine serum. In our hands, these cells can be easily mobilized by incubation for 15–20 min with 5 mM EDTA in a buffered salt solution at 37°C, then centrifuged (200g for 1 min) and resuspended in the same medium, without serum (38,39). Although trypsin is commonly used to

facilitate the release of cells from the plastic substrate, we found that incubation in a protease-free buffer ensures more consistent responses, probably because cell-surface molecules, including receptors, may be better preserved. Because of its red light absorbance, phenol red, or other pH indicators, should be avoided. Either phenol red-free tissue culture media or buffer solutions are suitable for these experiments. In our laboratory, we use a custom-made balanced salt solution, buffered with HEPES and supplemented with glucose (127 mM NaCl, 3.8 mM KCl, 1.2 mM KH_2PO_4 , 1.2 mM CaCl_2 , 0.8 mM MgCl_2 , 5 mM glucose, and 10 mM HEPES, adjusted to pH 7.4 with 1N NaOH).

At this point, the cells can be loaded with the fluorescent probe of choice. In most cases, loading is accomplished by incubating for 30–60 min with the membrane permeant acetoxymethyl (AM) ester derivative of the dye, for example, the Ca^{2+} sensitive dyes indo-1 and fura-2, and the pH-sensitive probe BCECF. The cells are then washed, resuspended in a buffered solution, and transferred to a plastic cuvette for reading in a spectrofluorometer. The final cell concentration in the cuvette should be around 2×10^6 cells/ml. When dyes that label the plasma membrane or that partition across the membrane—such as some potentiometric probes—are used, cell suspension can be briefly incubated with the dye of choice just before the experiment. The cell suspensions are stirred continuously during the experiment, and the cuvette holder is thermostatted at the appropriate temperature.

Cytosolic Calcium

A number of fluorescent probes that report free Ca^{2+} concentration have been used to study intracellular $[\text{Ca}^{2+}]_i$ homeostasis in osteoblasts and signal transduction mechanisms activated by calcitropic hormones. Dyes that shift their emission (indo-1) or excitation (fura-2) spectrum upon binding to Ca^{2+} are preferred over probes that simply change the emission intensity, that is, quin-2, now virtually abandoned, and fluo-3, whose spectral properties make it suitable for multiple dye-loading experiments. The spectral shift allows detection of intensity changes at two different wavelengths, which are selected so that the direction of the changes in emission intensity are opposite. This allows one to express the results as a ratio of intensities, thus providing a higher sensitivity and a correction for differences in dye concentration between cells, and within cytoplasmic compartments (40). In our studies on PTH signal transduction in osteoblastic and proximal tubule cells, we employed indo-1 by virtue of its emission spectrum shift (38,39,41–43). The good sensitivity and reproducibility of this method led to the identification and analysis of an alternative signal transduction path-

way that is activated by PTH and parathyroid hormone-related peptide in their target cells. These results have been reproduced by other investigators using different methods (44–46) and constitute the foundation of the current knowledge on the biologic action of PTH at the cellular level. The inconsistent results that were obtained in early studies using quin-2 as the Ca^{2+} indicator may reflect the use of a poorly sensitive system (47,48). Interestingly, Yamaguchi *et al.* (44,49), using fura-2 and a single excitation/single emission detection system, were able to detect results closely similar to ours in PTH-stimulated osteoblastic cells.

One of the problems frequently encountered with Ca^{2+} -sensitive dyes is the conversion of the fluorescent signal into $[\text{Ca}^{2+}]_i$ levels. Calibration curves based on fluorescence values against a known free Ca^{2+} concentration in a buffer can be used. However, the optical properties of most dyes change in the cytoplasmic environment, as compared to a protein-free solution. This may lead to erroneous estimations of $[\text{Ca}^{2+}]_i$ in some cases. We prefer an “internal” calibration for each experiment. Such a procedure is quite easy in cell suspensions, but it may present some difficulties in single-cell settings. In the case of indo-1, after subtraction of autofluorescence at each wavelength, the ratio of the emission at 400 nm to that at 490 nm can be calculated and the corresponding value of $[\text{Ca}^{2+}]_i$ determined from the relationship $[\text{Ca}^{2+}]_i = K_d[(R-R_{\min})(R_{\max}-R)]\beta$ (40), where R is the measured ratio, R_{\min} and R_{\max} are the values of R at very low and saturating concentrations of calcium, respectively, and β is the ratio of emission intensities at 490 nm in these two sets of conditions. Calcium saturation of indo-1 is achieved by adding 5 mM ionomycin to loaded cells, and effectively zero calcium by the further addition of 12.5 mM EGTA. Cells can be permeabilized with saponin or digitonin before the addition of EGTA to decrease the time necessary for $[\text{Ca}^{2+}]_i$ to reach a minimum value. K_d , the dissociation constant of indo-1 + Ca^{2+} , can be experimentally calculated for each batch of dye, or it can be reasonably assumed to be close to 250 nM (40). Similar methods can be used for fura-2, except that a dual excitation configuration is required, as detailed later.

Intracellular pH

The concentration of intracellular protons in osteoblasts can be monitored in a manner similar to that described for $[\text{Ca}^{2+}]_i$, using pH-sensitive probes. A certain number of these probes have been developed, and the most popular are derivatives of carboxyfluorescein, such as BCECF, and the newly introduced rhodamine-based SNAFL and SNAFR. Our group and others have used BCECF to study hormonal regulation of intracellular pH (pHi) in osteoblastic cells (50–52). Being available in an AM form, BCECF

is loaded using the same procedure described for the Ca^{2+} indicators (see earlier). Thus, cell suspensions can be prepared after a short (30–40 min) incubation with BCECF-AM. Although the excitation spectrum of BCECF shifts in relation to ambient pH, the emission intensity changes little at excitation wavelengths lower than the isobestic point. Because of this, dual-wavelength ratio recording is usually obtained by dividing fluorescence intensity at the pH-sensitive range (480–500 nm) to that at the isobestic point (435 nm). This method allows correction for dye concentration and signal stabilization and is also used for calibration. Fluorescence ratios can be converted to pHi using a calibration curve obtained from BCECF-loaded cells suspended in buffers containing high K^+ concentrations and the K^+ - H^+ ionophore nigericin (50). In these conditions, pHi is equal to the medium pH, which is measured with a pH electrode. An alternative method for calibration of BCECF fluorescence consists in lysing the cells with Triton X-100, followed by subsequent additions of hydrochloric acid. The two methods should give comparable results, but cell lysis results in the dilution of the cytoplasmic components. Since the optical properties of the dye may be different inside the cell than in a cuvette (53), the second method may lead to slight but significant errors in estimating the correct pHi.

Application of pH-sensitive probes has helped delineate the mechanisms by which pHi is regulated in osteoblasts. We have demonstrated that one such mechanism is mediated by the Na^+/H^+ antiporter, which is inhibited by PTH, thus leading to cell acidification (50). Green *et al.* (51,52) have defined the properties of the antiporter and its function in relation to $[\text{Ca}^{2+}]_i$ in osteoblastic cells. An important point to keep in mind in pHi studies, and which certainly applies to osteoblasts, is the presence of bicarbonate in the bathing buffer and the pCO_2 of the atmosphere above the sample. Most of the initial studies on pHi regulation by hormones or growth factors were performed in the absence of bicarbonate, and thus at a lower than physiologic pHi. Although this experimental condition allowed one to selectively study the function of the Na^+/H^+ antiporter without the interference of bicarbonate-dependent transport mechanisms, the pHi changes induced by growth factors are smaller than those produced by readdition of bicarbonate to the medium (24,54). These observations should lead to critical reconsideration of the results obtained in bicarbonate-free conditions as far as physiologic relevance.

Membrane Potential

Potentiometric dyes have been used in many fields of cell physiology for the last two decades. However, probably because bone cells are not considered “excitable” in classic terms, and because of the increasing popularity and

powerful potentials of electrophysiologic techniques using patch-clamp systems, the application of fluorescent indicators of membrane potential to bone cells has been very limited. Dyes that report membrane potential are usually classified as “fast dyes” and “slow dyes” (25). Fast dyes can monitor changes of membrane potential in the millisecond range, whereas slow dyes can report voltage changes in longer time frames, as in the case of slow responses to hormonal stimulation. These differences relate to the different mechanisms by which the two classes of dyes respond to voltage changes. Fast dyes incorporate into the membrane, and their spectral properties change when the transmembrane voltage is perturbed. This class of dyes is more suitable to track rapid voltage changes in excitable cells. Because they are membrane-bound, and some of them undergo voltage-dependent spectral shifts, they have been proposed for microscopic fluorescence applications, using ratio video imaging (25,55). Slow dyes are instead charged but very liposoluble fluorescent molecules that partition across the plasma membrane according to the voltage difference. Spectral changes, in most cases variations in emission light intensity, are produced by the physicochemical differences between the intracellular and extracellular environments.

We have applied one of the slow potentiometric dyes, di-BA-C₄(3), an oxonol derivative, to study the electrophysiologic characteristics of osteoblastlike cells (56). For measurement of steady-state membrane potential, cells are simply released from the tissue culture flask, as described in previous sections, and resuspended in the appropriate buffer. The voltage-sensitive dye is added to the cell suspension at a concentration that provides a readable signal without saturating the photomultiplier, so that minimal changes in fluorescence intensity can be detected. For di-BA-C₄(3) we found 2 μM to be a suitable concentration. The dye equilibrates across the plasma membrane very rapidly, and the experiments can be initiated a few minutes after labeling. Real-time changes of membrane voltage can be followed by monitoring di-BA-C₄(3) fluorescence (56), but calibration of the optical signal is difficult. In our original study, we developed a calibration method based on the calculation of the pH null point (56), after having found other methods unsuitable. In the presence of a protonophore, which allows protons to freely move across the membrane, the membrane potential is equivalent to H⁺ equilibrium potential, and can be calculated by the Nernst equation [see Ref. 56 for details]. A good estimation of membrane potential using this method implies the precise knowledge of both intracellular and extracellular pH. When a protonophore is present, intracellular pH changes linearly with extracellular pH, and such a correlation can be calculated for a specific cell type in separate experiments, by measuring

pHi using a fluorescent probe (see earlier), and extracellular pH using a microelectrode.

Despite this successful initial approach, the application of potentiometric fluorescent probes to study biologic phenomena in bone cells has not been developed. The difficulty in obtaining stable signals in many circumstances, the cumbersome calibration methods, and the requirement of keeping the extracellular concentration of the dye tightly controlled have perhaps discouraged investigators from pursuing further efforts with this method. It is fair to say that patch-clamp techniques offer undeniable advantages over fluorometric techniques. Nonetheless, potentiometric dyes can monitor membrane voltage in multiple cells at the same time, which is not possible with microelectrode-based techniques, and without the requirement of mechanically disrupting the cell membrane. Further development of this class of dyes currently under way should overcome many of the applicative problems of the first generation of voltage-sensitive indicators.

Cell-Cell Communication

Methodologies based on fluorescent indicators have been used for the study of intercellular communication through gap junctions. Gap junctions are transcellular channels, which are formed by juxtaposition of two hemichannels facing each other on the plasma membrane of two adjacent cells. Each hemichannel is composed by six subunits, or connexins. When two hemichannels on opposing membranes are in register, a channel is formed that provides effective continuity between two cells. The gap junction channels allow ions as well as small molecules (<1000 Da) to pass from cell to cell. It is becoming increasingly evident that the pores of the transcellular channel formed by the different connexins (a dozen have been cloned so far) may differ in size and electric charge, which could provide the connexin with specificity for certain molecules or ions (57,58). Studies performed by our group have demonstrated that normal and transformed osteoblasts express both connexin43 and connexin45 (59,60), but that the two different connexins impart different molecular permeabilities to the gap junction they form (60,61).

Although the methods commonly employed to study the function of gap junctions as transcellular channels are based on microscopic fluorescence (see the following) and electrophysiology, more recently a technique that takes advantage of flow cytometry has been proposed. This method consists of determining the transfer of calcein from donor to acceptor cells after double-dye loading (62). The donor population is loaded with a gap junction permeant dye, calcein, and the recipient cells are stained with a permanent nontoxic lipophilic dye that binds the membrane irreversibly, such as

PKH26. Labeling with PKH26 is performed in cell suspensions by brief (2 min) incubation with the dye, followed by extensive washes in serum-containing media. Calcein is introduced in donor cells either in suspension or in tissue culture dishes, by incubation with the membrane-permeant acetoxymethyl ester form of the dye for 30–60 min. The two cell populations are mixed in appropriate ratios (depending of the degree of dye coupling), reseeded, and incubated for 24–48 hr co-cultured cells are harvested by trypsinization and analyzed by flow cytofluorometry. If the cells have functional gap junctions, upon cell mixing calcein passes from the loaded cells (fluorescein emission) to cells labeled with PKH26 (red emission). By calculating the percentage of PKH26-labeled cells that accept calcein from donor cells one can quantitate the degree of dye coupling (61,62). Although it requires substantial manipulations, this method affords a precise and rapid quantitation of dye coupling in large numbers of cells, and it appears to be considerably more sensitive than dye diffusion after microinjection. Accordingly, it can be employed primarily to assess coupling in osteogenic sarcoma cells, or when cells are available in large numbers. We have found this method to be very well suited to compare dye coupling between connexin transfectants and parent cells. For example, cells that express connexin43 are highly coupled by this method, whereas cells that preferentially express connexin45 are not (61).

ANALYSES IN SINGLE CELLS

Applicative Consideration

The monitoring of intracellular events in live, individual cells has overcome most of the problems and limitations of the initial fluorometric techniques developed for cell population studies. Many of the manipulations required for releasing the cells from their culture substrate can be avoided by simply culturing the cells on solid-state media (usually glass coverslides) suitable for fluorescence microscopy. In this way, all the cell-to-cell interactions, the cell shape, and the cytoskeletal architecture are maintained, and so is their potential contribution to a cell's ability to respond to an external stimulus. This is particularly useful for cells that strongly attach to plastic plates, that is, osteoclasts. Single-cell preparations require a very small number of cells, compared to cell suspensions, thus allowing the study of cell types that are available in limited quantities. An additional advantage of these systems is the possibility to perform manipulations on individual cells, such as microinjection of fluorescent dyes, or of antibodies or nucleic acids. Furthermore, it is possible to couple a fluorometric system to a patch-

clamp apparatus for simultaneous assessment of ionic concentrations and membrane currents. The potential usefulness of such a system is easy to envision, but the complexity of the hardware necessary for the optical and electric detection systems greatly limits its applicability.

Single-cell monitoring of fluorescent indicators in live cells can be performed using two types of detection systems, photon counting and video image analysis. The two applications may be employed for very different purposes, which hinge on and take advantage of some essential features of each detection system. Photon counting is very sensitive, has a high temporal resolution, and data collection and analysis is rather straightforward. However, it does not offer any information about the spatial relationships among the cells being studied. A single cell at a time can be studied, but if the field of view is extended to multiple cells, the signal detected represents the summation of events occurring in that particular section of the culture. Therefore, unless single cells are monitored, photon counting on multiple cells offers limited advantage over cell suspensions. An example is provided by studying responses to hormonal stimulation. Heterogeneity of responses among cells can be better detected by single-cell studies exploiting the bidimensional spatial resolution of video imaging. However, if the aim is to establish average hormonal responses in a rather homogeneous tissue (i.e., parathyroid cells), a cell population approach is clearly more advantageous.

An imaging system offers the ability to monitor fluorescence in an entire microscopic field, thus providing information on individual cells within the area examined. In this fashion, all intercellular spatial relationships are maintained, and individual cell behavior can be assessed directly. Perhaps the major disadvantage of video imaging systems stems from their technical complexity and elevated equipment cost. Most of the complications arise from the necessity of handling large amounts of information in very short time frames, which requires a very efficient and fast computing capacity. Systems that allow the delivery of two independent excitation beams to the sample can provide fluorescence ratio imaging, a more sensitive method compared to a single-wavelength recording, but require on-line image processing for best results, which may substantially slow down the data acquisition rate. Imaging systems that can simultaneously detect fluorescence emitted at two different wavelengths have an added degree of complexity generated by the need of an absolutely precise overlap between the two images. A detailed description of fluorescence detection systems, for both photon counting or video imaging, can be found in several publications (63–67). We shall describe some applicative considerations as they pertain to studies in bone cells.

Sample Preparation

For single-cell studies, the cells are cultured directly on glass coverslips, whose size must fit a holder or tissue culture chamber that can be placed on the stage of an inverted microscope. Both osteoblast primary cultures and osteosarcoma cells can be grown on glass support, without coating (67–69). The preparation of osteoblastic cells presents the same problems as any other cell, except that cultures of normal cells require a long time (4–6 weeks) before they reach a suitable density in the coverslip. Because they do not replicate, osteoclasts seeded onto the coverslips can be loaded with fluorescent indicators and analyzed shortly after attachment to the glass substrate. Our experience with chicken osteoclasts suggests that seeding densities of 1 to 2×10^6 cells per coverslip are suitable (70–72). Because of the importance of matrix proteins for osteoclast attachment (70), one should consider coating the glass surface with a layer of matrix components or with a specific protein in order to simulate the natural microenvironment of the bone surface. This is especially important for studying signaling mechanisms that involve the cytoskeleton.

Cells lying on the coverslip should be immediately covered with buffer or media to avoid dehydration. The coverslips fitted onto the tissue culture chamber should be kept at constant temperature, usually 37°C , during the experiment. This is usually accomplished by an internal water circulation system, or by an electric heating system. The second is preferable because it avoids possible leakages of water into the sample chamber, and it affords a better control of the temperature in the sample.

The microscopic system should be equipped with optics suitable for fluorescent light. We have had a successful experience with the Nikon Diaphot inverted microscope and the Fluor objectives, which can be used with phase-contrast illumination for focusing and scanning of the sample before the fluorescence measurements (67).

Cytosolic Calcium

Because of the widespread availability of fluorescence microscopic systems with dual excitation capabilities, fura-2 has enjoyed larger popularity than other Ca^{2+} indicators in single-cell analyses. The excitation spectrum shift of fura-2 upon binding to Ca^{2+} allows ratio recordings, in manner similar to indo-1 (see earlier). The excitation shift offers the additional advantage of using a single detector for fluorescence emission, which makes it possible to obtain ratio images using a single camera. On the other hand, a fast switch between the two optimal wavelengths (340–350 and 380 nm) is necessary to obtain readings as close as possible in time.

The basic techniques used for loading osteoblasts and osteoclasts on glass coverslips are not dissimilar to what has been described for cell population analyses (see earlier discussion). One of the problems we encountered, especially for cells that required prolonged incubation with fura-2AM, was dye compartmentalization. We have managed to minimize this phenomenon by loading cells at a lower temperature, as originally suggested by Malgaroli *et al.* (73). Loading can be improved with a mild detergent, such as pluronic F-127. Incomplete hydrolysis of fura-2AM, which reduces the Ca^{2+} sensitivity of the dye, is a problem that can be overcome by prolonging the incubation during loading. We have incubated osteoclast cultures for as long as 2 hr without affecting the viability of these cells (35). Alternatively, fura-2 free acid can be directly microinjected into individual cells. Although this invasive method requires the proper hardware and technical skills, it can be used to study a few cells at a time. Fura-2-loaded cells in the microscopic field are excited by alternating between 340 and 380 nm every second, after filtration through a dichroic mirror with a cutoff wavelength close to 400 nm.

For photon counting, the optical signal is detected by a photomultiplier and relayed to a computer, which generates a real-time recording of fluorescence intensity for both 340- and 380-nm excitation wavelengths. After background subtraction, the fluorescence signal is calibrated according to the method of Grynkiewicz *et al.* (40), as detailed previously. Even in this case, our preference goes to a calibration for each experiment, usually performed at the end. Because EGTA tends to permeabilize the cells, in many cases rapid loss of fluorescence occurs shortly after addition of the chelator (35). The operator should be careful to select the appropriate concentration of EGTA for each cell preparation, and ensure that fluorescence recording is obtained before the signal loss is significant.

Video images of fura-2-loaded cells are collected at the two excitation wavelengths. In our laboratory, we use 340 and 380 nm. The two images are ratioed after background subtraction to yield a final image that represents $[\text{Ca}^{2+}]_i$ concentration, in a gray scale. The gray scale is usually converted to an arbitrary color scale for better appreciation of the ion distribution within the cytoplasm (67). Alternatively, fluorescence can be recorded at 340 and 360 nm, instead of 380 nm. Since at 360 nm excitation, the isosbestic point of fura-2, the emitted fluorescence does not change upon Ca^{2+} binding, the image obtained at 360 nm can be used to correct the Ca^{2+} -sensitive 340-nm image, thus providing a more stable image. This type of correction may be useful when the system cannot provide image recording fast enough to detect very rapid changes in $[\text{Ca}^{2+}]_i$. Faster data acquisition can be obtained by recording at a single Ca^{2+} -sensitive wavelength and switching to the Ca^{2+} -insensitive wavelength every few seconds. The changes of fluorescence at 360 nm can be considered negligible within

such a short time frame. The ratio images are further elaborated by background subtraction, masking, and, when required, correction for shading and uniformity. The reader is referred to our review on this topic, as applied to bone and kidney cells (67), and to other reviews on more specific methodological issues (65).

The same comments detailed for photon counting apply to calibration of video images, with additional considerations. Although even in this case an internal calibration is preferred, an unstable or weak fluorescent signal may hinder a good calibration in many instances. In these cases, the use of a predetermined conversion curve is advisable. Whereas many methods can be found in the literature, we propose the following, modified from Ogura *et al.* (74). Small droplets of 20 mM Pipes-NaOH buffer (pH 6.8) containing EGTA and CaCl_2 in calculated ratios and 10 μM fura-2 pentasodium salt are suspended in liquid paraffin and excited at 340 and 360 or 380 nm, alternatively. The ratio values (340/360 nm or 340/380 nm) are then plotted against Ca^{2+} concentration and a calibration curve is constructed. The limitations related to the value of K_d also apply to image-based data, which further complicates the calibration procedures. Nonetheless, a good estimation of the actual $[\text{Ca}^{2+}]_i$ levels in bone cells should be pursued, simply because osteoblasts and osteoclasts live in a microenvironment wherein massive movements of Ca^{2+} occur, and the function of these cells, particularly osteoclasts, is directly regulated by the levels of $[\text{Ca}^{2+}]_i$ (33,71,72,75). We have successfully applied video imaging of transformed and normal osteoblastic cells, and demonstrated that the $[\text{Ca}^{2+}]_i$ response to PTH is heterogeneous from cell to cell, probably reflecting a different degree of expression of PTH receptors (68,76).

Intracellular pH

One of the primary functions of the osteoclast is to acidify the sealed compartment below the ruffled border to allow matrix and mineral dissolution (77,78). Because acidification of the extracellular resorption compartment is an active process requiring secretion of protons (79), the osteoclast must compensate for the loss of hydrogen ions through complementary mechanisms, one of which is the chloride/bicarbonate exchanger (77). Regulation of pH is therefore paramount in osteoclast physiology. The development of single-cell techniques for monitoring pH_i has provided the appropriate tools to investigate pH_i homeostasis in isolated osteoclasts.

The experimental setting is the same as described for photon counting or imaging of $[\text{Ca}^{2+}]_i$. Osteoclasts are cultured on glass coverslips, following the methods detailed in the Cell Cultures section, and loaded with BCECF directly on the coverslip. Osteoclasts are very large and flattened cells, and

the fluorescence intensity in the periphery is usually low relative to the multinucleated area. This characteristic feature of osteoclastic cells imposes some limits to the use of video imaging, and in many instances photon counting is preferred. Because of the large size, the microscopic field can be framed to include only a single osteoclast. Thus, unless intracellular ionic gradients are to be studied, photon counting can provide as much information as video imaging, at least in quantitative terms. Recording and calibration of BCECF fluorescence are performed by applying the same principles and procedures described for cell population studies. Therefore, if a dual excitation system is available, the user can record fluorescence emission (around 505 nm) at excitation wavelengths of 495 (pH sensitive) and 440 (isosbestic point) nm. After background fluorescence subtraction, the 495/440 nm ratio is calculated. Ratio values are then converted to pHi by constructing calibration curves at the end of each experiment. Either the nigericin/high-potassium or cell lysis with Triton X-100 methods can be used to this end (see earlier). Members of our group have successfully used BCECF and fluorescence microscopy in isolated, avian osteoclasts, and defined the importance of pHi changes for cell attachment to bone matrix and their resorptive activity (70,80).

Intracellular Cyclic AMP

The recent development of a fluorescent indicator that reports cAMP concentrations, [cAMP], has allowed monitoring of real-time changes of this important second messenger in live cells (81,82). We have applied this new technology to osteoblastic cells to verify whether the heterogeneous response to PTH we had observed for the Ca^{2+} signaling system (68) could also be detected for the cAMP pathway. The cAMP indicator, FICRhR, consists of protein kinase A, whose catalytic subunit has been labeled with fluorescein (FIC) and the regulatory subunit is labeled with rhodamine (RhR). In the absence of cAMP, the two subunits are bound in a dimeric complex, which brings the two fluorophores in close proximity and allows resonance energy transfer between the two fluorophores. Therefore, by exciting the complex in the fluorescein range (450–490 nm), light will be emitted in the rhodamine range (560–590 nm). Conversely, in the presence of cAMP, the two subunits dissociate, resonance energy transfer does not occur, and the emission will be in the fluorescein range (500–530 nm). Details on the optical properties of FICRhR and on the theoretical bases of the technique can be found elsewhere (81–83).

For these experiments, coverslips with semiconfluent (50–60% confluent) monolayers of osteoblastic cells are placed in a custom-made holder and positioned on the stage of an inverted epifluorescence microscope (69).

Because the probe is a protein, it must be microinjected into individual cells. This is usually accomplished using micropipettes with a tip of approximately $0.5\ \mu\text{m}$ in diameter. Following microinjection, cells should be allowed to recover for at least 30 min. Not all the cells microinjected survive the invasive procedure, and only those showing no perturbation or loss of FICRHR fluorescence are used for the experiment.

Monitoring FICRHR fluorescence requires a high-speed laser scanning confocal microscope capable of dual emission ratio imaging (64). Although xenon light can be used as a source for the exciting light, laser-based systems may provide a better uniformity of illumination. FICRHR is excited at 460–490 nm, and emission is simultaneously collected at 500–530 nm (fluorescein emission band) and above 560 nm (rhodamine emission band). Image processing of FICRHR images is essentially the same as that described for fura-2 ratio imaging, with some differences. Because the ratio image is generated by two emission images, the system must provide a precise overlap of the two frames, which are taken simultaneously by two detectors. Following background subtraction, images corresponding to the 500–530/ >560 nm ratio are generated and displayed in pseudocolors, representing cAMP levels between zero and saturating cAMP concentration. Absolute calibration of ratio, or pseudocolor hues in terms of free [cAMP], can be accomplished using a principle similar to that applied to $[\text{Ca}^{2+}]_i$ calibrations (83). As the reference points for calibration, virtually 0 [cAMP] is simulated by addition of the cAMP antagonist $R_p\text{cAMPS}$, and maximal [cAMP] is achieved by cell exposure to high doses of forskolin ($10^{-5}\ \text{M}$). Calibration may be problematic in cells that do not give consistent or stable responses to the cAMP antagonist. Unfortunately, this proved to be the case in both osteogenic sarcoma and human trabecular bone cells (69). Nevertheless, because osteoblastic cells typically increase their ratio by 1.5- to 1.6-fold upon effective stimulation with PTH, in a typical experiment their protein kinase A must go from minimal to nearly complete activation of the kinase, which is half-maximally activated at 100–300 nM [cAMP] (81,83). Therefore, the changes that are observed can be considered physiologically relevant. Using this approach, we have demonstrated that the cAMP response to PTH in osteogenic sarcoma cells is much more homogeneous from cell to cell than the $[\text{Ca}^{2+}]_i$ response (69).

Although this technique requires a complex imaging system and mechanical injection of the probe into individual cells, the use of a recombinant protein kinase offers some peculiar advantages. The major advantage is the possibility of following the translocation of the catalytic subunit of protein kinase from the cytoplasm to the nucleus as an index of more downstream events following cAMP production. This can be accomplished by monitoring the intracellular distribution of the fluorescein-labeled cata-

lytic subunit using the individual fluorescence images acquired at 500–530 nm. The amount of catalytic subunit present in the nucleus relative to that in the cytoplasm is assessed by ratioing the average 500- to 530-nm fluorescence intensity in the nucleus to that in the cytoplasm. This measure reports the relative distribution of the subunit independently of factors such as illumination intensity, change of focus, or photobleaching.

Cell Coupling

The classic and still widely used method to assess cell coupling through gap junctions is the *intercellular transfer of microinjected dyes*, usually Lucifer yellow (84). The experimental system is straightforward, but requires a microinjector-micromanipulator. Cells adherent to glass coverslips are grown to a suitable degree of confluence that allows direct cell-to-cell contacts. The coverslips are mounted in a tissue chamber similar to those described previously, and placed on the stage of an inverted epifluorescence microscope. Cells from confluent areas of the culture are microinjected with the dye (1100–1200 psi applied for 0.2–0.3 sec), and fluorescence is monitored either by using a low-light silicon-intensified target camera normally used for video imaging or by taking snapshots of the microscopic field 3–5 min after the injection. This method allows monitoring of dye diffusion in adherent cells, which can maintain physical contact with their neighbors. Although the number of adjacent cells containing dye 3–5 min after the injection can be used as a measure of dye coupling, frequency distributions of coupled cells are usually skewed and quantitation is difficult. An alternative method for introducing fluorescent dyes into cells in *scrape loading* (85). With this technique, the cell layer in tissue culture dishes is subjected to multiple “scratches” using a rubber policeman in the presence of a fluorescent dye in the bathing solution. Although many of the cells will be fatally damaged, some of them will reseal, trapping the dye inside. After a few minutes, the dye will pass from the primary scrape-loaded cell to neighboring cells, if gap junctions are present. A large fluorescent molecule that does not diffuse through the junctions can be used to distinguish the primary loaded cells from those that receive the dye from their neighbors. The method has its obvious limitations, but it can be useful to rapidly screen cell lines for dye coupling.

Propagation of $[Ca^{2+}]_i$ waves may be used to study intercellular communication. This method takes advantage of the fact that osteoblasts, like other cell types, when mechanically stimulated generate a sudden and transient increase in $[Ca^{2+}]_i$. The $[Ca^{2+}]_i$ rise rapidly spreads to neighboring cells with a variable time lag (86). We have found that the $[Ca^{2+}]_i$ waves generated in cultures of cells that express primarily connexin43 are slower

to propagate and affect a limited number of cells, whereas those observed in cells expressing connexin45 more abundantly than connexin43 are much faster and tend to affect a larger number of cells (T. H. Steinberg and R. Civitelli, unpublished observations, 1994). Although the precise mechanisms at the basis of this phenomenon are still unknown, functional gap junctions are necessary for wave propagation (86,87). For these experiments, cells in monolayer are loaded with fura-2, and one cell is gently touched with a pipette. Because the readout is $[Ca^{2+}]_i$, fluorescence ratio imaging is required.

Additional methods have been used to assess intercellular communication, but they have not been applied to bone cells. One of these is *fluorescence recovery after photobleaching* (88), which requires a laser-based video imaging system. Cells grown on glass slides are loaded with a fluorophore that permeates gap junctions and that can be used as acetoxymethyl ester derivative, that is, 6-carboxyfluorescein. Using a high-intensity laser light pulse, the dye is selectively photobleached in an individual cell. If that cell is functionally coupled via gap junctions to neighboring cells, dye molecules will diffuse through the junctions from the neighbors into the cell that has been photobleached. The rate of fluorescence recovery after photobleaching can be used to quantitate the degree of cell–cell communication. The method is potentially useful because it can be quantitative, and it does not require disruption of the cell membrane. However, the requirement of costly and complex equipment and the number of alternative methods available to assess cell coupling greatly limit its applicability.

ACKNOWLEDGMENTS

Part of the work quoted in this chapter has been supported by NIH Grants AR41255, AR32087, and DK46686, NIH Training Grant AR07033, and a grant from Shriners Hospital for Crippled Children.

REFERENCES

1. M. Weinreb, D. Shinar, and G. A. Rodan, Different pattern of alkaline phosphatase, osteopontin, and osteocalcin expression in developing rat bone visualized by *in situ* hybridization. *J. Bone Miner. Res.* **5**, 831–842 (1990).
2. L. G. Raisz and G. A. Rodan, Cellular basis of bone turnover. In “Metabolic Bone Diseases and Clinically Related Disorders” (L. V. Avioli and S. M. Krane, eds.), pp. 1–41. Saunders, Philadelphia, Pennsylvania, 1990.
3. G. S. Stein, J. B. Lian, and T. A. Owen, Relationship of cell growth to the regulation of tissue specific gene expression during osteoblast differentiation. *FASEB J.* **4**, 3111–3123 (1990).

4. M. P. Mark, W. T. Butler, C. W. Prince, R. D. Finkelman, and J. V. Ruch, Developmental expression of 44-kDa bone phosphoprotein (osteopontin) and bone gamma-carboxyglutamic acid (Gla)-containing protein (osteocalcin) in calcifying tissues of rats. *Differentiation* **37**, 123–136 (1988).
5. T. A. Owen, M. S. Aronow, V. Shalhoub, L. M. Barone, L. Wilming, M. S. Tassinari, J. B. Lian, and G. S. Stein, Progressive development of the rat osteoblast phenotype *in vitro*: Reciprocal relationship in expression of genes associated with osteoblast proliferation and differentiation during formation of the bone extracellular matrix. *J. Cell. Physiol.* **143**, 420–430 (1990).
6. N. C. Partridge, D. Alcorn, V. P. Michelangeli, G. Ryan, and T. J. Martin, Morphological and biochemical characterization of four clonal osteogenic sarcoma cell lines of rat origin. *Cancer Res.* **43**, 4308–4314 (1983).
7. S. M. Forrest, K. W. Ng, D. M. Findlay, V. P. Michelangeli, S. A. Livesey, N. C. Partridge, J. D. Zajac, and T. J. Martin, Characterization of an osteoblast-like clonal cell line which responds to both parathyroid hormone and calcitonin. *Calcif. Tissue Int.* **37**, 51–56 (1985).
8. R. J. Majeska, S. B. Rodan, and G. A. Rodan, Parathyroid-hormone responsive clonal cell lines from rat osteosarcoma. *Endocrinology (Baltimore)* **107**, 1494–1503 (1980).
9. R. J. Majeska, B. C. Nair, and G. A. Rodan, Glucocorticoid regulation of alkaline phosphatase in the osteoblastic osteosarcoma cells ROS 17/2.8. *Endocrinology (Baltimore)* **116**, 170–179 (1985).
10. J. D. Fraser, Y. Otawara, and P. A. Price, 1,25-Dihydroxyvitamin D₃ stimulates the synthesis of matrix gamma-carboxyglutamic acid protein by osteosarcoma cells. *J. Biol. Chem.* **263**, 911–916 (1988).
11. N. Kurihara, S. Ishizuka, M. Kiyoki, Y. Haketa, K. Ikeda, and M. Kumegawa, Effects of 1,25-dihydroxyvitamin D₃ on osteoblastic MC3T3-E1 cells. *Endocrinology (Baltimore)* **118**, 940–947 (1986).
12. L. D. Quarles, D. A. Yohay, L. W. Lever, R. Caton, and R. J. Wenstrup, Distinct proliferative and differentiated stages of murine MC3T3-E1 cells in culture: An *in vitro* model of osteoblast development. *J. Bone Miner. Res.* **7**, 683–692 (1992).
13. S. B. Rodan, Y. Imai, M. A. Thiede, G. Wesolowski, D. D. Thompson, Z. Bar-Shavit, S. Shull, K. G. Mann, and G. A. Rodan, Characterization of a human osteosarcoma cell line (Saos-2) with osteoblastic properties. *Cancer Res.* **47**, 4961–4966 (1987).
14. B. Fournier and P. A. Price, Characterization of a new human osteosarcoma cell line OHS-4. *J. Cell Biol.* **114**, 577–583 (1991).
15. L. Rifas, A. Fausto, M. J. Scott, L. V. Avioli, and H. G. Welgus, Expression of metalloproteinases and tissue inhibitors of metalloproteinases in human osteoblast-like cells: Differentiation is associated with repression of metalloproteinase biosynthesis. *Endocrinology (Baltimore)* **134**, 213–221 (1994).
16. G. Kohler, V. Shen, and W. A. Peck, Adriamycin inhibits PTH-mediated but not PGE₂-mediated stimulation of cAMP formation in isolated bone cells. *Calcif. Tissue Int.* **36**, 279–284 (1984).
17. B. A. Ashton, F. Abdullah, J. Cave, M. Williamson, B. C. Sykes, M. Couch, and J. W. Poser, Characterization of cells with high alkaline phosphatase activity derived from human bone and marrow: Preliminary assessment of their osteogenicity. *Bone* **6**, 313–319 (1985).
18. S. Cheng, J. W. Yang, L. Rifas, S. Zhang, and L. V. Avioli, Differentiation of human bone marrow osteogenic stromal cells *in vitro*: Induction of the osteoblast phenotype by dexamethasone. *Endocrinology (Baltimore)* **134**, 277–286 (1994).
19. J. E. Wergedal and D. J. Baylink, Characterization of cells isolated and cultured from human bone. *Proc. Soc. Exp. Biol. Med.* **176**, 60–69 (1984).

20. B. Auf'mkolk, P. V. Hauschka, and E. R. Schwartz, Characterization of human bone cells in culture. *Calcif. Tissue Int.* **37**, 228–235 (1985).
21. P. Gehron Robey and J. D. Termine, Human bone cells *in vitro*. *Calcif. Tissue Int.* **37**, 453–460 (1985).
22. L. R. Halstead, M. J. Scott, L. Rifas, and L. V. Avioli, Characterization of adult rat osteoblasts *in vitro*. *Calcif. Tissue Int.* **50**, 93–95 (1992).
23. H. Chiba, N. Sawada, T. Ono, S. Ishii, and M. Mori, Establishment and characterization of a simian virus 40-immortalized osteoblastic cell line from normal human bone. *Jpn. J. Cancer Res.* **84**, 290–297 (1993).
24. M. B. Ganz, G. Boyarsky, R. B. Sterzel, and W. F. Boron, Arginine vasopressin enhances pHi regulation in the presence of HCO_3^- by stimulating three acid–base transport systems. *Nature (London)* **337**, 648–651 (1989).
25. L. M. Loew, Potentiometric membrane dyes. In “Fluorescent and Luminescent Probes for Biological Activity” (W. T. Mason and G. Relf, eds.), pp. 150–160. Academic Press, San Diego, 1993.
26. P. J. Marie, Human osteoblastic cells: A potential tool to assess the etiology of pathologic bone formation. *J. Bone Miner. Res.* **9**, 1847–1850 (1994).
27. G. R. Mundy and G. D. Roodman, Osteoclast ontogeny and function. In “Bone and Mineral Research” (W. A. Peck, ed.), pp. 209–280. Elsevier, Amsterdam, 1987.
28. T. Suda, N. Takahashi, and T. J. Martin, Modulation of osteoclast differentiation. *Endocr. Rev.* **13**, 66–80 (1992).
29. P. C. Marchisio, D. Cirillo, L. Naldini, M. V. Primavera, A. Teti, and A. Zambonin-Zallone, Cell–substratum interaction of cultured avian osteoclasts is mediated by specific adhesion structures. *J. Cell Biol.* **99**, 1696–1705 (1984).
30. A. Zambonin-Zallone, A. Teti, A. Carano, and P. C. Marchisio, The distribution of podosomes in osteoclasts cultured on bone laminae: Effect of retinol. *J. Bone Miner. Res.* **3**, 517–523 (1988).
31. T. J. Chambers, J. C. Chambers, J. A. Darby, and K. Fuller, The effect of human calcitonin on cytoplasmic spreading of rat osteoclasts. *J. Clin. Endocrinol. Metab.* **63**, 1080–1085 (1986).
32. T. J. Chambers, P. M. J. McSheehy, B. M. Thomson, and K. Fuller, The effect of calcium-regulating hormones and prostaglandins on bone resorption by osteoclasts disaggregated from neonatal rabbit bones. *Endocrinology (Baltimore)* **116**, 234–239 (1985).
33. A. Malgaroli, J. Meldolesi, A. Zambonin-Zallone, and A. Teti, Control of cytosolic free calcium in rat and chicken osteoclasts. *J. Biol. Chem.* **264**, 14342–14347 (1989).
34. N. Udagawa, N. Takahashi, T. Akatsu, T. Sasaki, A. Yamaguchi, H. Kodama, T. J. Martin, and T. Suda, The bone marrow-derived stromal cell lines MC3T3-G2/PA6 and ST2 support osteoclast-like cell differentiation in cocultures with mouse spleen cells. *Endocrinology (Baltimore)* **125**, 1805–1813 (1989).
35. C. Bizzarri, A. Shioi, S. L. Teitelbaum, J. Ohara, V. A. Harwalkar, J. M. Erdman, D. L. Lacey, and R. Civitelli, Interleukin-4 inhibits bone resorption and increases cytosolic calcium $[\text{Ca}^{2+}]_i$ in murine osteoclasts. *J. Biol. Chem.* **269**, 13817–13824 (1994).
36. G. D. Roodman, K. J. Ibbotson, B. R. McDonald, T. J. Kuehl, and G. R. Mundy, 1,25-Dihydroxyvitamin D_3 causes formation of multinucleated cells with several osteoclast characteristics in cultures of primate marrow. *Proc. Natl. Acad. Sci. U.S.A.* **82**, 8213–8217 (1985).
37. N. Kurihara, C. Chenu, M. Miller, C. Civin, and G. D. Roodman, Identification of committed mononuclear precursors for osteoclast-like cells formed in the long term human marrow cultures. *Endocrinology (Baltimore)* **126**, 2733–2741 (1990).

38. I. R. Reid, R. Civitelli, L. R. Halstead, L. V. Avioli, and K. A. Hruska, Parathyroid hormone acutely elevates intracellular calcium in osteoblast-like cells. *Am. J. Physiol.* **253**, E45–E51 (1987).
39. R. Civitelli, T. J. Martin, A. Fausto, S. L. Gunsten, K. A. Hruska, and L. V. Avioli, Parathyroid hormone-related peptide transiently increases cytosolic calcium in osteoblast-like cells. Comparison with PTH. *Endocrinology (Baltimore)* **125**, 1204–1210 (1989).
40. G. Grynkiewicz, M. Poenie, and R. Y. Tsien, A new generation of Ca^{2+} indicators with greatly improved fluorescence properties. *J. Biol. Chem.* **260**, 3440–3450 (1985).
41. K. A. Hruska, D. Moskowitz, P. Esbrit, R. Civitelli, S. L. Westbrook, and M. Huskey, Stimulation of inositol triphosphate and diacylglycerol production in renal tubular cells by parathyroid hormone. *J. Clin. Invest.* **79**, 230–239 (1987).
42. R. Civitelli, I. R. Reid, S. L. Westbrook, L. V. Avioli, and K. A. Hruska, Parathyroid hormone elevates inositol polyphosphates and diacylglycerol in a rat osteoblast-like cell line. *Am. J. Physiol.* **255**, E660–E667 (1988).
43. A. Fujimori, A. Miyauchi, K. A. Hruska, K. J. Martin, L. V. Avioli, and R. Civitelli, Desensitization of calcium messenger system in parathyroid hormone-stimulated opossum kidney cells. *Am. J. Physiol.* **264**, E918–E924 (1993).
44. D. T. Yamaguchi, T. J. Hahn, A. Iida-klein, C. R. Kleeman, and S. Muallem, Parathyroid hormone activated calcium channels in an osteoblast-like osteosarcoma cell line: cAMP-dependent and independent calcium channels. *J. Biol. Chem.* **262**, 7711–7718 (1987).
45. H. J. Donahue, M. J. Fryer, E. F. Eriksen, and H. Heath III, Differential effects of parathyroid hormone and its analogues on cytosolic calcium ion and cAMP levels in cultured rat osteoblast-like cells. *J. Biol. Chem.* **263**, 13522–13527 (1988).
46. J. P. Bidwell, M. J. Fryer, A. F. Firek, H. J. Donahue, and H. Heath III, Desensitization of rat osteoblast-like cells (ROS 17/2.8) to parathyroid hormone uncouples the adenosine 3',5'-monophosphate and cytosolic ionized calcium response limbs. *Endocrinology (Baltimore)* **128**, 1021–1028 (1991).
47. C. W. G. M. Löwik, J. P. T. M. van Leeuwen, J. M. van der Meer, J. K. van Zeeland, B. A. A. Scheven, and M. P. M. Herrmann-Erlee, A two-receptor model for the action of parathyroid hormone on osteoblasts: A role for intracellular free calcium and cAMP. *Cell Calcium* **6**, 311–326 (1985).
48. K. Meier, W. Knepel, and C. Schöfl, Potassium depolarization elevates cytosolic free calcium concentration in rat anterior pituitary cells through 1,4-dihydropyridine-sensitive, omega-conotoxin-insensitive calcium channels. *Endocrinology (Baltimore)* **122**, 2764–2770 (1988).
49. D. T. Yamaguchi, T. J. Hahn, T. G. Beeker, C. R. Kleeman, and S. Muallem, Relationship of cAMP and calcium messenger systems in prostaglandin-stimulated UMR 106-01 cells. *J. Biol. Chem.* **263**, 10745–10753 (1988).
50. I. R. Reid, R. Civitelli, L. V. Avioli, and K. A. Hruska, Parathyroid hormone depresses cytosolic pH and DNA synthesis in osteoblast-like cells. *Am. J. Physiol.* **255**, E9–E15 (1988).
51. J. Green, D. T. Yamaguchi, C. R. Kleeman, and S. Muallem, Cytosolic pH regulation in osteoblasts. Regulation of anion exchange by intracellular pH and Ca^{2+} ions. *J. Gen. Physiol.* **95**, 121–145 (1990).
52. J. Green, D. T. Yamaguchi, C. R. Kleeman, and S. Muallem, Cytosolic pH regulation in osteoblasts. Interaction of Na^+ and H^+ with the extracellular and intracellular faces of the Na^+/H^+ exchanger. *J. Gen. Physiol.* **92**, 239–261 (1988).
53. J. R. Chaillet and W. F. Boron, Intracellular calibration of a pH-sensitive dye in isolated perfused salamander proximal tubules. *J. Gen. Physiol.* **86**, 765–794 (1985).

54. M. B. Ganz and W. F. Boron, Long-term effects of growth factors on pH and acid–base transport in rat glomerular mesangial cells. *Am. J. Physiol.* **266**, F576–F585 (1994).
55. D. Gross and L. M. Loew, Fluorescent indicators of membrane potential: Microspectrofluorometry and imaging. In “Fluorescence Microscopy of Living Cells in Culture” (D. Lansing-Taylor and Y. Wang, eds.), pp. 193–219. Academic Press, San Diego, 1989.
56. R. Civitelli, I. R. Reid, L. R. Halstead, L. V. Avioli, and K. A. Hruska, Membrane potential and cation content of osteoblast-like cells (UMR 106) assessed by fluorescent dyes. *J. Cell. Physiol.* **131**, 434–441 (1987).
57. R. B. Stagg and W. H. Fletcher, The hormone-induced regulation of contact-dependent cell–cell communication by phosphorylation. *Endocr. Rev.* **11**, 302–325 (1990).
58. R. D. Veenstra, H. Wang, E. M. Westphale, and E. C. Beyer, Multiple connexins confer distinct regulatory and conductance properties of gap junctions in developing heart. *Circ. Res.* **71**, 1277–1283 (1992).
59. R. Civitelli, E. C. Beyer, P. M. Warlow, A. J. Robertson, S. T. Geist, and T. H. Steinberg, Connexin43 mediates direct intercellular communication in human osteoblastic cell networks. *J. Clin. Invest.* **91**, 1888–1896 (1993).
60. T. H. Steinberg, R. Civitelli, S. T. Geist, A. J. Robertson, E. Hick, R. D. Veenstra, H. Wang, P. M. Warlow, E. M. Westphale, J. G. Laing, and E. C. Beyer, Connexin43 and connexin45 form gap junctions with different molecular permeabilities in osteoblastic cells. *EMBO J.* **13**, 744–750 (1994).
61. M. Koval, S. T. Geist, E. M. Westphale, A. E. Kemendy, R. Civitelli, E. C. Beyer, and T. H. Steinberg, Transfected connexin45 alters gap junction permeability in cells expressing endogenous connexin43. *J. Cell Biol.* **130**, 987–995 (1995).
62. C. Tomasetto, M. J. Neveu, J. Daley, P. K. Horan, and R. Sager, Specificity of gap junction communication among human mammary cells and connexin transfectants in culture. *J. Cell Biol.* **122**, 157–167 (1993).
63. G. R. Bright, G. W. Fisher, J. Rogowska, and D. Lansing-Taylor, Fluorescence ratio imaging recording. In “Fluorescence Microscopy of Living Cells in Culture” (D. Lansing-Taylor and Y. Wang, eds.), pp. 157–192. Academic Press, San Diego, 1989.
64. R. Y. Tsien, Laser scanning confocal fluorescence microscopy at video rate (30 frames/sec) with dual-wavelength emission ratioing for quantitative imaging of intracellular messengers. *Proc. R. Microsc. Soc.* **25**, S53 (1990).
65. Z. Jericevic, B. Wiese, J. Bryan, and L. C. Smith, Validation of an imaging system: Steps to evaluate and validate a microscope imaging system for quantitative studies. In “Fluorescence Microscopy of Living Cells in Culture” (D. Lansing-Taylor and Y. Wang, eds.), pp. 48–83. Academic Press, San Diego, 1989.
66. J. F. Wampler and K. Kutz, Quantitative fluorescence microscopy using photomultiplier tubes and imaging detectors. In “Fluorescence Microscopy of Living Cells in Culture” (D. Lansing-Taylor and Y. Wang, eds.), pp. 239–267. Academic Press, San Diego, 1989.
67. R. Civitelli, A. Miyauchi, and K. A. Hruska, Monitoring cytosolic calcium in parathyroid hormone target cells: Osteoblasts and kidney epithelia. *J. Tissue Cult. Methods* **13**, 217–228 (1991).
68. R. Civitelli, A. Fujimori, S. Bernier, P. M. Warlow, D. Goltzman, K. A. Hruska, and L. V. Avioli, Heterogeneous $[Ca^{2+}]_i$ response to parathyroid hormone correlates with morphology and receptor distribution in osteoblastic cells. *Endocrinology (Baltimore)* **130**, 2392–2400 (1992).
69. R. Civitelli, B. J. Bacskai, M. P. Mahaut-Smith, S. R. Adams, L. V. Avioli, and R. Y. Tsien, Single-cell analysis of cyclic AMP response to parathyroid hormone in osteoblastic cells. *J. Bone Miner. Res.* **9**, 1407–1417 (1994).

70. A. Teti, H. C. Blair, P. Schlesinger, M. Grano, A. Zambonin-Zallone, A. J. Kahn, K. A. Hruska, and S. L. Teitelbaum, Extracellular protons acidify osteoclasts, reduce cytosolic calcium, and promote expression of cell-matrix attachment structures. *J. Clin. Invest.* **84**, 773–780 (1989).
71. A. Miyauchi, K. A. Hruska, E. M. Greenfield, R. L. Duncan, J. I. Alvarez, R. Barattolo, S. Colucci, A. Zambonin-Zallone, S. L. Teitelbaum, and A. Teti, Osteoclast cytosolic calcium, regulated by voltage-gated calcium channels and extracellular calcium, controls podosome assembly and bone resorption. *J. Cell Biol.* **111**, 2543–2552 (1990).
72. A. Miyauchi, J. I. Alvarez, E. M. Greenfield, A. Teti, M. Grano, S. Colucci, A. Zambonin-Zallone, F. P. Ross, S. L. Teitelbaum, D. Cheresch, and K. A. Hruska, Recognition of osteopontin and related peptides by an $\alpha_v\beta_3$ integrin stimulates immediate cell signals in osteoclasts. *J. Biol. Chem.* **266**, 20369–20374 (1991).
73. A. Malgaroli, D. Milani, J. Meldolesi, and T. Pozzan, Fura-2 measurement of cytosolic Ca^{2+} in monolayers and suspensions of various types of animal cells. *J. Cell Biol.* **105**, 2145–2155 (1987).
74. A. Ogura, Y. Myojo, and H. Higashida, Bradykinin-evoked acetylcholine release via inositol trisphosphate-dependent elevation in free calcium in neuroblastoma \times glioma hybrid NG108-15 cells. *J. Biol. Chem.* **265**, 3577–3584 (1990).
75. B. S. Moonga, A. S. M. Towhidul Alam, P. J. R. Bevis, F. Avaldi, R. Soncini, C. L. Huang, and M. Zaidi, Regulation of cytosolic free calcium in isolated rat osteoclasts by calcitonin. *J. Endocrinol.* **132**, 241–249 (1992).
76. R. Civitelli, A. Fujimori, S. Cheng, L. Rifas, L. R. Halstead, P. M. Warlow, K. A. Hruska, and L. V. Avioli, Single-cell analysis of the $[\text{Ca}^{2+}]_i$ response in normal rat and human bone cell cultures. In "Osteoporosis 1990" (C. Christiansen and K. Overgaard, eds.), pp. 277–279. Osteopress ApS, Copenhagen, Denmark, 1990.
77. R. Baron, L. Neff, D. Luovard, and P. J. Courtoy, Cell-mediated extracellular acidification and bone resorption: Evidence for a low pH in resorbing lacunae and localization of a 100-kD lysosomal membrane protein on the osteoclast ruffled border. *J. Cell Biol.* **101**, 2210–2222 (1985).
78. H. C. Blair, A. J. Kahn, E. C. Crouch, J. J. Jeffrey, and S. L. Teitelbaum, Isolated osteoclasts resorb the organic and inorganic components of bone. *J. Cell Biol.* **102**, 1164–1172 (1986).
79. H. C. Blair, S. L. Teitelbaum, R. Ghiselli, and S. Gluck, Osteoclastic bone resorption by a polarized vacuolar proton pump. *Science* **245**, 855–857 (1989).
80. A. Teti, H. C. Blair, S. L. Teitelbaum, A. J. Kahn, C. Koziol, J. Konsek, A. Zambonin-Zallone, and P. Schlesinger, Cytoplasmic pH regulation and chloride/bicarbonate exchange in avian osteoclasts. *J. Clin. Invest.* **83**, 227–233 (1989).
81. S. R. Adams, A. T. Harootunian, Y. J. Buechler, S. S. Taylor, and R. Y. Tsien, Fluorescence ratio imaging of cyclic AMP in single cells. *Nature (London)* **349**, 694–697 (1991).
82. P. J. Sammak, S. R. Adams, A. T. Harootunian, M. Schliva, and R. Y. Tsien, Intracellular cyclic AMP, not calcium, determines the direction of vesicle movement in melanophores: Direct measurement by fluorescence ratio imaging. *J. Cell Biol.* **117**, 57–72 (1992).
83. S. R. Adams, B. J. Bacskai, S. S. Taylor, and R. Y. Tsien, Optical probes for cyclic AMP. In "Fluorescent and Luminescent Probes for Biological Activity" (W. T. Mason and G. Relf, eds.), pp. 133–149. Academic Press, San Diego, 1993.
84. W. W. Stewart, Functional connections between cells as revealed by dye-coupling with a highly fluorescent naphthalimide tracer. *Cell (Cambridge, Mass.)* **14**, 741–759 (1978).
85. P. L. McNeil, Incorporation of macromolecules into living cells. In "Fluorescence Microscopy of Living Cells in Culture" (Y. Wang and D. Lansing-Taylor, eds.), Vol. 29, pp. 153–173. Academic Press, San Diego, 1989.

86. S. Xia and J. Ferrier, Propagation of a calcium pulse between osteoblastic cells. *Biochem. Biophys. Res. Commun.* **186**, 1212–1219 (1992).
87. M. J. Sanderson, A. C. Charles, and E. R. Dirksen, Mechanical stimulation and intercellular communication increases intracellular Ca^{2+} in epithelial cells. *Cell Regul.* **1**, 585–596 (1990).
88. M. H. Wade, J. E. Trosko, and M. Schindler, A fluorescence photobleaching assay of gap junction mediated communication between human cells. *Science* **232**, 525–528 (1986).

7

Measurement of Thyroid Hormones and Related Molecules

Edward J. Diamond

Department of Medicine

Division of Endocrinology

Mount Sinai School of Medicine

New York, New York 10029

INTRODUCTION

Laboratory evaluation of thyroid status centers around chemical measurements of thyroid gland secretory products present in the circulation, assessment of the hypothalamic–pituitary–thyroid axis, and measurement of related molecules that affect thyroid gland function, such as thyroid binding proteins and autoantibodies. During the past 10 to 15 years, many advances in thyroid testing have been made including the development of highly sensitive assays for thyroid stimulating hormone (TSH), new approaches to measuring free hormone concentrations, and automation of most routine thyroid assays. The goal of this chapter is to historically review the methods in use for measuring thyroid hormones and related substances in humans, and to focus on the merits and limitations of each approach. The intent is not to exhaustively review all available methods but to focus on those most commonly used. The literature references cited are representative for the topics covered but are not all-inclusive.

LABORATORY MEASUREMENTS TO ASSESS THYROID FUNCTION

Total Thyroxine (T4) and Triiodothyronine (T3)

Background

Thyroxine (T4) is the major secretory product of the thyroid gland and is present in the circulation at concentrations 50 to 100 times greater than triiodothyronine (T3). Total serum concentrations of total T4 and T3 range from about 4.5 to 12.5 $\mu\text{g}/100\text{ ml}$ and 70 to 200 $\text{ng}/100\text{ ml}$, respectively, depending on the measurement method used. Although T3 is present in much smaller amounts, it has about four times the biological activity of T4 and, in the circulation, represents the same level of biological activity as T4. The major source of T3 is from peripheral deiodination of T4, primarily in the liver. For these reasons and because it interacts with the T3 receptor, T3 is considered to be the primary thyroid hormone. Over 99% of both hormones are bound to protein in the blood and it is the unbound fractions that are considered to be biologically active. Both T4 and T3 function to control the rate of metabolic activity of most tissues and are required for physical and mental development during childhood. Total T4 measurements reflect the thyroid status in most individuals and most often parallel the free T4 levels. Serum T4 concentrations are usually elevated in hyperthyroidism and reduced in hypothyroidism. Total T3 measurements are used primarily to confirm hyperthyroidism in individuals with reduced levels of TSH and elevated concentrations of free T4 (FT4) (1).

Measurement of Total T4 and T3

Total T4 and total T3 are referred to as T4 and T3, respectively, and are measured by radioimmunoassay (RIA), enzyme immunoassay and a variety of automated immunoassay systems (2,3). RIA is still used extensively because it is sensitive, reliable, and inexpensive. Several of the available RIA kits offer simplified separation systems such as antibody-coated tubes or magnetic particles coated with antibody. T4 and T3 must first be released from their carrier proteins before they can react with antibody in the immunoassay. Chemical blocking agents such as 8-anilino-1-naphthalene sulfonic acid (ANS) (4) or salicylates (3), which release T4 and T3 from protein and prevent further binding, are incorporated into the assay reagents. Assay formats using nonradioactive labels such as fluorescent and chemiluminescent substances have been used and are currently available in some automated systems (5,6). The most widely used technology for measuring T4 and T3 in the United States is the fluorescence polarization immunoassay (7).

Influences on Measurement of Total T4 and T3

Measurements of T4 and T3 can be influenced by factors that limit their usefulness;

1. Abnormal concentrations of binding proteins in euthyroid individuals lead to high or low levels of T4 and T3, for example, pregnancy, oral contraceptives, and some drugs can cause increases in binding proteins. It is essential to know whether abnormal concentrations of T4 and T3 are due to variations in binding proteins; interpretation of total T4 and T3 concentrations requires this information (8).

2. Nonthyroidal illnesses (NTI) may cause decreases in T4 and T3 even when there is no thyroid abnormality. NTI refers to severe illnesses usually in hospitalized patients, that can affect thyroid hormone concentrations. NTI can lead to abnormalities in pituitary–thyroid function, in binding proteins, and in thyroid hormone metabolism.

3. Certain drugs may displace thyroid hormones from their protein binding sites and lead to decreases in T4 and T3 concentrations.

4. Situations in which T4 is normal and T3 is elevated (T3 toxicosis).

5. Thyroid hormone autoantibodies can interfere with RIA measurements of total and free concentrations of T4 and T3. When present they compete with the animal anti-thyroid antibodies used in the assay for radiolabeled T4 or T3. The presence of these autoantibodies can lead to incorrect assessment of thyroid status and inappropriate therapy. They can also bind endogenous T4 and T3 making them less available for metabolic action and leading to hypothyroidism (9–12).

Free Thyroid Hormone Measurements

Rationale for Measuring Concentrations of Free Hormone

Measurements of serum concentrations of free thyroxine (FT4) and free triiodothyronine (FT3) are believed to be better methods for assessing thyroid status than total hormone (bound + free hormone) measurements. The concentration of free hormone is more closely related to an individual's thyroid status than the total hormone concentration. Total T4 measurements are affected by variations in T4 carrier protein levels, which can change in response to estrogen administration, drugs, and other influences (13). Serum FT4 mirrors thyroid gland secretory activity and only the free hormone enters cells to exert its hormonal action (13). The view that the free hormone is the active form was advanced during the 1950s and is essentially held to today with few exceptions (14–16).

Thyroid Transport Proteins

The thyroid hormones T4 and T3 travel in the serum reversibly bound to transport proteins, which are synthesized in the liver. These proteins bind over 95% of the circulating hormone, the remaining 5% being carried primarily by lipoproteins. This leaves approximately 0.03% of the total thyroxine and 0.3% of the total triiodothyronine which circulates in the free form. The major thyroid binding protein is thyroxine binding globulin (TBG), followed by transthyretin (thyroid binding prealbumin, TBPA) and albumin. TBG binds 65% of the circulating T4 and 75% of T3, TBPA binds 10% of each, and albumin accounts for 20% of the T4 and 10% of T3 (17).

Circulating concentrations of TBG can be influenced by hormones, drugs, genetic factors and disease (18,19). Changes in carrier protein concentrations can elicit changes in total thyroid hormone concentration in the absence of thyroid disease (20,21). These changes in circulating levels of T4 and T3 occur without concomitant changes in FT4 and FT3 concentrations. This occurs because the bound hormone serves as a reservoir for the biologically active free form, and dissociation of hormone from its binding protein occurs rapidly (17).

Examples of Changes in Binding Proteins

TBG has a fairly high carbohydrate content (23%), which is increased under the influence of estrogens, as observed in pregnancy and during contraceptive use, and leads to increased clearance of the molecule and higher circulating concentrations of TBG. This is accompanied by increases in total T4 and T3, whereas free T4 and T3 levels do not change (22). In individuals with TBG deficiency, total T4 and T3 concentrations are decreased but the free hormone (FT4 and FT3) levels do not change, indicating that FT4 and FT3 concentrations are independent of TBG fluctuations (23,24).

Genetic variants of transthyretin with increased affinity for T4 show increased concentrations of T4 but normal FT4 (22). In the genetic disease familial dysalbuminemic hyperthyroxinemia (FDH), the serum albumin has increased affinity for T4. These individuals are euthyroid and have elevated T4 concentrations but normal FT4 (25). These observations show that total thyroid hormone concentrations are influenced by many factors even in euthyroid individuals, and that measurement of free hormone is almost always preferable.

Technical Difficulties with Free Thyroid Hormone Measurements

The main analytical problems involved in making reliable measurements of FT4 and FT3 are:

1. Measurement of free hormone in the presence of a very large excess of protein-bound hormones. There is 5000 times more protein-bound T4 than FT4 and 250 times more bound than free for T3.

2. Free hormones are present at very low concentrations (at the picomolar level), requiring very sensitive detection methods.

3. The manipulations of the procedure should not change the equilibrium that exists between the bound and free hormone in the serum.

4. Variations in thyroid hormone binding proteins or competitors for their binding sites should not interfere with free hormone measurement (16).

No one procedure is able to overcome all the technical problems encountered in measuring free thyroid hormone concentrations and both direct and indirect approaches have been developed. The direct techniques include equilibrium dialysis and ultrafiltration. The indirect methods are T3 uptake (T uptake), the free T4 index (FTI), T4/TBG ratio, two-step immunoextraction, one-step immunoassay analog, and the labeled antibody method. These approaches will be discussed in the following with emphasis on the major problems inherent in each.

Direct Measurements

Equilibrium dialysis and ultrafiltration are methods that directly measure the concentration of free hormone after it has been separated from its binding proteins. After separation, FT4 and FT3 are usually measured by sensitive RIA. Both methods are time-consuming and do not lend themselves to routine use in the clinical laboratory. However, they are considered to be the "gold standard" or reference method for the measurement of free thyroid hormones (26).

Equilibrium Dialysis Equilibrium dialysis for measurement of FT4 involves dialysis of an aliquot of serum against a volume of buffer until the concentration of free hormone reaches equilibrium on both sides of the dialysis membrane. The concentration of free T4 in the dialysis sac is then measured. In the earlier procedures iodinated T4 was added to the serum before dialysis and was used to quantitate FT4. In this approach, the radioactivity in the dialysate was divided by the total radioactivity in the dialysate plus bound fractions to give a "dialysis fraction" (DF). The total T4 concentration in the serum was then determined by RIA or by some other chemical means to give the actual concentration of FT4 (27). The major problem with this method was deiodination of the iodinated T4 during the procedure, some of the radioactivity was in the form of iodide and gave spurious results. This

problem was overcome by prior separation of T4 from iodide by dilution of serum (28) or by the use of magnesium to precipitate T4 (29). Today, quantitation with radioactivity has been replaced by sensitive immunoassays of free hormone in the dialysate (30). Improvements and variations of this basic approach have been developed, with the emphasis on improving accuracy, simplifying the procedure and trying to adapt methods for use in the clinical laboratory (24,31–36).

In their equilibrium dialysis assay for free T4 (FT4D), Helenius and Liewendahl (33) used disposable dialysis cells made of a thermoplastic resin that adsorbed less T4 than other materials. This FT4D assay was compared with five commercial one-step immunoassays using sera from euthyroid subjects with nonthyroidal illness or with abnormal TBG concentrations. A normal reference range was established for this method (9–21 pmol/Liter) that was similar to those of other FT4D methods (23,24). Individuals with inherited TBG abnormalities had normal FT4D values and abnormal free thyroxine index (to be discussed in a later section), showing that FT4 concentrations are independent of variations in TBG. Subjects with NTI had increased levels of dialyzable FT4, which occurred more often in individuals that had normal T4 than in those with low serum T4, suggesting the presence of an inhibitor of thyroid hormone binding in NTI. These same individuals with NTI had below normal levels of FT4 when measurements were performed with the one-step immunoassays (33).

Dilution of serum from healthy euthyroid individuals before dialysis appears to have little effect on FT4 concentration. However, it leads to decreases in FT4 in some individuals with NTI (36). Hence, FT4 measurements carried out on undiluted serum are probably more accurate (34). A dialysis method that minimizes changes in serum matrix by using undiluted serum and measurement of T4 by sensitive RIA has been described (36). FT4D reference ranges were established for euthyroid individuals (8–27 ng/Liter) as well as for hyper- and hypothyroidism, TBG excess and deficiency, hypothyroxinemias (low T4) of NTI, and hyperthyroxinemias (elevated T4) of familial dysalbuminemia. The major strength of this method is its ability to distinguish between the hypothyroxinemias of NTI (FT4D is normal or increased, 8–35 ng/Liter) and the TBG deficiencies (normal FT4D), which are usually due to changes in protein binding from primary hypothyroidism (low FT4D, <2–7 ng/Liter). The FT4 index and analog methods (to be discussed later) give low values in these situations; only membrane separation methods are able to distinguish between hypothyroxinemia of hypothyroidism and that observed in NTI (36,37). This method using undiluted serum is the most accurate and reliable for the measurement of FT4. Its

major drawbacks are that it uses radioactivity and it cannot be automated (36).

Ultrafiltration The technique of ultrafiltration refers to the physical separation of bound from free T4 or T3 by filtration of serum through a membrane by centrifugation. The free hormone passes through the membrane and can be measured in the ultrafiltrate (38,39). Most ultrafiltration methods use undiluted or minimally diluted serum so as not to disturb the existing equilibrium between bound and free hormone and to carry out the procedure at physiologic pH and temperature. Theoretically, ultrafiltration should be the most accurate method for measuring FT4 and FT3 because it does not alter the serum components and the procedure is carried out under physiologic conditions. In some methods, radioactive T4 or T3 is added to the serum followed by incubation, ultrafiltration, and separation of free radioactive hormone from iodide by sephadex (37) or paper chromatography (38). The radioactive hormone in the ultrafiltrate is used to determine the concentrations of FT4 or FT3. Another approach is to measure the concentrations of T4 and T3 in the ultrafiltrate by sensitive RIA (39,40).

Evaluation of thyroid status in individuals with nonthyroidal illnesses is a difficult analytical problem. Changes in hormone production, metabolism, and binding protein concentrations, as well as the presence of inhibitors of thyroid hormone binding, probably contribute to the confusing laboratory results reported in the literature. Both elevations and reductions in T4 and T3 have been reported, as well as inconsistent measurements of FT4 on diluted serum (32,34,38,41,42). In an attempt to resolve this confusion, a comparison of ultrafiltration with equilibrium dialysis was carried out in patients with severe nonthyroidal illnesses and with normal or below normal concentrations of T4 and no history of thyroid disease. FT4 levels in these patients, by either ultrafiltration (FT4U) or equilibrium dialysis (FT4D), in these did not differ from those of normal controls. The FT4 values were lower by equilibrium dialysis but the correlation between the two methods was excellent. Either method appears to be able to differentiate euthyroid hypothyroxinemic sick patients (FT4U = 34.7 ± 7.6 ; FT4D = 45.3 ± 5.1 pmol/Liter) from those with hypothyroidism (FT4U = 2.6; FT4D = 4.1) (38). Similar results using ultrafiltration in critically ill patients have also been reported (37). Tikanoja and Liewendahl (39) compared ultrafiltration with dialysis and found that, in contrast to Surks and coworkers (38), the FT4U concentrations were about two-fold higher than the FT4D values. They point out that FT4 results from other laboratories using ultrafiltration (40,43,44) are higher than results reported by others using

equilibrium dialysis (23,24,33,34). Both methods in this study showed elevated and depressed concentrations in hyper- and hypothyroid individuals, respectively, and reported most FT4 concentrations to be within the normal range in nonthyroidal illness. Several individuals with NTI had highly elevated levels of FT4 accompanied by increased circulating concentrations of unsaturated free fatty acids (FFA). FFA may be responsible for elevated FT4 levels sometimes observed in NTI (35,45–47]. FFA, probably enzymatically liberated *in vitro* (during the assay incubation), frees T4 from its carrier proteins. Ultrafiltration of undiluted serum using a commercially available filtration device and a sensitive radioimmunoassay appears to be the most accurate and least time-consuming of the direct methods currently available (39) and might be adaptable for use in the clinical laboratory.

Equilibrium dialysis and ultrafiltration are the most accurate and precise methods for measuring concentrations of free thyroid hormones compared to all other techniques (discussed in the following) for assaying FT4 and FT3. However, their use in the clinical laboratory is limited because:

1. They are technically difficult to carry out, are expensive and time-consuming, and require highly sensitive immunoassays.
2. Dilution of serum can affect the equilibrium between bound and free hormone, perhaps by altering serum factors that influence binding (16).
3. Considerable variability exists between laboratories. Some of this is probably due to methodological differences, however, all methods appear to be able to distinguish between euthyroid individuals and those with thyroid disease.
4. A serious disadvantage of the direct methods is that they do not lend themselves to automation at a time when endocrine testing is close to being completely automated.

Interlaboratory variability of free hormone measurements is more frequent when comparisons are made between groups of patients with nonthyroidal illnesses. NTI includes seriously ill hospitalized patients with dissimilar disease states and some of the variability might be due to individual differences within the NTI group. Direct methods for free hormone measurements essentially remain research tools, although most reports claim that they are adaptable for use in the clinical laboratory.

Indirect Measurements

Indirect measurements of free thyroid hormones do not actually measure free hormone concentrations but use assay parameters that are proportional to the concentrations of FT4 and FT3.

T3- or T4-Uptake Assays and the Free Thyroxine Index Variations in thyroid binding protein concentrations (predominantly TBG) can lead to changes in total T4 and T3 levels that may give a false indication of thyroid status in euthyroid individuals. The observation that an equilibrium exists between free thyroid hormones and the binding sites of plasma proteins and of red cells (48) led to the development of the T3-uptake methods. These assays indirectly assess the number of unoccupied T4 binding sites in a serum sample by incubating radioactive T3, originally with red blood cells (48) or presently with weak binders of high capacity such as ion-exchange resins or sephadex (49). Radioactive T3 is used because it binds less to serum proteins than does T4—in this way more counts are bound to the binder and fewer to the serum proteins. The uptake of T3 is inversely proportional to the unsaturated binding capacity of the T4 binding proteins, principally TBG; for example, hyperthyroid individuals when compared to euthyroids have increased uptake (most sites on TBG are filled), whereas hypothyroid subjects have decreased T3 uptake (most TBG sites are unoccupied) (42,49). T3 uptake is usually normalized by expressing it as a ratio of the patient result to the T3 uptake for a euthyroid serum pool and is referred to as the thyroid binding hormone ratio (THBR), expressed as percentage uptake and usually ranging between 25 and 35% (16,42). The uptake assay can also distinguish between euthyroid individuals with normal, low, or high concentrations of TBG; high levels of TBG show decreased T3 uptake and low levels show increased uptake. T3-uptake assays were developed even before the advent of T4 measurement by competitive binding assays and RIA and were extensively used because FT4 concentrations were difficult to measure. The T-3 uptake assays showed that individuals with abnormal concentrations of TBG could be euthyroid and reinforced the idea that the free hormone concentration determined thyroid status.

T3-uptake measurements, combined first with protein-bound iodine (PBI) levels (50) and later replaced with T4 concentration (51,52), give another estimate of the FT4 concentration, the free thyroxine index. The FTI is equal to the $T4 \times T3$ uptake, was shown to correlate with an individual's clinical state, and is a good estimate of the FT4 concentration (53). Knowledge of both T4 and T3 uptake allows one to distinguish between a protein binding abnormality or thyroid malfunction. FTI is used to interpret serum T4 values when serum concentrations of TBG are abnormal, as in estrogen administration, pregnancy, and genetic abnormalities of TBG synthesis; for example, in pregnancy, T4 and TBG levels are increased whereas in nephrosis both are decreased. The FTI in both these situations is normal (42). The FTI suffices as an estimate of FT4 if the individual is

subject to only small changes in TBG. However, it does not reflect FT4 concentration in patients with significant changes in binding protein concentrations or in those with NTI (54). The original T3 resin uptake assay used to calculate the FTI has been replaced by modern methods that measure unsaturated binding capacity of T4 binding proteins. Analogs of thyroxine bound to enzymes, chemiluminescent and fluorescent substances, and antibodies bound to solid-phase materials have been used.

Many of the methods are automated and are referred to as “T-uptake assays”; examples are the fluorescence polarization assay, where fluorescein-labeled T4 is used, and the use of a biotinylated T4 analog that does not bind to TBG but that competes with FT4 for an antibody bound to a polystyrene bead (7,55). Alkaline phosphatase coupled to the antibody enzymatically generates a chemiluminescent signal (56). Recently, in a comparative study, five automated T-uptake assays were used to calculate FTI under a variety of clinical situations. Results from euthyroid individuals were comparable. However, in some patients with abnormalities of thyroid hormone binding proteins, the FTI varied according to the method used (57). The T-uptake assays and the FTI may perform poorly in pregnant women, in women taking oral contraceptives, in euthyroid individuals with inherited abnormalities of TBG, and in NTI and familial dysalbuminemia (58). In spite of the problems involved in these clinical situations, the FTI is still in use in many laboratories because direct methods of FT4 measurement are too labor-intensive and many indirect methods (discussed in the following) have serious problems.

Direct Measurement of TBG and T4/TBG Ratio The T4/TBG ratio is another free thyroxine index that correlates with the FT4 concentration and came into use after the development of reliable methods for the measurement of TBG concentrations in serum (59–61). It is calculated by dividing serum T4 concentration by the total TBG concentration. The T4/TBG ratio gives good differentiation between euthyroid, hyperthyroid and hypothyroid individuals when TBG concentrations are within the normal range and is believed to be a better diagnostic index than the FTI based on T3 uptake (59,60,62). Although T3- or T4- uptake assays have been useful, they present disadvantages when compared to direct measurement of TBG. The relationship between T3 uptake and TBG concentration is not linear at high TBG concentrations and under these conditions the T3 uptake is less sensitive and may lead to spurious results. This explains why the T4/TBG ratio is better able to correct for elevated concentrations of TBG whereas the FTI is not (60). Other reports claim that the T4/TBG ratio is not accurate when TBG concentrations are elevated or depressed

(62). However, T₃-uptake values also vary with changing concentrations of endogenous T₄ and T₃, whereas the TBG levels remain constant regardless of the endogenous concentrations of T₄ and T₃. This can lead to an erroneous FTI (63). Because of cost, most laboratories prefer to use other indirect measurements of FT₄ rather than the T₄/TBG ratio and as a result there are only a few assays available commercially.

Two-Step Immunoextraction Assay In this method the binding proteins are separated from the free thyroid hormones by incubation with a solid-phase antibody, for example, an antibody-coated tube. The free hormone that binds to the antibody is directly proportional to its concentration in the serum. Subsequent washing of the solid phase removes the binding proteins. A second incubation with labeled T₄ or T₃ fills the unoccupied antibody binding sites. The amount of label bound to antibody is inversely proportional to the concentration of free hormone in the serum (64). The amount of antibody used is small so as to minimize antibody-induced release of T₄ from the binding proteins. In addition, the binding proteins cannot interfere with the binding of labeled T₄ to antibody because they are removed before the label is added (65,66). The two-step immunoextraction assays are less labor-intensive than the direct methods and less subject to errors caused by fluctuations in binding protein concentrations than the one-step analog methods to be discussed next (47,67).

Yet this approach also has its limitations. Several steps in the procedure (two incubations and a wash step) are susceptible to error owing to dissociation of T₄ from the antibody during the wash step and during the second incubation (64). The extracted fraction (antibody-bound fraction) is often greater than the true FT₄ concentration, suggesting that the free hormone equilibrium is altered by assay manipulations (47). However, the assay still gives a valid estimate of the FT₄ concentration because the number of antibody sites occupied by T₄ is proportional to the amount of FT₄ in the sample. The two-step protocol is relatively insensitive to changes in binding protein concentrations, is easy to carry out, and has made it possible to measure free thyroid hormones in the clinical laboratory.

One-Step T₄-Labeled Analog Methods In this approach, a labeled analog of the hormone is used that binds to the antibody used in the assay but is claimed to have low affinity or no affinity at all for the serum binding proteins. The assays are designed so that bound T₄ does not interfere with the measurement of free T₄. The anti-T₄ antibody is often bound to a solid phase, for example, a magnetic particle (68,69) and the antibody and analog are added simultaneously for a single incubation. Competition occurs between the free hormone in the serum and the labeled hormone analog for

antibody-binding sites. Concentration of free hormone is inversely proportional to the amount of antibody-bound analog. This type of assay usually uses a radioactive tracer, although enzymes (70) and chemiluminescent substances (71,72) have also been used as tracers. In one assay that was reported to correlate well with equilibrium dialysis, a chemiluminescent T4-immunoglobulin complex was used as tracer and was incubated with an anti-T4 antibody coupled to magnetic particles. After magnetic separation and chemical excitation of the label, light output was measured in a luminometer. The chemiluminescent tracer also failed to interact with endogenous T4 binding proteins (72).

The one-step analog approach has several advantages over previous methods. Fewer steps are involved, thereby reducing error and improving assay precision, and some procedures were able to give reliable estimates of FT4 and FT3 concentrations in the presence of varying amounts of TBG (73).

The FT4 analog assay is based on the premise that the analog-tracer binds to the anti-T4 antibody but not to the T4 serum binding proteins. Most analog-tracers are reported to bind at least to some extent to serum proteins (47,72). This is the major limitation of this assay format and may give erroneous results in individuals with abnormalities of T4 binding proteins (47). A second problem is that analog-tracers bind strongly to serum albumin and are sensitive to variations in albumin concentration. As a result, FT4 concentrations obtained with analog methods correlate with the extent of tracer binding to albumin (74). In addition, decreases in serum albumin concentration that can occur in NTI lead to less binding of analog-tracer to albumin and erroneously low estimates of FT4 (32,75). In familial dysalbuminemic hyperthyroxinemia, the albumin is abnormal and binds the analog (76,77). In FDH individuals, two different analog assays gave elevated concentrations of FT4 that were normal when measured by equilibrium dialysis (78). Falsely elevated values of FT4 can also occur as a result of dissociation of T4 from its binding proteins and subsequent binding to antibody in the analog-based assay (74). Some patients with NTI have elevated levels of nonesterified fatty acids (79), which compete with T4 for protein binding sites and lead to erroneously high FT4 levels in analog assays (67).

Labeled Antibody Method (One Step) This is a one step-procedure in which serum is incubated with an I-¹²⁵labeled anti-T4 antibody and an excess of an antigen (e.g., T3) bound to a solid state such as magnetic (T3-mag) particles. The antigen-solid state complex is designed in such a way as to prevent binding to thyroid carrier proteins. Competition between free T4 in the sample and the antigen complex takes place, followed by removal

of excess reagents by washing and quantitation of the labeled antibody. The concentration of free T4 is inversely proportional to the amount of labeled antibody bound to the exogenous antigen (80). An excess of T3-mag is used to achieve equilibrium in 30 min and there is little dissociation of T3-mag or FT4 from antibody. In addition, the FT4 concentration of the sample remains constant because the thyroid binding proteins release T4 and replace whatever binds to the antibody. This is a unique approach to the measurement of FT4 that appears to overcome most of the limitations of the one-step analog method, such as binding of tracer to carrier proteins, to serum albumin or to abnormal albumins (80).

Thyroid Stimulating Hormone (Thyrotropin)

Background

TSH is a glycoprotein (molecular weight of 23,300) secreted by the anterior lobe of the pituitary gland and it is composed of two different noncovalently bound peptides, the alpha and beta subunits. The alpha subunits are identical for the other pituitary glycoproteins. However, it is the beta subunit that determines the biologic and immunologic specificity of these hormones. TSH stimulates synthesis and secretion of T4 and T3 from the thyroid gland. Secretion of TSH is stimulated by the hypothalamic tripeptide thyrotropin releasing hormone (TRH). A negative feedback mechanism exists whereby increased serum levels of free T4 and T3 decrease secretion of TSH. In individuals with normal functioning pituitary glands, a dynamic equilibrium exists between the circulating free thyroid hormones and TSH.

A decrease in FT4 or FT3 stimulates TSH secretion and release and leads to release of thyroid hormones from the gland. An increase in FT4 has the opposite effect (81).

The Importance of TSH Measurements

Measurement of serum TSH is generally accepted as the most important test for determining an individual's thyroid status. FT4 is the biologically active thyroid hormone and small changes in its concentration elicit large changes in circulating TSH: a 2 fold decrease in FT4 is associated with an approximate 160-fold increase in circulating TSH levels (82). This log-linear relationship shows that the pituitary thyrotroph is a very sensitive monitor of biologically active circulating levels of T4 and T3. The extreme sensitivity of this negative feedback system has led to the suggestion that TSH be used as the primary thyroid function test [82–85]. The development of sensitive TSH assays (sensitive to 0.01 μ IU/ml) has reinforced this concept

(86). Measurement of FT₄ gives information about thyroid gland secretory activity. Measurement of TSH in combination with FT₄ gives information about biological activity of the hormone and secretory activity of the gland and appears to be the best approach for determining an individual's thyroid status (16,82).

Radioimmunoassay of TSH

Radioimmunoassays for TSH were first developed in the mid-1960s, were not very sensitive and could only detect TSH in 50% of the normal (euthyroid) individuals studied. However, TSH was detectable in the sera of hypothyroid patients (87,88). By the early 1970s, many technical improvements had been made so that TSH RIAs were being utilized clinically and 87% of the euthyroid individuals studied had measurable levels of TSH (89,90). These early TSH measurements could not be used as primary thyroid function tests because they suffered from sensitivity limitations (sensitivity = 1.0–2.0 μ IU/ml), but were used primarily to diagnose low-T₄–high-TSH states (hypothyroidism).

During the 1970s and 1980s, improvements continued to be made in TSH assay methodologies, including the use of monoclonal antibodies with improved affinity and specificity and the development of immunometric (“sandwich”) assays (discussed in the following). These advances have been discussed and summarized by Ridgway (91).

Immunometric TSH Assays: Improvements in Sensitivity and Specificity

The more sensitive immunometric methods have enlarged the role of TSH measurements by allowing the detection of suppressed concentrations of TSH such as those observed in hyperthyroidism (86).

Immunometric or “sandwich” assays use two or more antibodies directed against different epitopes of the TSH molecule, which assures a high degree of specificity; the TSH is “sandwiched” between the two antibodies. One of the antibodies is fixed to a solid support such as a polystyrene bead, a plastic tube, or magnetic particles to facilitate separation of antibody–antigen complexes. The second antibody has a signal molecule bound to it, either a radioisotope, an enzyme, or a fluorescent or chemiluminescent substance. This enables one to quantify the antibody-bound TSH. Excess antibody is used so that all the TSH present is extracted from the serum sample. The TSH molecules form a bridge between the antibodies and the magnitude of the signal is directly proportional to the concentration of TSH in the sample (86,91,92).

The different signal molecules used have given rise to several assay names: immunoradiometric (IRMA) when I^{125} is used, immunoenzymometric (IEMA) or enzyme immunometric assay (EIA) when enzymes are used, and immunochemiluminometric (ICMA) when chemiluminescent compounds are used. The immunometric technology has led to TSH assays with increased sensitivities because of:

1. the use of excess first antibody which extracts all the TSH from the sample;
2. the use of chemiluminescent labels, which have higher specific activities and better detection limits than radioisotopes and enzymes (93); and,
3. the ability to enhance and prolong the signal by enzymatic excitation of the chemiluminescent substrate, illustrated by the phosphorylated dioxetanes used in several immunometric TSH assays (56,94).

With the use of excess antibody, precision is improved because there are fewer critical pipeting steps, the detection range is increased, and incubation times are reduced. Table I summarizes the specifications of some commonly used commercially available non-isotopic immunometric TSH assays. (95–104).

To make sense out of a confusing terminology that has arisen around the sensitive assays, a new nomenclature has developed based on functional sensitivity defined as the lowest TSH concentration that gives an interassay coefficient of variation (CV) of 20% has been suggested. TSH assays used in the 1970s and early 1980s, which were too insensitive to detect hyperthyroidism and had functional sensitivities of 1.0 to 2.0 $\mu\text{IU/ml}$ (20% CV), are now referred to as first-generation assays. Each generation is 10-fold more sensitive than the preceding generation. The second- and third-generation assays are sensitive to 0.1–0.2 and 0.01–0.02 $\mu\text{IU/ml}$, respectively (82). The introduction of the third-generation TSH assay has expanded the clinical utility of TSH measurements and has essentially replaced all other methods. The following list summarizes the clinical usefulness of the sensitive TSH assays:

1. permit discrimination between euthyroid patients with low TSH concentrations and hyperthyroid individuals (86);
2. useful in monitoring thyroid hormone replacement therapy;
3. used to monitor T4-induced TSH suppression in patients with thyroid cancer;
4. allow better diagnosis of hyperthyroidism in nonthyroidal illnesses when T4 and FT4 may be inappropriately low; and
5. allow TSH measurement to be used as a first line test for determining thyroid status (16,83,105).

TABLE I. Commercial Nonisotopic Immunometric TSH Assays

Assay	Description	Functional Sensitivity ($\mu\text{IU/ml}$)
Magic Lite TSH (hs) Ciba Corning (95,96)	Manual, chemilum. (AE), monoclonal Ab bound to magnetic particles, 2-point daily calibration, range: to 50 $\mu\text{IU/ml}$	Not given
Nichols 3rd- Generation (86,97)	Manual, chemilum. (AE), Ab bound to bead, standard curve, range: 0.01–50 $\mu\text{IU/ml}$	0.01
Kodak Amerlite TSH-30 (98,99)	Semiautomated, two monoclonal Abs, one bound to microtiter well, enzyme-generated chemilum. (luminol), daily calibration, range: 0.03–100 $\mu\text{IU/ml}$	0.03
Abbott IMX Ultrasensitive hTSH (100,101)	Automated, monoclonal Ab bound to microparticles, fluorescent signal, calibration every 2 weeks, range: 0.03–100 $\mu\text{IU/ml}$	Not given
Immulite Diagnostic Products Corp. (56,97,102)	Automated, Ab bound to bead, enzyme-generated chemilum. (diox-P), 2-point calibration every 28 days, range: 0.01–75 $\mu\text{IU/ml}$	0.01
Access Sanofi Pasteur Diagnostic (103)	Automated, Ab bound to magnetic particles, enzyme-generated chemilum. (diox-P), calibration every 28 days, range: 0.02–100 $\mu\text{IU/ml}$	0.02
Delfia hTSH Ultra Wallac (104)	Manual, three monoclonal Abs, one bound to microtiter well, fluorescent signal, standard curve, range: 0.007–100 $\mu\text{IU/ml}$	0.007

Note: chemilum., chemiluminescence; AE, acridinium ester; diox-P, dioxetane phosphate. Functional sensitivities are based on manufacturer's claims.

Although sensitive immunometric TSH assays are widely used, they have certain limitations. Erroneously high values of TSH may be caused by heterophile antibodies, for example anti-mouse antibodies, present in some sera that form a bridge between the capture antibody, usually a mouse monoclonal, and the signal antibody that mimics TSH (106). The protein matrix, usually animal sera, used in the TSH assay defines the zero TSH concentration, and in some cases, when elevated can alter the assay sensitivity for detection of hyperthyroidism (97,107). Each laboratory should deter-

mine the functional sensitivity of the TSH assay that it plans to use. In a recent interlaboratory study comparing different commonly used immunometric assays, it was found that most laboratories could not replicate the manufacturer's stated functional sensitivity and some methods could not "reliably" distinguish abnormal from normal TSH levels (97).

Selection of TSH and FT4 Assays

The TSH method should be able to distinguish between the suppressed TSH levels detected in hyperthyroidism and the low values sometimes observed in euthyroid individuals (82). The FT4 method should give reliable results in individuals with abnormal T4 protein binding, such as in nonthyroidal illnesses (32), and in those with hereditary dysalbuminemias (77). If both assays are selected following these criteria and the results of each agree, then one can be sure of the individual's thyroid status. Used separately, greater than 90% diagnostic accuracy can be expected (108).

AUTOIMMUNE PROCESSES THAT AFFECT THYROID GLAND FUNCTION AND HORMONE MEASUREMENTS: SERUM THYROID AUTOANTIBODIES

The cause of most active and underactive thyroid disease is believed to be due to an inappropriate immune system response directed against the thyroid gland. Autoantibodies to specific thyroid proteins are often associated with autoimmune thyroid disease. The three proteins involved in autoimmune thyroid disease (AITD) are thyroglobulin (Tg), thyroid peroxidase (TPO), and the TSH receptor. Tg, synthesized by the thyroid cells, is a large glycoprotein (660,000 MW) and makes up the majority of the colloid within the thyroid follicles. Synthesis of thyroid hormones takes place within the colloid. Iodide combines with tyrosine residues on the Tg molecule, followed by coupling of the tyrosines to form T4 and T3. Iodination and coupling reactions are achieved by the microsomal enzyme peroxidase (8). TPO was referred to as the "microsomal antigen" before its identification as TPO (109). The third protein involved in AITD is the TSH receptor located on the surface of the thyroid epithelial cells; its interaction with TSH leads to thyroid gland stimulation.

Autoantibodies to Thyroid Peroxidase and Thyroglobulin

Anti-TPO and anti-Tg antibodies may not initiate AITD but appear to be a secondary phenomenon to lymphocytic infiltration and thyroid gland

injury. The following discussion highlights the reasons for measuring circulating thyroid autoantibodies: the major reason is to confirm the diagnosis of AITD. In Hashimoto's thyroiditis (autoimmune thyroiditis, hypothyroidism), the major clinical features are goiter and disturbance of thyroid function (low T4 and FT4, elevated TSH), and both antibodies to Tg and TPO are associated with the disease. In Grave's disease (Grave's hyperthyroidism), there is diffuse goiter and increased synthesis and secretion of thyroid hormones. Anti-TPO antibodies are more common than anti-Tg and are closely related to thyroid dysfunction. They are present in over 90% of Hashimoto's patients and about 80% of those with Grave's disease and correlate with damage to the thyroid gland (110). When anti-TPO is detected in early pregnancy it may predict post-partum thyroiditis (PPTD), hence it is used to screen for PPTD. About 30% of pregnant women with positive anti-TPO develop some form of PPTD (111). Anti-TPO measurements are also used to follow individuals at risk for thyroid failure (subclinical hypothyroidism; elevated TSH and normal FT4). Low titers of anti-TPO correlate with lymphocytic infiltration (early damage), high titers suggest AITD, and significant levels confirm AITD (110). Anti-TG is present in about 55% of Hashimoto's patients and in 25% of those with Grave's disease, and it is not as useful a measurement as anti-TPO. It is rarely present without anti-TPO (110). When measured by the more sensitive radioimmunoassays (discussed in the following) about 30% of individuals without thyroid disease have circulating anti-thyroid antibodies, therefore, their measurement is not overly helpful as a diagnostic tool but is more useful as a predictor of future thyroid disease and as a means of following the progression of the disease.

The methods for detection of autoantibodies to TPO and Tg are tanned red cell hemagglutination (HA), immunofluorescence on thyroid sections (IF), enzyme-linked immunoassay (ELISA), and radioimmunoassay. HA and IF assays (112,113) depend on indirect measurement of the autoantibodies, are subjective, and are not very sensitive. IF methods are less sensitive to Tg autoantibodies and are subject to interference from heterophile antibodies (110). HA assays that use tanned red cells coated with antigen are only semiquantitative, are unsuitable for large-scale screening of patients, and require making multiple dilutions of patient sera. Enzyme assays (ELISAs) are objective and quantitative, but also depend on indirect measurements. In addition, they have precision problems but are more sensitive than HA and IF and more specific than HA. The ELISA usually requires only a single dilution for both anti-Tg and anti-TPO, and when automated microplate washers and spectrophotometers are used they permit rapid processing of samples. Results are usually expressed in terms of

an optical density ratio compared to a positive control (109,114,115). Recently two ELISA methods have been developed using human recombinant TPO for the detection of anti-TPO (116,117). RIAs for anti-Tg and anti-TPO, in contrast to the other methods are based on direct interaction between ^{125}I -labeled autoantigens and autoantibodies present in patient sera. They are one order of magnitude more sensitive than the HA and ELISA methods, are highly specific (e.g., unlabeled Tg did not affect measurements of anti-TPO), and show good precision (118). The RIA should express the results in standardized units based on an international reference preparation available from the National Institute for Biological Standards in the United Kingdom (118). This facilitates comparisons of autoantibody measurements on the same individual over an extended time period.

Antibodies to the TSH Receptor

The major clinical symptom of Graves' disease is hyperthyroidism probably caused by stimulation of the thyrotropin receptor by autoantibodies (119,120). The autoantibodies seen in Graves' patients affect thyroid function in different ways (121). The TSH-stimulating antibodies (TSAb) stimulate thyroid function and can be identified using bioassays that measure adenylate cyclase activity and generation of cyclic AMP in human or rat thyroid cells (122–125). TSAb is present in over 90% of individuals with untreated Graves' disease (110). Another population of autoantibodies block (inhibit) the binding of TSH to its receptor and are referred to as TSH-blocking antibodies (TSH-binding inhibitory immunoglobulins, TBII); they are detected by their ability to inhibit the binding of radiolabeled TSH to solubilized porcine TSH receptors (binding inhibition assay) (119,126). TSAb is also identified in the binding inhibition (TBII) assay. However, some antibodies measured in this assay do not stimulate thyroid cells (110). The TBII assay is an indirect measurement but does not confirm the presence of TSAb, though it is relatively easy to perform. The cyclic AMP assays directly measure TSAb and confirm the diagnosis of Graves' disease. However, they are more difficult to perform and less widely used.

TBII and cyclic AMP assays are helpful in diagnosing AITD and are used to predict relapse or remission of disease after withdrawal of anti-thyroid drugs. High serum levels almost always predict relapse and suggest that the patient is unlikely to respond to anti-thyroid drug administration. Since TSH receptor antibodies cross the placenta and can stimulate the fetal thyroid gland, monitoring of TSAb or TBII in pregnant women with Graves' disease can be used to predict neonatal hyperthyroidism during pregnancy (120).

MEASUREMENT OF SERUM THYROGLOBULIN

Thyroglobulin plays a major role in the synthesis of T₄ and T₃ within the thyroid follicle and is also present in the circulation, gaining access either as a normal glandular secretory product or by leakage from the thyroid. Its functional significance outside of the thyroid gland is not known. Sensitive and specific assays showing no interference from the thyroid hormones have been developed for the measurement of serum Tg. Among the techniques described are double-antibody RIAs (127–129) ELISA (130,131), and IRMA (132,133). The sensitivity of most of these assays is between 1.0 and 5.0 ng/ml.

There is wide interlaboratory variability in serum Tg concentrations in normal individuals, which has been underscored by two international studies (134,135). Van Herle (9) attributes this variability to methodological differences and emphasizes the need for standardizing Tg assays by developing an international Tg standard.

It is well known that autoantibodies to Tg (anti-Tg) interfere with Tg immunoassays (128,136). Most laboratories screen samples for anti-Tg and do not attempt to measure Tg in the presence of anti-Tg. The effects of anti-Tg on the RIA of serum Tg have been studied extensively and involve a complex set of variables including the concentration of anti-Tg and the affinity of the autoantibody for antigen and for the tracer (127,128,136,137). Briefly, an elevated concentration of anti-Tg could bind the tracer (¹²⁵I-Tg) but would not be precipitated by the second antibody in the assay. This would lead to erroneously elevated concentrations of Tg. Some patient Tg could also be removed from the measurable Tg pool by binding to the anti-Tg, which would result in erroneously low levels of Tg. One could also have a combination of these two situations, which would further complicate interpretation of the assay (128,136).

Several studies have attempted to determine the degree of autoantibody interference by adding Tg to serum samples containing different concentrations of anti-Tg (128,136,137). In one such study, the data indicated that anti-Tg concentration alone was not sufficient to evaluate interference; the same concentrations of anti-Tg decreased recovery to different degrees (137). One has to conclude from most studies that anti-Tg interference in RIA can only be assessed by carrying out recoveries of different amounts of added Tg for each sample assayed. This approach is too time-consuming for the routine clinical laboratory.

A unique IRMA (Magnogel-IRMA-Tg) that eliminates anti-Tg interference uses five monoclonal antibodies directed against three epitopes on the Tg molecule that anti-Tg does not recognize. Four of these antibodies

are directed against two epitopes and are coupled to magnetic beads. Another antibody is iodinated and is directed against still another epitope and acts as the second antibody (133). This approach appears to reliably measure Tg in the presence of anti-Tg.

Thyroglobulin is elevated in Graves' disease, thyroiditis, and thyroid adenoma and carcinoma (9,138). Measurements of serum Tg are used to monitor thyroid activity in Graves' patients during anti-thyroid therapy (138) and to follow patients after total thyroidectomy and radioiodine ablation treatment of differentiated thyroid carcinoma. Presence of Tg in the serum after treatment for carcinoma indicates residual thyroid tissue metastases and recurrence of disease (9,139,140). In neonatal hypothyroidism, Tg measurements are helpful in determining the thyroid defect. Undetectable levels of Tg in the serum indicate absence of thyroid tissue (141). Patients treating themselves with thyroid hormones can be identified by suppressed concentrations of Tg in their serum, which rules out true thyroid overactivity.

Tg assays are widely used in most medical centers in spite of wide variations that exist between measurements carried out at different locations. This variability is most likely due to methodological differences and will probably be resolved by the establishment of a stable reproducible international standard. The problem of assay influence by anti-Tg autoantibodies awaits the development of a simple method to eliminate this interference.

CONCLUSIONS

In many instances the measurement of total thyroid hormone concentration reflects the functional status of the thyroid and in most individuals total T4 concentrations parallel free T4 measurements. However, variation in binding protein levels and problems associated with nonthyroidal illnesses may lead to erroneous results and the need to do further testing.

Biologically active free hormone concentrations would appear to be the best way to assess thyroid status. However, many of the methods are beset with technical difficulties or they involve time-consuming procedures that do not lend themselves to use in the busy clinical laboratory. The sensitive immunometric TSH assay is the most important clinical laboratory measurement for the assessment of thyroid status. This is so because of the negative feedback log-linear relationship that exists between circulating levels of TSH and FT4, making TSH a very sensitive monitor of thyroid gland secretory activity. A sensitive TSH measurement is all that is needed to monitor thyroid function in most ambulatory individuals. When used in

conjunction with a reliable FT4 assay, it becomes an even more powerful indicator of thyroid status.

Measurements of thyroid gland-related molecules such as anti-Tg, anti-TPO, and TSH-receptor autoantibodies give information concerning the cause of thyroid malfunction and can also be used to follow progression of disease. Serum thyroglobulin measurements are used to follow patients being treated for differentiated thyroid carcinoma, are used to monitor thyroid activity during treatment for hyperthyroidism, and help to determine the defect in neonatal hypothyroidism.

It should be kept in mind that many of the methods discussed in this review give useful diagnostic information, although some results may be unreliable in clinical situations such as nonthyroidal illnesses and in hereditary dysalbuminemias.

ACKNOWLEDGMENTS

The author wishes to thank Erlinda Concepcion and Margarita Kogan for help in the preparation of this manuscript.

REFERENCES

1. J. H. Oppenheimer and R. Volpe, Measurements of thyroid function. In "Thyroid Function and Disease" (G. N. Burrow, J. H. Oppenheimer, and R. Volpe, eds.), pp. 124–139. Saunders, Philadelphia, Pennsylvania, 1989.
2. U. Chopra, A radioimmunoassay for measurements of thyroxine in unextracted serum. *J. Clin. Endocrinol. Metab.* **34**, 938–947 (1972).
3. P. R. Larsen, J. Dockalova, D. Sipula, and F. M. Wu, Immunoassay of thyroxine in unextracted human serum. *J. Clin. Endocrinol. Metabol.* **37**, 177–182 (1973).
4. S. E. Evans, W. A. Burr, and T. C. Hogan, A reassessment of 8-anilino-1-naphthalene sulphonic acid as a thyroxine binding inhibitor in the radioimmunoassay of thyroxine. *Ann. Clin. Biochem.* **14**, 330–334 (1977).
5. R. G. Symons and R. F. Vining, An evaluation of A fluorescence polarization immunoassay of thyroxin-uptake. *Clin. Chem.* **31**, 1342–1348 (1985).
6. M. L. Sturgess, I. Weeks, C. N. Mpoko, I. Laing, and J. S. Woodhead, Chemiluminescent labeled-antibody assay for thyroxin in serum with magnetic separation of the solid phase. *Clin. Chem.* **32**, 532–535 (1986).
7. S. S. Levinson, J. O. Goldman, and P. A. Burch, Thyroid profile testing with the TDX and IMX: Improved low end accuracy for thyroxine. *J. Clin. Immunoassay* **15**, 127–132 (1992).
8. I. R. McDougall, "Thyroid Disease in Clinical Practice," pp. 16–20. Oxford Univ. Press, New York, 1992.
9. A. J. Van Herle, Clinical tests of thyroid function. In "The Thyroid Gland" (M. A. Greer, ed.), pp. 345–390. Raven, New York, 1990.

10. S. Benvenga, F. Trimarchi, and J. Robbins. Circulating thyroid hormone autoantibodies. *J. Endocrinol. Invest.* **10**, 605–619 (1987).
11. D. F. Wood, A. M. Zalin, W. A. Ratcliffe, and M. C. Sheppard, Elevation of free thyroxine measurements in patients without thyrotoxicosis. *Q. J. Med.* **65**, 863–870 (1987).
12. O. Isozaki, T. Tsushima, K. Sato, M. Saji, Y. Ohba, N. Emoto, and K. Shizume, Triiodothyronine binding immunoglobulin in a euthyroid man without apparent thyroid disease: Its properties and effects on triiodothyronine metabolism. *Acta Endocrinol.* **108**, 498–503 (1985).
13. R. Ekins, Measurements of free hormones in blood. *Endocrinol. Rev.* **11**, 5–46 (1990).
14. J. Robbins and J. E. Rall, The interaction of thyroid hormones and protein in biological fluids. *Recent Prog. Horm. Res.* **13**, 161–208 (1957).
15. J. Robbins and J. E. Rall. Proteins associated with the thyroid hormones. *Physiol. Rev.* **40**, 415–489 (1960).
16. I. D. Hay, M. F. Bayer, M. M. Kaplan, G. G. Klee, P. R. Larsen, and A. C. Spencer, American Thyroid Association assessment of current free thyroid hormone and thyrotropin measurements and guidelines for future clinical assays. *Clin. Chem.* **37**, 2002–2008 (1991).
17. L. Bartalena and J. Robbins. Thyroid hormone transport proteins. *Clin. Lab. Med.* **13**, 583–598 (1993).
18. M. Inada and K. Sterling, Thyroxine transport in thyrotoxicosis and hypothyroidism. *J. Clin. Invest.* **46**, 1442–1450 (1967).
19. J. S. Marshall, R. P. Levy, and A. G. Steinberg. Human thyroxine-binding globulin deficiency. A genetic study. *N. Engl. J. Med.* **274**, 1469–1473 (1966).
20. P. R. Larsen, In “The Thyroid” (J. B. Wyngaarden and L. H. Smith, eds.), Cecil Textbook of Medicine, 18th Ed., pp. 1315–1340. Saunders, Philadelphia, Pennsylvania 1988.
21. R. D. Utiger, In “The Thyroid: Physiology, Hyperthyroidism, Hypothyroidism, and the Painful Thyroid” (P. Felig, I. D. Baxter, A. E. Broadus, and L. A. Frohman, eds.), Endocrinology and Metabolism, 2nd Ed., pp. 389–472. McGraw-Hill, New York 1987.
22. R. Ball, D. B. Freedman, J. C. Holmes, J. E. M. Midgley, and C. P. Sheehan, Low-normal concentrations of free thyroxine in serum in late pregnancy; Physiological fact, not technical artefact. *Clin. Chem.* **35**, 1891–1896 (1989).
23. R. P. Ekins and S. M. Ellis, In “The Radioimmunoassay of Free Thyroid Hormones in Serum” (L. E. Braverman and J. Robbins, eds.), Thyroid Research, Proc. 7th Int. Thyroid Conf., Boston, 1975, pp. 597–600. Excerpta Medica, Amsterdam, 1975.
24. A. F. Giles, An improved method for the radioimmunoassay of free-thyroxine in serum dialysates. *Clin. Endocrinol.* **16**, 101–105 (1982).
25. I. W. Jensen and J. Faber, Familial dysalbuminaemic hyperthyroxinaemia. *J. R. Soc. Med.* **81**, 34–37 (1988).
26. R. P. Ekins, Methods for measurement of free thyroid hormones. “International Symposium on Free Thyroid Hormones,” pp. 72–92. Excerpta Medica, Amsterdam, 1978.
27. K. Sterling and A. Hegedus, Measurement of free thyroxine concentration in human serum. *J. Clin. Invest.* **41**, 1031–1040 (1962).
28. J. H. Oppenheimer, Distribution and metabolism of the thyroid hormones. In, “Thyroid Function and Disease” (G. N. Burrow, J. H. Oppenheimer and R. Volpe, eds.), pp. 65–70. Saunders, Philadelphia, Pennsylvania, 1989.
29. K. Sterling, and M. A. Brenner, Free thyroxine in human serum: Simplified measurement with aid of magnesium precipitation. *J. Clin. Invest.* **45**, 153–163 (1966).
30. S. Ellis, and R. Ekins. Direct measurement by radioimmunoassay of free thyroid hormone concentration in serum. *Acta Endocrinol. Suppl.* **177**, 106 (1973).

31. I. J. Chopra, A. J. Van Herle, G. N. Chua Teco, and A. H. Nguyen, Serum free thyroxine in thyroidal and nonthyroidal illness: A comparison of measurements by radioimmunoassay, equilibrium dialysis and free thyroxine index. *J. Clin. Endocrinol. Metab.* **51**, 135–143 (1980).
32. E. M. Kaptein, S. S. Macintyre, J. M. Weiner, C. A. Spencer, and J. T. Nicoloff, Free thyroxine estimates in nonthyroidal illness: Comparison of eight methods. *J. Clin. Endocrinol. Metab.* **52**, 1073–1077 (1981).
33. T. Helenius and K. Liewendahl, Improved dialysis method for free thyroxine in serum compared with five commercial radioimmunoassays in nonthyroidal illness and subjects with abnormal concentrations of thyroxine-binding globulin. *Clin. Chem.* **29**, 816–822 (1983).
34. J. C. Nelson and R. M. Weiss, The effect of serum dilution on free thyroxine (T₄) concentration in the low T₄ syndrome of nonthyroidal illness. *J. Clin. Endocrinol. Metab.* **61**, 239–246 (1985).
35. K. Liewendahl, H. Mahonen, S. Tikanoja, T. Helenius, M. Turula, and M. Vallimak, Performance of direct equilibrium dialysis assays, and analogue-type free thyroid hormone assays, and an immunoradiometric TSH method in patients with thyroid dysfunction. *Scand. J. Clin. Lab. Invest.* **47**, 421–428 (1987).
36. J. C. Nelson and R. T. Tomei, Direct determination of free thyroxin in undiluted serum by equilibrium dialysis/radioimmunoassay. *Clin. Chem.* **34**, 1737–1744 (1988).
37. J. Faber, C. Kirkegaard, B. Rasmussen, B. Westh, M. Busch-Sorensen, and I. W. Jensen, Pituitary–thyroid axis in critical illness. *J. Clin. Endocrinol. Metab.* **65**, 315–320 (1987).
38. M. I. Surks, K. H. Hupart, C. Pan, and L. E. Shapiro, Normal free thyroxine in critical nonthyroidal illnesses measured by ultrafiltration of undiluted serum and equilibrium dialysis. *J. Clin. Endocrinol. Metab.* **67**, 1031–1039 (1988).
39. S. H. Tikanoja and B. K. Liewendahl, New ultrafiltration method for free thyroxine compared with equilibrium dialysis in patients with thyroid dysfunction and nonthyroidal illness. *Clin. Chem.* **36**, 800–804 (1990).
40. J. Weeke, N. Boye, and H. Orskov, Ultrafiltration method for direct radioimmunoassay measurement of free thyroxine and free tri-iodothyronine in serum. *Scand. J. Clin. Lab. Invest.* **46**, 381–389 (1986).
41. M. F. Slag, J. E. Morley, M. K. Elson, T. W. Crowson, F. Q. Nuttall, and R. B. Shafer, Hypothyroxinemia in critically ill patients as a predictor of high mortality. *J. Am. Med. Assoc.* **245**, 43–45 (1981).
42. I. J. Chopra, G. N. Chue Teco, A. H. Nguyen, and D. H. Solomon, In search of an inhibitor of thyroid hormone binding to serum proteins in nonthyroidal illnesses. *J. Clin. Endocrinol. Metab.* **49**, 63–69 (1979).
43. Y. S. Wang, A. E. Pekary, M. L. England, and J. M. Hershman, Comparison of new ultrafiltration method for serum free T₄ and free T₃ with two RIA kits in eight groups of patients. *J. Endocrinol. Invest.* **8**, 495–500 (1985).
44. J. Faber, P. Rogowski, C. Kirkegaard, K. Sierback-Nielsen, and T. Friis, Serum free T₄, T₃, rT₃, 3,3'-diiodothyronine and 3',5'-diiodothyronine measured by ultrafiltration. *ACTA Endocrinol.* **107**, 357–365 (1984).
45. I. J. Chopra, G. N. Chua teco, T.-S. Huang, A. Bredo, and D. H. Solomon, Relationship between serum free fatty acids and thyroid hormone binding inhibitor in nonthyroid illnesses. *J. Clin. Endocrinol. Metab.* **60**, 980–984 (1985).
46. I. J. Chopra, T.-S. Huang, D. H. Solomon, G. Chaudhuri, and G. N. Chua Teco, The role of thyroxine (T₄)-binding serum proteins in oleic acid-induced increase in free T₄ in nonthyroidal illnesses. *J. Clin. Endocrinol. Metab.* **63**, 776–779 (1986).

47. S. H. Tikanoja, A. Joutti, and B. K. Liewendahl, Association between increased concentrations of free thyroxine and unsaturated free fatty acids in non-thyroidal illnesses: Role of albumin. *Clin. Chim. Acta* **179**, 33–44 (1979).
48. M. W. Homelsky, M. Stein, and A. S. Freedberg, The thyroid hormone-plasma protein complex in man. II. A new *in vitro* method for the study of “uptake” of labeled hormonal components by human erythrocytes. *J. Clin. Endocrinol.* **17**, 33–44 (1967).
49. D. B. Horn, Available assays for serum thyroxine and for serum uptake tests. *J. Clin. Pathol.* **28**, 218–224 (1975).
50. F. Clark and D. B. Horn. Assessment of thyroid function by combined use of the serum protein-bound iodine and resin uptake of L-Triiodothyronine. *J. Clin. Endocrinol.* **25**, 39–45 (1964).
51. P. J. N. Horworth and N. F. Maclagan, Clinical application of serum-total-thyroxine estimation, resin uptake, and free-thyroxine index. *Lancet* **1**, 224–228 (1969).
52. T. J. Wilke, Estimation of free thyroid hormone concentrations in the clinical laboratory. *Clin. Chem.* **32**, 582–592 (1986).
53. M. L. Wellby, M. W. O’Halloran, and J. Marshall, A comparison of effective thyroxine ratio, free thyroxine index and free thyroxine concentration in correcting for thyroxine-binding abnormalities in serum. *Clin. Endocrinol.* **3**, 63–68 (1974).
54. J. C. Nelson and R. T. Tomei, Dependence of the thyroxin/thyroxin-binding globulin (TBG) ratio and the free thyroxin index on TBG concentrations. *Clin. Chem.* **35**, 541–544, (1989).
55. P. Bodlaender, Immulite free T4: Design and complementary role to immulite third generation TSH. *Diagnostic Products Corp. Technical Bulletin* ZB128 (1994).
56. A. L. Babson, The cirrus immulite automated immunoassay system. *J. Clin. Immunoassay* **14**, 83–88 (1991).
57. J. D. Faix, H. N. Rosen, and F. R. Velazquez, Indirect estimation of thyroid hormone-binding proteins to calculate free thyroxine index: Comparison of nonisotopic methods that use labeled thyroxine (“T-uptake”). *Clin. Chem.* **41**, 41–47 (1995).
58. P. R. Larsen, N. M. Alexander, I. J. Chopra, I. D. Hay, J. T. Hershman, J. H. Oppenheimer, D. H. Solomon, and M. I. Surks, Revised nomenclature for tests of thyroid hormones and thyroid-related proteins in serum. *Clin. Chem.* **33**, 2114–2117 (1987).
59. R. P. Levy, J. S. Marshall, and N. L. Velayo, Radioimmunoassay of human thyroxine-binding globulin (TBG). *J. Clin. Endocrinol. Metab.* **32**, 372–381 (1971).
60. W. A. Burr, D. B. Ramsden, S. E. Evans, T. Hogan and R. Hoffenberg, Concentration of thyroxine-binding globulin: Value of direct assay. *Br. Med. J.* **1**, 485–488 (1977).
61. E. C. Attwood, R. M. Seddon, and D. E. Probert, The T4/TBG ratio and the investigation of thyroid function. *Clin. Biochem.* **11**, 218–221 (1978).
62. M. Lecureuil, G. Crouzat-Reynes, J. C. Besnard, and C. Choffel, Correlation of free thyroxine index and thyroxine: thyroxine-binding globulin ratio with the free thyroxine concentration as measured by the thyroxine and thyroxine-binding globulin radioimmunoassays. *Clin. Chem. Acta* **87**, 373–381 (1978).
63. W. DiGiulio, and S. T. Siebert, Thyroxine-binding globulin by competitive protein binding analysis (CPBA). Abstract. *J. Nucl. Med.* **14**, 392 (1973).
64. G. Hintze, E. Briehl, D. Jaworek, A. Kunst, and J. Koberling, Evaluation of new enzyme immunoassay system for free thyroxine (Enzymun-test FT4). *J. Clin. Chem.* **28**, 427–433 (1990).
65. T. J. Wilke, Estimation of free thyroid hormone concentrations in the clinical laboratory. *Clin. Chem.* **32**, 585–592 (1986).
66. P. Beck-Peccoz, P. B. Romelli, M. G. Cattaneo, G. Faglia, E. L. White, J. W. Barlow, and J. R. Stockigt, Evaluation of free thyroxine methods in the presence of iodothyronine binding autoantibodies. *J. Clin. Endocrinol. Metab.* **58**, 736–739 (1984).

67. G. Casco, M. H. Zweig, J. Glickman, M. Ruddel, and J. Kestner, Direct and indirect techniques for free thyroxine compared in patients with nonthyroidal illness. II. Effect of prealbumin, albumin and thyroxine-binding globulin. *Clin. Chem.* **35**, 1655–1662 (1989).
68. T. A. Wilkins and J. E. M. Midgley, New methods of free thyroid hormone assay. In “Physiological Peptides and New Trends in Radioimmunoassay” (A. Bizollon, ed.), pp. 215–234. Elsevier North Holland Amsterdam, 1981.
69. T. A. Wilkins, J. E. M. Midgley, and A. F. Giles, In “Theoretical Basis, Computer Simulation, Optimisation and Technical Validation of a New Direct Free Ligand Assay Principle with Particular Reference to the Measurement of Free Thyroxine,” pp. 221–240. Radioimmunoassay and Related Procedures in Medicine, IAEA, Vienna, Austria, 1982.
70. M. Ito, K. Miyai, K. Doi, I. T. Mitzota, and N. Amino, Enzyme immunoassay of free thyroxine in serum. *Clin. Chem.* **30**, 1682–1685 (1984).
71. J. Y. Bounard, M. P. Bounard, and F. Begon, One-step chemiluminescent immunoassay of free thyroxine with acridinium-ester-labeled thyroxin evaluated and compared with a two-step radioimmunoassay. *Clin. Chem.* **34**, 2556–2560 (1988).
72. J. Beaman, J. S. Woodhead, K. Liewendahl, and H. Mahonen, The evaluation of a chemiluminescent assay for free thyroxine by comparison with equilibrium dialysis in clinical samples. *Clin. Chem. Acta* **186**, 83–90 (1989).
73. J. A. Franklyn, M. C. Sheppard, D. B. Ramsden, and R. Hoffenberg, Free Triiodothyronine and free thyroxine in sera of pregnant women and subjects with congenitally increased or decreased thyroxine-binding globulin. *Clin. Chem.* **29**, 1527–1530 (1983).
74. J. R. Stockigt, V. Stevens, E. L. White, and J. W. Barrow, “Unbound analog” radioimmunoassays for free thyroxine measure the albumin-bound hormone fraction. *Clin. Chem.* **29**, 1408–1410 (1983).
75. K. Liewendahl, S. Tikanoja, T. Helenius, and M. Vitaki, Discrepancies between serum free triiodothyronine and free thyroxin as measured by equilibrium dialysis and analog radioimmunoassay in nonthyroidal illnesses. *Clin. Chem.* **30**, 760–762 (1984).
76. G. Henneman, R. Docter, E. P. Krenning, G. Bos, M. Otten, and T. J. Visser, Raised total thyroxine and free thyroxine index but normal free thyroxine. *Lancet* **1**, 639 (1979).
77. J. R. Stockigt, M. DeGaris, and J. W. Barlow, “Unbound analogue” methods for free T4: A note of caution. *N. Eng. J. of Med.* **307**, 126 (1982).
78. R. Rajatanavin, L. Fournier, D. DiCosimo, C. Abreau, and L. E. Braverman, Elevated serum free thyroxin by thyroxin analog radioimmunoassays in euthyroid patients with familial dysalbuminemic hyperthyroxinemia. *Ann. Intern. Med.* **97**, 865–860 (1982).
79. K. Liewendahl, S. Tikanoja, H. Mahonen, T. Helenius, M. Valimaki, and L. G. Tallgren, Concentrations of iodothyronines in serum of patients with chronic renal failure and other nonthyroidal illnesses: Role of free fatty acids. *Clin. Chem.* **33**, 1382–1386 (1987).
80. N. D. Christofides, C. P. Sheehan, and J. E. M. Midgley, One-step labeled-antibody assay for measuring free thyroxine. I. Assay development and validation. *Clin. Chem.* **38**, 11–18 (1992).
81. P. J. Snyder and R. D. Utiger, Repetitive administration of thyrotropin-releasing hormone results in small elevations of serum thyroid hormones and in marked inhibition of thyrotropin response. *J. Clin. Invest.* **52**, 2305–2312 (1973).
82. J. T. Nicoloff and C. A. Spencer, The use and misuse of the sensitive thyrotropin assays. *J. Clin. Endocrinol. Metab.* **71**, 553–558 (1990).
83. D. V. Becker, S. T. Bigos, E. Gaitan, J. C. Morris, M. L. Rallison, C. A. Spencer, M. Sugawara, L. V. Middlesworth, and L. Wartofsky, Optimal use of blood tests for assessment of thyroid function. *J. Am. Med. Assoc.* **269**, 2736–2737 (1993).
84. I. D. Hay and G. G. Klee, Linking medical needs and performance goals: Clinical and laboratory perspectives on thyroid disease. *Clin. Chem.* **39**, 1519–1524 (1993).

85. G. G. Klee and I. D. Hay, Role of thyrotropin measurements in the diagnosis and measurement of thyroid disease. *Clin. Lab. Med.* **13**, 673–682 (1993).
86. C. A. Spencer, J. S. LoPresti, A. Patel, R. B. Guttler, A. Eigen, D. Shen, D. Grey, and J. T. Nicoloff, Applications of a new chemiluminometric thyrotropin assay to subnormal measurement. *J. Clin. Endocrinol. Metab.* **70**, 453–460 (1990).
87. W. D. Odell, J. F. Wilber, and W. E. Paul, Radioimmunoassay of thyrotropin in human serum. *J. Clin. Endocrinol. Metab.* **25**, 1179–1188 (1965).
88. R. D. Utiger, Radioimmunoassay of human plasma thyrotropin. *J. Clin. Invest.* **44**, 1277–1286 (1965).
89. W. E. Mayberry, H. Gharb, J. M. Bilstad, and G. W. Sizemore, Radioimmunoassay for human thyrotropin: Clinical value in patients with normal and abnormal thyroid function. *Ann. Intern. Med.* **74**, 471–480 (1971).
90. J. M. Hershman and J. A. Pittman, Jr., Utility of the radioimmunoassay of serum thyrotropin in man. *Ann. Intern. Med.* **74**, 481–490 (1971).
91. E. C. Ridgway, Thyrotropin radioimmunoassays: Birth, life, and demise. *MAYO Clin. Proc.* **63**, 1028–1034 (1988).
92. G. G. Klee and I. D. Hay, Sensitive thyrotropin assays: Analytic and clinical performance criteria. *Mayo Clin. Proc.* **63**, 1123–1132 (1988).
93. R. Ekins, F. Chu, and J. Micallef, High specific activity chemiluminescent and fluorescent markers: Their potential application to high sensitivity and “multi-analyte” immunoassays. *J. Biolumin. Chemilumin.* **4**, 59–78 (1989).
94. I. Bronstein, J. C. Voyta, G. H. G. Thorpe, L. J. Kricka, and G. Armstrong, Chemiluminescent assay of alkaline phosphatase applied in an ultrasensitive enzyme immunoassay of thyrotropin. *Clin. Chem.* **35**, 1441–1446 (1989).
95. M. Romer and R. Haeckel, The analytical performance of the Ciba Corning ACS:180 automated immunoassay system. A multicentre evaluation. *Eur. J. Clin. Chem. Clin. Biochem.* **32**, 395–407 (1994).
96. J. Mora-Brugues, N. Gascon-Roche, J. Rodriguez-Espinosa, M. Cortes-Rius, and F. Gonzalez-Sastre, Evaluation of Ciba Corning ACS:180 automated immunoassay system. *Clin. Chem.* **40**, 407–410 (1994).
97. C. A. Spencer, M. Takeuchi, M. Kazarosyan, F. MacKenzie, G. J. Beckett, and E. Wilkinson, Interlaboratory/intermethod differences in functional sensitivity of immunoassay of thyrotropin (TSH) and impact on reliability of measurement of subnormal concentrations of TSH. *Clin. Chem.* **41**, 367–374 (1995).
98. E. Wilkinson, P. W. H. Rae, K. J. T. Thomson, A. D. Toft, C. A. Spencer and G. J. Beckett, Chemiluminescent third-generation assay (Amerlite TSH-30) of thyroid-stimulating hormone in serum or plasma assessed. *Clin. Chem.* **39**, 2166–2173 (1993).
99. C. R. Squire and W. D. Fraser, Improved sensitivity and precision of thyroid-stimulating hormone measurements by standardizing signal reagent addition in the Amerlite TSH-30 assay. *Clin. Chem.* **40**, 164–165 (1994).
100. M. Flore, J. Mitchell, T. Doan, R. Nelson, G. Winter, C. Grandone, K. Zeng, R. Haraden, J. Smith, K. Harris, J. Leszczynski, D. Berry, S. Safford, G. Barnes, A. Scholnick, and K. Ludington, The Abbott IMX automated benchtop immunochemistry analyzer system. *Clin. Chem.* **34**, 1726–1732 (1988).
101. G. Wiedenmann, L. Janetz-Mentzel, and R. Panse, Establishment of reference ranges for thyrotropin, triiodothyronine, thyroxine and free thyroxine in neonates, infants, children and adolescents. *Eur. J. Clin. Chem. Clin. Biochem.* **31**, 277–288 (1993).
102. E. J. Lamb, K. A. Noonan, and J. M. Burrin, Analytical Performance of immulite assay of thyroid-stimulating hormone. *Clin. Chem.* **40**, 1598–1600 (1994).

103. W. Patterson, P. Werness, W. J. Payne, P. Matsson, C. Leflar, T. Melander, S. Quast, J. Stejskal, A. Carlson, M. Macera, and F. W. Schubert, Random and continuous-access immunoassays with chemiluminescent detection by Access automated analyzer. *Clin. Chem.* **40**, 2042–2045 (1994).
104. E. Taimela, R. Tahtela, P. Koskinen, P. Nuutila, J. Forsstrom, S. Taimela, S. L. Karonen, M. Valimaki, and K. Irfala. Ability of two new thyrotropin (TSH) assays to separate hyperthyroid patients from euthyroid patients with low TSH. *Clin. Chem.* **40**, 101–105 (1994).
105. C. Spencer, J. Lopresti, L. V. Middlesworth, L. Wartofsky, D. Becker, T. Bigos, E. Gaitan, J. C. Morris, M. L. Railison, and M. Sugawara, Screening for thyroid dysfunction: Which test is best (in reply). *J. Am. Med. Assoc.* **270**, 2297–2298 (1993).
106. M. H. Zweig, G. Csako, J. C. Reynolds, and J. A. Carrasquillo, Interference by iatrogenically induced anti-mouse IgG antibodies in a two-site immunometric assay for thyrotropin. *Arch. Pathol. Lab. Med.* **115**, 164–168 (1991).
107. R. E. Gaines-Das, H. Brettschneider, and A. F. Bristow, The effects of common matrices for assay standards on performance of ultrasensitive immunometric assays for TSH. *Clin. Chem. Acta.* **201**, S5 (1991).
108. M. I. Surks, I. J. Chopra, C. N. Mariash, J. T. Nicoloff, and D. H. Solomon, American Thyroid Association guidelines for use of laboratory tests in thyroid disorders. *J. Am. Med. Assoc.* **263**, 1529–1532 (1990).
109. T. Kotani, K. Umeki, S. Matsunaga, E. Kato, and S. Ohtaki, Detection of auto-antibodies to thyroid peroxidase in autoimmune thyroid diseases by micro-Elisa and immunoblotting. *J. Clin. Endocrinol. Metab.* **62**, 928–933 (1993).
110. R. Volpe, Autoimmune endocrinopathies: Aspects of pathogenesis and the role of immune assays in investigation and management. *Clin. Chem.* **40**, 2132–2145 (1994).
111. A. Stagnaro-Green, S. H. Roman, R. H. Cobin, M. Alvarez-Marfany, and T. F. Davies, Detection of at-risk pregnancy by means of highly sensitive assays for thyroid autoantibodies. *J. Am. Med. Assoc.* **264**, 1422–1425 (1990).
112. I. Cayzer, S. R. Chalmers, D. Doniach, and G. Swana. An evaluation of two new haemagglutination tests for the rapid diagnosis of autoimmune thyroid diseases. *J. Clin. Pathol.* **31**, 1147–1151 (1978).
113. A. E. Ohwovoriole, T. J. Wilkin, L. Scott-Morgan, P. Johnston, and W. Mould, Improved ELISA for thyroid microsomal autoantibodies. Comparison with hemagglutination and immunofluorescent techniques. *Int. Arch. Allergy Appl. Immunol.* **86**, 183–189 (1988).
114. Y. Hoshijima, M. Kosaka, K. Okagawa, T. Goto, and S. Saito, A sensitive immunoassay for anti-thyroglobulin antibody using Fab'-horseradish peroxidase conjugate. *J. Immunol. Methods* **96**, 121–126 (1987).
115. S. H. Roman, F. Korn, and T. F. Davies, Enzyme-linked immunosorbent microassay and hemagglutination compared for detection of thyroglobulin and thyroid microsomal autoantibodies. *Clin. Chem.* **30**, 246–250 (1984).
116. H. Haubruck, L. Mauch, N. J. Cook, U. Steffens, N. Hunt, H. Berthold, H. Neiman, C. Wirbelauer, and W. Northemann, Expression of recombinant thyroid peroxidase by the baculovirus system and its use in ELISA screening for diagnosis of autoimmune thyroid disease. *Autoimmunity* **15**, 275–284 (1993).
117. D. L. Kendler, A. Martin, R. P. Magnusson, and T. F. Davies, Detection of autoantibodies to recombinant human thyroid peroxidase by sensitive enzyme immunoassay. *Clin. Endocrinol.* **33**, 751–760 (1990).
118. K. Beever, J. Bradbury, D. Phillips, S. M. McLachlan, C. Pegg, A. Goral, W. Overbeck, G. Felfel, and B. R. Smith, Highly sensitive assays of autoantibodies to thyroglobulin and to thyroid peroxidase. *Clin. Chem.* **35**, 1949–1954 (1989).

119. B. R. Smith, and R. Hall, Thyroid-stimulating immunoglobulins in Graves' disease. *Lancet* **2**, 427-431 (1974).
120. K. D. Burman, and J. R. Baker, Jr., Immune mechanisms in Graves' disease. *Endocr. Rev.* **6**, 183-232 (1985).
121. J. R. Baker, Jr., Immunological aspects of endocrine diseases. *J. Am. Med. Assoc.* **268**, 2899-2903 (1992).
122. S. Levinson, Organ specific autoimmune disease. *J. Clin. Immunoassay* **17**, 92-97 (1994).
123. J. Orgianzz, D. E. Williams, I. J. Chapran, and D. H. Solomon, Human thyroid adenyl cyclase-stimulating activity in immunoglobulin G of patients with Graves' disease. *J. Clin. Endocrinol. Metab.* **42**, 341-354 (1976).
124. A. Sugeno, A. Kidd, V. V. Raw, and R. Volpe, Correlation between thyrotropin-displacing activity and human thyroid-stimulating activity by immunoglobulins from patients with Graves' disease and other thyroid disorders. *J. Clin. Endocrinol. Metab.* **48**, 398-402 (1979).
125. T. F. Davies, M. Platzer, A. Schwartz, and E. Friedman, Functionality of thyroid-stimulating antibodies assessed by cryopreserved human thyroid cell bioassay. *J. Clin. Endocrinol. Metab.* **57**, 1021-1027 (1983).
126. G. Shewring, and B. R. Smith, An improved radioreceptor assay for TSH receptor antibodies. *Clin. Endocrinol.* **17**, 409-417 (1982).
127. A. J. Van Herle, R. P. Uller, N. L. Mathews, and J. Brown, Radioimmunoassay for measurement of thyroglobulin in human serum. *J. Clin. Invest.* **52**, 1320-1327 (1973).
128. P. Bodlaender, J. R. Arjonilla, R. Sweat, and S. L. Twomey, A practical radioimmunoassay of thyroglobulin. *Clin. Chem.* **24**, 267-271 (1978).
129. U. Feldt-Rasmussen, P. H. Petersen, and J. Date, Sex and age correlated reference values of serum thyroglobulin measured by modified radioimmunoassay. *Acta Endocrinol.* **90**, 440-450 (1979).
130. J. Kastrup, U. Feldt-Rasmussen, H. R. Bartram, J. Witten, and H. S. Hansen, An enzyme linked immunosorbent assay (ELISA) for measurements of human serum thyroglobulin auto-antibodies. *Scand. J. Clin. Lab. Invest.* **45**, 471-476 (1985).
131. H. Endo, J. Nakano, S. Ohtaki, M. Izumi, H. Hamaguchi, S. Yoshitake, and E. Ishikawa, An enzyme immunoassay for the measurement of thyroglobulin in human serum. *Clin. Chim. Acta* **95**, 325-336 (1979).
132. M. F. Bayer and J. P. Kris, Immunoradiometric assay for serum thyroglobulin: Semiquantitative measurement of thyroglobulin in antithyroglobulin-positive sera. *J. Clin. Endocrinol. Metab.* **49**, 557-564 (1979).
133. M. Piechaczyk, L. Baldet. B. Pau, and J.-M. Bastide, Novel immunoradiometric assay of thyroglobulin in serum with use of monoclonal antibodies selected for lack of cross-reactivity with autoantibodies. *Clin. Chem.* **35**, 422-424 (1989).
134. A. J. Van Herle, I. S. Van Herle, and M. A. Greipel, An international cooperative study evaluating serum thyroglobulin standards. *J. Clin. Endocrinol. Metab.* **60**, 338-343 (1985).
135. U. Feldt-Rasmussen, and M. Schlumberger, Interlaboratory comparison of serum thyroglobulin measurement. *J. Endocrinol. Invest.* **11**, 175-181 (1988).
136. A. B. Schneider and R. Pervos, Radioimmunoassay of human thyroglobulin: Effect of antithyroglobulin autoantibodies. *J. Clin. Endocrinol. Metab.* **47**, 126-137 (1978).
137. A. Ligabue, M. C. Poggioli, and A. Zacchini, Interference of specific autoantibodies in the assessment of serum thyroglobulin. *J. Nucl. Biol. Med.* **37**, 273-279 (1993).
138. S. Kawamura, B. Kishino, K. Tajima, K. Mashita, and S. Tarui, Serum thyroglobulin changes in patients with Graves' disease treated with long term antithyroid drug therapy. *J. Clin. Endocrinol. Metab.* **56**, 507-512 (1983).

139. A. J. Van Herle, and R. P. Uller, Elevated serum thyroglobulin: A marker of metastases in differentiated thyroid carcinomas. *J. Clin. Invest.* **56**, 272–77 (1975).
140. M. Ozata, S. Suzuki, T. Miyamoto, R. T. Liu, F. Fierro-Rewoy, L. J. DeGroot, Serum thyroglobulin in the follow-up of patients with treated differentiated thyroid cancer. *J. Clin. Endocrinol. Metab.* **79**, 98–105 (1994).
141. P. Czernichow, M. Schlumberger, R. Pomarede, and P. Fragu, Plasma thyroglobulin measurements help determine the type of thyroid defect in congenital hypothyroidism. *J. Clin. Endocrinol. Metab.* **56**, 242–245 (1983).

8

Uptake Measurements of Thyroid Hormones and Amino Acids in Cultured Cells

Vadivel Ganapathy
Puttur D. Prasad
Frederick H. Leibach
*Department of Biochemistry and
Molecular Biology
Medical College of Georgia
Augusta, Georgia 30912-2100*

INTRODUCTION

Thyroid hormones (T_3 and T_4) are iodine-substituted tyrosines, joined to an iodine-substituted phenol via an ether linkage (Figure 1). In the naturally occurring thyroid hormones, the alanine side chain exists in the L-configuration. The amino and carboxyl groups in T_3 and T_4 are ionized under physiological conditions, the amino group existing as NH_3^+ and the carboxyl group as COO^- . This imparts a zwitterionic character to these compounds. Thus, T_3 and T_4 are structurally very similar to neutral amino acids. This chemical nature of T_3 and T_4 is the basis for the relationship between the cellular uptake of these hormones and the cellular uptake of neutral amino acids observed in several studies. Therefore, the transport systems that are responsible for the cellular uptake of thyroid hormones can be classified as amino acid transport systems. Interestingly, several amino acids exhibit endocrine/neuroendocrine functions (e.g., glycine, taurine, proline, γ -aminobutyrate, homocysteate, aspartate, and glutamate). However, al-

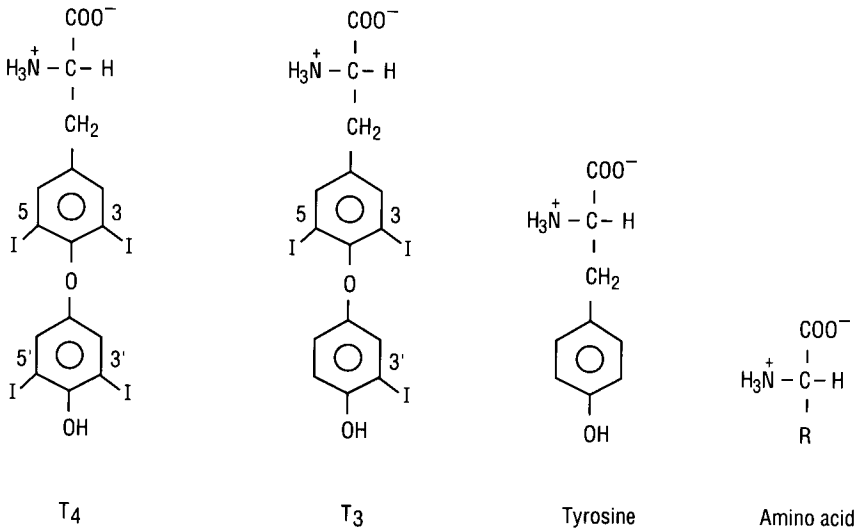


FIGURE 1. Chemical structures of thyroid hormones, tyrosine, and other amino acids.

though the receptors for thyroid hormones are located intracellularly, the receptors for the amino acids with endocrine/neuroendocrine functions are present in the plasma membrane. The transport systems available in cells for the uptake of thyroid hormones make it possible for these hormones to interact with the intracellular receptors. On the other hand, the transport systems available for other amino acids play a role in lowering the extracellular concentrations of these amino acids and consequently in reducing their interaction with the respective receptors in the plasma membrane. Therefore, the transport systems that are responsible for the cellular uptake of thyroid hormones and amino acids with endocrine/neuroendocrine functions are important determinants in the modulation of cellular signaling mediated by these compounds.

AMINO ACID TRANSPORT SYSTEMS

Substrate Specificity and Driving Forces

Amino acids vary widely in their physicochemical nature and it is not surprising that the cellular uptake of all amino acids is not mediated by a single transport system. The existence of multiple transport systems for amino acids in mammalian cells has been known for a long time. The initial classification of these transport systems was based on group specificity

because it was thought that distinct transport systems existed for the uptake of neutral amino acids, acidic amino acids, basic amino acids, and imino acids. It soon became apparent that the substrate specificity of the amino acid transport systems is far more complex than originally thought. At present, there are at least 20 different amino acid transport systems known to exist in mammalian cells (1–4). Even though there is considerable overlap in the substrate specificity of various amino acid transport systems, each system shows preference for certain specific amino acids. In addition to the differences in the substrate specificity, the transport systems also differ with respect to their driving forces. Some of them are facilitative transporters with no involvement of any driving force, whereas others are active transporters energized by membrane potential and/or ion gradients. At least four different ion gradients are known to participate in the energization of the amino acid transport systems: the Na^+ gradient, the Cl^- gradient, the K^+ gradient, and the H^+ gradient. In several instances, two or more ion gradients operate together as the driving force.

Interestingly, the spectrum of amino acid transport systems that are expressed in mammalian cells varies among different cell types. No single cell type expresses all the known amino acid transport systems. In this respect, three distinct groups become readily apparent: nonpolarized cells, polarized cells, and neuronal cells. Each of these cell types appears to possess a different set of amino acid transport systems (3–8).

Interaction between Thyroid Hormones and Amino Acids during Transport

The identity of the amino acid transport systems that mediate the cellular uptake of thyroid hormones has not been unequivocally established. Available evidence indicates that different systems may operate in different cell types. In erythrocytes, System T, which shows specificity toward aromatic amino acids, appears to mediate the uptake of T_3 and T_4 (9,10). In neuronal cells and in astrocytes, System L, which shows specificity toward branched chain and aromatic amino acids, seems to be involved (11,12). Studies in placental cells have shown that uptake of thyroid hormones occurs via a specific transport system that is unrelated to the amino acid transport systems T and L (13,14). In all of these cases, however, the transport systems mediating the uptake of thyroid hormones are Na^+ -independent and non-concentrative. In contrast, a Na^+ -dependent, active transport system for the uptake of T_3 and T_4 has been described in hepatocytes (15).

It appears that in most cell types the uptake of thyroid hormones is facilitative with no involvement of any driving force. Interestingly, the cellular uptake of other amino acids that exhibit endocrine/neuroendocrine

functions seems to be mediated by active transport systems involving multiple driving forces. For example, the transport systems available for taurine, glycine, proline, and γ -aminobutyrate are energized by three different driving forces, namely, a Na^+ gradient, a Cl^- gradient, and the membrane potential (8). This is an important difference that may be relevant to the physiological functions of these transport systems. Since the purpose of the transport systems for thyroid hormones is to make these hormones in the extracellular medium available to the intracellularly located receptors, there is hardly any need for these systems to be concentrative. On the other hand, the purpose of the transport systems for the amino acids with endocrine/neuroendocrine functions is to effectively reduce the concentrations of these amino acids in the extracellular medium in order to terminate their interaction with the respective receptors on the plasma membrane. This requires efficient and highly active transport systems that catalyze concentrative uptake. In neuronal cells, some of the amino acids (e.g., glycine, γ -aminobutyrate, and glutamate) that are transported actively into the cells are concentrated in storage granules for subsequent release into the extracellular medium to facilitate their interaction with the receptors.

Strategies to Establish the Identity of the Transport System for Any Particular Amino Acid

Elucidation of the substrate specificity of the transport system that catalyzes the uptake of a particular amino acid of interest and identification of the driving forces involved in the energization of the transport system are the two most important steps necessary to successfully establish the identity of the transport system. The substrate specificity studies are conveniently done by assessing the ability of various amino acids to inhibit the uptake of a particular amino acid. It is desirable to perform these inhibition experiments by using a wide range of concentrations of the potential inhibitors in order to determine whether the observed inhibition is complete or partial. This strategy will help in finding out whether or not a single transport system is responsible for the uptake of the particular amino acid, recognizing that any given amino acid may serve as a substrate for more than one transport system. Experiments designed to identify the driving forces should concentrate on the following ions: Na^+ , Cl^- , and H^+ . The ion dependence of an amino acid transport system is an important clue to the identity of the system (3–6). Certain amino acid transport systems are independent of any ion, whereas others are dependent on either Na^+ or H^+ . There are subclasses of Na^+ -dependent transport systems. Some systems are dependent solely on Na^+ with no involvement of other ions, whereas some have obligatory requirement for not only Na^+ but also Cl^- . In the latter case,

the presence of either Na^+ or Cl^- alone will not support the transport system. There are also other distinctive cases of Na^+ -dependent transport systems that, though not obligatorily dependent on other ions such as H^+ or K^+ for their activity, utilize these ion gradients as additional driving forces if they are present along with the Na^+ gradient.

An additional approach to identify the transport system responsible for the uptake of a particular amino acid is to use the so-called A-B-C test (2,16,17). This test is useful to establish whether or not two different amino acids share a common transport system. If the identity of the transport system mediating the uptake of one of the amino acids is known, the A-B-C test will assess the involvement of that particular transport system in the uptake of the other amino acid. According to this approach, if two amino acids, A and B, are transported via a common system, the uptake characteristics of these two amino acids should satisfy the following criteria. (a) Increasing concentrations of A should be able to block completely the uptake of B and vice versa. (b) Kinetic analysis should establish that the interaction between A and B during the uptake process is strictly competitive. (c) The dissociation constant (K_t) determined for A from its uptake measurements in the absence of B should be equal to the inhibition constant (K_i) determined for A from the uptake measurements of B in the presence of A. The same should be true for the K_t and K_i values determined for B. (d) Uptake of A and that of B should be inhibited to a similar extent by various other amino acids (designated as C) that share the common transport system.

UPTAKE MEASUREMENTS IN CULTURED CELLS

Cell Culture

When the functional expression of transport systems in cultured cells is investigated, it has to be remembered that the state of differentiation of the cells in culture profoundly affects the functional characteristics of these cells. The expression of transport systems is therefore dependent on culture conditions. Uptake measurements to assess transport functions are usually done after the cells reach confluence. The culture time needed for differentiation varies from cell type to cell type. In addition, it is influenced by the cell density during the initial seeding and also by the nature of the coating material on the culture dish. Several kinds of coating material are commercially available (e.g., collagen and Matrigel) and can be used to treat the culture dishes before seeding the cells. It is always advisable to study the dependence of the transport function on the culture time as an important

preliminary characterization. The pattern of expression with respect to culture time varies widely among different transport systems. Therefore, the optimal culture conditions have to be worked out independently for each transport system in question.

If the cells are polarized with functionally distinct apical and basolateral membrane domains (e.g., intestinal and renal epithelial cells, placental syncytiotrophoblast and thyroid follicular epithelium), differential expression of the transport systems in these two regions of the plasma membrane has to be taken into consideration. When these cells are cultured on a plastic dish, only the apical membrane is accessible for uptake measurements. The transport functions that are differentially expressed in the basolateral membrane cannot be studied with this experimental approach. To study independently the transport functions in the apical membrane and in the basolateral membrane, the cells can be cultured on permeable filters, which allows differential access to both domains (18).

Uptake Measurement

The following protocol is for the cells cultured on plastic support. The culture dishes containing confluent cells are taken out of the incubator and kept at room temperature for 30 min. The medium is aspirated and the cells are washed once with the uptake buffer. Care is always taken not to disrupt the cell layer during aspiration and washing. Aspiration can be conveniently done using a setup that operates under vacuum suction. The tube can be fitted with a Pasteur pipet and the medium in the culture dish can be removed fast and efficiently by placing the pipet tip at the edge of the dish and slightly tilting the dish as the medium is aspirated. Following the washing, 1 ml of uptake buffer containing radiolabeled amino acid substrate is added to the dish to initiate uptake. One milliliter of the uptake medium is enough for a 35-mm culture dish. If culture dishes of smaller areas are used as in 24-well culture plates, the volume of the uptake medium can be reduced. However, it is important that the volume is enough to cover the cell layer completely. The uptake is allowed to proceed for a desired time. For kinetic analysis of the transport system, it is necessary to choose a time period that represents a linear uptake rate. This can be done by first studying the dependence of uptake on the incubation time. At the end of incubation, uptake is terminated by aspirating the medium, followed by washing of the cells three times with fresh uptake medium that does not contain the uptake substrate. It may be preferable to use an ice-cold uptake medium for the washing procedure, which might eliminate or substantially reduce the efflux of the transported substrate during washing. After the washing, 1 ml of 0.2 *N* NaOH/1% SDS is added to the dish and

the incubation is continued at room temperature for 30 min. This results in the lysis of the cells. The lysate is transferred to scintillation vials for quantitation of radioactivity.

The composition of the uptake medium is 25 mM HEPES, 140 mM NaCl, 5.4 mM KCl, 1.8 mM CaCl₂, 0.8 mM MgSO₄, and 5 mM glucose, and the pH of the medium is adjusted to 7.4 with Tris base. This medium is used in most instances as a Na⁺- and Cl⁻-containing medium. However, when the influence of ion gradients on the transport function is assessed, the composition of the medium needs to be changed. A Na⁺-free medium is prepared by substituting NaCl with an equimolar concentration of one of the following: LiCl, choline chloride, or *N*-methyl-D-glucamine chloride. LiCl may not be suitable in some cases because Li⁺ can substitute for Na⁺ fully or partially as a cotransportable ion for certain transport systems. Choline chloride also is unsatisfactory in certain specific instances. Even though choline has not been shown to substitute for Na⁺ as a cotransported ion, it is known to interact with the Na⁺-binding site. Thus, choline chloride can be used in place of NaCl to assess the role of a Na⁺ gradient in a transport function. But when the dependence of a transport function on the concentration of Na⁺ is investigated, there is a need to replace NaCl isosmotically with another chloride salt to a varying degree. Choline chloride may not be desirable for this purpose because of the potential interaction of choline with the Na⁺-binding site. Such an interaction will lead to erroneous Na⁺-dependence kinetics. Because of these potential drawbacks associated with LiCl and choline chloride, *N*-methyl-D-glucamine chloride is frequently used as a substitute for NaCl. This salt is not readily available from commercial sources. However, it can be easily prepared by mixing equimolar concentrations of *N*-methyl-D-glucamine base and HCl. Thus, the Na⁺-free uptake buffer will contain 140 mM *N*-methyl-D-glucamine and 140 mM HCl in place of 140 mM NaCl. KCl should not be used to substitute for NaCl. Presence of high concentrations of K⁺ in the extracellular medium during uptake measurement will depolarize the cell and consequently interfere with the function of the transport systems, which are dependent on the membrane potential.

Certain amino acid transport systems are obligatorily dependent on Na⁺ as well as Cl⁻. Examples of this kind include the taurine transporter (19) and the glycine transport system GLYT1 (20). Therefore, it may be necessary in some instances to assess the role of Cl⁻ in the function of a transport system. This requires comparison of uptake values measured in the presence and in the absence of Cl⁻. The Cl⁻-free medium can be prepared by substituting NaCl, KCl, and CaCl₂ with isomolar concentrations of respective gluconate salts.

Determination of Incorporation of Amino Acids into Cellular Proteins during Uptake

Cellular metabolism, primarily incorporation into proteins, of transported amino acids during uptake measurements may make it difficult to calculate the uptake rates accurately. This problem is nonexistent or minimal in some cases where the amino acid substrates are not constituents of cellular proteins (e.g., taurine and γ -aminobutyrate). For most amino acids, however, incorporation into cellular proteins represents a primary metabolic pathway. Therefore, it may be necessary to determine the fraction of the transported amino acid substrate that gets incorporated into proteins. This can be assessed by measuring the radioactivity inside the cell, which can be precipitated with trichloroacetic acid (21). For this purpose, incubation of the cells with the radiolabeled substrate is carried out similar to the regular uptake measurement. At the end of incubation, uptake is terminated by aspirating the medium and then by washing the cells once with fresh uptake buffer. The cells are then washed four times with 10% trichloroacetic acid. This procedure leads to precipitation of cellular proteins. The precipitated proteins stay adhered to the dish while the amino acid pool that is not protein-bound is removed. The precipitate is washed once with ether-ethanol (1 : 3, vol/vol) and then solubilized with 1 ml of 0.2 N NaOH/1% SDS. The material is then transferred to scintillation vials for determination of radioactivity.

Differentiation between Transmembrane Transport and Cell-Surface Binding

When hydrophobic substrates such as aromatic amino acids and thyroid hormones are used, binding to the membrane sites not relevant to the transport systems may contribute significantly to the uptake values measured. In these circumstances it may be necessary to differentiate between transmembrane transport and cell-surface binding. Two procedures are generally employed for this purpose, an acidic saline wash or an alkaline saline wash of the cells at the end of incubation used for uptake measurement. Highly acidic or alkaline pH interferes with the cell-surface binding of the amino acid substrates. The radioactivity that is associated with the cell surface is released instantaneously when the cells are washed under these conditions, whereas the radioactivity present inside the cells as the result of transmembrane transport remains unaffected by the washing procedure. It has been shown in the case of thyroid hormones that the alkaline pH-sensitive component of uptake represents nonsaturable binding to the cell surface and has no relevance to transport (22). Similar procedures have proved to be useful in removing other ligands such as folate (23,24) and

epidermal growth factor (25) that are bound to the cell-surface receptors. The buffer used for acid wash is prepared by adjusting the pH of a 0.15 M NaCl/10mM Na acetate solution to 3.5 with acetic acid. The buffer used for alkali wash is prepared by adjusting the pH of a 0.15 M NaCl/50 mM glycine solution to 10.5 with NaOH. In both cases, the wash buffer is kept ice-cold and the cell layers are washed twice with the buffer.

Differentiation between Passive and Active Transport

Passive transport occurs down a concentration gradient with no involvement of any form of energy. In contrast, active transport occurs against a concentration gradient and requires energy in some form. The involvement of metabolic energy in a transport process can be assessed in intact cells by using reagents that will interfere with cellular metabolism (13,22,26). Commonly used reagents for this purpose are azide, cyanide, and carbonyl cyanide *p*-trifluoromethoxyphenylhydrazone. All of these compounds inhibit mitochondrial ATP production. Dinitrophenol, oligomycin, and antimycin are also used for this purpose. The cells have to be preincubated with these compounds for 30–60 min at room temperature prior to initiation of uptake measurements. The following concentrations have been shown to be effective: cyanide, 4 mM; azide, 0.25 mM; carbonyl cyanide *p*-trifluoromethoxyphenylhydrazone, 20 μ M; dinitrophenol, 2 mM; oligomycin, 50 μ M; and antimycin, 20 μ M. Additional approaches to determine the involvement of metabolic energy are to use a glucose-free medium for preincubation or to use phloridzin (2 mM), an inhibitor of cellular uptake of glucose. These manipulations lead to a decrease in the glycolysis-dependent ATP production in the cells. If a transport system is dependent on metabolic energy, interference with ATP production by any of these maneuvers will inhibit the transport function.

Most amino acid transport systems that are active utilize a transmembrane Na⁺ gradient as an obligatory energy source even though they may or may not use other ion gradients as additional energy sources. The Na⁺ gradient in cells is maintained by the Na⁺-K⁺-ATPase. Therefore, the role of a Na⁺ gradient in the function of a transport system can be investigated by using ouabain, which inhibits the Na⁺-K⁺-ATPase. Alternatively, ionophores such as gramicidin and monensin, which dissipate transmembrane Na⁺ gradients, can also be used. Collapse of the transmembrane Na⁺ gradient caused by these maneuvers will inhibit the function of Na⁺-dependent transport systems.

Determination of Cell Number and Protein Content

Uptake values measured in intact cells are generally expressed as moles per 10⁶ cells or moles per milligram of protein. To determine the cell

number and the protein content, cells that have been cultured under identical conditions as those for uptake measurements are used. The cells are released by treatment with trypsin and suspended in phosphate-buffered saline, and the cell number is determined with a Coulter counter. The optimal conditions for the release of the cells, such as the concentration of trypsin and the time of incubation, have to be independently worked out for each cell type.

Protein content of the cells is measured in the homogenate prepared from the cells. After aspirating the medium from the culture dish, 1 ml of deionized water is added to the dish. The cells are lysed by subjecting the dishes to freezing and thawing two times, following which the dish contents are suspended by passing through a 25-gauge needle several times to form the homogenate. The protein content of the homogenate can be determined by any of the routine protein determination methods.

PLASMA MEMBRANE VESICLES DERIVED FROM CULTURED CELLS FOR UPTAKE MEASUREMENTS

Advantages of the Use of Membrane Vesicles

Even though an intact cell system is convenient in a number of respects to characterize the transport systems for amino acids and thyroid hormones, it has certain drawbacks. Cellular metabolism of the transported substrates poses a significant problem in correctly interpreting the uptake data. Furthermore, the intact cell system places considerable restrictions in manipulating the ion gradients and membrane potential that exist across the plasma membrane. These drawbacks can be overcome by using purified plasma membrane vesicles for uptake measurements. With this membrane vesicle system, the transport of amino acids and thyroid hormones can be studied without the interference of the cellular metabolism. In addition, the transmembrane ion gradients and the membrane potential can be altered as desired in order to identify and analyze systematically the driving forces involved in the transport process.

Isolation of Plasma Membrane Vesicles from Cultured Cells

The cells have to be cultured in large flasks to provide enough starting material for the preparation of plasma membrane vesicles (27); 225-cm² culture flasks are convenient for this purpose. All steps involved in the membrane isolation procedure are carried out at 0–4°C. It may be desirable to include protease inhibitors in the lysis buffer to prevent possible proteoly-

sis of the transport proteins by endogenous proteases during membrane isolation. The culture medium is removed from the flasks and the cells are washed quickly with 10 ml of ice-cold phosphate-buffered saline. Following this, 25 ml of the lysis buffer (10 mM Tris/HCl buffer, pH 7.5) is added to the flask. The hypotonic buffer leads to the lysis of the cells. The contents of the flask are scraped by using a cell scraper and then transferred to a glass beaker. The lysate is homogenized for 30 s in an Ultra-Turrax Tissue-mixer. Other kinds of motor-driven homogenizers can also be used. The total volume of the homogenate is adjusted to 50 ml with the lysis buffer. The lysate from a number of flasks can be pooled at this stage. A stock solution of 1 M MgCl₂ is added to the homogenate to give a final concentration of 12 mM MgCl₂. The mixture is stirred at 0°C for 15 min. This step leads to preferential aggregation of nonplasma membrane fragments. The aggregated material is removed by centrifugation at 3000g for 15 min. The supernatant contains the plasma membranes, which can be collected by centrifuging the supernatant at 60,000g for 30 min. The membrane pellet is rinsed with and then suspended in the preloading buffer of desired composition. The membrane suspension is passed through a 25-gauge needle to obtain a homogeneous suspension. The preloading buffer used in general is either 10 mM HEPES/Tris, pH 7.5, containing 300 mM mannitol or 10 mM HEPES/Tris, pH 7.5, containing 150 mM mannitol plus 75 mM potassium gluconate. The protein content of the membrane suspension is determined and adjusted to a desired concentration. The membranes thus prepared exist in the form of vesicles possessing an osmotically responsive intravesicular space. The function of any transport system that is present in these membranes can be characterized by studying the uptake of suitable substrates into this intravesicular space. These membrane vesicles can be used fresh for uptake measurements or stored in aliquots in liquid nitrogen for later use. Purity of the membrane vesicles can be assessed by determining the enrichment of alkaline phosphatase activity in the membrane preparation compared to the activity in the original homogenate. Alkaline phosphatase is a marker enzyme for the plasma membrane. In place of alkaline phosphatase, 5'-nucleotidase can also be used for this purpose. The plasma membrane vesicles thus prepared are predominantly oriented right-side-out (i.e., the exoplasmic surface faces the outside and the cytoplasmic surface faces the inside).

Uptake Measurement in Plasma Membrane Vesicles

The plasma membrane vesicles can be used conveniently to study the transport of amino acids and thyroid hormones using a rapid filtration technique (27,28). Uptake is initiated by mixing in a small test tube 40 μ l of

the membrane suspension with 160 μl of a suitable uptake buffer containing radiolabeled substrate. Incubation is continued for a desired time. At the end of incubation, uptake is terminated by the addition of 3 ml of ice-cold stop buffer. The mixture is immediately filtered through a Millipore filter (DAWP type, 25 mm diameter, 0.45- or 0.65- μm pore size) under vacuum. The filtration apparatus from Micro Filtration Systems (cat. no. 311200; Model no. KG25) or any other similar setup can be used for this purpose. The membrane vesicles are retained on the surface of the filter during filtration. The filter is washed three times with 3 ml of the ice-cold stop buffer, following which the filter is transferred to a scintillation vial. Ten milliliters of scintillation cocktail is added to the vial and the radioactivity associated with the filter is counted.

The composition of the uptake buffer can be altered to suit the purpose of individual experiments. In general, a 10 mM HEPES/Tris buffer (pH 7.5) containing 150 mM NaCl is used. When the membrane vesicles are suspended in this buffer for uptake measurements, there exists an inwardly directed NaCl gradient across the vesicular membrane because the preloading buffer that is present in the intravesicular space contains neither Na^+ nor Cl^- . This uptake buffer is suitable for studies involving Na^+ -dependent transport systems. To assess the role of Na^+ and/or Cl^- in the transport function, these ions can be isosmotically replaced by other monovalent cations and/or anions. H^+ -dependent transport systems can also be investigated in these membrane vesicles by suitably altering the pH of the preloading buffer and the pH of the uptake buffer to produce desired transmembrane H^+ gradients (29,30). The stop buffer usually consists of 10 mM HEPES/Tris, 150 mM KCl, pH 7.5.

The role of membrane potential in the transport function can be studied in these membrane vesicles by using different approaches. The vesicles can be voltage-clamped by keeping K^+ in the intravesicular medium as well as in the uptake medium and by adding valinomycin (10 μM), a K^+ -ionophore. The same ionophore can also be used to generate an inside-negative or inside-positive membrane potential by altering transmembrane K^+ gradients. In the presence of an outwardly directed K^+ gradient, valinomycin facilitates the efflux of K^+ from the vesicles, generating an inside-negative membrane potential. When the K^+ gradient is inwardly directed, the ionophore generates an inside-positive membrane potential. Anions with varying membrane permeabilities are also useful for generating different degrees of inside-negative membrane potential across the vesicular membrane caused by the diffusion of the anions down their concentration gradients. Another approach is to use carbonyl cyanide *p*-trifluoromethoxyphenylhydrazone, a H^+ -ionophore, in combination with an inwardly directed or an outwardly directed transmembrane H^+ gradient (31,32).

Differentiation between Passive Transport and Active Transport

Unlike in intact cells, there is no cellular metabolism in purified plasma membrane vesicles. Therefore, the metabolic poisons such as cyanide or azide are not useful in differentiating between active transport and passive transport in these vesicles. Dependence of the uptake on some form of driving force (e.g., Na^+ gradient and H^+ gradient) is an indication that the uptake process is active. This characteristic can be easily identified in membrane vesicles. Another approach to determine whether an uptake process in membrane vesicles is active or not is to study the time course of the uptake. Since there is no cellular metabolism, the experimentally imposed driving forces (e.g., ion gradients) are not maintained in membrane vesicles for a long time. These gradients dissipate with time. Therefore, the rates of uptake are very high at early time periods because of the large magnitude of the driving forces. As these driving forces decrease in magnitude due to the gradual collapse of the ion gradients, the uptake rates also decrease with time. Thus, in the case of an active transport in membrane vesicles, the time course of uptake exhibits an “overshoot” where the uptake is very high at the initial periods of incubation but decreases afterward to reach the equilibrium. The collapse of the experimentally imposed ion gradients is complete at equilibrium and hence there is no driving force to maintain concentrative uptake. Therefore, the concentration of the uptake substrate is equal both inside the vesicles and in the uptake medium at equilibrium. The presence of an overshoot provides evidence for uptake against a concentration gradient at early time periods. The gradual disappearance of the driving forces causes efflux of the transported substrate to finally bring down the intracellular concentration of the substrate to be equal to the concentration in the uptake medium. Thus, the “overshoot” in the time course of uptake in membrane vesicles is indicative of active transport. Passive transport does not depend on the driving forces and hence is not influenced by the time-dependent collapse of the experimentally imposed ion gradients and/or membrane potential. Therefore, passive transport processes do not exhibit the “overshoot” phenomenon when studied in isolated membrane vesicles.

CONCLUSION

Cultured cells offer a convenient experimental system to study the uptake of thyroid hormones and amino acids. Various aspects of the uptake process, such as the identity, kinetics, and energetics of the transport systems mediat-

ing the uptake, can be investigated using this approach. Furthermore, cultured cells are also useful to delineate the role of hormones and cellular signaling pathways in the modulation of the transport systems. With this intact cell system, the regulation of the uptake process can be investigated at transcriptional, translational, and post-translational levels. Plasma membrane vesicles derived from cultured cells offer certain advantages over intact cells in the analysis of the driving forces involved in the energization of the uptake process. Thus, the intact cell system and the membrane vesicle system complement each other as extremely useful in the characterization of the uptake of thyroid hormones and amino acids.

ACKNOWLEDGMENTS

This work was supported by the National Institutes of Health Grant HD 24451. The authors thank Ida O. Thomas for expert secretarial assistance.

REFERENCES

1. H. N. Christensen, On the strategy of kinetic discrimination of amino acid transport systems. *J. Membr. Biol.* **84**, 97–103 (1985).
2. H. N. Christensen, Distinguishing amino acid transport systems of a given cell or tissue. *In* "Methods in Enzymology" (S. Fleischer and B. Fleischer, eds.), Vol. 173, pp. 576–616. Academic Press, San Diego, 1989.
3. L. J. Van Winkle, Endogenous amino acid transport systems and expression of mammalian amino acid transport proteins in *Xenopus* oocytes. *Biochim. Biophys. Acta* **1154**, 157–172 (1993).
4. J. D. McGivan and M. Pastor-Anglada, Regulatory and molecular aspects of mammalian amino acid transport. *Biochem. J.* **299**, 312–334 (1994).
5. M. S. Kilberg, B. R. Stevens, and D. A. Novak, Recent advances in mammalian amino acid transport. *Annu. Rev. Nutr.* **13**, 137–165 (1993).
6. V. Ganapathy, M. Brandsch, and F. H. Leibach, Intestinal transport of amino acids and peptides. *In* "Physiology of the Gastrointestinal Tract" (L. R. Johnson, ed.), pp. 1773–1794. Raven, New York, 1994.
7. S. Silbernagl, The renal handling of amino acids and oligopeptides. *Physiol. Rev.* **68**, 911–1007 (1988).
8. J. A. Clark and S. G. Amara, Amino acid neurotransmitter transporters: Structure, function, and molecular diversity. *BioEssays* **15**, 323–332 (1990).
9. Y. Zhou, M. Samson, J. Osty, J. Francon, and J. P. Blondeau, Evidence for a crosslink between the thyroid hormone transport system and the aromatic amino acid transport system T in erythrocytes. *J. Biol. Chem.* **265**, 17000–17004 (1990).
10. M. Samson, J. Osty, and J. P. Blondeau, Identification by photoaffinity labeling of a membrane thyroid hormone binding protein associated with the triiodothyronine transport system in rat erythrocytes. *Endocrinology (Baltimore)* **132**, 2470–2476 (1993).

11. M. Lakshmanan, E. Goncalves, G. Lessly, D. Foti, and J. Robbins, The transport of thyroxine into mouse neuroblastoma cells, NB41A3: The effect of L-system amino acids. *Endocrinology (Baltimore)* **126**, 3245–3250 (1990).
12. J. P. Blondeau, A. Beslin, F. Chantoux, and J. Francon, Triiodothyronine is a high affinity inhibitor of amino acid transport system L₁ in cultured astrocytes. *J. Neurochem.* **60**, 1407–1413 (1993).
13. P. D. Prasad, F. H. Leibach, V. B. Mahesh, and V. Ganapathy, Relationship between thyroid hormone transport and neutral amino acid transport in JAR human choriocarcinoma cells. *Endocrinology (Baltimore)* **132**, 574–581 (1994).
14. A. M. Mitchell, S. W. Manley, and R. H. Mortimer, Interactions between transport of triiodothyronine and tryptophan in JAR cells. *Mol. Cell. Endocrinol.* **101**, 203–210 (1994).
15. M. de Jong, T. J. Visser, B. F. Bernard, R. Docter, R. A. Vos, G. Hennemann, and E. P. Krenning, Transport and metabolism of iodothyronines in cultured human hepatocytes. *J. Clin. Endocrinol. Metab.* **77**, 139–143 (1993).
16. K. Ahmed and P. G. Scholefield, Biochemical studies on 1-aminocyclopentane carboxylic acid. *Can. J. Biochem. Physiol.* **40**, 1101–1110 (1962).
17. C. R. Scriver and O. H. Wilson, Possible locations for a common gene product in membrane transport of imino-acids and glycine. *Nature (London)* **202**, 92–93 (1964).
18. M. Hu and R. T. Borhardt, Transport of a large neutral amino acid in a human intestinal epithelial cell line (Caco-2): Uptake and efflux of phenylalanine. *Biochim. Biophys. Acta* **1135**, 233–244 (1992).
19. P. Kulanthaivel, D. R. Cool, S. Ramamoorthy, V. B. Mahesh, F. H. Leibach, and V. Ganapathy, Transport of taurine and its regulation by protein kinase C in the JAR human placental choriocarcinoma cell line. *Biochem. J.* **277**, 53–58 (1991).
20. W. Liu, F. H. Leibach, and V. Ganapathy, Characterization of the glycine transport system GLYT1 in human placental choriocarcinoma cells (JAR). *Biochim. Biophys. Acta* **1194**, 176–184 (1994).
21. M. Brandsch, Y. Miyamoto, V. Ganapathy, and F. H. Leibach, Regulation of taurine transport in human colon carcinoma cell lines (HT-29 and Caco-2) by protein kinase C. *Am. J. Physiol.* **264**, G939–G946 (1993).
22. J. P. Blondeau, J. Osty, and J. Francon, Characterization of the thyroid hormone transport system of isolated hepatocytes. *J. Biol. Chem.* **263**, 2685–2692 (1988).
23. B. A. Kamen and A. Capdevila, Receptor-mediated folate accumulation is regulated by the cellular folate content. *Proc. Natl. Acad. Sci. U.S.A* **83**, 5983–5987 (1986).
24. P. D. Prasad, V. B. Mahesh, F. H. Leibach, and V. Ganapathy, Functional coupling between a bafilomycin A₁-sensitive proton pump and a probenecid-sensitive folate transporter in human placental choriocarcinoma cells. *Biochim. Biophys. Acta* **1222**, 309–314 (1994).
25. H. T. Haigler, F. R. Maxfield, M. C. Willingham, and I. Pastan, Dansylcadaverine inhibits internalization of ¹²⁵I-epidermal growth factor in BALB 3T3 cells. *J. Biol. Chem.* **255**, 1239–1241 (1980).
26. D. R. Cool, F. H. Leibach, V. K. Bhalla, V. B. Mahesh, and V. Ganapathy, Expression and cyclic AMP-dependent regulation of a high affinity serotonin transporter in the human placental choriocarcinoma cell line (JAR). *J. Biol. Chem.* **266**, 15750–15757 (1991).
27. L. D. Jayanthi, S. Ramamoorthy, V. B. Mahesh, F. H. Leibach, and V. Ganapathy, Calmodulin-dependent regulation of the catalytic function of the human serotonin transporter in placental choriocarcinoma cells. *J. Biol. Chem.* **269**, 14424–14429 (1994).
28. M. E. Ganapathy, F. H. Leibach, V. B. Mahesh, J. C. Howard, L. D. Devoe and V. Ganapathy, Characterization of tryptophan transport in human placental brush border membrane vesicles. *Biochem. J.* **238**, 201–208 (1986).

29. S. Ramamoorthy, F. H. Leibach, V. B. Mahesh, and V. Ganapathy, Modulation of the activity of amino acid transport system L by phorbol esters and calmodulin antagonists in a human placental choriocarcinoma cell line. *Biochim. Biophys. Acta* **1136**, 181–188 (1992).
30. M. Brandsch, F. H. Leibach, V. B. Mahesh, and V. Ganapathy, Calmodulin-dependent modulation of pH sensitivity of the amino acid transport system L in human placental choriocarcinoma cells. *Biochim. Biophys. Acta* **1192**, 177–184 (1994).
31. S. Ramamoorthy, F. H. Leibach, V. B. Mahesh, and V. Ganapathy, Active transport of dopamine in human placental brush border membrane vesicles. *Am. J. Physiol.* **262**, C1189–C1196 (1992).
32. S. Ramamoorthy, P. D. Prasad, P. Kulanthaivel, F. H. Leibach, R. D. Blakely, and V. Ganapathy, Expression of a cocaine-sensitive norepinephrine transporter in the human placental syncytiotrophoblast. *Biochemistry* **32**, 1346–1353 (1993).

9

Two-Dimensional Gel Electrophoresis of Proteins¹

Chung Lee

Yi Qian

Julia A. Sensibar

Department of Urology

Northwestern University Medical School

Chicago, Illinois 60611

Harold H. Harrison

Genetrix, Inc. and Southwest Biomedical

Research Institute

Scottsdale, Arizona 85251

INTRODUCTION

Two-dimensional (2D) protein electrophoresis is a technique for separating individual proteins from a complex mixture. The first dimension separates proteins according to their relative charges—*isoelectric focusing*. The second dimension separates proteins according to their apparent molecular weights—*SDS-PAGE*. When used in conjunction with other techniques, such as *autoradiography* (or *fluorography*), *transfer blotting*, *amino acid sequencing*, *DNA cloning*, and *computer-based image analysis*, this technique is a powerful research tool in biological research. In *pharmacology* and *toxicology*, the investigation of *phenotypic changes* in protein composition and protein biosynthesis in body fluids or in specific tissues and cells can be done with ease by taking advantage of the techniques of 2D electrophoresis.

¹ Techniques described in this chapter were developed and are currently employed in the Two-Dimensional Electrophoresis Facility at Northwestern University Medical School, which is supported in part by NIH Grants HD-28148 and CA-60553.

In 1975, O'Farrell described a technique for separating proteins by 2D electrophoresis (1). Since then, this technique has received attention from scientists in all disciplines of biology. However, the operation of 2D electrophoresis remains labor-intensive and can be associated with large variation in results from one analysis to another. The advent of the ISO-DALT System (2,3), an apparatus that permits a streamlined operation of multiple specimens, has made it possible to significantly improve the resolution and reproducibility of the routine operation. This chapter describes the technical operation of 2D electrophoresis, mainly based on our experience from working with the ISO-DALT System and various associated techniques. For a comprehensive appreciation of 2D protein electrophoresis, readers are referred to many excellent reviews (4–6).

SAMPLE PREPARATION

Solubilizing Agents

For most samples, urea mix or SDS mix is used as the denaturing agent. Usually, urea mix is used for solid tissues, cell cultures, and urinary proteins, whereas SDS mix is used for body fluids, such as serum or plasma. The formula for 100 ml of urea mix consists of 9 *M* urea (Bio-Rad, Richmond, CA), 54 g; 4% Nonidet P-40 detergent (Sigma Chemical Co., St. Louis, MO), 4 ml; 2% ampholyte (pH 9–11, Pharmacia/LKB, Biotechnology, Inc., Piscataway, NJ), 10 ml; and 2% mercaptoethanol (Bio-Rad), 2 ml. Distilled water is added to make up to a final volume of 100 ml (pH 9.5 or greater). The formula for 10 ml of SDS mix consists of CHES (2-cyclohexylaminoethanesulfonic acid, Calbiochem, La Jolla, CA), 100 mg; SDS (Serva Biochemicals, Hauppauge, NY), 200 mg; DTT (Bio-Rad), 100 mg; and glycerol (Fisher Scientific Co., Pittsburgh, PA), 1 ml. Distilled water is then added to make up to 10 ml. Both urea mix and SDS mix should be stored in small aliquots at -70°C or lower.

Preparation of Solid Tissues for 2D

Tissue pieces are homogenized with a dual glass homogenizer set (Kontes, Chicago, IL), in three volumes of sample weight with phosphate-buffered saline (PBS, Sigma). An aliquot of the homogenized sample is mixed with 3 volumes of urea mix at room temperature for 2 hr with frequent vortexing, and centrifuged at 100,000*g* in an Airfuge (Beckman Instrument Co., Arlington Heights, IL) for 60 min. The resulting supernatant fraction is removed and stored at -70°C or lower for future 2D analysis. The protein content of the sample must be established prior to 2D.

Preparation of Cells for 2D

At least 1.5×10^6 cells are needed for each 2D gel if a nonisotopic staining method is used. At the end of the cell culture experiment, cells are washed with PBS and then scraped off the culture plate with a rubber policeman. The harvested cells are washed twice with 2 ml PBS and cells are pelleted in a conical centrifuge tube. The excess PBS above the cell pellet and on the inside wall of the tube is removed with a Q-tip without disturbing the cell pellet. The cells should be solubilized immediately with urea mix (approximately 30 μ l urea mix for 1×10^6 cells) for 2 hr and centrifuged at 100,000g. The supernatant fraction is collected and stored at -70°C for 2D analysis.

Preparation of Fluid Specimens for 2D

For fluid specimens, the volume of urea mix required will vary according to protein content of the sample, with a range from 1 to 3 parts for each part of the sample. The mixture is incubated at room temperature for 30 min and centrifuged at 100,000g. The supernatant is collected and stored at -70°C for 2D analysis. Alternatively, fluid specimens can be prepared by using the SDS mix for denaturing. Serum specimens can be mixed with SDS mix at a ratio of 1 to 3 by volume. The mixture is boiled at 95°C for 5 min, cooled at 4°C for 2 min, and centrifuged (100,000g) for 60 min. The supernatant is collected and stored at -70°C for 2D analysis.

The protein concentration of each specimen should be determined prior to 2D analysis in order to determine the exact quantity that will be loaded onto the gel. A modified Bradford method is recommended for protein determination for specimens in urea mix (7). Approximately 70–100 μg of total protein is loaded for complex protein mixtures such as tissue and cells. Semipurified and purified protein fractions require 20–40 μg and 2–5 μg of protein, respectively, for adequate detection by silver staining. For experiments where isotopically labeled proteins will be detected by autoradiography, less can be used but the amount varies by isotope, distribution, and dose and must be determined empirically.

THE FIRST DIMENSION: THE ISO SYSTEM

The first dimension of the classic O'Farrell 2D procedure is isoelectric focusing (IEF) under denaturing conditions in small diameter (1.5 mm) tube gels (18 cm or 7 inches long). The ISO system (Figure 1) (2) has been designed so that the diameter of the ISO tube gels is the same as the

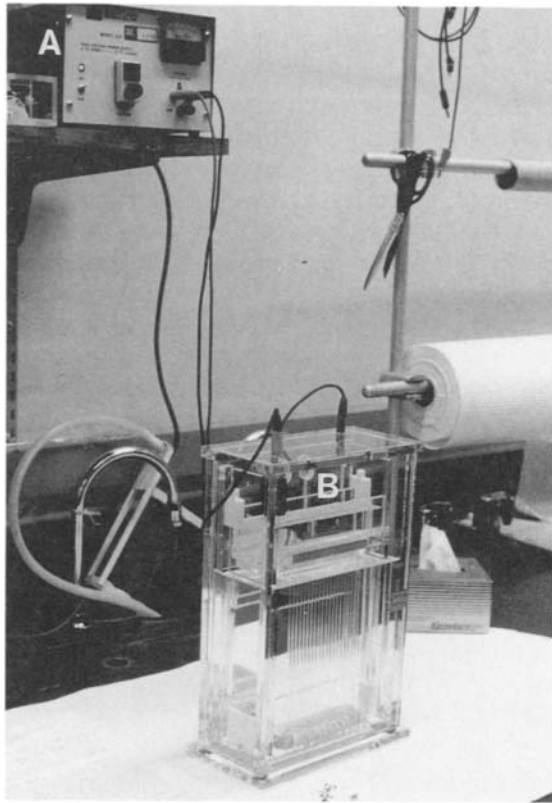


FIGURE 1. Photograph of the apparatus used in the authors' laboratories for first-dimension isoelectric focusing. (A) Power supply; (B) 20-gel isoelectric focusing apparatus.

thickness of the slab gels to be used for the second dimension. To prepare the isoelectric-focusing gel solution, the following chemicals are added into a 150-ml Erlenmeyer flask: urea, 8.25 g; ampholytes (320 μ l of Servalyt with pH 3–10, 320 μ l of Pharmalyte with pH 3–10, 160 μ l of LKB ampholyte with pH 5–7); 30% acrylamide with 1.8% Bis, 1.8 ml; and nanopure water, 6.2 ml. Dissolution of urea is aided by warming the flask and its contents with mildly warm water. The following chemicals are then added to solution: 0.3 ml of NP-40, nonidet P-40 detergent (Sigma), 50 μ l of 10% ammonium persulfate (Bio-Rad) in water, and 5 μ l of TEMED (Bio-Rad). The solution is mixed and cast into the first-dimension gel tubes, and the gels are allowed to polymerize for at least 1 hr. A polymerization line should be visible just below the meniscus of gels in the tubes.

The catholyte buffer in the upper chamber is CO₂-free sodium hydroxide solution. This is prepared by adding 0.5 ml of 6 *N* NaOH into 150 ml of degassed nanopure water. The anolyte buffer in the lower chamber box is 0.085% of H₃PO₄ solution. Any air bubble that remains in the upper portion of each tube gel is carefully removed by means of a hypodermic needle connected to a 100- μ l syringe that is filled with the upper chamber buffer. An aliquot of 5 μ l of SDS mix is loaded onto the top of each tube gel. Prefocusing is carried out at 100 V for 2 hr. Samples either in urea mix or in SDS mix can be loaded onto the gel in a volume no more than 35 μ l. Isoelectric focusing is run at 700 V for 20 hr. Carbamylated myoglobin (Sigma) or creatine phosphokinase can be used as the internal charge standards (8).

ALTERNATE FIRST-DIMENSION: THE IPG SYSTEM

The concept of an immobilized pH gradient (IGP) system was first introduced in 1982 (9). This system takes advantage of a stable pH gradient that is generated by the covalent anchoring of the ampholytes, which creates the pH gradient to a polymer matrix. Because the pH gradient is covalently bound onto immobilized matrix, one advantage of the IGP system is the creation of a stable pH gradient with time. As a result, the system improves the reproducibility of isoelectric focusing patterns. Another attractive feature of the IGP system is the practical feasibility of setting up very narrow pH gradients (0.5 pH per cm or less) in most regions of the pH scale, with a dramatic improvement in resolution for some applications. However, to achieve a streamlined operation and high resolution of 2D patterns with the IGP system as the first dimension, the classic ISO-DALT protocol must be modified, taking into account that IGP's behave differently as compared to the carrier ampholyte-generated pH gradients.

THE SECOND DIMENSION: THE DALT SYSTEM

The second dimension involves slab gel electrophoresis in the presence of SDS. In the ISO-DALT system (Figure 2) (3), the sample zone (the ISO gel) is small enough to serve as the stacking region following treatment in the equilibration buffer (10% glycerol, 4.9 mM DTT, 2% SDS, 0.125 *M* Tris-base, and trace of bromophenol blue, adjusted to pH 6.8 with 6 *N* HCl, stored at 4°C).

The second dimension slab gels are 7 \times 7 inches in size and 1.5 cm in thickness. The acrylamide/bis (27%/1.8%) system is used for casting the

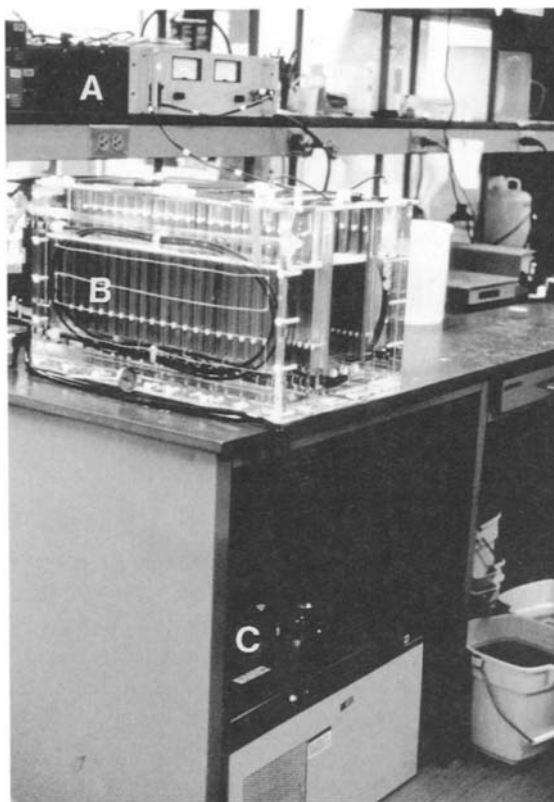


FIGURE 2. Photograph of the apparatus used in the authors' laboratories for second-dimension SDS-PAGE. (A) Power supply; (B) 20-gel SDS PAGE tank; (C) recirculating refrigerated water bath.

9–18% gradient gels. Both the light (9%) and the heavy (18%) solutions are prepared separately and 10% SDS, 10% ammonium persulfate, and TEMED are required for each of them. The apparatus required for casting gels includes gel plates (10 or 20 plates depending on experimental needs), a casting box, and a gradient maker. In the gradient maker, the light and heavy chambers are separated by a movable “tongue” whose shape directly defines the slope of the gradient. Because of the exothermic nature of acrylamide polymerization, the gradient must be made to solidify from the top downward, otherwise solution solidified first at the bottom would rise via thermal convection, upsetting the gradient. Filling of the 9 and 18% acrylamide into the respective chambers is done separately. The two cham-

bers are joined with a Y-connector and thoroughly mixed by a simple in-line mixer. Three spring clamps are used to control the flow at the exits from the light and heavy chambers and at the point distal to the mixer to regulate flow of acrylamide solution into the casting box. At least 1.5 hr are needed for polymerization.

The ISO tube gels, stored in equilibration buffer, are removed from the freezer one at a time and each gel is quickly thawed just before loading. Loading of ISO gels onto the top of DALT slabs should be done as soon as possible. The ISO gel is positioned so that it is extended along the loading ledge with the acid end to the left. Once it is positioned and air bubbles are removed, the ISO gel is overlaid with 0.8 ml melted 0.5% agarose made up in the DALT running buffer. This agarose will hold the ISO gels in position during electrophoresis in the DALT tank. The tank buffer consists of 26.8 mM Tris base, 192 mM glycine, and 3.5 mM SDS, pH 8.6. Electrophoresis is run at 180 V overnight at a constant temperature of 10°C. When the bromophenol blue line reaches the end of the gels, the run is done. Internal molecular weight standards (ranging from 10,000 to 200,000) can be applied at the acid end of the tube gel at the time of gel loading by incorporating the standards within agarose.

DETECTION OF PROTEINS IN 2D GELS

Proteins embedded in polyacrylamide gels can be detected by several methods. These include Coomassie blue dye staining, silver staining (Figure 3), protein blotting, and, if the proteins are radiolabeled, autoradiography and fluorography (Figure 4). These methods are briefly described in the following.

Coomassie Blue Dye Staining

Coomassie brilliant blue R-250 is a synthetic dye that binds strongly to most proteins. The composition for 1 liter of Coomassie blue solution contains 2 g Coomassie blue R-250, 22.75 ml of 85% phosphoric acid, 500 ml of ethanol, and the balance of the volume with nanopure water. The freshly run DALT gels are directly placed into this solution and stained for at least 4 hr. Destaining of these gels is done with 20% ethanol in water with frequent changing until the gel background is clear.

Silver Staining

Fixation of proteins in gels is necessary for silver staining and for fluorography. Containers to hold the gels can be common household plastic contain-

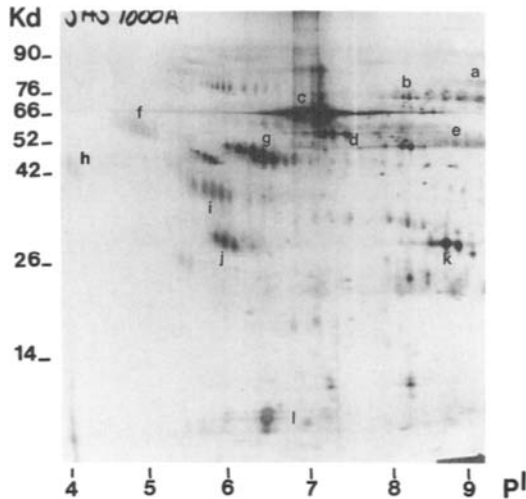


FIGURE 3. Photograph of a silver-stained, two-dimensional gel of human prostatic fluid proteins. Protein spots in the two-dimensional profile are defined by their relative molecular weight and approximate isoelectric points in the X and Y axis, respectively. Known proteins in the 2D profile are indicated by respective letters: (a) lactoferrin; (b) transferrin; (c) albumin; (d) IgM; (e) IgG; (f) α_1 antichymotrypsin; (g) prostatic acid phosphatase; (h) α_1 acidic glycoprotein; (i) prostatic acid phosphatase; (j) prostatic acid phosphatase; (k) prostate-specific antigen; (l) prostate binding protein.

ers (Rubbermaid, Servin' Saver, 10 × 10 × 4 inches) or glass containers (Corningware Corning Glass Co., Corning, NY). Freshly run DALT gels (four gels to a box) can be placed into the container for fixation with the following solutions. For gels with many low-molecular-weight proteins, the fixation solution consists of 0.1% formaldehyde in 50% ethanol (10.8 ml of 37% formaldehyde in 4 liters of 50% ethanol in water). The gels (four per staining dish) are placed in 1 liter of this solution for exactly 1 hr before subjecting them to the following general fixation procedures. For general fixation, the fixation solution is 2.5% sulfosalicylic acid (Sigma) and 5% acetic acid (Fisher) in 20% ethanol. After at least 4 hr of fixation, the gels are transferred to 20% ethanol overnight. The next morning, gels are transferred to fresh 20% ethanol twice with a 20-min interval in each. Other fixation protocols, for example, glutaraldehyde, can be used as the fixative in the solution. However, the present protocol will yield the lowest background upon silver staining.

Silver staining techniques are more sensitive than those using Coomassie blue dye staining. Therefore, this technique is useful for the detection of small amounts of proteins in the gel (10). Basically, the gels are soaked in

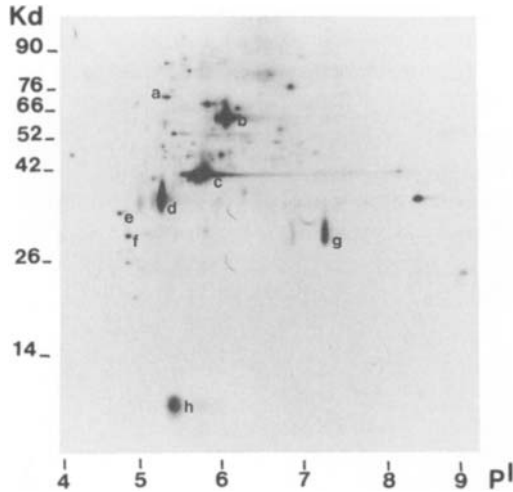


FIGURE 4. Photograph of a fluorograph developed from a two-dimensional gel of rat ventral prostatic tissue of a 2-day castrate rat following 4 hr of incubation with ^{35}S -labeled methionine. Protein spots in the two-dimensional profile are defined by their relative molecular weights and isoelectric points in the X and Y axis, respectively. Known proteins in the 2D profile are indicated by respective letters: (a) heat-shock protein 70; (b) clusterin precursor; (c) actin; (d) clusterin subunit; (e) tropomyosin; (f) tropomyosin-related protein (Tm:7); (g) clusterin subunit; (h) prostate binding protein.

basic silver diamine and developed in acidic (citric acid) formaldehyde solution. The silver staining solution is made in the following manner. First, 10 ml of 6 *N* NaOH and 42 ml of NH_4OH in 20% ethanol are vigorously mixed for 1–2 min. Then, 20 g AgNO_3 is dissolved in 200 ml of nanopure water. The latter is added into the alkaline solution slowly with vigorous stirring (this solution should be prepared away from NH_4OH vapor). The solution is then adjusted to 4 liters with 20% ethanol with continuing mixing for an additional 1–2 min. Batches of four gels per staining dish are soaked in 1 liter of the preceding solution for exactly 1.5 hr, and then rinsed with 1 liter of 20% ethanol three times with a 15-min interval between each rinse. Gels are then ready for treatment with developer, which is made up in two stages. The first stage involves dissolving 100 mg citric acid in 1 liter of 20% ethanol in nanopure water. The second stage is to add 1.5 ml of 37% formaldehyde into this solution with constant stirring immediately prior to soaking the gels for developing. Gels are soaked in this solution with constant shaking until the low-molecular-weight protein spots are visible. At that time, 5 ml of glacial acetic acid is added into this 1 liter solution to stop the reaction. Gels are transferred to another box containing 1 liter of 5% glacial acetic acid in 20% ethanol with constant shaking for

10 min. Finally, gels are rinsed with 1 liter of nanopure water three times with 15 min for each rinse. Gels are now ready for packaging, photographing, and storage. Routinely, gels are sealed in plastic bags with 10 ml of 5% acetic acid. Gels stored in this manner are ready for photographing as a hard copy record.

Past experience has indicated that, to enhance the number of protein spots detected, double staining procedures can be employed. A combination of Coomassie blue dye staining followed by silver staining or a repeat of the silver staining following the first staining yields detection of more protein spots than did the single staining procedures.

Fluorography

When protein spots are radiolabeled, fluorography is used to detect proteins in the gel. Gels must be prepared in the following manner prior to gel drying. Fresh gels are fixed for at least 4 hr as described earlier, and shaken in 20% ethanol overnight. The next morning, gels are rinsed twice with 20% ethanol with a 20-min interval for each rinse followed by three washings with nanopure water with a 15-min interval for each wash. Then, gels are incubated in auto-fluor solution (National Diagnostics, Atlanta, GA) with 5% glycerol for at least 30 min. Gel drying is carried out on a gel dryer at 50°C with vacuum (760 mm Hg) for at least 5 hr. Methanol and dry ice are used in the trapping system. Gels are placed face up on a sheet of thick filter paper and covered with a sheet of plastic wrap. At the end of the drying process, gels are transported to a dark room, where a preflashed XAR-2 film (Kodak, Rochester, NY) is pressed against the dried gel and placed in a Kodak X-omatic X-ray cassette. Several cassettes may be processed at the same time, wrapped with aluminum foil, and stored at -70°C for exposure. The length of exposure will depend on the type of isotope used, the amount of radioactivity incorporated into the protein, and the desired intensity of protein spots on the X-ray film. It is not unusual to re-expose the dried gel several times until a satisfactory image is obtained.

PROTEIN BLOTTING

Protein blotting involves transferring protein spots from an acrylamide gel onto a more stable and immobilizing medium, such as nitrocellulose membrane. A variety of procedures may be carried out once proteins are transferred onto the membrane, which otherwise would have proved difficult or impossible in the gel. Such procedures may include detection with antibodies or by other specific staining procedure.

Support Membranes and Transfer Buffer

Several kinds of membranes can be used for transferring proteins from the gel. Some examples include nitrocellulose (Bio-Rad), polyvinyl-difluoride (PVDF, Millipore, Bedford, NH), nylon (MSI, Wesboro, MA), and problot (Applied Biosystems, Foster City, CA). The size of these membranes is usually cut to 6.5×6.25 inches. Nitrocellulose membrane is most commonly used for Western blotting, whereas PVDF or problot is often used for amino acid sequencing. Transfer buffer consists of 0.192 M glycine (Sigma), 0.025 M Tris base, and 20% methanol (v/v, pH 8.3). Nitrocellulose and nylon are usually immersed in the transfer buffer directly before using. PVDF and problot membranes must be wetted with HPLC-grade methanol first, then they are rinsed with nanopure water before being immersed in the transfer buffer.

Electroblotting

Electroblotting was first described by Towbin *et al.* (11). Basically, proteins are transferred from the gel onto the membrane by electrophoresis. The advantage of this process is a short transfer time, which helps to reduce any diffusion effect. A TE 70 semiphor transfer unit (Hoefer, San Francisco, CA) is used as the transfer apparatus. The procedure is carried out by placing the membrane on top of filter papers that have already been saturated with the transfer buffer. The gel is placed face up, on top of the membrane, followed by a layer of cellophane sheet (Bio-Rad) and a further layer of filter paper soaked in the transfer buffer. This assembly, "the sandwich," is placed between two parallel flat electrodes inside the transfer apparatus. In this manner, current is passed through the sandwich by means of the electrodes from the top (the cathode) to the bottom (the anode). Transferring is performed at room temperature at 0.25 A for at least 2 hr. At the conclusion of transferring, the membrane is removed and marked with "X" at the lower right corner of the sheet to provide an orientation. Following rinsing with nanopure water to remove methanol, the membrane can be stored at 4°C or used immediately for further processing.

Staining for Total Proteins on Membranes

Several dyes can be used for the detection of total proteins on the membrane. Some examples are Coomassie blue, ponceau S, india ink, amido black, biotin-streptavidin, and colloidal gold. India ink, ponceau S, and Coomassie blue are the most commonly used dyes. India ink staining is carried out by first rinsing the membrane twice at 5-min intervals with 50

ml of 0.4% Tween-20 in PBS (Sigma), followed by soaking the membrane in 50 ml of 1% india ink (Faber-Castell Corp., Lewisburg, TN) in 0.4% Tween-20 in PBS for at least 1 hr without any shaking. At the end of the staining period, the membrane is rinsed with 50 ml PBS three times with a 10-min interval between each rinsing. Protein spots on the membrane are black against the white background. For ponceau S staining, the membrane is rinsed with 50 ml of 0.5% ponceau red in 1% acetic acid for a couple of minutes, followed by destaining with 50 ml of a solution of 10% acetic acid. The proteins are detected as red spots on the membrane. For Coomassie blue staining, the membrane is rinsed with 50 ml of 0.5% Coomassie blue in 40% methanol for several minutes followed by destaining with several changes of 50% methanol. The proteins are detected as blue spots on the membrane.

Detection of Specific Proteins by Western Blotting

For Western blotting, a primary antibody (polyclonal or monoclonal) for the specific protein (antigen) is used, followed by a second antibody that is species specific for the primary antibody and is labeled with a probe that permits its detection. The probe on the second antibody can be a number of substances, such as horseradish peroxidase, alkaline phosphatase, ^{125}I , ^{35}S , gold particles, biotin, and labeled F(ab) fragments. The use of horseradish peroxidase as the probe with either a colorimetric substrate or a chemiluminescent substrate will be discussed in this section.

There are many commonly used colorimetric substrates for horseradish peroxidase. They include 4-chloro-1-naphthol, 3,3-diaminobenzidine (DAB), and 3,5,5-tetramethylbenzidine (TMB). In the presence of horseradish peroxidase and hydrogen peroxide, these substrates yield insoluble precipitates at the site of the bound antibody. 4-Chloro-1-naphthol gives a purple precipitate and the reaction is easily controllable. DAB has a brown precipitate and intensification of the reaction product can be achieved by the addition of cobalt or nickel ions to the substrate solution, yielding a black precipitate that is more sensitive than 4-chloro-1-naphthol and DAB.

Chemiluminescent substrates for horseradish peroxidase are a relatively new detection system for Western blotting and kits for this technique are commercially available (Amersham, NEN, KPL, Bio-Rad). In the presence of hydrogen peroxide, horseradish peroxidase converts luminol, a cyclic diacylhydrazide, to an excited intermediate dianion, which emits light upon returning to its ground state. The reaction is visualized after exposure to X-ray film. The incorporation of enhancers such as phenols into the system can further increase the light output and extend the time of light emission. This system has the advantage of having the ability to achieve high levels

of sensitivity, fast processing time, and hard copy results on film, with low backgrounds.

To carry out Western blotting, efficient "blocking" of the membrane is essential to maximize the specific signal-to-noise ratio by minimizing nonspecific binding of the antibodies. The blocking buffer is made of 5% nonfat milk powder (Carnation brand) in PBS. The membrane is immersed in 50 ml of blocking buffer for at least 2 hr with shaking at room temperature, then the membrane is incubated with the specific primary antibody that is prepared in the blocking buffer at 4°C overnight. The concentration of the antibody varies according to each antibody used. Usually, a preliminary trial should be carried out to determine the optimal concentration of the primary antibody to use on a routine basis. At the end of incubation with the primary antibody, the membrane is rinsed with 50 ml of the blocking buffer three times with a 5-min interval for each rinse, before subjecting the membrane to 50 ml of horseradish peroxidase-conjugated second antibody prepared in the blocking buffer for 4 hr at room temperature. At the end of this 4-hr incubation with the second antibody, the membrane is rinsed with 50 ml of blocking buffer for 5 min, then with 50 ml of 0.4% Tween-20 in TBS (Tris-buffered saline) for another 5 min. When using 4-chloro-1-naphthol as the substrate, a color development solution for each membrane is prepared by mixing 10 ml of a 3 mg/ml solution of 4-chloro-1-naphthol in methanol together with 50 ml of 0.4% Tween in TBS and 0.3 ml 30–35% hydrogen peroxide just prior to use. The mixture should be cloudy. The membrane is incubated in this substrate solution for about 15 min and the reaction is stopped by washing the membrane with nanopure water. Positive spots on the membrane should be purple in color.

The preceding membrane can be reprobbed with another primary antibody with a different substrate solution, such as DAB or DAB with cobalt ion. Sodium azide (0.1%) is used to inactivate horseradish peroxidase left behind from the previous episode of blotting by incubating it with the membrane at room temperature for 10 min. The membrane is then rinsed twice with PBS (5 min each) and twice with the blocking buffer (10 min each). Another primary antibody, prepared in the blocking buffer, is then incubated with the membrane at 4°C overnight. The protocol for color development in Western blotting is then followed. Briefly, the developing solution is made up by mixing 25 mg DAB (with or without 2 ml of 1% cobalt chloride) in 50 ml PBS for each membrane, which is mixed with 0.3 ml of 30% hydrogen peroxide just prior to use. If positive, the new binding spots should be black or brown depending on whether the cobalt ion is present or not. There are now two different color spots on the same membrane. Again, the reaction is stopped by rinsing the membrane with nano-

pure water. If the reaction is negative, the reprobing technique can be repeated.

When TMB is used as the substrate, upon incubation with the secondary antibody, the membrane is rinsed once with 50 ml of the blocking buffer for 15 min and then with PBS five times for a 15-min interval each. The TMB substrate (Kirkegard & Perry Laboratories, Inc., Gaithersburg, MD) is warmed to room temperature and is used to cover the membrane surface for a few seconds, after which the spots will show up, if positive. The substrate reaction is stopped before the background becomes too intense by rinsing the membrane with nanopure water.

For use with the enhanced chemiluminescence (ECL) system, the membrane, following incubation with the secondary antibody, is rinsed three times with 50 ml of 0.4% Tween-20 in PBS with 5-min intervals for each rinse. The substrate is prepared by mixing equal volumes of chemiluminescent substrates A and B as provided by the supplier (KPL). The membrane is immersed in this substrate for 1 min and then is placed face up on a thin plastic sheet and, with the lights being turned off, transferred into the film cassette. In a dark room, a typical exposure time on the X-ray film is 5–15 min. The optimal exposure time should be determined for each experimental system. The film is developed to determine if the result is positive and to determine if the exposure is an appropriate one. Reprobing of the membrane with the same antibody or with a different antibody is possible by following the protocol for stripping and reprobing the ECL Western blots. The membrane may be stored in Saran Wrap at 2–8°C after immunodetection.

Detection of Glycoconjugates and Glycoproteins Using Digoxigenin-Labeled Lectins

Total glycoprotein detection on nitrocellulose membranes can be performed by taking advantage of the knowledge that adjacent hydroxyl groups in sugars of glycoconjugates are oxidized to aldehyde groups by mild periodate treatment.

The spacer-linked steroid hapten, digoxigenin, is then covalently attached to these aldehydes via a hydrazide group. Subsequently, digoxigenin-labeled glycoconjugates are detected in an antibody–horseradish peroxidase conjugate system. Briefly, the transferred membrane is first washed with PBS, and the adjacent hydroxyl groups in sugars of carbohydrate present on glycoproteins are then oxidized by incubation in 10 mM sodium metaperiodate in 0.1 M sodium acetate buffer (pH 5.5) for 30 min. The membrane is again washed in PBS, then covalently labeled via incubation with digoxigenin-conjugated succinyl- ϵ -aminocaproic acid hydrazide in 0.1

M sodium acetate for 1 hr. The membrane is then washed with TBS (50 mM Tris, 200 mM NaCl, pH 6.5) and blocked with a solution of 0.5% casein overnight. The next morning, the membrane is washed with TBS and incubated with anti-digoxigenin-horseradish peroxidase conjugate for 1 hr. The development of color is identical to that described for the Western blot. A positive protein spot should have a dark blue color.

In addition to total glycoprotein detection, specific terminal carbohydrate linkages on glycoproteins can be detected by lectin blotting analysis (12). A collection of five different digoxigenin-labeled lectins, *Datura stramonium* agglutinin (DSA), *Galanthus nivalis* agglutinin (GNA), *Maackia amurensis* agglutinin (MAA), *Peanut* agglutinin (PNA), and *Sambucus niger* agglutinin (SNA), which will recognize most common *N*- and *O*-glycosidic carbohydrate structures, is available in the form of a glycan-differentiation kit (Boehringer-Mannheim Biochemicals, Indianapolis, IN). The detection limit depends on the respective glycoprotein and varies with different lectins. Briefly, lectin blotting is carried out by rinsing the freshly transferred membrane with nanopure water. The membrane is incubated in a solution consisting of Tween-20 in TBS (0.5% Tween-20 in 150 mM NaCl, 50 mM Tris-HCl, pH 7.5) for overnight, and rinsed with 50 ml of TBS twice for 10 min each. The membrane is then incubated with 50 ml of lectin buffer (1 mM MgCl₂ · 6H₂O, 1 mM MnCl₂ · 4H₂O, 1 mM CaCl₂ in TBS, pH 7.5) once for 10 min. Following the constitution of the digoxigenin-labeled lectin solution, the following probes are added separately to 20 ml of lectin buffer in plastic bags: 20 μl of GNA, SNA, and DSA, 100 μl of MAA, and 200 μl of PNA. The membrane is incubated in the bag for at least 1 hr at room temperature, and rinsed with 50 ml of TBS three times for 10 min each. An aliquot of 100 μl of anti-digoxigenin-peroxidase solution is added to 20 ml of TBS and the membrane is incubated for at least 1 hr. Detection of color development is identical to that described for Western blotting.

ANALYSIS OF 2D PROTEIN PROFILES BY COMPUTER-BASED IMAGE ANALYSIS SYSTEMS

The technology of 2D gel electrophoresis is a powerful research tool in toxicology. However, the task of analyzing the vast amount of information contained in a complex 2D protein profile and comparing it with that of other profiles from related specimens has become overwhelming by manual observation. It is apparent that the field of 2D gel electrophoresis must resort to computer technology for a comprehensive analysis of protein profiles. Several mainframe, workstation, and PC computer-based systems have been developed for extracting information from the gels (13–16).

Basically, these systems offer the following capabilities. They include (1) image acquisition, (2) noise and background subtraction, (3) spot identification and quantitation, (4) spot editing, (5) profile matching and profile subtraction, (6) data and image output, and (7) data base management. A common problem with the existing systems is the need for extensive manual input and editing, making the technology difficult, if not impossible, for routine usage and mass production. However, as new technology in computer science and in 2D electrophoresis evolves, it is expected that current technical difficulties will be surmounted. Nevertheless, the present application of computer technology to 2D electrophoresis has created new and exciting opportunities in biomedical and toxicology research. A large data base can be created to examine inductive, suppressive, or other effects of specific pharmaceuticals or toxins on the array of proteins synthesized by a cell line or organism in a controlled experimental environment. Sets and subsets of proteins in the data base can then be examined for common or differential expression patterns (17–19).

SUMMARY

The foregoing discussion has provided technical procedures regarding the conduct of two-dimensional gel electrophoresis of proteins. These methodologies are currently used in the authors' laboratories (20–25). It should be pointed out that because technology is constantly evolving, procedures in two-dimensional electrophoresis will also change accordingly. This chapter covered basic topics such as sample preparation, running of two-dimensional electrophoresis, methods for the detection of proteins once separated in the gel, and obtaining information from the resulting protein profiles. Important aspects of two-dimensional electrophoresis that have not been discussed are the applications of this technology in biomedical research. Depending on individual circumstances and requirements, the various forms of application of this technology are adopted by virtue of its power to separate complex mixtures of proteins in a two-dimensional space according to their molecular weights and isoelectric points. The scope of application broadens when other methodologies such as computer technology, amino acid sequencing, and molecular biology techniques are used in conjunction with the two-dimensional gel electrophoresis technology. However, this technology is not without limitations. For example, the high resolution of the protein profiles and the high degree of reproducibility of this methodology are achieved at the expense of requirements of special equipment, skilled personnel, and large operating expenses. Unfortunately, these requirements may preclude access of this technology to many researchers

with small laboratories. Since the operation of two-dimensional electrophoresis is best carried out by a specialized, dedicated facility, we recommend that research institutions establish, as part of their operational strategy, a core facility for two-dimensional electrophoresis with centralized equipment and personnel so that every member within the institution will benefit.

REFERENCES

1. P. H. O'Farrell, *J. Biol. Chem.* **250**, 4007–4040 (1975).
2. N. G. Anderson and N. L. Anderson, *Anal. Biochem.* **85**, 331–340 (1978).
3. N. L. Anderson and N. G. Anderson, *Anal. Biochem.* **85**, 341–354 (1978).
4. L. Anderson, "Two-Dimensional Electrophoresis, Operation of the ISO-DALT System." Large Scale Biology Press, Washington, D.C., 1988.
5. J. E. Celis and R. Bravo, *In* "Two-Dimensional Gel Electrophoresis of Proteins" (J. E. Celis and R. Bravo, eds.), Academic Press, New York, 1984.
6. B. S. Dunbar, "Two-Dimensional Electrophoresis and Immunological Techniques." Plenum, New York, 1987.
7. L. S. Ramagli and L. V. Rodriguez, *Electrophoresis* **6**, 559–563 (1985).
8. N. L. Anderson and B. J. Hickman, *Anal. Biochem.* **93**, 312–320 (1979).
9. G. Angelika, P. Wilhelm, and G. Siegfried, *Electrophoresis* **9**, 531–546 (1985).
10. J. Henkeshoren and R. Dernick, *Electrophoresis* **6**, 103–112 (1985).
11. H. Towbin, T. Trachetin, and J. Gordon, *Proc. Natl. Acad. Sci. U.S.A.* **76**, 4350–4354 (1979).
12. J. A. Sensibar, Y. Qian, M. D. Griswold, S. R. Sylvester, C. W. Bardin, C. Y. Cheng, and C. Lee, *Biol. Reprod.* **76**, 233–242 (1993).
13. P. F. Lemkin, L. E. Lipkin, and E. P. Lester, *Clin. Chem.* **28**, 840–849 (1982).
14. J. I. Garrels, J. T. Farrar, and C. B. Burwell, *In* "Two-Dimensional Gel Electrophoresis of Proteins" (J. E. Celis and R. Bravo, eds.), pp. 37–91. Academic Press, New York, 1984.
15. N. L. Anderson, J. Taylor, A. E. Sandora, B. P. Coulter, and N. G. Anderson, *Clin. Chem.* **28**, 1807–1820 (1981).
16. C. Lee, E. R. Sherwood, J. A. Sensibar, L. A. Berg, Y. C. Chen, and C. C. Tseng, *BioTechniques* **7**, 374–378 (1989).
17. J. E. Celis, K. Dejgaard, P. Madsen, and H. Leffers, *Electrophoresis* **11**, 1072–1113 (1990).
18. J. E. Celis, H. H. Rasmussen, E. Olsen, and P. Madsen, *Electrophoresis* **14**, 1091–1198 (1993).
19. J. E. Celis and E. Olsen, *Electrophoresis* **15**, 309–344 (1994).
20. J. A. Daufeldt and H. H. Harrison, *Clin. Chem.* **30**, 1972–1980 (1984).
21. H. H. Harrison, K. L. Miller, C. Dickenson, and J. A. Daufeldt, *Am. J. Clin. Pathol.* **97**, 97–105 (1992).
22. H. H. Harrison, *Clin. Biochem.* **25**, 235–243 (1992).
23. C. Lee, Y. Tsai, J. A. Sensibar, L. Oliver, and J. T. Grayhack, *Prostate* **9**, 135–146 (1986).
24. C. Lee and J. A. Sensibar, *J. Urol.* **138**, 903–908 (1987).
25. C. Lee, M. Keefer, Z. W. Zhao, R. Kroes, L. Berg, X. Liu, and J. Sensibar, *J. Androl.* **10**, 432–438 (1989).

This Page Intentionally Left Blank

10

Effects of *in Vivo* Exposure to Glucocorticoids on Pituitary, Serum, and Messenger Ribonucleic Acid Levels of the Gonadotropin Hormones FSH and LH in Male and Female Rats

Joanne M. McAndrews
Sonia J. Ringstrom
*Department of Neurobiology and
Physiology,
Northwestern University
Evanston, Illinois 60208*

INTRODUCTION

The events of reproduction in mammals, including the production of gametes (ova in females and sperm in males), gestation, and birth of viable offspring, are controlled by hormones. The gonadotropin hormones, luteinizing hormone (LH) and follicle-stimulating hormone (FSH), are glycopro-

teins produced and secreted by gonadotrope cells of the anterior pituitary gland (1). Both LH and FSH are composed of two noncovalently linked subunits, a common subunit designated α and a unique β subunit that confers immunological and biological specificity to the hormone (2). These hormones regulate follicular development and ovulation in the female and spermatogenesis in the male, as well as steroid hormone production by the gonads of both sexes. The regulation of gonadotropin hormone secretion by the anterior pituitary gland is controlled for the most part by the secretion of hormones produced by hypothalamic neurons into the hypophysial–portal system, a vasculature that connects the hypothalamus and pituitary (3), and by negative feedback signals from the gonads to the hypothalamus and pituitary. The hypothalamic hormone, gonadotropin-releasing hormone (GnRH), stimulates the synthesis and secretion of FSH and LH (4). The gonadal steroids, estradiol, progesterone, and testosterone, are negative feedback signals for both gonadotropins, and the gonadal peptide inhibin is primarily a negative feedback regulator of FSH.

Exposure to a variety of stressors, both natural and experimental, can induce reproductive dysfunction in many species (5,6). Stress can disrupt the normal regulation of reproductive processes by GnRH and gonadal feedback. Physiological responses to stressors in both sexes may play a role in the regulation of some mammalian populations (5–8). Stress may also account for the reduction in successful reproduction reported in intensively managed domestic animals, such as bovines (6).

Attention has been focused on the role of adrenal glucocorticoids in mediating stress-induced reproductive failure ever since Selye (9) suggested that chronic exposure to stressors increased pituitary–adrenal secretion while decreasing pituitary–gonadal activity. Selye attributed this phenomenon to the necessity, in case of emergency, of maintaining adrenal cortex function at the expense of gonadal function. Stress can influence reproductive function at several different levels of the hypothalamic–pituitary–gonadal axis, including the (1) brain (to inhibit GnRH release), (2) anterior pituitary gland, and (3) gonads.

High levels of natural or synthetic glucocorticoids have been linked to reproductive disturbances in humans. These include reduced serum gonadotropin responses to an exogenous GnRH challenge, reduced basal secretion of LH and FSH, and amenorrhea in women (10,11). The effects of stress or elevated levels of glucocorticoids on reproductive processes have also been studied in rodents. The different methodologies used have been designed, in part, to explore different sites of action of glucocorticoids on the reproductive axis. Both adrenalectomy, which results in removal of corticosterone, and physical stress have effects at the level of the brain, including an increased secretion of the hypothalamic hormone CRF. During

a stress response, the anterior pituitary increases output of β -endorphins and prolactin. Elevated levels of CRF directly inhibit GnRH release, and both prolactin and β -endorphins suppress LH, and FSH to a lesser degree. Glucocorticoid treatment *in vivo* acts primarily, but perhaps not exclusively, at the level of the anterior pituitary gland. In this chapter, we describe the methodologies used to examine the effects of high levels (typical of a state of stress) of exogenous glucocorticoids on gonadotropin hormone parameters.

Several *in vivo* experiments were conducted that involved implanting male or female rats with pellets of either cortisol (Kendall's compound F) or corticosterone (Kendall's compound B) for short periods of time. These pellets delivered the high levels of glucocorticoids seen during a stress response. In some experiments, GnRH antagonist treatment was also used to determine if the glucocorticoid effects were occurring directly at the pituitary level by blocking the GnRH signal from the hypothalamus. After the *in vivo* treatment with glucocorticoids, FSH and LH immunoreactivity in the pituitary and serum, and gonadotropin hormone subunit messenger RNA levels were determined.

METHODOLOGIES

Hormone Pellet Construction

An adequate amount of glucocorticoid is not released by silastic capsules implanted *in vivo*, therefore, a method for making solid steroid pellet implants was developed. Cholesterol pellets are implanted as a control for the glucocorticoid since it is the common precursor for all steroid hormone biosynthesis.

Steroid and cholesterol pellets are made by pouring molten pellet material into paraffin molds. Histological paraffin preparation is melted in an oven and poured level with the tops of plastic disposable petri dishes. When the paraffin has cooled in the petri dishes, multiple holes are drilled into the hardened paraffin with a 1/4-inch drill bit. The drilled holes should be at least 1/4 inch apart. Excess paraffin should be removed from the drilled holes. Powdered steroid or cholesterol (Sigma Chemical Company, St. Louis, MO) is melted in a metal teaspoon over an alcohol flame, with care taken not to burn the material, and poured into the 1/4-inch paraffin molds, filling the mold to the top with one continuous pour. Once the pellets have cooled, the entire petri dish is placed in the melting oven to remelt the paraffin mixture. The liquid paraffin is poured off, leaving only the formed pellets in the petri dish. The pellets are then scraped to remove any remaining paraffin. The concentration of steroid in a pellet, and therefore the

dose of steroid delivered to an animal, can be controlled by mixing various proportions of steroid and cholesterol before melting. The corticosterone, cortisol, and cholesterol pellets weigh approximately 400 mg.

We preferred to use naturally occurring steroids rather than synthetic glucocorticoids such as dexamethasone, even though many of the synthetic compounds are extremely potent. We felt that using the natural steroids would enable us to make more reasonable assumptions about the effects of stress-induced, elevated levels of glucocorticoids in natural populations.

Surgeries

Pellet Implantation

Animals are anesthetized using metofane (Methoxyflurane, Pitman-Moore, Mundelein, IL) by placing them in an airtight glass jar with the bottom lined with cotton bedding that has been sprinkled with approximately 1.5 ml of the anesthetic. It normally takes a few minutes to achieve adequate anesthesia. All instruments and wound clips are sterilized by soaking in Nolvasan (Nolvasan Solution, chlorhexidine diacetate, Fort Dodge Laboratories, Fort Dodge, IA). The anesthetized animal is then placed dorsal side up and the area 4–5 cm behind the head is washed with 70% ethanol. An incision just large enough to admit the pellet is made in the skin with a pair of scissors. A hemostat is then inserted into the area of the cut and opened just under the skin, thereby creating a subcutaneous pocket at least 2.5 cm in length. The pellet or pellets are then pushed deep into the pocket to prevent their escape, and the wound is stapled shut with two or three 7.5-mm wound clips (Clay Adams, Parsippany, NJ).

Castration

A rat, anesthetized with metofane, is placed on his back and the hair is clipped from the scrotal area. The scrotal area is cleansed with 70% ethanol, and all instruments and wound clips are sterilized by soaking in Nolvasan solution. An incision is made through the scrotum on one side, a second incision is then made through the transparent tunica vaginalis, and the testis is pushed out with gentle pressure on the lower abdomen. A tie is made around the spermatic cord and blood vessels running parallel to the spermatic cord, thus interrupting the blood supply. The testis is removed by cutting close to the ligature. The second testis is removed in the same manner. The tunica is closed with suture and the skin is closed with two or more wound clips. Care is taken not to interfere with the rectum and anus. The rat is kept warm under a lamp until it is awake.

Subcutaneous Injections

Subcutaneous injections are administered with a 1-cc disposable tuberculin syringe and a 23-gauge, 1-inch needle (Becton Dickinson, Rutherford, NJ). Fully conscious animals are removed from their cages one at a time and placed dorsal side up and allowed to rest naturally. The animal is then immobilized with the left hand, and a triangle of skin is pinched from the rear dorsal area using the index finger and thumb of the left hand. The needle is then inserted just underneath the skin at the base of the pinch, and the plunger of the syringe depressed using the right hand. Animals receiving different kinds of injections should be housed separately since the rats tend to lick the injection sites of other animals.

Tissue Dissection and Serum Collection

Since there is a negative feedback relationship between corticosterone (secreted by the adrenal cortex) and both CRF (secreted by the hypothalamus) and ACTH (secreted by the anterior pituitary gland) (12), the weight of the adrenal glands after treatment with a glucocorticoid is an indication of the efficacy of glucocorticoid treatment. High levels of circulating glucocorticoids for 4 days or longer lead to a significant decrease in adrenal weight. The adrenal glands are removed at the time of sacrifice, the fat is dissected away, and the paired organ weight is recorded.

When the experimental manipulations are completed, unanesthetized rats are killed by decapitation using a rat guillotine. Exposure to anesthetic itself induces a stress response that could confound experimental results. Trunk blood is collected, allowed to clot at room temperature, and centrifuged for 20 min at 2500 rpm. Serum is aliquoted and stored at -20°C until RIA.

Pituitary Hormone Content Extraction

Pituitaries are collected at the time of sacrifice, snap frozen on dry ice, and stored at -70°C . Pituitaries are homogenized individually in 3 ml of 0.01 *M* phosphate buffer with 0.14 *M* NaCl and 1% (wt/vol) PBS-egg white, pH 7.6, with 1% (vol/vol) Triton X-100 added as a detergent [homogenization buffer (13)] with 25 strokes in glass pestles (Kontes Glass Company, Vineland, NJ). After the tissue is homogenized completely, the homogenate is poured into a 50-ml graduated cylinder and the volume is brought up to 50 ml with homogenization buffer. A 1:200 dilution of the final stock is made and aliquoted for future RIA for FSH, and a 1:1000 dilution of the final stock is made and aliquoted for subsequent assay of LH content by RIA. Dilutions are stored at -70°C until radioimmunoassay.

Radioimmunoassays

LH and FSH

Concentrations of LH in serum and pituitary homogenates are measured using an ovine:rat RIA, employing NIH S25 as a standard and LH S10 anti-rat antibody.

Concentrations of FSH in serum and pituitary homogenates are measured using a homologous RIA with reagents distributed by the National Hormone and Pituitary Distribution Program. NIH-FSH-RP-2 standard and FSH S11 anti-rat antiserum are used.

The assays are conducted in the following manner. The chloramine T method (14,15) is used to radioiodinate the antigen. A total incubation volume of 300 μl is used for the LH and FSH assays. Samples [50–100 μl serum (for LH), 25–100 μl serum (for FSH), 25 μl of a 1:1000 pituitary homogenate dilution (for LH), and 25–100 μl of a 1:200 pituitary homogenate dilution (for FSH)] or standards plus assay buffer (PBS-gel; phosphate-buffered saline, pH 7.6 + 0.1% gelatin) are added to achieve a volume of 150 μl . After the samples and standards have been pipetted, 50 μl anti-rat LH antibody (1:20,000) or anti-rat FSH antibody (1:1500) in PBS-(0.05 M) EDTA + 1% normal rabbit serum (NRS-EDTA-PBS) are added to all tubes except the total and nonspecific binding tubes. Nonspecific binding tubes receive 50 μl of NRS-EDTA-PBS only (without antibody). Tubes are incubated at 4°C for 24 hr. Next, 50 μl of ^{125}I -labeled rLH or rFSH containing 12,000–15,000 cpm in PBS-gel is added to all tubes and samples are incubated at 4°C for 24 hr. Sheep anti-rabbit gamma globulin (second antibody) (1:5–1:40 dilution in PBS-gel), at a volume of 50 μl , is added to all tubes except the totals and samples are incubated at 4°C for 24 hr. On the final day of the assay, 1 ml of PBS-gel is added to all assay tubes except totals. All tubes are centrifuged at 2500 rpm at 4°C for 40 min. The supernatant is carefully decanted, and tubes are inverted on paper toweling for approximately 3 min. The lip of each tube is blotted to remove any excess liquid. The tubes are then transferred into racks and counted for 1 min using a Micromedic Systems, Inc. (Horsham, PA) automatic gamma counter.

Corticosterone and Cortisol

Serum concentrations of corticosterone are measured using the Immuchem Double Antibody RIA ^{125}I kit for rats and mice (ICN Biomedicals, Costa Mesa, CA) and concentrations of cortisol in serum are measured with the Immuchem cortisol-coated tube ^{125}I RIA kit (ICN). The cortisol kit has been validated for use with rat serum. Rat serum did not interfere with

the standard curve for cortisol. Several serum pools were assayed for cortisol and corticosterone at several dilutions with both kits, and rabbit anti-cortisol-21 antibody produced similar and parallel values.

Pituitary Total RNA Extraction

Pituitaries are rapidly removed, immediately frozen on dry ice, and stored at -70°C until total RNA extraction. Initially, the method of Chomczynski and Sacchi (16) was used to extract total RNA from individual pituitaries. We have found, however, that the cesium chloride gradient centrifugation technique (17,18) results in better-quality total RNA and a better yield per pituitary.

A Polytron homogenizer (Brinkmann) is used to homogenize the tissues. Individual pituitaries are homogenized in 600 μl of 4 M GTC (guanidine isothiocyanate, Sigma) solution in 3-ml sterile plastic Falcon tubes (Becton Dickinson). To centrifuge the tissues, 400 μl of a 5.7 M CsCl solution is placed on the bottom of an 11 \times 34-mm Beckman (Palo Alto, CA) ultracentrifuge tube, and 600 μl of a 4 M GTC solution is carefully layered on top of the CsCl solution. Finally, the homogenized sample is very carefully placed on top of the two solutions already in the tube. Tubes are centrifuged at 50,000 rpm at 22°C for 4 hr in a Beckman tabletop ultracentrifuge (Model TL-100). When the centrifuge has stopped, the DNA, which is suspended in the center of the tube, is carefully removed with a 1.0-ml pipet tip and discarded. All of the remaining liquid is then removed from the tube and discarded. The semitransparent total RNA pellet is located at the bottom of the tube. One hundred microliters of DEPC (Sigma)-treated double-distilled water is added to the RNA pellet and incubated at room temperature for 10 min. The dissolved pellet is then transferred to a 1.5-ml sterile plastic eppendorf tube, and the centrifuge tube is rinsed with an additional 100 μl of ddH₂O and added to the eppendorf tube. The total RNA is ethanol precipitated by adding 10% of the total volume in the tube of 3 M Na acetate, pH 5.2 (i.e., 20 μl), and 2.5 volumes (i.e., 550 μl) of 100% ethanol. Tubes are gently inverted a few times to mix, vortexed, and stored at -20°C overnight. All samples are centrifuged at 10,000 rpm, 4°C , for 20 min and the supernatant is very carefully removed with a drawn-out glass pasteur pipette. The RNA pellet is carefully resuspended in 14 μl of DEPC-treated ddH₂O and is generally immediately prepared for electrophoresis.

Northern Blot Analysis

Ten micrograms (A_{260}) of total RNA from each sample is separated by electrophoresis on a 1% agarose-formaldehyde gel, diffusion-blotted onto

nylon membrane (ICN), and covalently attached by UV cross-linking. Blots are sequentially hybridized to the rat FSH β , LH β , and the common α subunit probes. Rat α (19) and LH β (20) cDNAs and rat FSH β genomic DNA (21) probes were the gift of Dr. William Chin (Brigham and Women's Hospital, Boston, MA). All probes are radiolabeled by random priming (United States Biochemical Corporation, Cleveland, OH). Specific activity of the probes is $0.75\text{--}1.0 \times 10^9$ cpm/ μg DNA. Blots are then rehybridized to a cDNA clone CHO-B (22), which detects the LLRep3 gene family (23), to assess the amount of RNA present in each lane. Probes for the mRNAs for β -actin, cyclophilin, or other housekeeping genes can also be used for this purpose. Blots are stripped between hybridizations with boiling 0.1% sodium dodecyl sulfate. Blots are subjected to both standard autoradiography and phosphorimaging (Molecular Dynamics, Sunnyvale, CA) following each hybridization. Quantification for each hybridized band for each probe is performed by image analysis. The amounts of each gonadotropin mRNA subunit are internally standardized by dividing the values for the subunit by the value for CHO-B in each lane. All mRNA data points are expressed as the means of normalized values \pm SEM in arbitrary phosphorimager units (APU).

EXPERIMENTAL PROTOCOLS

Experiment 1

The objective of this study was to test whether cortisol treatment *in vivo* increases pituitary content of FSH by selectively increasing FSH β mRNA. Adult male rats were implanted subcutaneously with a 400-mg pellet of either cortisol or cholesterol on Day 1 of the experiment. On Day 5, half of each implant group was orchidectomized under light metofane anesthesia and half remained intact. Animals were killed on Day 6. All procedures were performed at 0800 hr. There were 10–12 animals per treatment group. Pituitaries were collected at the time of sacrifice, snap frozen, and stored at -70°C until measurement of LH and FSH content ($n = 4$ or 5) or gonadotropin subunit mRNA levels ($n = 6$). Serum was stored at -20°C for subsequent hormone measurement by RIA. Some of the data presented here have been previously published (24).

Experiment 2

The objective of this study was to determine if the cortisol-induced increase in pituitary content of FSH was dependent on endogenous secretion of

GnRH. Adult female rats were implanted with 400-mg pellets of either cortisol or cholesterol on metestrus. At the same time, half of each implant group was given 100 μg of GnRH antagonist [WY 45760 ([Ac- β (2)-D-Nal¹,4-F-D-Phe,_D-Trp³,D-Arg⁶]LHRH), Wyeth Laboratories, Philadelphia, PA] suspended in 0.25 ml of sesame oil as a subcutaneous injection. The GnRH antagonist was weighed and placed in a small glass vial with the appropriate amount of oil and agitated with a small stir bar over very low heat for up to 1 hr until dissolved. Fifty to 100% more of the GnRH-oil solution than was needed was prepared each time to account for losses in filling the syringes. The other half of each group received injections of oil vehicle alone. Antagonist and control injections were given at 48-hr intervals beginning at the time of implantation until the animals were killed at 0800 hr, 5 days after the day of implantation. There were four animals per treatment group. At the time of sacrifice, pituitaries were collected and stored at -70°C until subsequent homogenization and measurement of hormone content by RIA. Some of the data from this experiment have been previously published (25).

Experiment 3

The objective of this study was to determine if *in vivo* treatment with corticosterone, the native glucocorticoid hormone in the rat, would have the same effects as cortisol in selectively increasing pituitary content of FSH and pituitary FSH β mRNA levels, and if so, whether or not these effects are dependent on a GnRH signal. Female rats were treated exactly as described in Experiment 2, except that corticosterone, instead of cortisol, pellets were implanted. There were 10 animals per treatment group. Pituitaries were collected at the time of sacrifice, snap frozen, and stored at -70°C until measurement of gonadotropin hormone subunit mRNA levels. The data from this experiment have been published (26).

RESULTS

Serum Levels of Cortisol (F) and Corticosterone (B)

Table I shows the serum levels of cortisol and corticosterone from animals treated with F, B, or cholesterol in all experiments discussed here.

In Experiment 1, treatment with cortisol significantly increased serum levels of cortisol ($P < 0.001$), as expected. There was also a significant effect of cortisol ($P < 0.001$) on lowering serum corticosterone levels.

Treatment of female rats *in vivo* with cortisol (Experiment 2) resulted in a significant increase in serum cortisol levels ($P < 0.0001$), as expected.

TABLE I. Serum Levels of Cortisol and Corticosterone^a

	Cortisol ($\mu\text{g}/\text{dl}$)	Corticosterone ($\mu\text{g}/\text{dl}$)
Experiment 1		
Cholesterol intact	0.94 \pm 0.07	13.57 \pm 3.38
Cortisol intact	20.07 \pm 1.75	2.02 \pm 0.20
Cholesterol castrate	1 \pm 0	26.55 \pm 5.01
Cortisol castrate	12.12 \pm 3.00	1.60 \pm 0.29
Experiment 2		
Cholesterol oil	1 \pm 0	
Cortisol oil	34.32 \pm 4.10	
Cholesterol GnRH Antag	1 \pm 0	
Cortisol GnRH Antag	21.60 \pm 3.26	
Experiment 3		
Cholesterol oil		33.68 \pm 6.24
Corticosterone oil		56.68 \pm 4.76
Cholesterol GnRH Antag		39.52 \pm 9.43
Corticosterone GnRH Antag		51.96 \pm 3.14

^a Data reprinted with permission from: S. J. Ringstrom, J. M. McAndrews, J. O. Rahal, and N. B. Schwartz, (1991). Cortisol *in vivo* increases FSH β mRNA selectively in pituitaries of male rats. *Endocrinology (Baltimore)* **129** (5): 2793–2795; S. J. Ringstrom, D. E. Suter, J. P. Hostetler, and N. B. Schwartz (1992). Cortisol regulates secretion and pituitary content of the two gonadotropins differentially in female rats: Effects of gonadotropin-releasing hormone antagonist. *Endocrinology (Baltimore)* **130** (6): 3122–3128; and J. M. McAndrews, S. J. Ringstrom, K. D. Dahl, and N. B. Schwartz, (1994). Corticosterone *in vivo* increased pituitary follicle-stimulating hormone (FSH)- β messenger ribonucleic acid content and serum FSH bioactivity selectively in female rats. *Endocrinology (Baltimore)* **134** (1): 158–164. Copyright of The Endocrine Society.

In Experiment 3, serum levels of corticosterone were significantly ($P < 0.01$) elevated in the animals that received corticosterone pellets, as expected. The levels seen in the corticosterone-treated animals are approximately those seen during a time of stress (50–60 $\mu\text{g}/\text{dl}$). The serum corticosterone levels in cholesterol-treated animals were also elevated. The control animals were moved from the animal room to the lab and handled prior to sacrifice, resulting in a mild and temporary state of stress.

Experiment 1

Serum FSH and LH Serum FSH and LH levels are presented in Figures 1A and 1B, respectively. Serum FSH levels doubled after castration ($P < 0.001$), as expected, and cortisol had no significant effect on serum FSH (27,28). Serum LH increased substantially after castration ($P < 0.001$) and

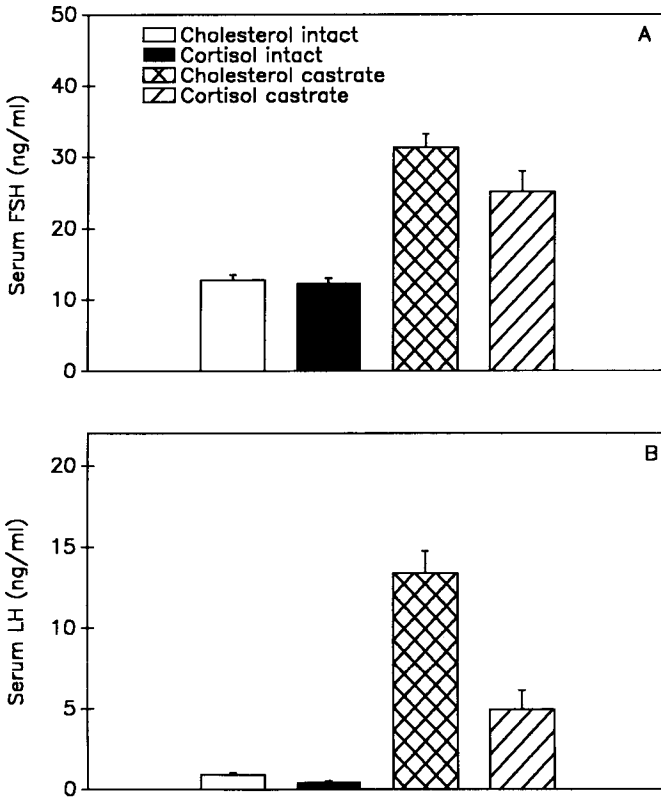


FIGURE 1. Serum FSH (A) and serum LH (B) from male rats implanted with cholesterol or cortisol on Day 1, castrated or left intact on Day 5, and killed on Day 6. Each bar represents the mean \pm SEM for an N of 10 animals. Reprinted with permission from S. J. Ringstrom, J. M. McAndrews, J. O. Rahal, and N. B. Schwartz (1991). Cortisol *in vivo* increases FSH β mRNA selectively in pituitaries of male rats. *Endocrinology (Baltimore)* **129**(5):2793–2795. Copyright of The Endocrine Society.

cortisol treatment significantly suppressed serum levels of LH ($P < 0.001$), as had been reported previously (27,28).

Pituitary Content of FSH and LH Pituitary content of FSH and LH is shown in Figures 2A and 2B, respectively. Treatment with cortisol significantly increased pituitary content of FSH, as shown previously (27,28). In contrast, there was no significant effect of cortisol on pituitary content of LH.

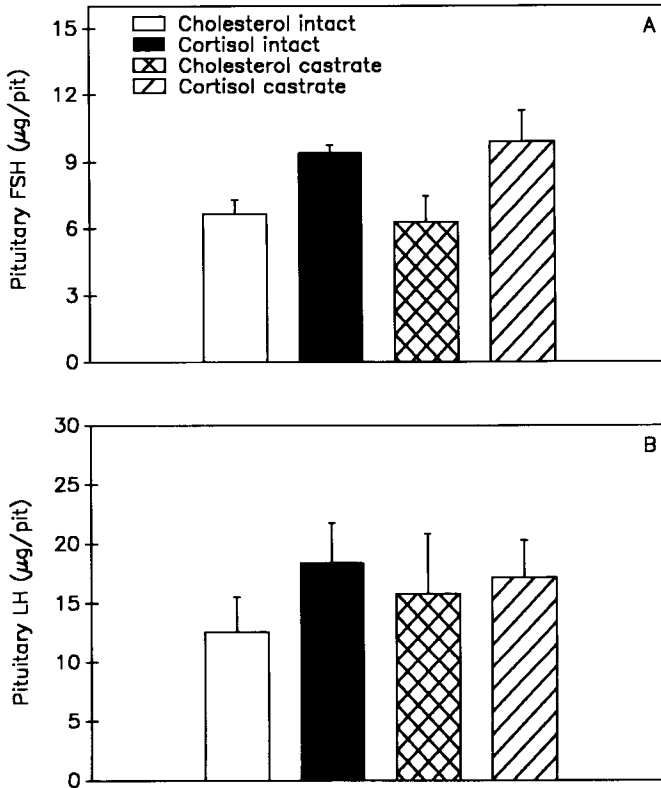


FIGURE 2. Pituitary content of FSH (A) and LH (B) from animals treated as described in the legend to Figure 1. Each bar represents the mean \pm SEM for an N of 4 animals. Reprinted with permission from S. J. Ringstrom, J. M. McAndrews, J. O. Rahal, and N. B. Schwartz (1991). Cortisol *in vivo* increases FSH β mRNA selectively in pituitaries of male rats. *Endocrinology (Baltimore)* **129**(5):2793–2795. Copyright of The Endocrine Society.

Gonadotropin Hormone Subunit Messenger RNA Levels

The combined data obtained by quantitative analysis of all Northern blots are presented in Figure 3. Treatment with cortisol significantly increased FSH β mRNA ($P < 0.01$) (Figure 3A), doubling levels in the castrate group. There were no significant effects of cortisol or castration on either LH β mRNA or α mRNA (Figs. 3B and 3C).

Experiment 2

Pituitary Content of FSH and LH Pituitary content of FSH and LH is presented in Figures 4A and 4B, respectively. Treatment with cortisol

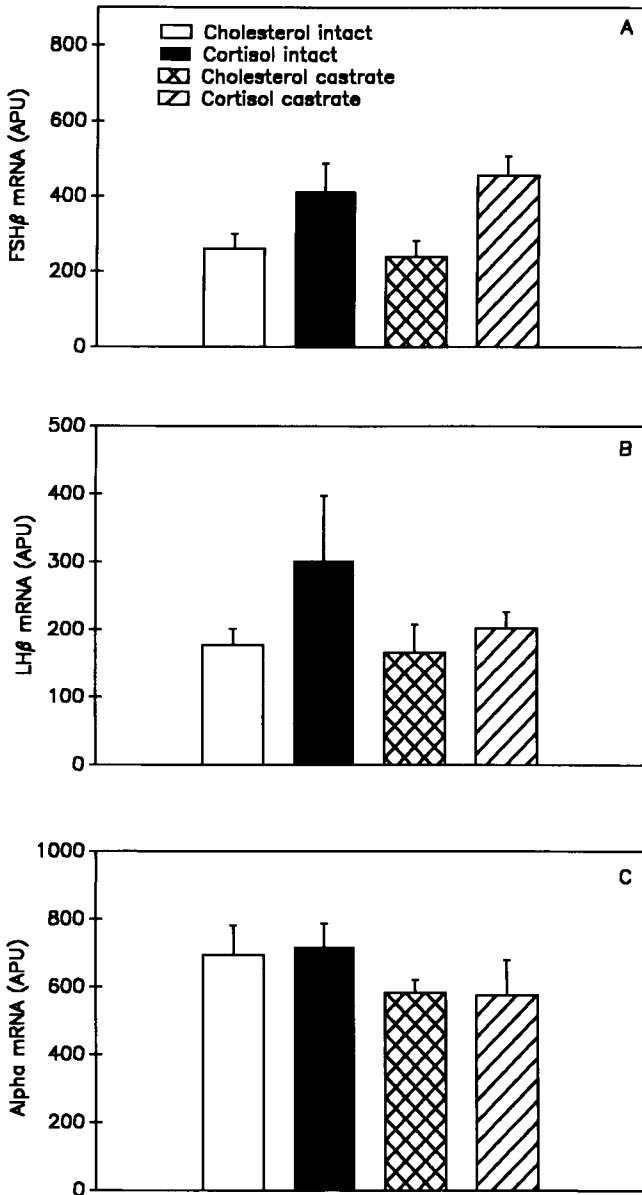


FIGURE 3. FSH β (A), LH β (B), and α (C) mRNA levels in pituitaries from animals described in the legend to Figure 1. Subunit mRNAs were measured in individual pituitaries by Northern blot hybridization analysis. Each bar represents the mean of values from six autoradiographic bands, measured by phosphorimaging, and standardized by dividing the values for the subunits by the values for CHO-B, \pm SEM. Reprinted with permission from S. J. Ringstrom, J. M. McAndrews, J. O. Rahal, and N. B. Schwartz (1991). Cortisol *in vivo* increases FSH β mRNA selectively in pituitaries of male rats. *Endocrinology (Baltimore)* 129(5):2793–2795. Copyright of The Endocrine Society.

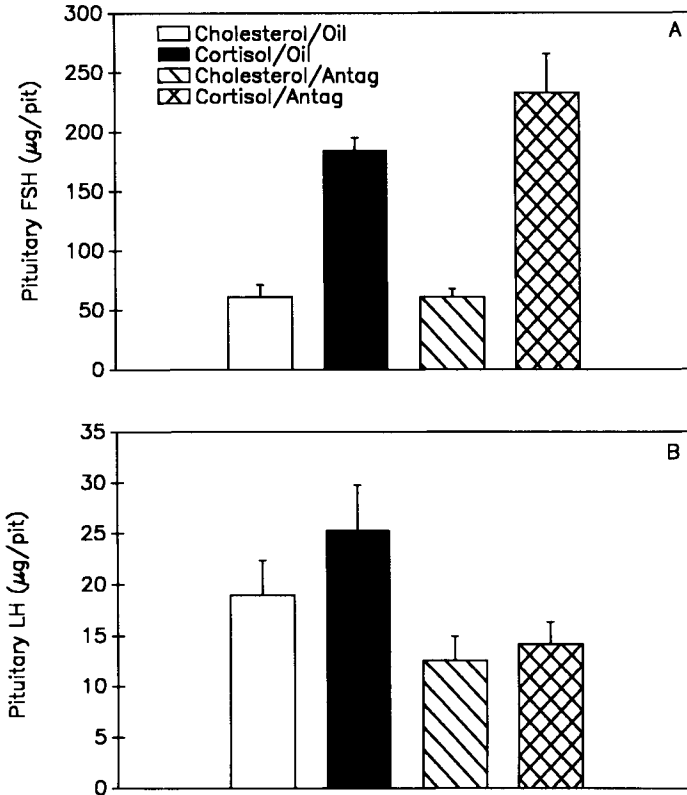


FIGURE 4. Pituitary content of FSH (A) and LH (B) from female rats implanted with cholesterol or cortisol on metestrus and given subcutaneous injections of 100 μg GnRH antagonist in oil or oil alone at 48-hr intervals beginning at the time of steroid implantation. Animals were killed 5 days after implantation. Each bar represents the mean ± SEM of values from 4 animals. Reprinted with permission from S. J. Ringstrom, D. E. Suter, J. P. Hostetler, and N. B. Schwartz (1992). Cortisol regulates secretion and pituitary content of the two gonadotropins differentially in female rats: Effects of gonadotropin-releasing hormone antagonist. *Endocrinology (Baltimore)* **130**(6):3122–3128. Copyright of The Endocrine Society.

significantly increased pituitary content of FSH ($P < 0.0001$). This effect of cortisol occurred in the presence or absence of the GnRH antagonist. GnRH antagonist treatment alone had no effect on pituitary content of FSH. In contrast, pituitary content of LH was significantly decreased by treatment with GnRH antagonist in the presence or absence of cortisol ($P < 0.02$). Treatment with cortisol alone had no significant effect on pituitary content of LH.

Experiment 3

Gonadotropin Hormone Subunit mRNA Levels The combined data obtained by quantitative analysis of all Northern blots are presented in Figure 5. Corticosterone treatment significantly increased FSH β mRNA in the presence or absence of the GnRH antagonist ($P < 0.01$) (Figure 5A). Treatment with GnRH antagonist tended to suppress LH β mRNA, but the effect was not significant. There were no significant effects of corticosterone or the two treatments in combination on LH β mRNA (Figure 5B). There was a tendency of GnRH antagonist treatment to suppress glycoprotein hormone α mRNA, but the effect was not significant. There were no significant effects of corticosterone or the two treatments in combination on α mRNA (Figure 5C).

SUMMARY

In the experiments described here and in others performed in this laboratory (24–28), we have consistently observed that glucocorticoids (both corticosterone, the native glucocorticoid in the rat, and cortisol) have different effects on the two anterior pituitary hormones, LH and FSH, that regulate reproductive processes. Sustained exposure to high levels of glucocorticoids, such as those present in a stress response, suppresses serum levels of LH while not affecting or only minimally affecting pituitary content of LH in both sexes. This suggests that glucocorticoids inhibit the release of LH from the gonadotropes. In contrast, high levels of circulating glucocorticoids do not affect or only slightly affect serum levels of FSH, but increase pituitary content of FSH in both sexes. This indicates that glucocorticoids either increase synthesis or block the degradation of FSH in the gonadotropes.

The specific purpose of the studies described in the chapter was twofold. We wanted to determine if glucocorticoid treatment affected the pituitary levels of the gonadotropin hormone subunit mRNAs. In addition, we wanted to block the action of GnRH, the hypothalamic signal that induces the secretion of LH and FSH, to see whether the glucocorticoids were acting directly at the level of the gonadotropes or indirectly by interfering with this hypothalamic signal to the gonadotropes.

Significant increases in pituitary FSH β subunit mRNA were observed with treatment of male rats with cortisol (Figure 3) and female rats with corticosterone (Figure 5), whereas α subunit and LH β mRNAs were not affected. Female rats treated with both corticosterone and a GnRH antagonist also showed a significant increase in FSH β mRNA at the level of

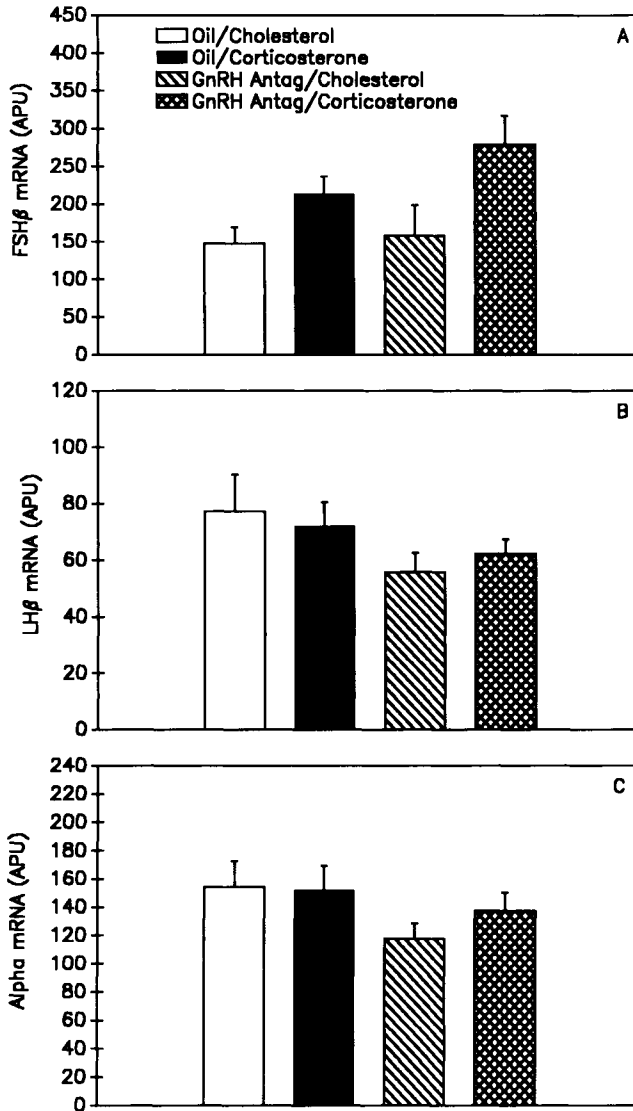


FIGURE 5. FSH β (A), LH β (B), and α (C) mRNA levels in pituitaries from female rats implanted with cholesterol or corticosterone on metestrus and given subcutaneous injections of 100 μ g GnRH antagonist in oil or oil alone at 48-hr intervals beginning at the time of steroid implantation. Gonadotropin hormone subunit mRNAs were measured in individual pituitaries by Northern blot hybridization analysis. Each bar presents the mean \pm SEM of values from five to six autoradiographic bands, as measured by phosphorimaging, and standardized by dividing the values for the subunits by the values for CHO-B. Reprinted with permission from J. M. McAndrews, S. J. Ringstrom, K. D. Dahl, and N. B. Schwartz (1994). Corticosterone *in vivo* increases pituitary follicle-stimulating hormone (FSH)- β messenger ribonucleic acid content and serum FSH bioactivity selectively in female rats. *Endocrinology (Baltimore)* 134(1):158–163. Copyright of The Endocrine Society.

the anterior pituitary. Thus, these data show that glucocorticoids act to selectively increase FSH β mRNA and that the steroids act directly at the level of the anterior pituitary gland.

Other effects of glucocorticoids on various gonadotropin hormone parameters were also observed. These data are generally consistent with those from previous studies (27,28). For example: treatment of male rats with elevated levels of cortisol caused a decrease in serum LH (Figure 1), but pituitary content of LH was not affected (Figure 2); immunoreactive serum FSH was not affected in males treated with cortisol (Figure 1); pituitary content of FSH was increased in male rats treated with cortisol (Figure 2); and cortisol treatment completely reversed the effects of a GnRH antagonist on pituitary FSH in female rats (Figure 4).

The findings described here also have adaptive significance implications, since high physiological levels of glucocorticoids, similar to those seen during a time of stress, were used to produce the effects. The suppression of LH release during a time of stress would result in blockade of ovulation in the female, and a subsequent decrease in serum testosterone and a loss of mating behavior in the male; thus reproduction would be blocked during the time of stress. This represents an important adaptive mechanism. When animals are experiencing a stress, such as overcrowding or food shortage, it is not advantageous for the population to keep reproducing. Inhibition of the release of LH by stress levels of glucocorticoids, therefore, serves to ensure that reproduction is halted. In addition, the increase in pituitary content of FSH by stress levels of glucocorticoids also has adaptive significance. The increased storage of FSH in the pituitary glands of both males and females would permit a rapid resumption of gametogenesis once the stress subsides, and enable reproduction to occur once again.

In summary, administration of glucocorticoid pellets that deliver high physiological levels of hormone similar to those seen during a time of stress was successfully used in these experiments to determine the effects on serum, pituitary content, and messenger RNA levels of the gonadotropin hormones in both male and female rats.

ACKNOWLEDGMENTS

The authors are extremely grateful to Dr. Neena B. Schwartz (Northwestern University, Evanston, IL), in whose lab these experiments were performed, for her support and guidance. The authors also thank Wyeth-Ayerst Research (Princeton, NJ) for the generous gift of the GnRH antagonist, the National Hormone and Pituitary Distribution Program for the gonadotropin RIA standards and antibodies, and Dr. William W. Chin (Brigham and Women's Hospital, Boston, MA) for the gift of the gonadotropin subunit probes. The technical assistance

of Brigitte Mann, William Talley, Robert Valadka, David Viet, Rachele Kardon, Bernadette Meberg, and Rosa Yueh is greatly appreciated.

REFERENCES

1. J. W. Everett, In "The Physiology of Reproduction" (E. Knobil and J. Neill, eds.), 2nd Ed., pp. 1509–1526. Raven, New York, 1994.
2. J. G. Pierce and T. F. Parsons, *Annu. Rev. Biochem.* **50**, 465–495 (1981).
3. R. B. Page, In "The Physiology of Reproduction" (E. Knobil and J. Neill, eds.), 2nd Ed., pp. 1527–1619. Raven, New York, 1994.
4. R. Geiger, W. Konig, H. Wissmann, K. Geisen, and F. Enzmann, *Biochem. Biophys. Res. Commun.* **45**, 767–773 (1971).
5. J. J. Christian, In "Populations of Small Mammals under Natural Conditions" (D. P. Snyder, ed.), pp. 143–158. University of Pittsburgh, Pittsburgh, Pennsylvania, 1978.
6. G. P. Moberg, *Oxford Rev. Reprod. Biol.* **9**, 456–496 (1987).
7. J. J. Christian, In "Hormonal Correlates of Behavior" (B. E. Eleftherious and R. V. Scott, eds.), pp. 205–209. Plenum, New York, 1975.
8. J. J. Christian, In "Biosocial Mechanisms of Population Regulation" (M. N. Cohen, ed.), p. 55. Yale Univ. Press, New Haven, Connecticut, 1980.
9. H. Selye, *J. Clin. Endocrinol. Metab.* **6**, 117–130 (1946).
10. G. Bocuzzi, A. Angeli, D. Bisbocci, D. Fonzo, G. P. Gaidana, and F. Ceresa, *J. Clin. Endocrinol. Metab.* **40**, 892–895 (1975).
11. J. P. Luton, P. Thiebolt, J. C. Valke, J. A. Mahoudeau, and H. Bricaire, *J. Clin. Endocrinol. Metab.* **45**, 488–495 (1977).
12. M. F. Dallman, S. F. Akana, C. S. Cascio, D. N. Darlington, L. Jacobson, and N. Levin, *Recent Prog. Horm. Res.* **43**, 113–173 (1987).
13. T. L. Spitzbarth, T. H. Horton, J. Lifka, and N. B. Schwartz, *J. Androl.* **9**, 294–304 (1988).
14. W. M. Hunter and F. C. Greenwood, *Nature (London)* **194**, 495 (1962).
15. F. C. Greenwood, W. M. Hunter, and F. S. Glover, *Biochem. J.* **89**, 114 (1963).
16. P. Chomczynski and N. Sachi, *Anal. Biochem.* **162**, 156–159 (1987).
17. V. Glisin, R. Crkvenjakov, and C. Byus, *Biochemistry* **13**, 2633–2637 (1974).
18. J. M. Chirgwin, A. E. Przybyla, R. J. MacDonald, and W. J. Rutter, *Biochemistry* **18**, 5294–5299 (1979).
19. J. E. Godine, W. W. Chin, and J. F. Habener, *J. Biol. Chem.* **257**, 8368–8371 (1982).
20. W. W. Chin, J. E. Godine, D. R. Klein, A. S. Chang, L. K. Tan, and J. F. Habener, *Proc. Natl. Acad. Sci. U.S.A.* **80**, 4649–4653 (1983).
21. S. D. Gharib, A. Roy, M. E. Wierman, and W. W. Chin, *DNA* **8**, 339–349 (1989).
22. M. M. Harpold, R. M. Evans, M. Salditt-Georgieff, and J. E. Darnell, *Cell (Cambridge, Mass.)* **17**, 1025–1035 (1979).
23. D. L. Heller, K. M. Gianola, and L. A. Leinwand, *Mol. Cell. Biol.* **8**, 2797–2803 (1988).
24. S. J. Ringstrom, J. M. McAndrews, J. O. Rahal, and N. B. Schwartz, *Endocrinology (Baltimore)* **129**, 2793–2795 (1991).
25. S. J. Ringstrom, D. E. Suter, J. P. Hostetler, and N. B. Schwartz, *Endocrinology (Baltimore)* **130**, 3122–3128 (1992).
26. J. M. McAndrews, S. J. Ringstrom, K. D. Dahl, and N. B. Schwartz, *Endocrinology (Baltimore)* **134**, 158–163 (1994).
27. S. J. Ringstrom and N. B. Schwartz, *J. Steroid Biochem.* **27**, 625–630 (1987).
28. D. E. Suter, N. B. Schwartz, and S. J. Ringstrom, *Am. J. Physiol.* **254**, E595–E600 (1988).

11

Glutamate Receptor Autoradiography and *in Situ* Hybridization

Rick Meeker

Department of Neurology

University of North Carolina

Chapel Hill, North Carolina 27599

INTRODUCTION

Glutamate Receptors and CNS Pathology

A large body of evidence now indicates that the excitatory amino acid glutamate is the most abundant excitatory transmitter in the hypothalamus (1–4) and brain in general (5–8). The excitatory amino acid (glutamate) receptors consequently have widespread involvement in normal CNS functions. However, under extreme conditions these receptors can become potent mediators of neurotoxicity. The association of glutamate receptors with neuronal damage has been extensively documented in response to traumatic events such as anoxic-ischemic insults (9–12), as well as in CNS disease states such as epilepsy (13–17), Huntington's disease (18–23), Alzheimer's (24–26), ALS (20,22,27,28), chronic pain (29,30), and human immunodeficiency virus infections (31). Because of the ubiquitous distribution of the glutamate receptors and their prominent role in synaptic plasticity, any disturbance of their function, even in the absence of neurodegeneration, would be expected to produce any of a vast array of undesirable effects. Glutamate receptors, particularly the *N*-methyl-D-aspartate (NMDA) sub-

type, have often played a pivotal role in the etiology of the neuronal damage in the foregoing examples and are thought to be necessary for normal expression of synaptic plasticity. Although less is known about the response of glutamate receptors to acute or chronic toxins, it is likely that these receptors play an equally important role in the evolution of neurotoxicological changes in the CNS. This is evidenced, in part, by the potent effects of naturally occurring glutamate receptor neurotoxins (18,27,28,32–34) and undesirable side effects that have been seen with glutamate receptor antagonists developed for therapeutic purposes (35). Given the widespread role of glutamate receptors in both normal brain function and neurodegenerative disease, evaluation of neurotoxicological changes in these receptors is likely to provide important insights into the impact of environmental insults on brain function.

Glutamate Receptor Neurotoxins

The proposed link between several environmental compounds that disrupt excitatory amino acid neurotransmission and either acute or progressive neurodegenerative diseases suggests that environmental toxins may participate in the etiology of neurodegenerative processes in the central nervous system (34). Several neurotoxins that are known to act directly through glutamate receptors are summarized in the following.

(S)- β -N-Oxalylamino(alanine) (β -ODAP or BOAA, also γ -ODAP)—is an AMPA receptor agonist (36) from the chick pea *Lathyrus sativus*, which causes neurolathyrism, a progressive spastic disorder (28). Descending pyramidal motor pathways appear to be a primary target of this toxin.

Willardiine—from the seeds of *Acacia* and *Mimosa*, is a potent and selective AMPA receptor agonist (37).

Domoic acid—a potent kainate receptor agonist from *Chordria armata* (seaweed) accumulates in mussels that eat the seaweed and causes a severe (limbic seizures, amnesia) and sometimes fatal neurological disorder in humans who eat the mussels (28). Primary targets for the excitotoxic damage in rats appear to be the hippocampus, amygdala, septum, thalamus, and frontal cortex. The hypothalamus, hippocampus, and area postrema are more susceptible to damage in primates (28).

(S)- β -N-Methylamino(alanine) (BMAA) and *cycasin*—from the seeds of *Cycas circinalis*, used to make flour in Guam, are thought to be major causal factors in Guamanian amyotrophic lateral sclerosis (ALS) (27). The carbamate derivative of BMAA is thought to be an agonist at NMDA and metabotropic glutamate receptors (38,39). However, the role of environmental exposure in the etiology of ALS is still unclear since large doses

are usually required to experimentally induce ALS-like effects in animal models and chronic administration of low doses is often without effect. Cycasin is converted to methylazoxymethanol (MAM), which is a strong DNA nucleotide alkylating agent to form 7-methylguanine. This compound may also contribute to neurodegeneration by causing long-term genetic damage or neuronal dysfunction (28). Degeneration is most prominent in the motor cortex, particularly Betz cells.

Ibotenic acid—from *Amanita muscaria*, is a potent agonist at NMDA and other glutamate receptors.

Argiope toxin—from the venom of *Argiope* spiders, blocks NMDA and AMPA receptor channels but is relatively insensitive at GluR-2 and NR2C subunits (40–42).

Philanthotoxin—from the venom of the digger wasp, *Philanthus triangulum*, is an antagonist at NMDA receptors as well as nicotinic cholinergic receptors (41–43).

Joro spider toxin—produces a long-lasting blockage of NMDA receptors (41).

Agatoxin—from the venom of the *Agelenopsis aperta* spider, is a potent and selective open-channel antagonist at NMDA receptors (44).

α -*Kainate*—an AMPA receptor agonist from *Digenaea simplex*, induces damage to hippocampal CA3 and other limbic structures (45).

Glutamate receptor function can also be influenced indirectly by a variety of challenges. Several compounds that interfere with metabolic or other cellular functions may promote excitotoxic damage by compromising the ability of the cell to keep NMDA receptor activity and Ca^{2+} influx in check (22). Several compounds that may indirectly promote excitotoxic damage are:

MPTP—converted to MPP^+ and taken up by substantia nigra neurons via dopamine transporter, inhibits mitochondrial respiration and facilitates NMDA receptor-mediated neurotoxicity (22,28).

Nitropropionic acid—is a suicide inhibitor of succinate dehydrogenase (also CO poisoning and formate poisoning from methanol intoxication). Neuronal degeneration is attenuated by MK-801, suggesting a role for NMDA receptor activation (22,28).

Cassavism—from cassava, which is commonly eaten in Africa, liberates CN and causes spastic disease similar to lathyrism. May also produce BOAA analogs [see earlier entry on (*S*)- β -*N*-oxalylamino(alanine)] and contribute directly to glutamate receptor overactivation (28).

The effects of these latter compounds illustrate that a wide variety of toxins may cause neural damage indirectly through glutamate receptors

by altering neuronal membrane potential, glutamate transporter function, calcium gating, or other cellular functions that influence glutamate receptor activity. The role of these and similar compounds in the etiology of long-term neurodegenerative changes is largely unknown. Thus far, the effects of each of these toxins appear to be limited to the duration of action of the compound and do not give rise to a progressive neurodegeneration that can be sustained in the absence of further exposure.

Neuroendocrine Effects of Excitotoxins

Every major subtype of glutamate receptor is present in the hypothalamus and particularly in regions associated with neuroendocrine functions (1–4,46,47). The density of glutamate synapses can be quite high in these systems relative to total synaptic density, reaching values as high as 38% of the total synapses (3). In addition, many neuroendocrine cells share features of functional activation with limbic cells, indicating that they may be similarly sensitive to glutamatergic stimulation (46,48–50). These observations are reinforced by functional data that demonstrate a role for glutamate receptors in the release of vasopressin, gonadotropin-releasing hormone (GnRH), and other peptides (51–60). The susceptibility of neuroendocrine regions to excitotoxic damage is amply demonstrated by the original excitotoxicity studies of Olney (61), which showed extensive medial hypothalamic damage and neuroendocrine dysfunctions in rats injected neonatally with monosodium glutamate. In addition, hypothalamic cells in monkeys have a relatively high sensitivity to the excitotoxin domoic acid (28). The sensitivity of neuroendocrine cells to excitatory activation is also underscored by the fact that neuroendocrine disturbances are a relatively common side effect of seizures (62). An important contribution of these observations is that they demonstrate that prolonged excitatory stimulation can lead to chronic neuroendocrine dysfunctions. Reproductive function may be particularly vulnerable (62). Thus, there is substantial data to suggest that neuroendocrine cells will be a sensitive target of compounds that pathologically activate glutamate circuits.

The mechanisms that lead to neuroendocrine dysfunctions are unknown and, although glutamate receptors are suspected to play an important role, it is difficult to predict how these receptors might change in response to excitatory challenges. Severe excitotoxic challenges are likely to lead to a loss of cells and their receptors, but even in this simple case, some caution is warranted. Little is known regarding how much of a role compensatory receptor proliferation may play in response to chronic, glutamate receptor activation (i.e., binding densities may not decrease if compensatory increases in glutamate receptors on the remaining cells parallel the loss of

neurons and their glutamate receptors). In many chronic neurodegenerative diseases such as Huntington's disease and Alzheimer's dementia, a correlation can be found in some brain regions between decreased glutamate receptor densities and disease (21,23,25). However, such correlations have been difficult to demonstrate, suggesting that substantial cell loss may be necessary to detect the decrease in glutamate receptors. This is particularly true in the absence of strict neurodegeneration, where the effects of neurotoxins have not yet been explored. If compensatory changes in glutamate receptors can be demonstrated to occur dynamically in response to over- or underactivation, this might provide a more sensitive index of progressing toxicity and be of more benefit than analyses of toxic challenges that kill neurons outright. Evidence to suggest that glutamate receptors may express this type of plasticity is reviewed next.

Receptor Plasticity

In addition to the role of glutamate receptors in the etiology of normal synaptic plasticity, a growing body of evidence suggests that the glutamate receptor itself may be subject to plastic changes in response to increases or decreases in activity. An increased density of NMDA receptors has been observed in neuroendocrine cells after chronic physiological activation (63). Limbic circuits display increases and decreases in the density of glutamate receptors in response to social stress (64), classical conditioning (65), long-term potentiation (66), and pathological activation through prolonged seizure activity (13,17,67–74). NMDA glutamate receptor blockade *in vitro* also induces a rapid compensatory increase in glutamate receptors (75). The specific circumstances that control these changes are unknown. These findings need to be extended to other systems, but provide good preliminary evidence that changes in the expression of glutamate receptors may be a common adaptive response to chronic stimulation by physiological or toxic stimuli. Thus, changes in glutamate receptor density may serve as a sensitive index of challenges to neuroendocrine (and other) systems.

Other plastic changes may be exerted in the form of changes in the subunit composition of the receptor, which in turn may change the properties of the receptor (5,76–84). These types of changes generally cannot be assessed by receptor binding studies that do not discriminate the molecular subunit structure of the receptor and must be evaluated using complementary approaches such as *in situ* hybridization with DNA or RNA probes. This latter approach has the potential to provide a sensitive and highly specific index of functional disruption of glutamatergic circuits in the CNS in the absence of neurodegeneration or changes in glutamate receptor density.

METHODS FOR STUDYING GLUTAMATE RECEPTOR EXPRESSION

Dealing with Multiple Receptor Subtypes

Several key questions are important before initiating an analysis of changes in glutamate receptors in response to toxic challenges. The type of analysis will ultimately be structured to meet the needs of the experimenter.

Which Receptor?

There are presently four major glutamate receptor subtypes with at least 9 identifiable ligand binding sites and 21 different subunit coding sequences (Figure 1). Hundreds of functional subunit combinations are theoretically possible, not including splice variants. Identifying a change in a particular type of glutamate receptor can therefore be a formidable challenge. Thus, one of the immediate problems faced when beginning to evaluate the effects of substances on glutamate receptors is to narrow down the type(s) of receptors that are most likely to be changed. This is particularly true in the hypothalamus, where the absolute density of glutamate binding sites is low relative to other brain regions, making it more difficult to detect changes in receptor density. Thus, the greater one can focus on a particular subtype and eliminate “background” due to subtypes that are not involved in the response of interest, the greater the chance of detecting significant changes. This problem will become less difficult as more information is generated on the functional role of different glutamate receptor subtypes in hypothalamic/neuroendocrine systems. A list of many of the ligands that are currently available for identification of glutamate receptor subtypes is provided in Table I (85–117). The pharmacology of glutamate receptors is expanding rapidly, and although the list provides information on many currently available ligands, it should be anticipated that new agonists and antagonists with greater receptor specificity will become available. In the absence of information implicating a specific receptor subtype, a general screen for glutamate receptor changes can be undertaken as described in a later section, although the specific conclusions one can draw will be limited.

Quantification or Localization?

A second question of major importance is whether it is more important to accurately determine the receptor density in the tissue of interest or localize the regions in which receptor changes might occur. The focus of the present methods on autoradiography is designed primarily for mapping studies,

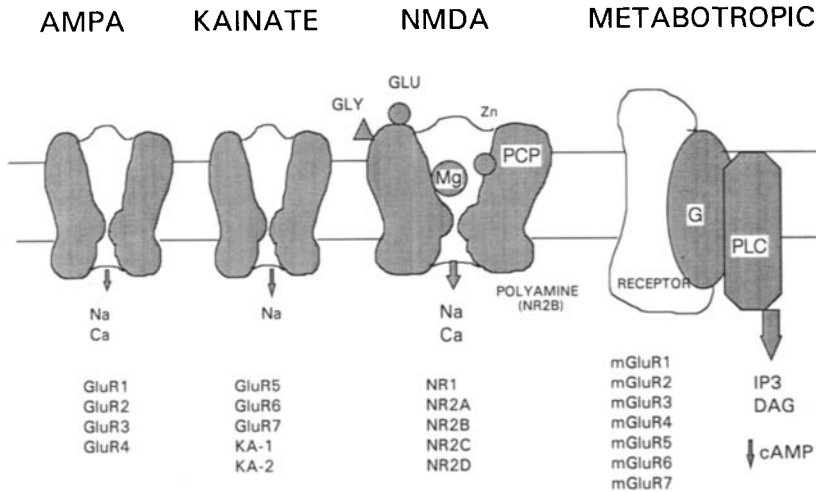


FIGURE 1. Diagrammatic representation of the ionotropic (AMPA, kainate, NMDA) and metabotropic glutamate receptors in brain. The ionotropic receptors are formed by combinations of at least four subunits (the same or combinations of different subunits), whereas the metabotropic receptors are individual proteins coupled to a GTP-binding protein (G) and an enzyme such as phospholipase C (PLC). A list of the major (not including splice variants) cloned receptor subtypes (metabotropic) or subunits that combine to form the functional receptor (ionotropic) are summarized below each receptor. The assembled subunits of AMPA and kainate receptors form ion channels that gate Na⁺ and in some cases Ca²⁺. The specific properties of these channels, such as the Ca²⁺ conductance, depend in part on the subunit combinations that make up the receptor. The NMDA receptor is formed by subunit NR1 in combination with NR2A, B, C, or D. Activation of the NMDA receptor is slow due in part to the Mg²⁺ block in the channel, but when opened the ion channel gates large amounts of Na⁺ and Ca²⁺. Several regulatory sites on the NMDA receptor modulate the binding of glutamate and the activation of the channel, including glycine, Zn²⁺, a site accessible in the open channel sensitive to PCPs, and a polyamine site thought to be on the NR2B subunit. The seven metabotropic receptors function to activate a G-protein coupled to activation of PLC or inhibition of adenylate cyclase (not shown). These actions result in the production of the second messengers inositol triphosphate (IP₃) and diacylglycerol (DAG) or a decrease in cyclic adenosine monophosphate (cAMP).

where it is assumed that localization is more important than a detailed analysis of receptor affinity and density. However, in some cases where there is a sufficient number of receptors, estimates of regional receptor densities can be achieved from sections using a modified saturation binding protocol. Both distribution and saturation binding analyses are generally not possible for hypothalamic regions owing to limitations in the number of matched sections that can be obtained. The details of each type of analysis are outlined in the methods that follow.

TABLE I. Glutamate Receptor Ligands and Their Properties^a

Receptor drug subtype	Binding site	K_D , K_I , or IC_{50} (μM)
All receptors		
L-Glutamate	All receptors	0.057–0.600 (47,85–90)
D-Glutamate		8.1 (88)
L-Aspartate		1.4–693 (85,88,90)
D-Aspartate		0.46–0.80 (86,88)
NMDA		
Glutamate	Agonist	0.192 (47)
NMDA	Competitive agonist	3.66–5.3 (88,91)
Glycine	Glycine site	0.18 (92), 204 (93)
D-AP5	Antagonist	0.350–1.50 (86,88,89,91,94)
L-AP5	Inactive isomer	29 (91)
D,L-AP7	Antagonist	0.90–8.9 (88,91)
MK-801	Noncompetitive, ion channel	2.2–8.4(high) (95,96) 40(low) (95)
CGS 19755	Antagonist	0.050–1.1 (97)
CGP 39653	Antagonist	0.007–0.230 (86)
CPP	Antagonist	0.105–0.820 (86,88,93,94,98,99)
Ifenprodil	Polyamine binding site	0.0367–0.45 (100,101), 0.34 (NR2B), 146(NR2A) (102)
Kynurenate	Glycine site antagonist	20–190 (88,93,103)
7-Chlorokynurenate	Glycine site antagonist	0.56 (92)
Ibotenate	Agonist	1.2–214 (85,90)
Quinolinate	Agonist	510 (88)
AMPA		
AMPA	Agonist	0.00026–0.011 (47,104–106)
CNQX	Competitive antagonist	0.067 (106), 0.340 (GluR7) (107), 1.2(GluR6) (107)
DNQX	Competitive antagonist	0.800 (103)
MNQX	Competitive antagonist	0.800 (103)
NBQX	Competitive antagonist	0.15 (108)
Kainate		
Kainic acid	Agonist	0.0039–0.070 (47,89,109,110), 0.070–0.073(GluR5) (107,110,111), 0.059 (GluR6) (107), 0.010–0.080(GluR7) (107), 0.0039–0.005(KA-1) (110), 0.015(KA-2) (111)
Domoate	Agonist	0.0005(GluR5) (111), 0.059(GluR6) (107), 0.010–0.080(GluR7) (107), 0.275(KA-2) (111)
Quisqualate	Agonist	58 (111), 1.1(GluR6) (107), 6.9(GluR7) (107)

(continues)

TABLE I. (Continued)

Receptor drug subtype	Binding site	K_D , K_I , or IC_{50} (μM)
Metabotropic		
Quisqualate	Agonist	3.9–655 (47,85)
(1 <i>S</i> ,3 <i>R</i>)ACPD	Agonist for mGluR2,3	0.187 (112)
L-AP4	Agonist, mGluR4,6,7	5.1 (113)
DCG IV	Agonist, mGluR2/3	1 (EC_{50}) (114)
3HPG	Agonist mGluR1/5	98(EC_{50}) (115,116)
L-AP3	Partial antagonist	313(47)
(+)MCPG	Antagonist, mGluR1,2,4,6	70 (116,117)
4CPG	Antagonist, mGluR1	40 (116,117)
3C4HPG	Antagonist, mGluR2	70 (116,117)

^a Abbreviations: (1*S*,3*R*)ACPD, 1-aminocyclopentane dicarboxylic acid; AMPA, α -amino-3-hydroxy-4-methyl-5-isoxazolepropionic acid; AP3, 2-amino-3-phosphonopropionic acid; AP4, 2-amino-4-phosphonobutyric acid; AP5, 2-amino-5-phosphonopentanoic acid; AP7, 2-amino-7-phosphonoheptanoic acid; 3C4HPG, 3-carboxy-4-hydroxyphenylglycine; 4CPG, 4-carboxyphenylglycine; CGP 39653, *D,L*-(*E*)-2-amino-4-propyl-5-phosphono-3-pentanoic acid; CNQX, 6-cyano-7-nitroquinoxaline-2,3-dione; CPP, 3-((*R*)-2-carboxypiperazine-4-yl)-propyl-1-phosphonic acid; DCG IV, (2*S*,1'*R*,2'*R*,3'*R*)-2-(2',3'-dicarboxycyclopropyl)glycine; DNQX, 6,7-dinitroquinoxaline-2,3-dione; 3HPG, 3-hydroxyphenylglycine; MCPG, α -methyl-4-carboxyphenylglycine; MNQX, 5,7-dinitroquinoxaline-2,3-dione; NBQX, 6-nitro-7-sulphamoylbenzo(*f*)quinoxaline-2,3-dione; CGS 19755, *cis*-4-phosphonomethyl-2-piperidine carboxylic acid; MK-801, 5-methyl-10,11-dihydro-5*H*-dibenzo-[*a,d*]cyclohept-5,10-imine maleate; NMDA, *N*-methyl-*D*-aspartic acid; TCP, *N*-(1-[2-thienyl]cyclohexyl)3,4-piperidine.

Receptor Binding or *in Situ* Hybridization?

The analysis of glutamate receptor binding sites and glutamate receptor mRNA levels provides two slightly different perspectives on glutamate receptor function, each with its own particular merits. Binding studies provide an indication of the receptor protein that is expressed in the cell membrane and is presumed to be a direct indication of the ability of the cell to respond to released transmitter. Binding measurements are sensitive to either (a) a loss of glutamate receptors resulting from down-regulation or neuronal loss or (b) compensatory changes in receptor density that may follow periods of underactivity or overactivity within a glutamatergic system. Ligands available for binding studies generally recognize only the major subtypes of glutamate receptors (NMDA, AMPA, kainate, and metabotropic) as indicated in Table I, with the possible exception of the drug ifenprodil and several new metabotropic receptor ligands. Recent studies suggest that high-affinity ifenprodil binding may be selective for the NR2B subunit of the NMDA receptor (102,118). In addition, several new ligands

have been identified that are partially selective for metabotropic receptor subtypes (114–117,119–124). These latter ligands are not yet available for direct radioisotope binding studies but may be used for competition binding.

In situ hybridization studies, in contrast to receptor binding, provide an indication of the level of demand for receptor (or receptor subunit) synthesis based on changes in mRNA content, but give no direct information on the actual level of functional receptor protein that is translated and expressed in the membrane. Although it is reasonable to expect that mRNA content and receptor protein expression are regulated in parallel, examples of mismatches between receptor binding and receptor mRNA are not uncommon and it should *not* be concluded that these two techniques provide the same information. Such mismatches are particularly true in some neuroendocrine cell populations such as the supraoptic nucleus, where high expression of mRNA is seen for NMDA receptor subunits but not for NMDA receptor-specific binding (e.g., contrast Figure 2 with Figure 6). One major advantage of *in situ* hybridization over traditional receptor binding approaches rests in the ability to assess specific receptor subunit mRNAs with cellular resolution (since the mRNA is largely restricted to the perikaryon cytoplasmic compartment). This level of resolution is difficult to achieve with current ligand binding techniques owing to the widespread distribution of receptors across the membrane, with the highest densities often in the dendritic neuropil. Because oligonucleotides identify selected mRNA sequences, no glutamate binding domain needs to be present and the contribution of all components of the functional glutamate receptor can be identified. Changes in receptor composition can dramatically alter the function of the ionotropic glutamate receptors (5,76–81) without major changes in binding of agonist. Plasticity of receptor subtype expression is just beginning to be assessed in various normal and pathological states and, though the extent and significance of these changes are not well understood, it seems likely that such changes will contribute to acquired pathology induced by chronic environmental challenges that target glutamatergic circuits. A growing body of evidence suggests that repetitive stimulation of excitatory circuits can induce long-term changes in gene expression (i.e., mRNA content) and that these changes are particularly notable within neuroendocrine cells (125). Since receptor binding analyses are relatively insensitive to changes in receptor composition, these types of plastic changes that may be independent of increases or decreases in receptor numbers would be overlooked. Thus, *in situ* hybridization studies provide a level of specificity and sensitivity that cannot be achieved with receptor binding and can be an invaluable supplement to receptor binding analyses.

THE GLUTAMATE RECEPTOR BINDING ASSAY

General Considerations

[³H]Glutamate is the ligand of choice if a general screen of glutamate receptor density is required and little information is available that would direct the experimenter to specific subtypes. Theoretically, binding to the tissue sections should be done under conditions of equilibrium, receptor saturation, and excess free ligand. Glutamate receptor assays rarely achieve these ideal conditions. To understand the limitations of the assay, it is therefore important to know the basic characteristics of binding for the chosen ligand: time to equilibrium, half-life of binding to the receptor ($t_{1/2}$), equilibrium dissociation constant (K_D), or inhibition constant (K_I) in competition binding. Estimates of K_D , K_I or IC_{50} for many agonists and antagonists are provided in Table I. Values not available in the literature for new ligands may need to be determined. Examples of the characterization of ligand binding are provided in many excellent papers (85,126–129) and will not be reviewed here.

Failure to meet the appropriate conditions for binding can lead to a variety of errors. Terminating binding prior to equilibrium can lead to high variability and an underestimate of the density of binding sites, whereas excessively long incubation can sometimes lead to a loss of binding. Knowledge of the $t_{1/2}$ is particularly important for glutamate receptors since most analyses are done with agonists that readily dissociate from the receptor. The rapid dissociation times (short $t_{1/2}$) necessitate that the wash times for elimination of unbound ligand and nonspecific binding be fast enough to minimize loss of binding to the receptor yet long enough to allow diffusion of the free ligand from the tissue. This is one of the more difficult aspects of the binding protocol because of the narrow window between removing the excess ligand and loss of the receptor binding. The loss at any given time point can be calculated from the rate equation $\ln(B/B_0) = -k_{-1}t$, where k_{-1} is the decay constant, B_0 is the bound ligand at time, $t = 0$, and B is the ligand bound at any time, t . Thus, for glutamate, with a calculated $t_{1/2}$ ($t_{1/2} = 0.693/k_{-1}$) as low as 1.2 min (85) at 2–4°C, approximately 26% of the binding can be lost within 30 sec. Consequently, several rapid washes for a total time of 15–20 sec are generally used to remove the excess ligand and retain most of the receptor binding. Carrying out the reaction and washes at 2–4°C is used to stabilize the binding by slowing down the dissociation rate. Because of the high amounts of radioactivity used for binding, too little washing results in unacceptably high background and a smeared pattern of radioactivity across the slide. Optimal wash times should be empirically determined with the understanding that it is generally best

to sacrifice some of the specific binding to eliminate the substantial interference that can accompany nonspecific binding.

To accurately determine the relative density of receptors in a tissue section it is important to ensure that all the receptors are saturated with radioligand, but this condition is almost never achieved for glutamate receptor binding. The low affinity of agonists typically used for binding require that large amounts of radioactive ligand ($>200 \times 10^6$ DPM/ml at 45 Ci/mmole) be applied to the tissue to attempt to achieve saturation. This high level of radioactivity produces unacceptably high background and cannot be reliably measured. Therefore, subsaturating concentrations have been used for most analyses, ranging from the K_D to two- to threefold greater than the K_D . Under these conditions, approximately 50–75% of the receptors will be occupied and limited conclusions can be drawn regarding low-affinity glutamate binding sites. For example, a relative decrease in receptor binding at subsaturating concentrations may be due to either a loss of receptors or a decrease in the affinity of the ligand for the receptor. These two options cannot be resolved with a single binding concentration used for most mapping studies. However, optional saturation binding analyses described in later sections can be performed that may help to distinguish between changes in receptor density or K_D .

As indicated earlier, [^3H]glutamate binding is insensitive to changes in specific glutamate receptor subtypes. However, indirect estimates of the density of specific subtypes can be obtained if the binding is done in the presence of the appropriate combination of ligands. Strategies for evaluating the contribution of various subtypes are discussed in the sections on indirect and direct glutamate receptor subtype analysis.

Materials

[^3H]-L-Glutamate from Amersham at a specific activity of 45 Ci/mmole, [^3H]kainic acid (New England Nuclear, 58.0 Ci/mmole), and [^3H]AMPA (New England Nuclear, 60.1 Ci/mmole) were used in the examples that follow. Several other reliable sources of radioligands are available, including Tocris-Cookson, ICN Biomedicals, and American Radiolabeled Chemicals. For direct assessment of glutamate receptor subtypes, a variety of radiolabeled, subtype-specific ligands are available. New England Nuclear carries many of these and offers a kit containing several ligands that are useful for screening multiple subtypes. Subtype-specific glutamate receptor agonists and antagonists were obtained from Sigma and Tocris-Cookson. Kodak X-omat AR X-ray film, Hyperfilm β max (Amersham), Ultrafilm ^3H (Leica), or NTB2 emulsion (Kodak) have been used in our lab for autoradiography. Similar types of film (e.g., Kodak SP5, fast with relatively large

grain; Kodak Industrex SR5, slow with very high resolution; EB1 Mammography film, medium speed with fine grain) and nuclear emulsions (e.g., Amersham, Hypercoat EM-1 and LM-1) are available from a variety of suppliers. The Hyperfilm β max and Ultrafilm are considerably more expensive than the Kodak X-omat-AR but will reduce the exposure time for hypothalamus by approximately one-half from 50–80 days to 25–30 days with slightly higher resolution and lower background.

Glutamate Receptor Autoradiography

The same general protocol for [^3H]glutamate binding has been used by most research groups with slight variations. The following procedure adapted from Greenamyre *et al.* (130) and Halpain *et al.* (98) provides a general protocol suitable for most receptor autoradiography with [^3H]glutamate.

1. Decapitate under deep isoflurane or pentobarbital anesthesia, remove the brain, and block in the reference plane for the atlas used [e.g., flat brain for Paxinos and Watson (131)].

2. Freeze in liquid nitrogen-cooled isopentane on a cryostat chuck. [The brain will crack if immersed totally in the isopentane. Let the brain freeze from bottom to top, keeping the isopentane level at the freezing line.]

3. Cut 12- to 20- μm -thick frozen sections in a cryostat at -12 to -14°C and thaw mount onto gelatin-chrome alum-coated slides.

4. Wash sections at 37°C for 30 min in 50 mM Tris-HCl binding buffer.

5. Incubate each section in 0.6–1 μM [^3H]glutamate in 50 mM Tris-HCl (pH 7.2) for 30 min at 4°C . Adjacent sections incubated with the same concentration of [^3H]glutamate in the presence of 1 mM glutamate are used to define nonspecific binding (see the following section, Nonspecific Binding). [The most uniform results are obtained if all slides are dipped in a solution containing the radioligand in the appropriate concentration. This method, however, requires the use of large amounts of radioligand for each assay and may not be practical for small runs. Satisfactory results can be obtained by applying enough solution on the slide to cover each section and then transferring the slides to the refrigerator to incubate in a protected container at 4°C . The slides must be kept perfectly flat and humidified to prevent either loss or concentration of the binding solution. A 150-mm culture plate works well for this with wet filter paper in the bottom and a pair of glass rods or pieces of a disposable plastic 1-ml pipette to support the slides.]

6. Terminate binding by rapidly washing three times (3 sec each) in ice-cold 50 mM Tris-HCl followed by ice-cold acetone containing 2.5% glutaraldehyde (5 sec) and ice-cold acetone (4 sec).

7. Dry the slides rapidly under a stream of warm air. [A hair drier on low heat works well, but care should be taken to ensure that the slides are well ventilated and far enough from the drier to eliminate any risk from the acetone.]

8. Place the dried sections and a slide containing ^3H standards in an X-ray cassette, place the X-ray film over the slides making sure that the emulsion side is in contact with the sections, and expose for approximately 50–90 days (Kodak X-omat-AR) or 20–40 days (Leica, Ultrofilm ^3H). [It is advisable to include a small set of extra slides in a separate cassette that can be developed independently to evaluate the adequacy of the exposure and fine-tune the exposure interval.]

9. Develop the film in D-19 for 4 min, wash in distilled water for 30 sec, and fix in Kodak General Fixer for 4 min.

Nonspecific Binding

Nonspecific binding determination is often given too little attention in binding studies but is of critical importance since specific binding to the receptor is not determined by the direct binding of the radioligand to the receptor but by the *displaceable binding* in the presence of unlabeled ligand (i.e., specific binding = total minus nonspecific). Unlabeled glutamate or the ligand used for binding is the preferred choice at concentrations that do not displace binding from nonreceptor sites. Under theoretical conditions with binding of the ligand to a single site, a 100-fold higher concentration of unlabeled ligand should be sufficient to displace >95% of the specific binding to the receptor. For ligands such as [^3H]glutamate, where binding occurs to multiple receptor subtypes with different affinities, the binding of glutamate spans a broader concentration range and at least a 1000-fold higher concentration provides a better estimate of total ligand binding. Most researchers have used a concentration of 1 mM glutamate to define nonspecific binding, which is approximately 5000-fold higher than the estimated K_D of 200–250 nM for glutamate binding in the hypothalamus (47).

Indirect Glutamate Receptor Subtype Analysis

Although as noted earlier, the binding of [^3H]glutamate alone provides little information regarding glutamate receptor subtypes, this binding can be used as a general screen and reference point for more detailed subtype analysis. Estimates of the major glutamate receptor subtypes can be obtained by using unlabeled ligands specific for each subtype to displace “nonspecific binding.” Under these circumstances, unlabeled excess glutamate is still used to define nonspecific binding to sites other than glutamate

receptors. The specific glutamate receptor ligands are used to limit total binding to the subpopulation of interest. This can be accomplished in two ways. First, specific agonists and antagonists can be used to block all receptor subtypes except the one of interest. This procedure can be helpful for direct comparison of relative binding densities and to minimize the cost of running many different radioligands when screening for multiple subtypes. Nonspecific binding in the presence of 1 mM glutamate is subtracted from the subtype-specific binding in the presence of blockers of all but one subtype to give a value that represents the binding of [^3H]glutamate to the unoccupied receptor (the receptor of interest). Some recommendations for agonist-antagonist combinations that define the four major glutamate receptor subtypes are provided in the following.

Subtype	Include in the assay (± 1 mM glutamate)
NMDA	100 μM AMPA + 100 μM kainate + 10 μM DCG IV + 200 μM (+)MCPG
AMPA	200 μM AP5 + 100 μM kainate + 10 μM DCG IV + 200 μM (+)MCPG + 100 mM potassium thiocyanate
kainate	200 μM AP5 + 100 μM AMPA + 10 μM DCG IV + 200 μM (+)MCPG
metabotropic	200 μM AP5 + 100 μM AMPA + 100 μM kainate

An example of autoradiograms generated in this fashion that illustrate binding to total and NMDA sites is provided in Figure 2.

The second indirect approach would use excess subtype-specific ligand to define "specific binding." In this case, the binding that remains represents

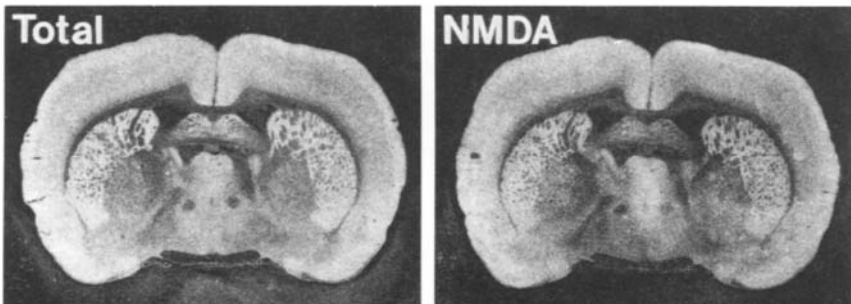


FIGURE 2. Autoradiogram illustrating binding of [^3H]glutamate to all glutamate receptors (Total) and to NMDA receptors. NMDA receptors were defined by binding in the presence of saturating concentrations of drugs for the AMPA, kainate, and metabotropic receptors. Nonspecific binding in the presence of 1 mM glutamate was negligible under the conditions used. A relatively low and diffuse pattern of binding is seen in the hypothalamus, with the highest levels in medial structures and the region of the supraoptic nucleus. A similar pattern but lower density was apparent for NMDA receptors. Kodak X-omat-XAR2 film.

all other glutamate receptors as well as binding to sites other than glutamate receptors, and the displaced binding represents the contribution of that subtype (i.e., $T - NS_{\text{sub}} = \text{subtype-specific binding}$, where $T = \text{total binding}$ and $NS_{\text{sub}} = \text{binding in the presence of the subtype-specific ligand}$). A disadvantage of this analysis is that the binding of interest cannot be visualized on the autoradiogram. Also, if the subtype-specific binding represents a small proportion of the measured values, estimates from this analysis may be subject to high relative error (i.e., if the subtype represents only 10% of the total glutamate receptors, an error of 5% in total binding would translate to an error of 50% in the difference score).

Direct Glutamate Receptor Subtype Analysis

It should be clear from the foregoing description of indirect glutamate receptor subtype analyses that there are many potential sources of error with these approaches. Consequently, if the investigator can focus on a particular subtype, then a direct analysis will usually provide far superior results than assays with [^3H]glutamate. Radioligands available for identification of the major glutamate receptor subtypes include the following: NMDA, competitive—[^3H]CPP, [^3H]AP5, [^3H]CGS 17955, [^3H]CGP 39653; NMDA, noncompetitive, ion channel—[^3H]MK-801; NMDA, polyamine site—[^3H]ifenprodil; NMDA, glycine regulatory site—[^3H]5,7-dichlorokynurenic acid; AMPA, agonist—[^3H]AMPA; AMPA, antagonist—[^3H]CNQX; kainate—[^3H]kainate; metabotropic—[^3H](\pm)*trans*-ACPD, [^3H]AP4. Many of these ligands are run under conditions similar to the general protocol described for [^3H]glutamate. An example of the binding of [^3H]AMPA and [^3H]kainate is provided in Figure 3. Binding conditions

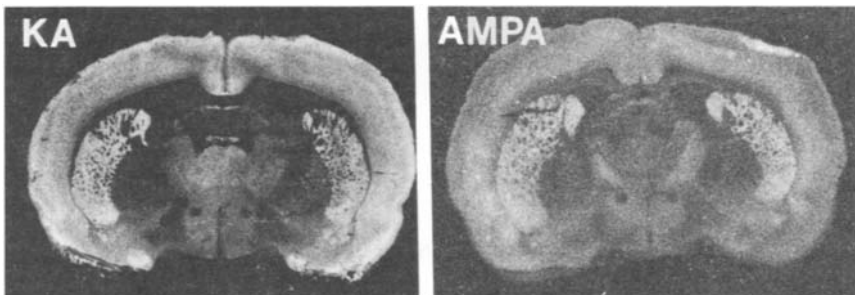


FIGURE 3. Autoradiogram illustrating the binding of [^3H]kainate and [^3H]AMPA in the rostral hypothalamus. Patterns of binding indicate a relatively uniform distribution throughout medial hypothalamic structures, with lower levels in lateral and supraoptic regions. Leica Ultrafilm ^3H .

used were the same as outlined except for the addition of 100 mM potassium thiocyanate to the [³H]AMPA binding buffer (132). Specific details for the binding of many of the other ligands can be found in the references cited in Table I.

Saturation Binding

If quantitative information is required regarding the density of glutamate receptors in the region(s) of interest, a saturation binding protocol can be run that will provide a rough estimate of K_D and B_{max} values. However, this procedure requires the use of many sections that are matched regionally. At least six ligand concentrations should be run, requiring a minimum of 12 sections per run; subtle changes in a single subtype would require at least 12 concentrations. This can be problematic for regions of the hypothalamus that are not large or are variable in the rostrocaudal plane of section. If sufficient sections can be obtained through the region of interest, the tissue should be run as outlined in the foregoing general protocol except that a series of concentrations should be used that span a range of at least 10-fold on either side of the anticipated K_D . Suggested concentrations that span the range of affinities for glutamate binding in the hypothalamus are: 10^{-9} , 3.2×10^{-9} , 10^{-8} , 1.78×10^{-8} , 3.2×10^{-8} , 5.62×10^{-8} , 10^{-7} , 1.78×10^{-7} , 3.2×10^{-7} , 5.62×10^{-7} and 10^{-6} M. Slides for total and nonspecific binding should be run at each concentration, in duplicate if possible. It is helpful to run an extra set of slides to check the exposure and make adjustments, which keep both the low and high concentrations on scale (see the Automated Densitometry and Grain Counting section). Generally the long exposure times that provide detectable exposure at the low concentrations will be adequate, since most hypothalamic structures are unlikely to produce a saturating autoradiographic signal even at the highest concentrations. An example of results obtained from a 6-point saturation binding analysis of hypothalamic ³H glutamate binding is illustrated in Figure 4. The resulting curvilinear Scatchard plot clearly highlights the complexity of the binding and the difficulty of trying to make quantitative comparisons. Even with 12 points per curve, adequate estimates of the various high- and low-affinity binding sites are difficult to achieve (129) and the identity of the contributing receptor subtype is still unknown.

As an alternative to the direct saturation binding analysis, a concentration-effect curve with subtype-specific ligands can also be used to provide specific information about the different glutamate subtypes. Using various concentrations of unlabeled drug (spanning approximately 10-fold on either side of the K_I) in the presence of near saturating concentration of ³H-labeled ligand, crude estimates of the density and apparent affinity of the

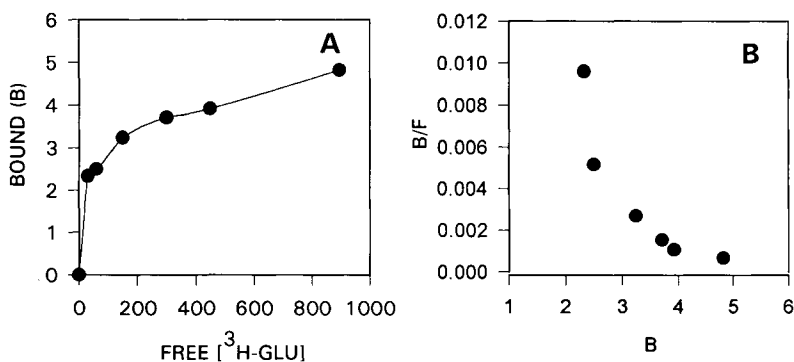


FIGURE 4. Saturation binding curve for specific binding of [³H]glutamate to the rostral hypothalamus. (A) Bound ligand (nCi/mg) was extrapolated from the density of the autoradiograms relative to ³H standards and plotted versus the free [³H]glutamate concentration (nM). (B) The curvilinear Scatchard analysis of the binding data illustrates the complex nature of glutamate binding to multiple subtypes in the tissue.

binding can be obtained. If accurate measures of receptor density are more important than regional localization and a sufficient supply of tissue can be obtained, membrane binding studies are recommended (47).

The Glutamate Transporter and Nonspecific Binding

A potential problem in glutamate binding assays is the uptake of glutamate into cells and terminals via the action of Na⁺-dependent high-affinity glutamate transporters, which are particularly active in astrocytes and glutamate presynaptic terminals. Because of the capacity of this system, it is possible to obtain a strong signal that is unrelated to receptor binding. Three major high-affinity transporters have recently been cloned: GLT-1 (133–136), a high-affinity glial transporter; EAAC1 (135,137), a high-affinity neuronal transporter; and GLAST (135,138–140), a low-affinity glial transporter. These transporters have approximate K_m values of 2, 12, and 77 μM respectively (135). Other clones that have been isolated include GluT ($K_m = 70 \mu M$) (141,142) and EAAT1-3 ($K_m = 19\text{--}97 \mu M$) (143). The K_m values for the high-affinity transporters are 10- to 60-fold greater than the K_D 's for glutamate binding to the glutamate receptors. Consequently, most contamination of binding assays from Na⁺-dependent uptake will occur in the evaluation of lower-affinity glutamate binding sites at glutamate concentrations greater than approximately 200 nM. Because the 1 mM glutamate concentration used to define nonspecific binding is sufficient to compete with almost all transport, any uptake of [³H]glutamate by the transporters

would be incorrectly recorded as specific binding. To minimize problems from transport, most assays are run in a sodium-free buffer at low temperatures. Under these conditions, the contribution from uptake is expected to be low. Nevertheless, if complications from uptake are suspected, the potential contribution from glutamate transport can be assessed by using specific uptake inhibitors in the binding protocol. Several inhibitors and their K_I values for inhibition are summarized in Table II. D,L-Threo- β -hydroxyaspartate and L-*trans*-pyrrolidine-2,4-dicarboxylic acid (PDC) are the most potent and specific inhibitors of high-affinity transport and are probably the best compounds to assess the contribution from transport. Presently there is no indication that these inhibitors will interfere with binding to the glutamate receptor.

Standards

A series of standards should be run with each binding experiment. A series of ^3H standards is available from Amersham with a tissue equivalent level of activity ranging from 1.3 to 33.1 nCi/mg for a 20- μm section. These standards can be purchased as a block and cut by the investigator or can be purchased precut. The polymer strips containing the ^3H can be float-mounted onto a coated slide, dried, and placed in the X-ray cassette with each set of tissue slides. A set of standards of lower activity (tissue equivalent of 0.072–6.2 nCi/mg) can also be purchased if the lower range of activities is required. An example of a standard curve obtained with this set of standards on Kodak Xomat X-ray film imaged with a Dage-MTI NC-70L camera using the Bioquant Image Analysis System (R&M Biometrics) is illustrated in Figure 5. Figure 5A illustrates the normal curvilinear response from the camera (gray level) expressed as the amount of light detected relative to the film background (transmittance). Transformation

TABLE II. Inhibitors of Glutamate Transporters

Inhibitor	Transporter	K_I
L- α -Amino adipate	EAAC1	165 μM
	GLT-1	10 μM
Dihydrokainate	EAAC1	>1 mM
	GLT-1	5–10 μM
D,L-Threo- β -hydroxyaspartate	EAAC1	7.1–65 μM
	GLAST	1 mM
	GLT-1	1.0 μM
L-Cysteine sulfate		80 μM
L- <i>trans</i> -Pyrrolidine-2,4-dicarboxylic acid (PDC)		4.6 μM

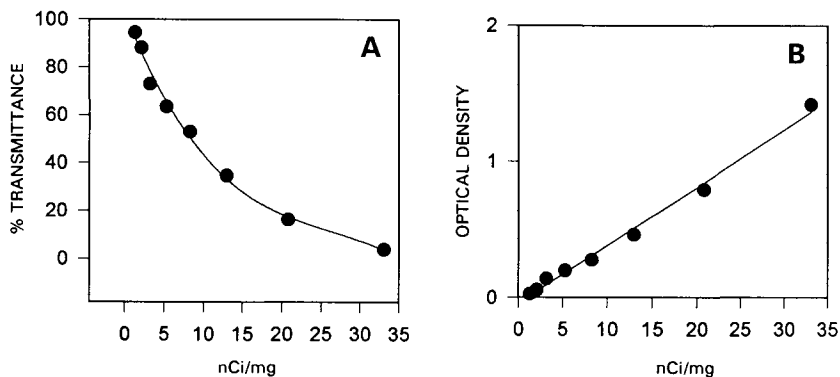


FIGURE 5. Videodensitometric analysis of standards exposed to Kodak Xomat-AR5 X-ray film. (A) The tissue-equivalent radioactive content of the standards is nonlinearly related to transmittance. (B) Conversion of gray level transmittance values to optical density (OD) units provides a linear relationship with tissue-equivalent radioactive content.

of the transmittance values to optical densities (OD, or absorbance) illustrated in Figure 5B provides a linear relationship between tissue-equivalent radioactive density and OD, which can be used for extrapolation to the tissue samples. If it is determined that high-resolution autoradiography is desired, a nuclear emulsion should be used. Because of the short $t_{1/2}$ for binding of glutamate receptor ligands, the sections cannot be dipped into liquid emulsion without loss and smearing of the signal. Consequently, it is best to use coverslips that have been precoated with liquid emulsion diluted 1 : 1 with distilled water and thoroughly dried in a light-tight environment (at least 2 hr). The coverslips are placed on top of the dry tissue sections and held in place by lightly glueing the top edge of the coverslip to the slide with a water, alcohol, and xylene-resistant cement such as Superglue. Only the very edge of the coverslip should be cemented. This allows the coverslip to be later lifted up for development of the emulsion layer opposed to the tissue. After photographic development, the sections can then be stained with a light autoradiography-compatible counterstain such as Giemsa, Pyronin Y, or the fluorescent stain Acridine Orange (0.0001%).

For *in situ* hybridization (see later section), a set of ^{14}C standards can be obtained from American Radiolabeled Chemicals, Inc., which range in activity from 0.035 to 400 $\mu\text{Ci/g}$ and provide a reasonably good approximation of the activity of the ^{35}S dATP-labeled oligonucleotide because of the similarities in the beta particle spectrum for ^{14}C (156 KeV) and ^{35}S (167 KeV).

Automated Densitometry and Grain Counting

A variety of imaging systems are available that will allow a semiquantitative analysis of the density of the autoradiographic image. Basic densitometry and morphometry (tracing the region of interest) used for analysis of autoradiograms are generally included in the simplest systems. The need for additional features depends on the applications of the investigator. Characteristics of these systems have been reviewed (144,145). Measurement of density changes are generally accomplished through a video camera capable of distinguishing 256 gray levels ranging from 0 to 255. These gray levels represent the amount of transmitted light entering the camera through the autoradiographic image and are not linearly related to the exposure of the film (i.e., the amount of radioactivity on the tissue; see Figure 5A). To obtain an approximate linear relationship between the film exposure and the camera response, the gray level values must be converted to optical density units. Some imaging programs will do this automatically, but it can also be done manually using Beer's Law: $O.D. = -\log T$, where O.D. is the optical density or absorbance and T is the transmittance. The transmittance can be calculated from a knowledge of the maximum gray level value obtained from the film background under the conditions of the analysis (100% transmittance) and the gray level value of the sample: $T = \text{sample gray value}/\text{background gray value}$. An example of the resulting curve relating optical density to tissue radioactivity is illustrated in Figure 5B.

Low-resolution images from X-ray film are usually sufficient to identify gross regional changes in binding densities in different hypothalamic areas. However, if one wishes to examine the density of glutamate binding with cellular resolution, high-resolution autoradiography is required. This technique will allow a much closer look at the binding distribution but also has significant limitations. Since glutamatergic synapses are abundant on dendrites, it is difficult to localize a binding site to individual cells. Nonspecific binding controls need to be carefully matched to the total binding sections to determine if significant changes in binding occur. In this case, an analysis of silver grain densities can be undertaken. The best signal-to-noise ratios are generally obtained under dark-field illumination, which can be combined with a fluorescent Nissl stain such as Acridine Orange (0.0001% in distilled water). Bright-field microscopy can also be used if the counterstain is sufficiently light to allow clear resolution of the silver grains (e.g., a light Giemsa or Pyronin Y stain). The silver grains are then highlighted with the thresholding feature of the image analysis system and the number of highlighted pixels (the smallest digitized unit) counted. Pixels can be converted to silver grain numbers by dividing by the average number of pixels in a silver grain (calibrated for each individual run). More advanced

imaging software may allow the automatic selection and counting of objects that meet the size and thresholding features of a silver grain. Silver grain densities for specific binding in individual sections should generally be at least two standard deviation units greater than the mean nonspecific binding. For example, if nonspecific binding is measured at a density of 8 ± 6 grains/square micron, specific binding should run at least 20 grains/square micron.

IDENTIFICATION OF GLUTAMATE RECEPTOR SUBTYPES BY *IN SITU* HYBRIDIZATION ANALYSIS

The Basic *In Situ* Hybridization Protocol for Glutamate Receptors

In situ hybridization is based on the ability of relatively short sequences of DNA or RNA to penetrate into cells and hybridize with complementary regions of RNA or DNA in the cell. Since conditions can be chosen that allow hybridization of perfect or near-perfect matches, a very high level of specificity can be achieved for identification of a target sequence that codes for a unique protein. Under ideal conditions, the binding of the labeled probe to the mRNA has a 1 : 1 stoichiometry and provides a direct quantitative assessment of the amount of the mRNA in the tissue. The mRNA content is assumed to be a marker of the level of expression of the protein for which the mRNA codes (although little information is actually available on the nature of the relationship between mRNA content and functional receptor protein expression). The ability to accurately estimate the amount of mRNA in the tissue is subject to a number of variables described in the protocol that follows. The protocol is divided into three separate procedures that describe each component of the assay: (1) preparation of the tissue, (2) labeling of the probe, and (3) hybridization of the probe specifically to the sequence of interest. Each protocol is followed by a detailed description of the purpose of key steps, as well as specific considerations and suggestions for optimizing the analysis. A list of oligonucleotide probes that have been used for various glutamate receptor subunits/subtypes is provided in Table III (146–151).

Perfusing and Sectioning the Brain

1. Perfuse with saline or balanced salt solution (approximately 20–40 ml in 0.5–1 min for rats). [If fresh brain is needed for parallel receptor binding or other analyses, skip steps 1, 2, and 4.]

TABLE III. Oligonucleotide Probes for Glutamate Receptor *in Situ* Hybridization^a

NMDA	
NR1 HUMAN*	5'-TCG CTG TTC ACC TTG AAC CGG CCG AAG GGG CTG AAG CGG TCC A-3'
NR1*	5'-CCT CAC TGT TCA CCT TGA ATC GGC CAA AGG GAC TGA AGC GGT CCA GC-3'
NR1	5'-TTC CTC CTC CTC CTC ACT GTT CAC CTT GAA TCG GCC AAA GGG ACT-3' (146)
NR1	5'-ATA GTT GGC AAA CTT CCG CTC CCC CAT CCT CAT TGA ATT CCA CAC G-3' (68)
NR2A	5'-AGA AGG CCC GTG GGA GCT TTC CCT TTG GCT AAG TTT C-3' (146)
NR2B	5'-GGG CCT CCT GGC TCT CTG CCA TCG GCT AGG CAC CTG TTG TAA CCC (146)
NR2C	5'-TGG TCC ACC AGG TTT CTT GCC CTT GGT GAG GTT CTG GTT GTA GCT-3' (146)
NR2C*	5'-TGC AGC ATC TTC AGC ACA TTG GCC TGG GCT-3'
NR2D	5'-CGT GGC CAG GCT TCG GTT ATA GCC CAC AGG ACT GAG GT-3' (146)
NR2D*	5'-CTG TGG CTC GAT GGG GCC GTA GTA TCG GTG GAA GCC GTC GGC TAT-3'
AMPA	
GluR1	5'-GTC ACT GGT TGT CTG GTC TCG TCC CTC TTC AAA CTC TTC GCT GTG-3' (104)
GluR2	5'-TTC ACT ACT TTG TGT TTC TCT TCC ATC TTC AAA TTC CTC AGT GTG-3' (104)
GluR3	5'-AGG GCT TTG TGG GTC ACG AGG TTC TTC ATT GTT GTC TTC CAA GTG-3' (104)
GluR4	5'-CTG GTC ACT GGG TCC TTC CTT CCC ATC CTC AGG TTC TTC TGT GTG-3' (104)
Metabotropic	
mGluR1	5'-CCC CAC GTG GAC ATA GTC ATA GCG ATT AGC TTC TGT GTA CTG CAG-3' (147)
mGluR1	5'-ACC CTT TAA GCA AGG CTC ACT GCA CAC AGA TCG TAC CAT TCC GCT-3' (68)
mGluR2	5'-GGT GAC AGC TGT AGG AGC ATC ACT GTG GGT GGC ATA GGA GCC ATC-3' (147)
mGluR3	5'-CTG AGA ATA GGT GGT TGC AGT TCC GCT GAC GCT GAA CCT GTT GAG-3' (147)
mGluR4	5'-GGT CTC CAG GTT CTC ACA CAG CTC TGA TTT GGC TTC CCC ATT GGG-3' (147)
mGluR5	5'-GGA GCG GAA GGA AGA AGA TCC ATC TAC ACA GCG TAC CAA ACC TTC-3' (147)
mGluR6	riboprobe to nucleotides 918-2418 or 1216-1973 (148)
mGluR7	riboprobe to nucleotides 177-1250, 945-2902 or 1251-2760 (149)
mGluR7*	5'-AAC TAC TTT CTC TGG CTT GAC GAA AAC CGG GGG CTC-3'
mGluR7*	5'-GGA TGG GAT CTC TCG GAC TCC TTT GCC CCA CTG CAT GTC CTC TAT-3'

(continues)

TABLE III. (Continued)

Kainate	
KA1	5'-CTT GTA GTT GAA CCG TAG GAT CTC AGC GAA CTC CTT GAG CAT GTC-3' (68)
KA2	5'-GTT CTC CAG GAT ATG GGG ACG CGC CCG AAG ACA CGG GTG AGG GTT-3' (111)
GluR5	full-length cRNA probe (150)
GluR6	N-terminal, 1000-base cRNA (151)

^a Antisense sequences shown are complementary to mRNAs for ionotropic (NMDA, AMPA, and kainate) glutamate receptor subunits and metabotropic receptor subtypes. Sequences are directed against rat mRNA unless otherwise indicated. Starred sequences indicate probes that may have utility based on initial studies in our laboratory but should not be considered proven until thoroughly tested. In cases where an oligonucleotide sequence is not yet available, the portion of the synthesized sequence used for *in situ* hybridization studies is given. References are given at the end of each sequence.

2. Follow immediately with 400–500 ml 4% paraformaldehyde (PF) in 0.1 M phosphate buffer (PB), pH 7.4, at room temperature for a minimum of 20 min.
3. Remove brain and block in the plane of the preferred atlas. Postfix in 4% PF, 0.1 M phosphate buffer, pH 7.4, for 1 hr at room temperature or overnight at 4°C.
4. Transfer the brain to 20% sucrose, 0.01 M phosphate buffer, pH 7.4, and store at 4°C until the brain sinks to the bottom of the vial (usually overnight). [This step can be omitted at the risk of introducing freezing artifact in the sections.]
5. Freeze the brain in isopentane (2-methylbutane) cooled in liquid nitrogen. [To prevent cracking, slowly lower the brain into the isopentane, allowing it to freeze from bottom to top. Use embedding compound to cement the brain to the chuck at the base.]
6. Cut immediately in a cryostat at approximately –15° to –20°C (–12° to –14°C for fresh brain) in 10- to 20- μ m sections. Thaw-mount sections on slides coated with gelatin-chrome alum or poly-*l*-lysine. [If the brain cannot be cut immediately, seal in a foil pouch and store in liquid nitrogen (do not let the brain thaw). Dry sections on the slides quickly at approximately 40°C. Section thickness should not exceed approximately 25 μ m, since the radioactive signal becomes nonlinear at greater thickness (152).] Fresh tissue should be fixed and washed immediately after cutting:
 - a. Immerse in 4% PF in 0.01 M PBS, pH 7.4, for 15 min. An alternative fixative is 100% ethanol:acetic acid [3:1 (v:v)] for 15 min (153).

- b. Wash 2×5 min in 0.01 M PBS.
- c. Dehydrate 2 min each in 70%, 95%, 100%, and 100% ethanol. After the slides are air-dried they can be stored frozen at -80°C sealed in a ziplock bag.

3' End-Labeling with Terminal Deoxynucleotidyl Transferase

Most terminal deoxynucleotidyl transferase enzyme purchased for 3' end-labeling now comes with all the necessary solutions to perform the reaction. Sources of enzyme include Boehringer Mannheim and Bethesda Research Labs. The following protocol describes the basic labeling procedure for a 50- μl reaction. The procedure may vary slightly depending on the source of the enzyme and buffer solutions.

1. Transfer 1 μl of oligonucleotide probe that has been reconstituted in distilled water to a concentration of 10 pmoles/ μl to a sterile plastic culture tube or microfuge tube.
2. Aliquot 50 μCi of [^{35}S]dATP (5 μl of 10 $\mu\text{Ci}/\text{ml}$ aqueous solution, free of DTT) into the sterile culture tube containing the oligonucleotide. [The final specific activity of the labeled probe depends on the stoichiometric ratio of [^{35}S]dATP to oligonucleotide. This procedure uses a ratio of 5:1, which will incorporate an average of 2.5 [^{35}S]dATPs per oligonucleotide at a reaction efficiency of 50%.]
3. Add 27 μl of distilled water.
4. Add 10 μl of $5 \times$ tailing buffer (final conc. = 200 mM K^+ -cacodylate, pH 7.2).
5. Add 5 μl of 25 mM CoCl_2 .
6. Mix and centrifuge briefly to collect liquid at bottom of tube.
7. Add 2 μl of terminal transferase (approx. 50 units). [The enzyme is not stable and care must be taken not to let it come to room temperature.]
8. Mix thoroughly, centrifuge briefly, and incubate for 1 hr at 37°C .
9. Stop the reaction by adding 400 μl of ice-cold Tris-TEA-EDTA buffer: 0.1 M Tris-HCl (pH 7.7), 10 mM triethylamine, and 1 mM tetrasodium EDTA.

The 3' end-labeled oligonucleotide is then purified using an NENsorb 20 cartridge from Dupont.

1. The column is first washed with 2 ml of methanol followed by 2 ml Tris-TEA-EDTA buffer at a flow rate of approximately 1 drop every 2 sec. [Care must be taken to ensure that the column does not dry out at any point in the purification procedure.]

2. Gently load the labeled probe onto the column until it just penetrates the column bed.
3. Wash with 2 ml of Tris-TEA-EDTA buffer. [Collect all wash solutions, which contain the free [³⁵S]dATP, for radioactive waste.]
4. Elute labeled probe with 1 ml of 20% ethanol (or 50% methanol if it tends to stick to the column). Collect five fractions of 4–5 drops each into sterile RNase-free 1.5-ml microfuge tubes. Count a 5- μ l aliquot from each vial. [A 5- μ l aliquot will contain approximately $1\text{--}3 \times 10^6$ CPM if the reaction is successful (specific activity of approx. $2\text{--}6 \times 10^8$ CPM/ μ g).] Store at -20°C in 20 mM DTT (approx. 5 μ l of 1 M DTT per vial). Use as fresh as possible.

In Situ Hybridization

1. Wash sections 2×5 min in sterile 0.01 M PBS + 0.3% Triton X-100. [Permeabilizes the tissue.]
2. Wash in 0.2% glycine in PBS for 5 min. [Inactivates reactive groups.]
3. Wash sections 2×5 min in sterile 0.01 M PBS + 0.3% Triton X-100.
4. Incubate 10 min in saline containing 0.1 M triethanolamine, 0.25% acetic anhydride. [Inactivates reactive groups.]
5. Dehydrate and delipidate in 50%, 70%, 95%, and 100% ethanol, 2 min each; chloroform, 5 min; 100% ethanol, 1 min; 95% ethanol, 1 min. Air-dry. [Removes lipids to which the oligonucleotide might bind.]
6. Prehybridize by applying fresh hybridization buffer to the sections (50 μ l/section) and incubating 1 hr at 44°C . For the hybridization buffer mix the following reagents in a clean, sterile tube. The approximate final concentration in the reaction is given in brackets.

250 μ l 1 M Tris-HCl, pH 8.0, at 22°C (pH 7.4 at 44°C)	[50 mM]
1.5 ml $20\times$ SSC	[6 \times]
50 μ l 0.5 M EDTA (pH 7.0)	[5 mM]
0.3 ml deionized sterile water	
0.5 g dextran sulfate (heating gently may help to dissolve the dextran)	[100 mg/ml]
Add 0.2 ml $25\times$ Denhardt's solution to the cooled mixture	[1 \times]

Add 2.5 ml of fresh deionized formamide containing:	
0.1% salmon sperm DNA	[0.5 mg/ml]
250 μ g/ml yeast tRNA	[125 mg/ml]

[Note: The prehybridization step is an optional procedure to help reduce background by using excess salmon sperm DNA and yeast tRNA to block sites that might interact with DNA or RNA probes. In some instances, more consistent hybridizations with no increase in background may be obtained if this step is eliminated.]

7. Drain slides thoroughly but do not let them dry. Apply freshly prepared hybridization buffer containing 5×10^5 – 2×10^6 CPM/100 μ l [35 S]dATP-labeled oligonucleotide to the sections. Place a Parafilm coverslip over the sections and incubate overnight at 44°C in humidified 150-mm petri dishes. [Plastic 1-ml pipettes on a wet filter paper disk work well for support of the slides in the petri dish.]
8. Remove coverslips by dipping slides into a beaker of 4X SSC at 44°C and allowing the coverslips to gently slide off the sections.
9. Wash sections 4 \times 15 min at 55°C in 1X SSC containing 10 mM sodium thiosulfate followed by 1 hr in 1X SSC at room temperature containing 10 mM sodium thiosulfate.
10. Dehydrate sections through a fresh graded ethanol series: 50%, 70%, 95%, 100%, 100% ethanol.
11. Air-dry sections for 1–2 hr.
12. Place the sections in an X-ray cassette and cover with X-ray film, making sure that the emulsion side is facing the tissue or dip slides in liquid emulsion (e.g., Kodak NTB-2) warmed to 42°C and diluted with an equal part of distilled water at 42°C (10 ml emulsion + 10 ml water using a small slide mailer or film canister). Dip each slide into the emulsion, invert onto a slide rack, and air-dry in complete darkness at room temperature for approximately 2 hr.
13. Wrap cassette or slide box with foil and expose at -80°C for approximately 30 days.
14. After exposure, develop film or slides for 4 min in Kodak D19 (1:1), wash for 30 sec in distilled water, and fix for 4 min in Kodak fixer.
15. Counterstain sections with a light Nissl stain such as Giemsa or Pyronin Y to allow clean imaging of the silver grains with minimal background. Dehydrate in an alcohol series, clear in xylene, and coverslip.

Maximizing the *in Situ* Hybridization Reaction

To ensure that there is no unnecessary degradation of RNA or DNA in the tissue, most solutions should be made in autoclaved deionized water treated with 0.02% diethylpyrocabonate (DEPC). The treated water is prepared by adding 200 μl fresh DEPC to each liter of deionized water, stirring vigorously until dissolved, and then autoclaving for 1 hr. *No DEPC-treated water* should be used for the terminal transferase labeling procedure since small traces of DEPC might inactivate the enzyme. A list of stock solutions used for *in situ* hybridization is provided at the end of this chapter.

If the tissue sections need to be stored before running *in situ* hybridization, it is best to store frozen at -80°C or below. Although we have seen good hybridization from tissue stored for up to 2 years in this fashion, we have also witnessed some degradation of mRNAs with extended storage, particularly for unfixed tissue. Very few hard data are available regarding the stability of mRNA in stored sections. Consequently, it is best if the tissue is used as quickly as possible to ensure the highest-quality hybridizations.

Specific hybridization of the oligonucleotide to the target mRNA in the tissue is dependent largely on the conditions of the assay. Conditions that destabilize the DNA–RNA hybrid are more stringent and provide greater specificity but must be balanced against potential loss of specific hybridization. If the probe has been properly selected and the conditions are sufficiently stringent, only the perfect match between the oligonucleotide (DNA) and messenger RNA of interest will form a stable hybrid. Three main variables control the assay stringency: salt concentration, temperature, and formamide concentration. Most assays keep the formamide concentration constant at 50% and vary the temperature and salt concentration. Hydrogen bonding between complementary nucleotides (two bonds per A–T pair, three bonds per G–C pair) is most stable at low temperatures, in an aqueous environment, and in the presence of high Na^+ . Under these conditions the negative charges of the phosphate backbone of the DNA/RNA are stabilized and hydrogen bonding by the nucleotides can proceed with minimal interference. Consequently, conditions of decreased salt, non-polar environment (formamide) and high temperature all decrease the stability of hybrid formation (increased stringency). Experimental choices for these conditions vary depending on the length of the oligomer and the relative G/C content. Probe length for oligonucleotides is generally between 30 and 50 bases with a G/C content of 50–70%. A G/C content of 50–70% ensures the strongest hydrogen bonding (three hydrogen bond pairs each) without excessive “stickiness.” Optimal conditions for specific hybridization can generally be predicted from a knowledge of the theoretical melting temperature of the hybrid. The approximate T_m or midpoint of the melting curve for hybrid formation can be calculated from the equation

$$T_m = 81.5 + 16.6 \log[\text{Na}^+] + 0.41(\% \text{G/C content}) - 1.2(\% \text{ mismatched pairs}) - 820/(\text{base length}) - 0.38(\% \text{ formamide}) \quad (152)$$

A temperature 20°–25° below the theoretical T_m is a good starting point for hybridization. Computer software designed to analyze short DNA sequences (e.g., OLIGO, National Biosciences Inc.) is also available for calculation of T_m in various solutions as well as many additional properties of the probe that might affect performance, such as formation of loops and self-hybridization.

A list of oligonucleotide probes that have been used for *in situ* hybridization to each major subunit or subtype of glutamate receptor is provided in Table III. Most of these probes have been run under conditions similar to our basic protocol. An example of hybridization of oligonucleotides to the NMDA glutamate receptor subunits NR1 and NR2D in the hypothalamus using the foregoing conditions is illustrated in Figure 6. However, different applications may require changes in the protocol and the reader is therefore encouraged to refer to specific papers for conditions that optimize the hybridization of selected oligonucleotides.

Autoradiography and Analysis

Autoradiography

Visualization of the oligonucleotide probe hybridized to the tissue is accomplished in much the same fashion as for receptor binding, by examining the silver grain density in the X-ray film (low resolution) or nuclear emulsion (high resolution). Since the relatively weak signal from glutamate receptor mRNAs will require long exposure times (3–6 weeks), an X-ray film with

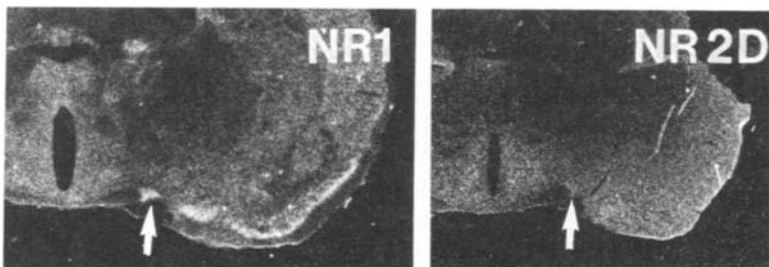


FIGURE 6. Example of the *in situ* hybridization of oligonucleotides that recognize the mRNA for NMDA receptor subunits NR1 and NR2D. NR1 mRNA is widespread throughout the hypothalamus, with a particularly high density in the supraoptic nucleus (arrow). Expression of NR2D is very low, with the highest expression in medial hypothalamic structures and low levels in the region of the supraoptic nucleus (arrow).

high sensitivity to ^{35}S and low background, such as Amersham Hyperfilm Betamax, is recommended. Other less expensive films, such as Kodak Xomat AR, can be used but will generally require 50–100% longer exposure times with slightly higher background. Densitometric analysis of the autoradiograms is the same as outlined in the Automated Densitometry and Grain Counting section.

Controls

To ensure that the autoradiographic signal is due to specific hybridization, controls should be included that give an estimate of nonspecific hybridization. Randomer oligonucleotides, sense sequence oligonucleotides, and sequences that do not recognize mRNAs in the brain have all been used for this purpose. Blockade of antisense hybridization by preincubation with excess sense sequence oligonucleotide has also been used as a control by several investigators but is not recommended since it provides no information on the nonspecific hybridization of antisense probe to targets in the tissue (it simply reaffirms that sense and antisense sequences will hybridize to each other to form double-stranded DNA). RNase treatment of the tissue has also been used to ensure that the probe does not bind nonselectively to non-RNA targets in the tissue. In addition, probes to different sequences in the target RNA or DNA can be useful to provide verification of the hybridization pattern or to enhance the sensitivity of the assay. The usefulness of this two-pronged approach will, however, depend on both probes having good target specificity. An additional control is to examine the hybridization of oligonucleotide to brain regions that express negligible amounts of the target mRNA (e.g., white matter). This provides an indication of nonspecific sticking of the probe to the tissue. Comparison to similar types of cells that do not express the mRNA is an even better control, but this is difficult with glutamate receptors owing to their ubiquitous distribution.

Troubleshooting and Elimination of Nonspecific Hybridization

Perhaps the greatest problem encountered with *in situ* hybridization studies is the production of a consistent, strong signal while keeping background down to reasonable levels. If probes are run at too low a stringency or have insufficient sequence specificity, a Nissl-like hybridization pattern results. This pattern is probably due to nonspecific hybridization to ribosomal RNA, which is abundant relative to mRNAs. The example in Figure 7 illustrates how the nonspecific hybridization pattern develops as the concen-

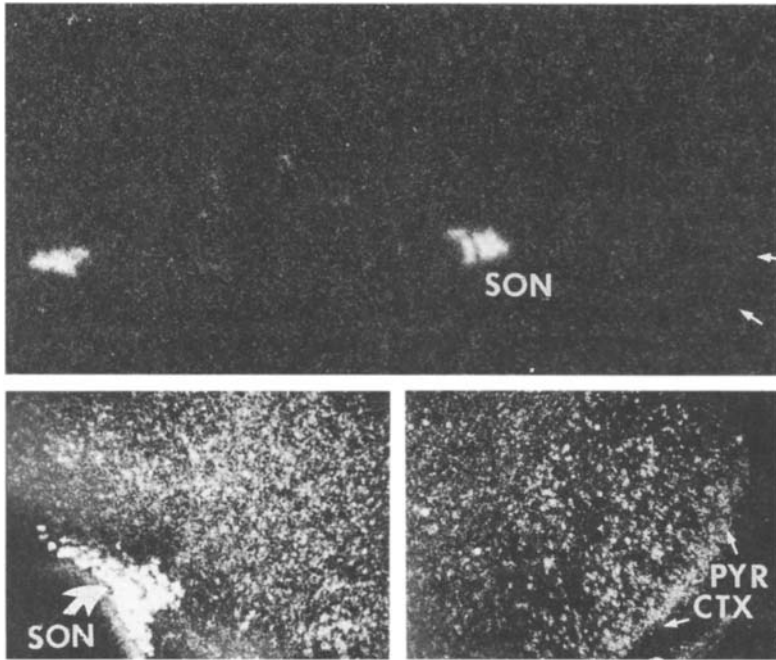


FIGURE 7. Example of nonspecific hybridization that appears with high oligonucleotide concentrations or insufficiently stringent hybridization conditions. Oligonucleotides that normally show highly specific and regionally discrete labeling in the supraoptic nucleus (top) will with insufficient stringency hybridize to all neurons, showing a Nissl-like staining pattern (bottom), as shown in the lateral hypothalamus (bottom left) and pyriform cortex (PYR CTX, bottom right) adjacent to the supraoptic nucleus. The location of the pyriform cortex in the top figure is indicated by small arrows for comparison. Vasopressin mRNA was targeted in the example because of its well-documented clean hybridization signal and discrete distribution under proper hybridization conditions.

tration of a vasopressin antisense probe is increased. The target mRNA in this case is restricted to relatively few cells and should provide a very discrete labeling pattern (Figure 7, top). The widespread labeling at higher concentrations clearly shows the pattern that can develop from nonspecific hybridization (Fig. 7, bottom). This is particularly troublesome for glutamate receptors, which are distributed in neurons throughout the brain. Few regions are available for comparison that are guaranteed not to have the target mRNA. Appropriate controls (see earlier) can help to detect and minimize this problem. The conditions described in the general protocol have been designed to provide a relatively high level of signal with minimal

background or nonspecific labeling. Still, problems will be encountered, the most common of which are summarized in the following.

<i>Problem</i>	<i>Possible solutions</i>
White matter labeling	Oligonucleotide sticking to lipid. Delipidation procedure may not have been adequate. Try fresh tissue or repeat alcohol/chloroform wash prior to fresh hybridization.
Nissl-like hybridization pattern	Stringency too low or probe has poor specificity. Compare with randomer probe of similar length and composition, decrease oligonucleotide concentration, increase hybridization or wash temperatures, decrease salt concentration, try probe targeted to a different sequence.
High tissue background	Desiccation of tissue during storage, hybridization solution dried during incubation, stringency too low, or chemography. Use fresh tissue, rehybridize, or increase stringency with fresh solutions.
High film background	Exposure to light, film or emulsion too old. Replace with fresh.
Nonneuronal localization	mRNA or oligonucleotide has been displaced, mRNA is expressed in glia, or nonspecific binding of oligonucleotide. Compare with immunohistochemistry, rerun at higher stringency.
Uneven pattern of hybridization	Labeled oligonucleotide was not uniformly applied to the tissue or ran off the slide. Rehybridize to fresh tissue, making sure the probe is evenly distributed and slides are flat, make sure coverslips cover sections, eliminate prehybridization step.

Stock Solutions for *in Situ* Hybridization

Tris-TEA-EDTA buffer:

- 0.1 M Tris-HCl, pH 7.7
- 10 mM triethylamine (TEA)
- 1 mM EDTA

Denhardt's solution:

- 5 g Ficoll
- 5 g polyvinylpyrrolidone
- 5 g BSA (Pentax fraction 5)
- Dilute to 55 ml with distilled water

Terminal transferase reaction buffer:

514 mM Na⁺ cacodylate in 9 ml distilled water
 adjust pH to 7.2 with 1 N HCl
 add deionized water to a final volume of 10 ml

20× standard saline-citrate (SSC):

3 M NaCl (175 g/liter)
 0.3 M sodium citrate · 2H₂O (88 g/liter)
 pH to 7.0 with HCl

Phosphate-buffered saline:

137 mM NaCl (8.0 g/liter)
 2.7 mM KCl (0.2 g/liter)
 4.3 mM Na₂HPO₄ · 7H₂O (1.15 g/liter)
 1.4 mM KH₂PO₄ (0.2 g/liter)

REFERENCES

1. R. B. Meeker, D. J. Swanson, and J. N. Hayward, Light and electron microscopic localization of glutamate immunoreactivity in the supraoptic nucleus of the rat hypothalamus. *Neuroscience (Oxford)* **33**, 157–167 (1989).
2. A. N. Van den Pol, J.-P. Wuarin, and F. E. Dudek, Glutamate, the dominant excitatory transmitter in neuroendocrine regulation. *Science* **250**, 1276–1278 (1990).
3. R. B. Meeker, D. J. Swanson, R. S. Greenwood, and J. N. Hayward, Quantitative mapping of glutamate presynaptic terminals in the supraoptic nucleus and surrounding hypothalamus. *Brain Res.* **600**, 112–122 (1993).
4. A. N. Van den Pol, Glutamate and aspartate immunoreactivity in hypothalamic presynaptic axons. *J. Neurosci.* **11**, 2087–2101 (1991).
5. B. Sommer and P. H. Seeburg, Glutamate receptor channels: Novel properties and new clones. *Trends. Pharmacol. Sci.* **13**, 291–296 (1992).
6. J. Boulter, M. Hollmann, A. O'Shea Greenfield, M. Hartley, E. Deneris, C. Maron, and S. Heinemann, Molecular cloning and functional expression of glutamate receptor subunit genes. *Science* **249**, 1033–1037 (1990).
7. M. Hollmann, A. O'Shea Greenfield, S. W. Rogers, and S. Heinemann, Cloning by functional expression of a member of the glutamate receptor family. *Nature (London)* **342**, 643–648 (1989).
8. D. T. Monaghan, R. J. Bridges, and C. W. Cotman, The excitatory amino acid receptors: Their classes, pharmacology, and distinct properties in the function of the central nervous system. *Annu. Rev. Pharmacol. Toxicol.* **29**, 365–402 (1989).
9. L. L. Dugan and D. W. Choi, Excitotoxicity, free radicals, and cell membrane changes. *Ann. Neurol.* **35** (Suppl.) S17–S21 (1994).
10. D. A. Kaku, R. G. Giffard, and D. W. Choi, Neuroprotective effects of glutamate antagonists and extracellular acidity. *Science* **260**, 1516–1518 (1993).
11. G. L. Westbrook, Glutamate receptors and excitotoxicity. *Res. Publ. Assoc. Res. Nerv. Ment. Dis.* **71**, 35–50 (1993).

12. J. McCulloch, Excitatory amino acid antagonists and their potential for the treatment of ischaemic brain damage in man. *Br. J. Clin. Pharmacol.* **34**, 106–114 (1992).
13. M. M. Okazaki, J. O. McNamara, and J. V. Nadler, *N*-Methyl-D-aspartate receptor autoradiography in rat brain after angular bundle kindling. *Brain. Res.* **482**, 359–364 (1989).
14. R. Dingledine, C. J. McBain, and J. O. McNamara, Excitatory amino acid receptors in epilepsy. *Trends Pharmacol. Sci.* **11**, 334–338 (1990).
15. D. D. Schoepp and P. J. Conn, Metabotropic glutamate receptors in brain function and pathology. *Trends Pharmacol. Sci.* **14**, 13–20 (1993).
16. A. I. Sacaan and D. D. Schoepp, Activation of hippocampal metabotropic excitatory amino acid receptors leads to seizures and neuronal damage. *Neurosci. Lett.* **139**, 77–82 (1992).
17. H. Lahtinen, E. Castren, R. Miettinen, A. Ylinen, L. Paljarvi, and P. J. Riekkinen, NMDA-sensitive [³H]glutamate binding in the epileptic rat hippocampus: An autoradiographic study. *Neuroreport* **4**, 45–48 (1993).
18. J. B. Martin and M. F. Beal, Huntington's disease and neurotoxins. *Ann. N.Y. Acad. Sci.* **648**, 169–175 (1992).
19. E. Storey, N. W. Kowall, S. F. Finn, M. F. Mazurek, and M. F. Beal, The cortical lesion of Huntington's disease: Further neurochemical characterization, and reproduction of some of the histological and neurochemical features by *N*-methyl-D-aspartate lesions of rat cortex. *Ann. Neurol.* **32**, 526–534 (1992).
20. M. F. Beal, Role of excitotoxicity in human neurological disease. *Curr. Opin. Neurobiol.* **2**, 657–662 (1992).
21. R. L. Albin, A. Reiner, K. D. Anderson, L. Dure, B. Handelin, R. Balfour, W. O. Whetsell, Jr., J. B. Penney, and A. B. Young, Preferential loss of striato-external pallidal projection neurons in presymptomatic Huntington's disease. *Ann. Neurol.* **31**, 425–430 (1992).
22. M. F. Beal, Does impairment of energy metabolism result in excitotoxic neuronal death in neurodegenerative illnesses? *Ann. Neurol.* **31**, 119–130 (1992).
23. A. B. Young, J. T. Greenamyre, Z. Hollingsworth, A. Albin, C. D'Amato, I. Shoulson, and J. B. Penney, NMDA receptor losses in putamen from patients with Huntington's disease. *Science* **241**, 981–983 (1988).
24. M. D. Carlson, J. B. Penney, Jr., and A. B. Young, NMDA, AMPA, and benzodiazepine binding site changes in Alzheimer's disease visual cortex. *Neurobiol. Aging* **14**, 343–352 (1993).
25. W. F. Marangos, J. T. Greenamyre, J. B. Penney, Jr., and A. B. Young, Glutamate dysfunction in Alzheimer's disease: An hypothesis. *Trends Neurosci.* **10**, 65–68 (1987).
26. D. Dewar, D. T. Chalmers, D. I. Graham, and J. McCulloch, Glutamate metabotropic and AMPA binding sites are reduced in Alzheimer's disease: An autoradiographic study of the hippocampus. *Brain. Res.* **553**, 58–64 (1991).
27. M. W. Duncan, Beta-methylamino-L-alanine (BMAA) and amyotrophic lateral sclerosis-parkinsonism dementia of the western Pacific. *Ann. N.Y. Acad. Sci.* **648**, 161–168 (1992).
28. P. S. Spencer, A. C. Ludolph, and G. E. Kisby, Are human neurodegenerative disorders linked to environmental chemicals with excitotoxic properties? *Ann. N.Y. Acad. Sci.* **648**, 154–160 (1992).
29. W. Zieglansberger and T. R. Tolle, The pharmacology of pain signalling. *Curr. Opin. Neurobiol.* **3**, 611–618 (1993).
30. S. B. McMahon, G. R. Lewin, and P. D. Wall, Central hyperexcitability triggered by noxious inputs. *Curr. Opin. Neurobiol.* **3**, 602–610 (1993).

31. S. A. Lipton, Models of neuronal injury in AIDS: Another role for the NMDA receptor: *Trends Neurosci.* **15**, 75–79 (1992).
32. M. Raditsch, J. P. Ruppersberg, T. Kuner, W. Gunther, R. Schoepfer, P. H. Seeburg, W. Jahn, and V. Witzemann, Subunit-specific block of cloned NMDA receptors by argitoxin636. *FEBS. Lett.* **324**, 63–66 (1993).
33. P. Krosggaard Larsen and J. J. Hansen, Naturally-occurring excitatory amino acids as neurotoxins and leads in drug design. *Toxicol. Lett.* **64–65** (Spec. No.) 409–416 (1992).
34. B. Meldrum, Amino acids as dietary excitotoxins: A contribution to understanding neurodegenerative disorders. *Brain. Res. Brain Res. Rev.* **18**, 293–314 (1993).
35. G. W. Albers, M. P. Goldberg, and D. W. Choi, *N*-Methyl-D-aspartate antagonists: Ready for clinical trial in brain ischemia? *Ann. Neurol.* **25**, 398–403 (1989).
36. R. J. Bridges, M. M. Kadri, D. T. Monaghan, P. B. Nunn, J. C. Watkins, and C. W. Cotman, Inhibition of alpha-amino-3-hydroxy-5-methyl-4-isoxazolepropionic acid binding by the excitotoxin beta-*N*-oxalyl-L-alpha,beta- diaminopropionic acid. *Eur. J. Pharmacol.* **145**, 357–359 (1988).
37. D. K. Patneau, M. L. Mayer, D. E. Jane, and J. C. Watkins, Activation and desensitization of AMPA/kainate receptors by novel derivatives of willardiine. *J. Neurosci.* **12**, 595–606 (1992).
38. J. H. Weiss and D. W. Choi, Beta-*N*-methylamino-L-alanine neurotoxicity: Requirement of bicarbonate as a cofactor. *Science* **241**, 973–975 (1988).
39. E. A. Mroz, Possible role of carbamates in neurotoxicity and neurotransmitter inactivation. *Science* **243**, 1615 (1988).
40. M. Raditsch, J. P. Ruppersberg, T. Kuner, W. Gunther, R. Schoepfer, P. H. Seeburg, W. Jahn, and V. Witzemann, Subunit-specific block of cloned NMDA receptors by argitoxin. *FEBS. Lett.* **324**, 63–66 (1993).
41. M. G. Jones and D. Lodge, Comparison of some arthropod toxins and toxin fragments as antagonists of excitatory amino acid-induced excitation of rat spinal neurones. *Eur. J. Pharmacol.* **204**, 203–209 (1991).
42. P. T. Brackley, D. R. Bell, S. K. Choi, K. Nakanishi, and P. N. Usherwood, Selective antagonism of native and cloned kainate and NMDA receptors by polyamine-containing toxins. *J. Pharmacol. Exp. Ther.* **266**, 1573–1580 (1993).
43. M. E. Eldefrawi, N. A. Anis, and A. T. Eldefrawi, Glutamate receptor inhibitors as potential insecticides. *Arch. Insect Biochem. Physiol.* **22**, 25–39 (1993).
44. N. I. Kiskin, I. V. Chizhnikov, A. Ya. Tsyndrenko, A. L. Mueller, H. Jackson, and O. A. Krishtal, A highly potent and selective *N*-methyl-D-aspartate receptor antagonist from the venom of the *Agelenopsis aperta* spider. *Neuroscience (Oxford)* **51**, 11–18 (1992).
45. B. Meldrum and J. Garthwaite, Excitatory amino acid neurotoxicity and neurodegenerative disease. In “TiPS Special Report: The Pharmacology of Excitatory Amino Acids” (D. Lodge and G. Collingridge, eds.), pp. 54–62. Elsevier Trends Journals, Cambridge, U.K., 1991.
46. B. Hu and C. W. Bourque, Functional *N*-methyl-D-aspartate and non-*N*-methyl-D-aspartate receptors are expressed by rat supraoptic neurosecretory cells *in vitro*. *J. Neuroendocrinol.* **3**, 509–514 (1991).
47. R. B. Meeker, R. S. Greenwood, and J. N. Hayward, Glutamate receptors in the rat hypothalamus and pituitary. *Endocrinology (Baltimore)* **134**, 621–629 (1994).
48. P. Legendre, D. A. Poulain, and J. D. Vincent, A study of ionic conductances involved in plateau potential activity in putative vasopressinergic neurons in primary cell culture. *Brain Res.* **457**, 386–391 (1988).

49. D. A. Poulain and J. B. Wakerley, Electrophysiology of hypothalamic magnocellular neurones secreting oxytocin and vasopressin. *Neuroscience (Oxford)* **7**, 773–808 (1982).
50. G. I. Hatton, Y. W. Ho, and W. T. Mason, Synaptic activation of phasic bursting in rat supraoptic nucleus neurones recorded in hypothalamic slices. *J. Physiol. (London)* **345**, 297–317 (1983).
51. F. J. Lopez, A. O. Donoso, and A. Negro-Vilar, Endogenous excitatory amino acids and glutamate receptor subtypes involved in the control of hypothalamic luteinizing hormone-releasing hormone secretion. *Endocrinology (Baltimore)* **130**, 1986–1992 (1992).
52. A. O. Donoso, F. J. Lopez, and A. Negro-Vilar, Cross-talk between excitatory and inhibitory amino acids in the regulation of luteinizing hormone-releasing hormone secretion. *Endocrinology (Baltimore)* **131**, 1559–1561 (1992).
53. A. O. Donoso, F. J. Lopez, and A. Negro-Vilar, Glutamate receptors of the non-*N*-methyl-D-aspartic acid type mediate the increase in luteinizing hormone-releasing hormone release by excitatory amino acids *in vitro*. *Endocrinology (Baltimore)* **126**, 414–420 (1990).
54. J.-P. Bourguignon, A. Gerard, J. Mathieu, J. Simons, and P. Franchimont, Pulsatile release of gonadotropin-releasing hormone from hypothalamic explants is restrained by blockade of *N*-methyl-D,L-aspartate receptors. *Endocrinology (Baltimore)* **125**, 1090–1096 (1989).
55. M. T. Price, J. W. Olney, and T. J. Cicero, Acute elevations of serum luteinizing hormone induced by kainic acid, *n*-methyl aspartic acid or homocysteic acid. *Neuroendocrinology* **26**, 352–358 (1978).
56. J. G. Ondo, D. D. Wheeler, and R. M. Dom, Hypothalamic sites of action for *N*-methyl-D-aspartate (NMDA) on LH secretion. *Life Sci.* **43**, 2283–2286 (1988).
57. V. L. Gay and T. M. Plant, *N*-Methyl-D,L-aspartate elicits hypothalamic gonadotropin-releasing hormone release in prepubertal male rhesus monkeys (*Macaca mulatta*). *Endocrinology (Baltimore)* **120**, 2289 (1987).
58. H. F. Urbanski and S. R. Ojeda, A role for *N*-methyl-D-aspartate (NMDA) receptors in the control of LH secretion and initiation of female puberty. *Endocrinology (Baltimore)* **126**, 1774–1776 (1990).
59. L. Cocilovo, V. deGennaro-Colonna, M. Zoli, G. Biagini, B. P. Settembrini, E.-E. Muller, and D. Cocchi, Central mechanisms subserving the impaired growth hormone secretion induced by persistent blockade of NMDA receptors in immature male rats. *Neuroendocrinology* **55**, 416–421 (1992).
60. F. Rage, A. Benyassi, S. Arancibia, and L. Tapia-Arancibia, Gramma aminobutyric acid–glutamate interaction in the control of somatostatin release from hypothalamic neurons in primary culture: *In vivo* corroboration. *Endocrinology (Baltimore)* **130**, 1056–1062 (1992).
61. J. W. Olney, Brain lesions, obesity and other disturbances in mice treated with monosodium glutamate. *Science* **164**, 719–721 (1969).
62. R. S. Greenwood, R. Meeker, and A. Abdou, Neuroendocrine pathologic plasticity in epilepsy. *Int. Pediatr.* **9**, 94–99 (1994).
63. R. B. Meeker, S. McGinnis, R. S. Greenwood, and J. N. Hayward, Increased hypothalamic glutamate receptors induced by water deprivation. *Neuroendocrinology* **60**, 477–485 (1994).
64. H.-J. Krugers, J.-M. Koolhaas, B. Bohus, and J. Korf, A single social stress-experience alters glutamate receptor binding in rat hippocampal CA3 area. *Neurosci. Lett.* **154**, 73–77 (1993).

65. G. Tocco, K. K. Devgan, S. A. Hauge, C. Weiss, M. Baudry, and R. F. Thompson, Classical conditioning selectively increases AMPA receptor binding in rabbit hippocampus. *Brain Res.* **559**, 331–336 (1991).
66. S. Maren, G. Tocco, S. Standley, M. Baudry, and R. F. Thompson, Postsynaptic factors in the expression of long-term potentiation (LTP): Increased glutamate receptor binding following LTP induction *in vivo*. *Proc. Natl. Acad. Sci. U.S.A.* **90**, 9654–9658 (1993).
67. G. D. Pratt, M. Kokaia, J. Bengzon, Z. Kokaia, J.-M. Fritschy, H. Mohler, and O. Lindvall, Differential regulation of *N*-methyl-D-aspartate receptor subunit messenger RNAs in kindling-induced epileptogenesis. *Neuroscience (Oxford)* **57**, 307–318 (1993).
68. M. Hikiji, H. Tomita, M. Ono, Y. Fujiwara, and K. Akiyama, Increase of kainate receptor mRNA in the hippocampal CA3 of amygdala-kindled rats detected by *in situ* hybridization. *Life Sci.* **53**, 857–864 (1993).
69. W. Kamphuis, T. C. De Rijk, L. M. Talamini, and F. H. Lopes da Silva, Rat hippocampal kindling induces changes in the glutamate receptor mRNA expression patterns in dentate granule neurons. *Eur. J. Neurosci.* **6**, 1119–1127 (1994).
70. G. C. Yeh, D. W. Bonhaus, J. V. Nadler, and J. O. McNamara, *N*-Methyl-D-aspartate receptor plasticity in kindling: Quantitative and qualitative alterations in the *N*-methyl-D-aspartate receptor–channel complex. *Proc. Natl. Acad. Sci. U.S.A.* **86**, 8157–8160 (1989).
71. J. B. Perlin, C. M. Gerwin, D. M. Panchison, R. S. Vick, E. R. Jakoi, and R. J. DeLorenzo, Kindling produces long-lasting and selective changes in gene expression of hippocampal neurons. *Proc. Natl. Acad. Sci. U.S.A.* **90**, 1741–1745 (1993).
72. M. Cincotta, N. Young, and P. Beart, Unilateral up-regulation of glutamate receptors in limbic regions of amygdaloid-kindled rats. *Exp. Brain Res.* **85**, 650–658 (1991).
73. H. Lahtinen, E. Castren, R. Miettinen, A. Ylinen, L. Paljarvi, and P. J. Riekkinen, NMDA-sensitive glutamate binding in the epileptic rat hippocampus: An autoradiographic study. *Neuroreport* **4**, 45–48 (1993).
74. R. A. Morrisett, C. Chow, J. V. Nadler, and J. O. McNamara, Biochemical evidence for enhanced sensitivity to *N*-methyl-D-aspartate in the hippocampal formation of kindled rats. *Brain Res.* **496**, 25–28 (1989).
75. K. Williams, M. A. Dichter, and P. B. Molinoff, Up-regulation of *N*-methyl-D-aspartate receptors on cultured cortical neurons after exposure to antagonists. *Mol. Pharmacol.* **42**, 147–151 (1992).
76. K. Kleinanen, W. Wisden, B. Sommer, P. Werner, A. Herb, T. A. Verdoorn, B. Sakmann, and P. H. Seeburg, A family of AMPA-selective glutamate receptors. *Science* **249**, 556–560 (1990).
77. B. Sommer, M. Kohler, R. Sprengel, and P. H. Seeburg, RNA editing in brain controls a determinant of ion flow in glutamate-gated channels. *Cell (Cambridge, Mass.)* **67**, 11–19 (1991).
78. B. Sommer, K. Keinanen, T. A. Verdoorn, W. Wisden, N. Burnashev, A. Herb, M. Kohler, T. Takagi, B. Sakmann, and P. H. Seeburg, Flip and flop: A cell-specific functional switch in glutamate-operated channels of the CNS. *Science* **249**, 1580–1585 (1990).
79. N. Burnashev, H. Monyer, P. H. Seeburg, and B. Sakmann, Divalent ion permeability of AMPA receptor channels is dominated by the edited form of a single subunit. *Neuron* **8**, 189–198 (1992).
80. M. Hollmann, M. Hartley, and S. Heinemann, Ca²⁺ permeability of KA-AMPA-gated glutamate receptor channels depends on subunit composition. *Science* **252**, 851–853 (1991).
81. H. Monyer, R. Sprengel, R. Schoepfer, A. Herb, M. Higuchi, H. Lomeli, N. Burnashev, B. Sakmann, and P. H. Seeburg, Heteromeric NMDA receptors: Molecular and functional distinction of subtypes. *Science* **256**, 1217–1221 (1992).

82. N. Brose, G. W. Huntley, Y. Stern-Bach, G. Sharma, J. H. Morrison, and S. F. Heinemann, Differential assembly of coexpressed glutamate receptor subunits in neurons of rat cerebral cortex. *J. Biol. Chem.* **269**, 16780–16784 (1994).
83. M. Sheng, J. Cummings, L. A. Roldan, Y. N. Jan, and L. Y. Jan, Changing subunit composition of heteromeric NMDA receptors during development of rat cortex. *Nature (London)* **368**, 144–146 (1994).
84. K. A. Wafford, C. J. Bain, B. Le Bourdelles, P. J. Whiting, and J. A. Kemp, Preferential co-assembly of recombinant NMDA receptors composed of three different subunits. *Neuroreport* **4**, 1347–1349 (1993).
85. S. Halpain, C. M. Wiczorek, and T. C. Rainbow, Localization of L-glutamate receptors in rat brain by quantitative autoradiography. *J. Neurosci.* **4**, 2247–2258 (1984).
86. M. A. Sills, G. Fagg, M. Pozza, C. Angst, D. E. Brundish, S. D. Hurt, E. J. Wilusz, and M. Williams, [³H]CGP 39653: A new *N*-methyl-D-aspartate antagonist radioligand with low nanomolar affinity in rat brain. *Eur. J. Pharmacol.* **192**, 19–24 (1991).
87. S. Grimwood, G. J. C. Wilde, and A. C. Foster, Interactions between the glutamate and glycine recognition sites of the *N*-methyl-D-aspartate receptor from rat brain, as revealed from radioligand binding studies. *J. Neurochem.* **60**, 1729–1738 (1993).
88. D. E. Murphy, A. J. Hutchison, S. D. Hurt, M. Williams, and M. A. Sills, Characterization of the binding of [³H]-CGS 19755: A novel *N*-methyl-D-aspartate antagonist with nanomolar affinity in rat brain. *Br. J. Pharmacol.* **95**, 932–938 (1988).
89. R. Dingledine, L. M. Boland, N. L. Chamberlin, K. Kawasaki, N. W. Kleckner, and S. F. Traynelis, Amino acid receptors and uptake systems in the mammalian central nervous system. *Crit. Rev. Neurobiol.* **4**, 1–96 (1988).
90. M. Baudry and G. Lynch, Characterization of two [³H]glutamate binding sites in rat hippocampal membranes. *J. Neurochem.* **36**, 811–820 (1981).
91. G. E. Fagg, H.-R. Olpe, M. F. Pozza, J. Baud, M. Steinmann, M. Schmutz, C. Portet, P. Baumann, K. Thedinga, H. Bittiger, H. Allgeier, R. Heckendorn, C. Angst, D. Brundish, and J. G. Dingwall, CGP 37849 and CGP 39551: Novel and potent competitive *N*-methyl-D-aspartate receptor antagonists with oral activity. *Eur. J. Pharmacol.*, 791–797 (1990).
92. J. A. Kemp, A. C. Foster, P. D. Leeson, T. Priestley, R. Tridgett, L. L. Iversen, and G. N. Woodruff, 7-Chlorokynurenic acid is a selective antagonist at the glycine modulatory site of the *N*-methyl-D-aspartate receptor complex. *Proc. Natl. Acad. Sci. U.S.A.* **85**, 6547–6550 (1988).
93. W. Danysz, E. Fadda, J. T. Wroblewski and E. Costa, Kynurenate and 2-amino-5-phosphonovaleate interact with multiple binding sites of the *N*-methyl-D-aspartate-sensitive glutamate receptor domain. *Neurosci. Lett.* **96**, 340–344 (1989).
94. D. Lodge, S. N. Davies, M. G. Jones, J. Millar, D. T. Manallack, P. L. Ornstein, A. J. M. Verberne, N. Young, and P. M. Beart, A comparison between the *in vivo* and *in vitro* activity of five potent and competitive NMDA antagonists. *Br. J. Pharmacol.* **95**, 957–965 (1988).
95. D. C. Javitt and S. R. Zukin, Interaction of [³H]MK-801 with multiple states of the *N*-methyl-D-aspartate receptor complex of rat brain. *Proc. Natl. Acad. Sci. U.S.A.* **86**, 740–744 (1989).
96. S. Subramaniam and P. McGonigle, Quantitative autoradiographic characterization of the binding of (+)-5-methyl-10,11-dihydro-5H-dibenzo[*a,d*]cyclohepten-5, 10-imine ([³H]MK-801) in rat brain: Regional effects of polyamines. *J. Pharmacol. Exp. Ther.* **256**, 811–819 (1991).
97. J. Lehmann, A. J. Hutchison, S. E. McPherson, C. Mondadori, M. Schmutz, C. M. Sinton, C. Tsai, D. E. Murphy, D. J. Steel, M. Williams, D. L. Cheney, and P. L. Wood,

- CGS 19755, a selective and competitive *N*-methyl-D-aspartate-type excitatory amino acid receptor antagonist. *J. Pharmacol. Exp. Ther.* **246**, 65–75 (1988).
98. K. Hatta, T. Yamamoto, T. Hori, M. Okuwa, and T. Moroji, 3-((±)2-Carboxypiperazine-4-yl)propyl-1-phosphonic acid (CPP) more potently antagonizes the high affinity Mg²⁺ binding site on the *N*-methyl-D-aspartate receptor ion channel complex than the L-glutamate recognition site. *Neurosci. Lett.* **124**, 229–231 (1991).
 99. E. W. Harris, A. H. Ganong, D. T. Monaghan, J. C. Watkins, and C. W. Cotman, Action of 3-((±)2-carboxypiperazin-4-yl)-propyl-1-phosphonic acid (CPP): A new and highly potent antagonist of *N*-methyl-D-aspartate receptors in the hippocampus. *Brain Res.* **382**, 174–177 (1986).
 100. C. Dana, J. Benavides, H. Schoemaker, and B. Scatton, Pharmacological characterisation and autoradiographic distribution of polyamine-sensitive ifenprodil binding sites in the rat brain. *Neurosci. Lett.* **125**, 45–48 (1991).
 101. H. Schoemaker, J. Allen, and S. Z. Langer, Binding of ifenprodil, a novel NMDA antagonist, to a polyamine-sensitive site in the rat cerebral cortex. *Eur. J. Pharmacol.* **176**, 249–250 (1990).
 102. K. Williams, Ifenprodil discriminates subtypes of the *N*-methyl-D-aspartate receptor: Selectivity and mechanisms at recombinant heteromeric receptors. *Mol. Pharmacol.* **44**, 851–859 (1993).
 103. D. Lodge and K. M. Johnson, Noncompetitive excitatory amino acid antagonists. In “TIPS Special Report: The Pharmacology of Excitatory Amino Acids” (D. Lodge and G. Collingridge, eds.), pp. 13–18. Elsevier Trends Journals, Cambridge, U.K., 1991.
 104. K. Keinänen, W. Wisden, B. Sommer, P. Werner, A. Herb, T. A. Verdooran, B. Sakmann, and P. H. Seeburg, A family of AMPA-selective glutamate receptors. *Science* **249**, 556–560 (1990).
 105. T. C. Rainbow, C. M. Wiczorek, and S. Halpain, Quantitative autoradiography of binding sites for [³H]AMPA, a structural analogue of glutamic acid. *Brain Res.* **309**, 173–177 (1984).
 106. E. O. Nielsen, J. Drejer, J. H. Cha, A. B. Young, and T. Honore, Autoradiographic characterization and localization of quisqualate binding sites in rat brain using the antagonist [³H]6-cyano-7-nitroquinoxaline-2,3-dione: Comparison with (*R,S*)-[³H]alpha-amino-3-hydroxy-5-methyl-4-isoxazolepropionic acid binding sites. *J. Neurochem.* **54**, 686–695 (1990).
 107. B. Bettler, J. Egebjerg, G. Sharma, G. Pecht, I. Hermans Borgmeyer, C. Moll, C. F. Stevens, and S. Heinemann, Cloning of a putative glutamate receptor: A low affinity kainate-binding subunit. *Neuron* **8**, 257–265 (1992).
 108. M. J. Sheardown, E. O. Nielsen, A. J. Hansen, P. Jacobsen, and T. Honore, 2,3-Dihydroxy-6-nitro-7-sulfamoyl-benzo(*F*)quinoxaline: A neuroprotectant for cerebral ischemia. *Science* **247**, 571–574 (1990).
 109. D. T. Monaghan and C. W. Cotman, The distribution of [³H]kainic acid binding sites in rat CNS as determined by autoradiography. *Brain Res.* **252**, 91–100 (1982).
 110. P. Werner, M. Voigt, K. Keinänen, W. Wisden, and P. H. Seeburg, Cloning of a putative high-affinity kainate receptor expressed predominantly in hippocampal CA3 cells. *Nature (London)* **351**, 742–744 (1991).
 111. A. Herb, N. Burnashev, P. Werner, B. Sakmann, W. Wisden, and P. Seeburg, The KA-2 subunit of excitatory amino acid receptors shows widespread expression in the brain and forms ion channels with distantly related subunits. *Neuron* **8**, 775–785 (1992).
 112. D. D. Schoepp and R. A. True, 1*S*,3*R*-ACPD-sensitive (metabotropic) glutamate receptor binding in membranes. *Neurosci. Lett.* **145**, 100–104 (1992).

113. D. T. Monaghan, M. C. McMills, A. R. Chamberlin, and C. W. Cotman, Synthesis of [³H]2-amino-4-phosphonobutyric acid and characterization of its binding to rat brain membranes: A selective ligand for the chloride/calcium-dependent class of L-glutamate binding sites. *Brain Res.* **278**, 137–144 (1983).
114. M. Ishida, T. Saitoh, K. Shigamoto, Y. Ohfune, and H. Shinozaki, A novel metabotropic glutamate receptor agonist: Marked depression of monosynaptic excitation in the newborn rat isolated spinal cord. *Br. J. Pharmacol.* **109**, 1169–1177 (1993).
115. E. F. Birse, S. A. Eaton, D. E. Jane, P. L. Jones, R. H. Porter, P. C. Pook, D. C. Sunter, P. M. Udvarhelyi, B. Wharton, P. J. Roberts, and *et al.*, Phenylglycine derivatives as new pharmacological tools for investigating the role of metabotropic glutamate receptors in the central nervous system. *Neuroscience (Oxford)* **52**, 481–488 (1993).
116. J. Watkins and G. Collingridge, Phenylglycine derivatives as antagonists of metabotropic glutamate receptors. *Trends Pharmacol. Sci.* **15**, 333–342 (1994).
117. Y. Hayashi, N. Sekiyama, S. Nakanishi, D. E. Jane, D. C. Sunter, E. F. Birse, P. M. Udvarhelyi, and J. C. Watkins, Analysis of agonist and antagonist activities of phenylglycine derivatives for different cloned metabotropic glutamate receptor subtypes. *J. Neurosci.* **14**, 3370–3377 (1994).
118. K. Williams, A. M. Zappia, D. B. Pritchett, Y. M. Shen, and P. B. Molinoff, Sensitivity of the *N*-methyl-D-aspartate receptor to polyamines is controlled by NR2 subunits. *Mol. Pharmacol.* **45**, 803–809 (1994).
119. M. Ishida, H. Akagi, K. Shimamoto, Y. Ohfune, and H. Shinozaki, A potent metabotropic glutamate receptor agonist: Electrophysiological actions of a conformationally restricted glutamate analogue in the rat spinal cord and *Xenopus* oocytes. *Brain Res.* **537**, 311–314 (1990).
120. V. Bruno, A. Copani, G. Battaglia, R. Raffaele, H. Shinozaki, and F. Nicoletti, Protective effect of the metabotropic glutamate receptor agonist, DCG-IV, against excitotoxic neuronal death. *Eur. J. Pharmacol.* **256**, 109–112 (1994).
121. F. Nicoletti, G. Casabona, A. A. Genazzani, M. R. Lepiscopo, and H. Shinozaki, (2*s*,1'*R*,2'*R*,3'*R*)-2-(2,3-Dicarboxycyclopropyl) glycine enhances quisqualate-stimulated inositol phospholipid hydrolysis in hippocampal slices. *Eur. J. Pharmacol.* **245**, 297–298 (1993).
122. D. D. Schoepp, B. G. Johnson, and J. A. Monn, Inhibition of cyclic AMP formation by a selective metabotropic glutamate receptor agonist. *J. Neurochem.* **58**, 1184–1186 (1992).
123. D. D. Schoepp, J. Goldsworthy, B. G. Johnson, C. R. Salhoff, and S. R. Baker, 3,5-Dihydroxyphenylglycine is a highly selective agonist for phosphoinositide-linked metabotropic glutamate receptors in the rat hippocampus. *J. Neurochem.* **63**, 769–772 (1994).
124. D. E. Jane, P. L. Jones, P. C. Pook, H. W. Tse, and J. C. Watkins, Actions of two new antagonists showing selectivity for different sub-types of metabotropic glutamate receptor in the neonatal rat spinal cord. *Br. J. Pharmacol.* **112**, 809–816 (1994).
125. R. S. Greenwood, R. B. Meeker, A. Abdou, and J. N. Hayward, Kindled seizures induce a long-term increase in vasopressin mRNA. *Mol. Brain Res.* **24**, 20–26 (1994).
126. F. J. Ehlert, W. R. Roeske, and H. I. Yamamura, Mathematical analysis of the kinetics of competitive inhibition in neurotransmitter receptor binding assays. *Mol. Pharmacol.* **19**, 367–371 (1981).
127. A. De Lean, A. A. Hancock, and R. J. Lefkowitz, Validation and statistical analysis of a computer modeling method for quantitative analysis of radioligand binding data for mixtures of pharmacological receptor subtypes. *Mol. Pharmacol.* **21**, 5–16 (1982).
128. G. A. Weiland and P. B. Molinoff, Quantitative analysis of drug–receptor interactions: I. Determination of kinetic and equilibrium properties. *Life Sci.* **29**, 313–330 (1981).

129. P. B. Molinoff, B. B. Wolfe, and G. A. Weiland, Quantitative analysis of drug-receptor interactions: II. Determination of the properties of receptor subtypes. *Life Sci.* **29**, 427-443 (1981).
130. J. T. Greenamyre, A. B. Young, and J. B. Penney, Quantitative autoradiographic distribution of L-[³H]glutamate-binding sites in rat central nervous system. *J. Neurosci.* **4**, 2133-2144 (1984).
131. G. Paxinos and C. Watson, "The Rat Brain in Stereotaxic Coordinates." Academic Press, Sydney, 1986.
132. E. O. Nielsen, J. H. Cha, T. Honore, J. B. Penney, and A. B. Young, Thiocyanate stabilizes AMPA binding to the quisqualate receptor. *Eur. J. Pharmacol.* **157**, 197-203 (1988).
133. B. I. Kanner, Glutamate transporters from brain. A novel neurotransmitter transporter family. *FEBS Lett.* **325**, 95-99 (1993).
134. B. I. Kanner, N. Danbolt, G. Pines, H. Koepsell, E. Seeberg, and J. S. Mathisen, Structure and function of the sodium and potassium-coupled glutamate transporter from rat brain. *Biochem. Soc. Trans.* **21**, 59-61 (1993).
135. Y. Kanai, C. P. Smith, and M. A. Hediger, A new family of neurotransmitter transporters: The high affinity glutamate transporters. *FASEB J.* **7**, 1450-1459 (1993).
136. G. Pines, N. C. Danbolt, M. Bjoras, Y. Zhang, A. Bendahan, L. Eide, H. Koepsell, J. Storm Mathisen, E. Seeberg, and B. I. Kanner, Cloning and expression of a rat brain L-glutamate transporter. *Nature (London)* **360**, 464-467 (1992).
137. Y. Kanai and M. A. Hediger, Primary structure and functional characterization of a high-affinity glutamate transporter. *Nature (London)* **360**, 467-471 (1992).
138. U. Klockner, T. Storck, M. Conradt, and W. Stoffel, Functional properties and substrate specificity of the cloned L-glutamate/L-aspartate transporter GLAST-1 from rat brain expressed in *Xenopus* oocytes. *J. Neurosci.* **14**, 5759-5765 (1994).
139. U. Klockner, T. Storck, M. Conradt, and W. Stoffel, Electrogenic L-glutamate uptake in *Xenopus laevis* oocytes expressing a cloned rat brain L-glutamate/L-aspartate transporter (GLAST-1). *J. Biol. Chem.* **268**, 14594-14596 (1993).
140. T. Storck, S. Schulte, K. Hofmann, and W. Stoffel, Structure, expression, and functional analysis of a Na⁺-dependent glutamate/aspartate transporter from rat brain. *Proc. Natl. Acad. Sci. U.S.A.* **89**, 10955-10959 (1992).
141. K. Tanaka, Pharmacological characterization of a cloned rat glutamate transporter (GluT-1). *Brain. Res. Mol. Brain Res.* **21**, 167-170 (1994).
142. K. Tanaka, Expression cloning of a rat glutamate transporter. *Neurosci. Res.* **16**, 149-153 (1993).
143. J. L. Arriza, W. A. Fairman, J. I. Wadiche, G. H. Murdoch, M. P. Kavanaugh, and S. G. Amara, Functional comparisons of three glutamate transporter subtypes cloned from human motor cortex. *J. Neurosci.* **14**, 5559-5569 (1994).
144. J. Wharton and J. M. Polak (eds.), "Receptor Autoradiography: Principles and Practice." Oxford Univ. Press, New York, 1993.
145. C. A. Boast, E. W. Snowhill, and C. A. Altar (eds.), "Quantitative Receptor Autoradiography." Alan R. Liss, New York, 1986.
146. H. Monyer, N. Burnashev, D. J. Laurie, B. Sakmann, and P. H. Seeburg, Developmental and regional expression in the rat brain and functional properties of four NMDA receptors. *Neuron* **12**, 529-540 (1994).
147. C. M. Testa, D. G. Standaert, A. B. Young, and J. B. Penney, Jr., Metabotropic glutamate receptor mRNA expression in the basal ganglia of the rat. *J. Neurosci.* **14**, 3005-3018 (1994).
148. Y. Nakajima, H. Iwakabe, C. Akazawa, H. Nawa, R. Shigemoto, N. Mizuno, and S. Nakanishi, Molecular characterization of a novel retinal metabotropic glutamate receptor

- mGluR6 with a high agonist selectivity for L-2-amino-4-phosphonobutyrate. *J. Biol. Chem.* **268**, 11868–11873 (1993).
149. N. Okamoto, S. Hori, C. Akazawa, Y. Hayashi, R. Shigemoto, N. Mizuno, and S. Nakanishi, Molecular characterization of a new metabotropic glutamate receptor mGluR7 coupled to inhibitory cyclic AMP signal transduction. *J. Biol. Chem.* **269**, 1231–1236 (1994).
 150. B. Bettler, J. Boulter, I. Hermans-Borgmeyer, A. O'Shea-Greenfield, E. S. Deneris, C. Moll, U. Borgmeyer, M. Hollmann, and S. Heinemann, Cloning of a novel glutamate receptor subunit, GluR5: Expression in the nervous system during development. *Neuron* **5**, 583–595 (1990).
 151. J. Egebjerg, B. Bettler, I. Hermans-Borgmeyer, and S. Heinemann, Cloning of a cDNA for a glutamate receptor subunit activated by kainate but not AMPA. *Nature (London)* **351**, 745–748 (1991).
 152. W. S. Young, *In situ* hybridization histochemistry. In "Handbook of Chemical Neuroanatomy" (A. Bjorklund, T. Hokfelt, F. G. Wouterlood, and A. N. van den Pol, eds.), pp. 481–506. Elsevier, New York, 1990.
 153. J. T. McCabe and D. W. Pfaff, *In situ* hybridization: A methodological guide. In "Gene Probes" (P. M. Conn, ed.), pp. 98–126. Academic Press, San Diego, 1989.

12

Chromatographic Methods for Analyzing β -Endorphin and Related Peptides

William R. Millington

Amy B. Manning

*Division of Molecular Biology and
Biochemistry*

*University of Missouri-Kansas City
Kansas City, Missouri 64108*

INTRODUCTION

β -Endorphin is a 31-amino-acid peptide that was initially isolated from porcine pituitary by Bradbury and co-workers in the mid-1970s (1). During the past two decades, β -endorphin(1-31)'s potent analgetic activity has stimulated intense research interest (2) and the peptide has become enconced in the popular imagination as the endogenous substance responsible for much that is deemed pleasurable in life (3). Largely forgotten, however, is that Bradbury and coworkers initially isolated not one, but two structurally related peptides, β -endorphin(1-31) and a shorter fragment, β -endorphin(1-27) (1). Later, Smyth *et al.* discovered four additional analogs: β -endorphin(1-26), α -N-acetyl- β -endorphin(1-31), α -N-acetyl- β -endorphin(1-27), and α -N-acetyl- β -endorphin(1-26) (4). Subsequent elucidation of the post-translational processing pathway for β -endorphin(1-31)'s precursor, pro-opiomelanocortin (POMC), confirmed that these carboxy-terminal-shortened and α -N-acetylated peptides are sequentially derived

from β -endorphin(1-31) (Figure 1) (5). Thus, in actuality, β -endorphin is not one, but a family of structurally related peptides.

From a practical, analytical standpoint, β -endorphin(1-31) processing is important to consider because most of the antisera used to measure β -endorphin immunoreactivity recognize all six β -endorphin analogs as well as β -lipotropin. This methodological detail complicates the analysis of β -endorphin, in part because β -endorphin(1-31) processing is tissue specific, which means that different tissues may synthesize completely different assortments of β -endorphin peptides yet, when measured by radioimmunoassay (RIA), contain equivalent amounts of β -endorphin immunoreactivity (2,6,7). This principle is clearly illustrated by β -endorphin(1-31) processing in the anterior and intermediate lobes of the rat pituitary (5,6). In the rat anterior lobe corticotrophs synthesize approximately equal amounts of β -endorphin(1-31) and β -lipotropin, whereas in the intermediate lobe, melanotrophs primarily express the α -N-acetylated congeners of β -endorphin(1-27) and β -endorphin(1-26) (Figure 2). Hence, the term “ β -endorphin

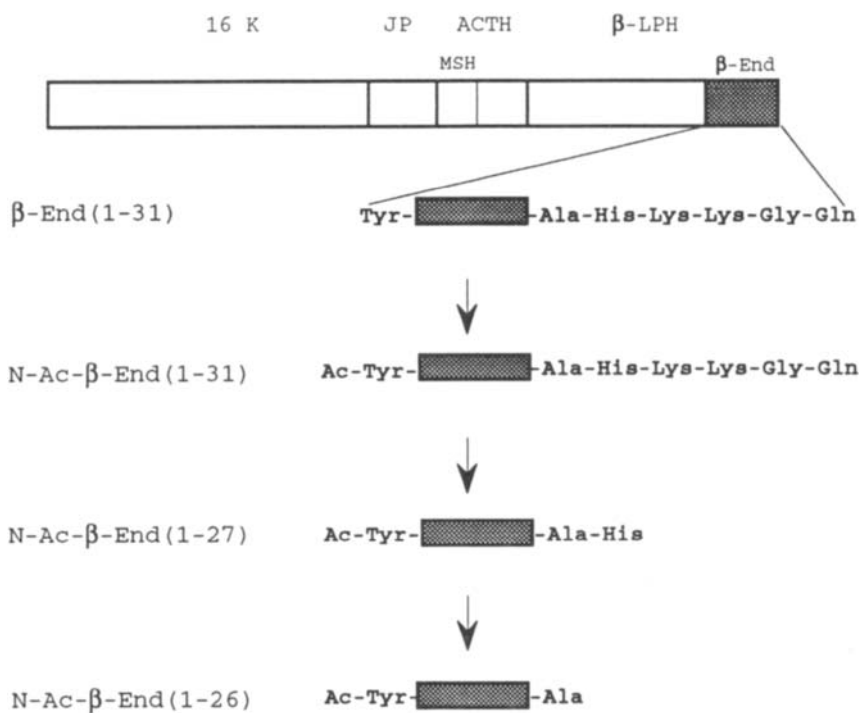


FIGURE 1. β -Endorphin(1-31) processing in the intermediate lobe of the rat pituitary.

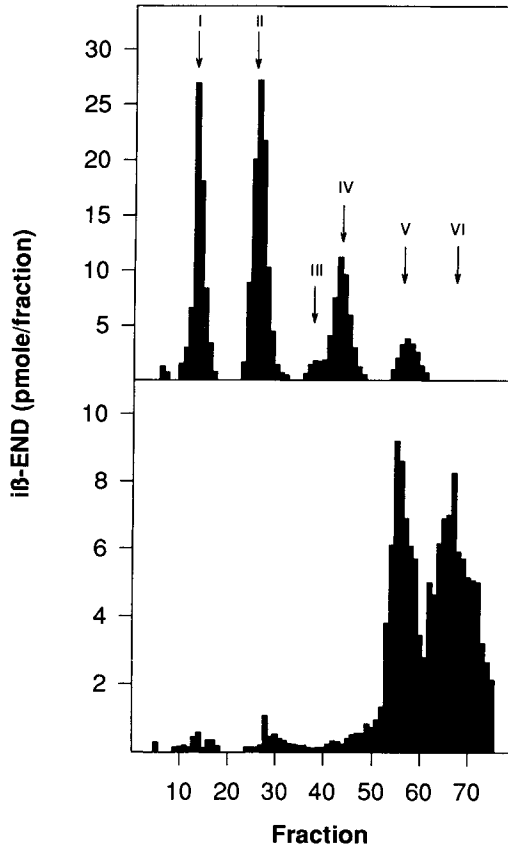


FIGURE 2. Analysis of β -endorphin peptides in the intermediate lobe (IL; upper panel) and anterior lobe (AL; lower panel) of the rat pituitary. β -Endorphin peptides were separated from acid extracts of rat IL or AL by cation-exchange chromatography using a SP-Sephadex C-25 column. The arrows mark the elution positions of α -N-acetyl- β -endorphin(1-26) (I), α -N-acetyl- β -endorphin(1-27) (II), β -endorphin(1-27) (III), α -N-acetyl- β -endorphin(1-31) (IV), β -endorphin(1-31) (V), and β -lipotropin (VI).

immunoreactivity” refers to entirely different peptides when crude extracts of the two pituitary lobes are analyzed by RIA.

β -Endorphin(1-31) also undergoes extensive post-translational processing in brain and in peripheral tissues that express the POMC gene (2,7). In brain, β -endorphin(1-31) processing is regionally selective; β -endorphin(1-31) is the major form localized throughout much of the forebrain, but α -N-acetylated, carboxy-terminal-truncated congeners predominate in the brain stem and several other regions (6–8). N- and C-terminally modi-

fied forms are also major end products in many peripheral tissues (7). In the heart, for example, β -endorphin(1-31) is almost entirely converted to α -N-acetylated, carboxy-terminal-shortened derivatives (Figure 3) (9); presumably these peptides are produced by cardiac myocytes, which have been shown to express POMC mRNA (10). Thus, virtually every tissue that synthesizes β -endorphin(1-31) further modifies the peptide, albeit to varying degrees.

A second important reason for identifying the specific β -endorphin peptides generated by POMC neurons and endocrine cells is that processing dramatically changes the peptide's biological activity (2,11). Indeed, only one of the six β -endorphin peptides, β -endorphin(1-31), produces analgesia at physiologically relevant doses (12). But far from being inactive, N- and C-terminally modified β -endorphin peptides produce a variety of effects in brain and peripheral tissues (2,7,11). β -Endorphin(1-27), for example,

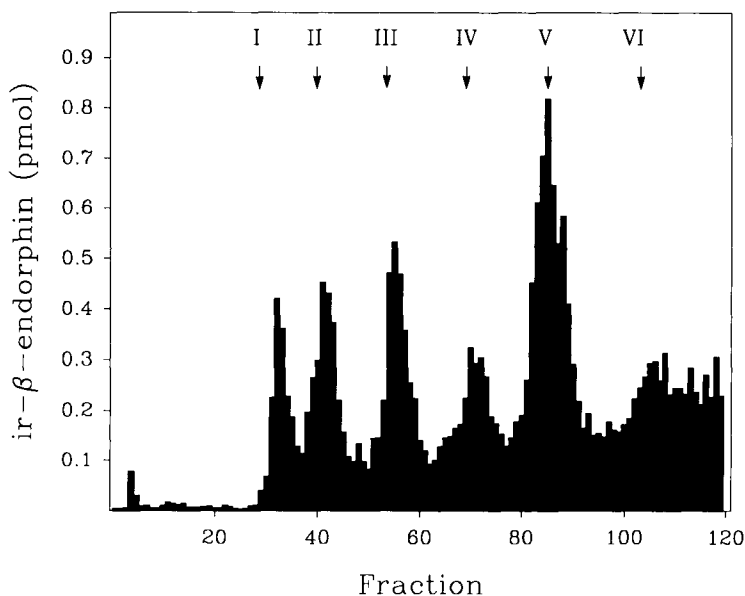


FIGURE 3. Cation-exchange HPLC separation of β -endorphin peptides in rat heart. An acid extract of five rat hearts was fractionated by size-exclusion chromatography, fractions containing β -endorphin-sized peptides were combined, and individual β -endorphin peptides were separated by cation-exchange HPLC. The arrows indicate the elution positions of α -N-acetyl- β -endorphin(1-26) (I), α -N-acetyl- β -endorphin(1-27) (II), β -endorphin(1-26) (III), β -endorphin(1-27) (IV), α -N-acetyl- β -endorphin(1-31) (V), and β -endorphin(1-31) (VI). [Reprinted with permission from W. R. Millington, V. R. Evans, L. J. Forman, and C. N. Battie (1993). *Peptides* **14**, 1141–1147.]

functions as an opioid receptor antagonist that, paradoxically, inhibits β -endorphin(1-31)-induced analgesia when centrally injected (12). Consequently, merely assaying tissue β -endorphin immunoreactivity by RIA provides little definitive information about either the structure or the function of β -endorphin peptides. Nevertheless, it is not unusual to encounter published studies in which RIA measurement of β -endorphin immunoreactivity in crude tissue extracts or unextracted plasma is tacitly assumed to represent the opioid form of the peptide.

In this chapter, we will review analytical methods commonly used to isolate β -endorphin-related peptides from biological tissues, including plasma. For the most part, these are relatively standard techniques for separating peptides, but like most “standard” methods, they provide a wealth of opportunities for technical problems and/or experimental error to occur, particularly for investigators new to the field of peptide analysis. In addition to providing an overview of procedures, the review will highlight problems that can arise and provide a brief description of alternative methods for achieving the same objectives.

PROCEDURES

Tissue Extraction Procedures

The extraction of neuroendocrine peptides from brain or other tissue can be a critical step in peptide analysis, particularly for tissues that contain low peptide concentrations. Ideally, the extraction procedure should recover the endogenous peptide quantitatively without generating artifactual structural modifications and should exclude as much unrelated protein, lipid, and nucleic acids as possible. Pituitary tissue, which contains relatively large amounts of β -endorphin and other POMC peptides, is often homogenized in acetic acid, or other weak acids (concentrations used vary from 0.5 *M* to 50% v/v), and following centrifugation, the extract can be diluted and assayed by RIA or applied directly to a size-exclusion or cation-exchange column. For brain and other tissues additional purification and sample concentration steps are usually required before meaningful data can be generated. For these applications extraction on small octadecylsilyl-silica (C-18) solid-phase extraction (SPE) columns is generally desirable (9,13,14).

Procedure

1. The tissue is homogenized in an ice-cold solution of 1% trifluoroacetic acid (TFA), 5% formic acid, 1 *M* HCl, and 1% NaCl (at least 5 ml/g tissue) and subsequently centrifuged at 100,000 *g* for 30 min.

2. The supernatant fluid is then loaded onto a C-18 SPE column (Sep Pak, Waters Associates, Milford, MA). The column is washed with 5 ml 0.05% TFA and then with 2 ml 0.05% TFA containing 10% acetonitrile and β -endorphin peptides are eluted with 4 ml 0.05% TFA containing 50% acetonitrile.

3. The 0.05% TFA/50% acetonitrile eluant is concentrated by rotary evaporation to remove acetonitrile and the remaining aqueous portion lyophilized.

Comments

β -Endorphin-related peptides are quite soluble in aqueous solvents at acid pH and are generally extracted from tissue homogenates with good recovery. Recovery from C-18 solid-phase extraction columns can vary, however, depending on the extraction medium used. Homogenization in acetic acid or other weak acids generally removes endogenous β -endorphin peptides from tissue adequately, but retention on C-18 SPE columns can be both low and variable (13,14). Extraction in TFA/formic acid/HCl/NaCl, as described earlier, produces considerably higher recovery from C-18 SPE columns, 90% or more, and consistently extracts β -lipotropin and other POMC peptides with equivalent recovery (13,14). The higher SPE column recovery is not entirely unexpected because a greater percentage of soluble protein is precipitated and because TFA acts as an ion pairing agent that facilitates peptide retention by the hydrophobic C-18 resin.

Peptide degradation by tissue proteases can also cause both low recovery and artifactual changes in peptide structure. β -Endorphin is not excessively vulnerable to tissue proteases however, and acid extraction is generally sufficient to prevent degradation. Nevertheless, some extraction procedures include protease inhibitors in the extraction medium or call for boiling the tissue or tissue homogenate to ensure protease inactivation. These are logical strategies but they do not necessarily lead to higher peptide recoveries. Protease inhibitors have been shown to be without effect on immunoreactive β -endorphin recovery from pituitary tissue (15), for example, and boiling can actually lower recovery of some peptides (16).

Selection of an extraction procedure must also consider subsequent steps in the overall analysis. TFA/formic acid/HCl/NaCl would seem to be an ideal extraction medium even if the SPE column step is omitted and the sample simply lyophilized and assayed. But despite its volatility TFA is difficult to remove by lyophilization and the traces that remain can interfere with subsequent RIA analysis if the sample is not diluted extensively with RIA assay buffer. Conversely, SPE can lead to a false sense of security because SPE column extracts can still contain relatively large amounts of

protein, including contaminants that may interfere with subsequent RIA analysis. This problem can be of particular concern when SPE columns are used to concentrate tissue extracts containing low concentrations of β -endorphin peptides.

Additional considerations must often be made if more than one peptide is to be analyzed from the same extract. Often overlooked is the importance of assessing the SPE column recovery for each peptide independently. Unexpected difficulties can also be encountered when an extraction system is optimized for one peptide, then used to extract multiple peptides simultaneously. Boiling tissue extracts in HCl may be an appropriate procedure for extracting β -endorphin, for example, but it reportedly converts *N,O*-diacetyl- α -MSH to α -MSH, complicating simultaneous analysis of β -endorphin- and α -MSH-related peptides (17). Finally, acid extraction oxidizes the methionine residues present in both the β -endorphin and α -MSH sequences; the inclusion of 1% 2-mercaptoethanol in the extraction medium reduces (but seldom eliminates) methionine sulfoxide formation (Figure 4).

Plasma Extraction

The measurement of peptide concentrations in plasma often provides the analytical biochemist with a special challenge, and so it is for β -endorphin, at least in human plasma. Measuring plasma β -endorphin immunoreactivity in the rat is relatively facile and with many β -endorphin RIAs extraction is not essential (18). Nevertheless, it may be desirable if mandated by low assay sensitivity and/or specificity, but a simple protein precipitation step will often suffice to concentrate and partially purify plasma β -endorphin peptides (19). Plasma β -endorphin concentrations are far lower in the human, however, and normally range no higher than 10 fmol/ml, approximately 5–10% of rat plasma concentrations. Extraction and concentration are therefore essential when measuring β -endorphin immunoreactivity in human plasma.

Naturally, a variety of procedures have been used to extract β -endorphin peptides from human plasma but many generate low and variable peptide recoveries. The highest and most consistent recoveries are attained by using a modification of the extraction procedure discussed earlier in which plasma is layered directly onto a C-18 SPE column (20,21). Recovery of β -endorphin immunoreactivity by these methods is reportedly 90% or higher, and by extracting 3–6 ml or more, plasma β -endorphin peptides are both purified and concentrated sufficiently to generate reproducible data with most available RIAs. Few other precautions must be taken to extract plasma other than even more dogged consistency when layering, washing, and eluting the sample. EDTA is generally used as an anticoagulant because heparin

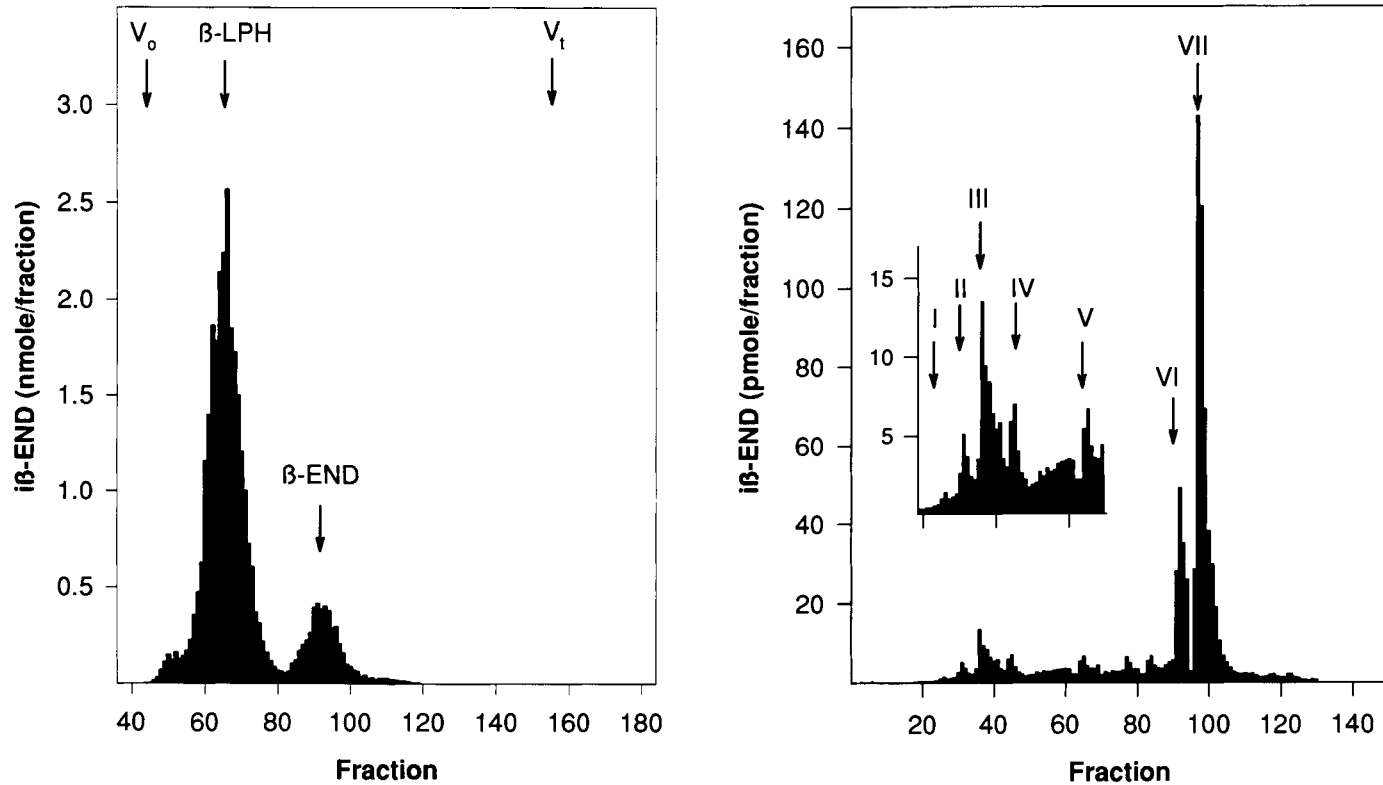


FIGURE 4. Analysis of β -endorphin-related peptides in the human pituitary gland by size-exclusion chromatography (left panel) and cation-exchange HPLC (right panel). (Left) an acid extract of a human pituitary gland was fractionated on a Sephadex G-50 fine column (1.5 \times 100 cm). β -LPH, β -lipotropin; β -END, β -endorphin; V_0 = void volume; V_t = total volume. (Right) Sephadex G-50 column fractions containing β -endorphin-sized peptides were combined and individual β -endorphin peptides were separated by cation-exchange HPLC. The arrows indicate the elution positions of α -N-acetyl- β -endorphin(1-26) (I), α -N-acetyl- β -endorphin(1-27) (II), β -endorphin(1-26) (III), β -endorphin(1-27) (IV), α -N-acetyl- β -endorphin(1-31) (V), β -endorphin(-1-31) methionine sulfoxide (VI), and β -endorphin(1-31) (VII). [Reprinted with permission from V. R. Evans, A. B. Manning, L. H. Bernard, B. M. Chronwall, and W. R. Millington (1994). *Endocrinology (Baltimore)* **134**, 97–106.]

reportedly interferes with the analysis of plasma β -endorphin (20), although this problem can apparently be circumvented by using low heparin concentrations (22). C-18 SPE columns can also be used to extract and concentrate cerebrospinal fluid (CSF) β -endorphin peptides, but since CSF contains little in the way of interfering protein or lipid, extraction is often unnecessary and adequate sample concentration can usually be achieved by lyophilization (19).

Recently, Monger and Olliff developed a modification of this procedure in which β -endorphin peptides are extracted from human plasma by cation exchange on silica, rather than C-18, SPE columns (22). Silica SPE columns generated higher β -endorphin recoveries than C-18 columns whether β -endorphin was extracted in physiologically relevant concentrations (250 pg) or higher amounts (4 μ g). Plasma samples were first acidified with 100 μ l 10% TFA which precipitates plasma proteins and enhances the capability of concentrating the sample—up to 20-fold. Although proteolytic degradation has also been of concern when analyzing plasma β -endorphin, rapid acidification obviates the need for protease inhibitors. Another advantage of this procedure is that β -endorphin peptides are eluted with low volumes (0.5 to 1.0 ml) of high-performance liquid chromatography (HPLC) mobile phase containing only 32% acetonitrile, and so the silica SPE column eluate can be layered directly onto a reverse-phase HPLC column without lyophilization; this is generally not possible with C-18 SPE columns, which require higher acetonitrile concentrations. Hence, this procedure generates excellent recoveries and offers several additional advantages that may make it the method of choice for extracting β -endorphin from human plasma.

Procedures for Separating β -Endorphin from β -Lipotropin and POMC

The large differences in molecular size between β -lipotropin and β -endorphin make size-exclusion chromatography (SEC) an ideal separation method. A large variety of resins, column sizes, elution rates, and so on have been used for this purpose, but essentially all utilize an acidic mobile phase, often containing bovine serum albumin (BSA) to reduce loss due to absorption to glass and reducing agents to prevent oxidation (23). One important variable is simply the degree of resolution achieved; somewhat surprisingly, many published methods fail to attain baseline separation between β -endorphin- and β -lipotropin-sized peptides. The following is a modification of commonly used procedure that produces good resolution between these and other POMC peptides (Figure 4) (14,24).

Procedure

1. Sephadex G-50 fine resin (Pharmacia Biotech, Piscataway, NJ) is equilibrated overnight in degassed column buffer (10% formic acid containing 10 $\mu\text{g/ml}$ bovine serum albumin and 0.1% 2-mercaptoethanol) at 4°C. The resin is then suspended in a 1.5 \times 100-cm column (Spectrum Medical Industries, Houston, TX), equilibrated with at least 10 column volumes of buffer at a flow rate of 3 ml/hr controlled by a peristaltic pump (Rainin Instruments, Emeryville, CA), and calibrated with blue dextran to mark the void volume and 75 μl 2-mercaptoethanol, which identifies the total volume. Close inspection of the blue dextran solution as it passes through the column aids in the detection of bubbles and other flaws in the resin packing.

2. The sample is lyophilized, reconstituted in 2.0-ml column buffer, and layered carefully on the resin. An aliquot is retained to determine total protein and peptide levels. The column is eluted at a flow rate of 3 ml/hr at 4°C and fractions are collected at 20-min intervals. Protein elution is monitored with a UV absorbance detector at 280 nm. Subsequently, the column is calibrated with β -lipotropin, β -endorphin(1-31), blue dextran, and 2-mercaptoethanol; alternatively, BSA (1 mg) and 2-mercaptoethanol (75 μl) can be layered with the sample to mark the void and total volumes during sample elution. Iodinated peptides are also commonly used for column calibration, although endogenous peptides do not strictly coelute with iodinated standards.

3. Column fractions are lyophilized and analyzed for β -endorphin immunoreactivity by RIA using an antiserum that cross-reacts equally with all six β -endorphin(1-31)-related peptides and β -lipotropin (18).

Comments

Sephadex G-50 SEC provides excellent resolution between β -endorphin- and β -lipotropin-sized peptides (Figure 4). The procedure is also capable of partially separating β -endorphin(1-31) from its carboxy-terminal-shortened congeners, although the resolution is quite poor (25). Like all SEC separations, column length and buffer flow rate are important determinants of peptide resolution. Acidic solvents, such as formic acid, can be used to reduce nonspecific peptide adsorption, which enhances recovery, and are sufficiently volatile to remove by rotary evaporation and/or lyophilization prior to RIA analysis. An additional, albeit obvious, asset is that other POMC-derived peptides can be analyzed in the same SEC column fractions, assuming that assay sensitivities and/or peptide concentrations are sufficient for multiple analyses.

A minor liability of the described procedure is that formic acid is rather unpleasant to work with and can be detrimental to metal surfaces. Furthermore, although formic acid is volatile, trace amounts may remain following lyophilization and can interfere with subsequent RIA analysis if the samples are not diluted sufficiently with buffer. A variety of alternative solvents are available; 50% acetic acid has also been widely used, for example, and offers many of the same advantages (23).

A second problem is simply the time required to complete the analysis. SEC HPLC columns overcome this problem; a full SEC analysis can be completed within 2 hr (14). Baseline resolution between β -endorphin(1-31) and β -lipotropin is difficult to achieve, however, and the necessity of using multiple columns makes the procedure somewhat costly (23). In our hands, coupling two or three Bio-Sil TSK SEC columns in series produces adequate resolution, but it is far from ideal (21). SEC HPLC columns specifically developed for peptide analysis have recently become available; polyhydroxyethyl aspartamide columns (Nest Group, Inc., Southborough, MA), for example, are exceptionally versatile although they have not, to our knowledge, been evaluated for separating β -endorphin-related peptides (26).

In theory, β -endorphin(1-31) might be distinguished from β -lipotropin by using selective antisera, although in practice this has not been a particularly fruitful strategy. Antisera directed against the N-terminal portion of β -lipotropin do not detect β -endorphin(1-31), of course, but they cross-react fully with γ -lipotropin, complicating the analysis (27). Conversely, antisera raised against the N-terminal of β -endorphin do not recognize β -lipotropin, but unfortunately cross-react with met-enkephalin; such antisera also fail to detect α -N-acetylated β -endorphin peptides. In theory, radioreceptor assays may also be useful for selectively detecting β -endorphin(1-31) but met-enkephalin and other opioid peptides interfere with this procedure, and again α -N-acetylated β -endorphin analogs will not be detected. A more successful alternative, developed by Krieger *et al.*, has been to separate β -endorphin peptides from β -lipotropin and γ -lipotropin by using a series of immunoaffinity columns coupled to β -lipotropin and β -endorphin-specific antisera (27). Nevertheless, SEC remains the most widely used procedure for separating β -endorphin peptides from β -lipotropin and POMC.

Analysis of Individual β -Endorphin Peptides

β -Endorphin peptides have been notably difficult to separate by reverse-phase HPLC, an otherwise standard method for analyzing neuropeptides, because the structural differences among them are relatively minor. Instead, most investigators in the field now use cation-exchange chromatography,

which exploits differences in charge at acidic pH generated primarily by basic amino acid residues in the β -endorphin sequence. Initially, this was achieved by using standard low-pressure SP-Sephadex C-25 columns. As one might predict, however, resolution between peptides with equivalent charge was limited; specifically, β -endorphin(1-26) and α -N-acetyl- β -endorphin(1-27) and β -endorphin(1-27) and α -N-acetyl- β -endorphin(1-31) were difficult to resolve (Figure 2). Smyth overcame this problem by using relatively long, narrow-bore columns (70×0.7 cm), by converting SP-Sephadex C-25 from the sodium to the pyridinium form, and by separating the peptides with a pyridine gradient (23). Excellent resolution of the six β -endorphin peptides is achieved with this procedure (6,23).

Subsequent development of ion-exchange HPLC columns has largely replaced SP-Sephadex C-25, providing comparable resolution with considerably faster run times (28–30). These columns provide adequate resolution of peptides with the same ionic charge, evidently through nonionic interactions with the column matrix. The first to become available were standard silica-based columns that provided good resolution but were susceptible to pressure changes and, overall, somewhat delicate to use. The nonporous, polymer-based columns currently available retain the resolving power but exhibit enhanced stability and even faster run times (24). The following method relies on a polymer-based column.

Procedure

1. Fractions from the SEC column containing β -endorphin immunoreactivity are pooled and lyophilized, and the sample is reconstituted in 45 mM sodium acetate (pH 2.5) containing 30% acetonitrile. Aliquots are removed for analysis of protein and peptide content.

2. The sample is applied to a 50×7.8 -mm MA7S cation-exchange column (BioRad Laboratories, Richmond, CA) equilibrated with 45 mM sodium acetate/30% acetonitrile, and β -endorphin peptides are eluted with a 60-min linear gradient to 355 mM sodium acetate/30% acetonitrile at a flow rate of 1 ml/min.

3. Fractions are collected at 0.5-min intervals and analyzed for β -endorphin immunoreactivity by RIA. Following each sample analysis, the column is calibrated with 2.0 μ g each of α -N-acetylated and des-acetyl β -endorphin(1-31), β -endorphin(1-27), and β -endorphin(1-26). If necessary, the elution positions of methionine sulfoxide β -endorphin derivatives are determined by incubating 2 μ g of each peptide standard in 100 μ l 10% hydrogen peroxide for 30 min before applying them to the column. Alternatively, all six β -endorphin peptides can be fully converted to their methionine sulfox-

ide derivatives by incubation in 1 mM sodium metaperiodate for 30 min (23).

Comments

Cation-exchange HPLC provides rapid, high-resolution separation of β -endorphin peptides (Figures 3 and 4). Nonporous, polymer-based cation-exchange columns are especially pleasurable to work with because they are resistant to pressure and pH fluctuations and less susceptible to contamination by extraneous proteins than porous, silica-based columns. In our hands, they are also less susceptible to "ghost peaks," that is, small amounts of peptide standards retained by the column and eluted by subsequent gradients, a common problem with HPLC peptide analysis (31). Nevertheless, this does occur with nonporous columns and must be carefully monitored. We routinely control for this problem by washing the column extensively and repeatedly with 0.5 M sodium acetate after each standard calibration, then confirm that peptide standards have been completely removed by running a sample blank, collecting fractions, and analyzing them as one would a sample. It is important that this procedure should precede each sample analysis. Alternatively, the column can be calibrated with lower amounts of peptide standards and detected by RIA. More extensive column regeneration procedures have also been recommended (30).

Despite the difficulties involved with reverse-phase HPLC analysis of β -endorphin peptides, several laboratories have been successful with this method. Reverse-phase HPLC may be particularly useful for analyzing β -endorphin peptides in brain regions, such as the hypothalamus, in which β -endorphin(1-31), β -endorphin(1-27), and β -endorphin(1-26) account for the major portion of β -endorphin immunoreactivity (32). Nevertheless, Wilkinson and Dorsa achieved quite good baseline separation of all six β -endorphin congeners by using a precisely controlled gradient, a slow flow rate (0.2 ml/min), and frequent fraction collection (33). These and other reports demonstrate that it is feasible to analyze β -endorphin peptides by using reverse-phase HPLC columns, which are generally available in most analytical laboratories.

Reverse-phase HPLC is also the method of choice for analyzing γ -endorphin [β -endorphin(1-16)], α -endorphin [β -endorphin(1-17)], and their α -N-acetylated congeners (33-35). These are relatively minor products of β -endorphin processing, comprising approximately 5% of β -endorphin immunoreactivity, in the intermediate pituitary and brain, that are not recognized by most midregion β -endorphin antisera. α -Endorphin and γ -endorphin can be separated relatively easily by using standard gradient elution procedures applicable for most peptide separations (34,35). Evans

et al. have recently published an excellent review of reverse-phase HPLC peptide analysis (36).

β -Endorphin peptides have also been separated by Sephadex G-50 SEC, although this procedure is only capable of separating β -endorphin(1-31) from β -endorphin(1-27) and β -endorphin(1-26) (37). SEC is adequate for discriminating opioid from nonopioid β -endorphin peptides, particularly if coupled with an immunoassay that uses an α -N-acetyl- β -endorphin selective antiserum (38), although it is incapable of distinguishing the individual molecular forms of β -endorphin. SEC and reverse-phase HPLC are thus useful methods, but the simplicity and resolving capability of cation-exchange HPLC continue to make it the method of choice for most applications.

Analysis of β -Endorphin Peptides in the Human Pituitary

Figure 4 provides an example in which the procedures for analyzing β -endorphin peptides, summarized in Table I, were used to investigate β -endorphin processing in the human pituitary. The adult human lacks a well-defined intermediate lobe, suggesting that, like the rat anterior pituitary (Figure 2), β -endorphin(1-31) is not further processed in the human pituitary. Alternatively, evidence that a few residual intermediate lobe cells remain in the human anterior lobe raises the possibility that small amounts of α -N-acetylated, carboxy-terminal-shortened β -endorphin peptides may be present in the gland.

To test these alternative hypotheses we analyzed the β -endorphin peptides present in a series of human pituitaries (24). In Figure 4, an individual

TABLE I. Summary of Extraction and Chromatographic Analysis of β -Endorphin Peptides

1. Extraction: Homogenize in 1% TFA, 5% formic acid, 1 M HCl, and 1% NaCl (5 ml/g) and centrifuge at 100,000g for 30 min. Extract β -endorphin peptides from the supernatant fluid with a C-18 SPE column and elute with 0.05% TFA/50% acetonitrile. Remove solvents by rotary evaporation and lyophilize. Reconstitute in 2 ml 10% formic acid buffer.
2. Size-exclusion chromatography: Load sample onto a Sephadex G-50 column (1.5 \times 100 cm) and elute with 10% formic acid buffer (3 ml/hr). Lyophilize fractions, reconstitute in RIA buffer, and assay for β -endorphin immunoreactivity. Pool peptide-containing fractions, lyophilize, and reconstitute in 1 ml 45 mM sodium acetate containing 30% acetonitrile.
3. Cation-exchange HPLC: Equilibrate MA7S cation-exchange HPLC column (50 \times 7.8 mm) with 45 mM sodium acetate (pH 2.5)/30% acetonitrile. Load sample and elute β -endorphin peptides with a 60-min linear gradient to 355 mM sodium acetate/30% acetonitrile. Analyze fractions for β -endorphin immunoreactivity by RIA.

human pituitary gland was homogenized and centrifuged, and the supernatant fluid was extracted by using a C-18 SPE column (Table I). Subsequent fractionation of the pituitary extract on a Sephadex G-50 fine column resolved two peaks of β -endorphin immunoreactivity coeluting with porcine β -lipotropin and camel β -endorphin(1-31) standards; the larger peak, containing approximately 80% of total immunoreactivity, coeluted with β -lipotropin. A third peak containing small amounts of higher-molecular-weight immunoreactive material—presumably POMC—eluted near the void volume. Thus, only a limited proportion of the β -lipotropin produced in the human pituitary is processed further to β -endorphin-sized molecules.

Fractions containing β -endorphin immunoreactivity were subsequently pooled, lyophilized, and reconstituted in 45 mM sodium acetate/30% acetonitrile and individual β -endorphin peptides were separated by cation-exchange HPLC (Table I). RIA using an antiserum that recognizes all six congeners and their methionine sulfoxide derivatives (18) revealed that the major portion of β -endorphin immunoreactivity eluted as a single peak coeluting with human β -endorphin(1-31) standards (Figure 4). Small amounts of immunoreactivity also coeluted with α -N-acetyl- β -endorphin(1-31), α -N-acetylated and des-acetyl β -endorphin(1-27), β -endorphin(1-26), and β -endorphin(1-31) methionine sulfoxide. The presence of small amounts of α -N-acetylated β -endorphin peptides was consistent with the results of immunohistochemical experiments showing that α -N-acetyl- β -endorphin immunoreactive cells were dispersed throughout the human anterior lobe (24). Hence, the human pituitary gland N- and C-terminally modifies a very small proportion of the β -endorphin(1-31) it synthesizes.

CONCLUSIONS

β -Endorphin(1-31) processing provides a clear-cut example of two general principles in peptide processing: first, that relatively minor changes in peptide structure, generated post-translationally, often produce profound changes in peptide bioactivity; and second, that peptide processing is often heterogeneous, producing stable assemblies of precursors, products, and intermediates rather than a single, final end product. β -Endorphin(1-31) processing in the rat intermediate lobe (Figure 2) and heart (Figure 3) are clear-cut examples that emphasize the necessity of separating individual β -endorphin peptides by chromatographic techniques to obtain definitive data regarding the functional significance of the β -endorphin peptides in a particular tissue. Moreover, these principles are by no means specific to β -endorphin, but extend to many other peptide families as well (11).

The importance of analyzing individual β -endorphin peptides is emphasized further by evidence that β -endorphin(1-31) processing can be modified by physiological stimuli and pharmacological treatments that affect the secretory activity of POMC neurons and endocrine cells. For example, stress alters the ratio of β -endorphin to β -lipotropin released from the anterior pituitary of rats (39) and selectively enhances the synthesis and release of nonopioid forms of β -endorphin in the intermediate lobe (38). Various drug treatments including dexamethasone (40), dopamine receptor ligands (36,41), and opioid receptor agonists (42) and antagonists (37), have also been shown to modify β -endorphin(1-31) processing in the pituitary and brain. This raises the possibility that drugs may affect synaptic transmission by peptidergic neurons, not only by modulating synthesis and secretion, but also by regulating the post-translational processing, and hence the biological activities, of the secreted peptides. Whether the processing of β -endorphin or other peptides is similarly regulated by toxic agents has not been extensively investigated and remains exciting territory for future exploration.

ACKNOWLEDGMENTS

This research was supported by grants from the National Institute on Drug Abuse (DA04598) and the U.S. Army Medical Research and Developmental Command (DAMD17-90-Z-0022).

REFERENCES

1. A. F. Bradbury, D. G. Smyth, and C. R. Snell, *Biochem. Biophys. Res. Commun.* **69**, 950-956 (1976).
2. Y. P. Loh, *Biochem. Pharmacol.* **44**, 843-849 (1992).
3. C. H. Hawkes, *J. Neurol. Neurosurg. Psychiatry* **55**, 247-250 (1992).
4. D. G. Smyth, D. E. Massey, S. Zakarian, and M. D. A. Finnie, *Nature (London)* **279**, 252-254 (1979).
5. R. E. Mains and B. A. Eipper, *J. Biol. Chem.* **256**, 5683-5688 (1981).
6. S. Zakarian and D. G. Smyth, *Proc. Natl. Acad. Sci. U.S.A.* **76**, 5972-5976 (1979).
7. A. I. Smith and J. W. Funder, *Endocr. Rev.* **9**, 159-179 (1988).
8. R. M. Dores, M. Jain, and H. Akil, *Brain Res.* **377**, 251-260 (1986).
9. W. R. Millington, V. R. Evans, L. J. Forman, and C. N. Battie, *Peptides* **14**, 1141-1147 (1993).
10. L. J. Forman and O. Bagasra, *Brain Res. Bull.* **28**, 441-445 (1992).
11. W. R. Millington and M. D. Hirsch, *In* "The Nucleus of the Solitary Tract" (R. A. Barraco, ed.), pp. 315-326. CRC Press, Boca Raton, Florida, 1994.
12. P. Nicolas and C. H. Li, *Proc. Natl. Acad. Sci. U.S.A.* **82**, 3178-3181 (1985).
13. H. P. J. Bennett, C. A. Browne, and S. Solomon, *J. Biol. Chem.* **257**, 10096-10102 (1982).
14. B. A. Eipper, C. C. Glembotski, and R. E. Mains, *J. Biol. Chem.* **258**, 7292-7298 (1983).

15. X. Zhu and D. M. Desiderio, *Anal. Lett.* **27**, 2267–2280 (1994).
16. O. J. Igwe, L. J. Felice, V. S. Seybold, and A. A. Larson, *J. Chromatogr.* **432**, 113–126 (1988).
17. M. E. Goldman, M. Beaulieu, J. W. Kebabian, and R. L. Eskay, *Endocrinology (Baltimore)* **112**, 435–441 (1983).
18. G. P. Mueller, *Proc. Soc. Exp. Biol. Med.* **165**, 75–81 (1980).
19. W. R. Millington, N. O. Dybdal, R. Dawson, C. Manzini, and G. P. Mueller, *Endocrinology (Baltimore)* **123**, 1598–1604, 1988.
20. C. A. Cahill, J. D. Matthews, and H. Akil, *J. Clin. Endocrinol. Metab.* **56**, 992–997 (1983).
21. K. M. Hargreaves, R. A. Dionne, and G. P. Mueller, *J. Dent. Res.* **62**, 1170–1173 (1983).
22. L. S. Monger and D. J. Olliff, *J. Chromatogr.* **577**, 239–249 (1992).
23. D. G. Smyth, *Anal. Biochem.* **136**, 127–135 (1984).
24. V. R. Evans, A. B. Manning, L. H. Bernard, B. M. Chronwall, and W. R. Millington, *Endocrinology (Baltimore)* **134**, 97–106 (1994).
25. W. R. Millington, N. O. Dybdal, G. P. Mueller, and B. M. Chronwall, *Gen. Comp. Endocrinol.* **85**, 297–307 (1992).
26. B.-Y. Ahu, C. T. Mant, and R. S. Hodges, *J. Chromatogr.* **594**, 75–86 (1992).
27. D. T. Krieger, H. Yamaguchi, and A. S. Liotta, in “Neurosecretion and Brain Peptides” (J. B. Martin, S. Reichlin, and K. L. Bick, eds.), pp. 551–556. Raven, New York, 1981.
28. R. B. Emeson and B. A. Eipper, *J. Neurosci.* **6**, 837–849 (1986).
29. W. R. Millington and D. L. Smith, *J. Neurochem.* **57**, 775–781 (1991).
30. D. W. Young and R. J. Kempainen, *Am. J. Vet. Res.* **55**, 567–571 (1994).
31. A. J. Fischman, A. J. Kastin, and M. V. Graf, *Peptides* **5**, 1007–1010 (1984).
32. S. B. Jaffee, S. Sobieszcyk, and S. L. Wardlaw, *Brain Res.* **648**, 24–31 (1994).
33. C. W. Wilkinson and D. M. Dorsa, *Neuroendocrinology* **43**, 124–131 (1986).
34. J. P. H. Burbach, H. H. M. Van Tol, V. M. Wiegant, R. A. Van Ooijen, and R. A. A. Maes, *J. Biol. Chem.* **260**, 6663–6669 (1985).
35. W. R. Millington, T. L. O’Donohue, and G. P. Mueller, *J. Pharmacol. Exp. Ther.* **243**, 160–170 (1987).
36. C. J. Evans, N. T. Maidment, and R. Newcomb, in “High Performance Liquid Chromatography in Neuroscience Research” (R. B. Holman, A. J. Cross, and M. H. Joseph, eds.), pp. 265–295. Wiley, New York, 1993.
37. D. M. Bronstein, N. C. Day, H. B. Gutstein, K. A. Trujillo, and H. Akil, *J. Neurochem.* **60**, 40–49 (1993).
38. H. Akil, H. Shiomi, and J. Matthews, *Science* **227**, 424–426 (1985).
39. E. A. Young, J. Lewis, and H. Akil, *Peptides* **7**, 603–607 (1986).
40. J. Ham and D. G. Smyth, *Neuroendocrinology* **44**, 433–438 (1986).
41. J. Ham and D. G. Smyth, *Neuropeptides* **5**, 497–500 (1985).
42. D. M. Bronstein, H. B. Gutstein, and H. Akil, *J. Neurochem.* **60**, 2304–2307 (1993).

This Page Intentionally Left Blank

13

Detection of Autoantibodies to the Thyrotropin Receptor

John S. Dallas¹ and Bellur S. Prabhakar²

Departments of ¹Pediatrics and

²Microbiology and Immunology

The University of Texas

Medical Branch

Galveston, Texas 77555

THE THYROTROPIN RECEPTOR AND NORMAL THYROID FUNCTION

The Structure of the Thyrotropin Receptor

The thyrotropin (TSH) receptor is a member of the large family of guanine-nucleotide-binding (G) protein-coupled receptors. The cDNA encoding the human TSH receptor has recently been cloned and characterized (1,2). As deduced from the cDNA sequence, the mature receptor is a glycoprotein with a single polypeptide chain of 744 amino acids (molecular weight of 120,000). Like all other G-protein-coupled receptors, the TSH receptor has an extracellular domain, seven transmembrane domains, and an intracellular domain. The TSH and other glycoprotein hormone [i.e., luteinizing hormone (LH)/chorionic gonadotropin (CG) and follicle-stimulating hormone (FSH)] receptors each have relatively large extracellular domains, and this characteristic differentiates them from the other G-protein-coupled receptors. The TSH, LH/CG, and FSH receptors are closely related structurally and share about 70% and 45% homology in their transmembrane and extracellular domains, respectively (3).

The extracellular domain of the TSH receptor (398 amino acids) represents the amino-terminal end, and the transmembrane and intracellular

domains (346 amino acids) represent the carboxyl-terminal end of the protein. The extracellular domain contains six potential N-glycosylation sites and nine leucine-rich repeats of a loosely conserved 25-amino-acid residue motif. Proper glycosylation appears to be important both for normal expression of the receptor on the thyroid cell and for normal hormone–receptor interactions (1,2). The leucine-rich repeats, which have the potential to form amphipathic α -helices, are believed to be involved in protein–protein or protein–membrane interactions. Recent studies have confirmed that both TSH and autoantibodies to the TSH receptor (TSHrAb) bind to the extracellular domain (1,2). The transmembrane and intracellular domains are involved in signal transduction, acting through G-protein to stimulate the cyclic AMP and phosphatidol–inositol pathways.

The Function of the Thyrotropin Receptor

Under normal physiologic conditions, TSH is produced by and secreted into the blood-stream from cells of the anterior pituitary known as thyrotrophs. Human TSH is a glycoprotein hormone with a molecular weight of 28,000. Like the other glycoprotein hormones (i.e., luteinizing hormone, follicle stimulating hormone, and chorionic gonadotropin), it is a heterodimer composed of an α -subunit and a β -subunit that are linked by noncovalent bonds. The α -subunit is common to the other glycoprotein hormones, whereas the β -subunit is distinct and confers the hormone's biologic specificity (4). Pituitary TSH synthesis and secretion are directly controlled by serum levels of free or unbound thyroxine (T_4) and triiodothyronine (T_3). This control occurs by negative feedback; that is, rising serum levels of free T_4 and T_3 inhibit, whereas decreasing levels of free T_4 and T_3 enhance TSH synthesis and secretion. Through thyrotropin-releasing hormone (TRH) and somatostatin secretion, the hypothalamus modulates this negative feedback system and determines the “set point” for TSH secretion (5). TRH secretion enhances TSH release, and somatostatin inhibits TSH release.

Circulating TSH binds to its receptor (approximately 10^3 – 10^4 receptors/cell) on thyroid epithelial cells, which in turn leads to activation of G-protein. The G-proteins are heterotrimers composed of an α -subunit and a tightly coupled β/γ -dimer. The α -subunit contains the guanine-nucleotide-binding site and has intrinsic GTPase activity. In the normal situation, the binding of TSH to its receptor facilitates the exchange of GTP for GDP in the guanine-nucleotide-binding site of the α -subunit (G_{sa}). This results in the release of the G-protein from the receptor and its dissociation into free G_{sa} -GTP and free β/γ -dimer. Free G_{sa} -GTP stimulates adenylyl cyclase activity, with the subsequent production of intracellular cAMP. After a preset time, the intrinsic GTPase activity of G_{sa} hydrolyzes GTP to GDP,

and the G_{sa} -GDP reassociates with the β/γ -dimer. The G-protein is thus returned to its inactive state and can now reassociate with the TSH receptor and participate in another cycle (6). Specific cellular processes that are activated as a result of increased intracellular cAMP include iodine uptake, tissue peroxidase activation, and protein synthesis, including thyroglobulin synthesis (7).

THE THYROTROPIN RECEPTOR AND AUTOIMMUNE THYROID DISEASES

Thyrotropin Receptor Antibody-Mediated Thyroid Diseases

The TSH receptor is the primary target antigen in several autoimmune thyroid disorders, including Graves' disease, primary myxedema, and diffuse nontoxic goiter (8). These diseases are among the most common endocrine disorders (9). Graves' disease, which is characterized classically by the clinical triad of diffuse thyromegaly, hyperthyroidism, and ophthalmopathy, occurs in approximately 0.4% of the population of the United States and represents the most common cause of hyperthyroidism in patients less than 40 years of age (9). Primary myxedema, or atrophic thyroiditis, is a leading cause of hypothyroidism in adults (9). The prevalence of diffuse nontoxic goiter is uncertain, but it probably accounts for a sizeable number of patients with asymptomatic thyromegaly (10). The peak age of onset for Graves' disease is between 20 and 40 years and for primary myxedema between 40 and 60 years (9). Both afflict women more often than men, in a ratio of 5:1 to 10:1 (9). Because TSHrAbs are IgG antibodies, they can be passed transplacentally to the baby of an affected woman and cause either neonatal hypo- or hyperthyroidism (11). Children and adolescents also develop Graves' disease and primary myxedema, and both disorders can cause school, behavioral, and growth problems (12). Therefore, there is appreciable morbidity associated with these diseases in individuals from all age groups.

TSHrAbs can be detected in sera from 80–100% of patients with active Graves' disease (13), up to 50% of patients with primary myxedema (14,15) and up to 60% of patients with diffuse nontoxic goiter (16). Current evidence suggests that TSHrAbs bind to the extracellular domain of the TSH receptor (17,18) and mediate their biologic effects on thyroid cells. For example, TSHrAbs in Graves' sera bind to the TSH receptor and mimic the stimulatory effects of TSH to produce the thyromegaly and hyperthyroidism that are characteristic of the disease. In primary myxedema, TSHrAbs bind to the TSH receptor and block the stimulatory effects of TSH, leading to

thyroid atrophy and hypothyroidism. In diffuse nontoxic goiter, TSHrAbs bind to the TSH receptor and stimulate thyroid cell growth, without affecting thyroid cell function.

Clinical Usefulness of Thyrotropin Receptor Antibody Assays

There are several areas in medical practice where the measurement of TSHrAb can be of clinical importance (7). Many clinicians feel that the routine measurement of TSHrAb for the diagnosis of Graves' disease is unnecessary, especially in those patients with hyperthyroidism, diffuse thyromegaly, and an elevated 24-hr thyroid radioiodide uptake. On the other hand, TSHrAb is the cause of hyperthyroidism and can be detected in >80% of patients with active, untreated Graves' disease. Because TSHrAb assays cost less than thyroid radioiodide uptake assays, other clinicians argue that the measurement of TSHrAb is useful in the diagnosis of Graves' disease. Measurement of TSHrAb is especially useful in determining the etiology of hyperthyroidism in pregnant patients, as radioiodide uptake tests are contraindicated in these individuals.

TSHrAb represents a biological marker for the activity of Graves' disease. Several studies have demonstrated that the short-term relapse rate for hyperthyroidism is significantly higher in patients with detectable TSHrAb at the end of antithyroid treatment compared to patients who are negative for TSHrAb at the end of treatment (19–21). Therefore, measurement of TSHrAb is useful for predicting relapse of hyperthyroidism and can help guide the medical management of Graves' disease.

Occasionally, TSHrAb levels can aid in the diagnosis of those patients who present with uni- or bilateral exophthalmos and normal thyroid function. A positive assay for TSHrAb will confirm the diagnosis of Graves' disease and avoid the need for a more aggressive evaluation (7).

Measurement of TSHrAb is indicated during the third trimester in pregnant patients with a past or present history of Graves' disease; several studies have shown that the presence of high maternal TSHrAb levels after 28–30 weeks of gestation increases the risk of fetal/neonatal hyperthyroidism (22). A highly positive result should lead to investigation and treatment, if indicated, for fetal thyroid dysfunction. Further, pregnant patients with a history of either Graves' or Hashimoto's disease can also pass thyroid-stimulating blocking antibodies (TSBAB) across the placenta, which can produce transient neonatal hypothyroidism. Measurement of TSBAB in either maternal or neonatal sera can aid in the medical management of these children.

METHODS TO DETECT AUTOANTIBODIES TO THE THYROTROPIN RECEPTOR

Radioreceptor Assays

Currently, two major types of assays are commonly used to measure TSH-rAbs. The first is a radioreceptor assay, which assesses the ability of TSH-rAbs to inhibit radiolabeled TSH from binding to solubilized TSH receptor preparations. Antibodies detected by this method have been designated as thyrotropin-binding inhibitory immunoglobulins or TBII. This method (outlined in the following), which was originally described by Rees Smith and Hall, is now commercially available (Kronus, Dana Point, CA) and employs a combination of detergent-solubilized porcine TSH receptors and receptor-purified ^{125}I -labeled bovine TSH (23). This method is sensitive and specific and provides a reproducible, inexpensive means of measuring TSHrAb in unextracted serum; however, this method gives no information about the functional (i.e., stimulatory versus inhibitory) effect of the antibody.

The assay procedure for the radioreceptor method originally described by Rees Smith and Hall employs either human or porcine thyroid tissue (23). Human TSHrAbs appear to interact with the human and porcine TSH receptors in a similar fashion; therefore, either can be used to prepare the TSH receptors for the assay. Once the thyroid tissue is obtained, it should be placed immediately in a beaker on ice, trimmed free of fat and connective tissue, and cut into pieces weighing 100–200 mg. If the tissue is not going to be used immediately, then it should be “quick frozen” (e.g., immersion in liquid nitrogen) and stored at -70°C . The TSH receptors in the frozen tissue will remain stable for several years.

To prepare the thyroid membranes for assay, the following steps should be performed at $0-4^{\circ}\text{C}$, unless otherwise indicated. First, weigh out the thyroid tissue. Approximately 200 mg tissue is required for each assay tube. If the thyroid tissue has been previously frozen, allow it to soften at room temperature. Cut the tissue into fine pieces with scissors and homogenize in 5–10 volumes of 10 mM Tris-HCl buffer (pH 7.5), using a mechanical homogenizer (e.g., Polytron) or an all ground-glass hand homogenizer. Centrifuge the homogenate at 500g for 5 min to remove large cell and tissue debris. Collect the supernatant from this spin and centrifuge at 15,000g for 15 min. Discard the supernatant from this spin and, with a Pasteur pipette, resuspend the pellet (thyroid particulate fraction) in buffer (pH 7.5) containing 50 mM NaCl, 10 mM Tris-HCl, and 0.1% Lubrol or Triton X-100. For each gram equivalent of membrane preparation, use 2 ml of the 0.1%

detergent buffer. One gram equivalent of membrane preparation is defined as that prepared from 1 g of thyroid tissue. Gently homogenize this suspension with an all ground-glass homogenizer and then centrifuge at 100,000g for 1 hr at 4°C. The supernatant is discarded and the pellet is rehomogenized in buffer (pH 7.5; 1 ml/gram equivalent) containing 50 mM NaCl, 10 mM Tris-HCl, and 1.0% Lubrol or Triton X-100. The mixture is centrifuged at 100,000g for 2 hr (4°C). The resulting supernatant is rich in TSH-binding activity and can be stored at -70°C for several months, without significant loss of binding activity.

The preparation of receptor-purified radiolabeled bovine TSH is a relatively complex and prolonged procedure, but can be carried out in most well-equipped laboratories. Alternatively, receptor-purified ¹²⁵I-labeled bovine TSH can be purchased commercially (Kronus) for use in the assay. Receptor purification increases the binding activity of the bovine TSH, and thereby improves the sensitivity and specificity of the assay. Several methods have been described for labeling TSH with ¹²⁵I, and these include the chloramine-T (24), lactoperoxidase (25), Bolton-Hunter (26), and iodogen methods (23). Our laboratory has found the Iodo-bead (Pierce Chemicals, Rockford, IL) method to be a gentle, efficient means of radioiodination; this method (Pierce Technical Bulletin) will be described here.

The Iodo-bead is washed with 50 mM disodium hydrogen phosphate buffer, pH 7.4, twice using 0.5 ml buffer per wash. The bead is then dried on Whatman #52 paper and added to a reaction vial containing 10 μl (1 mCi) ¹²⁵I solution (Radiochemical Center, Amersham), diluted with 50 μl of 0.1 M phosphate-buffered saline (PBS), pH 7.4. The bead is left in this solution at room temperature for 5 min. Highly purified bovine TSH (e.g., NIDDK-bTSH-11, AFP-555-B; National Hormone and Pituitary Program, NIDDK, Baltimore, MD), 25 μg/50 μl in 0.1 M PBS, is then added to the reaction vial for 5 min at room temperature. Iodination is terminated by removing the reaction mixture from the bead. An aliquot of the reaction mixture is taken to determine the percentage of incorporation of ¹²⁵I into TSH. A convenient method (23) is to dilute 1 μl of the reaction mixture in 10 ml of buffer (pH 7.5) containing 10 mM Tris-HCl, 50 mM NaCl, and 20 mg/ml bovine serum albumin (Tris/NaCl/BSA). Add 2 × 200 μl of this to 2 × 500 μl of 20 mg/ml BSA in 10-ml tubes. Count the tubes in a gamma counter, then add 3 ml 10% trichloroacetic acid (TCA) and 7 ml of H₂O, mix, centrifuge at 1000g for 5 min, and count the pellet. Percentage incorporation is determined by dividing the cpm pellet by the cpm total.

The radiolabeled hormone is purified by gel filtration. The reaction mixture is transferred directly to a Sephadex G-100 column (2.6 × 40 cm) that has been equilibrated with 10 mM Tris-HCl, 50 mM NaCl buffer (pH 7.5), containing 0.2 mg/ml NaN₃. Gel filtration should be done at 4°C at a

flow rate of 15 ml/hr. Two-milliliter fractions are collected and monitored for ^{125}I by counting small aliquots (10 μl) of each fraction. The fractions containing TSH monomer (as determined by the elution profile) are pooled and BSA is added to a final concentration of 1 mg/ml. The TSH is now ready to be receptor purified.

Thyroid particulate fraction is prepared from 5 g of porcine tissue as described earlier, except the final 15,000g pellets (in four 10-ml centrifuge tubes) are not suspended in buffer. Instead, the labeled TSH monomer is added to the pellets, and the pellets are suspended with a Pasteur pipette. These suspensions are incubated for 15 min at 37°C and then centrifuged at 17,000g for 15 min (4°C). The supernatant is removed from each of the four tubes, and 7.5 ml of ice-cold Tris/NaCl/BSA is added to each tube. The tubes are again centrifuged at 17,000g for 15 min. The supernatants are discarded, and all of the pellets are resuspended in a total volume of 8 ml of 2 M NaCl containing 1 mg/ml BSA. The combined pellets are gently homogenized with an all ground-glass homogenizer, and then centrifuged at 100,000g for 2 hr (4°C). The supernatant is collected and run on a second Sephadex G-100 column in Tris/NaCl at 15 ml/hr at 4°C. Two-milliliter fractions are collected and monitored for radioactivity, and the peak tubes are pooled. BSA is added to a final concentration of 1 mg/ml, and the purified, labeled TSH is stored in aliquots at -70°C. The preparation is usually stable for about 4 weeks.

To perform the assay, take 200 μl solubilized thyroid receptor preparation and mix it with 50 μl neat patient or control serum in a polypropylene tube (12 \times 75 mm). A serum pool from normal individuals should be established as a negative control for the assay. Serum samples should be centrifuged before assay to remove any particulate matter. Neither plasma samples nor grossly hemolyzed or lipemic serum samples should be used in the assay. To control for nonspecific binding (NSB), take 200 μl of the 1.0% detergent/Tris/NaCl buffer (pH 7.5) and mix with 50 μl negative control serum. Allow the serum to incubate with the solubilized receptors for at least 15 min at room temperature. The sensitivity of the assay can be enhanced by increasing the incubation time from 15 min to 2 hr (8). Following this incubation step, add 100 μl ^{125}I -labeled bovine TSH (approximately 10,000 cpm) to each tube. Allow the tubes to incubate for 2 hr at room temperature and then add 150 μl ice-cold buffer (pH 7.5) containing 50 mM NaCl, 10 mM Tris-HCl, and 0.1% bovine serum albumin. Immediately add 500 μl ice-cold polyethylene glycol (MW 4000; 30% w/v in 1 M NaCl). Vortex each tube for at least 15 sec, and then centrifuge at 1500g for 30 min (4°C). Aspirate the supernatant, being careful not to disrupt the pellet. The pellets are then counted for ^{125}I in a gamma counter; count each pellet for 5 min. In general, the total binding should be greater than

20–25% in the presence of normal control sera, and nonspecific binding should be less than 5%.

The results can be expressed qualitatively as a “thyrotropin binding inhibition index,” which is calculated in the following manner:

$$\left[1 - \frac{\text{CPM (sample)} - \text{CPM (NSB)}}{\text{CPM (negative control)} - \text{CPM (NSB)}} \right] \times 100$$

Normal individuals typically have a TBI index between –15 and 15%. Serum samples containing TSH in amounts over 100 $\mu\text{U/ml}$ may interfere (i.e., give elevated TBI indexes) with the assay.

Bioassay Methods

In Vivo Methods

Bioassay methods constitute the other major type of assay currently used to measure TSHrAbs. Adams and Purves described the first bioassay method in 1956 (27). Their assay employed live guinea pigs, and they measured the release of thyroid radioiodine in response to intravenous injection of sera from patients with Graves’ disease. They found that the release of radioiodine from the guinea pig thyroid was delayed in response to Graves’ sera as compared to the response observed with TSH preparations (9 hr versus 3 hr). The term “long acting thyroid stimulator” (LATS) was used to describe this serum factor, which was later shown to be an IgG, in patients with Graves’ disease. Because of the species specificity of the antibody for the human TSH receptor, this method detected TSHrAbs in only 20–30% of patients with Graves’ disease (7). Although *in vivo* bioassay methods for TSHrAbs are not currently being used for clinical purposes, research groups that are attempting to develop animal models of Graves’ disease may have an interest in this methodology. For this reason, the Adams and Purves method, as modified by McKenzie (28,29), will be presented. McKenzie’s assay employs albino mice (Swiss-Webster strain) instead of guinea pigs.

Mice weighing about 15 g each are maintained on a low-iodine diet (250 μg iodine/kg feed) throughout the assay period. After being on the low iodine diet for 8 days, each mouse is given an intraperitoneal injection of 8 μCi carrier-free radioiodine (^{131}I), followed immediately by a subcutaneous injection of 10 μg L-thyroxine. Subcutaneous injections of L-thyroxine (10 $\mu\text{g/day}$) are repeated on Days 9–11. The L-thyroxine is used to decrease the turnover of the radioiodine taken up by the mouse thyroid. By Day 12, the blood radioiodine will have been cleared by the kidneys and thyroid, and the animals are ready for assay.

On the day of assay (Day 12), blood is obtained by venipuncture of the tail veins. To facilitate bleeding, the animals are kept at a temperature of 29–31°C for 45 min before venipuncture. One hundred microliters of blood is obtained and counted for ^{131}I . Immediately following blood collection, the animal is given an intravenous injection of test material (0.2 to 0.5 ml serum or IgG preparation) through a tail vein. Following the intravenous injection of test material, repeat blood samples (100 μl) are obtained to measure the release of radioiodine from the thyroid. McKenzie found that TSH preparations produced a maximal increase in circulating radioactivity after a 2-hr interval, whereas Graves' sera produced a maximal increase after 12 hr (29). The increase in blood ^{131}I is calculated as a percentage increase of the initial radioactivity. Normal control samples should be tested to establish a normal range for the assay.

In Vitro Methods

For clinical purposes, current bioassay methods employ isolated thyroid cells in culture to assess the ability of immunoglobulin concentrates from patient sera to either directly stimulate cAMP production or inhibit TSH-mediated cAMP production by the thyroid cells. Antibodies that stimulate the production of cAMP have been designated as thyroid-stimulating antibodies (TSAb), whereas those that inhibit TSH-mediated cAMP production are known as TSBAb. A variety of cell types, including human, porcine, and murine, have been used in these assays. At present, however, the most widely used bioassay employs cell cultures of an immortalized line of rat thyroid cells. This cell line is known as FRTL-5 and is deposited in the American Type-Culture Collection (ATCC CRL# 8305, Rockville, MD). These cells have a TSH-responsive adenylate cyclase and an absolute growth requirement for TSH. They maintain the functional characteristics of iodide uptake, thyroglobulin synthesis, and cyclic nucleotide metabolism over prolonged periods of culture (30). These characteristics make the FRTL-5 cells ideally suited for assays that determine and quantify thyroid stimulatory and inhibitory factors. These factors may be evaluated by assays that measure cAMP production, iodide uptake, and thymidine incorporation. Several investigators have demonstrated that results from bioassays that utilize FRTL-5 cells to measure TSHrAbs correlate well with results from assays that use human thyroid cells in culture (31). For details regarding culture and maintenance, along with bioassay methods, of FRTL-5 cells, the reader is referred to the manual by Kohn and Valente (30). Details regarding the methods that assay for cAMP production in response to stimulatory and inhibitory TSHrAbs will be presented here.

FRTL-5 cells are grown either in sterile plastic culture dishes (100 mm) or tissue culture flasks in Coon's modified Ham's F-12 medium supplemented with 5% calf serum and a six-hormone mixture consisting of 10 $\mu\text{g}/\text{ml}$ insulin, 10^{-8} M hydrocortisone, 5 $\mu\text{g}/\text{ml}$ transferrin, 2 ng/ml glycy-L-histidyl-L-lysine acetate, 10 ng/ml somatostatin, and 1 mU/ml TSH. This medium is referred to as 6H medium. The cells are grown at 37°C in 95% air/5% CO₂. Once the cells reach confluence, they are seeded into 24-well culture dishes (5×10^4 – 10^5 cells/well) containing 1 ml of 6H medium/well. The 6H medium is replaced with fresh 6H medium every 3–4 days until the cells grow to near confluence.

Once the cells grow to near confluence, the medium is changed to Coon's modified Ham's F-12 medium supplemented with 5% calf serum and the hormone mixture outlined earlier, except without TSH (5H medium). The cells are maintained in the TSH-free medium for 7–10 days before assay; 5H medium is replaced with fresh 5H medium every 3–4 days. The maintenance of the cells in 5H medium allows for up-regulation of the TSH receptors and increases the sensitivity of the assay.

IgG extracts can be prepared from patient sera by several methods, including affinity chromatography (e.g., Protein G–Sepharose), ammonium sulfate precipitation, and polyethylene glycol (PEG) precipitation. The PEG precipitation method is relatively easy and allows for preparation of large numbers of crude IgG samples in a short period of time. To 1 ml of serum in a test tube, add 473 μl of 50% PEG (MW 4000). Allow the mixture to incubate for 30 min at 4°C, and then centrifuge at 3000g for 10 min (4°C). Remove the supernatant and wash the precipitate with 1 ml of 15% PEG. Recentrifuge, discard the supernatant, and resuspend the precipitate in 2 ml of Hanks' balanced salt solution (HBSS). It should be realized that PEG is also capable of precipitating 30–40% of the serum TSH content along with the IgG (8). Therefore, samples containing high TSH concentrations may give false-positive results with this method of IgG preparation.

On the day of assay, the 5H medium is removed from each of the wells. The cells are washed with 1 ml of HBSS without NaCl, which contains 10 mM HEPES, 0.4% BSA, and 220 mM sucrose (pH 7.4; hypotonic HBSS buffer). The sucrose is added to help maintain partial osmolarity for the NaCl-free HBSS. When assaying for stimulatory TSHrAbs, IgG preparations are prepared in the hypotonic HBSS buffer at concentrations between 250 and 500 $\mu\text{g}/\text{ml}$ (10-fold higher and lower concentrations of IgG can also be included to exhibit dose-dependent effects). When assaying for inhibitory IgG, IgG preparations are prepared in the hypotonic HBSS buffer at concentrations between 250 and 500 $\mu\text{g}/\text{ml}$, along with 10–100 μU bTSH/ml. IgG (and TSH) binding to the TSH receptor is enhanced in the presence of NaCl-free buffer. Further, the hypotonic medium allows

>95% of cAMP to move extracellularly into the incubation mixture. 3-Isobutyl-methyl-xanthine (IBMX) is added to the buffer at a final concentration of 0.5 mM to prevent degradation of cAMP by phosphodiesterases. The final volume of the incubation mixture is 250 μ l/well.

The plates are then incubated at 37°C in 95% air/5% CO₂ for 2–3 hr. The assay is terminated by aspiration of the incubation medium, which is saved and assayed for cAMP concentration. All assays normally include a positive TSH control, a buffer-alone control, and a normal IgG control prepared from a pool of 10–20 normal individuals. The patient's thyroid-stimulating activity is expressed as the percentage increase in cAMP over that of the normal control. The patient's thyroid-blocking activity is calculated as the percentage of inhibition of TSH-induced cAMP obtained with patient's IgG as compared to TSH-induced cAMP with normal pooled IgG. Individual laboratories will need to determine their own normal control ranges for both the stimulatory and inhibitory assays.

FRTL-5 cells can also be used to screen patient IgGs for thyroid cell growth activity by determination of labeled thymidine incorporation into DNA. The FRTL-5 cells are grown and prepared in 12-well plates as described earlier. The cells are grown in the presence of 6H medium until they reach approximately 70% confluence. The 6H medium is then removed, and the cells are washed once with 5H medium. After washing, the cells are maintained in 5H medium for 5–7 days, with the medium being replaced by fresh 5H medium every 3–4 days.

Under sterile conditions, the assay is started by adding 0.8 ml of 5H medium containing 1×10^6 cpm of tritiated thymidine to each well, along with patient IgG samples (in 0.2 ml). The IgG samples should be filtered through 0.22- μ m filters to avoid infecting the cells. Appropriate controls such as TSH-positive control, buffer-alone control, and a normal IgG control should be included in each assay. The cells are then incubated in the presence of the labeled thymidine, 5H medium, and patient IgG at 37°C in 95% air/5% CO₂ for 72 hr. When the incubation period is completed, the assay is terminated by washing each well three times with ice-cold HBSS (pH 7.4). One milliliter of ice-cold 5% TCA is added to each well to precipitate DNA and protein-containing material. After 10 min at 4°C, the supernatant is aspirated, and 1 ml of diphenylamine (DPA) reagent is added to each well. The DPA reagent is made as follows (30). Dissolve 5 g of DPA in 490 ml glacial acetic acid and 10 ml sulfuric acid; this is referred to as DPA solution and is stored in a brown bottle at room temperature. Make a 1% acetaldehyde solution in distilled water and store at 0–4°C. Acetaldehyde is highly volatile and irritating and should be prepared in a hood. Immediately before use, prepare fresh DPA reagent by mixing 20

volumes of DPA solution with 8 volumes of water and 0.1 volume of 1% acetaldehyde. Mix and use immediately.

After overnight development at room temperature, aliquots from each well are analyzed for DNA content by absorbance at 580 nm using spermine DNA standards (e.g., 1.25, 2.5, 5, 7.5, 10, and 12.5 $\mu\text{g}/\text{ml}$). An aliquot (100 μl) is also added to a liquid scintillation vial (along with a liquid fluor) to count tritiated thymidine in a liquid scintillation counter. Results are expressed as cpm [^3H]thymidine/ μg DNA.

The thymidine uptake assay should be considered a screening test for factors that affect thyroid cell growth. Increased [^3H]thymidine uptake values may result from increased amounts of tritium incorporated into proteins either from impurities of [^3H]thymidine or ^3H transferred to amino acids (32). Further, changes in thymidine uptake may reflect alterations in thymidine transport, metabolism, and other nonmitogenic processes in the cell cycle (33).

Correlations between Radioreceptor and Bioassay Methods

Several investigators have compared the results of TSHrAb activities measured by the two assay methods (8). Although some studies have demonstrated highly positive correlations between TSHrAb levels detected by the receptor and bioassay methods (31,34), most have demonstrated no such correlation (8). Early on, the poor correlation was felt to be due in part to the use of particulate thyroid membrane preparations in the assays (35). Furthermore, species differences (i.e., rat versus porcine) in the assay materials may also contribute to the differences observed between the methods (8). However, a recent study continued to show only a weak correlation ($r = 0.31$), despite using human thyroid cells in the bioassay and recombinant human TSH receptor in the radioreceptor assay (36). At present, it appears that the lack of correlation between the two assay methods is due to either the presence of different populations of TSHrAbs that exhibit different degrees of TSH agonist activity (37) or the coexistence of both stimulating and blocking TSHrAbs in patient sera (38).

The latter finding might be very critical in understanding the difference and a lack of complete correlation between these two sets of assays. The radioreceptor assay detects antibodies that can compete for and/or interfere with TSH binding to the TSHr. Such antibodies could potentially represent either blocking, stimulatory, or growth antibodies. However, bioassays detect the net effect of antibodies in the serum. For example, if a patient serum contains a mixture of stimulatory and blocking antibodies, the bioassay can detect the net effect of these Igs. These differences in the types of antibodies

detected might be a reason for the discrepancies sometimes noted between these two sets of assays.

FUTURE DIRECTIONS FOR DETECTION OF THYROTROPIN RECEPTOR ANTIBODIES

Mammalian cell transfection with the cDNA has resulted in expression of the human TSHr protein (39–41). This has allowed some elegant studies of mapping of the TSH and antibody binding sites on the TSHr (1,2,42). Transfection of COS-1 cells with TSHr cDNA altered by site-directed mutagenesis has led to several important findings with respect to the structure–function relationship of the TSHr. Deletion of amino acid residues 38–45 and 317–366 (two regions unique to the TSHr, when compared to other G-protein-coupled receptors) revealed that the former region, but not the latter, is important for TSH binding and for a response to TSH and thyroid-stimulating immunoglobulins (18). Reports from other laboratories (43) have shown that deletion of residues 308–410 resulted in loss of stimulatory TSHrAb activity but not in complete TSH binding. Deletion of residues 339–367 resulted in no loss of either TSH or stimulatory TSHrAb activity. Together, these studies suggest possible multiple (i.e., 38–45 and 308–410) stimulatory TSHrAb binding sites. Further studies using site-directed mutagenesis revealed that the first cytoplasmic loop, the carboxy-terminal domain of the second and third loops, as well as amino acid residues 171–260 of the extracellular domain, are important for TSH binding and cAMP production (17,44).

Other studies with chimeras of LH/CG and TSH receptors have suggested that residues 1–260 are important for signal transduction of the TSHr, but that several regions are important for TSH binding, with no single site being predominant (17). Another group, using a similar approach, suggested that residues 8–165 are important for stimulatory TSHrAb binding and cAMP response to stimulatory TSHrAb (42). The relevance of glycosylation in relation to the function of the TSHr has been demonstrated by studies using site-directed mutagenesis (43,45). These studies revealed the possible importance of glycosylation of asparagine at residues 77 and 113 of human TSHr and residues 77 and 198 of rat TSHr.

Another approach to define structure–function relationships has been to use peptides and antipeptide antibodies. Atassi *et al.* (46) suggested that residues 12–30 and 324–344 contain important TSH binding sites. A study by Endo *et al.* (47) demonstrated that antibodies to residues 29–57, from two rabbits, elicited antibody responses that contained primarily either blocking or stimulating TSHrAb activity, respectively. Another group of

workers has demonstrated that antibodies to residues 372–397 and 341–358 possess blocking TSHrAb and TBII activity, whereas antibodies to 649–661 had only blocking TSHrAb activity (48).

It should be apparent from this brief review that there is no general consensus on epitopes of TSHr involved in interactions with TSH or autoantibodies. In part, this may be due to the following reasons. Transfection studies that showed a complete lack of TSH or immunoglobulin binding provided no direct evidence to show that, in fact, the protein was produced and expressed on the cell membrane. Studies that used TSHr synthetic peptides to examine TSH or anti-TSHr binding did not evaluate affinities of those interactions. Moreover, none of the studies that evaluated the biological effects of antipeptide antibodies on thyroid cells showed whether these antibodies could interact with the native protein. Further, the specificities of the antibodies were not established by reversing the functional activity by preincubating with the immunizing peptide. This is particularly important, as immunization with some peptides can cause breakdown of tolerance to self TSHr, resulting in an immune response that is much more broad and not limited to one against the immunizing peptide. Another confounding factor is the use of polyclonal antibodies in all of these studies. This is an important consideration, since the net biological specificities and functional effects (17). Therefore, a more comprehensive approach could result in a clearer understanding of the TSHr structure. Such a study would require relatively pure TSHr protein. However, to date none of the mammalian or bacterial expression systems (49) has yielded large enough quantities of TSHr to facilitate either purification of the protein or detailed immunological studies.

One eukaryotic system that results in high levels of protein production is the baculovirus expression system, which has been used to express over 150 proteins, including G-protein-coupled receptors with appropriate post-translational modifications (50). These include functional receptors for β -adrenergic and muscarinic cholinergic, nerve growth factor, and human immunodeficiency virus (i.e., CD4) (50). The predicted structure of the TSHr suggested that TSH might bind to the extracellular domain. This speculation has been supported more recently by a number of transfection studies using either chimeras of luteinizing hormone–thyrotropin receptor (LH–TSHr) cDNAs or site-directed mutagenesis (1,2,42). Therefore, we employed the baculovirus expression system to produce very high levels of recombinant ETSHr protein (51). The protein was used along with Freund's complete adjuvant to immunize rabbits and mice, and resulted in high levels of anti-TSHr antibody production. TSHrAbs obtained from both rabbits and mice blocked the binding of [¹²⁵I]TSH to native TSHr in solubilized porcine thyroid membranes in a radioreceptor assay. These

studies showed that the ETSHr is capable of inducing antibodies reactive with the native TSHr and suggested strongly that the ETSHr is antigenically similar to the native protein. More recently, we purified the ETSHr protein to homogeneity on a C4 reversed-phase, semipreparative column using high-performance liquid chromatography (52). The recombinant protein was identified as ETSHr by immunoreactivity with antibodies prepared against TSHr-derived synthetic peptides, amino acid compositional analyses, and protein sequence analyses. The purified ETSHr was refolded in the presence of 1.5 M guanidine-HCl and 1 mM each of cystine and cysteine. [¹²⁵I]TSH bound to the refolded ETSHr *in vitro* in a dose-dependent manner and was specifically blocked by unlabeled TSH, but not luteinizing hormone or follicle-stimulating hormone. It was notable that a membrane requirement was not essential for TSH to bind to ETSHr (52).

To analyze the anti-TSHr antibody response and to map anti-TSHr antibody binding sites, we developed a model system using the ETSHr protein, synthetic peptides derived from two regions (AA21–46 and 316–397) that have the highest predicted immunogenicity, and polyclonal antibodies against the recombinant ETSHr and the synthetic peptides. Antibodies against ETSHr and synthetic peptides were evaluated for their biological activity on rat thyroid cells (53). Antibodies were ineffective in causing either cAMP release or increased iodide uptake by the thyroid cells. However, antibodies against peptide 3A (AA357–372), 2 (AA352–366), and 91 (AA32–46) and anti-ETSHr showed blocking TSHrAb activity of 76.9, 37.5, 35.9, and 79.7%, respectively. When these antibodies were tested for their ability to block TSH binding to TSHr, only anti-ETSHr, but none of the antipeptide antibodies, blocked TSH binding. These data strongly suggested that blocking of TSH-mediated function in thyroid cells involves at least two mechanisms. The first is direct blocking of TSH as seen with anti-ETSHr, and the second, a step subsequent to TSH binding, as reported with some of the antipeptide antibodies. Using these antibodies in a competitive binding assay, we identified an immunodominant epitope (367–372) within a highly immunogenic region (AA352–388) of the ETSHr. This peptide lies within a region unique to the TSHr compared to other G-protein coupled glycoprotein hormone receptors (54).

In a more recent study, we investigated relationships between the time of appearance, fine specificity, and the functional properties of antibodies to TSHr in rabbits (55). The antibody response in each rabbit was characterized by testing serial serum sample for IgG against ETSHr protein and 26 synthetic peptides (20mers) that span the entire length of the ETSHr (55). All four rabbits developed high serum titers (>1:100,000) of ETSHr antibodies. None of the rabbits developed significant IgG titers against 11 of the 26 peptides, but each showed persistently high titers of IgG against

several other peptides. After multiple doses of antigen inoculation, significant TBII activity was found in sera from three of the four rabbits. On the basis of the ability of synthetic peptides to reverse TBII activity, we identified three regions of the TSHr (i.e., AA292–311, 367–386, and 397–415) to which TBII bind. Moreover, antibodies purified on either peptide 292–311 or peptide 367–386 affinity columns had TBII activity, as well as potent thyroid stimulation blocking (TSBA_b) activity on thyroid cells in culture. Together, the data from studies in rabbits showed that there are multiple regions on the TSHr (i.e., AA34–46, 292–311, 352–366, 357–372, 367–386, and 397–415) that play a direct or an indirect role in modulating the stimulatory effects of TSH. Antibody binding to any of these sites will block either TSH binding or TSH-mediated activation of thyroid cells, and thus represent sites on TSHr through which TSH interacts. Further discussion concerning these observations can be found in our recently published reports (53–55).

Encouraged by the results from our studies in rabbits, we have begun to use the recombinant protein and synthetic peptides to evaluate the immune response against TSHr in patients with Graves' disease. Our results showed that the ETSHr protein can be used to analyze and quantitate isotype-specific antibody response against the TSHr (56). In another study, we used the ETSHr protein and showed that a higher frequency of cells capable of producing TSHrAbs was present in patients with Graves' disease, relative to normal controls (57). For example, at 2×10^5 cells per well, 100% of wells containing cells from either patients with Graves' disease or controls were positive for Ig production. In contrast, 27% of the wells containing cells from Graves' patients, and only 3% from controls, were positive for TSHrAb. Higher titers of TSHrAbs were produced in cultures containing lymphocytes from patients with Graves' disease and these were predominantly of the IgG isotype. All patients with Graves' disease who had high thyrotropin-binding inhibitory Igs (TBII) also had higher frequencies of TSHr-specific B cells. These findings showed that TSHrAb-producing B cells are present at a higher frequency in the peripheral circulation of patients with Graves' disease (57).

Studies using 12 overlapping peptides derived from two predicted immunogenic regions of TSHr (AA12–46 and 316–397) have identified some of the antibody-reactive sites on the TSHr (56). Sera from patients with Graves' disease showed stronger reactivity against peptides from a relatively narrow region (i.e., AA352–394) of the TSHr. In another study, the same peptides were used to evaluate both antibody reactivity as well as a cell proliferation response in patients with Graves' disease (58). These studies showed that 4 out of 9 patients had antibody and cellular responses to some of the same peptides, and suggested that these peptides might contain

both T- and B-cell epitopes (58). More recently, we collaborated with Dr. Morris (Mayo Clinic) in studies using a large panel of 29 synthetic peptides that span the entire TSHr to identify epitopes to which Ig from Graves' patients bind (59). Nine, eight, and six of ten sera tested reacted with peptides 187–200, 376–394, and 629–639 (EC3), respectively. In contrast, none of the controls reacted. Using affinity columns prepared with peptides 376–394 and EC3, we were able to enrich for stimulatory antibodies. Affinity purification of antibodies on peptide 181–200 column resulted in enrichment of blocking antibodies. These data showed that we not only could partially purify TSHr-specific antibodies, but also could separate some of the stimulatory antibodies from the blocking antibodies. These studies continue to show the potential usefulness of peptides, albeit limited, for epitope mapping.

It is apparent that further studies are needed to evaluate the clinical usefulness of various recombinant proteins and synthetic peptides. It is likely that continued systematic studies could result in development of assays to detect and quantitate various subpopulations of antibodies to the TSHr.

ACKNOWLEDGMENTS

The authors gratefully thank Mardelle Susman for her expertise in editing and Cathy Gehret for her clerical assistance in the preparation of this work.

REFERENCES

1. Y. Nagayama and B. Rapoport, The thyrotropin receptor 25 years after its discovery: New insight after its molecular cloning. *Mol. Endocrinol.* **6**, 145 (1992).
2. G. Vassart and J. E. Dumont, The thyrotropin receptor and the regulation of thyrocyte function and growth. *Endocr. Rev.* **13**, 596 (1992).
3. G. Vassart, M. Parmentier, F. Libert, and J. Dumont, Molecular genetics of the thyrotropin receptor. *Trends Endocrinol. Metab.* **2**, 151 (1991).
4. F. E. Wondisford, J. A. Magner, and B. D. Weintraub, Thyrotropin. In "Werner and Ingbar's The Thyroid" (L. E. Braverman and R. D. Utiger, eds.), 6th Ed., pp. 257–305. Lippincott, Philadelphia, Pennsylvania, 1991.
5. M. F. Scanlon, Neuroendocrine control of thyrotropin secretion. In "Werner and Ingbar's The Thyroid" (L. E. Braverman and R. D. Utiger, eds.), 6th Ed. pp. 230–256. Lippincott, Philadelphia, Pennsylvania, 1991.
6. W. F. Schwindinger and M. A. Levine, McCune–Albright syndrome. *Trends Endocrinol. Metab.* **4**, 238 (1993).
7. D. Rosenbaum and T. F. Davies, The clinical use of thyroid autoantibodies. *Endocrinologist* **2**, 55 (1992).

8. M. K. Gupta, Thyrotropin receptor antibodies: Advances and importance of detection techniques in thyroid diseases. *Clin. Biochem.* **25**, 193 (1992).
9. P. R. Larsen and S. H. Ingbar, The thyroid gland. In "Williams Textbook of Endocrinology" (J. D. Milson and D. W. Foster, eds.), 8th Ed., pp. 357–488. Saunders, Philadelphia, Pennsylvania, 1992.
10. D. A. Fisher, M. R. Pandian, and E. Carlton, Autoimmune thyroid disease: An expanding spectrum. In "Pediatric Clinics of North America" (C. P. Mahoney, ed.), pp. 907–918. Saunders, Philadelphia, Pennsylvania, 1987.
11. D. A. Fisher, Neonatal thyroid disease in the offspring of women with autoimmune thyroid disease. In "Thyroid Today" (J. H. Oppenheimer, ed.), Vol. 9, No. 4, pp. 1–7. Flint Laboratories, Inc., Deerfield, Illinois, 1986.
12. J. S. Dallas and T. P. Foley, Thyrotoxicosis in childhood. In "Pediatric Endocrinology" (F. Lifshitz, ed.), 2nd Ed., pp. 483–500. Dekker, New York, 1990.
13. J. M. McKenzie and M. Zakarija, Antibodies in autoimmune thyroid disease. In "Werner and Ingbar's The Thyroid" (L. E. Braverman and R. D. Utiger, eds.), 6th Ed., pp. 506–524. Lippincott, Philadelphia, Pennsylvania, 1991.
14. L. Chiovata, P. Vitti, F. Santini, *et al.*, Incidence of antibodies blocking thyrotropin effect *in vitro* in patients with euthyroid or hypothyroid autoimmune thyroiditis. *J. Clin. Endocrinol. Metab.* **71**, 40 (1990).
15. B. Y. Cho, Y. K. Shong, H. K. Lee, *et al.*, Inhibition of thyrotropin stimulated adenylate cyclase activation and growth of rat thyroid cells, FRTL-5, by immunoglobulin G from patients with primary myxedema: Comparison with activities of thyrotropin-binding inhibitor immunoglobulins. *Acta Endocrinol.* **120**, 99 (1989).
16. M. M. Wilders-Trusching, H. A. Drexhage, G. Leb, *et al.*, Chromatographically purified IgG of endemic and sporadic goiter patients stimulates FRTL-5 cell growth in a mitotic arrest assay. *J. Clin. Endocrinol. Metab.* **70**, 444 (1990).
17. Y. Nagayama, H. Wadsworth, G. Chazenbalk, *et al.*, TSH-LH/CG receptor extracellular domain chimeras as probes for TSH receptor function. *Proc. Natl. Acad. Sci. U.S.A.* **88**, 902 (1991).
18. H. L. Wadsworth, G. D. Chazenbalk, Y. Nagayama, *et al.*, An insertion in the human thyrotropin receptor critical for high affinity hormone binding. *Science* **249**, 1423 (1990).
19. R. Wilson, J. H. McKillop, D. W. M. Pearson, *et al.*, Relapse of Graves' disease after medical therapy: Predictive value of thyroidal technetium-99m uptake and serum thyroid stimulating hormone receptor antibody levels. *J. Nucl. Med.* **26**, 1024 (1985).
20. R. Wilson, J. H. McKillop, N. Henderson, *et al.*, The ability of the serum thyrotropin antibody (TRAb) index and HLA status to predict long term remission of thyrotoxicosis following medical therapy for Graves' disease. *Clin. Endocrinol.* **25**, 151 (1986).
21. T. Davies, D. Evered, B. Smith, *et al.*, Value of thyroid stimulating antibody determinations in predicting short term thyrotoxic relapse in Graves' disease. *Lancet* **1**, 1181 (1977).
22. J. M. McKenzie and M. Zakarija, The clinical use of thyrotropin receptor antibody measurements. *J. Clin. Endocrinol. Metab.* **69**, 1093 (1989).
23. B. Rees Smith and R. Hall, Measurement of thyrotropin receptor antibodies. In "Methods in Enzymology" (J. J. Langone and H. V. Vunakis, eds.), Vol. 74, p. 405. Academic Press, New York, 1981.
24. B. R. Smith and R. Hall, Thyroid-stimulating immunoglobulins in Graves' disease. *Lancet* **2**, 427 (1974).
25. E. D. Mukhtar, B. Rees Smith, G. A. Pyle, *et al.*, Relation of thyroid stimulating immunoglobulins to thyroid function and effects of surgery, radioiodine, and antithyroid drugs. *Lancet* **1**, 713 (1975).

26. J. C. Kermode and B. D. Thompson, Iodination of thyroid-stimulating hormone for receptor-binding studies with human thyroid membranes: Effects of specific activity and method of iodination. *J. Endocrinol.* **84**, 439 (1980).
27. D. D. Adams, Thyroid stimulating autoantibodies. *Vitam. Horm.* **38**, 119 (1980).
28. J. M. McKenzie, The bioassay of thyrotropin in serum. *Endocrinology (Baltimore)* **63**, 372 (1958).
29. J. M. McKenzie, Delayed thyroid response to serum from thyrotoxic patients. *Endocrinology (Baltimore)* **62**, 865 (1958).
30. L. D. Kohn and W. A. Valente, FRTL-5 manual: A current guide. In "FRTL-5 Today" (F. S. Ambesi-Impombato and H. Perrild, eds.), pp. 243–273. Elsevier, Amsterdam, 1989.
31. J. C. Morris III, I. D. Hay, R. E. Nelson, and N.-S. Jiang, Clinical utility of thyrotropin-receptor antibody assays: Comparison of radioreceptor and bioassay methods. *Mayo Clin. Proc.* **63**, 707 (1988).
32. J. E. Dumont, P. P. Roger, and M. Ludgate, Assays for thyroid growth immunoglobulins and their clinical implication: Methods, concepts, and misconceptions. *Endocr. Rev.* **8**, 448 (1987).
33. H. R. Maurer, Potential pitfalls of [³H] thymidine techniques to measure cell proliferation. *Cell Tissue Kinet.* **14**, 111 (1981).
34. F. Creagh, M. Teece, S. Williams, *et al.*, An analysis of thyrotropin receptor binding and thyroid stimulating activities in a series of Graves' sera. *Clin. Endocrinol. (Oxford)* **23**, 395 (1985).
35. B. Rees Smith, S. M. McLachlan, and J. Furmaniak, Autoantibodies to the thyrotropin receptor. *Endocr. Rev.* **9**, 106 (1988).
36. S. Filetti, D. Foti, G. Costante, and B. Rapoport, Recombinant human thyrotropin (TSH) receptor in a radioreceptor assay for the measurement of TSH receptor autoantibodies. *J. Clin. Endocrinol. Metab.* **72**, 1096 (1991).
37. J. Ginsberg, G. Shewring, and B. Rees Smith, TSH receptor binding and thyroid stimulation by sera from patients with Graves' disease. *Clin. Endocrinol. (Oxford)* **19**, 305 (1983).
38. M. Zakarija and J. M. McKenzie, The spectrum and significance of autoantibodies reacting with the thyrotropin receptor. *Endocrinol. Metab. Clin. North Am.* **16**, 343 (1987).
39. Y. Nagayama, K. D. Kaufman, P. Seto, and B. Rapoport, Molecular cloning, sequence, and functional expression of the cDNA for the human thyrotropin receptor. *Biochem. Biophys. Res. Commun.* **165**, 1184–1190 (1989).
40. F. Libert, A. Lefort, C. Gerard, M. Parmentier, J. Perret, M. Ludgate, J. E. Dumont, and G. Vassart, Cloning, sequencing and expression of the human thyrotropin (TSH) receptor: Evidence for binding of autoantibodies. *Biochem. Biophys. Res. Commun.* **165**, 1250–1255 (1989).
41. M. Misrahi, H. Loosfelt, M. Atger, S. Sar, A. Guiochon-Mantel, and E. Milgrom, Cloning, sequencing, and expression of human TSHR. *Biochem. Biophys. Res. Commun.* **166**, 394–403 (1990).
42. L. D. Kohn, S. Kosugi, T. Ban, *et al.*, Molecular basis for the autoreactivity against thyroid stimulating hormone receptor. *Int. Rev. Immunol.* **9**, 135–165 (1992).
43. S. Kosugi, T. Akamizu, O. Takai, B. S. Prabhakar, and L. D. Kohn, The extracellular domain of the TSH receptor has an immunogenic epitope reactive with Graves' IgG but unrelated to receptor function as well as determinants having different roles for high affinity TSH binding and the activity of thyroid-stimulating autoantibodies. *Thyroid* **1**, 321–330 (1991).
44. G. D. Chazenbalk, Y. Nagayama, D. Russo, H. L. Wadsworth, and B. J. Rapoport, Functional analysis of the cytoplasmic domains of the human thyrotropin receptor by site directed mutagenesis. *Biol. Chem.* **265**, 20970–20975 (1990).

45. D. Russo, G. D. Chazenbalk, Y. Nagayama, H. L. Wadsworth, and B. Rapoport, Site directed mutagenesis of the human thyrotropin receptor. Role of asparagine linked oligosaccharides in the expression of a functional receptor. *Mol. Endocrinol.* **5**, 29–33 (1991).
46. M. Z. Atassi, T. Manshour, and S. Sakata, Localization and synthesis of the hormone-binding regions of the human thyrotropin receptor. *Proc. Natl. Acad. Sci. U.S.A.* **88**, 3613–3617 (1991).
47. T. Endo, M. Ohmori, M. Ikeda, and T. Onaya, Thyroid stimulating activity of rabbit antibodies toward the human thyrotropin receptor peptide. *Biochem. Biophys. Res. Commun.* **177**, 145–150 (1990).
48. M. Ohmori, T. Endo, and T. Onaya, Development of chicken antibodies toward the human TSHR peptides and their bioactivities. *Biochem. Biophys. Res. Commun.* **174**, 399–403 (1991).
49. O. Takai, R. K. Desai, G. S. Seetharamaiah, C. A. Jones, G. P. Allaway, T. Akamizu, L. D. Kohn, and B. S. Prabhakar, Prokaryotic expression of the thyrotropin receptor and identification of an immunogenic region of the protein using synthetic peptides. *Biochem. Biophys. Res. Commun.* **179**, 319–326 (1991).
50. V. A. Lucknow and M. D. Summers, Trends in the development of baculovirus expression vectors. *Bio/Technology* **6**, 47–55 (1988).
51. G. S. Seetharamaiah, R. K. Desai, J. S. Dallas, K. Tahara, L. D. Kohn, and B. S. Prabhakar, Induction of TSH binding inhibitory immunoglobulins with the extracellular domain of human thyrotropin receptor produced using a baculovirus vector. *Autoimmunity* **14**, 315–320 (1993).
52. G. S. Seetharamaiah, A. Kurosky, R. K. Desai, J. S. Dallas, and B. S. Prabhakar, A recombinant extracellular domain of the thyrotropin receptor binds thyrotropin in the absence of membranes. *Endocrinology (Baltimore)* **134**, 549–554 (1994).
53. R. K. Desai, J. S. Dallas, M. K. Gupta, G. S. Seetharamaiah, J. L. Fan, K. Tahara, L. D. Kohn, and B. S. Prabhakar, Dual mechanism of perturbation of thyrotropin mediated activation of thyroid cells by antibodies to the thyrotropin receptor (TSHR) and TSHR derived peptides. *J. Clin. Endocrinol. Metab.* **77**, 658–663 (1993).
54. J. S. Dallas, G. S. Seetharamaiah, S. J. Cunningham, R. M. Goldblum, R. K. Desai, and B. S. Prabhakar, A region on the human thyrotropin receptor which can induce antibodies that inhibit thyrotropin-mediated activation of *in vitro* thyroid cell function also contains a highly immunogenic epitope. *J. Autoimmunity* **7**, 469–483 (1994).
55. J. S. Dallas, S. J. Cunningham, J. C. Morris III, G. S. Seetharamaiah, N. Wagle, R. M. Goldblum, R. K. Desai, and B. S. Prabhakar, Thyrotropin (TSH) interacts with multiple discrete epitopes on the TSH receptor: Antibodies to one or more of these epitopes can inhibit TSH binding and function. *Endocrinology (Baltimore)* **134**, 1437–1445 (1994).
56. J. L. Fan, G. S. Seetharamaiah, R. K. Desai, J. S. Dallas, N. M. Wagle, and B. S. Prabhakar, Analysis of autoantibody reactivity in patients with Graves' disease using recombinant extracellular domain of the human thyrotropin receptor and synthetic peptides. *Autoimmunity* **15**, 285–291 (1993).
57. J. L. Fan, R. K. Desai, J. S. Dallas, N. M. Wagle, G. S. Seetharamaiah, and B. S. Prabhakar, High frequency of B cells capable of producing anti-thyrotropin receptor antibodies in patients with Graves' disease. *Clin. Immun. Immunopathol.* **152**, 2555–2561 (1994).
58. J. L. Fan, R. K. Desai, G. S. Seetharamaiah, J. S. Dallas, N. W. Wagle, and B. S. Prabhakar, Heterogeneity in cellular and antibody responses against thyrotropin receptor in patients with Graves' disease detected using synthetic peptides. *J. Autoimmunity* **6**, 799–808 (1993).
59. J. C. Morris, J. L. Gibson, E. J. Haas, E. R. Bergert, J. S. Dallas, and B. S. Prabhakar, Identification of epitopes and affinity purification of thyroid stimulating auto-antibodies using synthetic human TSH receptor peptides. *Autoimmunity* **17**, 287–299 (1994).

14

Measurement of Intracellular Glucocorticoid and Mineralocorticoid Receptors

Andrew S. Meyer¹
Thomas J. Schmidt
*Department of Physiology and Biophysics
College of Medicine
The University of Iowa
Iowa City, Iowa 52242*

INTRODUCTION

Overall Goal

In writing this review chapter, our primary goal has been to critically evaluate several experimental techniques currently utilized by our laboratory for measuring the intracellular levels of the glucocorticoid and mineralocorticoid receptors (GR and MR, respectively) that mediate the effects of adrenal corticosteroids on gene expression in target cells. To accomplish this goal we first present an overview of the diverse physiological effects elicited by these two classes of adrenal steroids, as well as the mode of action and structures of their respective receptor proteins. We then focus on the description and evaluation of several biochemical and molecular techniques utilized for the detection and quantitation of GR and MR at the ligand binding, protein, and mRNA levels. For each of these methodolo-

¹ Present address: Department of Biology, Concordia College, 800 N. Columbia, Seward, NE 68434.

gies we address theoretical and practical strengths and/or advantages, as well as potential limitations and/or disadvantages. Experimental conditions or physiological factors that can potentially influence the outcome of these assays are also discussed. Finally, we present experimental data generated in our own laboratory that demonstrate the application of these techniques in testing specific hypotheses. More precisely, we have utilized these methodologies to investigate the *in vivo* hormonal regulation, including potential homologous as well as heterologous regulation, of GR and MR levels in epithelial cells of the rat distal colon. These colonic cells, which coexpress GR and MR and are physiologically responsive to both glucocorticoid and mineralocorticoid hormones, have served as a useful model system in which to investigate potential autoregulation of these steroid receptors at the ligand binding, protein, and message levels.

Physiological Effects of Adrenal Corticosteroids

Glucocorticoids

Adrenal corticosteroids, which include glucocorticoids such as corticosterone (rodents) and cortisol (humans), as well as mineralocorticoids such as aldosterone, exert profound effects on the growth, differentiation, and function of a wide variety of target tissues and cell types. Since these diverse physiological and pharmacological effects have been the subject of several excellent reviews (1–6), they will only be briefly reviewed in this chapter. Although the glucocorticoid hormones acquired their name based on their critical role in maintaining carbohydrate reserves and blood glucose levels, virtually every tissue in the body is affected by either an excess or deficiency of these adrenal steroids. Certainly the best-known metabolic effect of glucocorticoids is their ability to stimulate gluconeogenesis in the liver (7) while simultaneously reducing the rate of lipogenesis (8). This gluconeogenic effect is mediated via the ability of these adrenocorticosteroids to enhance the rate of transcription of the hepatic genes that encode for enzymes involved in amino acid metabolism and gluconeogenesis (9). Cortisol also causes mobilization of amino acids from extrahepatic tissue, especially from muscle. As a consequence, more amino acids become available in the plasma to enter the hepatic gluconeogenic pathway and thereby enhance the rate of formation of glucose. Clearly one of the effects of this increase in gluconeogenesis is a dramatic increase in glycogen storage in liver cells (7). This increased rate of gluconeogenesis, coupled with a cortisol-mediated reduction in the rate of glucose utilization by all cells, results in an elevation of blood glucose levels, which can ultimately result in adrenal diabetes (10).

Another major effect of cortisol is its ability to reduce protein stores in essentially all cells except those of the liver. This effect is achieved by both a decrease in protein synthesis, which occurs as a consequence of decreased transport of amino acids into extrahepatic cells, and an increase in the catabolism of preexisting proteins (10). In contrast, cortisol enhances synthesis of liver proteins and plasma proteins synthesized in the liver. These hepatic responses reflect the fact that cortisol enhances the transport of amino acids into hepatic cells (10). Just as this glucocorticoid hormone promotes amino acid mobilization from muscle, it also promotes mobilization of fatty acids from adipose tissue (8). This effect increases the concentration of free fatty acids in the plasma, which also increases their utilization as an energy source. Although the mechanism(s) underlying this response are not thoroughly understood, the effect may well result from diminished transport of glucose into fat cells (10).

In addition to their well-documented and diverse anti-inflammatory and immunosuppressive effects (reviewed in Refs. 1,11, and 12), glucocorticoids also exert profound effects on the growth and differentiation of a wide variety of tissues (reviewed in Ref. 1). The growth-inhibitory effects may reflect the fact that these steroids can either antagonize the anabolic effects of growth hormone or directly inhibit the secretion of growth hormone. However, glucocorticoids have also been shown to inhibit DNA synthesis in most target tissues. This inhibitory effect appears to be common not only in tissues in which glucocorticoids are catalytic, such as fibroblasts, thymocytes, lymphocytes, muscle, and skin, but also in tissues such as the liver, in which these adrenal steroids are anabolic. Examples of the effects of glucocorticoids on differentiation include the observations that these steroids induce the precocious *de novo* synthesis of glutamine synthetase in the embryonic chick retina (13), accelerate fetal lung development and the appearance of surfactant in fetal rabbit lung (14,15), and promote the accumulation of rough endoplasmic reticulum, which may be the prerequisite for casein synthesis, by mammary gland organ cultures (16).

Mineralocorticoids

Mineralocorticoids such as aldosterone are referred to as the “life-saving” portion of the adrenocortical hormones. Clearly the most important physiological function of aldosterone is to promote the absorption of sodium and the simultaneous excretion of potassium by the renal tubular epithelial cells, particularly by those in the collecting tubule but also to a lesser extent by those in the distal collecting tubule and collecting duct (10). The net response of these effects is an increase in extracellular fluid volume and systemic blood pressure. In addition to promoting potassium secretion into

the renal tubules in exchange for sodium, aldosterone also causes, although to a much lesser extent, the tubular secretion of hydrogen ions in exchange for sodium ions. These same basic effects of aldosterone on electrolyte balance are also mediated in the sweat glands and salivary glands. Interestingly, recent data have also demonstrated that intracerebroventricular administration of aldosterone to rats (17) is capable of inducing hypertension at doses that have no effect on blood pressure when administered systemically. Although the mechanisms underlying this phenomenon are not well understood, these data do indicate that aldosterone can exert significant effects on fluid volume independent of its direct effect on renal sodium retention. In addition to these renal responses to mineralocorticoids, glucocorticoids are also capable of mediating specific effects on kidney function. For example, it has been clearly demonstrated that glucocorticoids are capable of increasing Na/H antiport activity in the proximal tubule (18) and sodium/potassium ATPase activity in the distal collecting tubule and medullary ascending limb (19,20). Use of a pure glucocorticoid agonist has also revealed that glucocorticoids elicit “mineralocorticoid-like” effects on sodium transport in cultured epithelia that include the frog A6 renal cell line (21), cultured collecting duct cells from the rabbit kidney (22), and rat inner medullary collecting duct cells (23). Although these renal effects of glucocorticoids have not been as thoroughly studied as those of mineralocorticoids, it is clear that these epithelia are glucocorticoid-responsive.

Colonic Responses

Finally, with regard to the content of the last section of this chapter, it is relevant to stress that the mucosal epithelial cells of the distal colon are also responsive to both classes of adrenal corticosteroids. Since the initial observation that aldosterone is capable of stimulating sodium and water reabsorption in the human colon (24), the effects of aldosterone on colonic ion transport have been studied in great detail. Data generated in several laboratories have suggested that the mechanism of colonic sodium reabsorption appears to be analogous to the mechanism described for the kidney (reviewed in Ref. 25). The initial effect of aldosterone on colonic epithelia appears to be an increase in the number of apical sodium channels, although it is not clear whether this increase is the result of new channel synthesis or recruitment of latent channels (26,27). Chronic aldosterone treatment has also been shown to increase the surface area and sodium/potassium ATPase activity of the basolateral membrane (28). Interestingly, it has been demonstrated that although colonic ATPase activity is increased by aldosterone, it is the GR, not the MR, that is solely capable of regulating expression of the $\alpha 1$ and β subunits of the enzyme at the transcriptional level

(29). Other data have suggested that the aldosterone-mediated increases in ATPase activity in some segments of the nephron are secondary to an increased level of intracellular sodium resulting from the increase in apical sodium channels (30,31). One exception to this appears to be the collecting tubule of the rabbit nephron. In this tissue, aldosterone has been reported to increase sodium/potassium ATPase activity by inducing the appearance of new catalytic units (32), and this effect is blocked by inhibitors of protein synthesis (33), suggesting that aldosterone increases *de novo* synthesis of the enzyme.

Complete analysis of the effects of glucocorticoids on colonic transport has previously been hampered by the fact that ligands such as dexamethasone and methylprednisolone, which were thought to be selective for GR, were found to bind to MR and elicit agonist activity (34–36). To avoid these potential complications, Turnamian and Binder (37) utilized aldosterone and the pure GR agonist RU 28362 to delineate mineralocorticoid and glucocorticoid effects on ion transport in the distal colon. Their data indicated that infusion of aldosterone (7 days) causes changes in four specific transport processes: induction of active electrogenic sodium absorption and active potassium secretion; enhancement of active electroneutral potassium absorption; and inhibition of electroneutral sodium chloride absorption. They also found that infusion of the pure glucocorticoid agonist RU 28362 elicits only an increase in electroneutral sodium chloride absorption, which is the predominant transport process in the distal colon. Treatment with RU 28362, however, has no effect on either potassium secretion or absorption and does not induce electrogenic sodium absorption. Additionally, in a more recent study Bastl *et al.* (38) demonstrated that glucocorticoids can actually inhibit the colonic electrogenic sodium absorption that is induced by aldosterone. According to the working model proposed by these investigators (38), the circulating levels of corticosterone in an intact animal are not only sufficient to enhance electroneutral sodium chloride absorption, but also sufficient to mediate this repression of aldosterone-induced active sodium absorption. Thus it has become clear that colonic epithelial cells, like those of the kidney, are physiologically responsive to both classes of adrenal corticosteroids.

Intracellular Mode of Action of Adrenal Corticosteroids

Although a growing body of data suggests that glucocorticoids (reviewed in Refs. 39 and 40) as well as mineralocorticoids (41) (reviewed in Refs. 40 and 42) may mediate nontranscriptional effects via binding to distinct plasma membrane receptors, clearly many of the effects elicited by these adrenal steroids in target tissues, including colonic epithelial cells, are medi-

ated at the transcriptional level via binding to intracellular GR and MR, respectively. Despite the fact that the unliganded receptors for sex steroids have been shown to reside exclusively in the nucleus even in the complete absence of their ligands (43,44), immunofluorescence data generated using specific antibodies directed against the GR (45–47) or MR (47,48) demonstrate that these receptors are located primarily in the cytoplasm in the absence of their respective ligands. According to the widely accepted model, once these adrenal corticosteroids diffuse into these target cells and bind to their appropriate heterooligomeric receptors, these complexes undergo a temperature-dependent step called “activation” or “transformation.” This ligand-induced conformational change, which occurs *in vivo* under physiological conditions as well as under a variety of *in vitro* conditions (49,50) (reviewed in Ref. 51), results in the dissociation of a dimer of the 90-kDa heat-shock protein (hsp 90) (52,53) and an increased affinity of these GR– and MR–hormone complexes for DNA (50,51,54). Once activated, these GR– and MR–hormone complexes translocate into the nucleus (47,48), where they bind as homodimers (55) to specific DNA sequences called hormone response elements (HREs) (56,57). The net result of this nuclear translocation and binding is the enhancement or repression of the rate of transcription of genes that code for specific proteins that potentially include the GR and MR proteins themselves. Although both positive (56,58) as well as negative (59) glucocorticoid response elements (GREs) have been shown to be associated with glucocorticoid-responsive genes, unique mineralocorticoid response elements (MREs) have not been identified (57). However, since the DNA binding domain of the human and rat MR is highly homologous (approximately 94% at amino acid level) to that of the human and rat GR (60,61), it is not surprising that MR can bind to specific positive GREs (57) and potentially negative GREs and modulate the rate of transcription of several glucocorticoid-responsive genes.

This ability of GR and MR to regulate the expression of overlapping gene networks has been the focus of several laboratories. In their model, Arriza *et al.* (62) hypothesized that the MR may partially stimulate a GR-responsive gene network in response to low glucocorticoid (corticosterone or cortisol) levels, whereas maximal activation of the gene network may be dependent on the GR responding to the higher levels of glucocorticoids associated with the response to stress. According to this model, the MR could actually function as an alternate or high-affinity GR (63), and this concept is consistent with the older literature that referred to the MR as type I (high affinity for corticosterone) and the GR as type II (low affinity for corticosterone) intracellular corticosteroid binding proteins. At the molecular level, hormone-dependent regulation of gene expression by GR and MR has been addressed using cells cotransfected with either GR or MR

expression vectors and a well-described glucocorticoid-responsive promoter (murine mammary tumor virus 5'-flanking sequence) linked to the luciferase reporter gene. Using this approach, Arriza *et al.* (62) noted that although both the GR and MR are capable of activating transcription from the same promoter, the GR appears to be 10–20 times more effective as a positive transcription factor. Additional studies on the structure of the GR by Hollenberg and Evans (64) revealed that the amino-terminal domain, which shares essentially no homology with the MR amino-terminal domain (60,61), contains a transactivation domain responsible for this efficient enhancement of transcriptional activity. Rupprecht and colleagues (65) subsequently reported that in contrast to the GR, the MR lacks such transactivation domains in its amino terminus. Also, a recent study by Pearce and Yamamoto (66) has demonstrated that MR and GR interact differently with the AP-1 transcription factors *c-jun* and *c-fos* when repressing transcription of a reporter gene. They concluded that the GR is more effective at repressing transcription of a reporter gene and that this differential response is again due to differences in the amino-terminal domains of these two receptors. Thus, despite the fact that the MR and GR are very similar in their basic structures and amino acid sequences, their abilities to modulate the expression of specific genes are not identical and may reflect their abilities to differentially interact with other positive as well as negative transcription factors.

Finally, with regard to the intracellular mode of action of glucocorticoids and mineralocorticoids, it has become clear that the mere expression of functional MR in a tissue does not guarantee that it will be responsive to physiological concentrations of aldosterone. Numerous tissues and cell types coexpress GR and MR, but not all of these tissues represent classic mineralocorticoid target tissues. As already mentioned, colonic epithelial cells, like specific epithelial cells found in the kidneys and parotid glands, not only coexpress both receptors but are also physiologically responsive to both glucocorticoids and mineralocorticoids. The sensitivity of these particular cells to aldosterone stems from the fact that they not only express functional MR that bind aldosterone with high affinity, but also express the enzyme 11 β -hydroxysteroid dehydrogenase. This enzyme catalyzes the metabolism of endogenous glucocorticoids to their respective keto analogs, which bind poorly to the MR. This inactivation of corticosterone or cortisol, both of which bind to MR with the same high affinity as aldosterone but circulate at much higher concentrations (100-fold higher) than aldosterone (63), thus facilitates the binding of aldosterone to MR in these classic mineralocorticoid-responsive tissues (67). It has been suggested that in other tissues that fail to express this metabolizing enzyme, glucocorticoids may function as the physiological ligand for the MR. As previously men-

tioned, in these tissues the MR may actually function as a high-affinity GR and as such may be responsive to typical resting levels of circulating glucocorticoids (63).

Autoregulation of Corticosteroid Receptors

The GR and MR, like other members of the steroid receptor gene superfamily, are subject to ligand-mediated autoregulation (reviewed in Ref. 68). Since it is the level of expression of these two closely related intracellular receptors that plays a major role in determining cellular sensitivity to adrenal glucocorticoid and mineralocorticoid hormones (69–71), homologous as well as potential heterologous regulation of GR and MR levels represent important homeostatic events. At the physiological level, autologous down-regulation of receptor gene expression by its cognate ligand could potentially prevent overstimulation by elevated adrenocorticosteroid levels. Conversely, during periods of low circulating steroid levels, these receptors could potentially be up-regulated to maintain target tissue sensitivity. Numerous laboratories have studied autoregulation of GR in a wide variety of tissues and cell types (reviewed in Ref. 68). Despite the fact that agonist-mediated down-regulation of GR does appear to be the most frequently detected form of autoregulation, it is not common to all target cells. For example, agonist-mediated up-regulation of GR (positive autoregulation) has been reported in several cells lines, many of which are growth-inhibited by glucocorticoids (72–74). Although not as thoroughly studied, autoregulation of MR levels has been evaluated in a number of key tissues, including the kidney and the hippocampus (reviewed in Ref. 68). Even though there is some variability in the results obtained by different laboratories, the majority of published data suggest that MR are up-regulated following removal of endogenous aldosterone via adrenalectomy. Finally, although potential heterologous regulation of GR and MR in a target tissue that is physiologically responsive to both glucocorticoids as well as mineralocorticoids had not been extensively investigated prior to our studies in the distal colon (75), earlier observations made in brain tissue suggested that such heterologous regulation does occur. For example, Luttge *et al.* (76) reported that binding of aldosterone to hippocampal MR down-regulates hippocampal GR binding levels. Our own data, which will be discussed in detail in the last section of this chapter, suggest that binding of aldosterone to colonic MR may be capable of down-regulating colonic GR mRNA levels.

Although the homologous as well as potential heterologous regulation of GR and MR were traditionally evaluated exclusively at the level of ligand binding, the cloning of the genes for these corticosteroid receptors (60,61,77,78) and the development of specific antibodies (79,80) have facili-

tated detailed analyses of hormonal regulation of these receptors at the message and protein levels. Using these reagents, numerous laboratories have demonstrated that autoregulation of the GR is somewhat tissue specific and may be mediated at one or more molecular levels, including: the transcriptional level, as evidenced by the ability of ligand-bound GR to decrease the rate of receptor gene transcription (81,82); the post-transcriptional level, as evidenced by the ability of some ligands to alter the stability of their own receptor message during the initial phase of homologous down-regulation (83–85); and the post-translational level, as evidenced by the ability of agonists to shorten the half-life of their own receptor protein (81,86,87). With regard to the agonist-mediated effect on GR gene transcription, Cidlowski and colleagues have reported that the human GR cDNA contains specific intragenic sequences, which lie within the ligand-binding domain, that can bind GR complexes and are sufficient to confer hormonally induced down-regulation (88,89). The autoregulation of MR mRNA and/or protein levels has been evaluated less vigorously. Although several investigators have reported up-regulation of MR mRNA levels in the hippocampus (90,91) and kidneys (92) following adrenalectomy, others have failed to detect message up-regulation in these same tissues (93,94). Recent data demonstrate that in the hippocampus multiple MR mRNA subtypes possessing unique 5'-untranslated sequences are expressed at different levels ($\alpha = \beta \gg \gamma$) and that only the α MR mRNA levels are up-regulated following adrenalectomy (95). Although it would be logical to conclude that up-regulation of MR mRNA levels, like up-regulation of GR mRNA levels, occurs primarily as a consequence of enhanced MR gene transcription, this conclusion has not been proven experimentally. Finally, with regard to MR protein levels, immunocytochemical studies using specific anti-MR antibodies have failed to detect any increase in either renal (96) or cardiac (97) immunostaining following adrenalectomy. In our own laboratory we have utilized an anti-MR antibody (80) in immunoblotting protocols in an attempt to analyze potential autoregulation of rat colonic MR, and those experiments will be presented in the section entitled Autoregulation of Rat Colonic GR and MR.

MEASUREMENT OF INTRACELLULAR GR AND MR

Quantitation of GR and MR Binding Levels

Specificity of Ligands

The specific binding of tritiated ligands has been utilized extensively for the quantitation of whole-cell or cytosolic GR and/or MR levels. However,

distinguishing between GR and MR in tissues or cell types that express both receptors has presented technical problems. These problems stem largely from the high degree of amino acid homology (57%) between the carboxy-terminal ligand binding domains of the GR and MR (61). As already mentioned, in many early studies the MR were referred to as the type I corticosteroid receptors because they bound cortisol and corticosterone (endogenous glucocorticoids) with a high affinity equivalent to that of aldosterone (60,62). Conversely, the GR were referred to as type II corticosteroid receptors because they bound cortisol and corticosterone, as well as aldosterone (endogenous mineralocorticoid), with relatively lower affinities than the type I receptors (21,62). Additionally, both glucocorticoid hormones, and to a lesser extent aldosterone, are known to bind to transcortin, the plasma corticosteroid binding globulin. Hence any contamination of tissue cytosolic extracts with plasma proteins complicated interpretation of binding data generated using the available tritiated ligands. The subsequent development of more specific synthetic ligands, however, eliminated most of these potential technical problems. For instance, with regard to quantitation of cytosolic GR, tritiated dexamethasone and triamcinolone acetonide, which bind to the GR with high affinity but with negligible affinity to transcortin (98), became commercially available. However, one limitation to the use of tritiated dexamethasone was that it was later shown by several investigators to cross-over bind to the MR (60,62,98–100). Also, although triamcinolone acetonide was considered a pure, high-affinity GR agonist, our laboratory as well as others have detected cross-over binding of this synthetic ligand to the MR, although with relatively low affinity (80,101). These specificity-related problems have been more recently overcome through the development of even more specific synthetic ligands, including the pure GR agonist RU 28362 (98,102), the pure GR antagonist RU 38486 (80,102), reviewed in Ref. 103), and the pure MR antagonists RU 28318 and RU 26752 (17,104). With regard to the MR antagonists, RU 28318, which is the potassium salt of 7 α -propyl spironolactone, has been shown to function as an antagonist *in vivo* (17,104), whereas the lactonic form of RU 28318, called RU 26752, has been reported to have a higher *in vitro* affinity for the MR and a lower affinity for other sex steroid receptors (104). Our laboratory has utilized these specific compounds, which have been supplied by Roussel-UCLAF, in designing ligand binding assays for the quantitation of GR and MR in colonic cytosolic assays. It is important to emphasize that these same basic protocols can be utilized for quantitating GR and MR binding levels in any other tissues or cultured cells in which they are coexpressed.

Cytosolic Binding Assays

For quantitation of GR and MR binding levels, cytosolic extracts are prepared by homogenizing pooled segments of either proximal or distal colon from rats of various treatment groups in two volumes of ice-cold Buffer A (50 mM potassium phosphate, 10 mM Na₂MoO₄, 10 mM Na₂WO₄, 2 mM dithiothreitol, and 10 mM thioglycerol, pH 7.0) using a Brinkman Tissue Homogenizer. Various components of this buffer, including Na₂MoO₄, Na₂WO₄, and dithiothreitol, are included to stabilize the unbound GR and MR and minimize the loss of steroid binding referred to as "inactivation" (reviewed in Refs. 51,105–107). The crude colonic homogenates are subsequently centrifuged at 100,000g for 1 hr at 0–4°C in a Beckman L7 Ultracentrifuge and the resulting supernatant (cytosol) is assayed for specific GR and MR binding levels. All of these steps, as well as those that follow, are performed at 0–4°C to minimize inactivation and potential proteolysis of the receptor proteins.

For quantitation of GR and MR binding levels, aliquots of freshly isolated cytosol are incubated with a single, saturating concentration of either [³H]triamcinolone acetonide or [³H]-aldosterone, respectively. More precisely, specific GR binding is measured by incubating aliquots of cytosol with 30 nM [³H]triamcinolone acetonide in the presence (competed) or absence (uncompeted) of a 500-fold molar excess of unlabeled triamcinolone acetonide for 3 hr at 0–4°C. For this assay the cytosol also contains a 250-fold molar excess of the MR antagonist RU 28318 to block cross-over binding of the GR agonist to the MR. Unpublished data (personal communication from Dr. J. Raynaud, Roussel-UCLAF, 1990) suggest that RU 28318 functions *in vivo* as an MR antagonist because it is converted into RU 26752, and hence may not function as an MR antagonist *in vitro* if this conversion does not occur. However, we selected RU 28318 for our *in vitro* cytosolic assays because our preliminary experiments conducted using cytosols prepared from a variety of target tissues demonstrated that a 250-fold molar excess of this steroid is sufficient to saturate the MR and block any cross-over binding of [³H]triamcinolone acetonide. Additional preliminary experiments also indicated that a 250-fold molar excess of RU 26752 can actually cross-over bind to the GR. Finally, with regard to the GR binding assay, preliminary experiments indicated that a 3-hr incubation is sufficient to achieve binding equilibrium. For quantitation of specific MR binding levels, aliquots of cytosol are incubated with 10 nM [³H]aldosterone in the presence (competed) or absence (uncompeted) of a 500-fold molar excess of unlabeled aldosterone for 48 hr at 0–4°C. For this MR assay the cytosol also contains a 250-fold molar excess of RU 28362 to block cross-

over binding of [^3H]aldosterone to the GR. Again, preliminary experiments indicated that this concentration of the pure agonist is sufficient to completely inhibit binding of [^3H]triamcinolone acetonide to the GR and hence block cross-over binding of [^3H]aldosterone. Also, preliminary time course experiments indicated that a 48-hr incubation is necessary for cytosolic MR binding levels to achieve equilibrium.

To quantitate GR and MR binding levels at the conclusion of these incubations, it is obviously necessary to separate that portion of the ^3H -labeled ligand bound to the receptor from the unbound (free) ^3H -labeled ligand. A number of methods have been developed to accomplish this separation for several different steroid receptors. Some of these techniques include: adsorption to dextran-coated charcoal particles; gel filtration; agar gel chromatography or electrophoresis; DEAE (diethylaminoethyl)-cellulose chromatography; high-pressure liquid chromatography; and adsorption of the bound ligand-receptor complexes by glass beads, adenosine triphosphate-Sepharose, and DEAE-cellulose filter discs (reviewed in Ref. 108). In our experiments we separate the bound from free ^3H -labeled ligands by adsorption to hydroxylapatite using a batch assay as originally developed for quantitation of estrogen receptors (109). Using this technique the ^3H -labeled ligand-bound GR or MR are adsorbed and the unbound ^3H -labeled ligands are removed by washing the pellets. The advantages of this procedure include the facts that the assay is rapid and reproducible, the adsorption to a solid phase may offer protection from proteolytic enzymes in solution, and, unlike the charcoal adsorption method, this technique does not result in the stripping of bound ^3H -labeled ligand at low cytosolic protein concentrations (110). In our experiments, 50- μl aliquots of the labeled colonic cytosols are incubated in triplicate with 400 μl of a hydroxylapatite slurry (10% w/v in Buffer A minus thioglycerol) for 15 min at 0–4°C. The pellets are then washed three times with 2 ml of wash buffer (50 mM potassium phosphate, 10 mM Na_2MoO_4 , pH 7.0) at 4°C to remove the unbound [^3H]triamcinolone acetonide or [^3H]aldosterone. The washed pellets are then resuspended in Redi-Gel scintillation cocktail (Beckman) and transferred to 5-ml plastic vials. The bound tritium content of each vial is subsequently assayed using a Beckman LS 5801 scintillation spectrometer with a counting efficiency of approximately 30% for tritium. The GR and MR binding data are then expressed as specifically (uncompeted minus competed) bound dpm per milligram of cytosolic protein as assayed via the Bradford assay (111).

Although these straightforward one-point GR and MR binding assays, which are routinely performed using a single saturating concentration of the appropriate ^3H -labeled ligand, have generated useful information, they do have potential limitations. First, when using these assays one can never

be completely certain that endogenous hormone (corticosterone or aldosterone) bound to cytoplasmic unactivated receptors has fully exchanged with the ^3H -labeled ligand. Also, any cytoplasmic GR or MR that have been activated by endogenous hormones may be less capable of rebinding ^3H -labeled ligands (112). Additionally, any GR or MR that may have been activated and subsequently translocated into the nuclei by endogenous glucocorticoid or mineralocorticoid hormones will not be detected in low-salt cytosolic extracts. Finally, it can be argued that a "saturating" concentration can never actually be found, since it represents the concentration that elicits the binding corresponding to the point on a linear Scatchard plot that lies in the intersection with the X axis (coordinates of $B/F = 0$, $[B] = [B_{\text{max}}]$). Thus it has been concluded that one-point measurements, although convenient, are not the most accurate method for quantitating maximal binding levels (reviewed in Refs. 108 and 113). Because of these potential limitations associated with ligand binding assays, our laboratory has also quantitated GR and MR at the protein and mRNA levels.

Quantitation of GR and MR Protein Levels

Antibodies and Preparation of Cytosol

For quantitation of GR and MR protein levels, Western immunoblotting protocols are employed. For quantitation of the GR protein, our laboratory utilizes the anti-GR monoclonal antibody BuGR₂ (79). This antibody recognizes an epitope within the DNA binding domain of the GR and interacts with the cytoplasmic unliganded and liganded as well as nuclear-activated forms of the GR (114,115). For quantitation of MR protein levels, the anti-MR antibody hMRsN (80) is utilized. This monospecific polyclonal antibody was raised against an 11-amino-acid peptide located in the amino-terminal region of the human MR and also recognizes the rat MR. As previously mentioned, this antibody has been utilized in immunocytochemical studies to demonstrate that aldosterone promotes nuclear translocation of the MR in rat colonic epithelial cells (47).

Cytosolic extracts for analysis by Western blotting are prepared from the scraped epithelial cells of the distal colon as already described for the ligand binding assays. However, for these experiments the homogenization buffer (Buffer A) is supplemented with 1 mM phenylmethylsulfonyl fluoride and 5 mg/ml soybean chymotrypsin/trypsin inhibitor. These inhibitors are added to minimize proteolysis of both receptors but particularly the MR (50), which appears to be more susceptible to proteolytic degradation in crude cytosolic extracts. To facilitate quantitation of total cellular (cytoplasmic plus nuclear) GR or MR protein levels, the homogenization buffer

is also adjusted to 0.4 M NaCl. Buffer of this ionic strength has been shown to extract nuclear GR (81) as well as MR (116) and thus facilitate the detection of these receptors in cytosolic extracts. In a separate series of experiments, our laboratory has taken advantage of the fact that homogenization buffer of low ionic strength can be used to generate cytosolic extracts containing only cytoplasmic GR. More specifically, we have evaluated the potential abilities of several GR agonists as well as antagonists to activate and promote nuclear translocation of cytoplasmic GR in the PROb rat colonic adenocarcinoma cell line. Since nuclear translocation occurs immediately following *in vivo* activation of GR (reviewed in Refs. 51 and 117), the ability of a ligand to activate GR in this colonic cell line has been evaluated in terms of its ability to deplete the cytoplasm of GR protein as assayed via immunoblotting (91). Finally, regardless whether total GR (or MR) protein levels are being quantitated in cytosols prepared from scraped colonic epithelial cells or cultured PROb cells, the cytosols prepared in buffer of high ionic strength must be desalted by gel filtration on prepacked Sephadex G₂₅ columns prior to immunoprecipitations and/or subsequent gel analyses.

Immunoprecipitations

For quantitation of GR protein levels, cytosols from the various treatment groups in a given experiment are adjusted to equivalent protein concentrations, incubated with a final concentration of 8% (v/v) BuGR₂ at 0–4°C for 3 hr and subsequently precipitated with Protein A–Sephadex. The resulting immunoprecipitates are then washed three times with Buffer A supplemented with 1.0% (w/v) sodium deoxycholate and 0.1% (v/v) Triton X-100 as previously described by our laboratory (118). Subsequent experiments showed that the concentrations of these detergents can be reduced to only 10% of those just listed. Preliminary experiments in which GR were prelabeled with [³H]triamcinolone acetonide for 2 hr and subsequently immunoprecipitated with BuGR₂ demonstrated that this protocol routinely results in the immunoprecipitation of 40–50% of the labeled GR. Also, we find less than 5% variability when comparing the efficiency of the immunoprecipitations between different samples in a given experiment. The results obtained using this approach of immunoprecipitating GR with BuGR₂ prior to immunoblotting with the same monoclonal antibody have generated data that are essentially identical to those obtained using crude cytosols (not immunoprecipitated). Importantly, this protocol did not produce autoradiograms on which the GR protein band was obscured, since the heavy and light chains of the antibody are of lower molecular weight than the

intact GR (94,000). Using this same basic protocol (immunoprecipitation and subsequent immunoblotting with BuGR₂), Hutchinson *et al.* (115) were able to follow GR immunoreactivity from the cytoplasmic fraction into the nuclear fraction following treatment of rat kidney epithelial cells with the glucocorticoid agonist corticosterone. Their data verified that decreases in total GR protein immunoreactivity following steroid treatment are not due to the failure of this antibody to recognize the activated nuclear form of the receptor protein. Finally, for quantitation of MR protein levels, aliquots of crude cytosols were used directly for immunoblotting, since in our experiments we have noted the failure of the hMRsN antibody to immunoprecipitate [³H]aldosterone–MR complexes.

Polyacrylamide Gel Electrophoresis and Western Transfer

Prior to gel analysis, standard sample buffer [10% glycerol, 2% sodium dodecyl sulfate (SDS), 0.0625 M Tris-HCl, 5% β-mercaptoethanol, and 0.005% pyronin y] is added to either the GR immunoprecipitates, aliquots of cytosols containing equivalent protein concentrations (MR quantitation), or Amersham prestained molecular weight markers. The samples are then boiled for 4–5 min, mixed, and allowed to stand at room temperature for 5 min prior to being loaded on a gel (10% SDS–polyacrylamide slab gel with a 3% stacking gel). The samples are then electrophoresed for 40 min at 150 V using a Bio-Rad minigel apparatus and standard electrophoresis buffer. Following electrophoresis the proteins are transferred to nitrocellulose filters using a Bio-Rad minitransfer unit and standard transfer buffer [25 mM Tris-HCl, 192 mM glycine, 20% (v/v) methanol, and 0.01% (w/v) SDS, pH 8.3] at 100 V for 1.5 hr.

Western Immunoblotting

After transfer of the proteins, the filters are blocked overnight (1 hr is sufficient) at room temperature with 10% nonfat milk in Tris-buffered saline (TBS: 20 mM Tris-HCl, pH 7.6, containing 137 mM NaCl and 0.1% Tween-20) and washed by three quick rinses, followed by one 15-min and two 5-min washes with room-temperature TBS. For detection of the GR protein, filters are then incubated with a 1:300 dilution of BuGR₂ in TBS for 1 hr at room temperature and then washed as just described. Detection of MR protein is performed in essentially the same manner using 4 μg/ml of hMRsN supplemented with 5% normal goat serum in TBS. For quantitation of both GR and MR, the washes are followed by incubation for 45 min with an anti-mouse (GR) or anti-rabbit (MR) horseradish peroxidase-labeled

second antibody provided with the Enhanced Chemiluminescence (ECL) kit (Amersham) and the filters are again washed. Detection is performed using reagents that are provided with the ECL kit and Hyperfilm-MP. Although other detection protocols, including ^{125}I -labeled counterantibody (80,119), are available for visualization of GR and MR protein bands by autoradiography, our laboratory utilizes the ECL protocol for a number of reasons. In this system a horseradish peroxidase-conjugated second antibody is used to catalyze the oxidation of luminol, a cyclic diacylhydrazide, in the presence of hydrogen peroxide. Immediately following this oxidation the luminol is in an excited state that may decay to ground state via a light-emitting pathway (reviewed in Ref. 120). Some of the advantages associated with ECL Western blotting include the following: (1) ECL is a nonradioactive detection system that has been estimated to be at least 10 times more sensitive than other nonradioactive or radioactive systems; (2) ECL generates a high-contrast signal; (3) using the ECL protocol, specific protein detection can often be achieved in less than 1 min; (4) the signal generated with ECL can be quantitated with a densitometer; (5) the ECL can be used to detect low-abundance proteins in complex cell samples; (6) using ECL the antigen can be detected with a very small amount of antibody or with a low-affinity antibody; and (7) using this detection system the primary and secondary antibodies can be stripped from membranes and the antigen, which remains undamaged, can be reprobbed with different antibodies.

In our experiments utilizing the ECL detection system we have found that the exposure times for the autoradiograms range from 5 sec to 1 hr. The resulting autoradiograms are then subjected to densitometric scanning using an Ultrosan XL laser densitometer with an internal integration system. Although, as previously mentioned, proteolytic inhibitors are routinely added to the homogenization buffer used for isolation of cytosolic extracts, extensive proteolysis of both GR and MR was detected in our initial experiments. We concluded that this degradation was most likely due to the high levels of fecal and bacterial contamination in the distal colon. To minimize this problem in subsequent experiments, the distal colons as well as the scraped epithelial cells were washed extensively with ice-cold saline prior to homogenization. This procedure, coupled with the immunoprecipitation of GR prior to immunoblotting, facilitated the routine detection of the intact (94 kDa) GR. Detection of intact MR (116 kDa) in aliquots of crude cytosol using the hMRsN antibody proved more difficult. However, after adding 5% normal goat serum to the hybridization solutions to reduce nonspecific binding and further diluting the second antibody, we were successful at detecting the 116 kDa band as well as a major band at 70 kDa, which presumably represents a proteolytic fragment of the MR.

Quantitation of GR and MR mRNA Levels

Isolation of RNA

For quantitation of GR and MR mRNA levels, our laboratory performs ribonuclease protection assays (RPAs). To perform these assays, RNA is first isolated from distal colonic epithelia scraped from individual experimental rats. The scraped cells are first washed twice with 0.9% NaCl and total cellular RNA is subsequently isolated with the RNA_{zol} reagent (Tel-Test, Inc., Friendswood, TX), which is a modification of the single-step procedure originally developed by Chomczynski and Sacchi (121). First, the colonic cell pellets are homogenized in 1 ml of RNA_{zol} using a Kontes ground-glass homogenizer. In related experiments we have found that isolation of total RNA from cultured colonic cells (PROb cell line) does not require homogenization with a glass homogenizer and can be achieved by thoroughly mixing the cells with RNA_{zol}. The homogenates prepared from scraped epithelial cells are then mixed with 0.1 volume of chloroform, incubated on ice for 15 min, and subsequently centrifuged at maximum speed in a microcentrifuge at 0–4°C. The upper aqueous portion is then transferred to a fresh tube and mixed with one volume of isopropanol, and RNA is then precipitated during a 45-min incubation at –20°C. The resulting precipitate is then centrifuged for 15 min in a microcentrifuge at 0–4°C and the RNA pellet is washed twice with cold 80% ethanol, dried, and resuspended in 0.5% SDS. The concentration of RNA in each sample is then determined by spectrophotometry (optical density at 260 nm/optical density at 280 nm) (122). The quality of the RNA is routinely verified by electrophoresis on a 1.0% agarose/formaldehyde gel and subsequent visualization by ethidium bromide staining using standard techniques (122). Our laboratory has chosen this particular method of RNA isolation because of its simplicity and the fact that it is a rapid procedure that is ideal for isolating intact RNA from small cell pellets. Additionally, RNA isolated with the use of RNA_{zol} is undegraded, free of DNA and proteins, and contains the whole spectrum of RNA molecules, including small (4–5S) RNAs.

Design of Riboprobes

The diagram presented in Figure 1 illustrates the homology between the rat MR and GR cDNAs and the location of the probes that we utilize for synthesis of antisense [³²P]cRNA probes. The MR antisense RNA probe has been derived from the prMR_{EH} transcription vector (60) (gift from Dr. R. Evans), which contains a 513-base-pair insert in pGEM 4z corresponding to an *Eco*R1 fragment containing portions of the carboxy terminus and

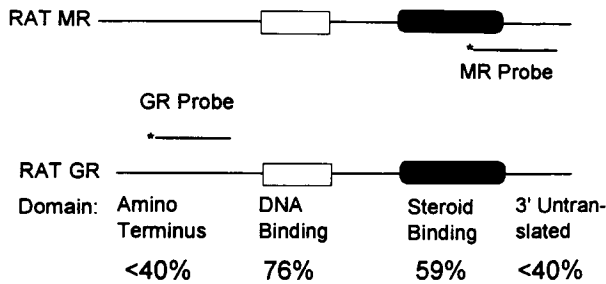


FIGURE 1. Linearized diagram depicting location of the cRNA probes used for quantitation of rat colonic epithelial cell MR and GR mRNAs. The upper panel depicts the MR cDNA and regions encoding the major receptor domains (amino terminus, DNA binding, ligand binding). The location of the cRNA probe specific for MR mRNA is also indicated. The lower panel depicts the GR cDNA and regions encoding the major receptor domains. The location of the cRNA probe specific for GR mRNA is also indicated. Beneath the receptor diagrams the locations of the basic domains are shown and the relative homology between the same domain of the two corticosteroid receptors is indicated. Note the low degree of cDNA homology between the two receptors in the domains that are targeted by the specific receptor probes.

3'-untranslated region of the rat MR cDNA. It is important to note that since this probe was generated from the 3' end of the MR cDNA, it would detect all possible 5'-untranslated splice variants of colonic MR mRNA if such message heterogeneity exists in that tissue. To confirm that this probe does not cross-hybridize to GR mRNA, the ribonuclease protection assay was performed utilizing this probe and 50 μg of total RNA prepared from the rat thymus. The thymus was selected for this important control experiment because it is known to express high GR levels but lacks detectable MR. The resulting autoradiogram revealed that although a strong protected fragment (513 nucleotides) could be detected with this probe and RNA isolated from rat colonic epithelia, no protected fragment of any size could be detected using thymus RNA. Subsequent probing with the β -actin and GR-specific probes resulted in strong protected fragments of the predicted size, indicating that the thymic RNA was intact.

The GR antisense RNA probe was derived from the pXGR14 transcription vector (gift from Dr. K. Yamamoto). This vector contains a 1.5-kb fragment of the GR cDNA in pBluescript that corresponds to sequences in the amino terminus as well as in the DNA binding domain of the GR. To synthesize an appropriate probe that would be specific for GR mRNA in ribonuclease protection assays, it was necessary to remove a *Sma*I–*Sma*I fragment (approximately 1 kb) that contains sequences encoding the GR DNA binding domain (76% homologous to MR DNA binding domain, see Figure 1). After removal of this fragment and religation of the vector, the

resulting cDNA insert was sequenced. Subsequent analysis indicated that this 446-nucleotide probe is less than 25% homologous to any MR cDNA sequences and hence cannot hybridize to MR mRNA in a ribonuclease protection assay. Although it would have been desirable to confirm this conclusion using RNA isolated from a rat tissue that expresses MR but not GR mRNA, such a tissue is not available. However, given the results of the sequence analysis and the high sensitivity of the ribonuclease protection assay (123), it is extremely unlikely that this probe can hybridize to MR mRNA. By utilizing this GR mRNA probe we were able to detect a single protected fragment in subsequent ribonuclease protection assays. Finally, the β -actin probe utilized in these experiments was purchased from Ambion Inc. (Austin, TX) and is provided in a linearized vector that contains promoters for several RNA polymerases. Although this probe is directed against sequences in the mouse β -actin cDNA, under our ribonuclease protection assay conditions it routinely facilitates detection of a strong protected fragment of the rat β -actin mRNA.

Synthesis of Riboprobes

The antisense [32 P]cRNA probes specific for the MR, GR, and β -actin mRNAs are synthesized using [32 P]UTP and the Riboprobe II Core System from Promega (Madison, WI). Briefly, 1 μ g of linearized template plasmid is incubated for 1–1.5 hr at 37°C in a reaction mixture containing 40 mM Tris-HCl, 6 mM MgCl₂, 10 mM dithiothreitol, 2 mM spermidine, 0.5 mM each of rATP, rCTP, and rGTP, 0.1 mM rUTP, 1 μ l of RNasin (RNase inhibitor from Promega), 2 μ l of [32 P]UTP, and 1 μ l of appropriate polymerase (T7 or SP6). The MR cRNA probe is synthesized via transcription of the *Hind*III linearized template with bacteriophage SP6 RNA polymerase to generate a 583-nucleotide antisense RNA probe containing 513 nucleotides that correspond to the MR cDNA sequences. The GR cRNA probe is synthesized via transcription of the *Xho*I linearized template with bacteriophage T7 polymerase, which generates a 550-nucleotide probe containing 446 nucleotides corresponding to GR cDNA sequences. The β -actin antisense RNA probe is transcribed using SP6 RNA polymerase to generate a 300-nucleotide probe containing 250 nucleotides corresponding to mouse β -actin cDNA sequences. Following synthesis, the reaction mixtures are incubated with 5 units of DNase I for 15 min at 37°C to digest template DNA. After DNase I digestion the riboprobes are gel-purified to remove fragments that are not of full length. Polyacrylamide (6%)/urea gels are subsequently utilized for both probe purification and final analysis of the ribonuclease protection assay and are run using a vertical gel apparatus (Bethesda Research Laboratories, Bethesda, MD) for 1 hr at 500 V as

described in the next section. Following electrophoresis, the gels used for probe purification are exposed to autoradiographic film for 1 min to determine location of the full-length probes, which are subsequently excised and eluted from the gel for several hours at 37°C using the elution buffer (0.5 M ammonium acetate, 1 mM EDTA, 0.2% SDS) included in the RPA II assay kit.

Ribonuclease Protection Assays

Ribonuclease protection assays are performed utilizing the Ribonuclease Protection Assay Kit (Ambion), which is a modification of the procedure originally described by Lee and Costlow (124). Briefly, 100,000 dpm of either the GR or MR [³²P]cRNA probes plus 60,000 dpm of the β -actin [³²P]cRNA probe are added to 20 μ g of epithelial cell total RNA. Preliminary experiments clearly demonstrated that these amounts of [³²P]cRNA probes are in excess of the amount of β -actin mRNA as well as the less abundant GR and MR mRNAs. The sample RNA and cRNA probes are then precipitated with 0.1 volume of 5 M NH₄OAc and 2.5 volumes of ethanol for 30 min at -20°C, and centrifuged at maximum speed in a microfuge at 4° for 15 min, and the supernatant is subsequently removed. The pellets are then resuspended in 20 μ l of hybridization buffer [80% formamide, 100 mM sodium citrate (pH 6.4), 300 mM sodium acetate (pH 6.4), and 1 mM EDTA], heated to 90°C for 3 min, and subsequently incubated overnight at 43°C. RNase digestion is performed the following morning by addition of 200 μ l of a 1 : 100 dilution (preliminary experiment indicated that this is the optimal concentration for total digestion of unprotected input probe) of RNase A/T1 mixture (250 units/ml RNase A, 10,000 units/ml RNase T1) and incubated for 30 min at 37°C. The protected fragments are subsequently precipitated by the addition of a proprietary RNase inactivation/precipitation mixture (Ambion). This mixture is then incubated for 15 min at -20°C and subsequently centrifuged at 4°C for 15 min. The supernatants are then removed and the pellets are resuspended in 8 μ l of loading buffer (80% formamide, 0.1% xylene cyanol, 0.1% bromophenol blue, and 20 mM EDTA). The pellets are heated at 90°C for 3 min prior to loading onto a 6% polyacrylamide/urea gel. The samples are electrophoresed at 400 V for approximately 1.5 hr using 1 \times TBE (50 mM Tris-base, 50 mM boric acid, 1 mM EDTA) running buffer.

Following electrophoresis, the gels are exposed to Hyperfilm-MP at -70°C for various periods of time. Two separate exposures are necessary for each gel to guarantee that both the β -actin mRNA signal and the MR or GR mRNA signal will fall within the linear range appropriate for densitometric scanning. This linear range was determined in a preliminary

experiment in which increasing amounts of total RNA from rat distal colon were utilized in the ribonuclease protection assay using the β -actin [^{32}P]cRNA probe. In most of our experiments, an overnight exposure has been sufficient for detection of the β -actin mRNA, whereas the receptor mRNA signals usually require 3- to 7-day exposures. The protected fragments on the resulting autoradiograms (see Figure 2) are then quantitated by densitometric scanning (LKB Ultrascan Scanning Densitometer) and the appropriate peak areas are automatically integrated. To ensure the reproducibility of the densitometric scanning, each band is scanned three separate times. For each sample the integrated area of the MR or GR mRNA protected fragment is normalized to the integrated area of the β -actin mRNA protected fragment. For our purposes, β -actin mRNA was selected for normalization because several laboratories have reported that this gene is unresponsive to corticosteroid treatment (81,82,88). Preliminary experiments conducted in our laboratory also demonstrated that adrenalectomy has no detectable effect on colonic epithelial cell β -actin mRNA levels. In each experiment the control treatment group (MR or GR mRNA/ β -actin mRNA) is normalized to 1.0 and the other treatment groups are expressed relative to the control group. For quantitation of GR and MR

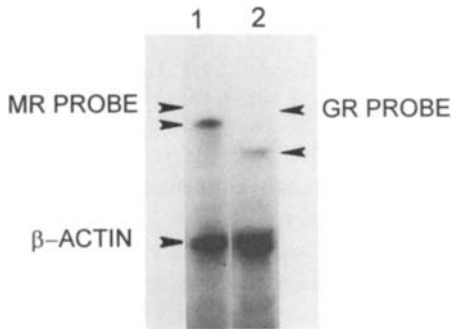


FIGURE 2. Example of ribonuclease protection assay (RPA) performed using total RNA from rat colonic epithelia. Total RNA (20 μg) isolated from the distal colon epithelia of 14-day adrenalectomized rats was used in the RPA with [^{32}P]cRNA probes for the MR mRNA (lane 1) or GR mRNA (lane 2) and the [^{32}P]cRNA probe for β -actin mRNA as described in the section entitled Quantitation of GR and MR mRNA Levels. For each lane, the upper arrow indicates the position of the intact MR (583-nucleotide) or GR (550-nucleotide) probe, the middle arrow indicates the position of the protected MR or GR mRNA fragment, and the lower arrow indicates the position of the protected β -actin mRNA fragment. The greater intensity of the MR mRNA protected fragment was due in part to the higher specific activity of the MR [^{32}P]cRNA probe. Separate exposures were normally used for detection of the protected GR, MR, and β -actin fragments to ensure that each signal fell within the linear range for densitometric scanning. Figure reproduced with permission from *Endocrinology* (75).

mRNA levels, all *in vivo* experiments are performed at least twice and the resulting data are pooled.

Finally, it is appropriate to emphasize that there are potential disadvantages as well as advantages associated with the use of the ribonuclease protection assay. In terms of potential disadvantages, this assay would fail to detect possible heterogeneity of GR or MR mRNAs as well as any differential hormonal regulation of those heterogeneous mRNA species. In contrast, there are numerous advantages associated with the use of this assay. First, it is an extremely sensitive procedure for the detection and quantitation of RNA species (usually mRNA) in a complex sample mixture of total cellular RNA. Second, compared to hybridization protocols that rely on RNA bound to a solid support (i.e., Northern blots), low-abundance mRNAs are detected more readily and quantitated more accurately using a solution hybridization procedure such as the ribonuclease protection assay (124). Finally, since the probes used in ribonuclease protection assays are generally significantly shorter than the mRNA species being quantitated, the target RNA preparation does not need to be completely intact. In other words, breaks in the mRNA that occur outside the region that hybridizes to the [³²P]cRNA probe will have no effect on the outcome of the ribonuclease protection assay, but will often result in band smearing on Northern blots.

AUTOREGULATION OF RAT COLONIC GR AND MR

Introduction

Having described in detail the specific protocols used for quantitation of GR and MR at the ligand binding, protein, and mRNA levels, we will focus in this last section on specific examples of how our laboratory has utilized these techniques to address specific hypotheses. Our major objective in the series of experiments that will be briefly reviewed here was to analyze hormonal regulation, both homologous as well as potential heterologous, of rat colonic GR and MR (75). As already mentioned in the section entitled Autoregulation of Corticosteroid Receptors, it is the level of expression of these two intracellular receptors that plays a major role in determining cellular sensitivity to adrenal glucocorticoid and mineralocorticoid hormones (69–71). Thus homologous as well as potential heterologous regulation of GR and MR levels are important events. As discussed earlier, the epithelial cells lining the rat distal colon have been utilized in our experiments because they represent an ideal target tissue in which to analyze hormonal regulation of GR as well as MR. These epithelial cells, which coexpress relatively high intracellular levels of GR and MR, can be easily

harvested as a relatively homogeneous cell population. Immunohistochemical studies have also shown that unliganded GR as well as MR are located primarily in the cytoplasm of these colonic cells and that both receptors are translocated into the nucleus following exposure to the appropriate ligand (47). Finally, as discussed earlier in the section entitled Physiological Effects of Adrenal Corticosteroids, MR and GR elicit distinct physiological responses in these colonic epithelial cells (37,38).

Effects of Adrenalectomy on GR and MR Ligand Binding Levels

The first basic question that we have addressed is whether endogenous corticosteroids (corticosterone and aldosterone) directly modulate GR and MR binding levels in colonic cells. Intact and adrenalectomized (14 days) Sprague-Dawley rats (175–200 g) were killed via anesthetization with methoxyflurane and subsequent decapitation. The colons were removed, opened longitudinally, and rinsed extensively with ice-cold 0.9% NaCl. The distal portion (4–5 cm) was considered to be the distal colon. The distal colons from the intact and adrenalectomized rats were pooled and homogenized in two volumes of ice-cold Buffer A and the cytosolic GR and MR specific binding levels were subsequently quantitated as described in the section entitled Quantitation of GR and MR Binding Levels. The data presented in Table I indicate that GR and MR binding levels were increased by 56 and 34%, respectively, 14 days following adrenalectomy. These data suggested that GR and MR binding levels may be coordinately up-regulated

TABLE I. Comparison of Cytosolic GR and MR Binding Levels in the Distal Colon of Intact versus 14-Day Adrenalectomized Rats

	dpm/mg protein ^a	
	GR ^b	MR ^c
Control	17,764 ± 391	7,896 ± 197
Adrenalectomized	27,643 ± 2119	10,630 ± 209
% increase	56 ^d	34 ^d

^a dpm specifically bound/mg cytosolic protein as assayed in triplicate by the hydroxylapatite batch assay (coefficient of variation consistently <5%).

^b Specific binding determined following a 3-hr incubation at 0–4°C.

^c Specific binding determined following a 48-hr incubation at 0–4°C.

^d Significant at $P < 0.05$ using Student's *t*-test.

in the distal colon following removal of endogenous corticosteroids. However, because of the potential limitations associated with ligand binding assays we felt that it was important to also address this question at the GR and MR protein and message levels.

Effects of Adrenalectomy on GR and MR Protein Levels

To test the hypothesis that the apparent up-regulation of both GR and MR binding levels detected postadrenalectomy are correlated with increases in total cellular (cytoplasmic plus nuclear) receptor protein levels, Western blotting experiments were subsequently performed. The data shown in Figure 3 were obtained in an experiment in which the total colonic epithelial cell GR protein levels were quantitated from three different treatment groups. The upper panel in Figure 3 is an autoradiogram of the immunoblot of the intact (approximately 94 kDa), previously immunoprecipitated GR protein detected using the BuGR₂ monoclonal antibody and the ECL reagents, whereas the lower panel illustrates the relative abundance of the GR protein levels as quantitated by densitometric scanning. In comparing the first two lanes it is clear that the total cellular GR protein level was up-regulated 14 days after adrenalectomy, which was consistent with the increase (up-regulation) in GR binding levels detected at this same time interval (see Table I). Since adrenalectomy eliminates both endogenous glucocorticoids and mineralocorticoids, it was also important as part of this experiment to demonstrate that administration of an exogenous GR agonist to adrenalectomized rats results in down-regulation of GR protein levels. As seen in Figure 3 (lane 3), three intraperitoneal injections of the pure GR agonist RU 28362 (1.0 mg/kg body weight) over a 24-hr period resulted in not only saturation of the GR based on binding assays but also down-regulation of the GR protein level to that detected in intact rats. Taken collectively, these data clearly demonstrated that colonic GR are autoregulated by their cognate ligand.

Western blotting experiments were also performed for quantitation of MR protein levels and the data are presented in Figure 4. The upper panel is an autoradiogram of the immunoblot of the intact MR protein (approximately 116 kDa) detected using the ECL reagents, whereas the lower panel illustrates the relative abundance of the MR protein bands as quantitated by densitometric scanning. The data demonstrate that MR protein levels were not increased 14 days after adrenalectomy, which was inconsistent with the increase (up-regulation) of MR binding levels detected at this same time interval (see Table I). These data thus suggested that the up-regulation of MR binding levels detected following adrenalectomy was not the direct consequence of increased MR protein levels. One plausible

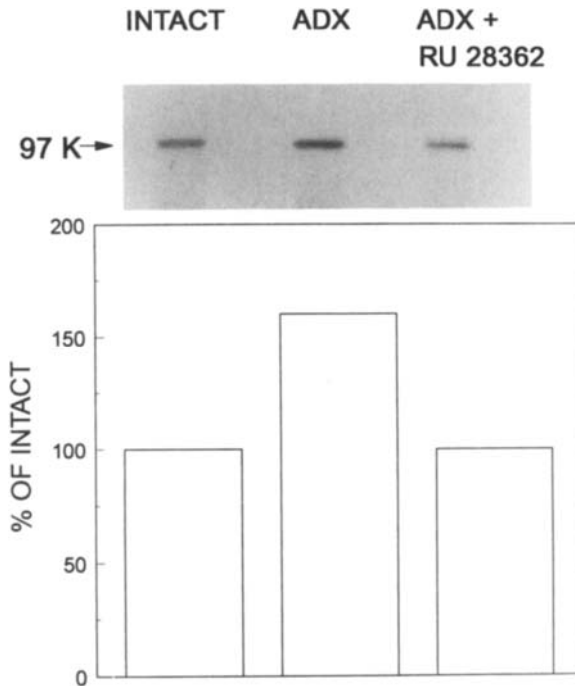


FIGURE 3. Western immunoblotting of colonic GR protein levels. Cytosol was prepared from the pooled distal colon epithelia (five animals per treatment group) from intact rats, adrenalectomized (14 days) rats, and adrenalectomized rats (14 days) that received multiple intraperitoneal injections of the pure GR agonist RU 28362 as outlined in the section entitled Effects of Adrenalectomy on GR and MR Protein Levels. Cytosols adjusted to equivalent protein concentrations were immunoprecipitated using the anti-GR monoclonal antibody BuGR₂, and Western blots were subsequently performed using BuGR₂ as outlined in the section entitled Quantitation of GR and MR Protein Levels. Detection of intact GR protein was performed using the enhanced chemiluminescence protocol also described in that section. The upper panel is a photograph of the resulting autoradiogram, and the lower panel indicates the relative abundance of the GR protein as quantitated by densitometric scanning of the autoradiogram. Figure reproduced with permission from *Endocrinology* (75).

explanation for the detected increase in MR binding levels after adrenalectomy is that activated nuclear receptors, which are incapable of rebinding steroid (125), are not detected in *in vitro* cytosolic binding assays. Because published data have suggested that in intact rats a significant fraction of MR are occupied by endogenous aldosterone (126) and presumably have undergone activation and nuclear translocation, removal of endogenous aldosterone via adrenalectomy would result in relocalization of these MR to the cytoplasm and subsequent detection in cytosolic binding assays. Thus

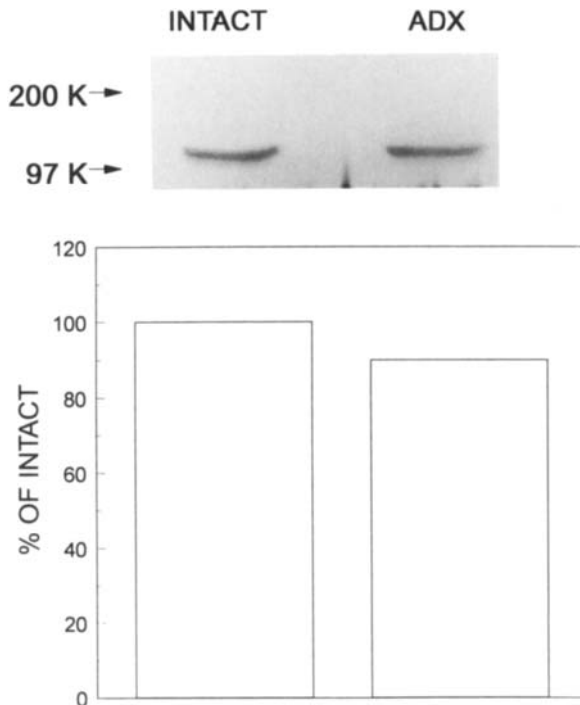


FIGURE 4. Western immunoblotting of colonic MR protein levels. Cytosol was prepared from the pooled distal colon epithelia (five animals per treatment group) from intact and adrenalectomized (14 days) rats. Equivalent amounts of cytosolic protein were subjected to Western blotting using the anti-MR monospecific polyclonal antibody hMRsN as outlined in the section entitled Quantitation of GR and MR Protein Levels. Detection of the intact MR protein was performed using the enhanced chemiluminescence protocol also described in that section. The upper panel is a photograph of the resulting autoradiogram, and the lower panel indicates the relative abundance of the MR protein as quantitated by densitometric scanning of the autoradiogram. Figure reproduced with permission from *Endocrinology* (75).

cytosolic binding could theoretically be increased after adrenalectomy as a consequence of receptor redistribution to the cytoplasm without any detectable up-regulation of MR protein levels. Although less likely, another possibility might be that following removal of endogenous corticosteroids including aldosterone, the total MR protein level in the cytoplasm may remain unaltered, but for unknown reasons (perhaps post-translational modifications such as enhanced phosphorylation or reduction of sulfhydryl groups) a higher fraction of the MR protein may be converted to an active binding form.

Effects of Adrenalectomy and Exogenous Ligands on GR and MR mRNA Levels

To test the hypothesis that the alterations in GR (increase) and MR (no change) protein levels detected following adrenalectomy are correlated with similar changes in receptor message levels, the effects of adrenalectomy as well as administration of exogenous glucocorticoid or mineralocorticoid ligands on GR and MR mRNA levels were then examined using ribonuclease protection assays as previously described. The data presented in Figure 5 demonstrate a significant 2.1-fold increase in colonic GR mRNA levels following 14 days of adrenalectomy, and this increase was consistent with the previously detected increase in GR protein levels (see Figure 3). In contrast, the data presented in Figure 5 show no detectable increase in MR mRNA levels following adrenalectomy, which was consistent with the observation that MR protein levels did not change following removal of endogenous corticosteroids (see Figure 4). Taken collectively, these data demonstrated that adrenalectomy results in differential regulation of rat colonic GR and MR at the mRNA as well as protein levels.

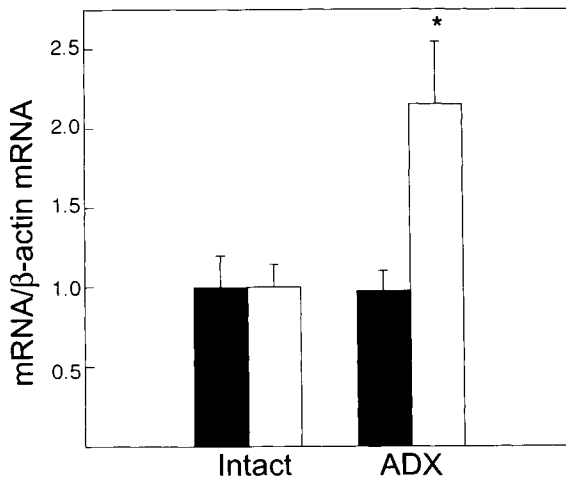


FIGURE 5. Effects of adrenalectomy on MR and GR mRNA levels. The RPA was performed for quantitation of both MR (■; $n = 6$) and GR (□; $n = 6$) mRNA levels using 20 μg total RNA isolated from the distal colon epithelia from either intact or adrenalectomized (14 days) rats. The scanned MR and GR mRNA/ β -actin mRNA ratios from the adrenalectomized animals were expressed relative to the control intact values. The n values represent the total number of animals used in two separate experiments. The asterisk indicates significantly different ($P < 0.05$) compared with control intact values. Figure reproduced with permission from *Endocrinology* (75).

Since adrenalectomy obviously removes endogenous glucocorticoids as well as aldosterone, a series of hormone replacement experiments were subsequently conducted to more precisely delineate which specific hormones (glucocorticoids versus mineralocorticoids) play a role in the regulation of GR mRNA levels. These experiments were also required for evaluation of potential homologous regulation of MR mRNA levels, because failure to detect an increase in these levels after adrenalectomy might have reflected the fact that this message is maximally expressed (up-regulated) in intact rats. Kalinyak *et al.* (127) have used this same logic to explain why GR mRNA levels are not apparently up-regulated in some rat target tissues following adrenalectomy. In the first series of hormone replacement experiments, multiple intraperitoneal injections of aldosterone (1.5 mg/kg body weight) or RU 28362 (1.0 mg/kg body weight) were administered over a 24-hr period. The multiple pharmacological injections of the pure GR agonist RU 28362 resulted in saturation of approximately 90% of the GR in the proximal colons of the same animals as measured by specific binding of [³H]triamcinolone acetonide. As the data in Figure 6 demonstrate, administration of this potent glucocorticoid agonist resulted in significant (approximately 80%) down-regulation of GR mRNA levels (homologous regulation), but did not result in any detectable change in MR mRNA levels (heterologous regulation). In the aldosterone replacement experiment it was necessary to administer an equimolar amount of the pure GR antagonist RU 38486 to block potential cross-over binding of aldosterone to the GR. These coinjections of aldosterone and RU 38486 (1.5 and 1.8 mg/kg body weight) saturated approximately 90% of the proximal colon MR and GR, respectively. Again, the data presented in Figure 7 demonstrate that multiple injections of the MR agonist failed to homologously regulate MR mRNA levels or heterologously regulate GR mRNA levels.

To test the hypothesis that autoregulation of MR mRNA levels might occur much more rapidly than homologous down-regulation of GR mRNA levels, a second series of hormone replacement experiments was performed. In these experiments, single injections of MR and GR agonists (same doses as previously indicated) were administered to adrenalectomized (14 days) rats and the animals were killed 6 hr later. A single injection of RU 28362 saturated approximately 45% of the GR in the proximal colons of the same animals as measured by the specific binding of [³H]triamcinolone acetonide. The resulting ribonuclease protection assay data (not shown) demonstrated that this single injection of agonist decreased GR mRNA levels by approximately 30%, but did not result in any detectable change in MR mRNA levels. A single injection of aldosterone administered without RU 38486 saturated approximately 90% of the MR in the proximal colons of these same animals. As seen in Figure 8, this single injection of aldosterone failed

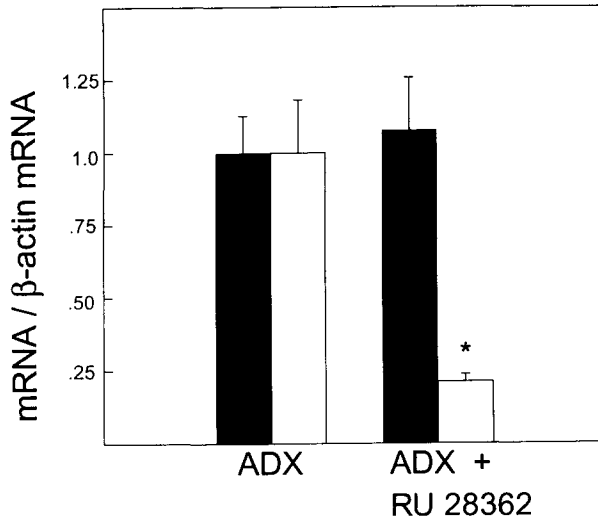


FIGURE 6. Effects of multiple injections of the pure GR agonist RU 28362 on MR and GR mRNA levels. The RPA was performed for quantitation of both MR (■; $n = 6$) and GR (□; $n = 6$) mRNA levels using 20 μ g total RNA isolated from the distal colon epithelia from either adrenalectomized (14 days) rats or adrenalectomized (14 days) rats that received multiple intraperitoneal injections of RU 28362 as outlined in the section entitled Effects of Adrenalectomy and Exogenous Ligands on GR and MR mRNA Levels. The scanned MR and GR mRNA/ β -actin mRNA ratios from the adrenalectomized animals were normalized to 1.0, and the MR and GR mRNA/ β -actin mRNA ratios from the RU 28362-injected animals were expressed relative to these normalized values. The n values represent the total number of animals used in two separate experiments. The asterisk indicates significantly different ($P < 0.01$) compared with control adrenalectomized values. Figure reproduced with permission from *Endocrinology* (75).

to homologously regulate MR mRNA levels, although it did elicit a 45% decrease (significant at $P < 0.05$) in GR mRNA levels. Although under these *in vivo* conditions cross-over binding of aldosterone to proximal colon GR was not detected, additional replacement experiments were performed to exclude this possibility. When aldosterone and RU 38486 were coinjected, approximately 90% of the MR and 80% of the GR in the proximal colons of the same animals were saturated as measured by steroid binding assays. The resulting message data (not shown) demonstrated that injection of the GR antagonist alone had no effect on GR mRNA levels and, most importantly, did not block the effect of aldosterone on GR mRNA levels. Taken collectively, these data demonstrated that although colonic MR–aldosterone complexes appear to be incapable of mediating homologous down-regulation of MR mRNA levels, these complexes do, under certain

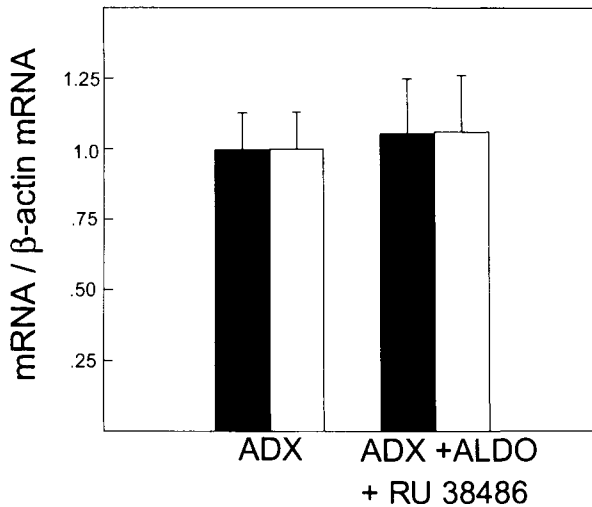


FIGURE 7. Effects of multiple injections of aldosterone (ALDO) on MR and GR mRNA levels. The RPA was performed for quantitation of both MR (■; $n = 6$) and GR (□; $n = 6$) mRNA levels using 20 μg total RNA isolated from the distal colon epithelia from either adrenalectomized (14 days) rats or adrenalectomized (14 days) rats that received multiple intraperitoneal injections of aldosterone in combination with the GR antagonist RU 38486 as outlined in the section entitled Effects of Adrenalectomy and Exogenous Ligands on GR and MR mRNA Levels. The scanned MR and GR mRNA/ β -actin mRNA ratios from the adrenalectomized animals were normalized to 1.0, and the MR and GR mRNA/ β -actin ratios from the animals injected with aldosterone plus RU 38486 were expressed relative to these normalized values. The n values represent the total number of animals used in two separate experiments. Figure reproduced with permission from *Endocrinology* (75).

in vivo situations, appear to be capable of mediating a reproducible heterologous down-regulation of GR mRNA levels. Whether this heterologous down-regulation results from a transient decrease in the rate of transcription of the GR gene mediated by binding of aldosterone–MR complexes to negative GRE sequences, a transient decrease in the stability of the GR message again mediated by aldosterone–MR complexes, or a combination of both mechanisms is not known. Obviously, experiments designed to address these underlying mechanisms would be technically difficult to perform *in vivo*.

Conclusions

In conclusion, the experimental data presented in the last section of this chapter have illustrated how specific techniques developed for the measurement of intracellular GR and MR at the ligand binding, protein, and mRNA

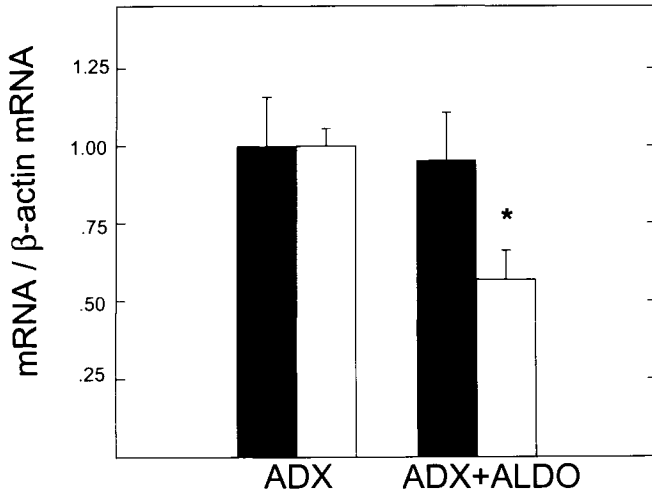


FIGURE 8. Effects of a single injection of aldosterone (ALDO) on MR and GR mRNA levels. The RPA was performed for quantitation of both MR (■; $n = 6$) and GR (□; $n = 4$) mRNA levels on 20 μg total RNA isolated from the distal colon epithelia of adrenalectomized (14 days) rats and adrenalectomized (14 days) rats that received a single intraperitoneal injection of aldosterone as outlined in the section entitled Effects of Adrenalectomy and Exogenous Ligands on GR and MR mRNA Levels. The GR and MR mRNA/ β -actin mRNA ratios for the adrenalectomized rats were normalized to 1.0, and the GR and MR mRNA/ β -actin mRNA ratios from the aldosterone-injected animals were expressed relative to these normalized values. The n values represent the total number of animals used in two separate experiments. The asterisk indicates significantly different ($P < 0.05$) compared with control (non-aldosterone-injected) values. Figure reproduced with permission from *Endocrinology* (75).

levels have been utilized by our laboratory to address fundamental questions concerning autoregulation of colonic corticosteroid receptors. Each of these techniques, including specific binding assays, Western blotting, and ribonuclease protection assays, has limitations as well as specific advantages and strengths, and when utilized in combination with each other they constitute a sound experimental approach. Hopefully our detailed discussion of these specific techniques will be not only informative but also of practical utility to endocrinologists interested in additional questions concerning the potential regulation of the expression of the GR and MR genes by corticosteroids as well as by other hormones and cytokines.

ACKNOWLEDGMENTS

The authors wish to express their appreciation to Dr. Rheem Medh for her helpful comments and suggestions during the preparation of this chapter and to Ms. Vicki Spenner for her

secretarial assistance. They would also like to thank Roussel-UCLAF in Romainville, France, for their generous gifts of RU 28362, RU 38486, and RU 28318. The research conducted in Dr. Schmidt's laboratory was supported in part by U.S. Public Health Service Grant HL-44546 (Hypertension SCOR) and by a Grant-in-Aid from the American Heart Association, Iowa Affiliate.

REFERENCES

1. E. B. Thompson and M. E. Lippman, *Metabolism* **23**, 159–202 (1974).
2. J. D. Baxter, *Pharmacol. Ther.* **2**, 605–659 (1976).
3. A. Munck and K. Leung, In "Receptors and Mechanism of Action of Steroid Hormones" (J. R. Pasqualini, ed.), Vol. 8 Modern Pharmacology—Toxicology, pp. 311–397. Dekker, New York, 1976.
4. A. Munck, P. M. Guyre, and N. J. Holbrook, *Endocr. Rev.* **5**, 25–44 (1984).
5. D. Marver and J. P. Kokko, *Miner. Electrolyte Metab.* **9**, 1–18 (1983).
6. C. P. Bastl and J. P. Hayslett, *Kidney Int.* **42**, 250–264 (1992).
7. G. R. Cahill, In "The Human Adrenal Cortex" (N. P. Christy, ed.), p. 205. Harper & Row, New York, 1971.
8. D. Rudman and M. Girolamo, In "The Human Adrenal Cortex" (N. P. Christy, ed.), p. 241. Harper & Row, New York, 1971.
9. P. Feigelson, F.-L. Yu, and J. Hanoune, In "The Human Adrenal Cortex" (N. P. Christy, ed.), pp. 257–272. Harper & Row, New York, 1971.
10. A. C. Guyton, In "Textbook of Medical Physiology" (A. C. Guyton, ed.), 8th Ed., pp. 842–854. Saunders, Philadelphia, Pennsylvania, 1991.
11. C. L. Cope, In "Adrenal Steroids and Disease" (C. L. Cope, ed.), 2nd Ed., pp. 232–253. Lippincott, Philadelphia, Pennsylvania, 1972.
12. R. M. Berne and M. N. Levy, "Physiology," 2nd Ed., p. 968. Mosby, St. Louis, Missouri, 1988.
13. A. A. Moscona and R. Piddington, *Science* **158**, 496–497 (1967).
14. R. V. Kotas and M. E. Avery, *J. Appl. Physiol.* **30**, 358–361 (1971).
15. E. K. Motoyama, M. M. Orzalesi, Y. Kikkawa, M. Kaibara, B. Wu, C. J. Zigas, and C. D. Cook, *Pediatrics* **48**, 547–555 (1971).
16. O. Takami and Y. J. Topper, *J. Natl. Cancer Inst.* **48**, 1225–1230 (1972).
17. E. P. Gomez-Sanchez, C. M. Fort, and C. E. Gomez-Sanchez, *Am. J. Physiol.* **258**, E482–484 (1990).
18. J. L. Kinsell, *Semin. Nephrol.* **10**, 330–338 (1990).
19. L. C. Garg, N. Narang, and C. S. Wingo, *Am. J. Physiol.* **248**, F487–F491 (1985).
20. A. I. Katz, *Semin. Nephrol.* **10**, 388–399 (1990).
21. T. J. Schmidt, R. F. Husted, and J. B. Stokes, *Am. J. Physiol.* **264**, C875–C884 (1993).
22. A. Naray-Fejes-Toth and G. Fejes-Toth, *Am. J. Physiol.* **259**, F672–F678 (1990).
23. R. F. Husted, J. R. Laplace, and J. B. Stokes, *J. Clin. Invest.* **86**, 498–501 (1990).
24. R. Levitan and F. J. Ingelfinger, *J. Clin. Invest.* **44**, 801–808 (1965).
25. G. I. Sandle and H. J. Binder, *Gastroenterology* **93**, 187–196 (1987).
26. H. Garty and I. S. Edelman, *J. Gen. Physiol.* **81**, 785–803 (1983).
27. A. Tousson, C. D. Alley, E. J. Sorscher, B. R. Brinkley, and D. J. Benos, *J. Cell Sci.* **93**, 349–362 (1989).
28. M. Kashgarian, C. R. Taylor, H. J. Binder, and J. P. Hayslett, *Lab. Invest.* **42**, 581–588 (1980).

29. P. J. Fuller and K. Verity, *Endocrinology (Baltimore)* **127**, 32–38 (1990).
30. D. Marver, *Am. J. Physiol.* **246**, F111–F123 (1984).
31. A. Doucet, *Kidney Int.* **34**, 749–760 (1988).
32. G. El Mernissi and A. Doucet, *Pfluegers Arch.* **402**, 258–263 (1984).
33. C. Barlet-Bas and A. Doucet, *J. Clin. Invest.* **79**, 629–631 (1987).
34. C. P. Bastl, *J. Clin. Invest.* **80**, 348–356 (1987).
35. C. P. Bastl, *Am. J. Physiol.* **255**, F1235–F1242 (1988).
36. E. S. Foster, T. W. Zimmerman, J. P. Hayslett, and H. J. Binder, *Am. J. Physiol.* **245**, G668–G675 (1983).
37. S. G. Turnamian and H. J. Binder, *J. Clin. Invest.* **84**, 1924–1929 (1989).
38. C. P. Bastl, G. Schulman, and E. J. Cragoe, *Am. J. Physiol.* **263**, F443–F452 (1992).
39. D. Duval, S. Durant, and F. Homo-Delarche, *Biochim. Biophys. Acta* **737**, 409–442 (1983).
40. I. Nemer, Z. Li-Xin, and A. W. Norman, *Receptor* **3**, 277–291 (1993).
41. M. Wehling, J. Kasmayr, and K. Theisen, *Am. J. Physiol.* **260**, E719–E726 (1991).
42. M. Wehling, In “Genomic and Nongenomic Effects of Aldosterone” (M. Wehling, ed.), pp. 109–149. CRC Press, Boca Raton, Florida, 1994.
43. M. Perrot-Applanat, F. Logeat, M. T. Groyer-Picard, and E. Milgrom, *Endocrinology (Baltimore)* **116**, 1473–1484 (1985).
44. W. V. Welshons, M. E. Lieberman, and J. Gorski, *Nature (London)* **307**, 747–749 (1984).
45. A.-C. Wilkstrom, O. Bakke, S. Okret, M. Bronnegard and J.-A. Gustafsson, *Endocrinology (Baltimore)* **120**, 1232–1242 (1987).
46. D. Picard and K. R. Yamamoto, *EMBO J.* **6**, 3333–3340 (1987).
47. G. Schulman, N. M. Robertson, B. Eifenbein, D. Eneanya, G. Litwack, and C. P. Bastl, *Am. J. Physiol.* **266**, C729–C740 (1994).
48. N. M. Robertson, G. Schulman, S. Karnik, E. Alnemri, and G. Litwack, *Mol. Endocrinol.* **7**, 1226–1239 (1993).
49. G. Schulman, V. Daniel, M. Cooper, E. S. Alnemri, A. B. Maksymowych, and G. Litwack, *Receptor* **2**, 181–194 (1992).
50. G. Schulman, A. Miller-Diener, G. Litwack, and C. P. Bastl, *J. Biol. Chem.* **261**, 12102–12108 (1986).
51. T. Schmidt and G. Litwack, *Physiol. Rev.* **62**, 1131–1192 (1982).
52. E. R. Sanchez, S. Meshinchi, W. Tienrungoj, M. J. Schlesinger, D. O. Toft, and W. B. Pratt, *J. Biol. Chem.* **262**, 6988–6991 (1987).
53. M.-E. Rafestin-Oblin, B. Couette, C. Radanyi, M. Lombes, and E.-E. Baulieu, *J. Biol. Chem.* **264**, 9304–9309 (1989).
54. C. Grillo, S. M. Vallee, G. Piroli, B. S. McEwen, and A. F. DeNicola, *J. Steroid Biochem. Mol. Biol.* **42**, 515–520 (1992).
55. J. Drouin, Y. L. Sun, S. Tremblay, P. Lavender, T. J. Schmidt, A. de Lean, and M. Nemer, *Mol. Endocrinol.* **6**, 1299–1309 (1992).
56. K. R. Yamamoto, *Annu. Rev. Genet.* **19**, 209–252 (1985).
57. M. Lombes, N. Binart, M.-E. Oblin, V. Joulin, and E.-E. Baulieu, *Biochem. J.* **292**, 577–583 (1993).
58. S. Argentin, Y. L. Sun, I. Lihmann, T. J. Schmidt, J. Drouin, and M. Nemer, *J. Biol. Chem.* **266**, 23315–23322 (1991).
59. J. Drouin, Y. L. Sun, M. Chamberland, Y. Gauthier, A. deLean, M. Nemer, and T. J. Schmidt, *EMBO J.* **12**, 145–156 (1993).
60. J. L. Arriza, C. Weinberger, G. Cerelli, T. M. Glaser, B. L. Handelin, D. E. Housman, and R. M. Evans, *Science* **237**, 268–275 (1987).

61. P. D. Patel, T. G. Sherman, D. J. Goldman, and S. J. Watson, *Mol. Endocrinol.* **3**, 1877–1885 (1989).
62. J. L. Arriza, R. B. Simerly, L. Swanson, and R. M. Evans, *Neuron* **1**, 887–900 (1988).
63. R. M. Evans and J. L. Arriza, *Neuron* **2**, 1105–1112 (1989).
64. S. M. Hollenberg and R. M. Evans, *Cell (Cambridge, Mass.)* **55**, 899–906 (1988).
65. R. Rupprecht, J. L. Arriza, D. Spengler, J. M. H. M. Reul, R. M. Evans, F. Holsboer, and K. Damm, *Mol. Endocrinol.* **7**, 597–603 (1993).
66. D. Pearce and K. R. Yamamoto, *Science* **259**, 1161–1164 (1993).
67. J. W. Funder, P. T. Pearce, R. Smith, and A. L. Smith, *Science* **242**, 583–585 (1988).
68. T. J. Schmidt and A. S. Meyer, *Receptor* **4**, 229–257 (1994).
69. J. N. Vanderbilt, R. Miesfeld, B. A. Maler, and K. R. Yamamoto, *Mol. Endocrinol.* **1**, 68–74 (1987).
70. D. L. Bellingham, S. Madhabananda, and J. A. Cidlowski, *Mol. Endocrinol.* **6**, 2090–2102 (1992).
71. S. Okret, Y. Dong, H. Tanaka, B. Cairns, and J.-A. Gustafsson, *J. Steroid Biochem. Mol. Biol.* **40**, 353–361 (1991).
72. L. P. Eisen, M. S. Elsasser, and J. M. Harmon, *J. Biol. Chem.* **263**, 12044–12048 (1988).
73. R. R. Denton, L. P. Eisen, and J. M. Harmon, *Endocrinology (Baltimore)* **133**, 248–256 (1993).
74. D. J. Gruol, F. M. Fajah, and S. Bourgeois, *Mol. Endocrinol.* **3**, 2119–2127 (1989).
75. A. S. Meyer and T. J. Schmidt, *Endocrinology (Baltimore)* **134**, 1163–1172 (1994).
76. W. G. Luttgé, M. E. Rupp, and M. E. Davda, *Endocrinology (Baltimore)* **125**, 817–824 (1989).
77. R. Miesfeld, S. Rosconi, P. J. Godowski, B. A. Maler, S. Okret, A.-C. Wilkstrom, J.-A. Gustafsson, and K. R. Yamamoto, *Cell (Cambridge, Mass.)* **46**, 389–399 (1986).
78. S. M. Hollenberg, C. Weinberger, E. S. Org, G. Cerelli, A. Oro, and R. Lebo, *Nature (London)* **318**, 635–641 (1985).
79. B. Gametchu and R. W. Harrison, *Endocrinology (Baltimore)* **114**, 274–279 (1984).
80. E. S. Alnemri, A. B. Maksymowych, N. M. Robertson, and G. Litwack, *J. Biol. Chem.* **266**, 18072–18081 (1991).
81. Y. Dong, L. Poellinger, J.-A. Gustafsson, and S. Okret, *Mol. Endocrinol.* **2**, 1256–1264 (1988).
82. S. Rosewicz, A. R. McDonald, B. Madduz, I. D. Goldfine, and R. L. Miesfeld, *J. Biol. Chem.* **263**, 2581–2584 (1988).
83. W. V. Vedecis, M. Ali, and H. R. Allen, *Cancer Res.* **49**(Suppl.), 2295s–2302s (1989).
84. M. Alksnis, T. Barkhem, P. E. Stromsted, H. Ahola, E. Kutoh, J.-A. Gustafsson, L. Poellinger, and S. Nilsson, *J. Biol. Chem.* **266**, 10078–10085 (1991).
85. A. S. Meyer and T. J. Schmidt, *76th Annual Meeting of the Endocrine Society (abstract)*, p. 318 (1994).
86. W. R. McIntyre and H. H. Samuels, *J. Biol. Chem.* **260**, 418–427 (1985).
87. T. J. Schmidt and A. S. Meyer, *J. Cell. Biochem. Suppl.* **18B**, p. 372 (abstract) (1984).
88. K. L. Burnstein, C. M. Jewell, and J. A. Cidlowski, *J. Biol. Chem.* **265**, 7284–7291 (1990).
89. K. L. Burnstein, C. M. Jewell, M. Sar, and J. A. Cidlowski, *Mol. Endocrinol.* **8**, 1764–1773 (1994).
90. J. M. H. M. Reul, P. T. Pearce, J. W. Funder, and Z. S. Krozowski, *Mol. Endocrinol.* **3**, 1674–1680 (1989).
91. J. P. Herman, P. D. Patel, A. Huda, and S. J. Watson, *Mol. Endocrinol.* **3**, 1886–1894 (1989).
92. J. E. Kalinyak, J. G. Bradshaw, and A. J. Perlman, *Horm. Metab. Res.* **24**, 106–109 (1992).
93. H. M. Chao, P. H. Choo, and B. S. McEwen, *Neuroendocrinology* **50**, 365–371 (1989).

94. K. M. Todd-Turla, J. P. Briggs, P. Killen, and J. Schnermann, *FASEB* (abstract), p. 1289 (1992).
95. S. P. Kwak, P. D. Patel, R. C. Thompson, H. Akil, and S. J. Watson, *Endocrinology (Baltimore)* **133**, 2344–2350 (1993).
96. Z. S. Krozowski, S. E. Rundle, C. Wallace, M. J. Castell, J. H. Shen, J. Dowling, J. W. Funder, and A. I. Smith, *Endocrinology (Baltimore)* **125**, 192–198 (1989).
97. M. Lombes, M.-E. Oblin, J.-M. Gasc, E.-E. Baulieu, N. Farman, and J.-P. Bonvalet, *Circ. Res.* **71**, 503–510 (1992).
98. T. Ojasoo and J.-P. Raynaud, *Cancer Res.* **38**, 4186–4198 (1978).
99. H. Coirini, A. M. Magarinos, A. F. DeNicola, T. C. Rainbow, and B. McEwen, *Brain Res.* **361**, 212–216 (1985).
100. C. Grillo, S. M. Vallee, G. Pirolì, B. S. McEwen, and A. F. De Nicola, *J. Steroid Biochem. Mol. Biol.* **42**, 515–520 (1992).
101. M. V. Govindan, S. Leclerc, R. Roy, P. Rathanaswami, and B. Xie, *J. Steroid Biochem. Mol. Biol.* **39**, 91–103 (1991).
102. G. G. Teutsch, G. Costerousse, R. Deraedt, J. Benzoni, M. Fortin, and D. Philibert, *Steroids* **38**, 651–665 (1981).
103. M. Moguilewsky and D. Philibert, *J. Steroid Biochem.* **20**, 271–276 (1984).
104. I. Perroteau, P. Netchitaïlo, C. Delarue, F. Leboulenger, D. Philibert, R. Deraedt, and H. Vandry, *J. Steroid Biochem.* **20**, 853–856 (1984).
105. J. J. Sando, N. D. Hammond, C. A. Stratford, and W. B. Pratt, *J. Biol. Chem.* **254**, 4779–4789 (1979).
106. J. J. Sando, C. J. Nielsen, and W. B. Pratt, *J. Biol. Chem.* **252**, 7579–7582 (1977).
107. M. E. Rafestin-Oblin, M. Lombes, P. Lustenberger, P. Blanchardie, A. Michaud, G. Cornu, and M. Claire, *J. Steroid Biochem.* **25**, 527–534 (1986).
108. S. Z. Cekan, *J. Lab. Clin. Med.* **124**, 606–622 (1994).
109. E. J. Pavlik and P. B. Coulson, *J. Steroid Biochem.* **7**, 357–368 (1976).
110. R. G. Smith and M. A. Sestili, *Clin. Chem.* **26**, 543–550 (1980).
111. M. Bradford, *Anal. Biochem.* **72**, 248–254 (1976).
112. J. A. Goidl, M. H. Cake, K. P. Dolan, L. G. Parchman, and G. Litwack, *Biochemistry* **16**, 2125–2130 (1977).
113. H. Braunsberg and K. D. Hammond, *J. Steroid Biochem.* **13**, 1133–1145 (1980).
114. E. H. Bresnick, E. R. Sanchez, and W. B. Pratt, *J. Steroid Biochem.* **30**, 267–269 (1988).
115. K. A. Hutchinson, L. C. Scherrer, M. J. Czar, Y. Ning, E. R. Sanchez, K. L. Leach, M. R. Deibel, and W. B. Pratt, *Biochemistry* **32**, 3953–3957 (1993).
116. D. Marver, D. Goodman, and I. S. Edelman, *Kidney Int.* **1**, 210–223 (1972).
117. A. Munck and R. Foley, *Nature (London)* **278**, 752–754 (1979).
118. E. E. Diehl and T. J. Schmidt, *Biochemistry* **32**, 13510–13515 (1993).
119. K. A. Hutchinson, M. J. Czar, L. C. Scherrer, and W. B. Pratt, *J. Biol. Chem.* **267**, 14047–14053 (1992).
120. D. F. Rosewell and E. H. White, In “Methods in Enzymology” (M. A. Deluca, ed.), Vol. 57, pp. 409–423. Academic Press, New York, 1978.
121. P. Chomczynski and N. Sacchi, *Anal. Biochem.* **162**, 156–159 (1987).
122. L. G. Davis, M. D. Dibner, and J. F. Battey, “Basic Methods in Molecular Biology,” p. 328. Elsevier, New York, 1986.
123. E. Winter, F. Yamamoto, C. Almoquera, and M. Perucha, *Proc. Natl. Acad. Sci. U.S.A.* **82**, 7575–7579 (1985).
124. J. J. Lee and N. A. Costlow, In “Methods in Enzymology” (S. L. Berger and A. R. Kimmels, eds.), Vol. 152, pp. 633–648. Academic Press, Orlando, Florida, 1987.

354 Chapter 14 Intracellular Glucocorticoid and Mineralocorticoid Receptors

125. R. L. Spencer, E. A. Young, P. H. Choo, and B. S. McEwen, *Brain Res.* **514**, 37–48 (1990).
126. P. C. Will, R. C. Delisle, J. G. Douglas, and U. Hopfer, *Am. J. Physiol.* **248**, G124–G132 (1985).
127. J. E. Kalinyak, R. I. Donn, A. R. Hoffman, and A. J. Perlman, *J. Biol. Chem.* **262**, 10441–10444 (1987).

15

Use of Transfection Techniques for Studying the Function of the D₂ Dopamine Receptors

Susan E. Senogles

Department of Biochemistry

University of Tennessee

Memphis, Tennessee 38163

Michael W. Quasney

Department of Pediatrics

Division of Critical Care

LeBonheur Children's Medical Center

University of Tennessee

Memphis, Tennessee 38103

INTRODUCTION

Importance of Dopamine in Regulating Prolactin Secretion from the Pituitary

The anterior lobe of the pituitary (adenohypophysis) secretes a number of hormones, including prolactin, thyrotropin stimulating hormone (TSH), adrenocorticotrophic hormone (ACTH), luteinizing hormone (LH), follicle stimulating hormone (FSH), and growth hormone (GH). Lactotroph cells, which comprise about 30% of cells in the anterior pituitary, are responsible for the production and secretion of prolactin. The secretion of prolactin is regulated partly in response to increasing levels of estrogen during pregnancy but can also be stimulated above basal levels in response to suckling and nipple stimulation. Hypothalamic regulation of the secretion of pituitary hormones has been the subject of intense research for years. Regulation of prolactin secretion by lactotrophs is unique among pituitary hormones because it has no specific releasing factor and is primarily under

tonic negative control. Dopamine, released by hypothalamic neurons into the portal blood system, functions as a dominant negative modulator of prolactin release from lactotrophs. Dopamine binds to a class of dopamine receptors, D₂ dopamine receptors, located on the lactotroph cells of the anterior pituitary (1–6), which are responsible for modulating both the basal and stimulated secretion of prolactin. In addition to the negative control by dopamine, prolactin secretion is also under the positive control of thyrotropin releasing hormone (TRH) released by the hypothalamus, though the physiological significance of this control is unclear.

Dopamine Receptor Signaling

The D₂ dopamine receptors are pleiotropic in their cellular signaling. These activated receptors have been shown to signal through adenylyl cyclase, phospholipase D, and various ionic channels to transduce their signals across cell membranes. The agonist-activated D₂ dopamine receptor has been shown to inhibit adenylyl cyclase in cells from the anterior and intermediate lobe of the pituitary (7,8). However, this effect of dopaminergic receptor activation does not account for all of the effects on prolactin secretion, as dopaminergic agonists inhibit prolactin release even in the presence of high cAMP (9). These data suggest that the inhibition of prolactin release by dopamine may be due to the interplay of one or more other signaling pathways. For example, it has been demonstrated that dopamine also will decrease intracellular [Ca²⁺]_i in primary lactotrophs and inhibit elevation of intracellular calcium by secretagogues, such as TRH (10). The apparent decrease of intracellular calcium may occur through the agonist-activated D₂ dopamine receptor modulation of K⁺ channels and Ca²⁺ channels. Agonist activation of the D₂ dopamine receptor has been shown to activate two distinct K⁺ channels in isolated lactotrophs (11–13). Other investigators have shown that dopamine can also inhibit two distinct voltage-gated calcium currents in isolated lactotrophs (14). Thus, negative modulation of prolactin secretion by dopamine may involve a complicated network of different signaling pathways.

Dopamine Receptor Expression

The D₂ dopamine receptor exists in two isoforms generated by the alternate splicing of mRNA, designated D_{2s} (short) and D_{2l} (long). These two isoforms differ only by the presence of a 29-amino-acid insert in the putative third cytoplasmic loop of the D_{2l} form (15). The two isoforms of the receptor are found colocalized in all tissues but in different expression ratios. For example, the intermediate and the anterior pituitary have a higher expres-

sion of the D₂ long form compared to the D₂ short form (15–17). However, the question arises as to whether the two isoforms of the receptor are functionally distinct. Recent evidence has suggested very few functional differences between the D₂ long and short forms of the dopamine receptor. Both isoforms of the D₂ dopamine receptor have been shown to inhibit adenylyl cyclase (15) and potentiate arachidonic acid release (18) with comparable potency of agonists. Reporter gene experiments suggest that the short form of the D₂ dopamine receptor is more potent at inhibiting adenylyl cyclase than the long form of the receptor (19). Evidence from our laboratory also demonstrates that the two isoforms of the receptor may couple through different G_{ia} subunits to the inhibition of adenylyl cyclase (20).

Why Use Transfection Techniques?

The study of the molecular mechanisms that govern dopamine mediation of prolactin release has been hampered by several factors. The anterior lobe of the pituitary is a heterogeneous population of secretory cells, only a portion of which secrete prolactin. Thus, the study of primary cells in culture is problematic owing to the difficulty in obtaining pure cultures of lactotrophs. From molecular cloning, it has become apparent that the effects of dopamine are mediated through two distinct D₂ dopamine receptors, which are coexpressed in tissues. Hence, determining the individual role of each of the alternate splice forms of the D₂ dopamine receptor in the control of prolactin secretion requires a system to dissect the contributions of each of the two isoforms. The ability to express the genes for the individual isoforms of the D₂ dopamine receptor in lactotroph cells would provide a unique opportunity to study the contributions of each D₂ dopamine receptor to the inhibition of prolactin secretion. We have utilized a transfection system to establish permanent cell lines that express each of two isoforms of the D₂ dopamine receptor.

TRANSFECTION OF CLONAL PITUITARY CELL LINES

Choice of Parent Cell Line

The GH4C1 cell line was chosen for the transfection studies in which a stable, permanent expression of the D₂ dopamine receptor gene was desired. This cell line was cloned from a pituitary tumor by Tashjian *et al.* (21). The GH4C1 cells synthesize and secrete prolactin and growth hormone, both basally and in response to secretagogue stimulation such as TRH. The

GH4C1 cells are an excellent model for studying lactotroph function and are ideal for transfection of either of the isoforms of the D₂ dopamine receptor, as the cells have lost the D₂ dopamine receptors during their transformation and do not respond to dopamine agonists (22) nor have detectable binding of D₂ dopamine ligands (23).

Stable Transfection in GH4C1 with Constitutive Expression

Culture Conditions for Parental Cell Line

GH4C1 cells (obtained from Dr. Agnes Schonbrun, University of Texas) were routinely cultured in Ham's F10 media supplemented with 7.5% heat-inactivated fetal bovine serum and 2.5% heat-inactivated horse serum in a humidified 5% CO₂ atmosphere at 37°C. Cells are plated at a density of 10 × 10⁶ cells/100-mm tissue culture dish 24 hr prior to transfection.

Preparation of Plasmid DNA and Transfection

Method We have used pZEM 228 D₂ long or short obtained from James R. Bunzow (Vollum Institute, University of Oregon Medical Sciences Center, Portland, OR) and Dr. Oliver Civelli (Hoffman-LaRoche, Basel, Switzerland). This vector contains the gene encoding resistance to G418 and the gene for the D₂ receptor under constitutive control.

1. Plasmid DNA prepared by cesium chloride gradient centrifugation (24) is precipitated with 0.1 volume of 5 M NH₄ acetate, pH 5.0, with 2 volumes of absolute ethanol at 4°C. Comments: The commercially available column purifications for plasmids are quite variable in terms of yielding plasmid capable of being used for transfection. Routinely, if plasmids prepared by this method are used, a phenol, phenol-chloroform, and chloroform extraction of the DNA is performed followed by ethanol precipitation.

2. The precipitate is collected by centrifugation at 13,000g for 20 min at 4°C and aspirated under sterile conditions in a tissue culture hood. The rest of the procedure is performed under sterile conditions.

3. The precipitated DNA is dissolved in 150 μl of sterile 10 mM Tris-HCl, pH 7.2, 150 mM NaCl, and 1 mM EDTA. This mixture is supplemented with 5 μg of sonicated calf thymus DNA.

4. Sterile 2 M CaCl₂ (25 μl) is added to the plasmid DNA, followed by a slow dropwise addition of 200 μl of 50 mM HEPES, pH 7.0, 2 mM NaPO₄, and 180 mM NaCl.

5. The mixture is allowed to stand at ambient temperature for 45 min, then 1–5 μg of either the $\text{D}_{2\text{S}}$ or the $\text{D}_{2\text{L}}$ isoform of the D_2 dopamine receptor is added.

6. The monolayer of cells is washed with Hank's Balanced Salt Solution (HBSS) to remove sera.

7. The transfection mixture is then added to the cells, which are incubated for 20 min. After this time, 2 ml of complete media is added. The cells are incubated for another 4 hr.

8. The media is removed after 4 hr and 1 ml of HBSS + 15% glycerol is added for 2 min at ambient temperature. Comment: This glycerol shock is important for reproducible transfections.

9. The cells are washed three times with HBSS, complete media is added, and the cells are allowed to recover for 48–72 hr.

10. At the end of this period, the cells are trypsinized (0.05% trypsin in 0.5 mM EDTA, Gibco) and plated in medium containing 400 $\mu\text{g}/\text{ml}$ of active G418 and 1 μM raclopride.

11. The selection media is changed every 3 days and potential clones are selected 14 days post-transfection.

12. Individual clones are obtained by the use of cloning cylinders or by limiting dilution. Comments: We have found that the D_2 dopamine receptor inhibits growth of cells, particularly in the early passages, presumably due to the catecholamines present in sera. We routinely use raclopride (a D_2 receptor antagonist) to facilitate growth of the clones.

Screening for Receptor Expression

To screen for the expression of the two isoforms of the D_2 dopamine receptor protein, we measure the binding of a dopamine antagonist, [^3H]-spiperone (NEN-DuPont), to the clonal cells.

[^3H]Spiperone Binding The various cell lines generated after transfection with either of the two isoforms of the D_2 dopamine receptor were characterized with respect to the amount of D_2 dopamine receptor expressed as determined by [^3H]-spiperone binding.

Method

1. Cells are scraped into microfuge tubes and crude membranes are prepared by centrifugation at 13,000g.

2. The crude membrane pellets are resuspended in 250 μl of 50 mM Tris-HCl, pH 7.4, 120 mM NaCl, 1 mM EDTA, and 10 mM MgCl_2 .

3. Binding reactions contain 50 μl of resuspended membranes with 500 pM of [^3H]spiperone.

4. Nonspecific binding is determined by inclusion of 1 μM (+)-butaclamol in parallel binding reactions.

5. The tubes are incubated at room temperature for 1 hr and the bound [^3H]spiperone is separated by filtration of the binding assay through GF/C glass fiber filters (Whatman) and quantified by liquid scintillation.

6. Specific binding is determined by subtraction of nonspecific binding determined by inclusion of 1 μM (+)-butaclamol in parallel incubations.

7. Total protein is determined by the method of Bradford (25). Comments: Many of the cell lines derived from GH4C1 cells expressed D₂ dopamine receptor ranging from 0.11 to 0.32 pmol/mg of protein. Occasionally a clonal line will show very high expression (>2 pmol/mg protein). However, these tend to grow slowly even in the presence of antagonist.

Southern Slot Blot Analysis The various cell lines generated after transfection with either of the two isoforms of the D₂ dopamine receptor were also characterized by Southern blot analysis using one of two oligonucleotides. The first probe, oligonucleotide 5'-ATGAACTCTGCACC-3', identified the D₂ long isoform of the receptor by annealing to sequences within the 87-nucleotide insert. The second probe, oligonucleotide 5'-CACTCAAGGATGCTG-3', spans one of the splice sites and is specific for the D₂ short isoform. This method is rapid and particularly useful for cotransfection strategies or for the screening of a large number of clones.

Method: Preparation of Sample for Slot Blot

1. The clonal lines to be screened are grown in 24-well cluster dishes in duplicate. We routinely plate 0.5×10^6 cells/well.

2. The media is aspirated and the cells are washed twice with phosphate-buffered saline (PBS).

3. The cell lysate is prepared by addition of 500 μl of 0.5 M NaOH and 1.5 M NaCl to the cell pellet.

4. The cells are scraped into microfuge tubes and heated to 100°C for 10 min and immediately transferred to ice for snap-cooling.

5. The samples are centrifuged for 20 min and the supernatants transferred to new microfuge tubes for storage until used. The samples can be stored at -80°C for extended periods of time until blotted.

Method: Preparation of Oligonucleotide Probe

1. The oligonucleotide (200 pmol) is added to a reaction mixture containing 100 mM cacodylate, pH 6.8, 1 mM CoCl₂, 0.1 mM DTT, 800 pmol of

biotin-21 dUTP, and 3 units of terminal deoxytransferase in a total volume of 10 μ l.

2. The reaction is incubated for 20 min at 37°C and stopped by the addition of 2.5 μ l 0.2 M EDTA, pH 7.0, and 39 μ l of water. The labeled oligonucleotide is purified by precipitation with 240 μ l 5 M ammonium acetate, pH 5.0, and 750 μ l of absolute ethanol.

3. The oligonucleotide reaction mixture is placed on ice for 30 min and centrifuged for 10 min at 4°C. The pellet is air-dried and resuspended in 100 μ l of water and stored at -20°C. Comment: To test whether the oligonucleotide was labeled, we routinely spot 5 μ l of the biotinylated probe onto Biotrans (+) membrane. After drying, this membrane can be prepared as discussed beginning at step 7 in the following.

Method: Preparation of Blot

1. The Southern blot is performed using Biotrans (+) membrane (ICN). The membrane is saturated with water and assembled into the slot blot apparatus (BioRad).

2. The samples are loaded by suction onto the membrane. Normally one-half of the sample generated as in the foregoing is sufficient to observe a signal on the Southern slot blot. After the samples are loaded, the wells are rinsed by addition of 500 μ l of 0.5 M NaOH and vacuum is applied until the wells are dry.

3. The membrane is removed from the apparatus and placed (DNA side up) for 5 min onto a piece of Whatman #1 filter paper that has been saturated with 2 \times SSC buffer. The membrane is air-dried and irradiated on a UV transilluminator for 5 min at maximum power.

4. The membrane is prehybridized at 42°C overnight by heat-sealing into a Kapak bag (Kapakorporation) with 2 ml of prehybridization solution: 5 \times SSC, 5 \times Denhardt's solution, 20 mM NaPi, pH 7.0, 5 mM EDTA, and 1% sodium dodecyl sulfate (SDS).

5. The labeled oligonucleotide (100 pmol) is added to the bag and incubated at 42°C for 2 hr.

6. The hybridization solution is removed and the blot is washed twice at 42°C for 15 min each with 2 \times SSC + 0.1% SDS.

7. The membrane is washed with 2 \times SSC + 0.1% SDS containing 20 ng/ml of streptavidin-horse radish peroxidase (Boehringer Mannheim) for 15 min at ambient temperature. Comment: Longer incubation times with the streptavidin conjugate will significantly increase the background.

8. The blot is washed once for 10 min at ambient temperature with a buffer containing PBS with 100 mM NaCl, 5% Triton-X-100, 1 M urea, and 1% dextran sulfate.

9. The blot is washed once for 10 min with a buffer containing 6.6 mM Na₂ citrate, 3.8 mM citric acid, and 10 mM EDTA.

10. The blot is placed on filter paper to remove excess moisture and placed in equal volumes of ECL detection reagents (Amersham) for 1 min.

11. The membrane is blotted with filter paper to remove excess reagent and exposed to XAR-5 film for 1–10 min. Comments: If quantitation is required, duplicate blots can be performed and one blot developed with an oligonucleotide specific for β -actin. A comparison of these blots will normalize for the amount of DNA that was originally applied to the Southern blot.

Screening for Functional Response

Adenylyl Cyclase Activity in Transfected GH4Cl Cells In addition to screening for dopamine receptor expression by ligand binding and Southern slot blots, clonal lines carrying the receptor can be screened for functional responses as well. The ability of dopamine to inhibit forskolin-stimulated and vasoactive intestinal peptide (VIP)-induced adenylyl cyclase is well documented (26–34). Nontransfected GH4Cl cells do not show a dopamine-mediated inhibition of forskolin-stimulated adenylyl cyclase, whereas clones expressing D₂ dopamine receptors show a 30–60% inhibition of forskolin-stimulated adenylyl cyclase. The highest percentage inhibition of adenylyl cyclase is obtained at concentrations of forskolin that are around the EC₅₀, which is approximately 15–25 μ M for GH4Cl cells. Basal cAMP can also be elevated by use of a stimulatory agonist, such as vasoactive intestinal peptide. Whereas forskolin will result in stimulations of >20-fold, VIP will usually give a 4- to 5-fold increase over basal levels of cAMP. Inhibition of stimulated adenylyl cyclase activity is routinely used for this assay because of the increased sensitivity. The assay of choice for screening for a functional response is the [³H]adenine assay. This method labels the pool of adenine nucleotides in the cell, and then determines the cAMP accumulation in intact cells. The cAMP produced in the cell can be normalized for the total adenine nucleotide pool in unstimulated control cells versus stimulated cells.

Method

1. Cells to be tested are plated at a density of 0.25–0.5 \times 10⁶/well. The cells are labeled in complete media with 1 μ Ci [³H]adenine (NEN-DuPont) overnight. Both GH4Cl and AtT20 cells are labeled efficiently by this process.

2. The cells are washed with PBS to remove excess label and placed in Dulbecco's Modified Eagle's Medium with high glucose (DMEM) containing 500 μM 1-isobutyl-3-methylxanthine.

3. The assay is initiated by simultaneous addition of 25 μM forskolin and dopaminergic agonist, such as *N*-propylnorapomorphine (NPA) at concentrations ranging from 10^{-10} to 10^{-6} *M*.

4. After 30 min of incubation at 37°C, the media is aspirated and the reaction stopped by the addition of 1 ml 10% trichloroacetic acid containing 1 *mM* cAMP and 1 *mM* ATP.

5. The cells are scraped into microfuge tubes and pelleted by centrifugation at 13,000*g* for 10 min and the supernatants are fractionated for [^3H]cAMP.

Method: Fractionation of [^3H]cAMP The 10% TCA extract of cells is chromatographed sequentially on Dowex (BioRad) and neutral alumina (ICN). The Dowex AG-50W-X4 columns are made by pouring 2 ml of a 50% v/v slurry into Polyprep columns (BioRad) and regenerated after each use by 1 reservoir 1 *N* HCl of water. The neutral alumina (ICN, Alumina N, Act.1) columns are prepared by dispensing 0.5 g of resin into the Polyprep columns and washing with 5 volumes of 0.1 *M* imidazole, pH 7.2.

Method: Chromatography of [^3H]cAMP

1. Place the 1 ml of TCA extract on the regenerated Dowex column. Collect the effluents into 20-ml scintillation vials.

2. Add 2 ml of water to each column and continue to collect the eluate in the same vials. These combined counts represent the [^3H]ADP + ATP pool of the cells.

3. Rack the Dowex columns over the columns containing the neutral alumina so that the Dowex columns elute directly onto the neutral alumina columns.

4. Add 4 ml of water to the Dowex and allow to completely drain through the Dowex and onto the alumina before removing the Dowex columns.

5. Remove the Dowex columns and place the alumina columns over another new set of scintillation vials.

6. Elute the [^3H]cAMP by adding 4 ml of 0.2 *M* imidazole to the alumina columns. Comment: The [^3H]cAMP accumulation can be corrected for recovery by inclusion of [^{14}C]cAMP in some samples. The [^3H]cAMP isolated by the chromatography is quantified by liquid scintillation counting. The results are expressed as the [^3H]cAMP/total [^3H]adenine. Total [^3H]adenine nucleotides is calculated by addition of [^3H]ATP + [^3H]ADP

+ [³H]cAMP. We routinely calibrate new Dowex and neutral alumina columns by chromatography of [³H]cAMP and run blanks for this assay by chromatography of the 1 ml 10% TCA stop solution.

Inducible Expression of D₂ Dopamine Receptors in AtT20 Cells

Often it is desirable to have a cell line in which the transfected gene of interest is inducible and is not constitutively expressed. This system allows the use of the stably transfected cell before induction as the control for the transfected cell after induction. The AtT20 cells are a mouse cell line derived from a pituitary tumor. This cell line is responsive to glucocorticoids, making it an ideal parent cell for use of the glucocorticoid-inducible expression vectors. The coding region for the two isoforms of the D₂ dopamine receptors was cloned into the pMAMneo vector (Clontech). This vector contains the MMTV (mouse mammary tumor virus) long terminal repeat, which contains the hormone response element for glucocorticoid. The vector also contains the gene that encodes for the resistance to G418.

Culture Conditions of Parental Cell Line

AtT20 cells (ATCC CCL 89) are grown in DMEM supplemented with 10% heat-inactivated fetal calf serum in a constant 37°C humidified incubator with 5% CO₂. Cells are plated at a density of 10×10^6 cells/100-mm tissue culture dish 24 hr prior to transfection.

Transfection of AtT20 Cells

Liposome-mediated transfection of AtT20 cells involves presenting the plasmid DNA as a DNA containing liposome. Lipofectin (Gibco-BRL) is a 1:1 mixed liposome containing *N*-[1-(2,3-dioleoyloxy)propyl]-*n,n,n*-trimethylammonium chloride (DOTMA) and dioleoyl phosphatidylethanolamine (DOPE) and has proven successful for the transfection of these cells.

Method

1. AtT20 cells are plated at a density of 1.0×10^7 /100-mm tissue culture dish.
2. Prepare plasmid DNA by ethanol precipitation as described in the section Preparation of Plasmid DNA and Transfection Dilute the plasmid DNA by adding 10 μg into serum-free Opti-MEM (Gibco-BRL) media in a final volume of 100 μl (sterile).

3. Dilute the lipofectin reagent by adding 100 μl of Opti-MEM media to 50 μg of lipofectin.
4. Combine the two solutions and allow to incubate for 15 min at ambient temperature.
5. Wash the attached cells with two washes of PBS and a final wash with serum-free Opti-MEM media.
6. Add 2 ml Opti-MEM to each tube of liposomes and gently overlay onto the cell layer.
7. Incubate for 8 hr at 37°C in a humidified CO₂ incubator.
8. Add 2 ml of 2× growth media to cells and allow cells to recover for 48 hr.
9. Select transfected cells by trypsinizing and replating in complete media containing 400 μg active G418 and 1 μM raclopride.
10. Individual colonies are usually visible 10–14 days after the transfection.
11. Create clonal lines by use of cloning cylinders to isolate individual colonies or by limiting dilution.

Screening for Expression

The cells lines can be screened for the inducibility of the expression of the D₂ dopamine receptor. This can be performed by [³H]spiperone binding as described in the foregoing section. The clones to be tested are plated in duplicate wells, and 100 nM dexamethazone is added to half of the wells. After 48 hr [³H]spiperone binding can be performed to determine the amount of D₂ dopamine receptor expression that occurs after induction with glucocorticoid treatment. Routinely, we observe no specific binding in the absence of glucocorticoid treatment and inductions of receptor-specific binding to 0.3–1.2 pmol/mg protein after glucocorticoid treatment.

Transient Expression in HEK 293 Cells

Human embryonic kidney cells (HEK 293) were chosen for the transfection studies in which we examined mutated D₂ dopamine receptors. The transient transfection technique has advantages over the generation of stable cell lines as it allows the rapid screening of a number of mutations.

Culture Conditions of HEK 293 Cells

HEK 293 cells are grown in DMEM supplemented with 10% heat-inactivated fetal calf serum in a constant 37°C humidified incubator with 5%

CO₂. Cells are plated at a density of 10×10^6 cells/100-mm tissue culture dish prior to transfection.

Transfection of HEK 293 Cells

Method

1. HEK 293 cells are grown to approximately 50% confluency in 100-mm tissue culture plates.
2. For each transfection, 1–10 μg of the D₂ dopamine receptor cloned into the plasmid pBC obtained from James R. Bunzow (Vollum Institute, University of Oregon Medical Sciences Center, Portland, OR) and Dr. Oliver Civelli (Hoffman-LaRoche, Basel, Switzerland) is diluted in 50 μl of serum-free media.
3. In a separate tube, 30 μl of lipofectin reagent (Gibco) is diluted into 50 μl of serum-free media.
4. The DNA and lipofectin dilutions are combined in a polystyrene tube, mixed gently, and incubated at room temperature for 15 min to allow the DNA–liposome complexes to form.
5. The cells are washed twice with serum-free media and 3 ml of serum-free media is added to each culture plate.
6. The DNA–liposome complexes are added to the culture plates, mixed gently, and incubated for 5 hr at 37°C with occasional mixing.
7. 7 ml of serum-containing media is added at the end of the incubation period and the cells are incubated overnight at 37°C. Comment: The use of lipofectin-mediated transfection was superior to use of DEAE-dextran and chloroquine.

Screening for D₂ Dopamine Receptor Expression

We have evaluated the expression of the D₂ dopamine receptors in transfected HEK 293 cells by both [³H]spiperone binding and adenylate cyclase activity as described earlier.

CONCLUSIONS

The Potential of Using Transfection for Study of Structure–Function Relationships of Receptors

One of the opportunities that transfection techniques allows is the study of mutated proteins to help delineate the structure–function relationships

of receptors as well as protein–protein interactions. Receptors in which mutations have been created can be transfected into cells to determine if the mutations affect various functions of the receptor. These include changes that might occur in the binding kinetics, activation of endogenous receptor enzyme activity, or the coupling to G-proteins and subsequent activation of specific signaling pathways.

We are currently using this approach to study regions of the D_2 dopamine receptor that are important for various functions. Mutated or chimeric D_2 dopamine receptors have been used to elucidate which regions may be important in the signaling of dopamine. Neve and co-workers have shown that aspartate at position 80 is important for the binding of agonist to the D_2 dopamine receptor (35). Our interests are focused on the regions of the D_2 dopamine receptor that are important in coupling with the G-protein. Malik and co-workers demonstrated attenuation of dopamine-inhibited adenylate cyclase activity in HEK 293 cell membrane preparations using synthetic peptides corresponding to various regions of the third cytoplasmic loop of the D_2 dopamine receptor (36). This observation suggested that the coupling of the D_2 dopamine receptor to the G-protein involved the third cytoplasmic loop. However, we wish to identify the amino acids involved in the process. More recently, Senogles (20) has demonstrated that the D_{2s} and D_{2l} isoforms signal through different G_i proteins using a cotransfection technique. We found that the D_{2s} isoform of the dopamine receptor signals through the $G_{i2\alpha}$, whereas the D_{2l} isoform signals through the $G_{i3\alpha}$ subunit in cotransfected GH4CL cells. Thus, the versatility of the transfection technique has allowed us to evaluate how these two isoforms of the D_2 dopamine receptor are coupled to specific $G_{i\alpha}$ subunits in a lactotroph cell model. However, the precise amino acids of the D_2 dopamine receptor responsible for the coupling of the receptor and the G-protein are unknown. We are currently placing single-site mutations within the third cytoplasmic loop of the D_2 dopamine receptor in an attempt to disrupt this coupling.

The Potential for the Study of Cellular Processes by Individual Receptor Subtypes

It is unknown why the various cell types studied thus far coexpress both the D_{2s} and D_{2l} isoforms of the D_2 dopamine receptor. Since evidence suggests that the two receptor isoforms signal through different $G_{i\alpha}$ subunits, they may be capable of activating distinct signaling pathways that are not yet identified. On the other hand, they may serve redundant functions within the cell. Because of the large number of isoforms that exist for various proteins, it is important to delineate the function of each of these.

The ability to transfect cells with one isoform at a time will allow researchers to evaluate if isoforms have distinct functions.

ACKNOWLEDGMENTS

This work was supported by USPHS Grant NS 28811 (S.E.S.) and a LeBonheur Children's Medical Center Small Grant Award (M.W.Q.).

REFERENCES

1. M. G. Caron, M. Beaulieu, J. Raymond, B. Gagne, J. Drouin, R. J. Lefkowitz, and F. Labrie, *J. Biol. Chem.* **253**, 2244–2253 (1978).
2. M. Munenura, T. E. Cote, K. Tsuruta, R. L. Eskay, and J. W. Kebejian, *Endocrinology (Baltimore)* **106**, 1676–1683 (1980).
3. C. Kohler and K. Fahlberg, *J. Neural Trans.* **63**, 39–52 (1985).
4. A. Pazos, M. E. Stoeckel, C. Hindelang, and J. M. Palacios, *Neurosci. Lett.*, **59**, 1–7 (1985).
5. E. B. DeSouza, *Endocrinology (Baltimore)* **119**, 1534–1542 (1986).
6. A. Mansour, J. H. Meador-Woodruff, J. R. Bunzow, O. Civelli, H. Akil, and S. J. Watson, *J. Neurosci.* **10**, 2587–2600 (1990).
7. W. M. McDonald, D. R. Sibley, B. F. Kilpatrick, and M. G. Caron, *Mol. Cell Endocrinol.* **36**, 201–209 (1984).
8. T. E. Cote, G. W. Greve, and J. W. Kebejian, *Mol. Pharmacol.* **22**, 290–297 (1982).
9. D. Delbecke, J. G. Scammell, A. Martinez-Campos, and P. S. Dannies, *Endocrinology (Baltimore)* **118**, 1271–1277 (1986).
10. A. Malgaroli, L. Vallar, F. R. Elahi, T. Pozzan, A. Spada, and J. Meldolesi, *J. Biol. Chem.* **262**, 13920–13927 (1987).
11. P. M. Lledo, P. Legendre, J. Zhang, J. M. Israel, and J. D. Vincent, *Neuroendocrinology* **52**, 545–555 (1990).
12. P. M. Lledo, V. Homburger, J. Bockaert, and J. D. Vincent, *Neuron* **8**, 455–463 (1992).
13. J. M. Israel, C. Kirk, and J. D. Vincent, *J. Physiol. (London)* **390**, 1–22 (1987).
14. P. M. Lledo, P. Legendre, J. M. Israel, and J. D. Vincent, *Endocrinology (Baltimore)* **127**, 990–1001 (1990).
15. R. Dal Toso, B. Sommer, M. Ewert, A. Herb, D. B. Pritchett, A. Bach, B. D. Shivers, and P. H. Seeburg, *EMBO J.* **8**, 4025–4034 (1989).
16. D. M. Weiner and M. R. Brann, *FEBS Lett.* **253**, 207–213 (1989).
17. K. L. O'Malley, K. J. Mack, K.-Y. Gandelman, and R. D. Todd, *Biochemistry* **29**, 1367–1371 (1990).
18. R. Y. Kanterman, L. C. Mahan, E. M. Briley, F. J. Monsma, D. R. Sibley, J. Axelrod, and C. C. Felder, *Mol. Pharmacol.* **39**, 364–369 (1991).
19. J. P. Montmayeur and E. Borrelli, *Proc. Natl. Acad. Sci. U.S.A.* **88**, 3135–3139 (1991).
20. S. E. Senogles, *J. Biol. Chem.* **37**, 23120–23127 (1994).
21. A. H. Tashjian, Y. Yasumura, L. Levine, G. H. Sato, and M. L. Parker, *Endocrinology (Baltimore)* **82**, 342–352 (1968).
22. W. B. Malarkey, J. C. Groshong, and G. E. Milo, *Nature (London)* **266**, 640–641 (1977).
23. M. J. Cronin, N. Faure, J. A. Martial, and R. I. Weiner, *Endocrinology (Baltimore)* **106**, 718–723 (1980).

24. J. Sambrook, E. F. Fritsch, and T. Maniatis, In "Molecular Cloning: A Laboratory Manual," 2nd Ed., pp. 1.42–1.52. Cold Spring Harbor Laboratory, Cold Spring Harbor, New York, 1989.
25. M. M. Bradford, *Anal. Biochem.* **72**, 248–254 (1976).
26. P. De Camilli, D. Macconi, and A. Spada, *Nature (London)* **278**, 252–254 (1979).
27. G. Giannattasio, M. E. De Farraei, and A. Spada, *Life Sci.* **28**, 1605–1622 (1981).
28. P. Onali, J. P. Schwartz, and E. Costa, *Proc. Natl. Acad. Sci. U.S.A.* **78**, 6531–6534 (1981).
29. M. J. Cronin and M. O. Thorner, *J. Cyclic Nucleotide Res.* **8**, 267–275 (1982).
30. K. P. Ray, and M. Wallis, *Mol. Cell. Endocrinol.* **27**, 139–155 (1982).
31. A. Spada, A. Nicosia, L. Cortelazzi, G. Pezzo, M. Bassetti, A. Sartolio, and G. Giannattasio, *J. Clin. Endocrinol.* **56**, 1–10 (1982).
32. L. Swennen and C. Denef, *Endocrinology (Baltimore)* **111**, 398–405 (1982).
33. A. Enjalbert and J. Bockaert, *Mol. Pharmacol.* **23**, 576–584 (1983).
34. G. Schettini, M. J. Cronin, and R. M. MacLeod, *Endocrinology (Baltimore)* **112**, 1801–1807 (1983).
35. K. A. Neve, B. A. Cox, R. A. Henningsen, A. Spanoyannis, and R. L. Neve, *Mol. Pharmacol.* **39**, 733–739 (1991).
36. D. Malek, G. Munch, and D. Palm, *FEBS Lett.* **325**, 215–219 (1993).

This Page Intentionally Left Blank

16

Quantitation of Metallothionein

Michael P. Waalkes¹

Inorganic Carcinogenesis Section

Laboratory of Comparative Carcinogenesis

Division of Basic Sciences

National Cancer Institute

Frederick Cancer Research and

Development Center

Frederick, Maryland 21702-1201

THE PHYSIOLOGY AND TOXICOLOGY OF METALLOTHIONEIN

Since they were initially detected in the late 1950s as cadmium-binding proteins in equine renal cortex (1), metallothioneins (MTs) have proven to be of great interest in a variety of scientific fields, including toxicology, biological and physical chemistry, molecular biology, and most recently cancer research. MTs, as a class of proteins, have several unique characteristics. MTs are low-molecular-weight, metal-binding proteins found in a wide variety of organisms (1–6). As the name implies, MTs contain numerous thiol groups, owing to their very high cysteine content, which provide the basis for high-affinity binding of certain metals, doubtlessly a major purpose of these proteins. MTs can in fact bind a variety of transition metals, including Cd, Cu, Hg, Ag, and Zn. These proteins are thought to have several, diverse, potential functions, including essential element homeostasis and toxic metal detoxication.

¹ Address all correspondence to the author at National Cancer Institute-FCRDC, Building 538, Room 205E, Frederick, MD 21702-1201.

Structure and Biological Characteristics

The distinguishing characteristics of MTs, listed in Table I, have been extensively examined (2–8). The structure of MT is characterized by a very high content of cysteine (up to 30% of the total amino acid residues) and a high content of serine and glycine. MTs also lack aromatic amino acids and histidine. Cysteinyll residues are arranged in a highly conserved manner and the 61-residue chain is interspersed with a series of C-X-C, C-X-X-C, and C-X-X-X-C units (C = cysteine; X = other amino acid). This confers the capacity to bind a high number of metal atoms (up to 7 in the case of Cd and Zn, 12 in the case of Cu) in two clusters. When seven metal atoms are bound they are chelated into MT in two clusters, one of three and one of four, with each metal ion coordinated tetrahedrally to cysteines. Binding of metals to each cluster is specific and is a function of the known differences in binding affinity, which may facilitate intermolecular metal ion transfer between MTs and other metal-requiring proteins, including enzymes. There are no disulfide bridges in MT, and all cysteinyll sulfurs participate in metal complexation. Generally, there are two major isoforms of MT that can be resolved by several chromatographic techniques and have a closely related but distinct sequence. MT is primarily an elongated, single-chain molecule with a high degree of random structure. MT is also a very heat-stable protein, and is stable at low pH, characteristics often used in purification or quantitation.

MT synthesis is highly inducible by metals, especially Cd and Zn (2–6,9,10) (see Table II). MT synthesis is also induced by other agents, such as hormones, pharmaceuticals, alcohols, cytokines, antibiotics, and other diverse chemical and physical treatments (6,8,11). These include ethanol (12), acetaminophen (13), urethane (14), formaldehyde (15), estradiol (16), ethionine (17), and D-penicillamine (18), several of which act as cytotoxic

TABLE I. Criteria for Classification as a Metallothionein^a

Molecular weight 6000–7000
Metal clusters with bridging thiolate ligands
High cysteine content (~30%)
High metal content
High metal affinity
Deficient in aromatic amino acids and histidine
Optical properties characteristic of metal–thiolate bonds
Highly ordered and conserved cysteine arrangement
Inducible by various chemicals and physical treatments, including metals
Typically polymorphic

^a See Refs. 2–8 for review.

TABLE II. Examples of Treatments That Induce Metallothionein Synthesis^a

Metals
Cd, Zn, Hg, Cu, Bi, etc.
Chemical agents
Acetaminophen
Alkylating agents
Angiotensin II
Ascorbic acid
Azacytidine
Bromobenzene
Butyric acid
Calmodulin inhibitors
Carbon tetrachloride
Carrageenan
Catecholamines
Chloroform
Dextran
Di(ethylhexyl)phthalate
Endotoxin
Estradiol
Ethanol
Ethionine
Formaldehyde
Glucocorticoids
Glucagon
Indomethacin
Insulin
Interleukin-1, -6
Interferon- α , - γ
Phorbol esters
2-Propanol
Progesterone
Streptozotocin
Tumor necrosis factor
Urethane
Stress-producing conditions
Food deprivation
Hypothermia
Infection
Inflammation
X irradiation
UV irradiation
Elevated oxygen tension

^a Modified from Refs. 6, 8, and 11.

hepatotoxins. Many of these compounds are involved in endocrine-mediated effects or would have potential endocrine-based toxic effects.

The molecular biology of the MT gene has received a great deal of attention (4,19–22). A remarkable property of the MT gene is the activation of its expression by exposure to a variety of agents, including metals and hormones. This inducibility is regulated at the transcriptional level by various cis-acting DNA sequences located in the promoter region of MT genes (19,20). Such sequences are responsible for MT induction by metals [metal regulatory elements (MREs)] and glucocorticoids [glucocorticoid regulatory elements (GREs)]. MT gene expression appears to be correlated with the methylation status of the DNA, as is the case with many other genes. Hypomethylating agents, such as 5-azacytidine, deoxyazacytidine, butyric acid, and dimethyl sulfoxide, cause enhanced synthesis of MT mRNA and MT protein and confer tolerance to Cd (19,23,24), whereas hypermethylation correlates with poor expression. Since expression of the MT gene is so readily induced by exposure to metals, the use of MT fusion genes has promise in genetic engineering (25).

Some of the highest MT concentrations found occur in the liver of mature animals after metal exposure (9,10) or livers of untreated perinatal animals (3,26,27). The pancreas and the kidney also contain high concentrations of MT following Zn or Cd exposure (9,10). The biological half-lives of MTs generally range from 1 to 4 days depending on the metal content. Degradation of MT is as yet poorly defined but may well be an important aspect of its physiological or toxicological functions (28). MTs have been characterized from a wide variety of mammalian and nonmammalian sources (2–8,29,30). MT has no known enzymatic activity.

Possible Functions

The normal physiological function of the MTs may be related to Zn and/or Cu metabolism and homeostasis. The highest tissue concentrations of these proteins occur during periods of high Zn demand such as during the perinatal period (31) or with tissue regeneration such as after partial hepatectomy (32). MT is thought to provide a supply of Zn within rapidly growing tissues (31). Zn is an essential element for various aspects of cell division, including DNA, RNA, and protein synthesis (31). In mammals, MT levels are very high near term and at birth in several tissues (3,26,27,31,33) and then rapidly decay during postpartum development. For instance, MT levels in human fetal liver correlate well with Zn levels and gestational age, reinforcing the concept that MT functions as a storage depot of Zn during periods of rapid growth (34).

Such a function may not always apply, however, during rapid growth associated with malignancy, as it has been shown that relatively low MT levels occur in the malignant portions versus the surrounding areas of surgically resected human livers (35), or in mouse liver tumors (36). This may depend on the tumor type, however, as elevated levels of MT expression have been detected in several tumors of nonhepatic origin, such as thyroid tumors (37), testicular embryonal carcinomas (38), and skin papillomas (39). MT concentrations are also elevated during regenerative proliferation induced after chronic exposure to the hepatotoxins and tumor promoters acetaminophen and di(2-ethylhexyl)phthalate (40). Tumor promoters that induce cellular enlargement (barbiturates), and not cellular hyperplasia, do not elevate hepatic MT, indicating a relationship to stimulation of compensatory cell division (40). Likewise, the tumor-promoting phorbol ester 12-*O*-tetradecanoylphorbol-13-acetate (TPA) enhances MT mRNA expression (39). The role of MT in tumor cell pathobiology requires further definition.

A potential role of MT as a donor of Zn or Cu to other sites within the cell has received frequent support (29). For instance, several apoenzymes that require Zn and/or Cu as cofactors, such as carbonic anhydrase, alkaline phosphatase, and superoxide dismutase, have been reactivated *in vitro* after incubation with Zn- and Cu-thioneins (41–43). Recently, it has also been shown that Zn-thionein in kidney activates aminolevulinic acid dehydratase, a Zn-requiring enzyme involved in heme biosynthesis, by donating Zn to the enzyme (44). Such enzymatic reactivation has yet to be shown using an *in vivo* model. Evidence suggesting that MT is not a critical component for direct metal donation to activate enzymes includes studies showing that cultured cells lacking MT can function normally (22,45).

Another possible role of MT may involve detoxication of reactive chemical intermediates. Thus, it is proposed that MT constitutes a cellular defense system acutely responsive to electrophilic agents or reactive metabolites. This is likely related to the high sulfhydryl content of MT, which could provide a high degree of “neutralizing” nucleophilic equivalents (8). MT is an effective scavenger of hydroxyl radicals *in vitro* (46). Preinduction of MT reduces the toxic effects of carbon tetrachloride or X irradiation, which are mediated by reactive metabolites and free radicals, respectively (47–49). It is also possible that MT may provide a storage depot for cysteine, particularly during development (50).

MT also appears to play a critical role in detoxication of Cd. Cellular tolerance to Cd is thought to occur through high-affinity sequestration of the metal by MT, and early on it was demonstrated that following Cd exposure the metal is, in fact, predominantly associated with MT (51). Subsequently it was shown that pretreatment with metals known to

stimulate MT synthesis prevents the toxicity of subsequent Cd exposure (52,53). This includes pretreatment with Zn and low, nontoxic doses of Cd (52,53). It is believed that after the initial pretreatment, the synthetic mechanisms for MT are induced, and newly synthesized protein provides the sequestrational capacity necessary to substantially reduce the toxic actions of Cd. A primary intended function for MT in Cd detoxication would seem unlikely. For a protein to evolve specifically for the protection from a metal that has only very recently been concentrated within the biosphere through industrialization seems improbable. Rather, it would appear to be a fortuitous, but unintentional, occurrence that MT is capable of reducing Cd toxicity. This is probably related to the chemical mimicry of Cd for Zn.

Previous research on MT has largely focused on its role in either metal homeostasis or toxicity and the molecular control mechanisms of its genetic expression. Recently another area has emerged concerning medical implications, including the roles of MT in disease and therapy (54). One of the primary areas in which MT may have an important role is in chemotherapy of certain cancers, both in the development of tolerance to chemotherapeutics and as a potential therapeutic adjunct to reduce toxic side effects (54–58). In particular, induction of MT in the kidney appears to reduce the renal toxicity of cisplatin (CDDP) (57), a primary limiting factor in its chemotherapeutic usefulness. It is also clear that MT gene expression is often a primary cause of tumor cell resistance to electrophilic antineoplastic agents, including CDDP (58). In this regard, a variety of human and animal tumor cell lines were shown to express large quantities of MT, again emphasizing its potential importance in tumor cell resistance to electrophilic chemotherapeutics. In mouse models of chemically induced liver and lung cancer, Cd can markedly reduce tumor incidence and multiplicity, a finding correlated with poor expression of MT in these particular tumors, creating a potential chemotherapeutic utility for Cd and a rational basis for its usage. A new form of MT, called growth-inhibitory factor (GIF) or MT-III (59,60), has been isolated specifically from the brain and its down-regulation in certain nervous cells may be an important factor in the pathogenesis of Alzheimer's disease. As the medical implications of MT continue to be explored, other important roles in the diagnosis and treatment of disease will doubtlessly continue to be discovered.

Despite all of these efforts, the exact function or functions of MT are not known, with any certainty. The recent introduction of animal models such as transgenic mice containing mutated MT genes may help to precisely define the physiological and toxicological functions of this remarkable protein (22,61,62).

Toxicity

Though the Cd–MT complex is essentially nontoxic when localized intracellularly, it becomes a potent nephrotoxin if it reaches the systemic circulation. Extracellular Cd–MT can become available to systemic circulation, and thus to the kidney, either through release from liver after toxic insult or after direct gastrointestinal absorption, since the Cd–MT complex is absorbed at least partially intact (63). The Cd–MT protein complex is highly toxic to the kidney after renal tubular reabsorption (64–66). Human Cd nephrotoxicity is likely related to Cd–MT since this may be a major form of Cd in the diet. Smoking, another major source of human exposure to Cd, results in elevated renal Cd–MT (67).

Cd absorbed from the gastrointestinal tract or lungs is initially transported to the liver, where it induces the synthesis of MT. Continual exposure to Cd results in liver injury with leakage of Cd–MT from damaged hepatocytes into the circulation (68). The metal–protein complex is transported to the kidney, filtered by the glomerulus, and subsequently reabsorbed by the proximal tubule cell in a manner similar to that of other low-molecular-weight proteins (66,68–71). The reabsorbed complex is rapidly degraded (69–71), which releases free Cd and induces the synthesis of renal MT. This process continues until the capacity of the kidney to synthesize MT is exceeded and Cd can readily react with sensitive biological target systems.

QUANTITATION OF METALLOTHIONEIN

General Comments

Quantitation of MT typically requires three discrete steps (Table III) (72). Since, in large part, MT is localized in the soluble portion of the cell, estimation of MT content is typically carried out after sample preparation by homogenization and centrifugation to obtain a cytosolic fraction (72). Separation of MT from other proteins is then required, and this can be carried out by a variety of methods, including several types of chromatography and acid, heat, and/or solvent treatments. Quantitation of MT can then be accomplished by direct measurement of this specific protein, as with immunological techniques (RIA, ELISA), or indirect measurement by determination of metal or thiol contents of the purified or semipurified MT. The levels of MT are then related back to the original grams of wet tissue. In the case of cultured cells, MT levels can be related to either number of cells or DNA or protein content of the cells. At present the most commonly used assays are RIAs or the Cd saturation assay (72,73).

TABLE III. Steps in Metallothionein Quantification^a

Sample preparation
Homogenization or cellular disruption
Centrifugation
Metal saturation (in some assays)
Purification or semipurification of MT
Acid treatment
Heat treatment
Solvent extraction
Chromatography
Electrophoresis
Quantification of MT
Indirectly (metal content; thiol groups)
Directly (immunological)

^a Modified from Ref. 72.

Metal Saturation Assays

Of the available assays for MT quantitation, some of the most popular take advantage of MT's ability to avidly bind certain metals. Thus, MT levels are measured indirectly by metal content after the addition to samples of an excess of a metal of known high affinity such as Cd (9,10,74,75), Hg (76), or Ag (77). Because of the high affinity of these metals for MT, displacement of endogenously bound metals, at least in the case of zinc, will occur. These saturation assays take advantage of known stoichiometric relationships between such metals and the MT protein, and the ratio of metal bound and MT protein (6–7 for Cd and Hg; 18 for Ag) is used as a basis for calculating MT values.

A key aspect of all metal saturation assays is that, after saturation, an effective separation of MT-bound metal and metal not bound to MT is obtained. Metal not bound to MT includes both any excess free metal and metal bound to other, often higher molecular weight, proteins. Often exogenous proteins or protein mixtures (9,10,74,75), such as hemoglobin or RBC hemolyate, are added to provide excess, relatively low affinity, binding sites for the metals. Common separation methods with metal saturation assays include heat treatment of cytosol or acid treatment of whole-tissue homogenates with subsequent centrifugation. These techniques take advantage of the fact that the MT proteins are quite heat stable (Cd or Ag saturation) and are stable at low pH (Hg saturation). The binding of Hg to MT is also unaffected by low pH.

Low-pressure liquid chromatography of cytosol, using Sephadex G75 or a similar gel filtration matrix, was once a common technique for determining MT with metal saturation assays, but it is time-consuming and does not lend itself well to assessment of large numbers of samples, and is now seldom used (72,73). This method can provide for the ready determination of endogenous metal content of the MT if run without prior metal saturation. Instead of the more cumbersome standard liquid chromatography techniques, high-performance liquid chromatography (HPLC) techniques are now frequently used. Such systems include anion-exchange HPLC (78) or gel filtration HPLC systems (79) and allow for rapid separation of MT at the isoform level. Electrophoresis can also be used as a separation technique either with or without prior metal saturation (72,73).

Metal can be determined by atomic absorption spectrometry (AAS) and inductively coupled plasma emission spectrometry (ICPES) or, if radioisotopic metal was originally used for saturation (e.g., ^{109}Cd or ^{203}Hg), by standard assessment of radioactivity (72). The relationship to original tissue weight or cell number is then defined. Coupled HPLC/AAS and HLPC/ICPES systems have been adapted to directly measure the metal content in the elution fluid. Alternatively, thiol groups could be measured as a means of quantification of the MT.

As an illustrative example, Table IV shows the Cd saturation assay (also known as the cadmium-hemoglobin or Cd-Hem assay) as applied to cytosols prepared from tissue samples using radioisotopic cadmium (75). The tissue samples would be first homogenized in appropriate buffer and cytosol would be derived by differential centrifugation. Similarly, for *in vitro* work, cells would be disrupted and then centrifuged to obtain samples for MT analysis.

The Cd-binding assay appears to be similar in precision and recovery of MT to assays that directly measure the protein moiety, such as RIA (80). Problems of over- or underestimation by metal saturation assays have occurred. Metal saturation assays also have a potential problem of nonspecificity, in which proteins or other moieties that would bind the particular metal would be detected with MT. Appropriate isolation and adequate separation of MT from other proteins is thus critical for these assays. Use of silver, with its very high affinity for sulfhydryls, in part alleviates the difficulties with nonspecificity (77). Copper-containing MTs are a problem for the cadmium saturation assay owing to the higher affinity of copper for MT, though is not as great a concern with silver or mercury saturation assays (72). Without an HPLC separation phase the metal saturation assays do not readily detect MT isoforms. The standard saturation assays have detection limits of ~ 700 ng for Hg, 10–100 ng for Cd, and ~ 100 ng for Ag, depending on the detection method used (72).

TABLE IV. Cadmium Saturation Assay for Metallothionein^a

A. Reagents

1. 10 mM Tris buffer (pH 7.4)
2. CdCl₂ solutions:
Stock: 200 μg Cd/ml; 32.6 mg CdCl₂; qs to 100 ml in 0.1 N HCl
Working: 2 μg Cd/ml; Dilute stock solution 1:100 in 10 mM Tris; add ~3 μCi ¹⁰⁹Cd/
10 ml working solution (check pH, if <7.4, hemoglobin may not precipitate).
3. 2.0% hemoglobin
2.0 g bovine hemoglobin; qs to 100 ml Tris buffer

B. Metallothionein assay

1. To 100 μl of cytosol or sample supernatant in a 400-μl polyethylene microcentrifuge tube add 100 μl of working ¹⁰⁹CdCl₂ solution; cap and vortex. Note: include background blanks (buffer added instead of tissue) and assay totals (buffer added instead of tissue and instead of hemoglobin).
2. Incubate at room temperature for 10 min.
3. Add 50 μl 2% bovine hemoglobin and mix. Note: add 50 μl buffer to Assay Totals.
4. Place samples in a boiling water bath for 1 min.
5. Cool samples on ice; centrifuge ~10,000g, 3 min at room temperature.
6. Repeat steps 3 to 5.
7. Either carefully decant total supernatant (be sure not to disturb pellet) or take a known aliquot (≤200 μl) and determine cpm ¹⁰⁹Cd. Note: samples in which over 40–50% of the total cpm are retained in the supernatant will grossly underestimate MT levels. For tissues with induced amounts of MT, samples may well need dilution.

C. Calculations

$$\text{nmoles Cd bound/g wet weight} = \frac{[\text{cpm (sample)} - \text{cpm (blank)}]}{[\text{cpm (total)} - \text{cpm (blank)}]} \times \frac{2000 \text{ ng Cd/ml}}{112.4 \text{ ng Cd/nmole Cd}} \times \frac{\text{ml}}{\text{g tissue}} \times \text{dilution factor (if any)}$$

Note: nmol Cd/g wet weight = μg MT/g wet weight, assuming ~6 moles of Cd are bound per mole of MT, and assuming the molecular weight of MT is ~6000.

^a After Refs. 9 and 10.

Immunological Assays

Immunological techniques of quantification have been applied to MT. The initial development of a specific antibody in rabbits to rat MT allowed the development of a sensitive RIA system for MT (81). This particular RIA for MT has been shown to have complete cross-reactivity to Cd–MT, Zn–MT, and apothioneins, as well as MT isolated from rat, hamster, human, and equine liver (81). Many other antibodies, generally polyclonal, have since been developed and utilized in either RIAs or enzyme-linked immunosorbent assays (ELISA) (72,79,82–84). Unlike the assays for MT that employ metal saturation, the RIA directly measures the protein moiety of

MT for purposes of quantification. Outside of the requirement for the specific MT antibody, MT RIAs or ELISAs are performed by standard techniques commonly used in such assays. Thus the critical aspect of the immunological assay for determining MT is the availability of the particular antibody and its cross-reactivity to MT containing differing metals or from different sources (72). Thus RIAs for MT might still not be considered of general use for screening for MT in various tissues, particularly those with high basal amounts or with high inducibility (72). However, the RIA can allow the determination of MT in the picogram range and is the only assay method currently available that is sensitive enough to detect MT in body fluids such as blood or urine (72). In fact, the clinical use of MT determination by RIA in urine of Cd-exposed individuals showed that elevated levels of urinary MT have potential as a biomarker indicative of Cd-induced renal damage (85). The value in prognostication of Cd-induced nephropathy has not been defined.

Immunohistochemical techniques also exist for the localization of MT in fixed tissues and the peroxidase-antiperoxidase method (86), using an antibody developed in rabbits to rat MT (84,86), is an excellent example. Briefly, paraffin-embedded blocks containing sections of the previously fixed tissue of interest are sectioned ($5\ \mu\text{m}$), deparaffinized, and incubated with 20% normal swine serum for 30 min to block nonspecific binding. Excess normal swine serum is then removed and the sections are layered with rabbit anti-MT serum (100-fold diluted) or control serum (normal rabbit serum). The sections are incubated for 16–18 hr at 4°C in a humid chamber, washed with Tris-HCl buffer (100 mM, pH 7.4), and incubated at room temperature with the following sequence of reagents: (1) swine antirabbit IgG; (2) peroxidase-antiperoxidase complex; and (3) 6 mg 3,3'-diaminobenzidine tetrahydrochloride in 10 ml Tris-HCl buffer (100 mM, pH 7.4) containing 3 drops of 3% H_2O_2 . Hematoxylin is used as a counterstain. The immunohistological techniques for localization of MT are largely semiquantitative in nature. However, they can be invaluable in defining the precise locale of MT and, in combination with other more quantitative techniques, are a powerful method for defining MT expression in a given tissue.

ANALYSIS OF METALLOTHIONEIN mRNA

Molecular biology techniques have been developed to determine MT gene expression via specific MT mRNA (22,87–89) and are now widely used (for details about general molecular biological methods see Refs. 90 and

91). Use of species-specific probes or knowledge of probe cross-reactivity are necessary.

For these methods, RNA must first be extracted. As an example, RNA can be extracted from tissue samples or cells using the RNazol method (Tel-Test, Inc., Friendswood, TX). RNA samples from at least two animals per group should be isolated and duplicate aliquots of each sample are assayed. Depending on the size of the original organs, tissues from multiple animals may require pooling. RNA samples are then denatured using the glyoxal method (92) and either resolved on a 1% agarose gel and transferred to Nytran (Schleicher and Schuell, Keene, NH) or slot-blotted onto Nytran. RNA integrity is then confirmed by electrophoresis.

For samples derived from rats, slot blots and Northern transfers can be probed for MT mRNA using a ^{32}P -labeled cDNA probe specific for the rat MT-1 gene (87) labeled by nick translation. MT mRNA expression can also be determined using isoform-specific oligonucleotide probes. RNA samples are denatured using the formaldehyde method (93) and either resolved on a 1% agarose gel and subsequently transferred to Zeta-Probe membranes (Bio-Rad, Richmond, CA) or slot-blotted directly onto Zeta-Probe membranes. Membranes are probed for MT-I or MT-II mRNAs using ^{32}P -labeled oligonucleotide probes 5'-end-labeled using a T_4 polynucleotide kinase reaction specific for rat MT-I [5'-GAGGGCAGCAGCACTGTTTCG-3'; (87)] or MT-II [5'-ACACCATTGTGAGGACGCC-3'; (88)]. The integrity of the RNA samples is confirmed by electrophoresis/Northern analysis. Blots can be quantified by densitometry and standardized to a house-keeping gene such as β -actin (94). Relative MT mRNA expression is then defined as the ratio of MT mRNA to β -actin mRNA. The combination of defining MT protein with one of the assays mentioned earlier and MT mRNA allows very definitive statements to be made about induction of MT gene expression. A careful analysis of the time course of MT mRNA expression should also be carried out after any treatment to define response as maximal.

In situ hybridization techniques for definition of localization of MT mRNA are also available (95,96). These can give valuable information concerning the tissue or cell localization of the MT gene transcript but are again largely semiquantitative in nature.

USE OF METALLOTHIONEIN ANALYSIS IN ENDOCRINE TOXICOLOGY

Many examples could be cited of the importance of MT in endocrine toxicity. MT is thought to be a primary component of native or acquired

cellular tolerance to toxic effects of cadmium (6,97,98), a metal with a variety of endocrine targets. In particular, the activity of the MT gene plays a critical role in determining the sensitivity or resistance of a given tissue or cell to cadmium toxicity. For instance, the inactivity of the MT gene in certain portions of the male reproductive system in rats may well allow a greater rate of carcinogenic transformation of target cells and/or allow transformation to occur after exposure to relatively low concentrations of cadmium (99).

In this regard, chronic carcinogenicity studies in rats have established that the rat ventral prostate is a target site for cadmium induction of neoplasia (100–106). Thus far, the carcinogenic effects of cadmium in the prostate of rats are uniformly confined to the ventral lobe and have not been detected in the dorsolateral lobe. *In vitro* studies have demonstrated induction of malignant transformation in primary cultures of rat prostatic epithelial cells upon exposure to cadmium, but only in cells isolated from the ventral lobe and not from the dorsolateral lobe (107,108). Cadmium can also enhance the formation of chemically induced prostatic tumors in rats, as the combination of intramuscular cadmium and 3,2'-dimethyl-4-aminobiphenyl given to rats acts synergistically to induce carcinomas of the ventral prostate (109).

Since the sensitivity to cadmium carcinogenesis within the rat prostate is clearly lobe specific, the possibility exists that the basis of this sensitivity may lie in MT expression. In fact, recent evidence indicates that the MT gene activity, as assessed by MT mRNA (Figure 1), is only minimally active and is not inducible by cadmium within the ventral lobe of the rat prostate, whereas the MT gene in the dorsolateral prostate was shown to have a very high basal activity (110). MT levels by Cd saturation assay show a similar pattern (110). Similarly, very low constitutive levels of MT mRNA are detected in the ventral prostate by *in situ* hybridization (96). A number of studies have also shown that, under normal circumstances, there is little immunohistochemical evidence of MT in the ventral lobe of the rat prostate, although the dorsal prostate often shows significant staining (96,111,112). These findings point to a correlation between a lobe-specific deficiency in expression of MT and lobe-specific sensitivity to cadmium carcinogenicity. The lack of responsiveness in this important cellular detoxication system for cadmium appears to be an important factor in determining final sensitivity to cadmium carcinogenesis, at least in the rat ventral prostate.

SUMMARY AND CONCLUSIONS

An accurate and sensitive method for quantification of MT has long been sought. Most methods of MT quantification measure the protein indirectly

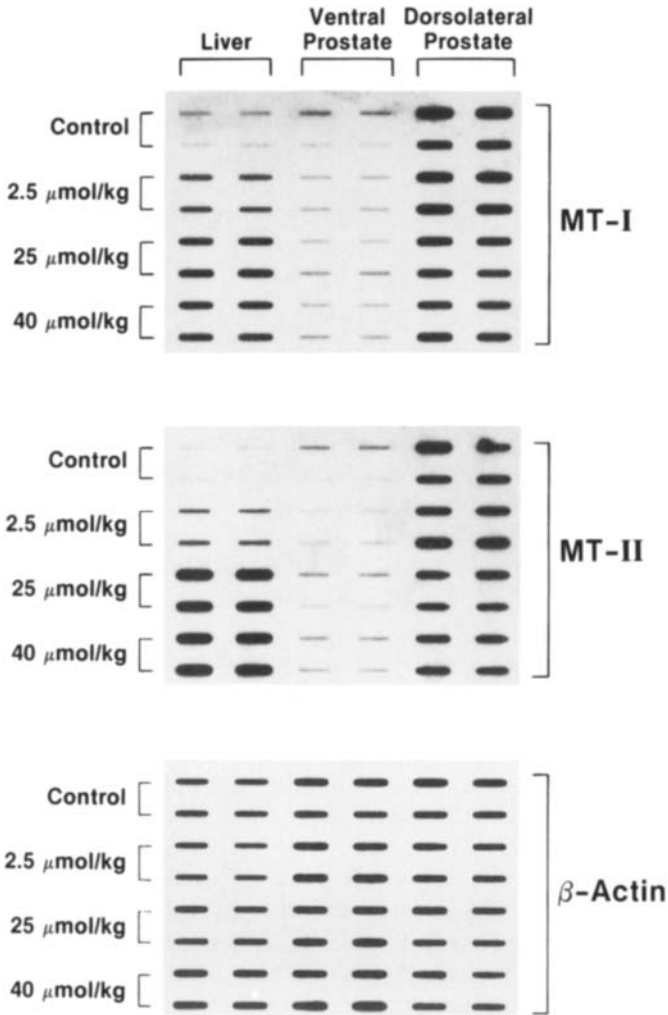


FIGURE 1. Slot-blot analysis of MT-I and MT-II mRNA accumulation in the liver, ventral prostate, and dorsolateral prostate after exposure to various doses of cadmium. Rats were exposed at time zero to 0, 2.5, 25, or 40 μmol Cd/kg, subcutaneously, and tissues were collected for RNA analysis 24 hr later. MT-I and MT-II mRNA were determined using specific oligonucleotides. MT expression was standardized against β-actin mRNA. From Ref. 110.

by measurement of its metal-binding capacity following saturation of the sample with a metal of known high affinity for MT, such as Ag, Hg, or Cd. Following saturation, the metal bound to MT is separated from non-MT-

bound metal (either free metal or that bound to other proteins). Several methods of separation have been employed, including gel filtration, HPLC, acid precipitation, and heat denaturation. However, overestimation of MT due to interfering substances should always be considered when employing any metal saturation assay because of a possible lack of specificity. Immunological techniques of quantification have also been applied to MT and the development of MT-specific antibodies preceded the development of sensitive RIAs for MT. Unlike metal saturation assays, the RIA directly measures the protein moiety of MT for purposes of quantification. The various assay systems can yield MT values that follow a similar intra-assay pattern, and although RIA is more sensitive, it is dependent on the availability of a specific antibody and does require considerable expertise. The RIA would appear to be the only choice where very high sensitivity is required, such as measurement of MT in plasma, since such concentrations are below the sensitivity of metal saturation assays. Neither RIA nor metal saturation assays will allow determination of endogenous metal content in MT. Molecular biological techniques are also available for determination of MT mRNA and are now widely used. In the final analysis, in order to define a biological response involving the MT gene, it is probably best to employ techniques that measure the MT protein, directly (RIA) or indirectly (metal saturation assays), in combination with measurement of MT mRNA.

REFERENCES

1. M. Margoshes and B. L. Vallee, A cadmium protein from equine kidney cortex. *J. Am. Chem. Soc.* **79**, 4813–4814 (1957).
2. J. H. R. Kagi and Y. Kojima (eds.), Metallothionein II. *Experientia Suppl.* **52**, (1987).
3. E. C. Foulkes (ed.), "Biological Rates of Metallothionein." Elsevier/North-Holland, Amsterdam, 1981.
4. D. H. Hamer and D. R. Winge (eds.), "Metal Ion Homeostasis." Molecular Biology and Chemistry, Alan R. Liss, New York, 1989.
5. J. H. R. Kagi, Overview of metallothionein. In "Methods in Enzymology" (J. F. Riodan and B. L. Vallee, eds.), Vol. 205, Metallobiochemistry, Part B, Metallothionein and Related Molecules, pp. 613–615. Academic Press, New York, 1991.
6. M. P. Waalkes and P. L. Goering, Metallothionein and other cadmium-binding proteins: Recent developments. *Chem. Res. Toxicol.* **3**, 281–288 (1990).
7. J. H. R. Kagi, M. Vasak, K. Lerch, D. E. O. Gilg, P. Hunziker, W. R. Bernhard, and M. Good, Structure of metallothionein. *Environ. Health Perspect.* **54**, 93–104 (1984).
8. J. H. R. Kagi and A. Schaffer, Biochemistry of metallothionein. *Biochemistry* **27**, 8509–8515 (1988).
9. S. Onosaka and M. G. Cherian, The induced synthesis of metallothionein in various tissues of rat in response to metals. I. Effects of repeated injection of cadmium salts. *Toxicology* **22**, 91–101 (1981).

10. S. Onosaka and M. G. Cherian, The induced synthesis of metallothionein in various tissues of rats in response to metals. II. Influence of zinc status and specific effect on pancreatic metallothionein. *Toxicology* **23**, 11–20 (1981).
11. J. H. R. Kagi, Evolution, structure and chemical activity of class I metallothioneins: An overview. In “Metallothionein III” (K. T. Suzuki, N. Imura, and M. Kimura, eds.), pp. 29–56. Birkhauser Verlag, Basel, 1993.
12. M. P. Waalkes, J. J. Hjelle, and C. D. Klaassen, Transient induction of hepatic metallothionein following oral ethanol administration. *Toxicol. Appl. Pharmacol.* **74**, 230–236 (1984).
13. U. Wormser and D. Calp, Increased levels of hepatic metallothionein in rat and mouse after injection of acetaminophen. *Toxicology* **53**, 323–329 (1988).
14. E. A. Brzezniczka, L. D. Lehman, and C. D. Klaassen, Induction of hepatic metallothionein following administration of urethane. *Toxicol. Appl. Pharmacol.* **87**, 457–463 (1987).
15. P. L. Goering, Acute exposure to formaldehyde induces hepatic metallothionein synthesis in mice. *Toxicol. Appl. Pharmacol.* **98**, 325–337 (1989).
16. S. Nishiyama, T. Taguchi, and S. Onosaka, Induction of zinc-thionein by estradiol and protective effects on inorganic mercury-induced renal toxicity. *Biochem. Pharmacol.* **36**, 3387–3391 (1987).
17. M. P. Waalkes, Elevation of hepatic metallothionein in rats chronically exposed to dietary ethionine. *Toxicol. Lett.* **26**, 133–138 (1985).
18. H. E. Heilmaier, J. L. Jiang, M. Greim, P. Schramel, and K. H. Summer, D-Penicillamine induces rat hepatic metallothionein. *Toxicology* **42**, 23–31 (1986).
19. D. H. Hamer, Metallothionein. *Annu. Rev. Biochem.* **55**, 913–951. (1986).
20. R. Palmiter, Molecular biology of metallothionein gene expression. *Experientia* **52**, (Suppl.), 63–80 (1987).
21. D. H. Hamer, Molecular genetics of metallothionein: An overview. In “Metallothionein III” (K. T. Suzuki, N. Imura, and M. Kimura, eds.), pp. 347–349. Birkhauser Verlag, Basel, 1993.
22. R. D. Palmiter, E. P. Sandgren, B. A. Masters, and R. L. Brinster, In “Metallothionein III” (K. T. Suzuki, N. Imura, and M. Kimura, eds.), pp. 399–406. Birkhauser Verlag, Basel, 1993.
23. S. J. Compere and R. D. Palmiter, DNA methylation controls the inducibility of the mouse metallothionein-I gene in lymphoid cells. *Cell (Cambridge, Mass.)* **25**, 233–240 (1981).
24. M. P. Waalkes, M. Miller, M. J. Wilson, R. M. Bare, and A. E. McDowell, Increased metallothionein gene expression in 5-aza-2'-deoxycytidine-induced resistance to cadmium cytotoxicity. *Chem.-Biol. Interact.* **66**, 189–204 (1988).
25. R. D. Palmiter, R. L. Brinster, R. E. Hammer, M. E. Trumbauer, M. G. Rosenfeld, N. C. Birnberg and R. M. Evans, Dramatic growth of mice that develop from eggs microinjected with metallothionein-growth hormone fusion genes. *Nature (London)* **300**, 611–615 (1982).
26. K.-L. Wong and C. D. Klaassen, Isolation and characterization of metallothionein which is highly concentrated in newborn rat liver. *J. Biol. Chem.* **254**, 12399–12403 (1979).
27. M. P. Waalkes and C. D. Klaassen, Postnatal ontogeny of metallothionein in various organs of the rat. *Toxicol. Appl. Pharmacol.* **74**, 314–320 (1984).
28. C. D. Klassen, S. Choudhuri, J. M. McKim, Jr., L. Lehman-McKeeman, and W. C. Kershaw, Degradation of metallothionein. In “Metallothionein III” (K. T. Suzuki, N. Imura, and M. Kimura, eds.), pp. 207–224. Birkhauser Verlag, Basel, 1993.
29. D. H. Petering and B. A. Fowler, Roles of metallothionein and related proteins in metal metabolism and toxicity, problems and perspectives. *Environ. Health Perspect.* **65**, 217–224 (1986).

30. H. C. Stone and J. Overnell, Non-metallothionein cadmium binding proteins. *Comp. Biochem. Physiol.* **80C**, 9–14 (1985).
31. F. O. Brady, The physiological function of metallothionein. *Trends Biochem. Sci.* **7**, 143–145 (1982).
32. H. Ohtake and M. Koga, Purification and characterization of zinc-binding protein from the liver of the partially hepatectomized rat. *Biochem. J.* **183**, 683–690 (1979).
33. G. K. Andrews, E. D. Adamson, and L. Gedamu, The ontogeny of expression of murine metallothionein: Comparison with α -fetoprotein gene. *Dev. Biol.* **103**, 294–303 (1984).
34. S. R. Clough, R. S. Mitra, and A. P. Kulkarni, Qualitative and quantitative aspects of human-fetal liver metallothioneins. *Biol. Neonate* **49**, 241–254 (1986).
35. S. Onosaka, K.-S. Min, C. Fukuhara, K. Tanaka, S.-I. Tashiro, I. Shimizu, M. Furuta, T. Yasutomi, K. Kobashi, and K.-I. Yamamoto, Concentrations of metallothionein and metals in malignant and non-malignant tissues in human liver. *Toxicology* **38**, 261–268 (1986).
36. M. P. Waalkes, B. A. Diwan, T. P. Coogan, C. M. Weghorst, J. M. Ward, J. M., Rice, M. G. Cherian, and R. A. Goyer, Tumor suppressive activity of cadmium. In “Metallothionein III” (K. T. Suzuki, N. Imura, and M. Kimura, eds.), pp. 303–328. Birkhauser Verlag, Basel, 1993.
37. T. E. Kontozoglou, D. Banerjee, and M. G. Cherian, Immunohistochemical localization of metallothionein in human testicular embryonal carcinoma cells. *Virchows Arch. A: Pathol. Anat. Histopathol.* **415**, 545–549 (1989).
38. N. Nartley, M. G. Cherian, and D. Banerjee, Immunohistochemical localization of metallothionein in human thyroid tumors. *Am. J. Pathol.* **129**, 177–182 (1987).
39. H. Hashiba, J. Hosoi, M. Karasawa, S. Yamada, K. Nose, and T. Kuroki, Induction of metallothionein mRNA by tumor promoters in mouse skin and its constitutive expression in papillomas. *Mol. Carcinog.* **2**, 95–100 (1989).
40. M. P. Waalkes and J. M. Ward, Induction of hepatic metallothionein in male B6C3F1 mice exposed to hepatic tumor promoters: Effects of phenobarbital, acetaminophen, sodium barbital and di(2-ethylhexyl)phthalate. *Toxicol. Appl. Pharmacol.* **100**, 217–226 (1989).
41. A. O. Udom and F. O. Brady, Reactivation of *in vitro* zinc-requiring apoenzymes by rat liver zinc-thionein. *Biochem. J.* **187**, 329–335 (1980).
42. T. Y. Li, A. J. Kraker, C. F. Shaw, and D. A. Petering, Ligand substitution reactions of metallothioneins with EDTA and apocarbonic anhydrase. *Proc. Natl. Acad. Sci. U.S.A.* **77**, 6334 (1980).
43. B. L. Geller and D. R. Winge, Metal binding sites of rat liver Cu-thionein. *Arch. Biochem. Biophys.* **219**, 109–117 (1982).
44. P. L. Goering and B. A. Fowler, Kidney zinc-thionein regulation of aminolevulinic acid dehydratase inhibition by lead. *Arch. Biochem. Biophys.* **253**, 48–55 (1987).
45. B. D. Crawford, M. D. Enger, B. B. Griffith, J. K. Griffith, J. L. Hanners, J. L. Longmire, A. C. Munk, R. L. Stallings, J. G. Tesmer, R. A. Walters, and C. E. Hildebrand, Coordinate amplification of metallothionein I and II genes in cadmium-resistant Chinese hamster cells: Implications for mechanisms regulating metallothionein gene expressions. *Mol. Cell. Biol.* **5**, 320–329 (1985).
46. P. J. Thornalley and M. Vasak, Possible role for metallothionein in protection against radiation-induced oxidative stress. Kinetics and mechanism of its reaction with superoxide and hydroxyl radicals. *Biochim. Biophys. Acta* **827**, 36–44 (1985).
47. S. Z. Cagen and C. D. Klaassen, Protection of carbon tetrachloride-induced hepatotoxicity by zinc: Role of metallothionein. *Toxicol. Appl. Pharmacol.* **51**, 107–116 (1989).

48. I. S. Clarke and E. M. K. Lui, Interaction of metallothionein and carbon-tetrachloride on the protective effect of zinc on hepatotoxicity. *Can. J. Physiol. Pharmacol.* **64**, 1104–1110 (1986).
49. J. Matsubara, Y. Tajima, and M. Karasawa, Promotion of radioresistance by metallothionein induction prior to irradiation. *Environ. Res.* **43**, 66–74 (1987).
50. S. H. Zlotkin and M. G. Cherian, Hepatic metallothionein as a source of zinc and cysteine during the first year of life. *Pediatr. Res.* **24**, 326–329 (1988).
51. M. Piscator, On cadmium in normal human kidney together with a report on the isolation of metallothionein from livers of cadmium exposed rabbits. *Nord. Hyg. Tidskr.* **45**, 7642 (1964).
52. A. P. Leber and T. S. Miya, A mechanism for cadmium and zinc-induced tolerance to cadmium toxicity: Involvement of metallothionein. *Toxicol. Appl. Pharmacol.* **37**, 403–414 (1976).
53. H. Yoshikawa, Preventive effects of pretreatment with cadmium on acute cadmium poisoning in rats. *Ind. Health* **11**, 113–119 (1973).
54. M. P. Waalkes, Medical implications of metallothionein. In “Metallothionein III” (K. T. Suzuki, N. Imura, and M. Kimura, eds.), pp. 243–253. Birkhauser Verlag, Basel, 1993.
55. A. Naganuma, M. Satoh, and N. Imura, Utilization of metallothionein inducer in cancer therapy. In “Metallothionein III” (K. T. Suzuki, N. Imura, and M. Kimura, eds.), pp. 255–268. Birkhauser Verlag, Basel, 1993.
56. Y. Kondo, K. Yamagata, M. Satoh, A. Naganuma, N. Imura, and M. Akimoto, Clinical use of a bismuth compound as an adjunct in chemotherapy with *cis*-DDP against human urogenital tumors. In “Metallothionein III” (K. T. Suzuki, N. Imura, and M. Kimura, eds.), pp. 269–278. Birkhauser Verlag, Basel, 1993.
57. N. Saijo, K. Miura, and K. Kasahara, The role of metallothionein for the reduction of adverse effect of cisplatin and the induction of resistance to cisplatin. In “Metallothionein III” (K. T. Suzuki, N. Imura, and M. Kimura, eds.), pp. 279–292. Birkhauser Verlag, Basel, 1993.
58. J. S. Lazo, Y.-Y. Yang, E. Woo, S.-M. Kuo, and N. Saijo, Regulation of metallothionein expression and cellular resistance to electrophilic antineoplastic agents. In “Metallothionein III” (K. T. Suzuki, N. Imura, and M. Kimura, eds.), pp. 269–278. Birkhauser Verlag, Basel, 1993.
59. Y. Uchida, Growth inhibitory factor in brain. In “Metallothionein III” (K. T. Suzuki, N. Imura, and M. Kimura, eds.), pp. 315–328. Birkhauser Verlag, Basel, 1993.
60. R. D. Palmiter, S. D. Findley, T. E. Whitmore, and D. M. Durnam, MT-III, a brain-specific member of the metallothionein gene family. *Proc. Natl. Acad. Sci. U.S.A.* **89**, 6333–6337 (1992).
61. R. D. Palmiter, E. P. Sandgren, D. M. Koeller, and R. L. Brinster, Distal regulatory elements from the mouse metallothionein locus stimulate gene expression in transgenic mice. *Mol. Cell. Biol.* **13**, 5266–5275 (1993).
62. A. E. Michalska and K. H. A. Choo, Targeting and germ-line transmission of a null mutation at the metallothionein I and II loci in mouse. *Proc. Natl. Acad. Sci. U.S.A.* **90**, 8088–8092 (1993).
63. D. Klein, H. Greim, and K. H. Summer, Stability of metallothionein in gastric-juice. *Toxicology* **41**, 121–129 (1986).
64. M. G. Cherian, R. A. Goyer, and L. Delaquerriere-Richardson, Cadmium-metallothionein-induced nephrotoxicity. *Toxicol. Appl. Pharmacol.* **38**, 399–408 (1976).
65. C. A. M. Suzuki and M. G. Cherian, Renal toxicity of cadmium-metallothionein and enzymuria in rats. *J. Pharmacol. Exp. Ther.* **240**, 314–319 (1987).

66. E. C. Foulkes, Renal tubular transport of cadmium metallothionein. *Toxicol. Appl. Pharmacol.* **45**, 505–512 (1978).
67. K. H. Summer, G. A. Drasch, and H. E. Heilmaier, Metallothionein and cadmium in human-kidney cortex: Influence of smoking. *Hum. Toxicol.* **5**, 27–33 (1986).
68. R. E. Dudley, L. M. Gammal, and C. D. Klaassen, Cadmium-induced hepatic and renal injury in chronically exposed rats: Likely role of hepatic cadmium-metallothionein in nephrotoxicity. *Toxicol. Appl. Pharmacol.* **77**, 414–426 (1985).
69. K. S. Squibb, J. W. Ridlington, N. G. Carmichael, and B. A. Fowler, Early cellular effects of circulating cadmium-thionein on kidney proximal tubules. *Environ. Health Perspect.* **28**, 287–296 (1979).
70. K. S. Squibb and B. A. Fowler, Intracellular metabolism and effects of circulating cadmium-metallothionein in the kidney. *Environ. Health Perspect.* **54**, 31–35 (1984).
71. K. S. Squibb, J. B. Pritchard, and B. A. Fowler, Cadmium metallothionein nephropathy: Ultrastructural/biochemical alterations and intracellular cadmium binding. *J. Pharmacol. Exp. Ther.* **229**, 311–321 (1984).
72. K. H. Summer and D. Klein, Quantification of metallothionein in biological materials. In “Metallothionein III” (K. T. Suzuki, N. Imura, and M. Kimura, eds.), pp. 75–86. Birkhauser Verlag, Basel, 1993.
73. M. P. Waalkes, J. S. Garvey, and C. D. Klaassen, Comparison of several methods of metallothionein quantitation: Cadmium-radioassay, mercury-radioassay and radioimmunoassay. *Toxicol. Appl. Pharmacol.* **79**, 524–527 (1985).
74. S. Onosaka, K. Tanaka, M. Doi, and K. Okahara, A simplified procedure for determination of metallothionein in animal tissues. *Eisei Kagaku* **24**, 128–133 (1978).
75. D. L. Eaton and B. F. Toal, Evaluation of the Cd/hemoglobin affinity assay for the rapid determination of metallothionein in biological tissues. *Toxicol. Appl. Pharmacol.* **66**, 134–142 (1982).
76. J. K. Piotrowski, W. Bolanowska, and A. Sapota, Evaluation of metallothionein content in animal tissues. *Acta Biochim. Pol.* **20**, 207–215 (1973).
77. A. M. Scheuhammer and M. G. Cherian, Quantification of metallothioneins by a silver-saturation method. *Toxicol. Appl. Pharmacol.* **82**, 417–425 (1986).
78. C. D. Klaassen and L. D. Lehman-McKeeman, Separation and quantification of isometalothioneins by high-performance liquid chromatography–atomic absorption spectrometry. In “Methods in Enzymology” (J. F. Riordan and B. L. Vallee, eds), Vol. 205, Metallobiochemistry, Part B, Metallothionein and Related Molecules, pp. 190–198. Academic Press, New York, 1991.
79. K. T. Suzuki, Detection of metallothioneins by high-performance liquid chromatography–inductively coupled plasma emission spectrometry. In “Methods in Enzymology” (J. F. Riordan and B. L. Vallee, eds.), Vol. 205, Metallobiochemistry, Part B, Metallothionein and Related Molecules,” pp. 198–205. Academic Press, New York, 1991.
80. H. H. Dieter, L. Muller, J. Abel, and K.-H. Summer, Determination of Cd-thioneine in biological-materials: Comparative standard recovery by 5 current methods using protein nitrogen for standard calibration. *Toxicol. Appl. Pharmacol.* **85**, 380–388 (1986).
81. R. J. Vander Mallie, and J. S. Garvey, Radioimmunoassay of metallothioneins. *J. Biol. Chem.* **254**, 8416–8421 (1979).
82. R. J. Cousins, Measurement of human metallothionein by enzyme-linked immunosorbent assay. In “Methods in Enzymology” (J. F. Riordan and B. L. Vallee, eds.), Vol. 205, Metallobiochemistry, Part B, Metallothionein and Related Molecules, pp. 131–140. Academic Press, New York, 1991.
83. Z. A. Shaikh, Radioimmunoassay for metallothionein in body fluids and tissues. In “Methods in Enzymology” (J. F. Riordan and B. L. Vallee, eds.), Vol. 205, Metallobio-

- chemistry, Part B, Metallothionein and Related Molecules, pp. 120–130. Academic Press, New York, 1991.
84. M. G. Cherian and D. Banerjee, Immunohistochemical localization of metallothionein. In "Methods in Enzymology" (J. F. Riordan and B. L. Vallee, eds.), Vol. 205, Metallobiochemistry, Part B, Metallothionein and Related Molecules, pp. 88–94. Academic Press, New York, 1991.
 85. C. Tohyama, Z. A. Shaikh, K. Nogawa, E. Kobayashi, and R. Honda, Elevated urinary excretion of metallothionein due to environmental cadmium exposure. *Toxicology* **20**, 289–297 (1981).
 86. D. Banerjee, S. Onosaka, and M. G. Cherian, Immunohistochemical localization of metallothionein in cell nucleus and cytoplasm of rat liver and kidney. *Toxicology* **24**, 95–105 (1982).
 87. R. D. Andersen, B. W. Birren, T. Ganz, J. E. Piletz, and H. R. Herschman, Molecular cloning of the rat metallothionein 1 (MT-1) mRNA sequence. *DNA* **2**, 15–22 (1983).
 88. R. D. Andersen, B. W. Birren, T. Ganz, J. E. Piletz, and H. R. Herschman, Rat metallothionein I structural gene and three pseudogenes, one of which contains 5'-regulatory sequences. *Mol. Cell. Biol.* **6**, 302–314 (1986).
 89. J. M. McKim, J. Liu, P. Liu, and C. D. Klaassen, Induction of metallothionein by cadmium-metallothionein in rat liver: A proposed mechanism. *Toxicol. Appl. Pharmacol.* **112**, 318–323 (1992).
 90. T. A. Brown (ed.), "Essential Molecular Biology; Volume I." IRL Press, New York, 1991.
 91. T. A. Brown (ed.), "Essential Molecular Biology; Volume II." IRL Press, New York, 1991.
 92. P. S. Thomas, Hybridization of denatured RNA and small DNA fragments transferred to nitrocellulose. *Proc. Natl. Acad. Sci. U.S.A.* **77**, 5201–5205 (1980).
 93. L. G. Davis, M. D. Dibner, and J. F. Battey, "Basic Methods in Molecular Biology," pp. 143–146, Elsevier, New York, 1986.
 94. N. Shiraishi and M. P. Waalkes, Enhancement of metallothionein gene expression in male Wistar (WF/NCr) rats by treatment with calmodulin inhibitors: Potential role of calcium regulatory pathways in metallothionein induction. *Toxicol. Appl. Pharmacol.* **125**, 97–103 (1994).
 95. G. K. Andrews, M. T. McMaster, S. K. De, B. C. Paria, and S. K. Dey, Cell-specific expression and regulation of the mouse metallothionein-I and -II genes in the reproductive tract and preimplantation embryo. In "Metallothionein III" (K. T. Suzuki, N. Imura, and M. Kimura, eds.), pp. 351–362. Birkhauser Verlag, Basel, 1993.
 96. C. Tohyama, J. S. Suzuki, N. Homma, N. Nishimura, and H. Nishimura, Regulation of metallothionein biosynthesis in genital organs of male rats. In (K. T. Suzuki, N. Imura, and M. Kimura, eds.), pp. 443–457. "Metallothionein III" Birkhauser Verlag, Basel, 1993.
 97. D. M. Templeton and M. G. Cherian, Toxicological significance of metallothionein. In "Methods in Enzymology" (J. F. Riordan, and B. L. Vallee, eds.), Vol. 205, Metallobiochemistry, Part B, Metallothionein and Related Molecules, pp. 613–615. Academic Press, New York, 1991.
 98. B. L. Vallee and W. Maret, The functional potential and potential functions of metallothioneins: A personal perspective. In "Metallothionein III" (K. T. Suzuki, N. Imura, and M. Kimura, eds.), pp. 1–28. Birkhauser Verlag, Basel, 1993.
 99. M. P. Waalkes, T. P. Coogan, and R. A. Barter, Toxicological principles of metal carcinogenesis with special emphasis on cadmium. *Crit. Rev. Toxicol.* **22**, 175–201 (1992).
 100. M. P. Waalkes and S. Rehm, Carcinogenicity of oral cadmium in the male Wistar (WF/NCr) rat: Effect of chronic dietary zinc deficiency. *Fund. Appl. Toxicol.* **19**, 512–520 (1992).

101. M. P. Waalkes and S. Rehm, Cadmium and prostate cancer. *J. Toxicol. Environ. Health* **43**, 251–269 (1994).
102. M. P. Waalkes, S. Rehm, C. W. Riggs, R. M. Bare, D. E. Devor, L. A. Poirier, M. L. Wenk, J. R. Henneman, and M. S. Balaschak, Cadmium carcinogenesis in the male Wistar [CrI:(WI)BR] rats: Dose–response analysis of tumor induction in the prostate and testes and at the injection site. *Cancer Res.* **48**, 4656–4663 (1988).
103. M. P. Waalkes, S. Rehm, C. W. Riggs, R. M. Bare, D. E. Devor, L. A. Poirier, M. L. Wenk, and J. R. Henneman, Cadmium carcinogenesis in the male Wistar [CrI:(WI)BR] rats: Dose–response analysis of effects of zinc on tumor induction in the prostate and in the testes and at the injection site. *Cancer Res.* **49**, 4282–4288 (1989).
104. L. Hoffmann, H.-P. Putzke, C. Simonn, P. Gase, R. Russbült, H.-J. Kampehl, T. Erdmann, and C. Huckstorf, Spielt Kadmium eine Rolle in der Ätiologie und Pathogenese des Prostatakarzinoms. *Z. Ges. Hyg.* **31**, 224–227 (1985).
105. L. Hoffmann, H.-P. Putzke, H.-J. Kampehl, R. Russbült, P. Gase, C. Simonn, T. Erdmann, and C. Huckstorf, Carcinogenic effects of cadmium on the prostate of the rat. *J. Cancer Res. Clin. Oncol.* **109**, 193–199 (1985).
106. L. Hoffmann, H.-P. Putzke, L. Bendel, T. Erdmann, and C. Huckstorf, Electron microscopic results on the ventral prostate of the rat after CdCl₂ administration. A contribution towards etiology of the cancer of the prostate. *J. Cancer Res. Clin. Oncol.* **114**, 273–278 (1988).
107. L. Terracio and N. Nachtigal, Transformation of prostatic epithelial cells and fibroblasts with cadmium chloride *in vitro*. *Arch. Toxicol.* **58**, 141–151 (1986).
108. L. Terracio and N. Nachtigal, Oncogenicity of rat prostate cells transformed *in vitro* with cadmium chloride. *Arch. Toxicol.* **61**, 450–456 (1988).
109. T. Shirai, S. Iwasaki, T. Masui, T. Mori, T. Kato, and N. Ito, Enhancing effect of cadmium on rat ventral prostate carcinogenesis induced by 3,2'-dimethyl-4-aminobiphenyl. *Jpn. J. Cancer Res.* **84**, 1023–1030 (1993).
110. T. P. Coogan, N. Shiraishi, and M. P. Waalkes, Minimal basal activity and lack of metal-induced activation of the metallothionein gene correlates with lobe-specific sensitivity to the carcinogenic effects of cadmium in the rat prostate. *Toxicol. Appl. Pharmacol.* **132**, 164–173 (1995).
111. T. Umeyama, K. Saruki, K. Imai, Y. Hidetoshi, K. Suzuki, N. Ikei, T. Kodaira, K. Nakajima, H. Saitoh, and M. Kimura, Immunohistochemical demonstration of metallothionein in the rat prostate. *Prostate* **10**, 257–264 (1987).
112. H. Nishimura, N. Nishimura, and C. Tohyama, Localization of metallothionein in the genital organs of the male rat. *J. Histochem. Cytochem.* **38**, 927–933 (1990).

This Page Intentionally Left Blank

17

Primary Culture of Bovine and Human Adult Adrenocortical Cells

Matthias M. Weber¹

Patrick Michl

Medical Department II

Laboratory of Endocrine Research

Klinikum Großhadern

University of Munich

81377 Munich

Germany

INTRODUCTION

Multiple pathways of steroidogenesis are present in the normal adrenocortical cell, primarily involving the formation of glucocorticoids, mineralocorticoids, and androgens. Histologically, the adult human adrenocortex is composed of three zones: an outer zona glomerulosa, a zona fasciculata, and a zona reticularis. However, the two inner zones appear to function as a unit. The mineralocorticoids, the main representative of which is aldosterone, are synthesized in the zona glomerulosa and regulated primarily by angiotensin II. The glucocorticoids, which are quantitatively the most important group of adrenal steroids, and the adrenal androgens are produced in the zonae

¹ Address correspondence to Dr. med. Matthias M. Weber, Medizinische Klinik II, Klinikum Großhadern, Marchioninistrasse 15, 81377 München, Germany.

fasciculata and reticularis. Adrenocorticotropin (ACTH) is the trophic hormone of these two inner zones and the major regulator of adrenal corticosteroid and androgen synthesis. Intracellularly, ACTH acts via cAMP-dependent protein kinase A, but involvement of other signal transduction pathways, including C kinase and Ca^{2+} /calmodulin-dependent protein kinase, have been postulated (1,2). The steroidogenic response of adrenocortical cells to ACTH is modified by a variety of hormones, growth factors, and cytokines, including angiotensin II, vasopressin, tumor growth factor (TGF), epidermal growth factor (EGF), insulinlike growth factor I (IGF I), and interleukin-6 (for review see Refs. 3,34).

Cultures of adrenocortical cells offer a useful model to study the regulation of metabolic pathways and enzymes involved in steroid formation and secretion. Since these cells are maintained in primary culture, their biochemical and proliferative function closely reflect the characteristics of normal adrenocortical cells. Their differentiated biochemical and morphological function *in vitro* renders them susceptible to biochemical perturbations. Therefore, primary cultures of adult adrenocortical cells seem to be well suited for the assessment of toxic effects of various agents on differentiated adrenocortical cell function.

MATERIALS AND REAGENTS

Equipment and Supplies

Five-hundred-milliliter sterile tissue containers (Sigma, Cat. No. Z14,229-8/4, Deisenhofen, Germany); 140 and 100- μm sieves (Bender & Hobein, Zürich, Switzerland); scalpels with No. 22 disposable blades; fine forceps without teeth; 50-ml centrifuge vials (Falcon GmbH, Cat. No. 2070, Heidelberg, Germany); sterile 10-ml plastic pipettes (Falcon, Cat. No. 7551); 100-mm tissue culture plates (Falcon, Cat. No. 3803); 22-mm 12-well tissue culture plates (Falcon, Cat. No. 3043); 15-mm 24-well tissue culture plates (Falcon, Cat. No. 3047); 9-mm 48-well tissue culture plates (Falcon, Cat. No. 3078); 25- cm^3 cell culture flasks (Falcon, Cat. No. 3013); sterile spoon for filtering (Falcon, Cat. No. 3085); bottle top vacuum sterile filter 0.22 μm (Falcon, Cat. No. 7105); cell counting vials (Sigma, Cat. No. Z35,349-3).

Reagents and Solutions

Phosphate-Buffered Saline (PBS)

Combine 0.877 g NaCl, 1.42 g Na_2HPO_4 , and 93 mg NaH_2PO_4 and add double-distilled water to a final volume of 1 liter, adjust the pH to 7.4, and sterilize the complete solution.

Fetal Calf Serum (FCS) and Horse Serum (HS)

Five-hundred-milliliter bottles of FCS (Biochrom, Cat. No. S0115, Berlin, Germany) are thawed, mixed, and divided into 50-ml aliquots in sterile 50-ml vials. The vials can be stored frozen at -20°C . Five-hundred-milliliter bottles of HS (Biochrom, S 9135) are thawed, mixed, and divided into 25-ml aliquots in sterile 50-ml vials. The vials can be stored frozen at -20°C . Because the composition of various lots of sera varies considerably, it is important to use only pooled sera to minimize variability of tissue culture conditions.

M-199 Cell Culture Medium

One hundred milliliters of the medium powder (M-199), containing Earle's salts without NaHCO_3 and L-glutamine (Biochrom, F0625), is diluted with 900 ml double-distilled and autoclaved water. NaHCO_3 (2.2 g/liter) is added to the solution and the pH is adjusted to values between 6.8 and 7.1 with NaOH. The solution is sterile-filtered through 0.2- μm filter units and stored in sterile 500-ml storage bottles at 4°C . Because of the lability of many medium components, the M-199 solution should not be kept for more than 4 weeks. Immediately before use the M-199 medium is substituted with L-glutamine (Gibco, Cat. No. 810-1051, Eggenstein, Germany) at a concentration of 290 ng/ml.

Enzymes

Collagenase II (Sigma, Cat. No. C-6885) and desoxyribonuclease I (DNase, Sigma, Cat. No. D-5025) are stored at -20°C and should be dissolved in PBS immediately before use.

Percoll

Percoll (Pharmacia GmbH, Freiburg, Germany) is a suspension of colloidal particles, 15–30 nm in diameter, which are coated with polyvinyl-pyrrolidone (PVD). Percoll can be used for purification and isolation of adrenocortical cells by sedimentation. Percoll has a density of 1.13 g/ml and the desired density of the isosmotic Percoll solution (ρ_o) can be obtained by dilution of Percoll stock solution with 1.5 M NaCl and double-distilled water. The volume of the percoll stock solution (V_s) can be calculated as

$$V_s = V_o \times \frac{\rho_o - (0.1 \times \rho_{\text{NaCl}}) - 0.9}{(\rho_s - 1)}$$

where

V_s = volume of Percoll stock solution (ml)

V_o = needed volume of the isosmotic Percoll solution (e.g., 100 ml)

ρ_o = density of the isosmotic Percoll solution produced (e.g.,
1.07 g/ml)

ρ_{NaCl} = density of 1.5 M NaCl (1.058 g/ml)

ρ_s = density of the Percoll stock solution (1.13 g/ml)

The following volumes of 1.5 M NaCl (V_{NaCl}) and double-distilled water ($V_{\text{H}_2\text{O}}$) are added to the Percoll (V_s) to obtain an isosmotic solution:

V_{NaCl} = volume of 1.5 M NaCl = 1/10 of V_o

$V_{\text{H}_2\text{O}}$ = volume of double-distilled water = $V_o - V_s - V_{\text{NaCl}}$

For example, to obtain 100 ml of 1.07 g/ml Percoll solution, combine 10 ml of 1.5 M NaCl with 49.3 ml Percoll stock solution (1.13 g/ml) and add 40.7 ml double-distilled water.

CELL CULTURE OF BOVINE ADRENOCORTICAL CELLS

Source of Bovine Adrenal Glands

Adrenal glands from 2- to 3-year-old steers are obtained from the local slaughterhouse. Once the animal has been killed, the adrenal gland should be removed as soon as possible. Using a sterile scalpel, and wearing surgical gloves, the organ is excised rapidly from the periadrenal fat tissue, leaving the entire adrenal capsule intact. Immediately after removal, the adrenal gland is placed in a 500-ml tissue container filled with 250 ml sterile ice-cold PBS containing gentamicin (52 $\mu\text{g/ml}$) and amphotericin B (0.5 $\mu\text{g/ml}$). The tissue container should be placed on ice in a second box and transferred to the laboratory as soon as possible. This procedure ensures rapid lowering of the organ temperature, and allows storage and transport of the tissue without loss of cell viability. It is important to use only intact adrenal glands, which are surrounded by enough periadrenal fat, to reduce the risk of contamination. In our hands, five adrenal glands are required for five confluent 12-well culture dishes.

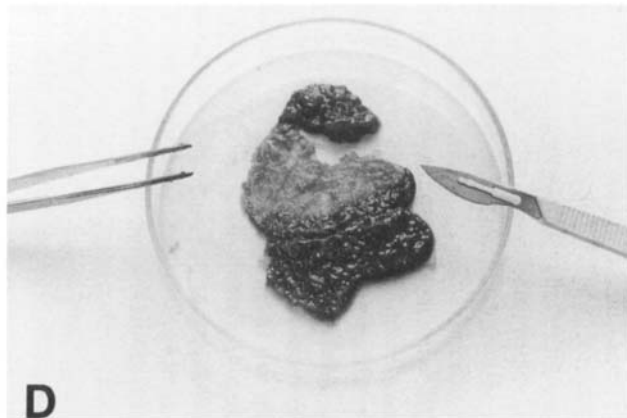
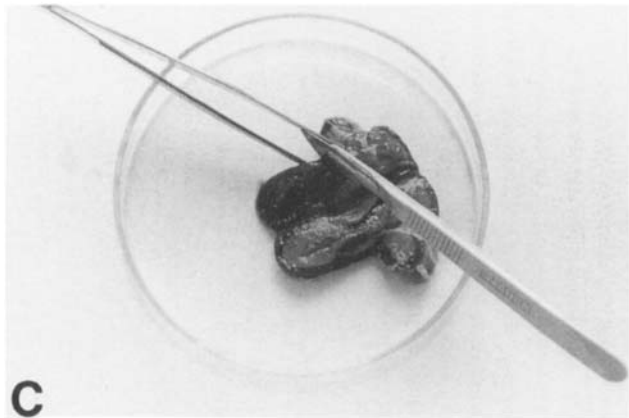
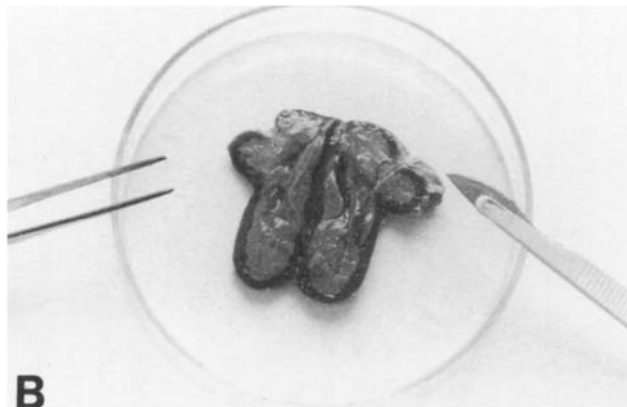
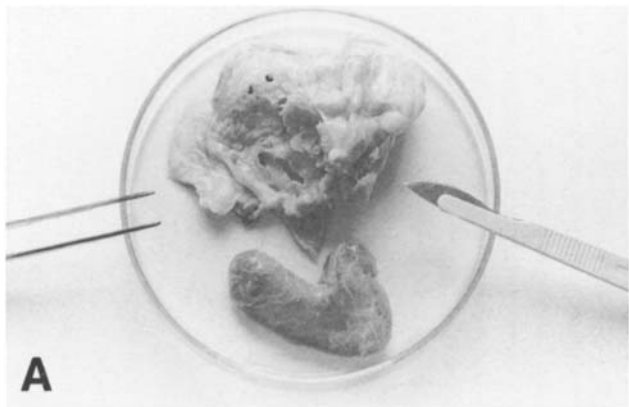
Dissection of Bovine Adrenocortical Tissue

The dissection of the adrenal glands should be performed in a designated tissue culture room equipped with an incubator, centrifuge, water bath, microscope, and laminar flow hood. On arrival, the adrenal glands are transferred to a second tissue container filled with 250 ml of sterile ice-cold PBS. All following preparation steps are performed under a laminar flow hood, using sterile glass and plastic ware.

One adrenal gland is removed from the tissue container and washed again with sterile ice-cold PBS. Before dissection, fat and extraneous tissue are removed carefully without injuring the capsule (Figure 1A). The adrenal gland is rinsed with PBS and placed on a sterile 10-cm tissue culture dish containing a small amount of serum-free tissue culture medium (see the following). Next, the adrenal gland is cut longitudinally with a sterile No. 22 scalpel (Figure 1B). In contrast to the yellow color of the adult human adrenal cortex, the bovine adrenocortex is of a dark red color. The bovine medulla is demarcated from the cortex as a pale gray tissue and can be easily scraped off with a scalpel and discarded (Figure 1C). All remaining adrenal glands are prepared as described, and the adrenocortical tissue is stored in a fresh container filled with sterile ice-cold PBS. In the following, the fasciculata/reticularis cells are separated from the capsule and attached glomerulosa cells by carefully scraping the adrenocortical tissue from the capsule with a sterile scalpel and a fine forceps (Figure 1D). Unless used for glomerulosa cell culture, the capsule with the attached glomerulosa cells is discarded and the fasciculata/reticularis tissue fragments of all adrenal glands are combined in a 10-cm tissue culture dish with a minimal volume of medium. Usually, the glomerulosa–fasciculata boundary is visible as an abrupt change in color from brown to red, and careful dissection of the zones is necessary to separate glomerulosa from fasciculata cells. If a more standardized method for separation of the cortical zones is required, the adrenal cortex can be cut by a microtome as described (4,5). Glomerulosa and fasciculata cells may also be separated by unit gravity sedimentation of adrenocortical cell suspensions (6). However, this size-fractionation of cells is time-consuming and limited by the small amounts of cells yielded by each run. Furthermore, it has been shown that *in vitro*, zona glomerulosa cells eventually behave functionally and morphologically exactly like cultures from the two other cortical zones (7,8).

Preparation of Bovine Fasciculata Cell Suspensions

The adrenocortical tissue fragments resulting from the dissection procedure are dissociated using collagenase II digestion. To facilitate enzymatic cell separation, the tissue is cut into very small fragments with a scalpel and transferred to a container containing tissue culture medium, gentamicin (52 $\mu\text{g}/\text{ml}$), and amphotericin B (0.5 $\mu\text{g}/\text{ml}$) with a final volume of 100 ml. Freshly prepared collagenase II (1 mg/ml) and desoxyribonuclease I (75 $\mu\text{g}/\text{ml}$) are added and the tightly closed container is incubated in a water bath at 37°C for 75 min with gentle shaking. DNase is added to digest DNA released from damaged cells, and the mechanical agitation helps to reduce incubation time and concentration of enzymes, resulting in a more



gentle digestion with decreased cytotoxic effects. At the end of the incubation time, the successful dissociation results in milky clouds of cells in the incubation medium and a reduction of the number of visible tissue fragments. After digestion, the cells are filtered twice through a sieve of 140- and 100- μm mesh opening, respectively. For this purpose, the digested tissue is poured onto the filter and gently stirred with a sterile spoon while washing with 300 ml of 37°C tissue culture medium containing antibiotics and FCS. It is important not to use mechanical force to avoid crushing the cells with consecutive cytotoxic effects of lysosomal enzymes. The filtering separates isolated cells from undigested tissue fragments and stops the digestion process by dilution with a large volume of tissue culture medium. Next, the 300-ml cell suspension is transferred to six 50-ml Falcon tubes and centrifuged for 5 min at 400g, and the cell pellet is resuspended in 50 ml of 37°C tissue culture medium and pelleted again for 5 min at 400g to clean the cell suspension of cell debris.

Purification of Bovine Fasciculata Cells by Percoll Centrifugation

To purify the dissociated cells, and to remove contaminating red blood cells and cell debris, a Percoll centrifugation is performed. For this purpose, the cell pellet, obtained after digestion and filtration, is resuspended in 20 ml of prewarmed (37°C) isosmotic Percoll solution (density: 1.07 g/ml), freshly prepared as described under Materials. In the following, the Percoll cell suspension is centrifuged in a horizontal swing bucket centrifuge (Mistral 3000, MSE Fison Inc., Oxford, Great Britain) for 10 min at 730g. After centrifugation, red blood cells and contaminating tissue fragments are pelleted at the bottom of the vials, whereas the fasciculata-reticularis cells are concentrated in a layer on top of the Percoll solution. This layer is carefully sucked off with a sterile 10-ml pipette, transferred to a 50-ml Falcon tube, brought to a final volume of 50 ml with tissue culture medium, and centrifuged for 5 min at 400g. The resulting cell pellet is washed twice in M-199 medium, to remove the remaining Percoll. After the last wash, the resulting supernatant is carefully discarded, and the final cell pellet is

FIGURE 1. Dissection of bovine adrenocortical tissue. (A) The periadrenal fat and extraneous tissue is removed carefully without injuring the capsule. (B) The adrenal gland is cut longitudinally with a sterile scalpel. (C) The medulla is scraped off the dark red cortex and discarded. (D) The fasciculata-reticularis cells are separated by carefully scraping off the adrenocortical tissue, leaving the glomerulosa cells attached to the capsule.

resuspended in a defined volume of serum containing growth medium (see the following). Using this Percoll centrifugation procedure, more than 70% of the red blood cells can be removed from the adrenocortical cell suspension, with only minor adverse effects on cell viability.

At this stage, the cells may be plated in culture dishes or may be frozen for long-term storage in liquid nitrogen. For the latter purpose, resuspend the resulting cell pellet of five adrenal glands in 8.5 ml of complete cell growth medium, add an extra 1 ml of FCS and 0.5 ml dimethyl sulfoxide (DMSO), and mix well by pipetting. As rapidly as possible, 1.8 ml of this cell suspension is put into each 2-ml freezing vial, closed carefully, and stored in liquid nitrogen after continuously lowering the temperature of the vials to -70°C .

Monolayer Cell Culture of Bovine Adrenocortical Cells

The final cell pellet is resuspended in complete growth medium, and an aliquot is counted in a hemocytometer. The viability is determined by the trypan blue exclusion test (9) and usually exceeds 90%. The cells are plated at a density of approximately 10^6 cells/ml in prewarmed M-199 medium supplemented with glutamine (290 ng/ml), gentamicin ($52\ \mu\text{g/ml}$), amphotericin B ($0.5\ \mu\text{g/ml}$), 10% fetal calf serum, and 5% horse serum (complete growth medium) and incubated at 37°C in a moist atmosphere with 5% CO_2 .

Depending on the nature of the experiment, a variety of plastic tissue culture plates can be chosen. We usually plate approximately 10^6 cells in 1 ml of incubation medium in 3.8-cm^2 12-well plates, or 0.5×10^6 in 1.8-cm^2 24-well plates. However, lower cell densities may be appropriate for long-term proliferation studies. In our hands, the preparation of five bovine adrenal glands yields approximately 6×10^7 cells, which is sufficient for plating five 12-well plates. Before plating, the cell suspension must be thoroughly mixed by pipetting up and down to obtain a homogeneous cell suspension and to ensure an even distribution of cells into each well. For this purpose, the stock vial with the cell suspension must be kept in a swirling motion by one hand, while pipetting the cells into the tissue culture plates with the other hand.

To further enhance cell growth, fibroblast growth factor (FGF) and/or IGFs, the most important mitogenic factors for bovine adrenocortical cells, can be added in a concentration of 100 ng/ml. Furthermore, a significant increase in cell growth has been reported when tissue culture dishes are coated with fibronectin ($2\ \mu\text{g/cm}^2$). However, the growth-promoting effect of fibronectin is relevant predominantly in long-term cultures of bovine adrenocortical cells (10).

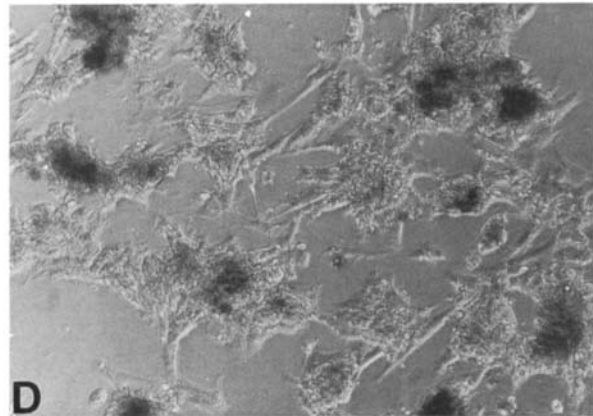
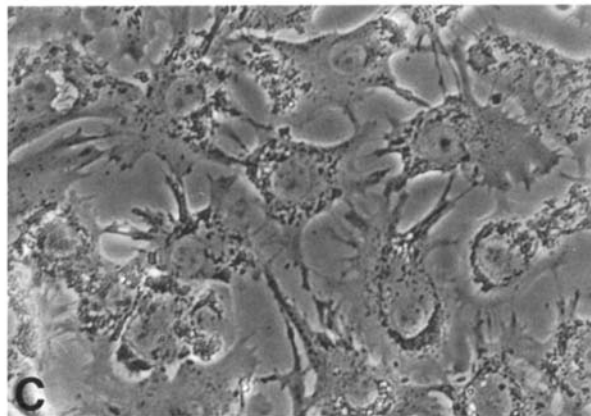
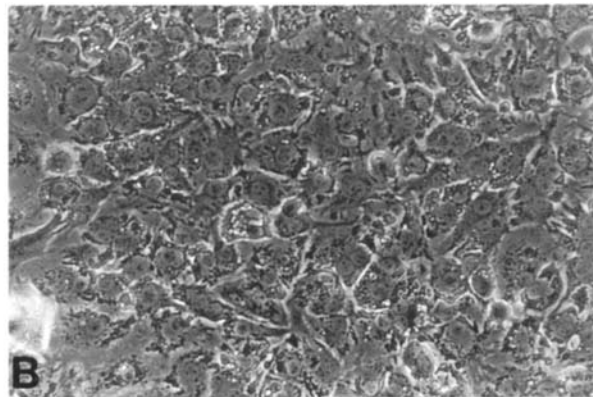
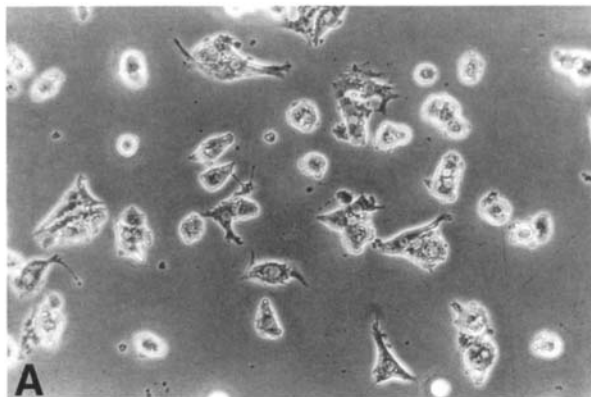
After plating, cells are allowed to grow undisturbed for 24 hr to facilitate cell attachment. Initially, media are changed after 24 hr to remove cell debris and unattached cells. More than 80% of all seeded cells do not attach during the first 24 hr and are removed with the first change of medium. A longer incubation period before the first wash is of no benefit, as this increases the cytotoxic effect of the damaged cells in the supernatant (Figure 2A). During the following days, medium is replenished every 24–72 hr, depending on the schedule of the experiments. Cells usually reach confluence after 72–96 hr of incubation in serum containing growth medium (Figure 2B). At this time, cell density is approximately 1.6×10^5 cells/well (12-well plate) as determined by Coulter counting (see the following) and cell viability is 95% as determined by trypan blue exclusion. The primary monolayer adrenocortical cell cultures can be maintained in the same tissue culture dish for up to 120 hr while still retaining their differentiated cell function and morphology. The morphology of the cell culture is monitored daily using phase-contrast microscopy. When bovine adrenocortical cells are treated with ACTH or cAMP, they change their morphological appearance and cells become more rounded or retracted.

Although adult bovine adrenocortical cells can easily be subcultured and maintained in monolayer culture for up to 60 generations (11), we do not use passaged cells for experiments. In our experience, subcultured cells change their biochemical and functional behavior already after one passage, and eventually are overgrown by fibroblasts (5).

A variety of medium formulations for bovine adrenocortical cells are described in the literature. An alternative basal medium is a 1:1 mixture of Dulbecco's modified Eagle's medium (DMEM) with Ham's F12 medium. Although serum-free media have been described, which support the long-term proliferation of adrenocortical cells (10), the use of serum-containing medium is still superior in promoting cell growth (12).

CELL CULTURE OF HUMAN ADRENOCORTICAL CELLS

Primary cultures of fetal human adrenocortical cells have been used for proliferation and functional studies (13–16). However, the fetal adrenal gland differs morphologically and biochemically from adult adrenocortical cells. In the fetal adrenal gland the outer fourth of the cortex consists of the small definitive zone, which eventually develops into the adult adrenocortex and produces predominantly cortisol. The major part of the fetal adrenal gland, however, consists of the fetal zone, which shows a relative lack of 3β -hydroxysteroid dehydrogenase (3β -HSD) expression and therefore synthesizes mainly dehydroepiandrosterone (DHEA) and its sul-



fate (DHEAS). Immediately after birth, the fetal zone degenerates and the definitive zone steadily grows until it shows the typical zonation of the adult cortex during puberty (17).

Although human adult adrenocortical cells do not grow as easily *in vitro* as do human fetal zone cells, they can be maintained in primary monolayer cell culture, where they still retain many differentiated cell functions like steroidogenesis and trophic responses to various growth factors and cytokines (14,18,19). Primary cultures of human adult adrenocortical cells therefore represent a useful system to evaluate toxicological effects on differentiated cell function in human endocrine cells.

Source of Human Adrenal Glands

Adult human adrenal glands are usually obtained from patients with renal neoplasm, undergoing a tumor nephrectomy with ipsilateral adrenalectomy. If the renal tumor is located at a distant site to the adrenal gland, and no infiltration of the organ is to be assumed, the part of the adrenal gland that is not required for pathological examination can be used for cell culture. An alternative source of adult adrenal glands is brain-dead patients who have given written consent for removal of organs for renal transplantation. In any case, the recommendations of the local ethical committee should be followed.

The combined weight of the adrenal glands from human adults is about 8 g, but the weight and size of the glands vary considerably with age and physical condition. Usually, the amount of tissue that is available for tissue culture purposes is very small, and a careful tissue dissection must be performed to obtain enough cells for adrenocortical cell culture.

Dissection of Human Adrenocortical Tissue

Primary cultures of adult human adrenocortical cells are prepared essentially as described for bovine adrenocortical cells. However, fatty tissue

FIGURE 2. Morphological appearance of bovine and human adrenocortical cells in primary monolayer cell culture. (A) Bovine adrenocortical cells are plated at a density of 10^6 cells/ml and allowed to grow for 24 hr (magnification, $\times 200$). (B) After 4 days of incubation in serum-containing medium, bovine adrenocortical cells reach confluence (magnification, $\times 200$). (C) Morphological appearance of semiconfluent bovine adrenocortical cells grown for 3 days under serum-free conditions without addition of ACTH (magnification, $\times 400$). (D) Morphological appearance of human adrenocortical cells grown for 6 days in serum-containing medium (magnification, $\times 200$).

such as the human adrenal cortex must be handled more carefully than nonfat tissue such as the bovine adrenal cortex. In particular, any crushing of the tissue with large scissors or forceps should be avoided (12). As the adrenal glands are removed under sterile conditions, the contamination risk should be low.

After careful removal of periadrenal fat tissue, the gland is cut longitudinally with a No. 22 scalpel. In section, the cortex, which represents 90% of the weight of the organ, appears yellow as human adrenocortical cells are packed with numerous large lipid droplets. In contrast, the medulla, owing to the larger number of blood vessels, is of a brown or dark red color. In the human adrenal gland, the boundary between cortex and medulla is not as clearly demarcated as in the bovine gland. However, human cortical tissue is of a more solid consistency than the tissue of the medulla, and the latter can be easily scraped off with a scalpel and discarded. Fasciculata-reticularis tissue is separated from the capsule and attached glomerulosa cells as described earlier.

Isolation and Purification of Human Fasciculata Cells

The enzymatic digestion is performed with collagenase II (1 mg/ml) and desoxyribonuclease I (100 $\mu\text{g/ml}$) in a final volume of 30 ml of PBS at 37°C for only 40 min in a gently shaking water bath. To minimize the mechanical forces used, the digest is filtered only once (100- μm mesh opening) and the cells are harvested by gentle centrifugation at 250g for 7 min. The Percoll purification step is performed in analogy to the bovine fasciculata-reticularis cells, with the exception that the Percoll-cell suspension is centrifuged at 650g for 10 min, and the resulting adrenocortical cell suspension is washed only once.

Monolayer Cell Culture of Human Adrenocortical Cells

After digestion and purification of the adrenocortical cells, the resulting cell pellet is resuspended in medium containing a higher serum concentration than growth medium for bovine adrenal cell culture [M-199 substituted with L-glutamine (290 ng/ml), gentamicin (52 $\mu\text{g/ml}$), amphotericin B (0.5 $\mu\text{g/ml}$), 15% FCS, and 7.5% HS]. The yield of adrenocortical cells largely depends on the quantity of the obtained adrenal tissue and varies considerably from preparation to preparation. Usually, the cells are plated in 15-mm 24-well culture dishes (1 ml medium per well) at a cell density of approximately 4×10^4 cells/ml. When 9-mm 48-well plates are used, 2×10^4 cells are seeded in 0.5 ml of medium/well. The first change of medium is performed after 24 hr of incubation, and thereafter every other day.

Usually, adult human adrenocortical cells show a significantly better plating efficiency than bovine adrenocortical cells (more than 90% attach after 24 hr). However, adult human fasciculata–reticularis cells do not grow as fast as fetal human or bovine adult adrenocortical cells, and confluence ($3\text{--}4 \times 10^4$ cells/cm²) is reached after about 6 days of culture in serum-containing medium.

DIAGNOSTIC EVALUATION OF ADRENOCORTICAL CELL CULTURES

Because well-defined secretion products and well-characterized responses to hormones are present *in vitro*, adrenocortical cells are especially suited for testing the influence of toxic substances. In the described *in vitro* cell system, a variety of diagnostic end points for toxicity can be measured, including adrenocortical cell proliferation and differentiation.

Proliferation Studies

The relative simplicity of culturing adrenal cells makes adult bovine adrenocortical cells an excellent primary-cell model for investigating the mechanism of action of growth-promoting or growth-inhibiting substances *in vitro*. Normal bovine and, to a lesser extent, human adrenocortical cells grow and proliferate well in culture with the addition of growth factors and supplements (for review see Ref. 12). Bovine adrenocortical cells can be maintained in culture for several months, and clonal cell lines have been obtained (20). Like many normal cell lines, bovine adrenocortical cell cultures progressively decline and reach senescence, resulting in a loss of responsiveness to growth stimulators and secretagogues (21). To avoid this phenomenon, we use only primary cultures of adrenocortical cells that are not older than 8 days for our experiments.

A variety of hormones, neuropeptides, and growth factors have been found to be mitogenic for adrenocortical cells *in vitro*, including angiotensin II, FGF, vasopressin, insulin, IGF I, thrombin, transferrin, EGF, antioxidant nutrients (ascorbic acid, α -tocopherol, selenium), bovine serum albumin (BSA), and fibronectin (10). In contrast, transforming growth factor- β (TGF β) and prostaglandin E₁ have been reported to have an inhibitory effect on adrenal cell proliferation (21,22).

Surprisingly, ACTH, which *in vivo* causes cellular hypertrophy and hyperplasia of the adrenal cortex, *in vitro* has an antimitogenic effect on bovine, rat, human, and tumorous adrenocortical cells. This effect is dose dependent, appears to be correlated with the steroidogenic response to

ACTH, and can be mimicked by the addition of cAMP and forskolin, an activator of adenylate cyclase (21). A possible explanation for this paradox is that ACTH *in vivo* may be an indirect mitogen that stimulates local production of growth factors that then induce adrenocortical cell division by paracrine effects (17,21).

Experimental Design

Adrenocortical cells can be tested for either mitogenic or antimitogenic properties of an exogenous reagent. For proliferation studies, freshly prepared cells are plated in 24-well plates at a somewhat lower cell density (e.g., 0.5×10^6 cells/ml) to allow “room” for the cells to divide. Cells are allowed to attach and grow in serum containing growth medium for 24 hr as described earlier. It is necessary to culture some more wells so that the cell number after the initial day of culture prior to the addition of test agents can be determined. At this time point, the old medium is removed and serum-reduced or serum-free defined medium is added together with the substance to be tested. The cells are incubated for another 24 to 144 hr, and medium is refreshed every 48 hr. At the end of the incubation period, cell viability is assessed by trypan blue exclusion, and protein synthesis or cell number can be determined.

Growth Medium

If the cells are continuously incubated in serum-reduced medium (growth medium with only 5% FCS and 2.5% HS), the cells proliferate actively with a doubling time of 48 hr (Fig. 3). Whereas ACTH, in a concentration of 10^{-8} M, completely inhibits cell growth, the addition of FGF and other growth-promoting factors significantly enhances cell growth (10) (Figure 4). A serum-containing cell system may not be the most sensitive for testing the inhibitory or stimulatory potential of specific agents upon adrenocortical cell proliferation. Furthermore, the exact interaction of the various growth-promoting factors and the substance under investigation cannot be exactly delineated when serum is present in the experimental setting. To circumvent this, a serum-free defined medium can be used. When cells are incubated with serum-free induction medium (M-199 with L-glutamine and antibiotics) without any growth-promoting additives, they remain growth arrested in the G1 phase (22). Although this is ideal for testing induction of cell differentiation, this may not be adequate for cell proliferation assays. Therefore a minimal serum-free defined medium that has limited growth-promoting activity should contain FGF (100 ng/ml) and insulin (1 μ g/ml) or IGF-I (100 ng/ml). A more sophisticated serum-free defined medium

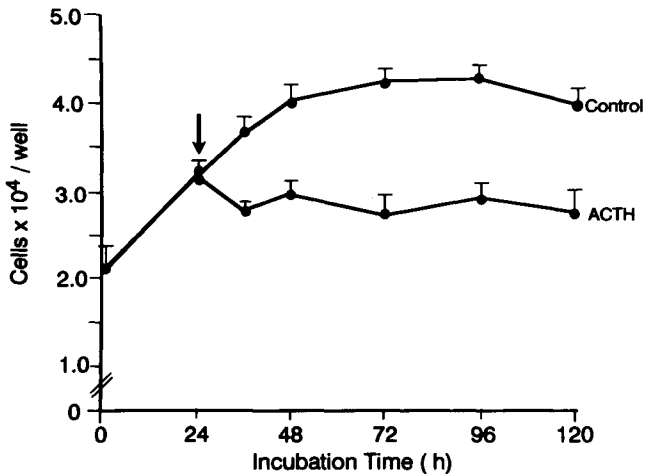


FIGURE 3. Proliferation of bovine adrenocortical cells. Bovine adrenocortical cells (24-well plates) were cultured in medium containing 10% FCS and 5% HS. After 24 hr, medium was exchanged to serum-reduced medium with or without ACTH (10^{-8} M). At each time point, cells were removed and counted using a hemocytometer. Each point represents the mean \pm SEM from 12 independent wells. After 48 hr, cells reached confluence and no further cell growth was observed. The addition of ACTH (arrow) completely inhibited cell growth.

that supports continuous proliferation and passaging of adrenocortical cells, similar to serum-supplemented medium, includes the following additives: FGF (4 nM), insulin (2 nM), thrombin (100 mU/ml), low-density lipoproteins (LDL, 10 μ g/ml), transferrin (100 μ g/ml), fatty acid-free BSA (500 μ g/ml), ascorbic acid (100 μ M), α -tocopherol (1 μ M), selenium (50 nM), and antibiotics. This medium can be used for long-term culture in combination with fibronectin (10 μ g/ml)-coated tissue plates (10).

Determination of Cell Number

Conventionally, cell number is determined by removing cells from the substratum and counting them with either a hemocytometer (e.g., Neubauer counting chamber) or an electronic particle counter (Coulter Counter, Coulter Electronics Ltd., Luton, Great Britain). Cell counts are obtained by removing the treatment medium and adding 0.3 ml of PBS with trypsin (0.25%) and EDTA (5 mM) to each well. The plates are returned to the incubator for 5 min (7 min for human adrenocortical cells). The digestion is stopped by the addition of 0.7 ml medium containing 10% FCS to each well. When using a Coulter Counter, 0.5 ml of each well is transferred to

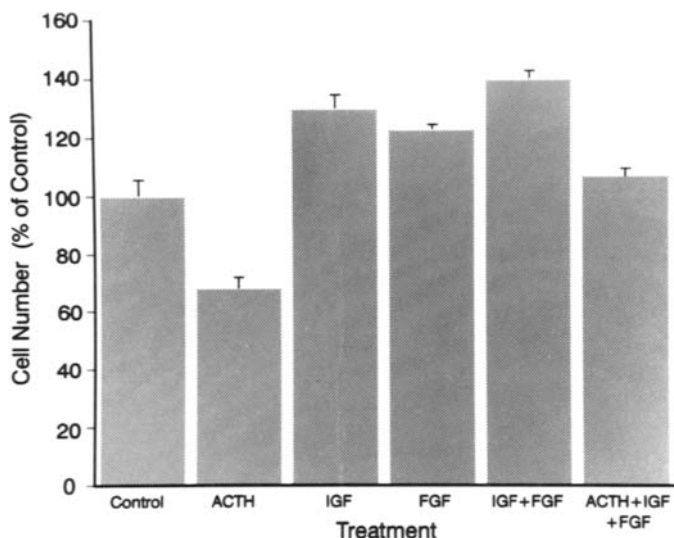


FIGURE 4. Effect of various growth factors on bovine adrenocortical cell proliferation. Bovine adrenocortical cells (24-well plates) were cultured in medium containing 10% FCS and 5% HS. After 24 hr, medium was exchanged to serum-reduced medium (5% FCS and 2.5% HS) in the presence of growth factors in the following concentrations: ACTH (10^{-8} M), IGF I (100 ng/ml), FGF (100 ng/ml). After an incubation time of 48 hr, cells were removed and counted using a hemocytometer. Each point represents the mean \pm SEM from 12 independent wells. Whereas the addition of ACTH led to a reduction in cell numbers to 68% of control, IGF I and FGF induced cell proliferation to 130 and 123% of control, respectively. The proliferative effect of IGF I and FGF was further enhanced when both growth factors were present (141% of control) and was abolished by the addition of ACTH.

a cell-counting vial containing 20 ml of PBS. Samples should be counted in triplicate immediately after removal and each treatment group should consist of at least six independent wells (Figure 3). The major drawback to these techniques is that they are laborious and time-consuming, and require relatively large numbers of cells.

[³H]Thymidine Incorporation Assay

An alternative and more convenient method for the estimation of cell growth is the [³H]thymidine incorporation assay. Depending on incubation time of the cells with the radiolabeled precursor and the extraction method used, a variety of protocols are available (23,24). The following protocol can be used to measure [³H]thymidine incorporation by adrenocortical cells in primary culture and the results are proportional to adrenocortical cell number and growth (Figure 5).

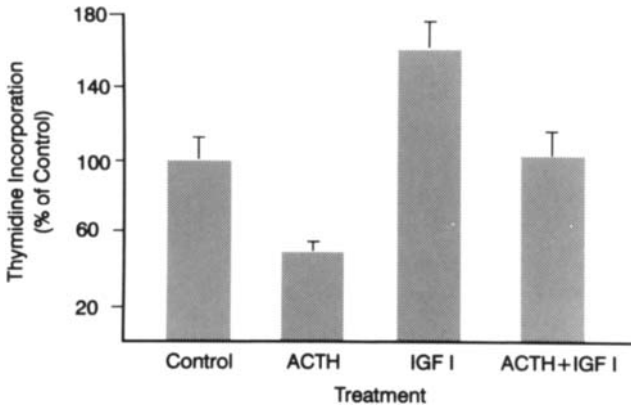


FIGURE 5. Effect of various growth factors on [^3H]thymidine incorporation by bovine adrenocortical cells. Bovine adrenocortical cells (24-well plates) were cultured in medium containing 10% FCS and 5% HS. After 24 hr, medium was exchanged to serum-reduced medium (5% FCS and 2.5% HS) in the presence of ACTH (10^{-8} M) and/or IGF I (100 ng/ml). After 36 hr, [^3H]thymidine (1 $\mu\text{Ci}/\text{ml}$) and cells were incubated for another 12 hr. At the end of the incubation period the radioactive medium was removed, cells were washed and lysed, and the incorporated radioactivity was counted in a scintillation counter. In parallel to the effect on cell growth, ACTH reduced the [^3H]thymidine incorporation by adrenocortical cells to 51% of untreated control, whereas IGF I induced an increase to 166% of control. The stimulatory effect of IGF I was abolished when ACTH was present at the same time.

After 36 hr of incubation with various test substances, [^3H]thymidine (Amersham TRA 310, 1 mCi; 10 μl contains 1 μCi) at a concentration of 1 $\mu\text{Ci}/\text{ml}$ is added to each well. When incubation medium that contains thymidine is used, the concentration of the labeled precursor should be 5 $\mu\text{Ci}/\text{ml}$. After an incubation period of 12 hr in the incubator, the radioactive medium is removed carefully and discarded into the liquid radioactive waste and the cells are washed once with PBS. Then, 400 μl of cold 10% trichloroacetic acid (TCA) is added to each well. After an incubation for 20 min at 4°C , the TCA is removed, and cells are incubated with TCA for 5 min two more times. The cells are lysed by incubation with 1 N NaOH (500 μl per well) for 30 min at 37°C under mechanical agitation. Finally, 450 μl of each well is collected and counted in a scintillation counter (Figure 5).

Steroidogenic Response

Multiple steroidogenic pathways are present in the normal adrenal cortex, primarily involving formation of glucocorticoids, mineralocorticoids, and to a lesser extent androgens. Because adrenocortical cells in monolayer

culture retain their capacity for synthesizing steroids from internal as well as from exogenous precursors and respond to ACTH stimulation, adult human and bovine adrenocortical cells are a useful cell system for the study of the influence of various substances on well-defined differentiated cell functions.

Upon stimulation, adrenocortical cells synthesize and secrete various steroid hormones that can be measured in the medium by radioimmunoassay. The induction of key-enzyme genes of the steroidogenic pathway can be monitored by Northern blotting of RNA, extracted from adrenocortical cell cultures before and after treatment (25). Furthermore, the expression and regulation of many growth factor receptors can be assessed by radioligand assay and Scatchard analysis (26).

Bovine and human fasciculata-reticularis cells secrete mainly cortisol, and to a lesser extent corticosterone, 11-deoxycorticosterone, 11-deoxycortisol, 17OH-progesterone, androstenedione, and DHEA (5,11, 18,27). The androgen DHEA is the main secretion product of fetal zone cells cultured from human fetal adrenal glands (28). Although bovine adult adrenocortical cells can be maintained in long-term monolayer cell culture for up to 60 generations, they eventually become resistant to the growth inhibitory effect of ACTH, and progressively higher concentrations of ACTH are required for stimulation of steroidogenesis (11). As soon as after 1 week, bovine adrenocortical cells start to lose their responsiveness to ACTH, primarily due to a loss in 11 β -hydroxylase activity. Furthermore, a substantial overgrowth of adrenal cell cultures by fibroblasts has been observed (5). In view of these results, it appears that *in vitro* studies investigating the regulation of adrenal steroidogenesis should be confined to confluent primary cultures during the first week.

Experimental Design

Primary bovine or human adrenocortical cells are prepared as described earlier. For initial experiments it is advisable to use larger wells to assess the magnitude of the response and to establish proper techniques. Because the human cell culture secretes larger amounts of steroids per number of seeded cells, we use 24-well or 48-well plates for human and 12-well or 24-well plates for bovine adrenal cell culture. Cells are initially plated for 2 to 6 days in serum-containing medium, until confluence is reached. Medium is exchanged after the first 24 hr of incubation in order to remove cell debris and unattached cells, thereafter every 24 hr. If possible, the following experiment should be performed under serum-free conditions, both to avoid the potential effect of unknown substances in the serum and to reduce pseudosubstrate effects. As soon as the confluent cells are incubated in

serum-free medium (induction medium, see the following) they become growth arrested, and induction experiments can be started by adding the various substances to the medium. For each treatment group at least six wells should be evaluated to obtain representative and reproducible results. To avoid any systematic error by uneven evaporation of the medium in the multiwell plates, the wells with various treatment groups should be randomly distributed on the plate, with an even number of each group on each plate. At the end of the incubation period the medium is collected, centrifuged to remove cellular material, and stored frozen for radioimmunoassay at -20°C . After the medium has been removed, cell viability is assessed and cells are counted by one of the previously described methods.

Cortisol is the major steroid secreted by both human and bovine adrenocortical cells in primary culture (5,27). We therefore assay cortisol secretion into the medium by radioimmunoassay as a measure of the steroidogenic response of adrenocortical cells to various stimuli. As a positive control, ACTH is included with each incubation experiment. Figure 6 shows the results of a time course and dose-response experiment with ACTH.

ACTH is the main inducer of adrenocortical steroidogenesis via activation of cAMP-dependent protein kinase. Because the increase of cAMP in the medium reflects the intracellular action of adenylate cyclase due to ACTH stimulation (29), cAMP can be measured by specific RIA in the medium as an indicator for ACTH receptor-mediated stimulation of adrenocortical steroidogenesis ($[^{125}\text{I}]\text{cAMP}$ assay, Amersham, Braunschweig, Germany). Besides ACTH, a variety of growth factors, cytokines, and hormones have been found to play a role in the regulation of adrenocortical steroidogenesis (for review see Ref. 3), either through synergistic action with ACTH (e.g., IGF I) or through ACTH/cAMP-independent pathways (e.g., interleukin-6). Therefore, to assess an inhibitory or synergistic effect of an unknown substance on adrenocortical steroidogenesis, each substance should be tested in the presence and absence of ACTH. Figure 7 depicts the influence of various growth factors on cortisol and cAMP secretion after an incubation time of 48 hr.

Induction Medium

Although adrenocortical cells grow best in serum-containing medium, all the following experiments are performed under serum-free defined conditions. As a serum-free induction medium we use M-199 substituted with L-glutamine (290 ng/ml), gentamicin (52 $\mu\text{g}/\text{ml}$), and amphotericin B (0.5 $\mu\text{g}/\text{ml}$). The absence of any additives except for antibiotics in the induction medium excludes an interaction of the tested substance with unknown serum factors, reduces the risk of pseudosubstrate effects, in-

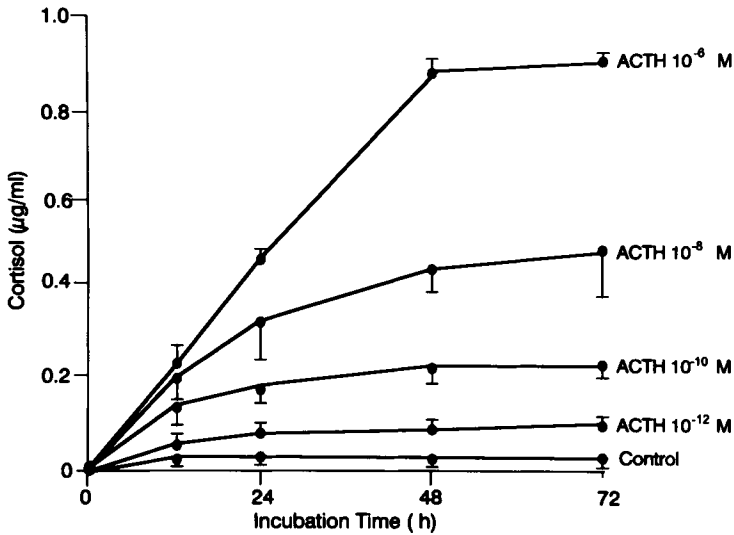


FIGURE 6. Effect of ACTH on cortisol secretion from bovine adrenocortical cells in monolayer culture. Bovine adrenocortical cells were grown to confluence in serum-containing growth medium. After 4 days, medium was exchanged to serum-free medium in the presence or absence of ACTH at the indicated concentrations. At each time point, medium was aspirated and assayed for cortisol by RIA. Each point represents the mean \pm SEM of six independent wells. ACTH stimulates cortisol secretion from adrenocortical cells in a dose- and time-dependent way. The stimulatory effect is significant already after 3 hr (data not shown) and reaches its maximum after 48 hr. Although physiological concentrations of ACTH already show a significant effect, the maximum 35-fold stimulation of basal cortisol secretion is reached by 10^{-6} M of ACTH.

creases the sensitivity for detecting specific actions of the examined agents, and facilitates interpretation of the data. Pseudosubstrate effects arise when high concentrations of steroids accumulate in the culture environment and interact with steroidogenic enzymes. Antioxidant nutrients [ascorbic acid ($100 \mu M$), α -tocopherol ($1 \mu M$), and selenium (50 nM)] have been found to reduce pseudosubstrate effects and therefore are added to the induction medium by some groups (12). LDL has been reported to be the principal source of cholesterol used for steroid biosynthesis by cultured bovine adrenocortical cells (30). However, the addition of LDL may increase pseudosubstrate effects, and primary adrenocortical cells grown under serum-free conditions are capable of a substantial steroidogenesis using endogenous sources of cholesterol. We therefore do not routinely add LDL to the medium for induction experiments. If appropriate, BSA at low concentra-

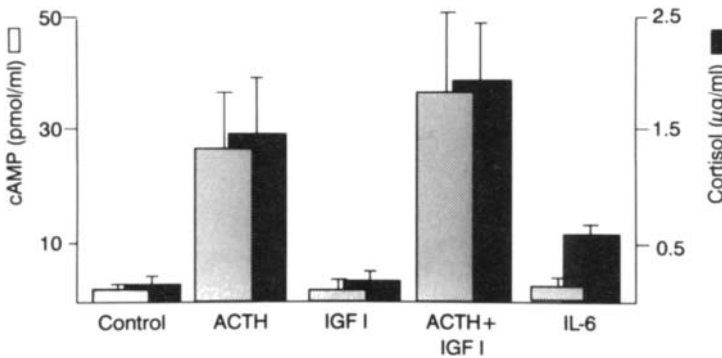


FIGURE 7. Effect of growth factors on cortisol and cAMP secretion from bovine adrenocortical cells in monolayer culture. Bovine adrenocortical cells were grown to confluence in serum-containing growth medium. After 4 days, medium was exchanged to serum-free medium in the presence of ACTH (10^{-8} M), IGF I (100 ng/ml), or IL-6 (100 ng/ml). After 36 hr, medium was aspirated and assayed for cortisol and cAMP by RIA. Each point represents the mean \pm SEM of six independent wells. Although IGF I alone does not show any significant effect, a synergistic effect on cAMP and cortisol secretion can be observed in combination with ACTH. In contrast to ACTH, IL-6 stimulates cortisol secretion without affecting the cAMP accumulation in the medium (34).

tions (500 μ g/ml) can be added to the medium, but one should keep in mind that BSA by itself has a slight mitogenic effect in bovine adrenocortical cells (10).

Cortisol Radioimmunoassay

In our laboratory, cortisol is measured in the supernatant by a specific radioimmunoassay with double-antibody precipitation, which accelerates the formation of precipitable complexes. The specific cortisol antiserum was a kind gift from O. A. Müller of Munich and is highly specific for cortisol (31). For the assay the following reagents are required: [125 I]cortisol as tracer (Sorin Biomedica AG, Düsseldorf, Germany), citrate buffer (0.1 M Na-citrate adjusted to pH 4.3), polyethyleneglycol (6% PEG solution in PBS) as second antibody anti-rabbit-IgG (Paesel, Cat. No. 14-102-00016, Frankfurt, Germany), and rabbit-y-globuline (7 μ g/ml, Serva, Cat. No. 22540, Heidelberg, Germany). An antibody mixture (50 ml) that is sufficient for 500 test tubes is prepared, containing 45.6 ml 0.9% NaCl solution, 2.4 ml of cortisol antiserum (1:100), 1.0 ml of the second antibody (anti-rabbit-IgG 1:25), and 0.5 ml of rabbit-y-globuline (7 μ g/ml).

For the standard curve a dilution series of standard cortisol concentrations in citrate buffer (0.78–1000 ng cortisol/ml) is prepared. In each test tube the following solutions are combined: 10 μl of sample (usually pure supernatant medium, which can be diluted if appropriate), pure medium (B0) or 10 μl of the standard curve, 100 μl of citrate buffer, 100 μl of antibody mixture (cortisol antibody and second antibody), and 100 μl of cortisol tracer (8000 cpm) in citrate buffer. The test tube for unspecific binding (N) contains no cortisol and no cortisol antiserum. After an overnight incubation at 4°C, the free hormone is separated from the bound hormone by addition of polyethyleneglycol (1.5 ml 6% PEG/tube) and centrifugation at 1500g for 20 min. The supernatant, containing the unbound hormone and tracer, is removed by soft vacuum aspiration. Subsequently, the pellet is washed with 1 ml distilled water per tube and recentrifuged at 1500g for 20 min. After aspiration of the supernatant the bound fraction of labeled cortisol is counted in a γ -counter. The standard curve demonstrates an ED₂₀ of 500 ng/ml and an ED₈₀ of 5 ng/ml. All samples are diluted to fall on the linear part of the curve between these two values, and are measured in duplicate. The intra- and interassay coefficients of variation of this assay were less than 10%. The cortisol antiserum donated by O. A. Müller cross-reacted with 11-deoxycortisol, the precursor of cortisol, to an extent of 25%, and with corticosterone 2.5%. The cross-reactivity with other naturally occurring steroids, including pregnenolone, deoxycorticosterone, estradiol, progesterone, DHEA, androstenedione, and testosterone, was less than 1%.

Alternatively, the steroidogenic response of adrenocortical cells can be assessed by the addition of labeled precursors (e.g., [³H]pregnenolone or [³H]progesterone) to the cells. At the end of the incubation period, steroids are extracted and separated by thin-layer and gas chromatography, and the synthesized radioactive metabolites are quantified by scintillation counting (27,32,33). This method allows one to study the biosynthesis of a variety of adrenal steroids. Furthermore, the action of stimulating or inhibiting substances can be assessed at different levels of the steroidogenic pathway. Figure 8 shows the inhibiting influence of the imidazole drugs ketoconazole and etomidate on the steroid production of human adrenocortical tissue in short-term incubation.

CONCLUSIONS

Bovine and human adult adrenocortical cells *in vitro* are shown to be responsive to the antimitogenic and steroidogenic effect of ACTH. In this cell system the action of various substances on proliferation and cell-differentiated function can be assessed easily by various methods. We there-

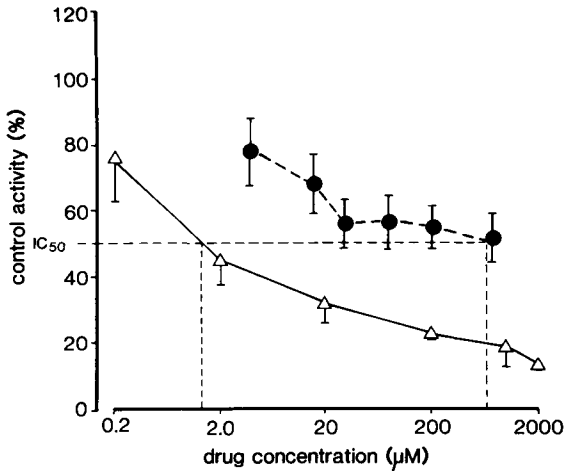


FIGURE 8. Effect of increasing concentrations of etomidate (●) and ketoconazole (Δ) on the formation of [^3H]androstenedione after incubation of human adrenal tissue with [^3H]17 α -hydroxyprogesterone, reflecting the effect of the drugs on C17,20-desmolase activity. 100% control represents the activity of [^3H]androstenedione production by human adrenal tissue in the absence of imidazole drugs. Values are means \pm SEM of at least three independent incubation experiments. These results indicate that both imidazole drugs block the conversion of 17 α -hydroxyprogesterone to androstenedione by the C17,20-desmolase. However, ketoconazole seems to be much more potent than etomidate, explaining the strong inhibitory effect of ketoconazole on human androgen biosynthesis *in vivo* (33).

fore believe that primary cultures of bovine or human fasciculata cells offer a convenient and sensitive *in vitro* system for testing the effect of toxic substances on specific endocrine cell function under a variety of well-defined conditions.

ACKNOWLEDGMENTS

We wish to express our appreciation to all individuals who have helped us to develop the methods described here: Prof. Dr. D. Engelhardt, Barbara Adelman, Thomas Beikler, Pia Simmler, and Christian Fottner.

REFERENCES

1. I. Vilgrain, C. Cochet, and E. M. Chambaz, *J. Biol. Chem.* **259**, 3403–3406 (1984).
2. V. Papadopoulos, A. Shane Brown, and Peter F. Hall, *Mol. Cell. Endocrinol.* **74**, 109–123 (1990).

3. A. Penhoat, W. E. Rainey, I. Viard, and J. M. Saez, *Horm. Res.* **42**, 39–43 (1994).
4. A. Penhoat, C. Jaillard, A. Crozat, and J. M. Saez, *Eur. J. Biochem.* **172**, 247–254 (1988).
5. C. G. Goodyer, J. S. Torday, B. T. Smith, and C. J. P. Girond, *Acta Endocrinol.* **83**, 373–385 (1976).
6. J. F. Crivello, P. J. Hornsby, and G. N. Gill, *Endocrinology (Baltimore)* **111**, 469–479 (1982).
7. A. McNicol, In “The Adrenal Gland” (V. H. T. James, ed.), 2nd Ed., p. 1–42. Raven, New York, 1992.
8. S. J. Quinn and G. H. Williams, In “The Adrenal Gland” (V. H. T. James, ed.), 2nd Ed., pp. 159–189. Raven, New York, 1992.
9. R. E. Duerst and C. N. Frantz, *J. Immunol. Methods* **82**, 39–46 (1985).
10. M. H. Simonian, M. L. White, and G. N. Gill, *Endocrinology (Baltimore)* **111**, 919–927 (1982).
11. P. J. Hornsby and G. N. Gill, *Endocrinology (Baltimore)* **102**, 926–927 (1978).
12. P. J. Hornsby and J. M. McAllister, In “Methods in Enzymology” (M. R. Waterman and E. F. Johnson, eds.), Vol. 206, pp. 371–380. Academic Press, San Diego, 1991.
13. P. J. Hornsby, *J. Biol. Chem.* **255**, 4020–4027 (1980).
14. R. Quali, M. C. LeBrethon, and J. M. Saez, *Endocrinology (Baltimore)* **133**, 2766–2772 (1993).
15. H. D. Mason, B. R. Carr, and W. E. Rainey, *Endocr. Res.* **12**, 447–467 (1986).
16. S. Mesiano, and R. B. Jaffe, *J. Clin. Endocrinol. Metab.* **77**, 754–758 (1993).
17. J. S. D. Winter, In “The Adrenal Gland” (V. H. T. James, ed.), 2nd Ed., pp. 87–104. Raven, New York, 1992.
18. M. T. Pham-Huu-Trung, J. M. Vilette, A. Bogyo, J. M. Duclos, J. Fiet, and M. Binoux, *J. Steroid Biochem. Mol. Biol.* **39**, 903–909 (1991).
19. V. Ilvesmäki, W. F. Blum, and R. Voutilainen, *Mol. Cell. Endocrinol.* **97**, 71–79 (1993).
20. M. H. Simonian, P. J. Hornsby, C. R. Ill., M. J. O’Hare and G. N. Gill, *Endocrinology (Baltimore)* **105**, 99–108 (1979).
21. F. E. Estivariz, P. J. Lowry, and S. Jackson, In “The Adrenal Gland” (V. H. T. James, ed.), 2nd Ed., pp. 43–70. Raven, New York, 1992.
22. M. H. Simonian and G. N. Gill, *Endocrinology (Baltimore)* **104**, 588–595 (1979).
23. R. I. Freshney, “Culture of Animal Cells,” pp. 237–238. Alan R. Liss, New York, 1987.
24. R. L. P. Adams, In “Laboratory Techniques in Biochemistry and Molecular Biology” (R. H. Burdon and P. H. van Knippenberg, eds.), 2nd Ed., Vol. 8, pp. 239–249. Elsevier, Amsterdam, New York, and Oxford, 1990.
25. S. A. Naseerudin and P. J. Hornsby, *Endocrinology (Baltimore)* **127**, 1673–1681 (1990).
26. M. M. Weber, W. Kiess, T. Beikler, P. Simmler, M. Reichel, B. Adelman, U. Kessler, and D. Engelhardt, *Eur. J. Endocrinol.* **130**, 265–270 (1994).
27. D. Engelhardt, M. M. Weber, T. Miksch, F. Abedinpur, and C. Jaspers, *Clin. Endocrinol.* **35**, 163–168 (1991).
28. M. Serón-Ferré, C. C. Lawrence, P. K. Siiteri, and R. B. Jaffe, *J. Clin. Endocrinol. Metab.* **47**, 603–609 (1978).
29. B. P. Schimmer and P. Schulz, *Endocr. Res.* **11**, 199–209 (1985).
30. M. S. Brown, P. T. Kovanen, and J. L. Goldstein, *Recent Prog. Horm. Res.* **35**, 215–257 (1979).
31. G. K. Stalla, G. Giesemann, O. A. Müller, W. G. Wood, and P. C. Scriba, *J. Clin. Chem. Clin. Biochem.* **19**, 427–434 (1981).
32. M. M. Weber, A. Will, B. Adelman, and D. Engelhardt, *J. Steroid. Biochem. Mol. Biol.* **38**, 213–218 (1991).
33. M. M. Weber, J. Lang, F. Abedinpur, K. Zeilberger, B. Adelman, and D. Engelhardt, *Clin. Invest.* **71**, 933–938 (1993).
34. M. M. Weber, P. Simmler, C. Fottner, and D. Engelhardt, *Endocrinology (Baltimore)* **136**, 3714–3720 (1995).

18

Assays for Vasopressin

Arnold M. Moses

Carol Jones

Department of Medicine

State University of New York

Syracuse, New York 13210

BACKGROUND

Until the late 1960s, the assessment of arginine vasopressin (antidiuretic hormone; AVP) concentration or amount in humans was determined by use of indirect methods based on the effects of the hormone on water excretion using parameters such as urine volume, concentration, and free water clearance (1–3). Direct determination of vasopressin activity could be performed with difficulty by bioassay of extracts of tissue, plasma, or urine, with the most sensitive method based on the antidiuretic effect of the hormone injected intravenously into the hydrated alcohol-anesthetized rat (4,5). A less sensitive but less difficult method for determining tissue content of vasopressin utilized the pressor action of the hormone in the anesthetized rat (6,7). Both assays were time-consuming, technically demanding, and lacked specificity, and only a relatively few samples could be assayed in a test animal. Another problem was that large amounts of blood had to be obtained and concentrated. These assays have been abandoned almost completely. Nonetheless, studies performed by bioassay helped to validate the radioimmunoassays (RIAs) for AVP, and still provide much of the basic information for our understanding of neurohypophysial function.

Application of immunoassay techniques to the assay of vasopressin had an inherent difficulty. The small size of the peptide hormone (molecular

weight 1084) resulted in its poor antigenicity. This was true for both the lysine vasopressin (LVP) extracted from the pig and AVP from humans and mammals other than the swine family. In 1966, Roth *et al.* described an antibody to vasopressin in a patient with diabetes insipidus who had been treated with a mixture of pork and beef posterior pituitary powder (8). The same year, Utiger reported an RIA for vasopressin utilizing an antiserum obtained from immunization of rabbits with LVP covalently conjugated to bovine serum albumin (9). This assay was used to determine the amount of AVP in extracts of a tumor from a patient with the syndrome of inappropriate antidiuresis. Substantial amounts of AVP were found in the tumor, none in the uninvolved lung, and much greater amounts in the normal pituitary gland. Two years later, Vorherr *et al.* used an antiserum prepared the same way to perform RIAs and bioassays to quantitate the amount of AVP in extracts of malignant tumors of 10 patients with the syndrome of inappropriate antidiuresis (10).

In 1969, our laboratory reported an RIA for AVP also using an antibody obtained from rabbits injected with LVP conjugated with bovine serum albumin (7). Simultaneous immunoassays and pressor bioassays for AVP were performed on posterior pituitaries of normally hydrated rats and rats subjected to varying periods of dehydration. There was a high degree of correlation between the bioassays and RIAs and each changed appropriately with dehydration (7) (Figure 1). These studies demonstrated that an RIA for AVP could be a reliable and specific method for measuring the relatively large amounts of AVP present in pituitary glands, and demonstrated appropriate changes under physiological conditions known to affect AVP content. The following year the same assay was utilized to demonstrate changes in pituitary AVP in normal rats and rats heterozygous for diabetes insipidus during periods of water deprivation and subsequent periods of rehydration (11). These experiments also demonstrated a good correlation between biologically and immunologically measurable AVP.

Problems arose in applying the RIA for AVP to plasma. These difficulties were reviewed by Robertson *et al.* (12). In an effort to bypass these problems and take advantage of the relatively large amount of AVP in urine, and the fact that urinary hormone levels reflect an integrated function of hormone secretion over time, methods were developed for the assay of AVP in extracted urine (13–15) and unextracted urine (16). Immunoassay and antidiuretic bioassays performed on aliquots of the same urine were in excellent agreement. Urinary AVP excretion accurately reflected the release of AVP from the neurohypophysis of the rat in response to physiological stimuli known to influence AVP release. We also demonstrated that the Brattleboro rat heterozygous for diabetes insipidus had a defect in AVP release as well as synthesis (13). The RIA for AVP was applied to urine

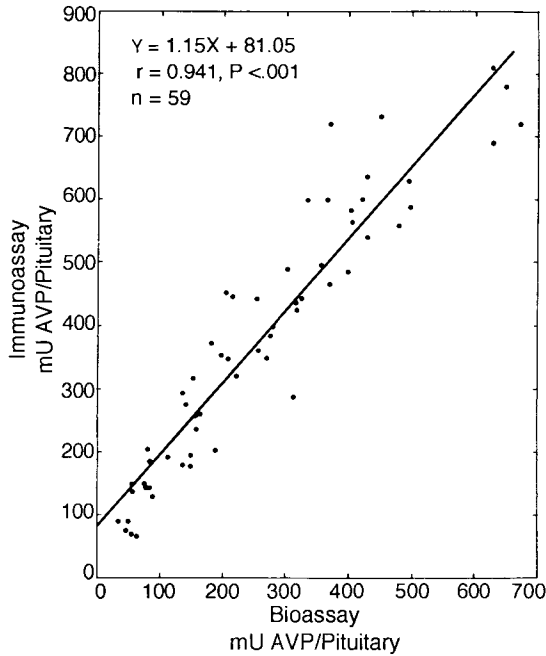


FIGURE 1. Relationship between pituitary AVP content of rats either hydrated or subjected to varying periods of water deprivation using the pressor bioassay and RIA for AVP (7). Procedures such as these were necessary to validate the biological significance of the RIA for AVP. To convert mU to ng, multiply by 2.5.

from normal subjects and revealed that physiological changes such as water loading and dehydration caused appropriate changes in AVP (14). The same year our RIA for AVP was used to assay urine from patients with polyuric disorders and inappropriate antidiuresis (15). The assay revealed appropriate abnormalities in AVP excretion during hydration and dehydration, and elevated AVP excretion in relation to plasma osmolality in patients with the syndrome of inappropriate antidiuresis. These studies helped to validate the value of urinary AVP measurements in determining physiological and pathophysiological abnormalities in humans. The following year the RIA was used to assay AVP in human urine to clarify the mechanisms by which chlorpropamide and clofibrate affected their antidiuretic actions (17,18).

The advantages of measuring urinary AVP (relative ease of assay and an integrated excretion rate) still make the measurement of urinary AVP attractive when not attempting to determine rapid changes in the release

of AVP and when renal function is normal. Urinary clearance and excretion of AVP is increased by plasma volume expansion and decreased by plasma volume contraction (19). However, this generally does not detract from the value of measuring urinary AVP as a means of assessing neurohypophysial function.

Robertson *et al.* were the first to report on the measurement of AVP concentrations in plasma that appeared to accurately reflect physiological stimuli (12). They described the presence of large quantities of cross-reactive materials in plasma that were higher in molecular weight than AVP. These cross-reactive substances did not fluctuate either in response to physiological stimuli known to alter AVP secretion or in disease states with AVP abnormalities. In order to assay AVP, they first filtered the plasma through G-25 Sephadex, which separated the hormonally active and inactive peptide peaks. Shortly thereafter, Beardwell used floracil to extract AVP from human plasma (20). The RIA from the eluate gave results that correlated with plasma osmolality in dehydrated subjects, the antidiuretic response to nicotine, and the expected marked elevation of plasma AVP in patients with inappropriate antidiuresis. Other studies at about the same time reported on the use of acetone, glass beads, Fuller's earth, and bentonite to eliminate nonspecific interference with the RIA for plasma AVP (21). Typical data were reported by Skowsky and Fisher, who found resting plasma AVP levels of 3.1 pg/ml in normal hydrated subjects, which increased to 22 pg/ml with dehydration (22). The status of the RIA for plasma AVP as of 1973 was summarized by Robinson and Frantz (21).

The assessment of current RIA techniques for measurement of AVP, and some of the physiological and pathophysiological information that has been revealed in the past 20 years, will be considered in the sections Methodology and Application of RIA for Vasopressin.

METHODOLOGY

Immunoradiometric assays (IRMA) using two different monoclonal antibodies have been developed for the assay of parathyroid hormone (PTH), adrenocorticotrophic hormone (ACTH), thyroid stimulating hormone (TSH), and other peptide hormones. These assays have provided remarkable sensitivity and specificity for the measurement of hormone concentrations and amounts. An IRMA has been described for AVP (23). However, that assay was considerably less sensitive than RIAs, probably because the antibody to the ring structure of AVP had a low affinity constant for radioactive antibody. Improvements in this technique have not yet been described. Others have attempted to develop an assay for AVP by using

indirect biotinylation and noncompetitive enzyme immunoassay (24). This method has not yet been applied to the measurement of AVP in plasma or in urine because it is time-consuming and less sensitive than the RIA.

Currently, RIA is the method used for the assay of AVP in scientific and medical work. A discussion of the various aspects of the RIA for AVP follows.

Handling of Specimens

Urine

Acidify urine to a pH of 3 to 4 with glacial acetic acid as soon as possible to prevent a decrease of AVP immunoreactivity (25). Urine stored at room temperature for 24 hr, without acidification, shows no loss of AVP activity, but after 3 weeks shows a 40% decrease in activity. If the urine is immediately acidified and kept at room temperature, it is stable for 3 weeks (25). Urine, acidified and frozen at -20°C , is stable for 2 months (25). Studies in our laboratory show that AVP in urine immediately acidified and frozen at -20°C is stable for at least 6 months.

Plasma

In processing of blood for the assay of AVP, the choice of anticoagulant, usually heparin or EDTA, may depend on the extraction procedure. When heparinized plasma is used and extracted on octadecylsilica (C_{18}) cartridges, the cartridges may clog; therefore, we use Na_2EDTA . When other extraction procedures are used, either heparin or EDTA will serve the purpose. Blood of pregnant women contains high concentrations of cystine aminopeptidase, which can inactivate large quantities of AVP (26). If blood is collected with a syringe containing 0.1 ml of a phenanthroline (1,10-phenanthroline monohydrate) solution (60 mg/ml), the breakdown of AVP is inhibited.

Whole blood, left at 20°C for 3 hr, loses 40% of its immunoreactivity (27). Beardwell finds that there is a 25% loss after 4 hr at 20°C (20). These observations demonstrate the importance of cooling and separating samples quickly. We recommend that blood be put into chilled tubes and centrifuged within 30 min, and the plasma separated and frozen immediately. If plasma is thawed and extracted within 2 weeks and stored at -20°C , there is no breakdown of AVP immunoactivity for at least 6 months.

When processing blood samples for assay of AVP, there should be no platelets in the plasma to be assayed. If platelets are not excluded, up to 90% of the circulating AVP measured by RIA may be associated with

platelets (28,29). Routine methods of centrifugation (2500 rpm for 20 min) do not completely separate platelets from the plasma (28,29).

The range of AVP in plasma containing platelets is much greater than that of platelet-free plasma. We collected blood samples from ten normal subjects using EDTA as anticoagulant and centrifuged the blood at 4°C for 20 min at 2500 rpm. The plasma, approximately 3 ml, was carefully separated into three layers: top, middle, and bottom. Each layer was assayed for AVP. Our findings are similar to those of Sadler *et al.* (30), who find the bottom layer to contain almost twice the amount of AVP as the other two layers. We find no difference between the top and middle layers, but the bottom layer contains three times the amount of AVP as the other two layers. Preibisz *et al.* use heparin tubes and report that the bottom 1 ml of 6 ml of plasma contains about seven times more AVP than the top 4 ml (28). These findings show that differential centrifugation is the best method of processing blood for AVP. If differential centrifugation is not used, the bottom 1 ml of plasma should be discarded.

Tissue

Tissue to be assayed for AVP is generally homogenized with a dilute acid, usually HCl or acetic. The homogenates are centrifuged and the supernatant is assayed directly (31), or further purified by an extraction procedure. Octadecylsilica cartridges are used by many investigators (32,33).

Extraction Procedures

Accurate measurement of AVP is difficult because of small amounts of AVP that are often present, particularly in the plasma, and because of interfering substances in plasma and urine. Because of these factors, both urine and plasma must be extracted before performing the RIA (25,34). The main object is to effectively separate AVP from interfering substances and to have a high recovery of AVP. The different extraction procedures currently being used are shown in Table I. Many investigators have changed to C₁₈ cartridges. These cartridges separate the active AVP from the AVP-like factors in both urine and plasma and, therefore, do not show falsely high AVP values (34,35). Bodola and Benedict find that most other extraction procedures are accompanied by poor and variable recoveries and that C₁₈ cartridge extraction is a more selective method for isolating AVP (36). The C₁₈ cartridges also allow the extraction of large amounts of plasma, urine, or tissue extract, and thus concentrate the AVP to a level that can be accurately measured with the RIA. The extraction procedure with the C₁₈ cartridges is simple and, with the use of a multisample manifold (Waters

Associates, Milford, MA), many samples can be processed rapidly. The C₁₈ extraction provides consistent, reproducible results and excellent recoveries (see Table I). The C₁₈ cartridges can be reused up to four times when extracting urine, but only once for plasma (37).

Several recent studies describe AVP methods for unextracted urine (38,39) and for unextracted plasma (40), using highly specific and sensitive antibodies.

Radioimmunoassay

Antibodies

There are three basic methods for developing antibodies to AVP. AVP may be coupled to (a) albumin by a carbodiimide reaction (20), (b) albumin with glutaraldehyde (16), and (c) thyroglobulin (41).

The coupled AVP is combined with Freund's complete adjuvant and injected subcutaneously into rabbits or guinea pigs at biweekly or monthly intervals. Blood is drawn for antibody testing after three or more injections. The antibodies are tested for titer, sensitivity, and cross-reaction to possible interfering substances, such as desmopressin, lysine vasopressin, oxytocin, arginine-vasotocin (AVT), angiotensin I and II, and bradykinin (42). Baylis suggests cross-reaction studies on luteinizing hormone releasing hormone (LHRH), thyrotropin releasing hormone (TRH), luteinizing hormone (LH), follicle stimulating hormone (FSH), human growth hormone (HGH), prolactin, and human chorionic gonadotropin (HCG) (27). Individual investigators may find it necessary to test other specificities to suit their requirements.

An antibody must have an extremely high equilibrium constant for a sensitive AVP immunoassay since AVP concentrations are usually low. It is difficult to produce sensitive antibodies for AVP that in addition have little cross-reactivity with related compounds. For instance, the structure of AVP differs from oxytocin in only two amino acids, and both are present in plasma at similar low concentrations. Also, the antibody should not measure the biologically inactive metabolites of AVP that are frequently present in the urine.

The amount of antibody used in the assay influences the sensitivity. Too much antibody decreases the sensitivity of the assay, and too little decreases the precision. The most desirable antibody concentration is where the zero binding falls between 35 and 40% of the total counts.

The measurement of AVP has become simpler in the last decade by the availability of commercial antibodies that are highly specific, well characterized, and reasonably priced. These antibodies can be purchased from many

TABLE I. Current Utilized Methods for RIA of AVP

Author, year	Extraction		Antiserum to AVP (combined with, or obtained from)	$[^{125}\text{I}]\text{AVP}$ (method or source) ^a	AVP standard	Separation	Sensitivity
	Method	% recovery					
Ervin (1991) (82)	Bentonite (83)	65	Conjugated to bovine thyroglobulin (41)	Iodinated with iodogen (83)	Bachem Chemicals (82)	Not stated	0.2 pg/ml (84)
McLeod (1993) (85)	Acetone- ether (86)	100	Coupled to bovine serum albumin (26)	Chloramine T without metabisulfite (43)	Ferring Arzneimittel (26)	PEG (86)	0.25 pg/tube (86)
Crofton (1990) (87)	C ₁₈ cartridge (37)	85	Coupled to thyroglobulin (88)	Amersham Corp., personal communication	USP Posterior Pituitary Ref. Std. (37)	BSA-coated charcoal (37)	Not stated
Stern (1986) (89)	C ₁₈ cartridge (34)	85	Conjugated to rabbit serum albumin (90)	Lactoperoxide method (44)	Pierce Chemical Co. (34)	PEG (34)	<0.4 pg/tube (34)
Verbalis (1986) (91)	Acetone- ether (92)	73	Coupled to egg albumin (93)	Chloramine T without metabisulfite (94)	Bachem Chemicals (92)	PEG (92)	0.5 pg/ml (91)
Robinson (1990) (95)	Acetone- ether (86)	96	Coupled to egg albumin (93)	Chloramine T without metabisulfite (92)	Not stated	PEG (93)	0.5 pg/ml (93)
Faull (1993) (96)	Florisil (54)	72-86	Coupled to bovine thyroglobulin (54)	Modified chloramine T (91)	Vasopressin International Std. (54)	Second antibody (54)	0.6 pg/ml (96)

Moses (1993) (49)	C ₁₈ cartridges (48)	89	Arnel Products (48)	Dupont NEN Research Products (48)	Sigma Chemical Co. (48)	BSA-coated charcoal (48)	0.5 pg/ml (48)
Ysewijn-Van Brussel (1985) (97)	C ₁₈ cartridges (97)	87	Coupled to bovine thyroglobulin (97)	Modified Chloramine T (97)	Not stated	Second antibody (97)	0.3 pg/ml (97)
Carman (1988) (98)	C ₁₈ cartridges (98)	81	Calbiochem-Behring (98)	Dupont NEN Research Products (98)	Calbiochem- Behring (98)	PEG (98)	0.5 pg/tube (98)
Bodola (1988) (36)	C ₁₈ cartridges (36)	89	Calbiochem-Behring (36)	Amersham Corp. (38)	U.S. Pharmacopeia (36)	Second antibody (36)	0.13 pg/ tube (36)
Sadler (1986) (99)	C ₁₈ cartridges (30)	89	Coupled to bovine thyroglobulin (30)	Modified Chloramine T (99)	Ferring Arzneimittel (30)	Second antibody (30)	0.2 pg/ml (30)
Garland (1985) (55)	C ₁₈ cartridges (34)	85	Calbiochem-Behring (55)	Chloramine T (55)	Calbiochem- Behring (55)	PEG (55)	Not stated
Camps (1983) (100)	Cold 98% ethanol (100)	65	Calbiochem-Behring (100)	Modified Chloramine T (100)	Calbiochem- Behring (100)	Dextran- coated charcoal (100)	0.31 pg/ tube (100)

^a [¹²⁵I]AVP—Both Amersham Corporation and Dupont NEN Research Products use the chloramine T method. All authors used a phosphate buffer except Camps (barbital), McLeod (veronal), Faull (Tris-HCl), and Sadler (Tris-HCl).

companies, including Mitsubishi Petrochemical Company Ltd., Arnel Products (New York, NY), Peninsula Laboratories Inc. (Belmont, CA), Calbiochem-Behring (San Diego, CA), Amersham Corporation (Arlington Heights, IL), Ferring Pharmaceuticals (New York, NY), and Incstar (Stillwater, MN).

Radioactive AVP

In earlier years, each laboratory iodinated its own AVP. The two most commonly used methods were the chloramine T without *meta*-bisulfite (43) and the lactoperoxidase method (44). Preparation and purification of [¹²⁵I]AVP requires HPLC (high-pressure liquid chromatography) equipment and specialized hoods to protect laboratory workers from exposure to ¹²⁵I. Fortunately, [¹²⁵I]AVP is now available from companies such as Dupont NEN Research Products (Boston, MA), Amersham Corporation, and Peninsula Laboratories Inc.

The amount of radioactivity used in an assay has a direct influence on the sensitivity of the assay. A lower amount of tracer increases the sensitivity. We suggest using only 3000 cts/min per assay tube and counting for 10 min. The long counting time is necessary to avoid variability owing to the small amount of tracer. The higher the specific activity of the tracer, the more sensitive the assay.

Standards

The early assays of AVP used standards prepared from extracts of bovine pituitary powder, the USP Reference Standard. The amount of AVP in the unknown was expressed in units of biological activity. Synthetic AVP standards are now available. Conversion from units to weight can be accomplished by recognizing that there are 400 rat pressor units of AVP per milligram. Therefore, microunits of AVP can be converted to picograms or milliunits converted to nanograms by multiplying by 2.5. Synthetic preparations contain varying amounts of impurities; however, most companies report the actual peptide content.

Because AVP is very stable at acidic pH, AVP standards should be stored in 0.2 mol/liter glacial acetic acid at a concentration of 1 mg/ml. AVP stored in this way at -25°C has no loss of immunoreactivity over a 7-year period (45). Synthetic AVP can be purchased from many companies, including Bachem Chemicals (Torrance, CA), Pierce Chemical Company (Rockford, IL), Calbiochem-Behring, Sigma Chemical Company (St Louis, MO), Ferring Arzneimittel (Wittland, Sweden), and United States Pharmacopia (Rockville, MD).

Buffering

The most commonly used buffer for AVP assays is sodium phosphate. Tris and barbiturate buffers are also used (Table I). The buffer must be concentrated enough to maintain the pH of the reaction mixture between 6.0 and 8.6, considering the variability between the various extraction procedures. However, increasing the molarity of the buffer can decrease both the antigen-antibody binding and the sensitivity of the assay. NaCl is usually added to the buffer to make the molarity of the buffer similar to that of plasma. Bovine serum albumin (BSA) is commonly used in the buffer to stabilize the reagents and prevent losses due to adsorption. It is important to use a high grade of BSA. Some investigators add enzyme inhibitors such as EDTA, PMSF (phenylmethylsulfonylfluoride), or phenanthroline. Others add bacteriostatic agents, such as neomycin, thiomersal, or sodium azide.

Incubation

The AVP assays are incubated at 4°C for 2–7 days, because small concentrations of reagents require this time to reach equilibrium. Increasing the temperature reduces the time required to reach equilibrium; however, this also increases both enzymatic destruction of the antigen and bacterial growth in the assay.

Disequilibrium incubation, or later addition of tracer, increases the sensitivity of the assay. The antibody is added to the unlabeled antigen and allowed to reach partial equilibrium before the tracer is added. After tracer is added, the bound and free antigens are separated before the tracer-antibody reaction reaches equilibrium. Crofton *et al.* (37) have increased the sensitivity of the AVP assays approximately four times by incubating the antibody and cold antigen for 24 hr at 4°C before the addition of [¹²⁵I]AVP, and further incubation of 24 hr at 4°C before the separation of free and bound antigens (37).

Separation Techniques

The three basic techniques for separating bound from free [¹²⁵I]AVP are adsorption of the free antigen, precipitation of the antigen-antibody complex, and solid-phase separation. Charcoal is most commonly used to adsorb the free antigen. Charcoal is inexpensive, but demands close attention to molarity, temperature (4°C), and protein concentration (see the section Currently Utilized Methods). Careful timing is important to prevent disassociation of [¹²⁵I]AVP from the antibody.

Polyethylene glycol (PEG) and a second antibody are the most commonly used techniques for precipitation of the antigen–antibody complex. The PEG method is inexpensive, fast, and highly reproducible, and batch-to-batch variation is small. The second-antibody method is more expensive, requires an additional incubation of 3 to 24 hr, and often produces a high degree of batch-to-batch variation.

With the solid-phase separation method, the antibody is coated directly to the inner walls of the test tube. This method eliminates a time-consuming step that can introduce a major error. The solid-phase method has been used for urine (46) and plasma (40,47). It is highly efficient, having low-assay blanks and complete separation of the bound fraction. However, immunoreactivity of the antibody is decreased through coating, and this greatly decreases the sensitivity of the method. Therefore, this method cannot be used unless the concentration of AVP in the sample is high and/or the antibody is very sensitive.

Techniques of Determining Amount of Unknown AVP Following Gamma-Counter Counting

Chapter 1 details the theory for calculating RIA assays. The most common methods for plotting AVP data are:

1. Ratio of bound activity to free radioactivity (B/F).
2. Ratio of free activity to bound activity (F/B).
3. Ratio of bound activity to total activity (B/T).
4. Ratio of bound activity to bound activity in the zero standard (B/B_0).

One of these variables is plotted on the y axis, and the concentration of AVP on the x axis is plotted.

The traditional standard curves were drawn manually; however, currently, they are more often constructed by computer programs. The same programs calculate the values of the unknown.

Normal Values in Humans

Under conditions of hydration, AVP in blood and urine usually becomes unmeasurable at plasma osmolalities in the range of 280–286 mmol/kg (48,49) (Figures 2 and 3). Under basal conditions, plasma AVP concentrations are approximately 1.5–2.5 pg/ml (50–55).

Johnson *et al.* studied 45 normal younger adults (35 ± 9 years) and 41 healthy elderly subjects (78 ± 3 years) (56). The younger adults had AVP values of 2.1 ± 0.2 pg/ml. In contrast, the elderly adults had significantly

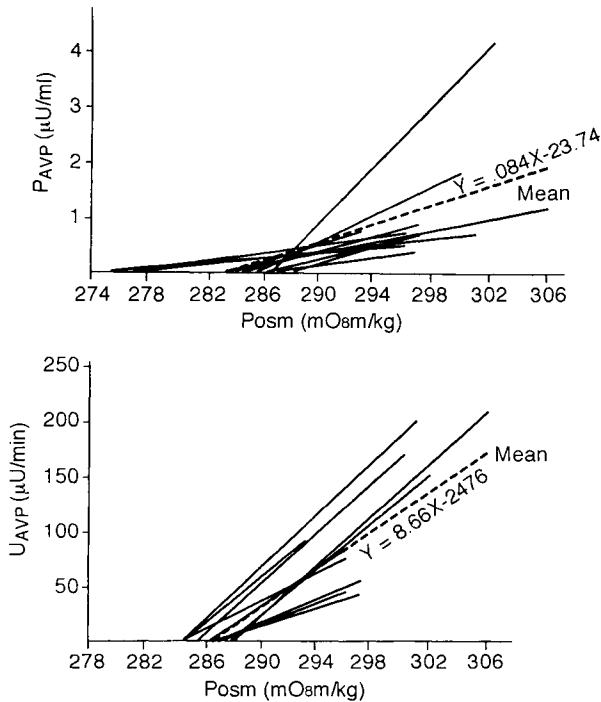


FIGURE 2. Variation between individual hydrated normal subjects in osmotic thresholds for AVP release (abscissal intercepts) and rates of rise of plasma (top) and urine AVP (bottom) when infused with hypertonic saline (48). To convert μU of AVP to pg, multiply by 2.5.

higher concentrations (4.7 ± 0.7 pg/ml). Other researchers do not find higher AVP values in older subjects (57–59).

When the hydrated adult is infused with hypertonic saline, plasma and urine AVP increase as demonstrated in Figures 2 and 3.

In our laboratory, 10 normal subjects, dehydrated for 12 hr, had urinary AVP of 2.48 ± 1.78 ng/hr. These values reflect improved techniques for the RIA of AVP and are lower than corresponding values reported 15–20 years ago (42).

Currently Utilized Methods in the Authors' Laboratory

Introduction

The following materials and method for performing RIA of plasma and urine AVP were developed at the laboratory in the Clinical Research Unit,

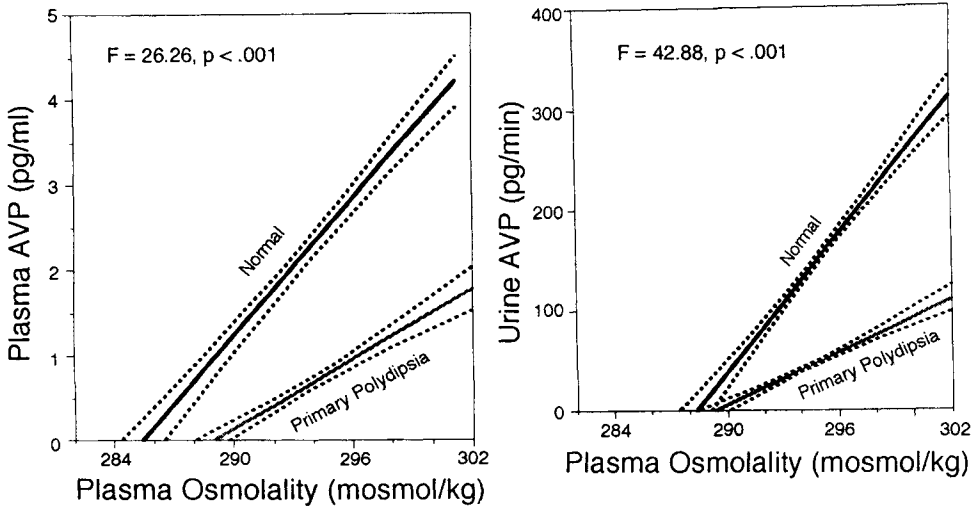


FIGURE 3. Mean and 95% confidence intervals of the linear regression lines relating plasma osmolality to plasma (left) and urine AVP (right) in normal subjects and patients with primary polydipsia hydrated and infused with hypertonic saline. The osmotic threshold for AVP release is the plasma osmolality at the abscissal intercepts. The mean osmotic threshold is higher and rate of rise of AVP is lower in patients with primary polydipsia (49).

University Hospital, SUNY Health Science Center, Syracuse, New York. The extraction procedure, buffer, and separation techniques are similar to those of Crofton *et al.* (37). The assay uses commercially available reagents, antibodies, and isotope.

Materials

- 12 × 75-mm borosilicate culture tubes (Corning Incorporated, Corning, NY)
- AVP standard (Sigma Chemical Company)
- [¹²⁵I]AVP (Dupont NEN Research Products; specific activity of 2200 Ci/mol).
- Antibodies for urine (Ferring Pharmaceuticals)
- Antibodies for plasma (Arnel Products, New York, NY)
- Bovine serum albumin (RIA Grade Fraction V Powder; Sigma Chemical Company)
- C₁₈ cartridges (C₁₈ Sep-Pak; Waters Associates)
- Charcoal (Nocit "A" Neutral Pharmaceutical Grade Decolorizing Carbon; Amend Drug and Chemical Company, Irvington, NJ)

Buffers

- Stock solution I = 0.2 M Na₂HPO₄ (MW 141.96). Weigh 28.39 g Na₂PO₄ and dilute to 1 liter distilled H₂O.
- Stock solution II = 0.2 M Na₂HPO₄ · H₂O (MW 137.998). Weigh 27.599 g Na₂HPO₄ · H₂O and dilute to 1 liter distilled H₂O.
- Assay buffer = 0.1 M PO₄, 0.3% NaCl, 0.1% BSA, pH 7.6.

Perform the following:

1. Add 1800 ml of stock solution I and 225 ml stock solution II to 2025 ml distilled H₂O, and add 12.15 g NaCl.
2. Adjust pH to 7.6, if needed.
3. Add BSA to the buffer to make a final concentration of 0.1% on day assay will be performed.

[¹²⁵I]AVP

The [¹²⁵I]AVP is diluted, aliquoted, and frozen at -20°C according to the manufacturer's directions. It is reconstituted in assay buffer the day of the assay.

Antibody Dilution

Antibodies are stored at a concentration of 1:100 with assay buffer and reconstituted in assay buffer on the day of the assay as follows for a 100-tube assay:

- (a) For plasmas, dilute 0.05 ml of Arnel Products antibody (1/100 dilution) to 5 ml with assay buffer.
- (b) For urines, dilute 0.15 ml of Ferring Pharmaceuticals antibody (1/100 dilution) to 5 ml with assay buffer.

Standards

Synthetic AVP is reconstituted in 0.25% glacial acetic acid, aliquoted, and stored at a concentration of 1 mg/ml at -20°C. The AVP stock standard is diluted the day of the assay with assay buffer to yield the necessary concentrations for the standard curve (range is 0.5–100 pg/ml).

Charcoal

Four grams of charcoal are placed into a 50-ml centrifuge tube with 40 ml of assay buffer without BSA, mixed well, and centrifuged at 1000 rpm for

10 min. The supernatant is discarded and the charcoal is resuspended in 480 ml of assay buffer and 0.8 g of BSA.

Sample Collection

Blood is put into chilled EDTA tubes and centrifuged within 15 min at 2500g for 20 min at 4°C. The platelet-free plasma is stored in polypropylene tubes at -20°C.

Extraction Procedure

The AVP is extracted from plasma using C₁₈ cartridges by adsorption as follows:

1. Acidify 2 ml of plasma to a pH of 2 to 3 by adding 0.2 ml of 1 N HCl (0.1 ml HCl/1 ml plasma).
2. Centrifuge for 15 min at 2000g.
3. Prime the cartridges with 5 ml MeOH followed by 20 ml distilled water.
4. Using a manifold (from Waters Associates) extract eight samples at the same time.
5. Pass the acidified plasma through the cartridge for 2 to 3 min.
6. Wash the cartridge with 20 ml of 4% acetic acid.
7. Elute vasopressin from the cartridge with 4 ml of 90% methanol over a period of 3 to 5 min.
8. Evaporate eluates to dryness under a stream of air, and store at -20°C until assayed. Average recovery of vasopressin is 89%.

Urine samples are extracted as shown for plasma, except the urine has already been acidified. The amount of urine extracted varies from 1 to 10 ml depending on the concentration of expected AVP in the sample.

When extracting plasma samples, use the cartridges one time. When extracting urine or tissue samples, reuse C₁₈ cartridges up to four times by priming them with 5 ml 8 M urea followed by 20 ml H₂O and 5 ml MeOH.

Assay Conditions

For plasma, provide conditions as follows:

1. On Day 1 of the assay, reconstitute the dried plasma extract to 1.0 ml with assay buffer.
2. Add 0.4 ml of extract or standard to each tube in duplicate.
3. Add 0.05 ml of antibody, vortex the tubes, and incubate for 24 hr at 4°C.

4. On Day 2, add 0.05 ml of [¹²⁵I]AVP (3000 cts/min), vortex tubes, and incubate for an additional 24 hr.

For urine, provide conditions as follows:

1. On Day 1, reconstitute extracted urine to 1 ml with assay buffer. The amount of urine assayed varies from 0.1 to 0.4 ml depending on the expected concentration and amount of urine extracted.
2. Add assay buffer to all tubes to make the volume equal to 0.4 ml.
3. Add 0.4 ml of standard to the standard tubes.
4. Add 0.05 ml of antibody (Ferring Pharmaceuticals) and 0.05 ml [¹²⁵I]AVP to the assay tubes (3000 cts/min).
5. Incubate the assay for 48 hr at 4°C.

Separation of Free and Bound Antigen

Free and bound [¹²⁵I]AVP is separated by adding 1.0 ml of charcoal mixture as follows:

1. Keep both the charcoal mixture and the assay tubes on ice during this procedure.
2. Using no more than 100 tubes at one time, rapidly add charcoal, vortex, and after 5 minutes centrifuge at 2000g for 25 min in a cold centrifuge (timing is very important).
3. Aspirate the supernatant and count the pellet in a gamma counter for 10 min.

Calculations

We express binding as a percentage of the amount of tracer bound in the absence of AVP and plot it against the log of the AVP standard (B/B_0). We read sample values from the curve and then correct for amount of sample extracted and assayed.

APPLICATION OF RIA FOR VASOPRESSIN

The RIA for vasopressin has been used to investigate many problems, involving *in vivo* and *in vitro* techniques, and utilizing fluids, tissues, and cells from many animal species. The applications chosen for review largely reflect the personal experiences of the authors. To obtain a better idea of the vast range of studies that have been addressed by RIAs for vasopressin (AVP, LVP, desmopressin, arginine vasotocin, etc.), the reader is advised

to refer to a book such as "The Neurohypophysis: Window on Brain Function," published by the New York Academy of Sciences in 1993.

Normal Regulation of Arginine Vasopressin Secretion

The secretion of AVP is influenced by a number of stimuli. Under normal conditions, AVP release is primarily regulated by osmoreceptors in the anterior hypothalamus. Changes in concentration of plasma solutes to which the cellular membrane is impermeable cause alterations in the volume of the osmoreceptor cells, which in turn alter electric activity of the neurons that control AVP release (and synthesis). The servomechanism between effective plasma osmolality and AVP release normally maintains plasma osmolality within a very narrow range. In humans, at plasma osmolalities below approximately 280 mmol/kg, AVP secretion is almost completely suppressed and plasma AVP concentrations are usually undetectable by current RIA techniques. The plasma osmolality that initiates antidiuresis during infusion of hypertonic saline into hydrated subjects is approximately 287 mmol/kg (2,3,48,49,60). This was called the osmotic threshold for vasopressin release (2,3,48,49,60). Above this threshold, plasma and urine AVP concentrations are directly related to plasma osmolality. The secretion of AVP is also regulated by changes in plasma volume and by activation of carotid and aortic baroreceptors. Many other factors, such as stress, pain, drugs, age, and temperature, can also regulate the release of AVP. The influence of these factors on the release of AVP has also been studied by the measurement of plasma and urine AVP by RIA.

The RIA for AVP has been critical in defining the properties of the osmoregulation of AVP release. Even though the osmotic threshold for AVP release was first determined by free water clearance changes, it was not until the RIA for AVP was available that AVP in plasma or urine could be correlated to plasma osmolality. The infusion of hypertonic saline confirmed the threshold concept of AVP release by relating plasma and urine AVP levels to plasma osmolality under the same conditions as were used for studies on free water clearance changes (48). The abscissal intercept of the line relating plasma osmolality to either plasma or urine AVP results in very similar values for the osmotic threshold for AVP release as that obtained by free water clearance changes (Figure 2). These studies demonstrated that individual subjects' relationship of AVP to plasma osmolality is quite precise, although there is substantial variability from person to person (Figure 3). This same general approach has been useful in investigating the solute specificity of the osmoregulatory system. Solutes of interest can be infused and related to the associated changes in AVP levels, osmolality, and specific solutes such as sodium. These studies show that the relation-

ship of plasma AVP to plasma osmolality is similar during the infusion of hypertonic mannitol and saline, even though mannitol depresses and saline increases plasma sodium concentrations. This demonstrates that the control mechanism behaves as an osmoreceptor and not as a sodium receptor (61). Similar studies also show that the osmoreceptor varies in sensitivity to different solutes. For example, the infusion of hypertonic urea had only a weak stimulatory effect on plasma AVP. Eventually we understood that the ability of different plasma solutes to release AVP varies inversely to the ability of the solutes to penetrate into the osmoreceptor cells. Determination of the relationship between plasma osmolality and AVP has been and is utilized to detect nonosmotic influences on vasopressin release. Previous to performing the RIA for AVP, hypovolemia and hypotension were known to stimulate secretion of AVP. However, these effects could not be defined reliably by measuring changes in urine osmolality or free water clearance, because a decrease in glomerular filtration rate may concentrate the urine independently of plasma AVP levels. These studies demonstrate that hemodynamic stimuli do not disrupt but simply reset the osmoreceptor system.

Several hormones, including glucocorticoids, atrial natriuretic hormone, and angiotensin, were shown to modulate the release of AVP. The present discussion will be confined to the role of glucocorticoids. Hormones of the adrenal cortex and posterior pituitary have long been known to be antagonistic in terms of water excretion. Glucocorticoids enhance a diuresis by inhibiting the secretion of AVP and protect against the impaired response to water loading and water intoxication in adrenal insufficiency. In the 1960s, using bioassays, glucocorticoids were found to inhibit AVP release from the rat pituitary during water deprivation (62), and to raise the osmotic threshold for AVP release in hydrated normal subjects being infused with hypertonic saline (2). A large number of animal and human studies, using RIA, confirm and expand these observations. The inhibitory effect of glucocorticoids was specific for AVP, since oxytocin levels are not affected. Other studies indicate an inhibitory action of cortisol on both basal and osmotically stimulated AVP release (63,64). In addition, cortisol inhibits AVP secretion in response to hypoxia and hypotension (65), stimuli independent of osmoreceptor input.

Metabolism of AVP

The metabolism and inactivation of vasopressin occur largely in liver and kidney, a major mechanism being the cleavage of the terminal glycnamide to produce a biologically (and immunologically) inactive substance.

Until 1986 there were no detailed data on the relationship between plasma and urine AVP levels and on urinary and metabolic clearances of AVP in normal humans during steady-state conditions of AVP infusion. Moses and Steciak demonstrated that there was a rapid rate of increase of urine AVP and a constant fraction of AVP excreted at various infusion rates (66). These data support the value of measuring AVP in urine. Measurement of urinary AVP avoids the problem of widely fluctuating plasma AVP values, since it represents an integrated value of the secretion or infusion of the hormone over time. Infusion of AVP at different rates demonstrated that urinary AVP increases linearly with increasing infusion rates, and that the concentration of AVP in urine increases 120 times more rapidly than plasma AVP. Urinary and metabolic clearances of AVP also increased linearly, with the maximum urinary clearance being 60.6% of the creatinine clearance (66). The metabolic clearance of AVP (including urinary clearance) was 18 times that of the urinary clearance of AVP alone. Subsequent studies investigated the role of sodium excretion, solute excretion, urine volume, plasma volume, atrial natriuretic (ANP) and plasma renin activity (PRA) on the metabolic (nonurinary) and urinary clearances of infused AVP in hydrated normal subjects (19). These experiments demonstrated that in hydrated normal subjects infused with AVP, the urinary clearance of AVP correlated positively with plasma ANP concentration, but not with urine volume, sodium, or solute excretion or PRA (19) (Figure 4). The infusion of physiological amounts of human ANP increased urinary clearance and perhaps metabolic clearance of AVP, leading to the conclusion that ANP plays a role in modulating the renal action of AVP (19) (Figure 5). These observations also indicated the importance of considering ANP levels when using plasma or urinary AVP as an indicator of AVP release from the neurohypophysis. Follow-up studies using the RIA for AVP in the isolated perfused rat kidney expanded and clarified these observations (67).

Role of AVP in Disease States

Disease states manifested by hypotonic polyuria have been clarified by the use of plasma and urine AVP levels. Central diabetes insipidus is characterized by low levels of AVP in relation to plasma osmolality, whereas patients with nephrogenic diabetes insipidus have normal to increased plasma and urine AVP levels in relation to plasma osmolality. Patients with primary polydipsia have a somewhat more complicated pattern. At times the chronic overhydration may cause a low set osmoreceptor mechanism with a relatively normal rate of rise of AVP levels in relation to plasma osmolality. More often chronic overhydration causes a modest increase in the osmotic

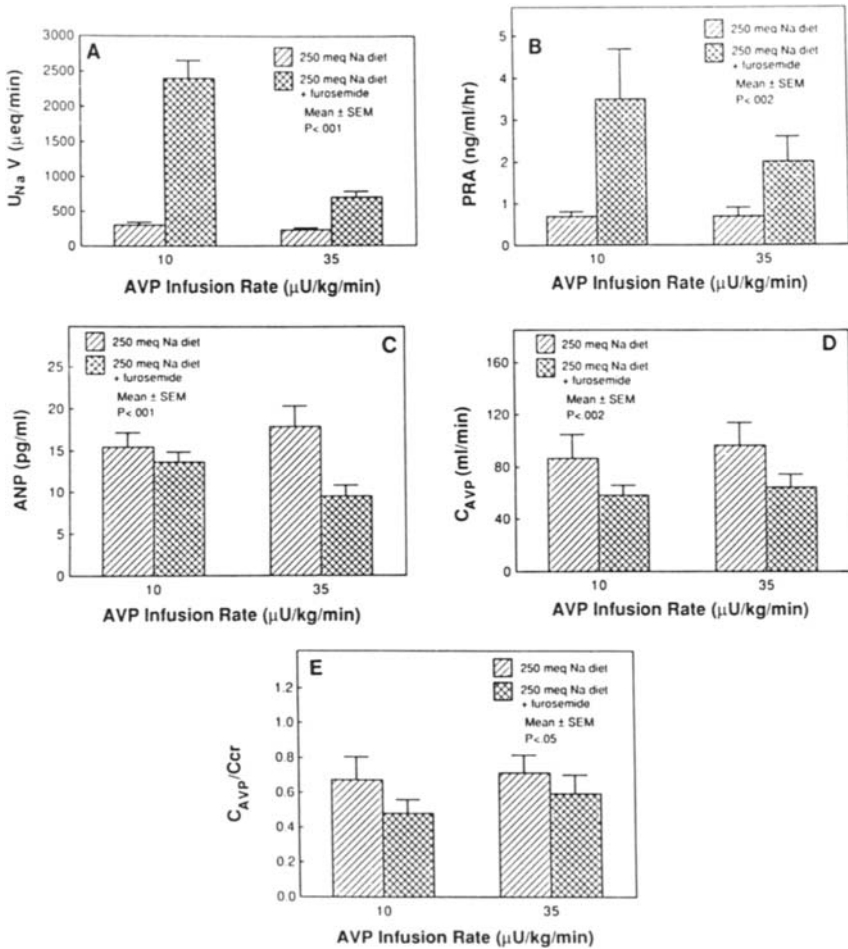


FIGURE 4. The effect of furosemide on response to the infusion of AVP at two different rates. These studies disproved the postulate that the urinary excretion of AVP was positively correlated with excretion of saline. Rather, the urinary excretion and clearance of AVP were found to be positively correlated with plasma atrial natriuretic peptide (ANP) levels (19).

threshold for AVP release and a diminished rate of rise of AVP in plasma and urine (Figure 3). The RIA for AVP has been useful in determining renal sensitivity to AVP by relating AVP to osmolality in the same urine specimen (68).

The syndrome of inappropriate antidiuresis (SIAD) is one of several clinical situations in which there is a subnormal serum sodium (and osmolal-

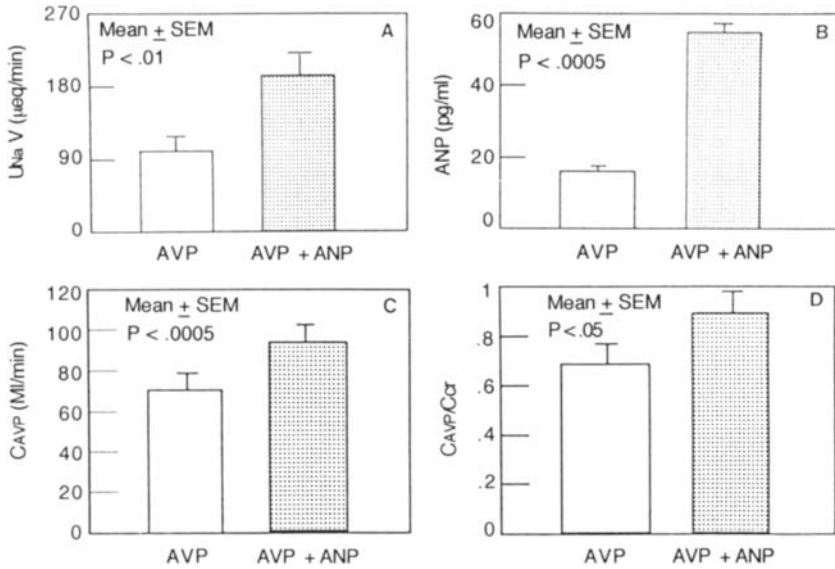


FIGURE 5. The effect of infusing 20 µg ANP over 1 hr on the response to AVP infused at the rate of 88 pg/kg/min. These data demonstrate that the correlation demonstrated in Fig. 4 represents a cause-and-effect relationship (19).

ity) associated with a less than maximally dilute urine. There are many intracranial disease states that cause increased AVP release from the neurohypophysis (69). In addition to disease states, drug-induced SIAD occurs when the pharmacological action of a drug either stimulates AVP release or potentiates the action of released AVP at the level of the renal tubule (17,18,70). Some of the most classic cases occur in patients who have ectopic release of AVP from extracranial neoplasms. A variety of pulmonary infections also cause the syndrome of SIAD. The measurement of AVP by RIA is rarely necessary to establish the diagnosis. However, investigators interested in determining the osmoregulatory dysfunction in patients with SIAD have infused hypertonic saline and related the rise in plasma osmolality to plasma AVP levels. These studies revealed that some patients have random fluctuations of plasma AVP without any relationship to plasma osmolality. Other patients have an AVP “leak” in which plasma AVP is present in increased but constant amounts at low plasma osmolalities, whereas it increases appropriately at higher plasma osmolalities (71). In some patients, plasma AVP is not elevated in relation to plasma osmolality (71). These patients may have impaired water excretion because of in-

creased renal sensitivity to AVP. The V2 receptor antagonist OPC-31260 may be found to be of therapeutic value in treatment of SIAD (72).

Studies in human subjects and experimental animals have provided evidence that AVP plays a major role in water retention in cirrhosis of the liver, congestive heart failure, and hypothyroidism (73,74). We will focus on hypothyroidism to illustrate the problem. Patients with hypothyroidism, particularly when hyponatremic, have diminished ability to excrete free water, fail to achieve maximum urinary dilution, and have delayed excretion of a water load (75). The two major postulated causes for the abnormal water retention are decreased renal blood flow and glomerular filtration rate, and excessive AVP secretion in response to nonosmotic stimuli.

Hypothyroid rats and sheep have increased circulating levels of AVP, and AVP production rates are increased 10-fold in thyroidectomized sheep (76). Some hypothyroid patients have increased plasma AVP concentrations that do not suppress normally following water ingestion (75), whereas others have non-AVP-mediated defects in water excretion. Nonetheless, osmotic regulation of AVP secretion is normal in patients with severe primary hypothyroidism infused with hypertonic saline (77). The general belief is that the elevated plasma AVP levels and failure to suppress with hydration are a consequence of the hypovolemia, which is well documented in patients with hypothyroidism (78,79). This mechanism may release AVP, concentrating the urine, even when the plasma is hypotonic. Our understanding of the metabolism of AVP in hypothyroidism will be improved when well-designed studies are conducted in hypothyroid patients on the release of AVP in response to nonosmotic stimuli, and on the urinary and metabolic clearances of AVP. All of these studies will undoubtedly use the RIA for AVP.

Some evidence for hemodynamic causes of the impaired ability of patients with hypothyroidism to excrete dilute urine is based on the RIA for AVP. Plasma AVP concentrations correlate poorly with the efficiency with which a water load is excreted in hypothyroid patients, and plasma AVP concentrations are not always increased in hyponatremic patients with hypothyroidism (77, 80). Plasma AVP concentrations may decline appropriately during water loading, even in patients who have hyponatremia and mild diluting defects during water loading (77). The physiological role of elevated plasma AVP concentrations in hyponatremic patients with hypothyroidism will be more clearly defined when these patients are studied with specific antidiuretic antagonists of AVP (72).

***In Vitro* Studies**

There are innumerable instances where the RIA for AVP has been applied to *in vitro* studies. We will confine this review to two recent examples.

Fitzsimmons *et al.* have conducted studies of AVP content of rat pituitaries to develop a model to obtain information on the regulation of the gene for AVP synthesis (31). They have attempted to explain why hormone release and synthesis eventually come into equilibrium following the induction of hypo- or hypernatremia and the role of age in this process. Using the RIA for the measurement of pituitary AVP, studies such as these will be able to improve our understanding of the relationship between synthesis and release of AVP by relating physiological regulation of AVP release and molecular control of the AVP gene.

Terasaki *et al.* have established a cell line from the tumor obtained from a patient with SIAD owing to small cell carcinoma of the lung (81). AVP was observed in cultured cells by means of immunohistochemistry, and AVP was extracted from the cells and assayed by RIA. Other marker substances indicative of small cell carcinoma of the lung were also found in both tumor and cell lines. Large amounts of AVP were produced by the cell lines even after 121 passages. Studies such as these will undoubtedly be applied in the future to help clarify the mechanism by which the production and secretion of AVP are controlled in cancer cells.

ACKNOWLEDGMENTS

The authors wish to acknowledge the excellent secretarial assistance of Patricia Gee and Julie Hartsell and the expert editorial collaboration of Miriam Weiner.

REFERENCES

1. A. C. Carter and J. Robbins, The use of hypertonic saline infusions in the differential diagnosis of diabetes insipidus and psychogenic polydipsia. *J. Clin. Endocrinol.* **7**, 753–766 (1947).
2. R. H. Aubry, H. R. Nankin, A. M. Moses, and D. H. P. Streeten, Measurement of the osmotic threshold for vasopressin release in human subjects, and its modification by cortisol. *J. Clin. Endocrinol.* **25**, 1481–1492 (1965).
3. A. M. Moses and D. H. P. Streeten, Differentiation of polyuric states by measurement of responses to changes in plasma osmolality induced by hypertonic saline infusions. *Am. J. Med.* **42**, 368–377 (1967).
4. S. Yoshida, K. Motohashi, H. Ibayashi, and S. Okinaka, Method for the assay of antidiuretic hormone in plasma with a note on the antidiuretic titer of human plasma. *J. Lab. Clin. Med.* **62**, 279–285 (1963).
5. J. W. Czaczkes, C. R. Kleeman, and M. Koenig, Physiologic studies of antidiuretic hormone by its direct measurement in human plasma. *J. Clin. Invest.* **43**, 1625–1640 (1964).
6. A. M. Moses, T. F. Leveque, M. Giambattista, and C. W. Lloyd, Dissociation between the content of vasopressin and neurosecretory material in the rat neurohypophysis. *J. Endocrinol.* **26**, 273–278 (1963).

7. M. Miller and A. M. Moses, Radioimmunoassay of vasopressin with a comparison of immunological and biological activity in the rat posterior pituitary. *Endocrinology (Baltimore)* **84**, 557–562 (1969).
8. J. Roth, S. M. Glick, L. A. Klein, and M. J. Petersen, Specific antibody to vasopressin in man. *J. Clin. Endocrinol.* **26**, 671–675 (1966).
9. R. D. Utiger, Inappropriate antidiuresis and carcinoma of the lung: Detection of arginine vasopressin in tumor extracts by immunoassay. *J. Clin. Endocrinol.* **26**, 970–974 (1966).
10. H. Vorherr, S. G. Massry, R. D. Utiger, and C. R. Kleeman, Antidiuretic principle in malignant tumor extracts from patients with inappropriate ADH syndrome. *J. Clin. Endocrinol.* **28**, 162–168 (1968).
11. A. M. Moses and M. Miller, Accumulation and release of pituitary vasopressin in rats heterozygous for hypothalamic diabetes insipidus. *Endocrinology (Baltimore)* **86**, 34–41 (1970).
12. G. L. Robertson, L. A. Klein, J. Roth, and P. Gorden, Immunoassay of plasma vasopressin in man. *Proc. Nat. Acad. Sci. U.S.A.* **66**, 1298–1305 (1970).
13. M. Miller and A. M. Moses, Radioimmunoassay of urinary antidiuretic hormone with application to study of the Brattleboro rat. *Endocrinology (Baltimore)* **88**, 1389–1396 (1971).
14. M. Miller and A. M. Moses, Radioimmunoassay of urinary antidiuretic hormone in man: Response to water load and dehydration in normal subjects. *J. Clin. Endocrinol. Metab.* **34**, 537–545 (1972).
15. M. Miller and A. M. Moses, Urinary antidiuretic hormone in polyuric disorders and in inappropriate ADH syndrome. *Ann. Intern. Med.* **77**, 715–721 (1972).
16. S. N. Oyama, A. Kagan, and S. M. Glick, Radioimmunoassay of vasopressin: Application to unextracted human urine. *J. Clin. Endocrinol.* **33**, 739–744 (1971).
17. A. M. Moses, P. Numann, and M. Miller, Mechanism of chlorpropamide-induced antidiuresis in man: Evidence for release of ADH and enhancement of peripheral action. *Metabolism* **22**, 59–66 (1973).
18. A. M. Moses, J. Howanitz, M. van Gemert, and M. Miller, Clofibrate-induced antidiuresis. *J. Clin. Invest.* **52**, 535–542 (1973).
19. A. M. Moses, C. Jones, and C. B. Yucha, Effects of sodium intake, furosemide, and infusion of atrial natriuretic peptide on the urinary and metabolic clearances of arginine vasopressin in normal subjects. *J. Clin. Endocrinol. Metab.* **70**, 222–229 (1990).
20. C. G. Beardwell, Radioimmunoassay of arginine vasopressin in human plasma. *J. Clin. Endocrinol.* **33**, 254–260 (1971).
21. A. G. Robinson and A. G. Frantz, Radioimmunoassay of posterior pituitary peptides: A review, *Metabolism* **22**, 1047–1057 (1973).
22. W. R. Skowsky and D. A. Fisher, Vasopressin (VP) kinetics in man and the rhesus monkey fetus using radioimmunoassay (RIA) measurements. *J. Clin. Invest.* **51**, 91a (1972).
23. S. C. Smith, A. Smith, K. James, and N. McIntosh, A two-site immunometric assay for arginine vasopressin. *Biochem. Soc. Trans.* **18**, 1273–1274 (1990).
24. E. Ishikawa, K. Tanaka, and S. Hashida, Novel and sensitive noncompetitive (two-site) immunoassay for haptens with emphasis on peptides. *Clin. Biochem.* **23**, 445–453 (1990).
25. A. Tausch, H. Stegner, R. D. Leake, H. G. Artman, and D. A. Fisher, Radioimmunoassay of arginine vasopressin in urine: Development and application. *J. Clin. Endocrinol. Metab.* **57**, 777–781 (1983).
26. J. M. Davison, E. A. Gilmore, J. Durr, G. L. Robertson, and M. D. Lindheimer, Altered osmotic thresholds for vasopressin secretion and thirst in human pregnancy. *Am. J. Physiol.* **246**, F105–F109 (1984).

27. P. H. Baylis and D. A. Heath, The development of a radioimmunoassay for the measurement of human plasma arginine vasopressin. *Clin. Endocrinol.* **7**, 91–102 (1977).
28. J. J. Preibisz, J. E. Sealey, J. H. Laragh, R. J. Cody, and B. B. Weksler, Plasma and platelet vasopressin in essential hypertension and congestive heart failure. *Hypertension* **5** (Suppl 1), I-129–I-138 (1983).
29. C. M. Chesney, J. T. Crofton, D. D. Pifer, D. P. Brooks, K. M. Huch, and L. Share, Subcellular localization of vasopressin-like material in platelets. *J. Lab. Clin. Med.* **106**, 314–318 (1985).
30. W. A. Sadler, C. P. Lynskey, N. L. Gilchrist, E. A. Espiner, and M. G. Nicholls, A sensitive radioimmunoassay for measuring plasma anti-diuretic hormone in man. *N. Z. Med. J.* **96**, 959–963 (1983).
31. M. D. Fitzsimmons, M. M. Roberts, and A. G. Robinson, Control of posterior pituitary vasopressin content: Implications for the regulation of the vasopressin gene. *Endocrinology (Baltimore)* **134**, 1874–1878 (1994).
32. F. Holmquist, S. Lundin, B. Larsson, H. Hedlund, and K.-E. Andersson, Studies on binding sites, contents, and effects of AVP in isolated bladder and urethra from rabbits and humans. *Am. J. Physiol.* **261**, R865–R874 (1991).
33. J. S. Simon, M. J. Brody, and B. G. Kasson, Characterization of a vasopressin-like peptide in rat and bovine blood vessels. *Am. J. Physiol.* **262**, H799–H805 (1992).
34. F. T. LaRochelle, Jr., W. G. North, and P. Stern, A new extraction of arginine vasopressin from blood: The use of octadecasilyl-silica. *Pflugers Arch.* **387**, 79–81 (1980).
35. J. R. Claybaugh and A. K. Sato, Factors influencing urinary vasopressin concentration. *Fed. Proc.* **44**, 62–65 (1985).
36. F. Bodola and C. R. Benedict, Rapid, simplified radioimmunoassay of arginine-vasopressin and atrial natriuretic peptide in plasma. *Clin. Chem.* **34/35**, 970–973 (1988).
37. J. T. Crofton, L. Share, B. C. Wang, and R. E. Shade, Pressor responsiveness to vasopressin in the rat with DOC-salt hypertension. *Hypertension* **2**, 424–431 (1980).
38. M. Bald and W. Rascher, Determination and characterization of arginine-vasopressin in extracted and unextracted urine and its urinary excretion in normal children and adolescents. *Horm. Res.* **34**, 60–65 (1990).
39. A. Panzali, C. Signorini, R. Ferrari, and A. Albertini, Direct determination of arginine-vasopressin in urine. *Clin. Chem.* **36**, 384–385 (1990).
40. H. P. Henneberry, J. D. H. Slater, V. Eisen, and S. Fuhr, Arginine vasopressin response to hypertonicity in hypertension studied by arginine vasopressin assay in unextracted plasma. *J. Hypertens.* **10**, 221–228 (1992).
41. W. R. Skowsky and D. A. Fisher, The use of thyroglobulin to induce antigenicity to small molecules. *J. Lab. Clin. Chem.* **80**, 134–144 (1972).
42. K. Glanzer, M. Appenheimer, F. Kruck, W. Vetter, and H. Vetter, Measurement of 8-arginine-vasopressin by radioimmunoassay. *Acta Endocrinol.* **106**, 317–329 (1984).
43. W. M. Hunter and F. C. Greenwood, Preparation of iodine-131 labelled human growth hormone of high specific activity. *Nature (London)* **194**, 495–496 (1962).
44. J. I. Thorell and B. G. Johansson, Enzymatic iodination of polypeptides with ¹²⁵I to high specific activity. *Biochim. Biophys. Acta* **251**, 363–369 (1971).
45. J. Mohring, P. Bohlen, J. Schoun, M. Mellet, U. Suss, M. Schmidt, and V. Pliska, Comparison of radioimmunoassay, chemical assay (HPLC) and bioassay for arginine vasopressin in synthetic standards and posterior pituitary tissue. *Acta Endocrinol.* **99**, 371–378 (1982).
46. P. Larose, J. Gutowska, P. du Souich, and H. Ong, Development of a solid-phase radioimmunoassay for the determination of arginine-vasopressin in urine. *J. Immunoassay* **6**, 207–225 (1985).

47. J. Burd, D. R. Weightman, B. A. Spruce, and P. H. Baylis, A solid phase radioimmunoassay for human plasma arginine vasopressin. *Clin. Chim. Acta* **136**, 251–256 (1984).
48. A. M. Moses, Osmotic thresholds for AVP release with the use of plasma and urine AVP and free water clearance. *Am. J. Physiol.* **256**, R892–R897 (1989).
49. A. M. Moses and B. Clayton, Impairment of osmotically stimulated AVP release in patients with primary polydipsia. *Am. J. Physiol.* **265**, R1247–R1252 (1993).
50. R. A. Donald, I. G. Crozier, S. G. Foy, A. M. Richards, J. H. Livesey, M. J. Ellis, L. Mattioli, and H. Ikram, Plasma corticotrophin releasing hormone, vasopressin, ACTH, and cortisol responses to acute myocardial infarction. *Clin. Endocrinol.* **40**, 499–504 (1994).
51. S. J. Holmes, C. M. Florkowski, M. J. Evans, M. J. Ellis, J. H. Livesey, R. A. Donald, and E. A. Espiner, Metyrapone induced increase in plasma corticotropin is not associated with changes in peripheral venous arginine vasopressin or corticotropin releasing factor. *J. Endocrinol. Invest.* **16**, 787–792 (1993).
52. A. L. Gerbes, R. Witthaut, W. K. Samson, W. Schnizer, and A. M. Vollmar, A highly sensitive and rapid radioimmunoassay for the determination of arginine⁸-vasopressin. *Eur. J. Clin. Chem. Clin. Biochem.* **30**, 229–233 (1992).
53. B. M. Wall, H. H. Williams, D. N. Presley, J. T. Crofton, E. G. Schneider, L. Share, and C. R. Cooke, Altered sensitivity of osmotically stimulated vasopressin release in quadriplegic subjects. *Am. J. Physiol.* **258**, R827–R835 (1990).
54. P. Rooke and P. H. Baylis, A new sensitive radioimmunoassay for plasma arginine vasopressin. *J. Immunoassay* **3**, 115–131 (1982).
55. R. Garland, A. Sanmanti, R. Catalan, S. Schwartz and J. M. Castellanos, Study of different factors affecting arginine-vasopressin radioimmunoassay. *Clin. Chim. Acta* **145**, 119–128 (1985).
56. A. G. Johnson, G. A. Crawford, D. Kelly, T. V. Nguyen, and A. Z. Gyory, Arginine vasopressin and osmolality in the elderly. *J. Am. Geriatr. Soc.* **42**, 399–404 (1994).
57. J. Duggan, S. Kilfeather, S. L. Lightman, and K. O'Malley, The association of age with plasma arginine vasopressin and plasma osmolality. *Age Ageing* **22**, 332–336 (1993).
58. P. A. Phillips, M. Bretherton, J. Risvanis, D. Casley, C. Johnston, and L. Gray, Effects of drinking on thirst and vasopressin in dehydrated elderly men. *Am. J. Physiol.* **264**, R877–R881 (1993).
59. P. Chiodera, L. Capretti, M. Marchesi, A. Caiazza, L. Bianconi, U. Cavazzini, C. Marchesi, R. Volpi, and V. Coiro, Abnormal arginine vasopressin response to cigarette smoking and metoclopramide (but not to insulin-induced hypoglycemia) in elderly subjects. *J. Gerontol.* **46**, M6–M10 (1991).
60. A. M. Moses and M. Miller, Osmotic threshold for vasopressin release as determined by saline infusion and by dehydration. *Neuroendocrinology* **7**, 219–226 (1971).
61. G. L. Robertson, Physiology of ADH secretion. *Kidney Int.* **32**, S20–S26 (1987).
62. A. M. Moses, Adrenal neurohypophyseal relationships in the dehydrated rat. *Endocrinology (Baltimore)* **72**, 230–236 (1963).
63. P. E. Papanek and H. Raff, Chronic physiological increases in cortisol inhibit the vasopressin response to hypertonicity in conscious dogs. *Am. J. Physiol.* **267**, R1342–R1349 (1994).
64. H. Raff, M. M. Skelton, D. C. Merrill, and A. W. Cowley, Jr., Vasopressin responses to corticotropin releasing factor and hyperosmolality in conscious dogs. *Am. J. Physiol.* **251**, R1235–R1239 (1986).
65. H. Raff, M. M. Skelton, and A. W. Cowley, Jr., Cortisol inhibition of vasopressin and ACTH responses to arterial hypotension in conscious dogs. *Am. J. Physiol.* **258**, R64–R69 (1990).

66. A. M. Moses and E. Steciak, Urinary and metabolic clearances of arginine vasopressin in normal subjects. *Am. J. Physiol.* **251**, R365–R370 (1986).
67. M. R. Lebowitz, A. M. Moses, and S. J. Scheinman, Effects of atrial natriuretic peptides on metabolism of arginine vasopressin by isolated perfused rat kidney. *Am. J. Physiol.* **263**, R273–R278 (1992).
68. A. M. Moses, S. J. Scheinman, and A. Oppenheim, Marked hypotonic polyuria resulting from nephrogenic diabetes insipidus with partial sensitivity to vasopressin. *J. Clin. Endocrinol. Metab.* **59**, 1044–1049 (1984).
69. D. H. P. Streeten and A. M. Moses, The syndrome of inappropriate vasopressin secretion. *Endocrinologist* **3**, 353–358 (1993).
70. A. M. Moses and M. Miller, Drug-induced dilutional hyponatremia. *N. Engl. J. Med.* **291**, 1234–1239 (1974).
71. R. Zerbe, L. Stropes, and G. Robertson, Vasopressin function in the syndrome of inappropriate antidiuresis. *Annu. Rev. Med.* **31**, 315–327 (1980).
72. A. Ohnishi, Y. Orita, R. Okahara, H. Fujihara, T. Inoue, Y. Yamamura, Y. Yabuuchi, and T. Tanaka, Potent aquaretic agent: A novel nonpeptide selective vasopressin 2 antagonist (OPC-31260) in men. *J. Clin. Invest.* **92**, 2653–2659 (1993).
73. P. Gines, W. T. Abraham, and R. W. Schrier, Vasopressin in pathophysiological states. *Semin. Nephrol.* **14**, 384–397 (1994).
74. F. Salerno, A. DelBo, A. Maggi, M. Marabini, M. Maffi, G. M. Borroni, and P. Moser, Vasopressin release and water metabolism in patients with cirrhosis. *J. Hepatol.* **21**, 822–830 (1994).
75. W. R. Skowsky and T. A. Kikuchi, The role of vasopressin in the impaired water excretion of myxedema. *Am. J. Med.* **64**, 613–621 (1978).
76. W. R. Skowsky and D. A. Fisher, Arginine vasopressin secretion in thyroidectomized sheep. *Endocrinology (Baltimore)* **100**, 1022–1032 (1977).
77. Y. Iwasaki, Y. Oiso, K. Yamauchi, K. Takatsuki, K. Kondo, H. Hasegawa, and A. Tomita, Osmoregulation of plasma vasopressin in myxedema. *J. Clin. Endocrinol. Metab.* **70**, 534–544 (1990).
78. H. H. Parving, J. M. Hansen, S. L. Nielsen, N. Rossing, O. Munck, and N. A. Lassen, Mechanisms of edema formation in myxedema-increased protein extravasation and relatively slow lymphatic drainage. *N. Engl. J. Med.* **301**, 460–465 (1979).
79. R. W. Schrier and J. P. Goldberg, The physiology of vasopressin release and the pathogenesis of impaired water excretion in adrenal, thyroid, and edematous disorders. *Yale J. Biol. Med.* **53**, 525–541 (1980).
80. Y. Koide, K. Oda, K. Shimizu, A. Shimizu, I. Nabeshima, S. Kimura, M. Maruyama, and K. Yamashita, Hyponatremia without inappropriate secretion of vasopressin in a case of myxedema coma. *Endocrinol. Jpn.* **29**, 363–368 (1982).
81. T. Terasaki, Y. Matsuno, Y. Shimosato, K. Yamaguchi, H. Ichinose, T. Nagatsu, and K. Kato, Establishment of a human small cell lung cancer cell line producing a large amount of anti-diuretic hormone. *Jpn. J. Cancer Res.* **85**, 718–722 (1994).
82. M. G. Ervin, R. Castro, D. J. Sherman, M. G. Ross, J. F. Padbury, R. D. Leake, and D. A. Fisher, Ovine fetal renal and hormonal responses to changes in plasma epinephrine. *Am. J. Physiol.* **260**, R82–R89 (1991).
83. M. G. Ervin, R. D. Leake, M. G. Ross, G. C. Calvario, and D. A. Fisher, Arginine vasotocin in ovine fetal blood, urine, and amniotic fluid. *J. Clin. Invest.* **75**, 1696–1701 (1985).
84. R. E. Weitzman, A. Reviczky, T. H. Oddie, and D. A. Fisher, Effect of osmolality on arginine vasopressin and renin release after hemorrhage. *Am. J. Physiol.* **238**, E62–E68 (1980).

85. J. F. McLeod, L. Kovacs, M. B. Gaskill, S. Rittig, G. S. Bradley, and G. L. Robertson, Familial neurohypophyseal diabetes insipidus associated with a signal peptide mutation. *J. Clin. Endocrinol. Metab.* **77**, 599A–599G (1993).
86. G. L. Robertson, E. A. Mahr, S. Athar, and T. Sinha, Development and clinical application of a new method for the radioimmunoassay of arginine vasopressin in human plasma. *J. Clin. Invest.* **52**, 2340–2352 (1973).
87. J. T. Crofton and L. Share, Sexual dimorphism in vasopressin and cardiovascular response to hemorrhage in the rat. *Circ. Res.* **66**, 1345–1353 (1990).
88. W. R. Skowsky, A. A. Rosenbloom, and D. A. Fisher, Radioimmunoassay measurement of arginine vasopressin in serum: Development and application. *J. Clin. Endocrinol. Metab.* **38**, 278–287 (1974).
89. J. E. Stern, T. Mitchell, V. L. Herzberg, and W. G. North, Secretion of vasopressin, oxytocin, and two neurophysins from rat hypothalamo-neurohypophyseal explants in organ culture. *Neuroendocrinology* **43**, 252–258 (1986).
90. J. J. Morton, P. L. Padfield, and M. L. Forsling, A radioimmunoassay for plasma arginine-vasopressin in man and dog: Application to physiological and pathological states. *J. Endocrinol.* **65**, 411–424 (1975).
91. J. G. Verbalis, E. F. Balwin, and A. G. Robinson, Osmotic regulation of plasma vasopressin and oxytocin after sustained hyponatremia. *Am. J. Physiol.* **250**, R444–R451 (1986).
92. S. M. Seif, A. G. Robinson, T. V. Zenser, B. B. Davis, A. B. Huellmantel, and C. Haluszczak, Neurohypophyseal peptides in hypothyroid rats: Plasma levels and kidney response. *Metabolism* **28**, 137–143 (1979).
93. R. M. Carey, A. J. Johanson, and S. M. Seif, The effects of ovine prolactin on water and electrolyte excretion in man are attributable to vasopressin contamination. *J. Clin. Endocrinol. Metab.* **44**, 850–858 (1977).
94. F. C. Greenwood and W. M. Hunter, The preparation of ¹³¹I-labelled human growth hormone of high specific radioactivity. *Biochem. J.* **89**, 114–123 (1963).
95. A. G. Robinson, M. M. Roberts, W. A. Evron, J. G. Verbalis, and T. G. Sherman, Hyponatremia in rats induces downregulation of vasopressin synthesis. *J. Clin. Invest.* **86**, 1023–1029 (1990).
96. C. M. Faull, J. A. Charlton, T. J. Butler, and P. H. Baylis, The effect of acute pharmacological manipulation of central serotonin neurotransmission on osmoregulated secretion of arginine vasopressin in the rat. *J. Endocrinol.* **139**, 77–87 (1993).
97. K. A. R. N. Ysewijn-Van Brussel and A. P. De Leenheer, Development and evaluation of a radioimmunoassay for arg⁸-vasopressin, after extraction with Sep-Pak C₁₈. *Clin. Chem.* **31**, 861–863 (1985).
98. F. S. Carmen III, C. E. Dreiling, and D. E. Brown, Preparation of serum oxytocin and arginine vasopressin prior to radioimmunoassay: Simultaneous extraction and separation on C18 Sep-Pak cartridges. *Clin. Biochem.* **21**, 265–269 (1988).
99. W. A. Sadler, C. P. Wright, and J. H. Livesey, Preparation of ¹²⁵I-labelled arginine vasopressin for radioimmunoassay. *Clin. Chim. Acta* **155**, 61–68 (1986).
100. J. Camps, A. Martinez-Vea, R. M. Perez-Ayuso, V. Arroyo, J. M. Gaya, and F. Rivera-Fillat, Radioimmunoassay for arginine-vasopressin in cold ethanol extracts of plasma. *Clin. Chem.* **29**, 882–884 (1983).

This Page Intentionally Left Blank

INDEX

A

- A-B-C-test, amino acid system transport determination, 191
- Adenylyl cyclase, activity response analysis, 362–363
- Adrenal corticosteroid receptors, *see* Glucocorticoid receptors; Mineralocorticoid receptors
- Adrenocortical cells, primary culture technique, 393–415
 - bovine cell culture, 396–401
 - adrenal gland sources, 396
 - fasciculata cells
 - purification, 399–400
 - suspension preparation, 397–399
 - monolayer culture, 400–401
 - tissue dissection, 396–397
 - diagnostic evaluation, 405–414
 - cortisol radioimmunoassay, 413–414
 - proliferation studies, 405–409
 - steroidogenic response, 409–414
 - [³H]thymidine incorporation assay, 408–409
 - equipment, 394
 - human cell culture, 401–405
 - adrenal gland sources, 403
 - fasciculata cell purification, 404
 - monolayer culture, 404–405
 - tissue dissection, 403–404
 - overview, 393–394
 - reagents, 395–396
- Adrenocorticotrophic hormone
 - bioassay, 6
 - marker assay, 64
 - radioimmunoassay, 11, 18
 - radioreceptor assay, 6
 - steroidogenic response pathway, 393–394, 405–406, 411
- Allografts, pituitary/renal capsule hypophysial grafts, 101–113
 - future research directions, 113
 - historical perspective, 101–104
 - in situ versus in vitro* models, 104–105
 - technique, 105–113
 - allograft tissue removal, 112
 - control tissue allografts, 112
 - donor tissue selection, 110–112
 - host selection, 108–110
 - host status, 113
 - methodology, 105–108
- Amino acids, *see also specific types*
 - thyroid hormone uptake measurement, 187–200
 - amino acid transport systems, 188–191
 - amino acid identification strategies, 190–191
 - driving forces, 188–189
 - substrate specificity, 188–189
 - transport interactions, 189–190
 - cultured cell systems, 191–196
 - active transport, 195
 - amino acid incorporation determination, 194
 - cell count, 195–196
 - cell culture, 191–192
 - cell-surface binding, 194–195
 - passive transport, 195
 - protein content, 195–196
 - protocol, 192–194
 - transmembrane transport, 194–195
 - plasma membrane vesicle culture, 196–199
 - active transport, 199

- Amino acids (*continued*)
- advantages, 196
 - passive transport, 199
 - protocol, 197–198
 - vesicle isolation, 196–197
- Antibodies
- adrenal corticosteroid receptors,
 - intracellular protein level
 - quantitation, 331–332
 - bound-from-free hormone separation, 21–26
 - prolactin plaque assay preparation, 118–119
 - radioimmunoassay technique, 13–18, 26–28
 - thyroglobulin autoantibody measurement, 174–175
 - thyroid peroxidase autoantibody measurement, 174–175
 - thyrotropin antibody measurement, 175–176
 - thyrotropin receptor autoantibody measurement
 - assay method correlations, 310–311
 - autoimmune thyroid diseases, 301–302
 - bioassays
 - in vitro* methods, 307–310
 - in vivo* methods, 306–307
 - future research directions, 311–315
 - radioreceptor assays, 303–306
 - receptor structure and function, 299–301
- Arginine vasopressin, concentration
- detection, 417–440
 - methodology, 420–433
 - currently utilized methods, 429–433
 - extraction procedures, 422–423
 - human normal values, 428–429
 - radioimmunoassay, 423–428
 - specimen care, 421–422
 - unknown quantity determination, 428
 - overview, 417–420
 - radioimmunoassay applications
 - disease states, 436–439
 - in vitro* studies, 439–440
 - methods, 423–428
 - normal metabolism, 435–436
 - normal secretion regulation, 434–435
- Autoradiography, glutamate receptor
- detection
 - in situ* hybridization method, 267–268
 - nonspecific binding, 252, 256–257
 - protocol, 251–252
 - quantitative analysis, 259–260
 - saturation binding, 255–256
 - standards series, 257–258
 - subtype analysis
 - direct, 254–255
 - indirect, 252–254
- B**
- Binding assay
- glucocorticoid receptor measurement, 329–331
 - glutamate receptor analysis
 - expression study methods, 244–248
 - identification, 244
 - localization, 244–246
 - quantification, 244–246
 - study method choice, 247–248
 - overview, 239–243
 - central nervous system pathology, 239–240
 - excitotoxin effects, 242–243
 - neurotoxins, 240–242
 - receptor plasticity, 243
 - protocol, 249–260
 - autoradiography, 251–252
 - considerations, 249–250
 - materials, 250–251
 - nonspecific binding, 252, 256–257
 - quantitative analysis, 259–260
 - saturation binding, 255–256
 - standards, 257–258
 - subtype analysis
 - direct, 254–255
 - indirect, 252–254
 - transport, 256–257
 - thyroid hormone measurement, 165–166
- Bioassays
- methodology, 3–6
 - thyrotropin receptor detection
 - in vitro* method, 307–310
 - in vivo* method, 306–307
 - radioreceptor assay compared, 310–311
- Bone biology
- fluorescence assays, 131–150
 - bone cell cultures, 132–135
 - osteoblastic cells, 132–134
 - osteoclastic cells, 134–135

- cell population analysis, 135–142
 - applicative considerations, 135–136
 - cell-cell communication, 141–142
 - cytosolic calcium, 137–138
 - intracellular pH, 138–139
 - membrane potential, 139–141
 - sample preparation, 136–137
 - single cell analysis, 142–150
 - applicative considerations, 142–143
 - cell coupling, 149–150
 - cytosolic calcium, 144–146
 - intracellular cyclic AMP, 147–149
 - intracellular pH, 146–147
 - sample preparation, 144
 - longitudinal bone growth, 81–87
 - growth plate infusion, 85–87
 - measurement, 82–85
 - principles, 81–82
- C**
- Calcitonin, marker assay, 65
 - Calcium ion, concentration analysis,
 - osteoblast cells
 - populations, 137–138
 - single cells, 144–146
 - Central nervous system, glutamate receptor
 - pathology, 239–240
 - Chemiluminescent assays, methodology, 51–55
 - Chorionic gonadotropin, human, marker
 - assay, 65–66
 - Chromatography
 - adenylyl cyclase activity analysis, 363
 - β -endorphin separation, 281–296
 - analysis, 291–294
 - human pituitary peptide analysis, 294–295
 - overview, 281–285
 - separation procedure, 289–291
 - tissue extraction, 285–289
 - Colon
 - adrenal corticosteroid effects, 322–323
 - intracellular corticosteroid receptor
 - autoregulation, rat models, 340–348
 - ligand binding level, 341–342
 - mRNA levels, 345–348
 - protein level, 342–345
 - Colorimetric assays, methodology, 3
 - Computers, two-dimensional protein
 - analysis, 217–218
 - Coomassie blue dye, protein detection, 209
 - Corticosterone, radioimmunoassay, 226–227, 229–231
 - Cortisol
 - marker assay, 60–61
 - radioimmunoassay, 226–231, 413–414
 - Cunningham chamber, prolactin plaque
 - assay preparation, 119
 - Cyclic AMP
 - concentration analysis, osteoblast cells, 147–149
 - Graves' disease detection, 175–176
- D**
- DALT system, gel electrophoresis protein
 - separation, 207–209
 - D₂ Dopamine receptors, transfection
 - techniques, 355–367
 - clonal pituitary cell lines, 357–366
 - AtT20 cells, 364–365
 - GH4C1 cells, 357–358, 362–363
 - HEK 293 cells, 365–366
 - inducible expression, 364–365
 - parent cell line choice, 357–358
 - stable transfection, 358–363
 - transient expression, 365–366
 - future research directions, 366–367
 - overview, 355–357
 - prolactin secretion regulation, 355–356
 - receptor expression, 356–357
 - receptor signaling, 356
 - technique rational, 357
 - Dehydroepiandrosterone
 - marker assay, 61–62
 - steroidogenic response pathway, 410–411
 - Dehydroepiandrosterone sulfate, marker
 - assay, 61–62
 - Digoxigenin, glycoprotein detection, 216–217
 - Dihydrotestosterone, marker assay, 62
 - 1,25-Dihydroxyvitamin D, marker
 - assay, 63
 - DNA, steroid receptor binding,
 - measurement, 89–99
 - DNase I footprinting, 94–97
 - methylation interference, 97–100
 - mobility shift analysis, 90–94

DNase I, steroid receptor/DNA binding measurement, 94–97

E

Electroblotting, protein detection, 213

Electrochemical immunoassays, methodology, 57–58

Electrophoresis, *see* Polyacrylamide gel electrophoresis; Two-dimensional gel electrophoresis

β -Endorphin, chromatography separation, 281–296

analysis, 291–294

human pituitary peptide analysis, 294–295

overview, 281–285

separation procedure, 289–291

tissue extraction, 285–289

Enzyme immunoassay

methodology, 32–35, 39–44

thyrotropin measurement, 170–173

Enzyme-linked immunosorbent assay

metallothionein quantitation, 380–381

methodology, 32–35, 39–44

Enzyme multiplied immunoassay,

methodology, 40

Equilibrium dialysis, free thyroxine

measurement, 161–163

Estradiol, marker assay, 62

Excitotoxins, neuroendocrine effects,

242–243

F

Fluorescein, fluorescence assay applications, 47–48

Fluorescence assays

bone studies, 131–150

cell cultures, 132–135

osteoblastic cells, 132–134

osteoclastic cells, 134–135

cell population analysis, 135–142

applicative considerations, 135–136

cell-cell communication, 141–142

cytosolic calcium, 137–138

intracellular pH, 138–139

membrane potential, 139–141

sample preparation, 136–137

single cell analysis, 142–150

applicative considerations, 142–143

cell coupling, 149–150

cytosolic calcium, 144–146

intracellular cyclic AMP, 147–149

intracellular pH, 146–147

sample preparation, 144

methodology, 44–51

protein detection, 212

Follicle-stimulating hormone

bioassay, 5–6

glucocorticoid effects, rat studies, 221–237

experimental protocols, 228–229

methodologies, 223–228

hormone pellet construction, 223–224

Northern blot analysis, 227–228

pituitary hormone content

extraction, 225

pituitary total RNA extraction, 227

radioimmunoassay, 226–227

serum collection, 225

surgical methods, 224–225

tissue dissection, 225

overview, 221–223

results, 229–235

corticosterone serum levels, 229–231

cortisol serum levels, 229–231

messenger RNA subunit levels, 232–235

marker assay, 65–66

pituitary graft models, 102, 111

G

Gammaglobulin, radioimmunoassay, 13–18

Gap junctions, fluorescence studies

cell-cell communication, 141–142

cell coupling, 149–150

Gel electrophoresis, *see* Polyacrylamide gel electrophoresis; Two-dimensional gel electrophoresis

Glucocorticoid receptors, intracellular measurement techniques, 319–349

binding level quantitation, 327–331

cytosolic binding assay, 329–331

ligand specificity, 327–328

mRNA level quantitation, 335–340

ribonuclease protection assay, 338–340

- riboprobe design, 335–337
 - riboprobe synthesis, 337–338
 - RNA isolation, 335
 - overview, 319–327
 - autoregulation mechanisms, 326–327
 - corticosteroid physiology, 320–323
 - intracellular mode of action, 323–326
 - protein level quantitation, 331–334
 - antibodies, 331–332
 - cytosol preparation, 331–332
 - immunoprecipitation, 332–333
 - polyacrylamide gel electrophoresis, 333
 - Western immunoblotting, 333–334
 - Western transfer, 333
 - rat colonic hormone autoregulation, 340–348
 - ligand binding level, 341–342
 - mRNA levels, 345–348
 - protein level, 342–345
 - Glucocorticoids
 - gonadotropin hormone effects, rat studies, 221–237
 - experimental protocols, 228–229
 - methodologies, 223–228
 - hormone pellet construction, 223–224
 - Northern blot analysis, 227–228
 - pituitary hormone content extraction, 225
 - pituitary total RNA extraction, 227
 - radioimmunoassay, 226–227
 - serum collection, 225
 - surgical methods, 224–225
 - tissue dissection, 225
 - overview, 221–223
 - results, 229–235
 - corticosterone serum levels, 229–231
 - cortisol serum levels, 229–231
 - gonadotropin hormone subunit messenger RNA levels, 232–235
 - physiological effects, 320–321
- Glutamate receptor
 - binding assay, 249–260
 - autoradiography, 251–252
 - considerations, 249–250
 - materials, 250–251
 - nonspecific binding, 252, 256–257
 - quantitative analysis, 259–260
 - saturation binding, 255–256
 - standards, 257–258
 - subtype analysis
 - direct, 254–255
 - indirect, 252–254
 - transport, 256–257
- expression study methods
 - multiple receptor subtypes, 244–248
 - identification, 244
 - localization, 244–246
 - quantification, 244–246
 - study method choice, 247–248
- in situ* hybridization analysis, 260–271
 - autoradiography, 267–268
 - nonspecific hybridization elimination, 268–270
 - protocol, 260–266
 - brain sectioning, 260–263
 - hybridization technique, 264–265
 - 3' end-labeling, 263–264
 - reaction maximization, 266–267
 - stock solution preparation, 270–271
- physiology, 239–243
 - central nervous system pathology, 239–240
 - excitotoxin effects, 242–243
 - neurotoxins, 240–242
 - receptor plasticity, 243
- Glycoprotein, detection, digoxigenin-labeled lectins, 216–217
- Gonadotropin hormones, *see* Follicle-stimulating hormone; Luteinizing hormone
- Gonadotropin-releasing hormone, pituitary stimulation, 222–223
- Graves' disease
 - thyrotropin antibody measurement, 175–176
 - thyrotropin receptor role, 301–302
- Growth hormone
 - marker assay, 65
 - pituitary graft models, 103
- Growth hormone releasing hormone, pituitary graft models, 102–103
- Growth plate, longitudinal bone growth, 81–87
 - infusion, 85–87
 - measurement, 82–85
 - principles, 81–82
- ## H
- Hemolytic plaque assays, *see* Reverse hemolytic plaque assays

- Hormones, *see also specific types*
 bound-from-free antibody separation,
 21–26
 marker assay, methodology, 60–68
 lipid-soluble hormones, 60–64
 water-soluble hormones, 64–68
 Human chorionic gonadotropin, marker
 assay, 65–66
 25-Hydroxy vitamin D, marker assay, 63
 Hypothyroidism, thyrotropin receptor role,
 301–302

I

- Immobilized pH gradient system, isoelectric
 focusing, 207
 Immunoassay, *see specific type*
 Immunoextraction assay, thyroid hormone
 measurement, 167
 Immunofluorometric assays
 methodology, 44–51
 thyrotropin measurement, 170–173
 Immunoglobulin F-1, marker assay, 67
 Immunoglobulin G, radioimmunoassay,
 13–18
In situ hybridization, glutamate receptor
 analysis, 260–271
 autoradiography, 267–268
 expression study methods, 244–248
 identification, 244
 localization, 244–246
 quantification, 244–246
 study method choice, 247–248
 nonspecific hybridization elimination,
 268–270
 overview, 239–243
 central nervous system pathology,
 239–240
 excitotoxin effects, 242–243
 neurotoxins, 240–242
 receptor plasticity, 243
 protocol, 260–266
 brain sectioning, 260–263
 hybridization technique, 264–265
 3' end-labeling, 263–264
 reaction maximization, 266–267
 stock solution preparation, 270–
 271
 Insulin, marker assay, 66

- Iodine isotopes, radioimmunoassay
 radiolabels, 19–21
 Isoelectric focusing
 immobilized pH gradient system, 207
 ISO system, 205–207

L

- Ligands
 DNA binding measurement
 intracellular corticosteroid receptor
 autoregulation
 ligand specificity, 327–328
 measurement technique, 341–342
 technique, 89–99
 DNase I footprinting, 94–97
 methylation interference, 97–100
 mobility shift analysis, 90–94
 Luteinizing hormone
 bioassay, 5–6
 glucocorticoid effects, rat studies,
 221–237
 experimental protocols, 228–229
 methodologies, 223–228
 hormone pellet construction,
 223–224
 Northern blot analysis, 227–228
 pituitary hormone content
 extraction, 225
 pituitary total RNA extraction, 227
 radioimmunoassay, 226–227
 serum collection, 225
 surgical methods, 224–225
 tissue dissection, 225
 overview, 221–223
 results, 229–235
 corticosterone serum levels, 229–231
 cortisol serum levels, 229–231
 gonadotropin hormone subunit
 messenger RNA levels, 232–235
 marker assay, 66
 pituitary graft models, 102, 111
 Luteinizing hormone releasing hormone,
 pituitary graft models, 102, 110–111
- M
- Marker assays, methodology
 lipid-soluble hormones, 60–64
 water-soluble hormones, 64–68

- Membrane potential, osteoblast cells, 139–141
- Metallothionein, quantitation methods, 371–385
 immunological assay, 380–381
 mRNA analysis, 381–382
 physiology, 371–376
 biological characteristics, 372–374
 functions, 374–376
 structure, 372–374
 saturation assay, 378–380
 toxicology, 377, 382–383
- Metal saturation assays, metallothionein quantitation, 378–380
- Methylation interference assay, steroid receptor/DNA binding measurement, 97–100
- Mineralocorticoid receptors, intracellular measurement techniques, 319–349
 binding level quantitation, 327–331
 cytosolic binding assay, 329–331
 ligand specificity, 327–328
 mRNA level quantitation, 335–340
 ribonuclease protection assay, 338–340
 riboprobe design, 335–337
 riboprobe synthesis, 337–338
 RNA isolation, 335
 overview, 319–327
 autoregulation mechanisms, 326–327
 corticosteroid physiology, 320–323
 intracellular mode of action, 323–326
 protein level quantitation, 331–334
 antibodies, 331–332
 cytosol preparation, 331–332
 immunoprecipitation, 332–333
 polyacrylamide gel electrophoresis, 333
 Western immunoblotting, 333–334
 Western transfer, 333
 rat colonic hormone autoregulation, 340–348
 ligand binding level, 341–342
 mRNA levels, 345–348
 protein level, 342–345
- Mobility shift assay, steroid receptor/DNA binding measurement, 90–94
- N**
- Nephelometry, methodology, 59–60
- Neurotoxins, glutamate receptor toxins, 240–242
- Nonradiometric assays, methodology, 32–44
 enzyme-linked immunosorbent assay, 35–37
 heterogeneous assay, 37–40
 homogeneous enzyme assay, 40–44
- Northern blot analysis, gonadotropin hormone RNA separation, 227–228
- O**
- Osteoblastic cells, *see* Bone biology
- Osteocalcin, marker assay, 66
- P**
- Parathyroid hormone
 cyclic AMP analysis, 147–149
 marker assay, 67
- Particle-enhanced immunoassay, methodology, 60
- Patch-clamp technique, membrane potential measurement, osteoblast cells, 139–141
- pH, intracellular concentration analysis, osteoblast cells
 populations, 138–139
 single cells, 146–147
- Pituitary gland
 β -endorphin peptide analysis, 294–295
 hormone regulation, *see specific hormone*
 renal capsule hypophysial grafts, 101–113
 future research directions, 113
 historical perspective, 101–104
in situ versus in vitro models, 104–105
 technique, 105–113
 allograft tissue removal, 112
 control tissue allografts, 112
 donor tissue selection, 110–112
 host selection, 108–110
 host status, 113
 methodology, 105–108
 total RNA extraction, 227
 transfection techniques
 AtT20 cells, 364–365
 GH4C1 cells, 357–358, 362–363
 HEK 293 cells, 365–366
- Plasma membrane vesicles, amino acid and thyroid hormone uptake measurement, 196–199
 active transport, 199
 advantages, 196

Plasma membrane vesicles (*continued*)

- passive transport, 199
- protocol, 197–198
- vesicle isolation, 196–197

Polyacrylamide gel electrophoresis, glucocorticoid receptors measurement, 333

Potentiometric immunoassay, methodology, 58

Progesterone, marker assay, 62

Prolactin

- marker assay, 67
- pituitary graft models, 102–104, 108–111
- regulation, dopamine role, 355–356
- reverse hemolytic plaque assays, 115–128
 - advantages, 125–126
 - assay establishment, 117
 - procedure, 117–124
 - antibody preparation, 118–119
 - blood cell conjugation, 118
 - cell acquisition, 119–120
 - equipment, 118
 - incubation times, 121–122
 - materials, 117–118
 - monolayer formation, 121
 - reagents, 117
 - reagent sequence, 121–122
 - results assessment, 122–124
 - slide chamber preparation, 119
 - toxic influence assessment, 126–128

Pro-opiomelanocortin, chromatography separation, 281–296

- overview, 281–285
- separation procedure, 289–291
- tissue extraction, 285–289

R

Radioimmunoassay

- adrenocortical cells, steroidogenic response assessment, 413–414
- arginine vasopressin analysis
 - disease states, 436–439
 - in vitro* studies, 439–440
 - methods, 423–428
 - normal metabolism, 435–436
 - normal secretion regulation, 434–435
 - overview, 417–420
- corticosterone measurement, 226–227, 229–231
- cortisol measurement, 226–231, 413–414

gonadotropin hormone measurement, 226

- historical perspective, 2–3
- metallothionein quantitation, 380–381, 385

methodology, 9–32

- antibodies, 13–18
- antibody/receptor binding characteristics, 26–28
- bound-from-free fraction separation, 21–26

data display, 26–28

radiolabels, 18–21

validation, 28–32

thyroid hormone measurement, 158, 161

thyrotropin measurement, 170

Radioreceptor assays

methodology, 6–9

thyrotropin receptor detection, 303–306, 310–311

Receptor proteins, *see also specific receptors*

DNA binding measurement, 89–99

DNase I footprinting, 94–97

methylation interference, 97–100

mobility shift analysis, 90–94

Renal capsule, pituitary hypophysial grafts, 101–113

future research directions, 113

historical perspective, 101–104

in situ versus *in vitro* models, 104–105

technique, 105–113

allograft tissue removal, 112

control tissue allografts, 112

donor tissue selection, 110–112

host selection, 108–110

host status, 113

methodology, 105–108

Reverse hemolytic plaque assays, prolactin

secretion, 115–128

advantages, 125–126

assay establishment, 117

procedure, 117–124

antibody preparation, 118–119

blood cell conjugation, 118

cell acquisition, 119–120

equipment, 118

incubation times, 121–122

materials, 117–118

monolayer formation, 121

reagents, 117

reagent sequence, 121–122

- results assessment, 122–124
 - slide chamber preparation, 119
 - toxic influence assessment, 126–128
- Rhodamine, fluorescence assay
 - applications, 47–48
- Ribonuclease protection assay, corticosteroid receptor mRNA
 - quantitation, 338–340
- Riboprobes, corticosteroid receptor mRNA
 - quantitation, 335–340
 - probe design, 335–337
 - probe synthesis, 337–338
 - ribonuclease protection assay, 338–340
 - RNA isolation, 335
- RNA
 - corticosteroid receptor mRNA
 - quantitation
 - autoregulation, 345–348
 - ribonuclease protection assay, 338–340
 - riboprobe design, 335–337
 - riboprobe synthesis, 337–338
 - RNA isolation, 335
 - gonadotropin hormone analysis
 - messenger RNA subunit levels, 232–235
 - Northern blot analysis, 227–228
 - total RNA extraction, 227
 - metallothionein mRNA analysis, 381–382
- S**
 - Saturation assay, metallothionein
 - quantitation, 378–380
 - Sex hormone binding globulin, marker assay, 67
 - Silver stain, protein detection, 209–212
 - Skeletal system, *see* Bone biology
 - Somatomedin C, marker assay, 67
 - Somatotropin, marker assay, 65
 - Southern slot blot, d_2 dopamine receptor analysis, 360–362
 - Steroid receptors, *see also specific types*
 - DNA binding, measurement, 89–99
 - DNase I footprinting, 94–97
 - methylation interference, 97–100
 - mobility shift analysis, 90–94
- T**
 - Testis-stimulating hormone, bioassay, 6
 - Testosterone, marker assay, 63
 - [^3H]Thymidine incorporation assay,
 - adrenocortical cell evaluation, 408–409
 - Thyroglobulin
 - marker assay, 67
 - measurement, 176–177
 - thyroid gland autoantibody measurement, 174–175
 - Thyroid gland
 - autoimmune disorders
 - thyrotropin antibody measurement, 175–176
 - thyrotropin receptor role, 301–302
 - hormone measurement, *see specific hormone*
 - serum thyroid autoantibody
 - measurement, 173–176
 - thyroglobulin autoantibodies, 174–175
 - thyroid peroxidase autoantibodies, 174–175
 - thyrotropin antibodies, 175–176
 - Thyroid hormones, *see specific type*
 - Thyroid peroxidase, thyroid gland autoantibody measurement, 174–175
 - Thyroid-stimulating hormone, *see* Thyrotropin
 - Thyrotropin
 - marker assay, 68
 - measurement, 169–173
 - assay selection, 173
 - immunometric assay, 170–173
 - overview, 169–170
 - radioimmunoassay, 170
 - thyroid gland autoantibody measurement, 175–176
 - Thyrotropin receptor, autoantibody
 - detection, 299–315
 - assay method correlations, 310–311
 - autoimmune thyroid diseases, 301–302
 - bioassays
 - in vitro* methods, 307–310
 - in vivo* methods, 306–307
 - future research directions, 311–315
 - radioreceptor assay, 303–306
 - receptor structure and function, 299–301
 - Thyroxine
 - marker assay, 63–64
 - measurement, 158–169
 - free concentrations, 159–169
 - binding protein change, 160

Thyroxine (*continued*)

- direct measurement, 161–164
 - equilibrium dialysis, 161–163
 - immunoextraction assay, 167
 - indirect measurement, 164–169
 - labeled analog method, 167–168
 - labeled antibody method, 168–169
 - rationale, 159
 - technical difficulties, 160–161
 - thyroid transport proteins, 160
 - thyroxine binding globulin ratio, 166–167
 - ultrafiltration, 163–164
 - uptake assay, 165–166
 - influencing factors, 159
 - overview, 158
 - total count, 158
 - uptake measurement, 187–200
 - amino acid transport systems, 188–191
 - amino acid identification strategies, 190–191
 - driving forces, 188–189
 - substrate specificity, 188–189
 - transport interactions, 189–190
 - cultured cell systems, 191–196
 - active transport, 195
 - amino acid incorporation determination, 194
 - cell count, 195–196
 - cell culture, 191–192
 - cell-surface binding, 194–195
 - passive transport, 195
 - protein content, 195–196
 - protocol, 192–194
 - transmembrane transport, 194–195
 - plasma membrane vesicle culture, 196–199
 - active transport, 199
 - advantages, 196
 - passive transport, 199
 - protocol, 197–198
 - vesicle isolation, 196–197
 - Thyroxine-binding globulin, thyroid hormone measurement, 166–167
- Toxicology
- assay techniques, 1–69
 - bioassays, 3–6
 - chemiluminescent assays, 51–55
 - colorimetric assays, 3
 - electrochemical immunoassays, 57–58
 - fluorescence assays, 44–51
 - future research directions, 68–69
 - hormone marker assays, 60–68
 - lipid-soluble hormones, 60–64
 - water-soluble hormones, 64–68
 - nephelometry, 59–60
 - nonradiometric assays, 32–44
 - enzyme-linked immunosorbent assay, 35–37
 - heterogeneous assays, 37–40
 - homogeneous enzyme assays, 40–44
 - particle-enhanced immunoassays, 60
 - potentiometric immunoassays, 58
 - radioimmunoassay, 9–32
 - antibodies, 13–18
 - antibody/receptor binding characteristics, 26–28
 - bound-from-free fraction separation, 21–26
 - data display, 26–28
 - radiolabels, 18–21
 - validation, 28–32
 - radioreceptor assays, 6–9
 - glutamate receptor toxins
 - excitotoxins, 242–243
 - neurotoxins, 240–242
 - metallothionein, 377, 382–383
 - toxic influence, prolactin plaque assay, 126–128
- Transfection techniques, d₂ dopamine receptor studies, 355–367
- clonal pituitary cell lines, 357–366
 - AtT20 cells, 364–365
 - GH4C1 cells, 357–358, 362–363
 - HEK 293 cells, 365–366
 - inducible expression, 364–365
 - parent cell line choice, 357–358
 - stable transfection, 358–363
 - transient expression, 365–366
 - future research directions, 366–367
 - overview, 355–357
 - prolactin secretion regulation, 355–356
 - receptor expression, 356–357

- receptor signaling, 356
 - technique rational, 357
 - Tri-iodothyronine
 - marker assay, 63–64
 - measurement, 158–169
 - free concentrations, 159–169
 - binding protein change, 160
 - direct measurement, 161–164
 - equilibrium dialysis, 161–163
 - immunoextraction assay, 167
 - indirect measurement, 164–169
 - labeled analog method, 167–168
 - labeled antibody method, 168–169
 - rationale, 159
 - technical difficulties, 160–161
 - thyroid transport proteins, 160
 - thyroxine binding globulin ratio, 166–167
 - ultrafiltration, 163–164
 - uptake assay, 165–166
 - influencing factors, 159
 - overview, 158
 - total count, 158
 - uptake measurement, 187–200
 - amino acid transport systems, 188–191
 - amino acid identification strategies, 190–191
 - driving forces, 188–189
 - substrate specificity, 188–189
 - transport interactions, 189–190
 - cultured cell systems, 191–196
 - active transport, 195
 - amino acid incorporation
 - determination, 194
 - cell count, 195–196
 - cell culture, 191–192
 - cell-surface binding, 194–195
 - passive transport, 195
 - protein content, 195–196
 - protocol, 192–194
 - transmembrane transport, 194–195
 - plasma membrane vesicle culture, 196–199
 - active transport, 199
 - advantages, 196
 - passive transport, 199
 - protocol, 197–198
 - vesicle isolation, 196–197
- Two-dimensional gel electrophoresis,
 - methodology, 203–219
 - blotting techniques, 212–217
 - digoxigenin-labeled lectins, 216–217
 - electroblotting, 213
 - support membranes, 213
 - total protein staining, 213–214
 - transfer buffer, 213
 - Western blotting, 214–216
 - computer-based image analysis systems, 217–218
 - first dimension
 - IPG system, 207
 - ISO system, 205–207
 - future research directions, 218–219
 - overview, 203–204
 - protein detection, 209–212
 - coomassie blue dye staining, 209
 - fluorography, 212
 - silver staining, 209–212
 - sample preparation, 204–205
 - second dimension, DALT system, 207–209
- U**
- Ultrafiltration technique, thyroid hormone measurement, 163–164
 - Umbelliferone, fluorescence assay
 - applications, 47–48
 - Uptake assays
 - amino acid and thyroid hormone uptake measurement, 187–200
 - amino acid transport systems, 188–191
 - amino acid identification strategies, 190–191
 - driving forces, 188–189
 - substrate specificity, 188–189
 - transport interactions, 189–190
 - cultured cell systems, 191–196
 - active transport, 195
 - amino acid incorporation
 - determination, 194
 - cell count, 195–196
 - cell culture, 191–192
 - cell-surface binding, 194–195
 - passive transport, 195
 - protein content, 195–196

Uptake assays (*continued*)

- protocol, 192–194
- transmembrane transport, 194–195
- plasma membrane vesicle culture,
196–199
 - active transport, 199
 - advantages, 196
 - passive transport, 199
 - protocol, 197–198
 - vesicle isolation, 196–197
- thyroid hormone measurement, 165–166

V

- Vasopressin, *see* Arginine vasopressin
- Vitamin D, marker assay, 63

W

- Western blot
 - corticosteroid receptor quantitation,
333–334
 - protein detection, 214–216

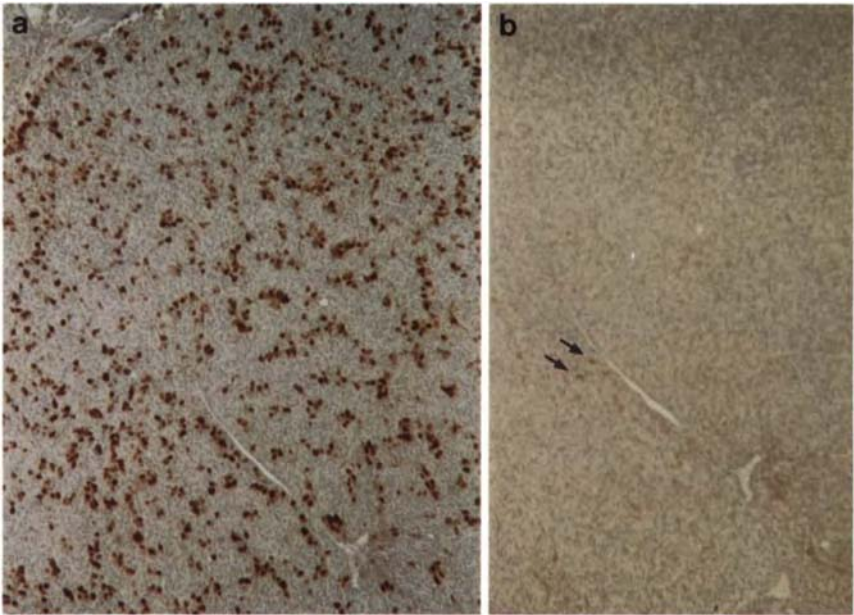


Figure 1. Photomicrographs of sections of an allograft of neonatal hypophysial tissue in place beneath the renal capsule of an intact female host for 322 days. Figure 1a depicts cells stained immunohistochemically for LH. Figure 1b shows the few cells (arrows) which are positive for FSH. Sections were counterstained with hematoxylin. Magnification is approximately 50 \times .



Figure 2. A prospective host hamster with the right kidney exposed. Note the light-colored piece of pituitary tissue (beneath the renal capsule) directly under the tip of the forceps in the right hand.